CRANFIELD INSTITUTE OF TECHNOLOGY

COLLEGE OF AERONAUTICS

Ph.D. THESIS

D.M. AHN

INVESTIGATION OF THE STRUCTURAL INTERACTION BETWEEN THE WING AND BODY OF A CLASS OF SIMPLE REMOTELY PILOTED AIRCRAFT

SUPERVISOR: K.H. GRIFFIN

OCTOBER, 1982

SUMMARY

Effects of various wing-body interaction design parameter variations on the structural behaviour of a small RPV have been investigated using the finite element method on an adhoc basis rather than a classical analytic approach.

The method in use is based on the substructuring displacement method considering the body and the wing as two major substructures. The elastic coupling effect of wing stiffness on the body structural behaviour also examined.

By comparing classical analysis methods to the present investigation, comments are made upon the use of those methods in the design analysis of the RPV class of structure. From the calculated results, general guidelines on the structural wing-body interaction analysis or design of this class of vehicle have been proposed.

A set of finite element programs have been developed for the present investigation, and relevant finite elements based on the displacement assumption have been formulated.

ACKNOWLEDGEMENT

I would like to express my deepest gratitude to my supervisor Mr. K.H. Griffin without whose sustained encouragement and guidance this work would not have been possible.

I am also extremely grateful to Prof. D. Howe for his sincere encouragement during this work and review of the manuscript.

I would like to thank Korea Agency for Defence Development for granting me study leave during the course of my research.

I express my grateful thanks to my parents for their patience and understanding during my study.

I also gratefully acknowledge help given by my friend Mr. R. Langley.

I express my sincere appreciation to my wife for her patient encourgement and understanding during our stay in England, and also for her very special care of the preparation of this text.

CONTENTS

LIST OF FIGURES

LIST OF TABLES

NOTATION

a	Length of shell element in longitudinal direction. Unknown coefficient matrix for finite element displacement assumption.
A	Cross sectional area of beam element.
A_f, A_r, A_s	Cross sectional area of frame element, ring element, and stringer element respectively.
b	Length of shell element in circumferential direction.
B	Strain-displacement relation matrix.
c	Shell element bending rigidity to extedsional rigidity ratio; $= t^2/12$.
C	Shell element extensional rigidity; $C = Et/(1-\gamma^2)$ Nodal displacement matrix for the shell element formulation.
C_{fx}, C_{fr}, C_{ft}	Frame internal force coefficients in X, R, and θ direction respectively. C_f=FR/PL$_c$
C_{mx}	Frame internal inplane moment coefficient C_{mx}=M/PR.
C_{ux}, C_{ur}, C_{ut}	Frame displacement coefficients in X, R θ direction respectively. C_u=uGtR/PL$_c$
C_{px}	Frame internal inplane rotation coefficient. $C_{px}=\phi_x GtR^2/PL_c$
C_g, C_p, C_t, C_f	Load factors for unit normal acceleration, unit pitching acceleration, tail load, and fin load respectively.
C.G.	Centre of gravity of the vehicle.

d	Depth of the deep frame.
D	Shell element bending rigidity. $D = Et^3/12(1-\nu^2)$
	Stress-strain relation matrix of finite element formulation.
E	Young's modulus.
F	Load vector for system equations.
	Internal forces of frame or stiffeners.
$F_{b\ fw}$, $F_{b\ rw}$	Interaction load vectors at forward and rear wing attachment respectively.
g	Gravitational acceleration.
G	Shear modulus of rigidity.
I	Second moment of inertia.
I_f, I_r, I_s, I_{sh}	Second moment of inertia of loaded frame, rings, stringers, and body cross section respectively.
I_x, I_y, I_{xy}	Beam element second moment of inertia normal, lateral respectively.
J	Torsional constant of beam element.
K	Shear coefficient of beam element with shear deformation effect.
	Stiffness matrix.
K_b, K_w	Condensed stiffness matrix of total body and wing respectively.
K_e	Element stiffness matrix.
L_c, L_f, L_r	Length of centre body, forward body, and rear body respectively.
L_{rsp}	Standard ring spacing.
m	Harmonic number in analytic formulae.
	Master degree of freedom.
M	Concentrated moment load on loaded frame in harmonic analysis.
	Mass matrix.
	Internal moment of frame or stiffeners.
Mb, M_{BT}	Bending moment on the body cross-section.

$M_x, M_\theta, M_{x\theta}$	Bending moment in longitudinal direction, in circumferential direction, and twesting moment of shell element. (= M_x, M_t, M_{xt} in graphs)
M_x, M_y, M_z	Bending moment about normal axis, lateral axis, and axis along shear centre of beam element.
N	Stress resultants vector of shell element.
N_{str}	Number of stringers in body cross section.
$N_x, N_\theta, N_{x\theta}$	Direct stress resultant, hoop stress resultant, and shear stress resultant of shell element. (= N_x, N_t, N_{xt} in graphs)
o	Fictitious member.
O	Null matrix or vector.
P	Concentrated radial load on loaded frame or reaction load at wing pick up point.
	Element load vector or matrix.
P_t	Total normal force on the tail plane.
$\overline{P}$	Condensed load matrix.
Q	Shear flow on the frames.
q	Distributed load vector.
R	Radius of body.
	Circumferential curvature of shell element.
R_B, R_W	Resultant reaction load vectors of body and wing respectively.
R_g, R_p, R_t	Reaction load vectors on wing pick up points due to unit normal acceleration, load, unit pitching acceleration load and tail load respectively.
r_c, r_s	Curvature of beam element centroid and shear centre respectively.
t	Thickness of body skin or shell element.
t'	Effective thickness of body skin in extension.
T_o	Concentrated tangential load on frame.
u	Displacement along body longitudinal axis.
u_e	Element displacement vector.

u_e, u_w	Displacement vector of body and wing.
U	Strain energy.
U_b	Interaction displacement vector.
U_g, U_p, U_t	Interaction displacement components by body loads of 1 g inertia, 1 rad/sec^2 pitching, and unit tail load respectively.
v	Circumferential displacement of shell element.
w	Radial displacement of shell element.
$\bar{x}, \bar{y}$	Offset of stiffening element shear centre from shell middle surface.
x_c, y_c	Dislocation between shear centre and centroid.
$Z(L), Z(Lc)$	Parameters in ESDU and Chpater 7; GtR^4/EI_fL .
α	Semiarc angle of shell element or beam element.
β	Twisting angle of beam element.
β_o	Opening angle of cutout.
γ	Shear strain of shell element.
γ_{xz}, γ_{yz}	Shear strain of beam element.
ε	Strain vector.
ε_o	Normal strain of beam element at centroid.
$\varepsilon_x \; \varepsilon_\theta$	Strain along longitudinal axis and circumferential axis respectively.
$k_x, k_\theta, k_{x\theta}$	Change of curvature about longitudinal axis, circumferential axis, and twisting of shell element.
θ	Circumferential angle.
ρ	Specific weight.
σ	Normal stress of beam element.
ϕ	Rotation of beam element about shear centre.
ϕ_x, ϕ_z	Curvature about longitudinal axis and circumferential axis of the shell or beam elementary respectively.
ν	Poisson's ratio.
ξ	$1/(\pi+2A_s/Rt)$

Subscripts and others

c	Centre body.
f	Frame or forward body.
r	Standard ring stiffeners or rear body.
s	Longitudinal stringers or booms.
rsp	Ring spacing.
str	Stringers.
w	Wing structure.
72-12-60	Representation of body substructure length; L_f=72.0 in. L_c=12.0 in. and L_r=60.0 in.
$[\ ]$	Matrix
$[\ ]^T$	Transposed matrix.
$\{\ \}$	Vector.
$\lfloor\ \rceil^T$	Transposed vector.

CHAPTER 1

INTRODUCTION

The demands on the unmanned reusable or disposable flight vehicle are rapidly growing due to the escalating costs of aircraft and their increasing vulnerability to the modern anti-air defence weapon systems. One type of unmanned flight vehicle, the remotely piloted vehicle (RPV), previously used mainly as a drone, has had its typical mission extended to the tasks of reconnaissance, decoy, harassment and attack (Ref.1-4) in the military purpose as well as being developed into a highly maneuverable research aircraft (Ref.5).

Despite major development of electronic devices for use of in this class of unmanned vehicle, little has been reported on the structural design and analysis of an RPV. Those reports which have appeared are not concerned with the overall structural behaviour, but mainly with the use of composite materials for the wing structure (Ref.6, 7) or components (Ref.8).

The wing-body interaction of an RPV has not only a major influence on the stress distributions in the overall structure, as on a usual aircraft, but also most frequent structural redesigns and reanalyses involving in during the preliminary design phase, because of the major structural assembly and the large concentrated load transmission.

From the extensive investigation of existing aircrafts and RPVs (Appendix A), typical characteristics of the existing and possible RPV structural designs can be summarized as follows:

i) Simple shell structure of the body around the wing attachment.

ii) One piece of the wing structure which is attached to the various positions of the body structure (low/high or mid-wing) and use of extreme low or high wing pick up.

iii) Simple wing assemblage and detachment using small number of pick up points.

iv) Small number of longitudinal stiffeners (stringers) and transverse stiffeners (rings), and wing pick up load frames which are relatively deeper or heavier than the frames used in the transport type fuselage.

These structural characteristics are quite different from those of the transport type of aircraft structure with the exception of the cross sectional shape. The sort of structural simplicities listed above are mainly the results of cost effectiveness and the requirement for the replacement of parts, both for disposable and reusable vehicle.

From the structural analysis point of view, whereas the large number of stiffeners in the monocoque fuselage of an orthodox transport vehicle distributes the concentrated wing load smoothly over the fuselage and enables the use of the assumption of stiffeners which are smeared out to the skin structure, the small number of stiffeners or wing pick up frames in the RPV produce abrupt changes in the stress distributions around them, consequently preventing the use of above assumption.

In particular the small number of wing pick up frames and attachment points will transfer severely concentrated wing loads to the body structure, while the large number of these wing-body connections used in transport or military fighter aircraft will provide smooth wing load transfer to the body structure.

The relatively smaller chord length or frame spacing due to the smaller wing taper ratio of this class of vehicle compared to those of aircraft, subjects the body to highly cocentrated shear loads and large bending moments around the wing attachments due both to wing loads and distributed body loads.

The question arises as to whether the classical design formulae used for a transport type semi-monocoque fuselage are resonably applicable to the simpler RPV body structural design, and whether simple design guidelines are available for the design and analysis of this type structure.

In the present research, the structural characteristics of RPV wing-body interaction have been investigated on an adhoc basis using the finite element method and the simple design of RPV which is shown in Appendix B.

As in the case of aircraft, numerous designs for the wing and body shape are possible. For the present analysis a simple body of circular cross section and a two spar wing have been chosen. This enables a comparison to be made with results yielded by the classical analysis methods or formulae which are used for transport type aircraft.

The effect of various wing-body design parameters, such as frame properties and the wing positions etc., on the body structural behaviour has been investigated, extensively using a set of developed finite element method body analysis computer programs which use the substructuring displacement method.

The influence of the wing stiffness on the body structural behaviour by the elastic coupling between these two substructure has been also examined and results are evaluated against the body alone analysis. The wing matrix has been condensed using the PAFEC 75 (Ref.9) program package, in lieu of developing another computer program.

Further parametric investigations are performed for more general discretely stiffened body shell structures. These include dimensional changes in the above RPV design.

Classical analytic or empirical methods which are used for the transport type of fuselage have been evaluated by comparison with the present results in order to asses the limitations of their application to small simple shell structures of an RPV body. Using the results of the present investigation, an attempt has been made to draw general guidelines on the wing-body intersection design and analysis of a class of small RPV structure.

Although only the case of simple structural wing-body interaction for a small RPV is considered here, the method used can be applied to the general wing-fuselage interaction analysis of any aero-space vehicle.

The set of specially developed cylindrical shell analysis finite element programs can be readily used for the preliminary phase of an RPV type body structure or for the analysis of similar type of shell structure without depending on the expensive general purpose structural analysis programs, such as PAFEC or NASTRAN (Ref.10) , The development of finite element method investigation program includes the element formulations for the shell, stiffeners and loaded frames. Especially the deep stiffneners or frames, due to the small size of RPV class compared to the aircraft structure, requires the use of deep beem elements which are connected to the shell skin with large eccentricities.

The aim of this research is to find the general trends of such simple structural design of RPV type wing-body interaction and expecting complicated structural behaviour, in contrast with those in an aircraft wing-body interaction structure.

CHAPTER 2

BACKGROUND STUDIES

2.1 Introduction

Typical wing-body interaction designs of existing aircraft and RPVs have been investigated in Appendix A, prior to the numerical investigation of the structural wing-body interaction of the RPV. The characteristics of the RPV class of vehicle have been described in the previous chapter.

The relevant classical analysis methods or design formulae for transport type aircraft fuselages have been surveyed, as there has been no previous investigation into the RPV type of vehicle. Several finite element approaches to the analysis of aircraft wing-fuselage interaction effects have also been surveyed.

In conjunction with the development of the finite element method body analysis program, subjects such as shell elements,beam elements and solution techniques have been briefly reviewed.

2.2 Classical Analyses and Design Formulae for Transport Type Fuselages

The salient feature of the general structural characteristics of most aircraft fuselage is that it consists of an outer skin of comparatively thin sheet which is stiffened in the longitudinal direction by stringers around the circumference, transverse rings to maintain the cross section, and heavier frames to distribute concentrated load into the skin. For such a structure, engineering beam theory approaches, such as the loaded frame analyses (Ref.11, 12) or shell analysis (Ref.13) for the fuselage, are no longer applicable due to the importance of shear deformation and the consequent warping of cross sections which gives rise to axial constraint stresses.

The flexibility of a frame produces much higher shear stresses in the skin due to transverse loads on the frame, than those predicted by the engineering beam theory, while the bending moments in the frame may be reduced. The presence of cut-outs in an aircraft fuselage reduces the applicability of these elementary theories.

The first theoretical solution for the flexible framed shell type of structure was developed by Wignot, Comb, and Ensrud (Ref.14). Their model of the shell assumes that there are no transverse stiffeners except the loaded frame. Hoff presented an analysis (Ref.15) based on the assumption that the unknown quantities are harmonic in polar angle of the shell. Kempner and Duberg (Ref.16) produced a recurrence formula for the stress analysis of reinforced cylinders loaded in the planes of their rings, using two design parameters of R^6t'/IL^3 and GtR^3/EIL^3. The structural model of the shell in references 15 and 16 considers the shell ring stiffeners to be equally spaced and to have second moments of inertia equal to that of the loaded frame.

Since the time that the matrix method of structural analysis introduced to aircraft structures by Argyris and Kelsey (Ref.17), this method has been used almost exclusively and MacNeal and Bailie's consecutive reports (Ref.18-20) are virtually the last analytical approaches for the aircraft fuselage analysis. In their harmonic analysis of a cylindrical fuselage with a single loaded frame, all structural behaviors are expressed as a function of harmonic coefficient Kn which relates the engineering beam theory values to those of each harmonic term. Using the basic long shell solution, Kn has been modified for various frame conditions.

These analyses are used extensively in design manuals such as ESDU (Ref.21). Kuhn (Ref.22) developed an analysis formula for the four longeron shell with or without cut-outs using empirical data. Argyris and Kelsey (Ref.17) have given a detailed review of aircraft fuselage analysis methods for more general shapes in their work.

The presence of the wing structure has always been neglected to minimize analytical complexity in the classical analyses. The shell is also assumed to be very long so as to neglect the clamped end reactions due to the self-equilibrating harmonic load terms.

The other important assumption made in the classical analyses is that of the role of the longitudinal and the transverse stiffeners. Usually the cross sectional area of these members are smeared out to the skin, which increases extentional stiffnesses of the shell, while bending and torsional properties are neglected.

However when the shell skin is very thin and the stiffeners are very sturdy, the contribution of these stiffeners to the bending rigidity of the shell becomes more important. In particular the major contribution of local twisting rigidity of a thin stiffened shell comes from the torsional rigidity of the stiffeners as desribed by Flügge (Ref.23).

2.3 Wing-Fuselage Interaction Analysis by the Finite Element Method

Although the simplified classical fuselage analysis methods or engineering beam theory are still useful for the preliminary analysis or design of semi-monocoque fuselages (Ref.13, 24, 25), the rapid development of large digital computers and the development of the finite element method have enabled a more rigorous analysis of the total aircraft structure to be performed.

Argyris and Kelsey (Ref.17, 26) applied the matrix force method to a general shape of aircraft fuselage, assuming the cross section to be a polygon of shear pannels with direct stress carrying longitudinal members at the vertices. The ring stiffeners were represented by beam elements to make a polygonal frame.

Using the substructuring technique proposed by Prezemieniecki (Ref.27), Taig (Ref.28) gave a multi-level substructuring analysis of an aircraft structure. Later Hansen et al. (Ref.29) gave their Boeing 747 wing-body intersection structural analysis using this substructuriing technique.

Kalev, Baruch and Blaso (Ref.30) proposed a wing-fuselage static interaction analysis by the combination of experimental results and the finite element method. They have used the substructuring force method (Ref.31) for the Kfir aircraft structure with the refined wing NASTRAN model and the beam type fuselage model. Numerical analyses and full scale separate structural tests for the wing and fuselage have been performed to obtain wing-fuselage interaction for any symmetric load conditions of the fuselage model. The calculated results of the fuselage disagreed with the test results due to its simple modeling.

2.4 Finite Element Shell Analysis Pertinent to Present Work

The most important factors in the finite element method of analysing shell structures are the adequate idealization of the shell geometry, the choice of the finite element formulation method and the use of an effective solution algorithm for the computer program. These factors are briefly discussed in their relation to the development of a cylindrical body analysis program in the following sections.

2.4.1 Shell Structural Idealization and Shell Elements

Numerous methods of finite element shell structure analysis have been reported in static, stability and dynamic analyses. Gallagher (Ref.32) and Zienckiewicz (Ref.33) summarized numerous thin shell idealizations and the shell finite element formulations which have been proposed in the literatures based on the direct displacement approach, hybrid or mixed formulation.

The common structural idealizations used in the finite element analysis of shell structures, such as the fuselage of an aerospace vehicle, a cooling tower, a pressure vessel etc, are as follows:

i) Polygonal representation using triangular or rectangular membrane or plate elements (Ref.26, 34-37).

ii) Axisymmetric representation using Fourier harmonic axisymmetric elements for the shell of revolution (Ref.38-42).

iii) Usage of triangular or rectangular curved shell elements to represent the shell curvature with or without the shallow shell assumption (Ref.43-52).

Usually the first type of representation requires the coordinate transformation of the element matrices to the global coordinate system during assemblage of the elements, while the second and the third do not need to be transformed.

When the shell is stiffened by many stringers and rings, as in a transport fuselage or the booster structure of a space vehicle, the structural idealization can be more simplified by the use of anisotropic axisymmetric element (Ref.38), shear panel or membrane elements for the skin and simple three degrees of freedom for the stiffeners (Ref.26, 53), or plate elements and ordinary beam elements (Ref.54).

2.4.2 Beam Elements

For the representation of stiffeners and frames, numerous beam elements are available. They are mostly based on the beam theory or the isoparametric formulation method. The straight beam element with shear deformation effect (Ref.55) is one of the basic elements which can be used for an idealization of the stringer members by applying the appropriate transformations and assumptions.

Curved thin-walled beams have been frequently used for the idealization of bridge girders (Ref.56-59). The effect of cross sectional warping due to torsion is commonly included in these formulations. These elements can be used to model ring stiffeners, discarding warping terms for the present structure. Curved beam elements which include the shear deformation effect (Ref.60-62) are also useful elements for the idealization of the ring stiffeners.

Most of those elements do not include the centroid-shear centre dislocation which is likely to happen in the present structure. The effect of eccentricity between the shell middle surface and the shear centre of the element can be incoorporated into these general elements by a simple transformation of coordinates.

2.4.3 Solution Routines

In the structural parametric study, due to the numerous design possibilities, it is anticipated to have many different proportions of the structural system equations.

Numerous effective solution techniques are available based on the direct or iterative method for the finite element method of structural analysis, as summarized in the Meyer's paper (Ref.63). The basic solution techniques for the systems of equations are incore solution techniques such as a band solver (Ref.64). For large systems of equations which are too large to be solved within the given computer central memory, it is common to use an out of core solver, such as Iron's frontal solution technique and its variations (Ref.65-67). The partitioning method or the substructuring technique (Ref.27, 28, 68-72) are also effective solution methods, which reduce the large systems of equations to systems which can be handled within the central memory.

The efficiency of those solution routines for large structural systems will usually depend upon the ratio of the incore usage, which is much faster but usually limited in size, to the use of the peripheral processor as a backing storage system, which is usually slower but no limitation in memory size.

When changes in structural geometry or material properties are involved as in the present design parameter changes, either substructuring techniques or reanalysis techniques (Ref.73, 74) using series expansion of sensitivity vectors will be neccessary. As pointed out by Meyer (Ref.63), these reanalysis techniques are sometimes error-prone or ineffective in reducing the computing time, so that substructuring techniques or complete reanalyses are preferable. Large finite element structural analysis packages, such as NASTRAN, have substructuring as a standard capability.

CHAPTER 3

SCOPE OF INVESTIGATION AND METHOD OF ANALYSIS

3.1 Introduction

The tasks herein are the investigation of general trends in the structural behaviour of small RPV's due to various wing-body interaction design parameter changes, and the formulation of general guidelines for the future structural design of this class of vehicles.

A small slender RPV model design has been chosen (Fig.3.1) to accomplish these tasks effectively. Detailed descriptions of the chosen RPV design are given in Appendix B. Given the basic dimensions of this structure, major design parameter variation effects have been investigated using a fixed body configuration and considering various positions of the wing around the circumference of the body cross section.

A set of finite element method cylindrical body analysis programs has been developed for the present investigations of the body structural behaviour. Since the concentrated wing loadings are transfered to the body through the wing pick up frames, the investigations are focused on the effect of design variations in the pick up frames and the centre body, such as the frame stiffness and the centre body cutout.

The body structure has been subdivided into three major shells in the longitudinal direction, and two frames.

The elastic coupling effect between the two major substructures, the body and the wing, has been investigated using a substructuring technique. The stress distributions in the total body structure and the wing structure have been examined and compared with the results obtained from a body alone or a wing alone analysis.

Other important wing-body interaction parameters, such as the pick up frame pitch, have been investigated in accordance with changes in the basic body shell dimensions. Alterations were made in the properties and dimensions of the original structure including a change in the relative positions of the wing and the tail planes and a change in the stiffener properties. Effect of number of stiffeners also examined.

The classical design formulae which are used for the analysis of transport type fuselages are evaluated against the results of the present investigations in order to asses the limitations in their application to RPV design.

The major items which are investigated are as follows:

i) Axial and circumferential distributions of displacements and stresses in the skin and stiffeners of the body.

ii) Circumferential distribution of internal loads in the loaded frames.

3.2 General Assumptions and Load Conditions

The general assumptions made in the present investigation into the wing-body interaction of a class of small RPV are as follows:

i) Nonstructural members at the nose and tail sections of the body are neglected, so that the body is a cylindrical shell.

ii) The same isotropic material is used for all structural members.

iii) The circumferential and the longitudinal stiffeners are spaced regularly throughout the body structure, and the number of stiffeners is so small that their properties are not smeared to the skin properties.

iv) Wing and body are joined together at two positions along the body axis, and at a single point along the semicircumference through the frames in a statically determined manner for the symmetric load cases.

v) The angle of wing incidence is assumed to be zero so that the plane of the wing is parallel to the vehicle longitudinal axis.

vi) The tail units and the fin are connected to the body by a single point at the end circumference, and their stiffnesses are negligible.

vii) The inplane stiffness of the wing structure along the wing span is very large compared to the shell stiffness.

viii) The total structure is symmetric about the global X-Y plane of symmetry (Fig.3.2) as in orthodox aircraft.

ix) The centre of gravity of the vehicle is located at the forward frame centre.

The basic loadings considered here are the distributed and concentrated vertical loads due to normal acceleration or symmetric pull up which are symmetric, and the torsion load on the body due to roll which is antisymmetric about the plane of symmetry. The symmetric load on the vehicle is assumed to be balanced by the combinations of wing normal forces, body normal acceleration inertia, pitching acceleration inertia, and normal force on the tail plane.

Thus, in the investigation of the body structural behavior, the following three symmetric load conditions (Fig.3.3) have been considered:

i) The structural inertia load due to unit normal acceleration which will be multiplied by the appropriate mass ratio of total vehicle mass to structural mass.

ii) The structural inertia load due to unit pitching acceleration of structural mass.

iii) The tail normal force which is reacted by the concentrated wing normal loads at the pick up frames.

The total wing reactions at the wing pick-up points will be the algebraic sum of the above three loads. Although there is the obvious disadvantage of another step to arrive at the actual wing-body interaction forces due to these resolved symmetric load sources, the structural behavior under each load condition will give a clear quantitative idea of the interaction forces.

In the case of the antisymmetric loading due to roll produced by aileron deflection, which is the most important load source of the body torsion, it is assumed that the reactions are carried by the tail plane and the fin only (Fig.3.4). Therefore, the rolling inertia terms of the wing and body as well as the changes in the normal force distribution on the wing is balanced by the normal forces on these tail unit.

According to the above chosen load conditions, the boundary conditions are applied along the plane of symmetry of the structure in the usual manner. The restraints on the plane of symmetry are all inplane degrees of freedom for the symmetric load conditions, and all out of plane displacement constraints for the antisymmetric load.

3.3 Finite Element Structural Idealization

The total RPV structure has been subdivided into three major substructures of the body shell, the loaded frames and the wing. The tail plane and fin structure stiffness effects have been neglected while the loads on these structures are transfered to the body shell as described in the previous section.

The body shell structure consists of the skin, the ring stiffeners, and the longitudinal stringers as shown in Fig.3.5. The body structure is further subdivided into the forward body, the centre body in which the wing is attached, and the rear body.

Using the symmetry of the structure about the vertical plane of symmetry, only one half of the structure has been modeled and analysed. One of the finite element structural models for the total vehicle is shown in Fig.3.6. Details of the body and the wing finite element idealizations are given in Chapters 4 and 5 respectively.

3.3.1 Body Shell Structure Finite Element Idealization and Elements Used

The basic structural components of the body shell are the direct stress carrying skin member and two types of stiffening members, one in the longitudinal and the other in the transverse direction.

Among the numerous methods of shell element formulation, Sabir and Ashwell's strain element formulation method (Ref.50) with Novozhilov's shell theory (Ref.75) has been chosen to represent the shell skin. In this formulation, the simple strain functions are found from the shell compatibility equations, instead of using the usual displacement assumptions or stress assumptions along the boundaries of element (Appendix C). This strain assumption enables the use of an explicit integral for the formulation of the element matrices, and has shown a high level of accuracy when a smaller number of degrees of freedom are considered. The cylindrical shell geometry of this element does not require the transformation process of the element matrices.

The transverse ring stiffeners have been modeled using the curved thin-walled beam element which is given in Appendix D. This curved beam element has been modified to a straight thin-walled beam element and used for modeling the longitudinal stringers. This element allows for a centroid-shear centre offset as well as for the dislocation of the shell middle surface and the beam shear centre.

3.3.2 Loaded Frame Considered and Finite Element Modeling

The flexibility of the loaded frame is a major cause of deviation of the body structural behaviour from that predicted by elementary beam theory, as is also the case for the transport type fuselage. The choice of frame design for a small RPV is much greater than that available for the transport type fuselage. A limited number of frame designs have been selected for the present investigation.

The typical types of loaded frame design which are considered in the present investigation (Fig.3.7) are as follows:

i) A rigid diaphragm or bulkhead which has much greater stiffness in its plane than the radial and tangential stiffnesses of the shell element, while it has negligible out of plane stiffnesses so as to allow warping of the cross section of the shell. This type of frame has been modeled by rigid spring elements which completely prevent inplane displacements and rotations along the circumference.

ii) A simple circular ring frame which has constant cross sectional properties around the circumference. Depending on the depth and eccentricity of this type of frame, it can either be a simple ring frame, a ring frame with eccentricity or a boom-web-boom construction annular frame.

iii) Finally a noncircular frame whose properties are not constant around the circumference. This radial unsymmetry results from heavy local reinforcements around the wing attachments. This frame can have two variations depending upon the frame depth.

The possible radial unsymmetry of the frame design and the number of stringers in the body shell were the main obstructions to the use of an axisymmetric analysis.

The booms of the loaded frame are modeled by the same curved beam element which is used to model the ring stiffeners. The web member in the boom-web-boom type frame is idealized by the isoparametric inplane element (Ref.76).

3.3.3 Wing Structure

The wing configuration, which is shown in Fig.3.1, has the leading edge sweep back angle of 2.7 degrees, the quater chord sweep back angle of zero degree and the trailing edge sweep forward angle of eight degrees. The aileron is located outside of the 79% semi-wing span and afterward of the 70% chord line.

The convential torsion box type wing has been used. The wing structure consists of six ribs and two spars, using isotropic material. The main forward spar is placed at the quater chord line, while the auxiliary rear spar is placed at the 70 per cent chord line.

The wing skin is modeled by the isoparametric plate bending element. The spars and ribs are idealized by using simple beam elements for the lower and upper booms and an isoparametric membrane element for the web.

Unlike the previous body and frame modeling and analysis, the PAFEC 75 program has been used for the condensation of the wing structure. The finite element model of the wing is shown in Fig.5.1.3. The aileron structure is neglected. The same wing model has been used for the various wing-body attachment position design.

3.3.4 Structural Symmetry and Antisymmetry

The body and the frame structures have been assumed to be symmetrical about the vertical plane of symmetry as in many aerospace, civil engineering, and marine structures. This structural symmetry permits a complete structural analysis to be made by considering only a portion of the total structure (Ref.77).

Although the use of the horizontal plane of symmetry is possible when considering the shell only, this is not the case when the wing structure is included. It is also precluded by the requirements of a further transformation procedure to match with the unsymmetric system equations of the possible unsymmetric loaded frame case.

3.4 Analysis and Parametric Variation Study of Chosen RPV Body Structure

As a first step to the present investigation, the effect on the body structural behaviour due to the change of wing-body design in the following ways, has been examined:

i) Position of the wing in the circumference of the body, which is varying five different circumferential angle from 180 degree position (low/high wing) to 90 degree position (mid wing) with variation of 22.5 degree.

ii) Variation of the frame type as discussed in section 3.3.2 and changes in the frame stiffness properties, such as second moment of inertia and eccentricity etc.

iii) Consideration of the centre body cutout, which is neccessary in order to assemble the wing structure.

iv) Different combinations of frame types for the forward and rear frame, such as diaphragm-ring frame and deep noncircular frame-ring frame etc..

Due to the long shell geometry of the body, differences in structural behaviors from those predicted by beam theory will be most noticeable near to the frame stations. Thus the present investigations are mainly concerned with the centre body shell and the loaded frames. The outer bodies have been assembled as substructures.

3.5 Static Wing-Body Interaction Analysis

The wing interaction effects occuring in the body shell, have been examined by assembling the condensed wing stiffness to the centre body. The condensed wing matrix is obtained from the eigen value calculation routine in the PAFEC 75. The influence of the body structure on the wing structural behaviour can be analysed by PAFEC program using the interaction displacements which are obtained from the body analysis. However, the wing analysis is excluded in the present investigation.

Including the basic wing-body interaction of the normal force and displacement, other types of possible interactions , such as axial force and moments, also have been examined.

Details of the wing structural model and the usage of PAFEC program for the condensation of wing stiffness matrix are given in Chapter 5 and Appendix F respectively.

3.6 Further Investigation of Body Shell Design Parameters

The investigations were extended to a more general design of cylindrical RPV body in order to examine the effect of varying the following design parameters:

i) The slenderness ratio of each substructure of the cylindrical body, including the frame spacing.
ii) The number of stiffeners and their properties.
iii) The position of tail plane around the circumference of the body.

By comparing the results of the present investigation with those given by classical analytic methods, the applicability of those methods to the present type of shell structure has been examined.

3.7 Development of the Computer Program

Although a very useful finite element structural analysis package, PAFEC 75, was readily available at the beginning of this research, it was considered to be uneconomical to use such a general purpose computer program to investigate the structure, considering the number of runs neccessitated by the so many design parameters and variations.

In order to perform an efficient investigation, a set of small finite element cylindrical RPV wing-body interaction analysis program has been developed on the basis of substructuring technique, although the PAFEC 75 program was used for the analysis of the wing structure.

As shown in Appendix H, the complete package used is devided into several small modular programs to achieve maximum substructuring efficiency. They are interfacing each other through the backing storage disc files.
A brief summary of the developed modular programs, together with the externally supplied PAFEC 75 role in the analysis, is as follows:

i) ELMAT; Element stiffness and distributed inertia load matrices generation routine for the four noded cylindrical shell element and the curved or straight thin walled beam used for stiffeners.

ii) CONSH; To obtain the condensed structural matrices of the forward and rear body, and the displacement/stress solution of these structures by back-substitution.

iii) LOADFR; To obtain the structural matrices for the various types of loaded frame which are assembled to the centre body.

iv) PAFEC 75; To obtain the condensed wing stiffness matrix and to analyse the wing structural behavior under the body structure presence.

v) CENSOL; The main centre body solution routine for various centre shell design options. This program reads in the condensed structural matrices of the other substructures, solves for the displacements and stresses in the centre body, and back-substitutes the boundary displacement data for the outer shells and the wing structures.

3.8 Units and Coordinate System Used

Throughout the present research, the imperial units have been used in pound force (lbf) and inch system.

Cartesian coordinates are used for the general description of the structural system and loads. However, in the actual displacement and stress calculation, the cylindrical polar coordinates have been used in order to exploit the cylindrical geometry which does not need to be transformed to assemble element matices. Thus the load matrices which are in the global cartesian coordinates of the vehicle, such as the vertical inertia load or the wing load matrices, are transformed to the cylindrical polar coordinates in the program. The coordinate system used for the general description of the vehicle is shown in Fig.3.2.

The sign conventions used for the stress resultants, internal forces, and displacements of the shell and ring elements in the cylindrical coordinates are shown in Fig.C.1 and Fig.D.1 respectively.

3.9 General Notes on the Graphic Outputs

Most of the results are plotted using a CALCOMP plotter and the GINO graphic subroutines. The automatic scaling routine in the graphic subroutines produces odd scale factors for many graphic outputs. Furthermore, the small number of circumferential mesh (mostly eight elements per semi-circumference) and the curve fitting routine make some results be more complicated. However, unless there are sharp changes of displacement or stress distributions, the results are fair enough to show trends and relative magnitudes of the finite element output.

As the structural behaviour near the wing pick up is of primary intrest, most graphic outputs are drawn for the structure between two standard ring stiffeners which are located either side of the two loaded frames. The results are generally represented circumferentially (in degrees or Y/R) as well as longitudinally (in body station number or relative position from the frames). Generally the horizontal axis is used for the circumferential nodal position.

The major graphic outputs can be represented by the following categories:

i) Displacement distributions of the type of Fig.4.3.10: These are generally plotted using a single scale which is taken from the maximum value of displacement present. This scale is shown at the bottom left of vertical axis. The longitudinal body positions are shown along the right hand side vertical axis. A zero displacement line for each is drawn as a solid hozontal line. The results for the forward body are drawn at the bottom, while those for rear body are on the top of graphs.

ii) Stress distributions of the type of Fig.4.3.13: These are also plotted in one scale as the displacement distributions, but the results are drawn mostly on the separate graph for each of longitudinal body position. The order of this body station appearing is usually from the bottom of page to the top and from the left to the right side. Therefore the graph at bottom left represents the circumferential stress distribution at the standard ring position forward of the forward pick up frame, while the graph on the top represents the opposite case.

iii)Stress distributions of the type of Fig.4.4.1; When the general trends of stress distribution are shown for the variation of a single design parameter, the same graphic representation as the displacement distributions are used. However, the shell stress distributions at both both sides of each frame are drawn separately.

iv) Stress distributions of the type of Fig.4.4.21: Another set of graphs for the stress distributions is used to show a schematic comparison along the circumference and longtitude of body. The relative magnitude of stress is represented by the radially distorted shape of the original semi-circle. The scale for stress level is shown in one inch length scale.

v) Stress distributions of the type used in Chapter 5: The membrane and bending stress of the shell around the circumference of two frame positions and the middle of two frames are plotted on separate page for each stress. Comparisons are made between two different wing pick up conditions side by side for each case of stress. The individual scale for each stress is used. Therefore the maximum value of vertical axis represents 1.2 times of the maximum stress in each type of stress resultant

vi) Shear flow distributions of the type of Fig.4.3.19; The shear flow distributions on the two loaded frames are plotted mostly in nondimensionalized coefficient form. The results for the forward frame are drawn on the left side and for the rear frame on the right side. Unless there are sharp variations of shear distributions, the smooth curve fitting subroutine in GINO is used.

The structural dimensions and design variables which are constant are placed at the top of each page, and the variation of a design variable is indicated at the bottom, in most graphic comparisons.

CHAPTER 4

ANALYSIS AND DESIGN PARAMETER VARIATION STUDIES OF WING PICK UP STRUCTURES

4.1 Introduction

A cylindrical body structure of small RPV in Appendix B under the distributed and concentrated load has been analysed using the finite element method. This analysis has led to the investigation of structural behaviour of the wing attachment structure due to various design parameter variations. Analysis and investigation are mainly concerned about the wing pick up structures, such as the centre body shell and the loaded frames.

The wing loading is assumed as balanced reactions of distributed body loads and concentrated tail load for the case of symmetric loading by constraining the assumed wing attachment points. The antisymmetric load due to the aileron deflection is assumed to be balanced by the tail plane and fin normal forces. Forces on those tail units are assumed to be transmitted to the body as concentrated loads.

The effect of concentrated wing loads and flexibility of the loaded frames die out more or less rapidly increasing the distance from the wing pick up frames according to the Saint-Venant principle. Consequently stresses and displacements approach the values predicted by elementary beam theory.

To concentrate the investigation on this disturbed region, the substructuring technique has been used deviding the body into three major shells. The stiffnesses and load matrices of the outer body shells have been condensed, and they are assembled to those of the centre body to which the wing is attached through the frames. One diameter's length of the outer shell has been taken to be the centre body in order to compare the disturbed structural behavior with that predicted from elementary theory.

The calculated stresses and forces at nodal points are averaged in most cases except shear stress around the loaded frames. The shear flow load on the frames has been found from the difference in shear stress resultants in the skin elements at each side of the frame as usual.

Details of dimensions and general assumptions are given in Appendix B and in the previous chapter. The basic structural dimensions and assumptions for finite element idealization of the body structure are briefly summarized as follows:

i) Thin body shell skin with radius of 6.0 inch and thickness of 0.06 inch.

ii) Two main wing spars are attached to the loaded frames by a single point at each semicircle.

iii) Transverse ring stiffeners are placed at equal intervals of 12.0 inch, L_{rsp}, and they are identical throughout the body.

iv) Four longitudinal booms (stringers) are placed at equal intervals, at 45^{o}, 135^{o}, 225^{o} and 315^{o} angles respectively.

v) Total length of the body is 144 inch which is divided into 72 inch length of the forward body, L_f, 60 inch length of the rear body, L_r, and the centre body, L_c.

vi) The centre of gravity, C.G, of the vehicle is located at the X=72 inch position on the longitudinal axis (forward frame).

vii) The inplane stiffness of the wing structure in its spanwise direction, Z, is rigid, but it is negligible in the chord wise, X, direction.

viii) The wing pick-up positions are constrained in a statically determined manner to prevent rigid body motion in the vertical direction and to simulate the wing normal force. The axial restraint is applied on the forward pick up position.

ix) Using the structural symmetry about the vertical Y-Z plane, half of the body has been modeled with appropriate boundary conditions along that plane.

A simplified finite element model of the total body structure without the wing and the tail unit is shown in Fig.4.1.1. One of the idealized centre body structures is also shown in Fig.4.1.2. Most of graphic representation of results are plotted in accordance with the notes in section 3.9.

4.2 Design Parameters to be Investigated

The classical design parameters, for the shell structure with single loaded frame are GR^4t/EI_fL of Kempner's (Ref.16) or ESDU (Ref.21) and $R[t'R^2L_{rsp}/I_R]^{\frac{1}{4}}/\sqrt{6}$, $R\sqrt{Et'/Gt}/2$ of MacNeal's (Ref.18-20). They cannot be evaluated in the present finite element analysis for the two-framed body structure.

Although those parameters are related to the properties of all the parts of the shell structure (i.e., shell, ring stiffener, stringers and frame), the major differences from the beam theory arise from the frame stiffness I_f as shown in Appendix E.

Another important factor is the wing attachment points on the circumference of body, because the radial and the tangential load components on the frame due to the wing load depend on this position.

A possible structural discontinuity in the centre body also contribute significantly to the body structural behaviour. This discontinuity may arise from the cutout made for joining the wing structure to the inside the centre body.

Rather than examining the classical collective form of design parameter, the specific effects of the following design parameters on the body structural behavior have been examined in the present investigation:

i) Position of the wing attachment points around the circumference of body with two relatively heavy ring frames (I_f=0.1 in^4).
ii) Inplane bending stiffness of the loaded frame varying from the same second moment of inertia of the standard ring stiffener to the rigid diaphragm which has infinite inplane bending stiffness.
iii) Variation of the frame depth.
iv) Local reinforcement around the wing pick up points of the loaded frame.
v) Difference in the stiffnesses of two frames.
vi) Cutout of the centre body shell below the wing plane with an intermediate wing pick up at 135^o.

The other parameters relating to more general shell structures and the stiffeners are examined in Chapter 6.

4.3 Effect of the Wing Pick Up Position Variations Around the Circumference of the Shell

The wing attachment position on the fuselage of the aerospace vehicle affects not only an aerodynamic wing body interference (Ref.78), but also the internal load distributions of the fuselage structure. Many important design factors are involved in determination of this position, such as the requirements of internal payload arrangement, aerodynamics and performance, and structure etc.

Various positions of the wing attachment around the circumference of the body have been investigated in the structural point of view. This position is defined as the angle from the vertex of the circular cross section in the present work. Thus the mid-wing is assumed to be located at the 90 degree position, while the low-wing and the high wing are assumed to be at the top and the bottom vertices of the body circumference respectively. The intermediate positions between those extreme cases are also considered at equal intervals of 11.25 degrees.

The high wing or the low wing are extreme cases of the wing attachment but they affect the body structural behavior in the same manner. Therefore in the present investigation, both of them have been taken account of the low wing which is attached to the body at the 180 degree position of the circumference. A general description of the wing pick up position is given in Fig.3.2.

The loaded frames considered in this investigation are mainly rigid diaphragms or relatively heavy circular rings which have constant section properties around the circumference.

Because the wing loads are transmitted to the body structure as normal forces on the plane of the wing through the frames, change of the wing pick up position leads to the variation of the magnitude of radial and tangential force components on the frame. The low/high pick up is assumed to be subjected to pure radial loads, and the mid wing pick up to two pure tangential loads.

4.3.1 Displacements

For the case of mid wing pick up in the present analysis, the structural behavior of the body structure will be similar to that of the deep beam in which shear deformation effects are important, because the constraints are applied along the neutral axis of the body shell. The transverse frames and ring stiffeners will have negligible effect on the radial deformation of the circumference and warping of the cross section of body with the mid wing pick up under the symmetrical load conditions.

The vertical displacement and the inclination angle of the cross sections of the body with the mid wing pick up, are compared with the solutions of simple beam element and Timoshenko beam finite element analyses (Ref.31, 53) in Fig.4.3.1 and Fig.4.3.2 respectively. Tangential displacements and rotations of the ring stiffeners and the frames under the end tail load have been used in those comparison, and they are taken from the points along 90 degree position of the body circumference.

The shear coefficient K in the Timoshenko beam element, which is dependent upon the cross sectional shape, has been chosen from Cowper's theory (Ref.79, 80). This theory considers the lateral deflection and the inclination angle of the cross section of the beam to be the average values occuring in the section, while Timoshenko (Ref.81) and Roark (Ref.82) defined them at the neutral axis. In those figure, K=0.5306, is from $2(1+\nu)/(4+3\nu)$ for the cylindrical tube, and K=0.4355 from $20(1+\nu)/(48+39\nu)$ for the thin walled square tube of Cowper's formulae.

As shown in those comparison, it is interesting to note that K=0.4355 for the square tube gives closer agreement with the shell finite element analysis for mid wing pick up than K=0.5306 for the circular tube. This could be due to the presence of the longitudinal stringers which form a square within the shell.

Displacement distributions in the centre body with mid wing pick up under symmetric loads, form trigonometric curves around the circumference, as shown in Fig.4.3.3-4.3.5. These are nearly the same as the results given by beam theory. Consequently the stresses in the shell will have the same pattern as predicted by beam theory. Therefore no frame flexibility effects appear in the displacement and stress distributions of the body with the mid wing pick up, and beam theory can be used without any problems.

On the other hand, when the wing is attached at the top or bottom (0 or 180 degree position) of the circumference, it is no longer possible to predict displacements and stresses of the shell using a beam theory, due to the frame flexibility effect and shifting of restraining points from the neutral axis of cross section. The concentrated wing loads will be resisted by the flexible frames and adjacent shell skin as highly concentrated membrane and bending stresses.

Comparing Fig.4.3.6-4.3.8 for the low wing pick up with Fig.4.3.3-4.3.5 for the mid wing pick up, amount of cross sectional distortion (differences between the maximum and minimum axial deflection), the radial and tangential deformations of the body circumference can be noticed. These are mainly caused by the flexibility of loaded frame.

To illustrate the effect of wing pick up position change on the body circumference in another way, the ring frames have been replaced by the rigid diaphragms. The axial displacement under the tail load is also increased by increasing the pick up angle, but it is nearly the rigid body shift as shown in Fig.4.3.10.

However, despite of the pick up position changes, the radial and tangential displacement distributions in the centre body shell (Fig.4.3.11-4.3.12) show no difference at all. Furthermore these inplane diplacements are almost similar to those in the body having a mid wing attachment.

Thus when the loaded frame has an infinite stiffness in its plane and negligible stiffness in its normal direction, such as a rigid diaphragm or bulkhead, no effect of the wing position changes on the body structural behaviour can be expected, and the stresses in body shell skin can be predicted by elementary beam theory as they are in the case of mid wing pick up.

4.3.2 Stresses in the Shell

The larger distance between the wing pick up position and the neutral axis of body cross section produces the greater perturbation of displacements predicted by elementary theory. This will lead to the same tendencies in the shell stress distributions.

The effect of wing position change on the stresses in shell is examined in this section. This investigation includes the bending moments in shell element, which are mostly ignored in the classical wing body interaction analyses or design formulae for an aircraft structure.

4.3.2.1 Direct Stress Resultants (Fig.4.3.13)

As expected from the displacement results in the previous section, the cosine distribution of axial displacements gives the same pattern of direct stress distributions around the circumference of body shell having the mid wing attachment. Furthermore this direct stress distribution due to the mid wing pick up is almost identical to that predicted by beam bending theory.

The large axial deformation due to the low wing attachment not only increases the direct stress level, but also noticeably changes the stress distributions in the circumferential direction as well as in the longitudinal direction. Especially at the forward frame station, where beam theory does not predict any bending moment and direct stress under the tail load, the radial reaction due to low wing pick up produces a near cosine distribution of direct stress having a considerable magnitude.

The maximum direct stress due to the low wing pick up at the rear frame has been increased drastically, while opposite side compression stress has been reduced. It is noticeable that this effect dies out as the distance from the frames increases, and that the frame effects cancell out at the middle of those frames, showing a similar distribution to that predicted by elementary theory.

The intermediate pick up position (135 degree) affects the axial stress distribution slightly through a reduction of radial loads and a shifting of the loading point toward the neutral axis of the body.

The direct stress level of the low wing at the forward frame is almost purely a radial local reaction effect, while the distribution at the rear frame station is a combination of the overall bending action result and the local radial load effect.

4.3.2.2 Hoop Stress Resultant (Fig.4.3.14)

As a consequence of the large deformations due to the increasing wing pick up angle, the hoop stresses in the shell are also greatly disturbed from the usual cosine curve of the mid wing pick up case. These changes are especially significant around the pick up frames.

At the forward frame station where the overall bending is negligible, the radially inward local reaction load effect is predominant, due to zero curvature about the axial axis, for the case of the low wing. The combined effect of the overall bending and local radial load at the rear frame reduces the loading point stress but increases the peak value.

These local effects are nearly cancelled out at the middle of the frames as in the previous case of direct stress, by reaction loads occuring in opposite directions. However the tendency for these effects to die out away from the frame station is much less than in the direct stress case.

4.3.2.3 Shear Stress Resultant (Fig.4.3.15)

In the case of the mid wing pick up, the regular sine and cosine distributions of the body displacements give the same sine curve pattern of shear stress distribution as elementary beam theory.

On the other hand, large radial and tangential displacements due to the low wing pick up induce considerable changes in the shear stress distribution. The position of the peak stress is shifted away from the centres towards the loading points, and the maximum stress level is increased by more than 50 per cent over the mid wing case.

Under tail loading, the shear stress distribution between the two frames is nearly constant, as would be predicted by elementary beam theory. Except the mid wing pick up case, considerable shear stresses are found in the forward body where according to elementary beam theory shear force does not exist.

4.3.2.4 Bending Stress Resultants

As in the previous membrane stress resultant distributions, the low wing pick up produces very large bending moments in contrast with negligible bending in the mid wing pick up case. Large concentrated local bending stresses due to the low wing pick up can be observed at the 180 degree position for the axial and circumferential bending moment distributions in the skin (Fig.4.3.16, 4.3.17).

The effect of the stringers on the twisting moment of the skin is apparently an abrupt reduction along the 45 degree and 135 degree positions of the circumference, where the stringers are placed, as can be seen in Fig.4.3.18. Even if this effect of stringers are appeared in circumferential bending moment distribution also, it has been disappeared when the frames or rings are placed.

Although the magnitudes of these bending moments are small, the additional stresses at the extreme fiber of the shell element which are induced by these bending terms are very large due to the thin shell thickness. The maximum increased stresses due to bending are about 25 per cent in direct stress, 70 to 150 per cent in hoop stress and about 30 per cent in shear stress for the low wing pick up case.

4.3.3 Shear Flow on the Frame

In classical theory, the loads on the shell stiffening frame are found from the difference in shear flow between the adjacent skin members.

The same method has been used to find the shear flow from the shell to the frames using the shear stress resultant distribution in the skin. These shear flow distributions in the two loaded frames are shown in Fig.4.3.19 for three different positions of the wing position. The sign difference between the shear flow in the two frames results from the direction of the local reaction force under tail loading. It is noticeable that the forward frame is subjected to a slightly greater shear flow than the rear frame by the low wing pick up. This is caused by the presence of the elementary shear stress distribution in the rear body skin due to the end tail load.

4.3.4 Antisymmetric Loading

The antisymmetric load has been applied to the present structure at the end circumference where the tail plane and the fin are assumed to be attached. It consists of 100 lbf for each of the tail plane normal forces and the same amount for the fin load.

As shown in Fig.4.3.20, the axial shell stress is not affected considerably. The stress distribution for the low wing slightly differs from that for the mid wing. Direct stresses gradually increase from the negligible level in the forward body up to the rear frame position. The overall bending stress due to the end fin normal force predominates this direct stress distribution.

In Fig.4.3.21, the hoop stress distributions at the frame stations show the strong effect of the local pick up constraints. The hoop stress resultants at station 78 and 90, where there are no stiffeners, show the effect of the stringers between the 45 degree and 135 degree positions. This stress rapidly dies out away from the forward frame.

The shear stresses in the centre body are shown in Fig.4.3.22. The effect of the fin loading, although small, can be seen on the rear body shear stress distribution, shifting the zero stress point towards opposite side of the fin. This fin effect becomes negligible in the centre body due to the large wing reaction loads at the pick up frames. Constant shear stress is produced between the two frames as it is in the symmetric loading case. Changing the pick up position from the mid wing case, the shear stress distribution is shifted by a nearly constant amount unlike the other stresses.

The difference between the results of the 135 degree wing pick up and the low wing pick up is very small, as was the case for the results of the mid wing pick up and the 135 degree wing pick up under symmetric loading. Also, the low wing pick up produces greater shear and hoop stresses in the shell as in the case of symmetric loading.

4.4 Effect of Frame Properties Variation

The stiffness of the ring frame is mainly dependent upon the cross sectional area for tangential displacement, and the second moment of inertia and curvature for radial displacement. The case of low/high wing attachment, which is the most critical case of pick up conditions as discussed in the previous section, has been investigated.

Although the cross sectional area of the curved beam affects the bending behavior of the frame (Appendix D), the more dominant parameter is the second moment of inertia of the frame cross section, due to the severe radial load applied by the low/high wing attachment to the frames. Therefore this section investigates the effect on the centre body structural behaviour due to variations in second moment of inertia of the frame.

4.4.1 Shell Stresses under Symmetric Loadings

When the frame bending stiffness is infinite (rigid diaphragm), the displacement distributions are exactly the same as the results of beam theory as shown in Fig.4.3.9-4.9.12. This leads the similar shell stress distributions as are obtained from the mid wing pick up.

In Fig.4.4.1-4.4.5, two different values of the frame bending stiffness are compared with the rigid diaphragm, to see the frame flexibility effect on the shell stress distributions. One is a relatively stiff ring frame with large second moment of inertia (0.1 in^4) as used in section 4.3, and the other is a light ring frame which has the same second moment of inertia as the standard ring stiffener (0.01 in^4).

As a consequence of the frame flexibility, the light frame produces the highest stress resultants around the low wing pick up points. It also causes a very gradual reduction in membrane stresses with increasing distance from the frames. This is as expected from the classical analyses of the aircraft fuselage.

A considerable increases in the shell bending moments are observed for the flexible frame cases. On the other hand, the negligible shell bending moments are present for the rigid diaphragm case.

4.4.2 Stresses in the Body Skin under Antisymmetric Load

The presence of the fin normal force effects on the body stress distributions not only in the manner of bending action but also in the torsion. The pure coupling due to the tail plane produces additional torsion on the body.

In the direct stress distributions (Fig.4.4.6, 4.4.9), the light frame produced approximately 10 per cent higher maximum stress for the low wing pick up and about 30 per cent higher maximum stress for the mid wing pick up than the heavy ring frame. This frame flexibility effect is apparent in the forward body where no internal forces appear according to beam theory.

The rigid diaphragm frame produces the ordinary sine curves of the direct stress distribution, and no direct stress in the forward body. These are mainly due to the bending action of the fin normal force and the constrained inplane displacements of the frames.

The out of plane force and moment about the plane of symmetry due to antisymmetric wing load reaction affect significantly on the hoop stress and the shear stress distributions as in the case of the flexible frame with the different wing pick up positions (section 4.3.4). These significant changes are appeared more clearly by the light frame.

Especially the hoop stresses at the frame stations (Fig.4.4.7, 4.4.10) show significant difference between two flexible ring frames. The maximum stress due to the light frame show more than 250 per cent greater stress than that due to the heavier ring frame.

The shear stress distributions in the rear body are affected by the torsion and the bending. While the coupling due to the tail plane produces pure torsion on the rear body, the fin normal force produces not only the torsion but also the bending moment and the shear force.

The dominant bending action is observed in the centre body because the constant shear stress around the circumference according to elementary torsion is negligible in this region, especially for the case of the diaphragm frame.

The magnitude of the maximum shear stress is almost unchanged in the centre body by the change of the frame stiffness, but the overall circumferential distribution is considerably affected by the frame flexibility (Fig.4.4.8, 4.4.11). The light frame produces near sine curve distributions of shear stresses in the body semicircle for the mid wing pick up case, while the diaphragm frame produces cosine curves.

Therefore the maximum stresses in the body under the antisymmetric load are predominated generally by the fin bending action as well as by the frame flexibility.

4.4.3 Frame Loads and Displacements

The frame shear loads from the shell are shown in Fig.4.4.12 - 4.4.13. The lighter frame increases the shear flow drastically near the low wing pick up points under the symmetric loading, while reducing the stress opposite the pick up points. It is interesting to note that the increased area of the shear flow distribution curves due to the flexible frames from the regular sine curve due to the diaphragm frame, is nearly the same as that obtained from the reduced area opposite sides.

On the other hand, the shear flow due to the anti-symmetric loading with a mid wing pick up does not show any great dependence upon the frame stiffness. Because of the unsymmetric end fin loading and its bending action, the rear frame shear flow is slightly different from a cosine curve, while the shear flow on the forward frame is almost exactly a cosine curve.

Circumferential displacements and inplane internal forces in the forward ring frames are shown in Fig.4.4.14 and Fig.4.4.15 respectively, in which nondimensional co-efficients are used to compare the effect of frame stiffness. Significant reduction of the inplane and out-of-plane displacements are achieved by increasing the frame stiffness, whereas the stiffer frame absorbs the greater internal loads.

4.4.4 Annular Frame

An alternative way of increasing the bending stiffness of the frame is the use of an annular type ring frame. Because of the relatively small radius of the RPV type body structure, this type of the deep frame is more likely compared to the frames in the conventional transport type fuselage.

The deep annular frame has been examined in comparison with the relatively stiff ring frame in Fig.4.4.16-4.4.20. The low wing pick up position and the tail loading condition have been considered in order to clearly illustrate the effect. A web of depth 1.0 inch and thickness 0.1 inch has been considered.

The deep frame shows very similar patterns of stresses to the diaphragm, producing near cosine curves for direct stress and hoop stress, and near sine curves for shear stress distribution, together with zero bending moments. These results are mainly due to the increased frame inplane bending and the frame extensional stiffness in its plane, while the normal stiffness of this frame is negligible.

Schematic comparisons of this frame and the other types of frame are shown in Fig.4.4.21 for the direct stress and Fig.4.4.22 for the shear stress resultants. A symmetric tail load and low wing pick up position have been used in these comparisons.

4.5 Effect of Local Reinforcement at the Vicinity of Wing Attachment Position

It is often necessary to locally reinforce the frame which is subjected to large concentrated loads or moments. To examine this reinforcement effect, reinforcement has been applied to the light ring frame, whose bending stiffness is same as the standard ring stiffeners.

The bending stiffness of the reinforced element is ten times that of the unreinforced member, and a concentrated tail load condition with low wing pick up position has been considered. Two types of the strengthened region in the loaded frames are compared with the unreinforced pure ring frame. The one is in the region of ± 22.5 degrees and $\pm$ 45.0 degrees around the loading points.

The effects of this local reinforcement are far greater than might be expected. As shown in Fig.4.5.1 - 4.5.2, the stress concentrations around the loading points are considerably reduced. Comparing the shear flow distributions on the locally stiffened frames with that on the unstiffened ring frame in Fig.4.5.3, the peak value of shear flow on the heavily reinforced frames (135 - 225 degree) is much less than that occuring on the ring frames.

The displacements and internal loads in the frames have been compared in Fig.4.5.4 and Fig.4.5.5 respectively. It can be seen that there are enormous reductions in the radial displacement and the inplane curvature around the pick up position.

Another type of local reinforcement is considered for the annular frame with depth of 1.0 inch. In Fig.4.5.6 and Fig.4.5.7, the direct stress and shear stress in the centre body shell have been plotted for the symmetric annular frame of the previous section together with those for a frame having heavy local reinforcement (between 135 degree and 215 degree). Small reductions of the shell stresses can be seen.

4.6 Effect of Stiffness Difference Between Two Frames

In the actual design of aerospace vehicles, it is likely that the two loaded frames will have different stiffnesses due to the requirements of strength and load.

The heavy forward ring frame has been combined with various sizes of the rear frame. Also, combinations of the diaphragm and flexible ring frames have been investigated.

When the rear frame reaction load is small, as in the 1 g load case, the flexibility of the rear frame does not significantly effect (Fig.4.6.1, 4.6.2) the shell behaviour. On the other hand, when the rear frame reaction is as large as in the case of tail loading, the stress distributions are severely influenced by the flexibility of the rear frame (Fig.4.6.3, 4.6.4) even though this is less stiff than the forward frame. As shown in Fig.4.6.5, the shear flow on the both the flexible frames under tail load are entirely dependent on the rear frame flexibility.

In contrast with the above frame combination, when the forward frame is replaced by a rigid diaphragm or bulk-head, the influence of the restrained local deformations at the forward frame station reduces the maximum stress (Fig. 4.6.6 - 4.6.8) by approximately 10 per cent compared to the results in Fig.4.1.1 and Fig.4.1.2.

On the other hand the reverse combination, a forward ring and a rear diaphragm, reduces the maximum stresses by about 20 per cent (Fig.4.6.9-4.6.10).

Displacements and inplane internal loads on the forward frame are shown in Fig.4.6.11 and 4.6.12. Although the inplane displacements are mainly reduced by its large bending stiffness, the out of plane displacement of the frame is influenced by the rear frame flexibility.

Therefore the use of diaphragm for any one frame reduces the maximum stresses considerably, due to the reduction of the frame flexibility effects on the body stresses.

4.7 Effect of Centre Body Cut-Out under the Wing Plane

Unlike large aircraft structures, the class of small remotely piloted vehicles does not need many small cutouts in the body which cause structural discontinuity and con-sequently stress redistribution around the cutout.

The one structural discontinuity considered here is that small portion of the centre body skin which is taken out from the lower quadrant for assembling the wing structure. It is assumed that this cutout is located between the two bottom stringers in the circumferential direction, and between the two loaded frames in the longitudinal direction. Therefore an intermediate wing pick up position (135 degree) has been assumed.

In the finite element analysis of this cutout problem, the missing members are taken to be fictitious elements in order to preserve the constant band width and the solution efficiency. The imaginary nodes in the cutout are completely constrained, as described in Appendix G. During the forward elimination and back-substitution procedures, the constrained degrees of freedom have been omitted since these imaginary elements are not related to the remaining structural elements.

Structural discontinuity due to the cutout leads to irregular displacements and stresses around cutout. The centre body axial displacement distribution is a typical example of disturbed deformations. As shown in Fig.4.7.1 and Fig.4.7.2, the axial displacements around the cutout have been greatly increased due to the loss of the structural members.

This sort of large displacement leads to heavy local stress concentrations. Fig.4.7.3 shows that the major axial stress concentration occurs along the lower boom, and zero stress occur at the free vertex (180 degree position of the frame). These effects are noticeable especially at the corners of cutout, where the axial stresses are more than twice those occuring in the regular shell. Hoop stress concentrations appear at the 112.5 degree position of the shell, between two frames (Fig.4.7.4).

It is also noticeable that the shear stress directions have been changed at the vicinity of the cutout along the frame station (Fig.4.7.5).

In Fig.4.7.6 and 4.7.7, schematic diagrams of stress distributions under tail loading are shown. Because of the coarse mesh used in the model, serious stress concentrations do not occur.

CHAPTER 5

WING-BODY INTERACTION ANALYSIS OF COMBINED STRUCTURE

5.1 Introduction

In the previous investigation of the body structural behaviour and its response to changes in the various design parameters, the stiffness of the wing structure was neglected except for the inplane stiffness of the mid wing structure which was assumed to be infinite in its spanwise direction. The wing load was simulated as a combination of the reactions due to each loading condition on the body.

To investigate the influence of wing stiffness to the body structure, they have been assembled together for the analysis of this chapter. Fig.5.1.1 and Fig.5.1.2 show the finite element models of the combined structure of the wing and the centre body, for the mid wing and low wing pick up cases respectively. A finite element model of the wing structure for the static condensation is shown in Fig.5.1.3.

The investigations are carried out by using the PAFEC 75 for the wing substructuring together with the developed body analysis programs which have been used in the previous chapter. The main solution program for the centre body analysis has been slightly modified to cope with the wing stiffness assembly.

The interactions between the two structures are as assumed primarily to be wing normal forces through the wing attachment points. Single point interaction for each semicircle of the loaded frame is assumed, as in the previous chapter. A simple ring framed body shell model is used to illustrate the wing effect on the body structural behaviours, and the results are compared then with those in the previous chapter. The form of the graphic plots used in this chapter is described in paragraph (v) of section 3.9.

5.2 Body Structural Idealization

The outer body matrices have been condensed to the positions of the loaded frames. To prevent rigid body motion due to releasing the constraints at the wing attachment points, four fictitious beam elements have been added to the loaded frames. These connect the two vertices of the loaded frame to the centre of the body. These beam elements are assumed to have very small cross sectional area and second moment of inertia. Constraints are then applied to the centre of shell where these fictitious beam elements are joined together (Fig.5.2.1).

Wing load components due to the distributed body and the concentrated tail reaction loads have been applied to the wing attachment points. The magnitudes of the wing load components are found directly from the reaction forces produced by the assumed body load conditions at wing pick up points, which were found from the body alone analysis in the previous chapter.

The condensed wing stiffness which is found by using the PAFEC 75 has been assembled to appropriate degrees of freedom of the centre body system stiffness matrix. This assemblage of the wing stiffness, which is similar to a simple two noded beam element, leads to an enlargement of the band width in the system equations and consequently longer CPU time. The number of degrees of freedom between the two loaded frames in the centre body, is the maximum band width in the system equations to be solved. Thus, to reduce the computing time and the scratch file disc block size, a coarse mesh model of the centre body is used.

5.3 Modeling and Static Condensation of the Wing Structure

The wing structure was idealized as an assembly of isoparametric plate elements and beam elements, PAFEC 75 computer program was used to perform the static condensation of the wing matrices and the structural analysis (see Appendix F). To avoid complexity in the comparison of results, the same wing structural model has been used for the various wing attachment positions to the body.

The display picture of the finite element model is shown in Fig.5.1.3. The finite element model excludes the aileron structure; fitting and all mechanisms (N.B. there are no other control surfaces except the aileron in the wing). The upper and lower skins are represented by the isoparametric quadrilateral plate bending element to cope with the distributed aerodynamic pressure load. The transverse ribs and the spars are modeled by using simple beam elements for the upper and lower booms, and the triangular or quadrilateral membrane elements for the webs. A coarse mesh model has been used to reduce computing costs. It consists of 180 nodes, 824 degrees of freedom and 327 elements.

In order to investigate the wing stiffness effect on the body structural behaviour, the condensed wing stiffness matrix is extracted from the PAFEC 75 eigen-value solution routine by choosing the interaction nodes in the two main spars, for each wing pick up position, as the master nodes. The master degrees of freedom are then selected under the present assumption of wing-body interaction, i.e., Y and Z direction forces interact only in global coordinates. The other degrees of freedom for the wing itself are chosen as the slaves. During the eigen value calculation in PAFEC, the master degrees of freedom are retained, whereas the slave degrees of freedom are eliminated to form the effective stiffness and mass matrices in eigen value economization scheme.

A brief description of the use of PAFEC program for the condensation of wing stiffness matrix is given in Appendix F, and the detail of eigen value economization scheme in the PAFEC 75 can be refered to Ref.9.

5.4 Formulation of the Wing-Body Interaction Equation

As mentioned in the previous sections, the condensed stiffness and load matrices of the wing, loaded frames and outer shells are assembled to the centre body matrices without reducing the centre body stiffness and loads to the boundary nodes.

It has been found that the centre shell substructuring needs much greater computer CPU time than does the direct solution, due to the elimination of the internal degrees of freedom and the back-substitution process required for solving the internal displacements. Furthermore the substructuring of centre body needs a large backing storage disc blocks in order to store the elimination of internal degrees of freedom which are related to the outer degrees of freedom in both directions of the body axial axis towards the two boundaries at the loaded frames. Once the reduction is proceeded in one direction, it still requires another transformation process in order to obtain the terms for the other side and the coupling terms between two boundaries.

Thus, a coarse mesh model in the axial direction together with a direct solution method has been used to minimize programming efforts and computing costs.

The final equilibrium equation of the centre body with the wing stiffness effect included can be written as follow:

$$\left[\bar{K}_b + \bar{K}_w\right]\{u\} = \{F\} \quad \ldots\ldots\ldots\ldots\ldots\ldots\ldots (5.4.1a)$$

Details of each of the terms appearing in the above simple equation are given in eq. (5.4.1b) on next page. The load vectors on the wing pick up, $F_{b\ fw}$ and $F_{b\ rw}$ in eq. (5.4.1b), are the same forces as the reaction forces of the body alone analysis with constraints at these points. Exactly the same load conditions as were used in the previous chapter have been used for the other loading terms.

The fictitious displacements corresponding to the fictitious beam elements at the centre line of frame stations are prescribed as zeroes in appropriate directions to prevent the rigid body motion of total body structure.

$$\begin{bmatrix} Koo_{f} & & & & & \text{SYMMETRIC} & \\ Kob_{f} & Kb_{f} & & & & & \\ 0 & Kb_{fw,f} & Kb_{fw}+Kw_{f} & & & & \\ 0 & Kcb_{f} & Kcb_{fw} & Kc & & & \\ 0 & 0 & 0 & Kbc_{r} & Kb_{r} & & \\ 0 & 0 & Kw_{r,f} & Kbc_{rw} & Kb_{rw,r} & Kb_{rw}+Kw_{r} & \\ 0 & 0 & 0 & 0 & 0 & Kob_{r} & Koo_{r} \end{bmatrix} \begin{Bmatrix} 0 \\ u_{b\,f} \\ u_{b\,fw} \\ u_{c} \\ u_{b\,rw} \\ u_{b\,r} \\ 0 \end{Bmatrix} = \begin{Bmatrix} 0 \\ F_{b\,f} \\ F_{b\,fw} \\ F_{c} \\ F_{b\,r} \\ F_{b\,rw} \\ 0 \end{Bmatrix} \quad \text{.................................. (5.4.1b)}$$

in which the subscripts indicate the following:-

o; fictitious beam member to constrain rigid body motions,

b; boundary with forward or rear body and frames,

w; condensed wing, c; centre body internal degrees of freedom,

f; forward boundary, fw; forward wing pick up,

r; rear boundary, rw; rear wing pick up.

5.5 Effect of the Wing Stiffness on the Body Structure

Using the centre body model described in section 5.2 and solving eq.(5.4.1), the body structure has been analysed including the wing stiffness effect. The typical low and mid wing pick up cases have been examined under the 1 g loading and the tail loading conditions. Comparisons are made mainly for the shell stress resultant distributions between the two loaded frames.

When the wing is attached at the low/high pick up, the influence of the wing inplane stiffness is nill. The only contribution of the wing stiffness to the body is via the normal displacement terms affecting the body radial displacements. As shown in Table 5.1a, the normal stiffnesses of the condensed wing are very small compared to those of the shell and ring frame element stiffnesses.

Thus no effect of the wing stiffness on the body can be expected for the low wing pick up case, and as shown in Fig.5.5.1 for the circumferential distributions of direct stress and in Fig.5.5.2 for the bending stress resultants, no wing structure effect on the body stress distribution can be seen in these comparisons of the two types of body analysis.

In the mid wing position, the radial and tangential stiffnesses of the wing are no longer negligible. In particular, the inplane stiffness of the wing (radial stiffness of the body) has a comparable order of magnitude to those of the shell element or the frame element. However, this stiffness is not so great as was considered in the previous chapters, where it was assumed to be infinite. This increment to the radial stiffness of the body at the frame stations slightly affects the hoop stress distribution of the shell near the forward frame, although it makes no difference to the other membrane stresses of the shell as shown in Fig.5.5.3 and Fig.5.5.5.

Even though the bending moments in the skin are very much affected by this additional stiffness at shell neutral axis (Fig.5.5.2 and 5.5.4), he overall stress resultants are not significantly influenced by the presence of the wing structure. For example in the case of concentrated load at atil, the maximum direct stress at the pick up position due to bending (Fig.4.5.2) is about 40 per cent of the membrane stress at that point (Fig.4.5.1).
The shear stress due to twisting also has nearly the same magnitude as the direct stress.

Two cases of the wing pick up variation are compared in Fig.5.5.7 and Fig.5.5.8. The large increases in the hoop stress and bending moments in the centre body shell having the low wing pick up can be seen compared to the mid wing pick up as they are in the body alone structure.

In Fig.5.5.9 and Fig.5.5.10, the direct and shear stresses in the whole body shell under the three symmetric loading cases are plotted and comparisons are made with the results from the body alone analysis. Almost identical stress distributions can be noticed except the pitching moment loading case in which the body alone analysis show approximately 15 per cent higher maximum stresses in the centre body.

5.6 Variation of the Wing-Body Interaction Type

So far, it has been assumed that the wing-body interaction occurs only in the normal forces and displacements of the wing. Two other possible interaction types are invetigated in this section. The first type is that the wing attached to the body tightly in the longitudinal direction as well as previous normal and spanwise interaction, and the second is a complete interaction, except the moment about the lonitudinal axis which is usually avoided in most aerospace wing-body interactions.

When the first type interaction is used for the low wing pick up, the direct stresses in the body are only affected by the additional axial stiffness caused by the wing. Slight changes in the maximum direct stress can ben seen in Fig.5.6.1 and 5.6.2, while the other stresses and bending moments are not affected at all compared to previous normal force interaction. However this change in direct stress is also negligible for the mid wing pick up (Fig.5.6.3-5.6.4).

On the other hand, when the second type of wing-body interaction is in use for the mid wing pick up (Fig.5.6.5-5.6.6), significant increases of the membrane stresses and bending moments can be seen. Especially drastic changes of stresses around pick up position are noticeable. Consequently this type of bending interaction also show considerable disadvantages for the body stress distributions.

CHAPTER 6

FURTHER INVESTIGATIONS OF THE BODY SHELL DESIGN PARAMETER VARIATION

6.1 Introduction

The effects of various design parameter changes have been investigated in the previous two chapters using the chosen RPV model design which has given dimensions for the body and wing structures. In this chapter the investigations are extended to cover more general cylindrical body design paremeter variations, which are as follows:

i) The number of longitudinal stringers and their properties.

ii) The ring stiffener sectional properties and spacing.

iii) The loaded frame spacing and variations in its properties which were not covered in Chapter 4.

iv) The slenderness (L/R) of body sections, especially for the rear body under the tail loading case.

v) The position of the tail around the end circumference.

The results obtained after having varied one of the above parameters are compared with those obtained for body structure dimensions and properties. The investigations are primarily focused on the behaviour of the centre body shell, as in the previous chapters. In most cases, the simple ring type of loaded frame and the low/high wing pick up have been considered in order to illustrate more clearly the effect of variations in the parameters.

The unit tail load was chosen as the load condition, in order to enable an easy comparison to be made to the results of elementary theories.

The basic shell dimensions, radius and thickness, have also been altered from their previous values in many of the parameter variations. The arrangements of displacement and stress output are explained in section 3.9.

6.2 Effect of the Stringer Design Parameters

In the classical analysis of a shell having many stringers and flexible load frames, the stringers are smeared out to the shell skin which causes an increase in the effective extensional stiffness of the skin in membrane action. Unless the stringers are very closely spaced, this will lead to errors in the prediction of the local shell behavior. The effect of the stringer area has been examined in two ways - keeping the total stringer area constant while changing the number of stringers, and vice versa.

6.2.1 Variation in the Number of Stringers (N_{str})

A common way of dealing with stringers in an analytical solution is to smear them into an equivalent thickness of skin which only posseses axial direct stiffness. In an attempt to see the likely effect of such an assumption, the standard four stringer solution has been compared with two others, each aiming to represent the same total stringer area. One of the solutions is for the case of 16 stringers each of one-quarter of the basic stringer area.

The other is where no stringers have been incorporated in the finite element model, but the skin thickness has been increased to represent the effective stringer area. This is not the classical case of smearing, as the additional skin is isotropic and therefore adds to the circumferential and shear stiffness as well as that in the axial direction. This is referred to as the zero stringer case.

In section 4.3, it has been shown that, when the wing is attached at the middle of the shell circumference, the shell having four stringers undergoes almost the same vertical displacement along the neutral axis as a square tubular beam. However, this vertical displacement distribution in the case of zero stringer is a little larger than in the case of tubular beam having circular cross section, as shown in Fig.6.2.1. The maximum vertical displacement of centre body of zero stringer case is approximately 12 per cent higher than those of the other types of stiffened shell. On the other hand, the shell having 16 stringers produced almost the same vertical displacement as the four stringered shell or square tube. The circumferential displacement distributions of these shells show the same trends as the vertical displacements as shown in Fig.6.2.2-6.2.4.

As a consequence of the larger axial displacement by the zero stringer shell(Fig.6.2.2), the highest direct stress also produced by this shell (Fig.6.2.5). It can also be seen from this figure that the direct stress produced by the sixteen stringer shell is considerably lower than both that in the four stringered shell or zero stringer shell. Therefore the use of the zero stringer shell (or smeared shell) for the present class of shell having small number of stringers is conservative to predict direct stresses. On the other hand, the distributions of radial and tangential displacements(Fig.6.2.3-6.2.4), consequently shear stress(Fig.6.2.6), do not show any sigificant differences by the change of number of stringers.

When these shells are subjected to a radial load (low or high wing pick up condition), the sparsely stiffened shell (N_{str}=4) produces higher direct stress near the pick up point, while the shell having many evenly distributed stringers (N_{str}=16) produces less concentrated stress, as shown in Fig.6.2.7. This would not be predicted by elementary beam theory, since the second moment of area of the four stringer shell is slightly larger than that of the 16 stringer shell.

This can be explained by examining the local stiffness of shell. While none of the stringers are located at the loading point for the four stringer shell, a longitudinal member is placed at the wing pick up position in the case of 16 stringer shell causing a reduction in the local direct stress. The increase in skin thickness by the zero stringer shell also reduces the direct stress level, but it is not as effective as using stringers.

For the cases of hoop stress(Fig.6.2.10) and shear stress distribution between two frames (Fig.6.2.8), they show the same trends as the direct stress. The shear flow distributions on the frame do not show any significant differences as shown in Fig.6.2.9. The effect of stringer positions can be seen clearly in the bending stress resultant distributions in Fig.6.2.11 to Fig.6.2.13. In particular, the shell having zer stringers shows a significant rise in the twisting moment along the stringer line (45 and 135 degree positions).

6.2.2 Variation of the Stringer Properties

As a second alteration of the stringer properties, the area of the stringers is increased. All other variables are kept constant, and four stringers are considered.

The increase in extensional stiffness caused by the enlargement of the stringer cross sectional area naturally reduces the direct stress level (Fig.6.2.14). However, the shear and hoop stresses are not so affected by the change in the stringer area, as shown in Fig.6.2.15-6.2.16. This is due to the negligible contribution of the stringers to the shell radial and circumferential stiffnesses.

The effect of the stringer area change has been examined for the intermediate wing pick up case (135 degree), with and without cutout of the lower body. The apparent effect of increasing the stringer area on the local direct stress concentration for the shell with cutout is shown in Fig.6.2.17a.

When there is no cutout in the shell (Fig.6.2.17b), the ratio of the direct stress level at the two boom positions is 57.3% and 56.2% respectively, while this ratio is approximately 61% and 63% at the upper and bottom quadrant of the shell (Table 6.1).

Although it may be small, the local stress reduction due to the changes in the stringers can be seen from these comparisons. The coarse mesh used in the finite element model would not be expected to show up the effect of stringer area variation clearly.

In contrast to the significant influence of the stringer area on the direct stress distribution, the effect on the shear stresses is almost negligible Fig.6.2.18.

This is because the shear strain in the shell is related to the change in tangential displacement along the longitudinal direction and the change in axial displacement along the circumferential direction, and the stringers provide a negligible contribution to the circumferential stiffness.

The longitudinal distribution of axial force in the two types of stringer is examined in Fig.6.2.19 which concerns a shell having a cutout at the bottom quadrant. While the two boom areas show the same force distribution trends and a similar ratio of the total second moment of inertia of the cross section along the upper boom, the larger stringer carries much higher axial loads along the lower boom, which is located at the edge of the cutout. Consequently the direct stress in the shell skin reduced, as shown in Fig.6.2.17.

When the bending stiffness of the stringer is changed as well as its cross sectional area, there is a gradual reduction in the shear flow at the frame as these properties are increased, as shown in Fig.6.2.20. Comparing this result with that in Fig.6.2.18, in which the second moment of inertia of the stringer is kept constant (I_s=0.08 in^4), it can be noticed that the changes in stringer bending stiffness also affect the shear flow distributions. Thus, whereas the cross sectional area of stringer is affecting mainly on the shell direct stress, the second moment of that influences primarily on the shear stresses.

6.3 Effect of Ring Stiffener Design Parameters

The presence of ring stiffeners near the loaded frame will restrain the displacements of the shell and will consequently increase the local shell stresses caused by the flexibility effect of the loaded frames. Thus the stiffer ring stiffener will produce higher stresses in the shell around the loaded frame than the lighter ring stiffener.

Fig.6.3.1-6.3.3 show the effect of the ring bending stiffness on the stress distributions in the centre section of the body shell, under an end tail load. As shown in these figures, an increase in the bending stiffness of the ring produces slightly higher direct and shear stresses and reduces the maximum hoop stress in the shell.

The cross sectional area and second moment of inertia of the ring stiffener are altered simultaneously, and the results are presented in Fig.6.3.4 and Fig.6.3.5. These figures show that the shear stress is entirely dependent upon the bending stiffness, while the area of ring has no effect on the shear stress distribution. This indicates that the shear stresses are more affected by the bending stiffness of the ring than the cross sectional area.

The effect of ring stiffner spacing change on the shell stresses are examined in Fig.6.3.6-6.3.8. Two types of spacing are used in those figures. The one is a radius length and the other is a diameter length. The larger spacing produces the greater direct stress at the frame stations, while it does the smaller shear flow on the frames than the narrow spacing. Approximately 30 per cent higher maximum direct stress and 15 per cent lower maximum shear flow are found.

The above results indicate that the frame flexibility effect is more localized around the frames by either the large ring stiffener bending stiffness or narrow spacing. In other words, the ring bending stiffness per unit length of the shell apparently affects the shell behaviour more than the cross sectional area of the ring stiffeners.

6.4 Effect of Frame Pitch

In the classical analysis method, the frame spacing is considered to be large enough to allow the fuselage to be treated as a single framed shell. However, as shown in the previous chapters this is not strictly applicable to the small class of RPV bodies which have very narrow frame spacing.

Because of the narrow spacing of the two flexible frames, the adjacent shells are affected by these frames in three distinct manners. The first one is the usual flexibility effect of one frame. The second effect is a result of the displacements or stresses transfered from the other frame, which rapidly die out with increasing distance from the frame. The third type is where one frame acts towards the other as a ring stiffener as described in the previous section.

The second and the third effects are equivalent in most classical analyses, since the loaded frame is assumed to have the same properties as a ring stiffener.

However, they are treated separately in the present investigation due to the great difference in the stiffnesses of the rings and the frames.

Two types of the frame spacing are compared in Fig.6.4.1-6.4.4. One spacing is considered to be small being equal to the diameter of the shell, whereas the other is twice this value. The wider frame pitch shows a much lower and smoother stress distribution than the smaller one. This indicates that the effect of the other load frame is greatly reduced and that fundamental beam bending action predominates as frame spacing increase.

Fig.6.4.1 shows that the effect of the flexible frame on the direct stress in the shell nearly vanishes at one diameter length away from the frame. Fundamental beam bending action is dominant at the middle of the two frames due to the cancelling effect of the two frames having opposite radial faces.

In constrast, as shown in Fig.6.4.2, the shear stress distribution shows neither rapid decaying outside the two frames nor does it show dominant bending action at the middle of the two frames. Although the ratio of the shear force in the centre shell is two to one for the two lengths of centre body, the maximum shear stress resultant ratio is approximately 2.5 to one due to the effect of other frame.

In Fig.6.4.4, the frame spacing has been examined in conjunction with the radius of shell. Despite changing the shell thickness, the shear flow distributions are entirely governed by the ratio of the frame pitch to the shell radius. As shown in Fig.6.4.4a and 6.4.4b, shells of the same L_c/R ratio produce almost identical circumferential distributions of shear flow.

Shear flow distributions of shells which have the same cross sectional dimensions are collected in Fig.6.4.4d. This shows a significant reduction in the stress level as this ratio increases, and ultimately the results approach to the case of shell with a single flexible loaded frame under the concentrated radial load.

6.5 Other Frame Design Parameter

The frame has been assumed to be a simple ring type frame having a large bending stiffness in the previous section. In Chapter 4, the effect of various frame design parameters has been examined in conjunction with the investigation into the effect of the chosen body structure design variables.

More parameters concerning the frame design are examined in the present section. The effect of the frame depth is again considered, using a smaller value than previously.

Various types of eccentricity in the frame design are also examined. The effect of the frame cross sectional area is also investigated.

6.5.1 Effect of the Frame Depth

In the previous investigation of the loaded frame effects, the deep symmetric and unsymmetric boom-web-boom type frame produced a similar shell structural behaviour to the rigid diaphragm frame, due to its large inplane bending stiffness.

The same type of frame, but having a smaller depth (1.0 inch for the previous case and 0.5 inch for the present case) has been analysed and compared to the simple ring type of frame and the previous deeper frame. The basic dimensions considered here are 0.04 inch web thickness and a beam second moment of inertia of 0.0002 in^4, as before.

Despite the symmetry of frame, the frames which have a shallow depth affect the shell stresses in the same way as the deeper annular frame (Fig.6.5.1-6.5.2). Whereas the highest direct stress is induced by the shallow annular frame, the deep annular frame causes the highest shear stress resultant. It can be seen that the shear distribution is a near sine curve for the deep frames, whereas this curve is deviated towards the wing loading points for the shallow frames.

When compared to the relatively stiff ring frames, it can be seen that these frames cause a sharp reduction in the direct stress at the loading points (Fig.6.5.1), and a considerable reduction in the frame shear flow (Fig.6.5.3).

Thus the boom-web-boom type frames are very effective in reducing the shell stresses over those produced by the ring type frame, the frame inplane stiffnesses.

This sort of deep frame is much more realistic in practical design than a ring frame with large bending stiffness. From these investigations into the effect of frame depth, it can be concluded that it is rather conservative to use the simple ring element idealization for the loaded frames for the present class of small RPV.

6.5.2 Effect of the Ring Frame Eccentricities

Idealizing the circular loaded frame as a ring, it is usually neccessary to take account of the eccentricity caused by the shear centre the centroid dislocation, as well as the offset of the shear centre from the shell middle surface, where the frame is assumed to be attached to the skin.

Using the curved beam element of Appendix D, the effect of these eccentricities in the ring frame have been examined. The parameter considered here is the relative position of the frame shear centre to the centroid or skin middle surface, radial and axial direction of the shell. The effects of these eccentricities on the shell stresses are shown in Fig.6.5.4-6.5.5. A constant value of eccentricity (0.083R) has been used.

As shown in these figures, the axial direction eccentricities cause a considerable reduction in direct stress, whereas they do not effect the shear stress resultants. These results are due to the increased rotational stiffness about the circumference and negligible contribution to the radial stiffness caused by the longitudinal eccentricity.

Conversely, when the radial eccentricities are imposed upon the frame shear center the two types of radial dislocation affect the shell stress distribution in quite a different manner. Fig.6.5.4 shows the effect of the frame shear centre offset on the shell direct stress distribution, while, as can be seen from Fig.6.5.5, the shear centre-centroid dislocation has much more effect than the others on the shear stress (Fig.6.5.5) due to the increased inplane stiffness of the frame.

Thus it would appear to be desirable to consider the effect of eccentricity of the ring type loaded frame from the beginning of design or analysis in structure of RPV type.

6.5.3 Effect of the Frame Cross Sectional Area

As the area of the ring stiffener does not affect the shell shear distribution, this will also be true of the frame cross sectional area. In Fig.6.5.6, the frame area and bending stiffness have been changed simultaneously. Frames having the same bending rigidity but different area show exactly the same shear distribution curve, while other cases show significant differences.

Thus it can be seen that cross sectional area of the loaded frame does not contribute noticeably either to resisting warping of the shell cross section or to the frame inplane displacements.

6.6. Effect of the Rear Body Length

When the end tail load is applied to a shell having a long rear body length, no local tail load effect will be transfered to the centre body, where the highest concentrated wing load and body bending moment are applied. Thus examine the tail load effect on the centre body, a shell having a short length has been analysed.

Comparisons are made in Table 6.2 for the stress distributions in the centre body under tail loading for various lengths of rear body. The direct stress at the rear loaded frame and the shear stress at the middle of the two frames have been factorized by the maximum beam theory bending moment and shear force respectively to exclude the overall bending effect on the stress distribution.

Approximately 25 per cent higher direct stresses can be seen to occur in the centre body of the longer shell. These are the results from the difference of local radial reaction loads, which has the ratio of two to one for the two shell structures. Therefore the local effect of end tail load influences seriousely on the direct stresses in the shell having short rear body length.

On the other hand, the shear stress distribution is not affected much by the rear body length variation, this indicates that the shear stress is related more to the radial reaction forces on the frame than the overall bending action.

6.7 Effect of the Tail Position

So far, the position of the tail plane has been located on the global X-Z plane (90 degree and 270 degree).

To examine more closely the effect of a short rear body under concentrated end tail load, the position of the tail plane on the circumference of the body has been altered from the mid tail to both the top and the bottom of the end circumference (high and low tail). The short rear body (L_f=24, L_c=12, L_r=24 inch) with the low wing (180 degree) has been considered.

In the region between the rear pick up frame and the end circumference, the opposite directions of the tail load and the rear pick up reaction of the high tail-low wing combination distort the rear body into a shape having an oval vertical cross-section. This produces a higher hoop tensile stress and shear stress in this region (Fig.6.7.2-6.7.3).

The higher local deformation along the bottom line due to the low wing-low tail combination gives a significant rise in the direct stress along pick up line, while the compression stress along the opposite side is reduced (Fig.6.7.1).

This large local radial and tangential deformation also effect the maximum shear stress between the two loaded frames.

Although greater membrane stress resultants are produced by the low wing-low tail combination, the high tail-low wing positioning effect has a great influence on the bending stress distributions of the rear body (Fig.6.7.4-6.7.6). The maximum stress resultants at the extreme fiber of the skin due to these bending terms, when expressesed as a percentage of the maximum stress resultants due to the membrane terms, are 30 per cent for the direct stress, 50 per cent for the hoop stress and 50 per cent for the shear stress.

However, since the maximum bending stress resultants mainly appear at the rear frame position and have the same magnitude for each tail position, the low wing-low tail combination gives the most severe stress distribution.

6.8 Decay Length

In appendix C of Ref.18, the decay length of shell having flexible loaded frame has been defined as the distance from the frame to undistorted shell section under the self-equilibrating harmonic loading terms. Using the method in Ref.18, the decay length of 30.7 inches has been found for the body structure in Appendix B and given in Appendix E.

The radial displacement distribution along the body longitudinal axis is shwn in Fig.6.8, in which the radial displacement at 180 degrees becomes the same as that at zero degree of the body circumference approximately 36 inches away from the two frames with the low wing pick up. Because of the constant radial displacement beyond these points, the shear and hoop stresses will be the same as those predicted by beam theory. Comparing this value with 30.7 inches predicted by the method in Ref.18, a comparatively good agreement is found.

However, from the results in chapters 4 and 6, the following characteristics of the perturbed stresses from beam theory is summarized:

i) The direct stress and axial bending moment die out at approximately one diameter length away from the loaded frames.

ii) The other stresses reduce more slowly and die out approximately three diameter length away from the loaded frames.

Because of the above two points, the method given in Ref.18 gives better agreement for the shear and hoop stresses than for the direct stress or axial bending moment distributions of the present structure.

6.9 Stress Concentration Around the Cutout

Using the empirical formula for the shell with cut out in Ref.22, the stress distribution around the circumference has been calculated as shown in Appendix E. Comparing these results to those shown in Fig.6.2.17, there is generally good agreement except at the edge of the cut out, at which the maximum direct stress by the present method is approximately 70 per cent of that predicted by the empirical formula.

These results, for the stresses at the middle of two frames, are shown in Fig.6.9.1. The smaller stress resultants given by the finite element method solution may be caused by the coarse mesh used in the circumferential direction, together with the flexibility of the loaded frames which can not be predicted from the formula in Ref.22.

To clarify these effects, the stresses in the ring framed shell are compared to those in the shell having two diaphragm frames in Fig.6.9.2 and 6.9.3, As can be seen from Fig.6.9.2, The axial stress at the middle of the two frames is not affected by the frame stiffnes difference. Therefore increasing the number of elements would be expected to give a closer result to that predicted by the method in Ref.22.

The redistribution of stresses due to the structural discontinuity can be seen to take place around the cut out. The change of shear stress direction on the lower skin outside the frames, is particulary noticeable.

CHAPTER 7

EXAMINATION OF THE DESIGN PARAMETERS USED IN CLASSICAL METHODS OF ANALYSIS

7.1 Introduction

Classical analyses of a cylindrical fuselage have produced design charts, formulae or tables for use on fuselage structures having large numbers of closely spaced stringers and rings. These analytic formulae have limitation in their application to the present class of small cylindrical RPV bodies, because of their analytical assumptions and the simple structural model which they use, as explained in Appendix E. Thus only a limited number of cases covered in the previous investigations can be compared with the results predicted by analytical methods.

As ESDU (Ref.21) uses a simple explicit design variable, namely GtR^4/EIL and allows the non-uniformity of ring spacing or different frame stiffness from the rings based on Ref.16 and Ref.20, the investigations are mainly carried out according to the effect of this parameter variation on the shell and loaded frames. The solutions of the finite element method analysis of the wing pick up structure, here developed, are compared to the results predicted by the method in Ref.21 and elementary theory. The comparisons are mainly concentrated on (i) the direct stress distributions at the rear pick up frame and (ii) the shear flow loading on this frame, under the case of a concentrated load at the tail plane. The structural model considered and symbols used are shown in Fig.7.1.1.
The structural model used in this cahpter has the forward body length of 72 inches and 60 inches length of the rear body as constants. The length of centre body varies in most cases, therefore the symbol in the graphic outputs 72-Lc-60 represents the geometry of model considered in longitidinal direction.

The relatively coarse finite element mesh used in the calculations appears to give sufficiently accurate distributions of stress. However, the overall magnitude of stress is overestimated in about five per cent of the case considered and under-estimated in about 10 per cent. In order to make fair comparisons, results in this chapter have been scaled, where it is noted, so that the comparison may be made between distributions having equal static resultants. The scale factors neccessary have differed from unity by no more than 10 per cent in most cases.

7.2 Examination of Parameter GtR^4/EIL

The inplane structural behaviour of flexible circular loaded frames supported by a shell has been evaluated against an explicit parameter GtR^4/EIL in Ref.21, for the shell having no other rings or stiffeners than a single loaded frame as used in Ref.14.

However based on the analyses of Ref.16 and Ref.21, the section 03.06.17 of Ref.21 recommends to use the stiffness of loaded frame (I_f) for I allowing nonuniformity of the ring stiffness (I_r) and frame stiffness. It also allows the nonuniformity of ring spacing by taking L as the harmonic mean of distances to the adjacent rings, and the effect of smeared stringers by using correction parameter R^6t'/IL^3 in which the variable t' represents the effective stress carrying thickness including shell skin.

Using the present notation of frame stiffness I_f, the validity of this parameter GtR^4/EI_fL, which for convenience is denoted by the symbol Z(L) from here on, to the present type of wing pick up structure having two identical flexible frames is examined.

First of all, the variable L in the parameter Z has been examined performing a series of calculations by use of different pairs of values of the frame stiffness(I_f) and frame spacing(Lc) which have the same product and therefore making a constant value of Z(Lc). The results are shown in Fig.7.2.1(a) for the low wing pick up(180 deg) and in Fig.7.2.1(b) for the intermediate pick up(135 deg). The ring spacing is kept constant. Even though two shells have same Z(Lc) value, the results show quite different magnitudes. The peak shear flow produced by the shell having smaller frame spacing (Lc=R) shows about 17 per cent higher than that produced by the shell having wider spacing (Lc=4R) for the case of low wing pick up(Fig.7.2.1(a)). However, the difference of two cases of 135 degree pick up is about 6 per cent(Fig.7.2.1(b)). This trend is also showing for the case of doubled and quadrupled value of Z(Lc) in Fig.7.2.1(c) and Fig.7.2.1(d) respectively.

On the other hand, when the harmonic mean of the frame spacing and standard ring spacing is in use for the case of smallest Z(Lc) value(25) as recommended by Ref.21, the values of Z(L) become near zero for both of shells, consequently producing greatly under-estimated shear flow distribution similar to that predicted by elementary theory(Z=0). The nearest values of Z(L) producing similar shear flow distributions to the solutions produced by the finite element method are obtained using the variable L as the frame spacing Lc for the shell having narrow frame spacing, and as twice the frame spacing for the shell having the wider spacing, in the case of low wing pick up. Although there are about five per cent differences in the maximum values of shear flow, this trend of coincidence is also shown in the case of larger values of Z(Lc). Therefore the parameter Z(L) in Ref.21 cannot predict explicitly the structural behaviour of the present type of shell, without considering the effect of frame spacing to radius ratio.

The other variable involved in determining the value of Z in Ref.21 is effective skin thickness t' in correction parameter $R^6 t'/I_f L$, which is derived from the stringer area per unit length of circumference. The shear flow distributions produced by two sizes of shells having two different stringer areas in each have been tabulated in Table 7.1. Because of the small number of stringers used($N_{str}=4$), doubling the stringer areas increases the value of t' by 15 per cent for the shell having the larger radius (R=12) and 8 per cent for the smaller shell (R=3) respectively. However, no effects of increase in this stringer area are found. This table also shows that the same L_c/R ratio gives nearly same value of peak shear flow coefficient compared to the results in Fig.7.2.1(a).

The effect of variations in the stringer area appears in the direct stress distribution as shown in Fig.7.2.2. The larger stringer areas of each shell give about 6 per cent higher maximum direct stress at 180 degree position. However, these differences are less than that predicted by engineering beam theory which shows 11 per cent for the larger shell (Fig.7.2.2(a)) and 7 per cent for the smaller shell(Fig.7.2.2(b)) from the stringer contribution to the total second moment of area of shell cross section $(1/(\pi+2A_s/Rt)$. Futhermore, although two shells have same value of $Z(L_c)$, the direct distribution is also affected by the variable L_c/R producing 40 per cent higher maximum direct stress by the larger shell ($L_c/R=1$) than that by the smaller shell ($L_c/R=4$). While the larger L_c/R gives about 20 per cent higher maximum direct stresses than that by engineering beam theory, the smaller L_c/R gives about 80 per cent larger maximum stresses.

7.3 Variation of Frame Spacing (Lc)

It has been shown that in the previous section that it is desirable to use the frame spacing rather than the standard ring spacing for the variable L in evaluating Z when using Ref.21 for the case of wing pick up structure having small frame spacing. This parameter $Z(L_c)$ is further examined in this section, changing the frame spacing and basic dimensions of shell. The ratio of shell radius to thickness, stringer area to product of radius and thickness, and ring stiffness to frame stiffness are kept constant.

The direct stress distributions on the rear pick up having a small value of Z(Lc) have been plotted in Fig.7.3.1. Two sizes of shells having two different pick up positions are plotted for the various L_c/R ratios. As shown in Fig.7.3.1(a) for the smaller shell and Fig.7.3.1(b) for the larger shell, although the maximum stress at 180 degree shows only 5 per cent difference in the relative value compared to that predicted by beam theory for the case of the smallest L_c/R, (1.), this difference is getting larger by increasing L_c/R ratio. The case of Lc/R equal to two has about 10 per cent difference between the results for two shells compared to that predicted by beam theory, and 37 per cent for the case of Lc/R equal to four. However, for the case of smaller shell in Fig.7.3.1(a), maximum direct stress produced by the largest Lc/R shows about 25 per cent higher than that predicted by beam theory, while the smallest Lc/R gives about 80 per cent higher value for the case of low wing pick up which is subjected to the concentrated load at tail.

On the other hand, when the intermediate wing pick up at 135 degree is used, the difference of maximum stress from that predicted by beam theory is noticeably affected by neither the change of Lc/R ratio nor the size of of shell, producing nearly same magnitude of 20 per cent difference, but the stresses at zero degree position show these effecs.

The effect of the ratio of Lc/R also appears in the shear flow distributions in Fig.7.3.2. The increases from the value predicted by elementary theory vary from minimum about 30 per cent for the case of L_c/R equal to 4, to the maximum about 50 per cent for the case of L_c/R equal to 1.0, when the low wing pick up is in use (Fig.7.3.2(a) and Fig.7.3.2(b)). For the case of intermediate wing pick up, these differences are much less than the low wing pick up case varying from about 20 per cent to about 30 per cent (Fig.7.3.2(c) and Fig.7.3.2(d)). The trend due to the change of L_c/R ratio and effect of shell size in shear flow distribution is same as those in the case of direct stress distribution. Therefore, the shear flow distribution can be predicted by using the parameter Z.

When the value of $Z(L_c)$ is doubled and quadrupled, the effect of L_c/R is even greater. While the maximum direct stress produced by the shell having smallest frame spacing ($L_c/R=1$) produces about 250 per cent for the quadrupled and 210 per cent for the doubled Z value of that predicted by beam theory, the largest spacing ($L_c=4$) produces about 130 per cent and 170 per cent respectively. for the case of smaller shell (R=6) having low wing pick up, as shown in Fig.7.3.3. The lightest frame (Z=100) may be seen to show departure from the trend observed for the stiffer frame near the wing loading point at 180 degree. This would seen to be due to the local distortion.

The significant effect of frame spacing on the light frame also appears in the shear flow distribution for the same structure (Fig.7.3.4). Doubling the value of $Z(L_c)$ increases nearly 30 to 40 per cent of the maximum shear predicted by elementary theory for each case of the frame spacing considered. However, corresponding distributions produced by Ref.21 always give overestimations as shown in Fig.7.3.4(d) by 5 per cent to 20 per cent depending on the frame spacing.

The direct stresses at the low wing pick up position (180 degree) have been plotted in Fig.7.3.5 for the various values of L_c/R and $Z(L_c)$. It is noticeable that increasing either the frame spacing or frame stiffness (in other words decreasing Z value), causes the maximum direct stress to approach that predicted by elementary theory. Two types of shell, R=6 and R=12, show this trend in a similar manner except that the smaller shell having the lightest frame stiffness produces a sudden drop of direct stress at the loading point as described before. However, in general, the larger shell produces about 10 per cent higher stresses than the smaller shell for the case of small L_c/R ratio ($L_c/R=1$) and about 25 per cent for a large L_c/R ratio ($L_c/R=4$, $Z=50$). Comparing the results to that predicted by elementary beam theory, the results for the small frame spacing shows about 180 per cent to 250 per cent, while the results for the largest spacing shows about 120 per cent to 200 per cent higher direct stresses.

Even though the increase of frame spacing also reduces the maximum shear flow level as shown in Fig. 7.3.6(b), the proportional reduction of maximum shear is not so great as in the case of the direct stresses in Fig.7.3.5(b). It is more affected by the variation of frame stiffness as can be observed in Fig.7.3.6(a). The larger shell (R=12) also gives the higher maximum value of shear flow on the frame. This is more significant for the case of a shell having the larger frame spacing (L_c/R) varying about 110 per cent to 140 per cent of the maximum shear produced by the smaller shell.

Examining the values of maximum shear flow predicted by the design chart in Ref.21, it can be noticed that the ESDU results everywhere overestimate this value as shown in Fig.7.3.6(b). Therefore, the chart in ESDU can be used for the prediction of shear flow distribution and give conservative value, it significantly overestimates the peak value for some practical cases. It does, of of course, not provide direct stress distributions.

7.4 Examination of Variables Relating to Ring Stiffeners

In the previous section, the larger shell (R=12) produces higher maximum stresses than the smaller shell (R=6). The only variable which is not taken into account in nondimensionalized form is the properties of standard ring stiffeners which has constant spacing of 12 inches. Therefore, the ratio of ring spacing to shell radius for those shells are 1.0 and 2.0 respectively. The stiffness per unit length (I_r/L_{rsp}) is 0.00333 for the smaller shell and 0.1333 for the larger shell respectively. These parameters related to the ring stiffeners are examined in this section using the smaller shell (R=6) having constant value of $Z(L_c)$ (Z=25.0) keeping the other basic variables constant.

As shown in Fig.7.4.1, the stiffness ratio of ring to frame shows no great influence on the stress distributions. The differences in maximum stresses are less than five per cent, comparing the result produced by the smallest value of I_r/I_f ratio (0.02) with that by the quadrupled one (I_r/I_f=0.2). Whereas the maximum shear flow produced by the shells having the larger ring spacing are approximately 10 per cent higher than that predicted by Ref.21(Fig.7.4.1(c)), the smaller spacing gives nearly same results as ESDU prediction (Fig.7.4.1(d)).

Therefore, for the shells having closer ring spacing which is approaching the smeared ring assumption, the method in Ref.21 can give more accurate prediction of frame shear flow distribution.

The effect of ring spacing change is examined keeping the ring stiffness per unit length (I_r/L_{rsp}) constant in Fig.7.4.2. Whereas the smallest ring spacing gives the highest direct stress and shear flow maximum, the largest spacing gives the lowest maximum direct stress and shear flow on the frame. The relative magnitude of changes in maximum stresses produced by these two kinds of ring spacing is approximately 10 per cent. It is also can be seen that the shear flow distribution predicted by ESDU gives very good approximation for the shell having a smaller ring spacing.

7.5 Summary of Examination

The parameter Z in Ref.21 has been used exclusively to represent the structural behaviour of flexible circular loaded frames supported by a shell. Although it has obvious limitations for the application to the shell having structural discontinuity due to cutouts and the loaded frame with local reinforcement or eccentricity etc., the present examination reveals other limitations in use for the wing pick up structure having two loaded frames and small number of circumferential and longitudinal stiffeners.

The most important discrepancy arises from the definition of ring spacing variable L. Especially when the harmonic mean of the ring spacing and the frame spacing for the case of small value of $Z(L_c)$, it gives significant underestimination of frame shear flow. On the other hand, when the frame spacing is used, it also gives a significant overestimation for the shell having larger ratio of the frame spacing to shell radius. Therefore, other than the case of shell having very small frame spacing which is desirable to use L_c instead of the mean value, the result produced by this parameter will not give an accurate shear flow distribution on the frame (Fig.7.3.6).

The variable L_c/R performs an important role in the direct stress distribution in accordance with this $Z(L_c)$ parameter. The smaller L_c/R and the larger $Z(L_c)$ provide the greater perturbed direct stress.

Even though the correction parameter in Ref.21 includes the effect of smeared stringer area, the effect of this area of stringers is not significant in the shear flow distribution for the present type of structure. However, this effect is distinct in the direct stress distribution as a form of nearby proportional contribution to the total second moment of area of shell cross section.

Another important variable relating to the ring stiffeners are the spacing of them. Although the ring stiffness also important in the stress distribution, the wider spacing gives the larger overestimation by Ref.21. Therefore,unless the rings are closely spaced, the result predicted by Ref.21 provide considerable overestimation. This also affects the direct stress distribution giving the closer spacing the higher direct stress.

CHAPTER 8

SUMMARY AND DISCUSSION OF RESULTS

Parametric studies of the wing-body interaction design variables have been performed using the finite element method. The wing attachment structure consists of basically two loaded frames and a body shell which is stiffened by a small number of standard transverse unloaded rings and longitudinal stringers. The details of each design variation effect of comments on them are given in Chapters 4 to 7. The effects of important design parameter variations are now summarized from those noted in earlier chapters.

1) The perturbation of the internal force distributions in the wing attachment structure of the RPV from those predicted by basic beam theory, has mainly arisen because of the inplane flexibilities of the wing pick up frame, as in the transport type of aircraft fuselage. The pick up frame for the unmanned RPV class of vehicle has more design choices available than there are for that of the transport type of vehicle. It can vary from a rigid bulkhead to a light gauge ring type frame.

   When the wing pick up frames have nearly infinite inplane stiffnesses as in the case of a rigid bulkhead or diaphragm, the structural behaviour of the body without cutouts becomes nearly the same as that of beam bending action (Fig.4.4.1-4.4.13).

   This is caused by the prevention of radial and tangential displacements at the wing load transmitting points.

These displacements are the major source of the perturbed hoop and shear stresses in the shell, while the axial displacement dut to the cross sectional warping is the major source of the perturbed direct stress in the shell from those predicted by elementary theory.

2) When flexible ring frames have been used for the loaded frames, the body structural behaviour has been predominately affected not only by the flexibility of the frames but also by the wing pick up position and the frame spacing in the body. Severe disturbances of the stress distributions in the body skin from those predicted by the elementary theory have arisen due to the local radial and tangential displacement of the wing attachment points.

A combination of the flexible ring frames and the low or high wing pick up positions illustrates clearly the discrepancy of the body structural behaviour from that predicted by the elementary theory of bending and torsion. Although it cannot be stated in terms of a single parameter, as much as 100 per cent increase in the maximum direct stress and shear stress in the body skin has been observed (Fig.7.2.1, 7.2.2).

This is especially noticeable when end tail vertical forces are applied to the body, for whereas beam theory predicts zero direct stress around the circumference of the forward frame due to zero bending moment, a near cos2θ curve for the distribution the direct stress is predicted by the present analysis. The magnitude of this curve is approximately 40 per cent of the maximum direct stress level predicted by beam bending theory (Fig.6.2.7).

Large local radial and tangential displacements at the pick up points tend to produce such great differences from the elementary theory.

The significance of the frame flexibility effect can be reduced by placing the wing near to the middle of body cross section. The mid wing pick up in this case shows almost the same pattern as beam theory (Fig.4.3.2-4.3.4), despite the flexibility of the frames. The present investigation has revealed that the ring framed body with mid wing pick up behaves like a square tubular beam rather than the circular tublar beam (Fig.4.3.1, 4.3.2, 6.2.1).

The similar behaviour to that predicted by the elementary theory is a result of the fact that the body horizontal plane is the neutral plane of the bending action of the beam. Even the intermediate pick up at 135 degrees shows a considerable reduction of the stress level from that of the low wing pick up (Fig.4.3.10-4.3.22).

3) The effect of the frame spacing appears as its ratio to the shell radius. Low wing pick up structures which have the same frame spacing to radius ratio, show almost the same shear stress distributions (Fig.6.4.3). Approximately 20 per cent reductions in the maximum direct stress and shear stress are achieved by increasing this ratio from two to four for the model design.

These are due to the propagations of the locally disturbed stress system in the longitudinal direction, which decrease with increasing distance from the loaded frame.

4) The significant effect of the cutout on the body skin stress distributions has been shown. Even if the present investigation could not show clear stress concentrations around the cutout due to the coarse mesh and the large number of design variables involved, serious increases in stresses can be noticed around the edge of cutout (Fig.4.7.3-4.7.5).

The maximum stresses are increased by more than 100 per cent by the cutout in the centre shell due to the abrupt structural discontinuity and the consequent stress concentrations caused by the removal of the load carrying members.

The maximum direct stress resultant appears at the rear frame corner of the model RPV cutout. It is 230 per cent of the beam theory result at this point (135°) and 162 per cent of the maximum value of the beam (180) theory under the tail load (Fig.6.9.2).

These increases are caused by both the reduction of the section's second moment of inertia and the structural irregularity.

It was found that the flexibility of the frames does not noticeably affect on the maximum direct stress in the shell when the cutout is present as it does for the complete shell (Fig.6.9.2, Fig.4.4.1).

An approximate increase in maximum shear stress of 30% is found when using a flexible frame as apposed to a rigid diaphragm (Fig.6.9.3). The change in the shear stress direction at the bottom quadrant of the outer shell caused by the cutout is another interesting result (Fig.4.7.5).

5) The simple ring type frames of an unmanned RPV would be likely to be relatively deeper than those of a transport type fuselage due to its smaller radius. The annular frame having an inch depth and a 0.1 inch thickness shows nearly same tendency as the diaphragm frame (Fig.4.4.16-4.4.20) when compared to the ring frame with second moment of inertia of 0.1 in^4.

Although the annular type frame has a smaller second moment of inertia than the heavy ring frame, the effect of eccentricity together with the inplane stiffness of membrane reduces the radial displacement of frame. About 10 per cent of the maximum direct stress (Fig.6.5.1) and 80 per cent of the maximum shear flow on the frame (Fig.6.5.3) have been reduced by the use of a 0.083R depth of annular frame with a 0.1 inch thick web, as apposed to relatively heavy ring frame (I_f=0.1 in^4). Thus a considerable overestimate in the stresses is likely to be made by the classical formula in which this frame depth has not been taken into account.

6) Other practical designs of the loaded frames are the use of local reinforcement and different stiffnesses for each frame. Approximately 20 and 30 per cent reduction of the maximum shear flow have been achieved by the reinforcement of a bottom octant (Fig.4.5.1-4.5.2) of the frame where the wing is attached, and by replacement of the forward light frame by a diaphragm (Fig.4.6.1-4.6.10) respectively. The first reduction is due to the decrease in the frame local radial and tangential displacement caused by the increased stiffness, and the second reduction is caused by the absence of a disturbed stress system due to the forward frame.

7) In the classical analyses and design formulae, the effect of stringer stiffness is represented by increasing the effective skin thickness carrying direct stress.

However, the samll number of longitudinal booms in the present type of RPV body shell structure behaves in a quite different manner. Although average direct stress is nearly proportional to the stringer area contribution, the local stresses are affected by thise stringer presence in conjunction with the position of wing attachment. Especially when stringers are placed at different position from the wing pick up circumferentially, the shell having four stringers produces approximately 20 per cent higher direct stress than the shell having equivalent thickness (Fig.6.2.7).

Although the shell having equivalent thickness produces produces a lower direct stress than the four stringered shell, they give a good agreement with the shell having sixteen stringers, which is more similar to the smeared shell assumption, in the shear stress distribution (Fig.6.2.9). Therefore the smearing assumption can predict the shear stress without great loss of accuracy. However, when the twisting moment of shell is considered, the resultant shear stress predicted by the smeared stringer or shell having equivalent thickness gives a great overestimation(Fig.6.2.13).

8) The effect of ring stiffener is mainly dependent upon the spacing of the stiffeners. Although the ratio of stiffness of ring to frame affects the shell stresses (Fig.7.4.1), the closer spacing produces the higher stresses(Fig.7.4.2) so that the shear flow distribution approaches to that predicted by the smeared ring assumption. Therefore the use of classical methods for the present type of shell structure will produce overestimated result.

9) The effect of wing stiffness on the body stresses is generally negligible (Fig.5.5.9-5.5.10). Whereas longitudinal interaction of the wing and the body slightly affects only the direct stress distribution, the bending type interaction gives significant rises of stresses in the shell (section 5.6).

10) Although the bending moments in the shell are comparatively small in most cases, the contribution of these bending moments to the extensional or shear stresses at the extreme fiber of the skin element are considerable due to the thin skin thickness. Nearly the same order of stresses are produced by 4.3.4, the membrane terms and the bending terms (section 4.3.4, 4.4, 6.2.1, 6.7).

A reduction of these bending stresses can be achieved by adding stiffeners or increasing their stiffness. The use of simple diaphragm frames or a mid wing pick up makes these bending stress resultants become negligible.

11) Another important design variable is the position of the tail plane which reacts the wing normal force by its nose down moment. Whilst the oval shape displacement of the low wing-high tail combination produces the highest hoop and shear stresses in the rear body, the local radial and tangential deformations caused by the low wing-low tail combination produces the highest longitudinal direct stress resultant (section 6.7).

12) In an ordinary transport type of fuselage, the use of extreme positioning of wing (high/low) is usually avoided to prevent highly concentrated stresses due to the flexible pick up frame, as discussed previously.

However, the simplicity of design of the present type of RPV would not exclude use of an extreme wing positioning, with appropriate local reinforcement.

13) When the tail plane and fin are reacting the roll of vehicle produced by the aileron deflection, the body shell behaviour is predominated by the overall bending action due to the unbalanced fin normal force rather than the overall torsion due to the tail plane and fin normal forces of the body structure investigated (section 4.3.4 and 4.4.2).

14) While reducing the longitudinal distance between the wing and tail leads to the decrease of overall bending stresses in the shell, the influence of local deformation at the tail position increases the stresses at the wing pick up position (section 6.6)

15) When the simple ring type frames are in use, the design charts in ESDU can give a maximum possible value of the frame shear flow distribution using the frame spacing and second moment of area rather than using the standard ring properties (Fig.7.3.5).

CHAPTER 9

CONCLUSIONS AND RECOMMENDATIONS FOR FURTHER WORK

9.1 Conclusions

A numerical method has been used to investigate the effect of variations in the wing-body interaction structural design parameters on the structural behaviour of a class of small RPVs. A set of computer programs using the developed finite element method of investigation has been based on the concept of substructuring. This program development includes appropriate element formulations. The elastic coupling between the wing and the body has also been examined. Examining a classical design parameter and analytical methods, the applicability of such methods to the RPV type wing body interaction structure is investigated. The application of the present method of analysis and developed programs is not restricted to the present type of structure but can also be used generally for the wing-fuselage interaction analysis of an aircraft in which the wing attachment is by frame pick ups only.

Based on the wide range of investigations of the effect of design parameter variation on the structural behaviour, the following characteristics of the most important design variables which should be taken into account for the design or analysis of the wing-body interaction of RPV class are found:

1. The inplane bending stiffness of a loaded frame does influence the structural behaviour of wing pick up in the form of stiffness ratio to the shell cross section second moment of area. The smaller ratio produces the larger deviation from the value predicted by elementary theory.

2. The ratio of loaded frame spacing to shell radius: A small value of this ratio produces a larger perturbed stress system from that predicted by elementary theory, and closer results to that predicted by analytical formuae for the shell having a single loaded frame.

3. The position of wing attachment to the body circumference: Placing the wing near to the middle of body cross section allows the use of elementary theory, while an extreme positioning (low or high wing pick up) gives highly perturbed stress system.

4. The overall effect of direct stress carrying longitudinal stringers is acting as beam theory, even though the number of stringers are small, as a ratio of total area of stringers to the product of radius and thickness of shell. However, the local membrane and bending stresses are quite different from the results predicted by elementary theory or analytical methods.

5. The most important variable related to the standard ring stiffener is the spacing. The closer spacing produces the higher shell stresses than the wider spacing, even though they have same stiffness per unit length.

6. Placing the tail plane to the opposite side of the wing around the body circumference produces lower stress than placing them in same position, for the case of body having a short distance between them.

The parameter $Z = GtR^4/EI_fL$ used in Ref.21 has been examined to see the validity of this parameter to the present type of wing pick up structure having small radius, small number of stiffeners and two loaded frame. From the present investigation, it has been found that there are other limitations in use of this parameter, even though having no cutout or no eccentricity and local reinforcement of the loaded frames have been employed.

The following variables also have great influence on the structural behaviour of wing pick other than the parameter Z.

i. The spacing of two loaded frames: When this variable is in use for L, Ref.21 could give very good approximation in the distribution of frame shear flow for the case of the shell having large frame stiffness (or large radius) and small value of ratio of this variable to radius ratio. However, for the case of the having larger ratio of frame spacing to radius, Ref.21 gives a significant over-estimation.

   This ratio performs also an important role in the direct stress distribution in accordance with this parameter variation. The smaller ratio and the larger value of Z provide the greater perturbed direct stress from that predicted by elementary theory.

ii. Although the change of stresses are not inversely proportional to the contribution of stringer area to the total second moment of area of shell cross section and the effect of this stringer area does not affect the shear flow distribution for the shell having small value of this parameter, the influence of this stringer area is shown noticeably in the direct stress distribution though not in the shear flow distribution.

iii. When the parameter Z has small constant value, the smeared ring assumption in Ref.21 provides very similar result of shear flow distribution for the case of closer spacing of rings. However, for the case of shell having wide spacing, this Z again gives considerable overestimation.

9.2 Recommendations for Further Work

Although the structural behaviours of a small RPV class wing body interaction structure under the investigation have been extensively examined, there are still important areas where the investigation can be extended by removing the limitations imposed on the present work or by confining the investigation to a certain parameter only. The wide range of parameters to be considered was a major factor prevented the use of fine mesh model or a general purpose analysis package which has generally more flexibility than the program used in the geometric representation of structures.

The use of refined mesh for the shell having cutout can extend the investigation to the study of stress concentration problem of an RPV type body structure having small number of stiffeners.

A slight modification of subroutines in the main solution program could lead the investigation to the more complicated wing-body interaction problems, such as multiple points wing attachment. An alteration of the cylindrical shell element by a doubly curved shell element in the program used could extend the present investigation to the structure having non-circular cross section.

The actual smeared shell element can be formulated by a slight modification of the stress-strain relation in Appendix C, without any difficulty. Then the smeared stringers or rings can be readily employed if it is nec neccessary.

The general trends of shell having various combination of frame spacing and stiffness relating them to the radius and second moment of area of shell cross section, for the limited number of cases. Performing further examination for the larger variable, more general design informations for a large aircraft can be found.

REFERENCES

1. BROWN, R.B. — Compass Cope Airframe Design History. Journal of Aircraft, vol.17, no.12, pp.867-874, Dec. 1980.

2. JANE'S — JANE'S All the World Aircraft, 1976 - 1979.

3. Aviation Week and Space Technology. "Remotely Piloted Vehicles and Drones", pp.140-142, Mar. 12 1979. "Israel IAI Scout", June 11 1979. "D-21 Drone Feature", Oct. 31 1977. "Compass Cope seen in Anti-Tank Roll", Dec. 1 1980. "Drone to Simulate Cruise Missile Threat", Feb. 27 1978. "Remotely Piloted Vehicle Effect Pressed", pp.170-173, Feb. 6 1978.

4. AL-SHOURBAJI, M.N. — Remotely Piloted Vehicle Design for Offensive Operations. MSc. Thesis, Cranfield Inst. Tech., 1976.

5. LOCKENOUR, J.L., LAYTON, G.P. — RRPV Research Focus on HiMAT. Aeronautics & Astronautics, vol.14, pp.36-41, Apr. 1976.

6. McQUILLEN, E.J. — Graphite Epoxy Wing for BQM-34E Supersonic Aerial Target. Journal of Aircraft, vol.8, no.6, pp.480-486, June 1971.

7. EL-TANTAWAY, B.J. — Design and Testing of a Wing Suitable for an RPV. MSc. Thesis, Cranfield Inst. Tech., 1978.

8.	MERTSOY, E.L.	Design and Construction of RPV Components from Non-Metallic Material. MSc. Thesis, Cranfield Inst. Tech., 1980.
9.	HENSHELL, R.D.	PAFEC 75 a) Theory and Result Manual. b) Data Preparation Manual.
10.	MacNEAL, R.H.	a) NASTRAN Theoretical Manual, Lev.16, NASA SP-221(3),1976 b) The NASTRAN Computer Program for Structural Analysis. Computers & Structures, vol.1, pp.389-412, 1971.
11.	WISE, J.A.	Analysis of Circular Rings for Monocoque Fuselage. Journal of the Aeronautical Science, vol.6, pp.460-463, 1939.
12.	WALTERS, E.R.	Stresses in a Ring Loaded Normal to Its Plane. Journal of the Aero. Science, vol.12, pp.235-240, 1945.
13.	ROTHWELL, A.	Specimen Calculation for Stress Distribution in Fuselage Section. DES 8116/1, College of Aeronautics, Cranfield Inst. Tech.,
14.	WIGNOT, J.E. COMB, H. ENSRUD, A.F.	Analysis of Circular Shell Supported Frames. NACA TN 929, Jul. 1943.
15.	HOFF, N.J.	Stresses in a Reinforced Monocoque Cylinder under Concentrated Symmtric Transverse Load. Jour. Appl. Mech., vol.11, no.4, pp.A-235, Dec. 1944.

16. KEMPNER, J. DUBERG, J.E. — Stress Analysis by Recurrence Formula of Reinforced Circular Cylinder under Lateral Loads. NACA TN 1219, 1947.

17. ARGYRIS, J.H. KELSEY, S. — Modern Fuselage Analysis and the Elastic Aircraft. Butterworth, London, 1963.

18. MacNEAL, R.H. BAILLE, J.A. — Analysis of Frame Reinforced Cylindrical Shells. Part I; Basic Theory. NASA TN D-400.

19. — Part II ; Discontinuities of Circumferential Bending Stiffness in Axial Direction. NASA TN D-401.

20. — Part III; Applications. NASA TN D-402.

21. ESDU — Engineering Science Data Unit. Item 03.06.11 - 03.06.17. Structural Analysis Series.

22. KUHN, P. — Stresses in Aircraft and Shell Structure. Chapt.9, McGraw-Hill, New York, 1956.

23. FLÜGGE, W. — Stresses in Shell. 2nd Ed., Springer-Verlag, New York, 1973.

24. BRUHN, E.F. — Analysis and Design of Airplane Structures. Tri-State Offset Co., 1973.

25. SHEPS, Z. Computer Analysis of Semi-Monocoque Shell Sections. Computers & Structures, vol.9, pp.305-313, 1978.

26. ARGYRIS, J.H. Continua and Discontinua. Proc. of Conference on Matrix Methods in Structural Mechanics, AFFDL-TR-66-80, pp.11-119, W.P.A.F.B., Dayton, 1965.

27. PRZEMIENIECKI, J.S. Matrix Structural Analysis of Substructure. AIAA Journal, vol.1, no.1, pp.138-147, Jan. 1963.

28. TAIG, I.C. Automated Stress Analysis using Substructures. Proc. of Conference on Matrix Methods in Structural Mechanics, AFFDL-TR-66-80, pp.225-274, W.P.A.F.B., Dayton, Ohio, 1965.

29. HANSEN, S.D.
ANDERTON, G.L.
CONNACHER, N.E.
DOUGHERTY, C.S.
Analysis of the 747 Aircraft Wing-Body Intersection. Proc. of 2nd Conference on Matrix Method in Structural Mechanics, AFFDL-TR-68-150, W.P.A.F.B., Dayton, Ohio, 1968.

30. KALEV, I.
BARUCH, M.
BLASS, E.
Structural Wing-Fuselage Static Interaction by a Combined Method of Tests and Numerical Analysis. Journal of Aircraft, vol.14, no.12, pp.1186-1191, Dec. 1977.

31. PRZEMIENIECKI, J.S. Theory of Matrix Structural Analysis. McGraw-Hill, New York, 1968.

32. GALLAGHER, R.H. Shell Elements. World Conference on Finite Element Methods in Structural Mechanics, Bournemouth, 1975.

33. ZIENKIEWICZ, O.C. — The Finite Element Method. 3rd Ed. pp.329-331, McGraw-Hill(UK), 1977.

34. ARGYRIS, J.H. — Matrix Displacement Analysis of Anisotropic Shells by Triangular Elements. Journal of Royal Aero. Society, vol.69, pp.801-805, 1965.

35. CLOUGH, R.W. JOHNSON, C.P. — A Finite Element Approximation for the Analysis of Thin Shell. Int. Journal of Solids and Structures, vol.4, pp.43-60, 1968.

36. CHU, T.C. SCHNOBRICH, W.C. — Finite Element Analysis of Translational Shells. Computers & Structures, vol.2, pp.197-222, 1972.

37. HERRMANN, L.R. CAMPBELL, D.M. — Finite Element Analysis for Thin Shells. AIAA Journal, vol.6, no.10, pp.1842-1847, Oct. 1968.

38. GRAFTON, P.E. STROME, D.R. — Analysis of Axisymmetric Shells by Direct Stiffness Method. AIAA J. vol.1, no.10, pp.2342-2347, Oct. 1963.

39. SVALBONAS, V. — Numerical Analysis of Stiffened Shells of Revolution. vol.I, NASA CR-2273, Sep. 1973.

40. CALLADINE, C.R. — A New Finite Element Method for Analysing Symmetrically Loaded Thin Shells of Revolution. Int. Journal for Numerical Methods in Eng., vol.6, pp.475-487, 1973.

41. WEBSTER, J.J. — The Accuracy of Finite Element Solution for the Modal Characteristics of Shells of Revolution. Int. Jour. of Mechanical Science, vol.12, pp.157-168, 1970.

42. DELPAK, R. — Static Analysis of Thin Rotational Shells. Computers & Structures, vol.11, pp.305-325, 1980.

43. CONNOR, J.
BREBBIA, C. — A Stiffness Matrix for a Shallow Rectangular Shell Element. Journal of Engineering Mech. Div., Proc. ASCE, vol.93, EM5, pp.43-65, 1967.

44. TAHIANI, C.
LACHNCE, L. — Linear and Non-Linear Analysis of Thin Shallow Shells by Mixed Finite Element. Computers & Structures, vol.5, pp.167-177, 1975.

45. EGGATOUDIS, I.
IRONS, B.M.
ZIENKIEWICZ, O.C. — Curved Isoparametric, Quadrilateral Elements for Finite Element Analysis. Int. Journal of Solids & Strucures, vol.4, pp.519-531, 1971.

46. HENSHELL, R.D.
NEALE, B.K.
WARBURTON, G.B. — A New Hybrid Cylindrical Shell Finite Element. Jour. Sound & Vib., vol.16, no.4, pp.519-531, 1971.

47. EDWARDS, G.
WEBSTER, J.J. — Hybrid Cylindrical Shell Finite Elements. Finite Elements for Thin Shells & Curved Members, Ch.6(Eds. Ashwell and Gallagher),Wiley, 1976.

48. SABIR, A.B.
LOCK, A.C. — A Curved, Cylindrical Shell Finite Element. Int. J. Mech. Science, vol.14, pp.125-135, 1972.

49. SABIR, A.B. — Finite Element Analysis of Arch Bridges. Finite Element Methods for Thin Shells & Curved Members, Ch.12(Eds. Ashwell and Gallagher), Wiley, 1976.

50. ASHWELL, D.G.
SABIR, A.B. — A New Cylindrical Shell Finite Element Based on Simple Independent Strain Functions. Int. J. Mech. Sci., vol.14, pp.171-183, 1972.

51. ASHWELL, D.G. — Strain Elements with Application to Arches, Rings and Cylindrical Shells. Finite Elements for Thin Shells & Curved Members, Ch.6(Eds. Ashwell and Gallagher), Wiley, 1976.

52. RAJU, J.S.
RAO, V.
RAO, P.
VEKATARMANA, J. — A Conical Shell Finite Element. Computers & Structures, vol.4, pp.901-915, 1974.

53. S-SOBIESK, J.
BHAT, R.B. — Adaptable Structural Synthesis Using Advanced Analysis and Optimization Coupled by Computer Operating System. Journal of Aircraft, vol.18, no.2, pp.142-149, Feb. 1981.

54. YURKOVICH, R.N.
SCHMIDT, J.H.
ZAK, A.R. — Dynamic Analysis of Stiffened Panel Structures. Journal of Aircraft, vol.8, no.3, pp.149-151, Mar. 1971.

55. DAVIS, R.
HENSHELL, R.D.
WARBURTON, G.B. — A Timoshenko Beam Element. Journal of Sound & Vibration, vol.22, no.4, pp.475-487, 1972.

56. EL-AMIN, F.M. BROTTON, D.M.	Horizontally Curved Beam Finite Element Including Warping. Int. J. Num. Meth. Eng., vol.10, pp.1397-1428, 1976.
57. THORNTON, W.A. AVIS, R.T.	Comment on 'Horizontally Curved Beam Finite Element Including Warping'. Int. J. Num. Meth. Eng., vol.14, pp.621-623,1979.
58. CHAUDHURI, S.K. SHORE, S.	Thin-Walled Curved Beam Finite Element. Journal of Eng. Mech. Div., Proc. ASCE, EM5, pp.921-937, Oct. 1977.
59. YOO, C.H.	Matrix Formulation of Curved Girders. J. Eng. Mech. Div., Proc. ASCE, EM6, pp.971-988, Dec. 1979.
60. DAVIS, R. HENSHELL, R.D. WARBURTON, G.B.	Curved Beam Finite Element for Coupled Bending and Torsional Vibration. Earthquake Engineering and Structural Dynamics, vol.1, pp.165-172, 1972.
61. FERGUSON, G.H. CLARK, R.D.	A Variable Thickness, Curved Beam and Shell Stiffening Element with Shear Deformations. Int. J. Num. Meth. Eng., vol.14, pp.581-592, 1979.
62. JIROUSEK, J.	A Family of Variable Section Curved Beam and Thick-Shell Isoparametric Elements. Int. J. Num. Meth. Eng., vol.17, pp.171-186, 1981.
63. MEYER, C.	Special Problems Related to Linear Equation Solver. J. Str. Div., Proc. ASCE, ST4, pp.869-890, Apr. 1975.

64. COLLINS, R.J. — Band Width Reduction by Automatic Renumbering. Int. J. Num. Meth. Eng., vol.6, pp.345-356, 1973.

65. IRON, B.M. — Frontal Solution Program for Finite Element Analysis. Int. J. Num. Meth. Eng., vol.2, pp.5-32, 1970.

66. LOCK, A.C., SABIR, A.B. — Algorithm for the Large Deflection Geometrically Nonlinear Plane and Curved Structures. The Mathmatics of Finite Element and Applications, pp.483-494(Ed. Whitemen), Academic Press, 1973.

67. WILSON, E.L., BATHE, K.J., DOHERTY, W.P. — Direct Solution of Large Systems of Linear Equations. Comp. & Str., vol.4, pp.363-372, 1974.

68. GUYAN, R.J. — Reduction of Stiffness and Mass Matrices. AIAA journal, vol.3, no.2, pp.380, 1965.

69. KAMEL, H.A., LIU, D., McCABE, W., PHILIPPOPOULOS, V. — Some Development in the Analysis of Complex Ship Structure. Advances in Computational Method in Structural Mechanics and Design, pp.703-726(Ed. Oden), Univ. of Alabama Press, 1972.

70. FURUIKE, T. — Computerized Multiple Level Sub-Structuring Analysis. Comp. & Str., vol.2, pp.1063-1073, 1972.

71. UTKU, S. — Systematic Substructuring. J. Str. Div., Proc. ASCE, ST4, pp.717-730, Apr. 1975.

72. NOOR, A.K. — Substructuring Techniques- Status and Projections. Comp. & Str., vol.8, pp.621-632, 1978.

73. MELOSH, R.J.
LUIK, R.
Multiple-Configuration Analysis of Structures. J. Str. Div., Proc. ASCE, ST11, pp.2581-2596, Nov. 1968.

74. NOOR, A.K.
LOWDER, H.E.
Approximate Reanalysis Techniques with Substructuring. J. Str. Div., Proc. ASCE, ST8, pp.1687-1698, Aug. 1975.

75. NOVOZHILOV, V.V.
The Theory of Thin Shells. Sec.10, P. Noordhoff Ltd., Gronningen, The Netherlands, 1959.

76. CHEUNG, Y.K.
YEO, M.F.
A Practical Introduction to Finite Element Analysis. Ch.3, Pittman, London, 1979.

77. McGUIRE, W.
GALLAGHER, R.H.
Matrix Structural Analysis. Sec.10.6, Wiley, 1979.

78. NICOLAI, L.M.
Fundamentals of Aircraft Design. Ch.11, Mets Inc., Ohio, 1975.

79. COWPER, G.R.
The Shear Coefficient in Timoshenko's Beam Theory. Trans. ASME, J. App. Mech., pp.335-340, June 1966.

80. COWPER, G.R.
On the Accuracy of Timoshenko's Beam Theory. J. Eng. Mech. Div., Proc. ASCE, EM6, pp.1447-1453, 1968.

81. TIMOSHENKO, S.P.
Strength of Materials - Part 1, 3rd Ed., pp.170-172, Van Nostrand Co., New York, 1955.

82. ROARK, R.J. Formula for Stress and Strain.
YOUNG, W.C. 5th Ed., pp.185, McGraw-Hill, 1975.

83. DOMMASCH, D.O. Airplane Aerodynamics. 2nd Ed.
SHERBY, S.S. pp.120, 536-537, Pittman, New York, 1957.

84. TIMOSHENKO, S.P. Theory of Plates and Shells, 2nd Ed.
WOINOWSKY-KRIEGER, Ch.15, McGraw-Hill Kogakusa Ltd., 1959.

85. CHENEY, J.A. Bending and Bulking of Thin-Walled Open-Section Rings. J. Eng. Mech. Div., Proc. ASCE, EM5, pp.17-43, Oct. 1963.

APPENDIX A

SURVEY OF THE STRUCTURAL WING-BODY INTERACTION TYPES OF EXISTING AIRCRAFTS AND RPVS

The general characteristics of the wing body interaction design of existing aircrafts have been surveyed. This survey covers various types of an aircraft and unmanned vehicle. The structural descriptions of the surveyed vehicles are based on schematic diagrams of each vehicle in most cases. The purpose of this survey is to get an idea for the design of an RPV wing-body interaction structure and for the generalization of the existing design types.

The detail description of the surveyed aircraft structures are given in Table A.1. The following simple classifications are used in the survey, on the bases of the size of aircraft and the structural types of wing-body intersection.

i) Small or medium sized transport type aircrafts, such as a light short haul transport, which have mostly large one piece wing attached to the top or bottom of the fuselage.

ii) Large military or civil transport type aircrafts which have usually a shell type fuselage and a torsion box type wing structure.

iii) Military fighter type of aircrafts which have many wing spars and fuselage frames.

iv) Unmanned aircrafts, such as a target drone or an RPV, which mostly have a very simple and small body and wing.

The typical characteristics of a small class of RPV structure have been chosen from this survey as follows:

i) A simple and small radius axisymmetric body which has very small number of transverse stiffeners to simplify manufacturing and access.

ii) A simple two spar torsion box type one piece wing structure construction.

iii) Small number of the longitudinal stiffeners using full length extrusion for the purpose of primary longerons, body sheets assemblage, and hard points for the wing and tail attachments.

iv) Small number of the wing pick up frames and pick up points for an easy assembly or replacement of wing structure.

v) No undercarriage in the body due to its mid-air retrieval system or parachute landing.

vi) Auxiliary power units for take-off, which is mounted on the longitudinal booms.

A small body radius of RPV makes the stiffeners and the wing attachment frames relatively deeper, compared to a conventional transport type fuselage. A use of more extreme wing positioning on the body circumference is another possible feature of an RPV type wing-body intersection, unlike the wing attachment to the fuselage of aircraft.

Table A.1 (continue)

I. LARGE CIVIL JET TRANSPORT

	NAME	TYPE	WING STRUCTURE					FUSELAGE	MAIN
			No. OF SPAR	TYPE	POSITION	¼ CHORD SWEEP	MAJOR SUBSECTION	TYPE, CROSS SECTION & WING ATTACHMENT	UNDER CARRAGE
1	AEROSPATIALE- - SE210, CARAVELLE	MEDIUM RANGE AIRLINER	3			20	2 PIECES HINGED AT CENTRE LINE	SEMI-MONOCOQUE, FRAME SPAR LUG, FWD SPAR	INSIDE FUSE. BEHIND REAR SPAR
2	DASSALUT-BREGUET : MERCURE	SHORTHAUL LARGE TRANSPORT	2	TORSION BOX	LOW	25			WING/FUSELAGE CENTRE SECT. FAIRING
3	AIRBUS - A300	WIDE BODIED SHORT/MEDIUM RANGE TRANSPORT	2 MAJOR	"	"	28			INSIDE FUSE. BEHIND REAR SPAR
4	AERSPATIALE/ BAC-CONCORDE	SUPERSONIC TRANSPORT	MULTI	"	"	-	3 PIECES	S-M, CENTRE WING SPAR & ASSOCIATED BODY FRAME BUILT AS SINGLE ASSY	FUSE. INSIDE & WING
5	BAe(BAC)-111	SHORT/MEDIUM RANGE TRANSPORT		3 SHEAR WEB TORSION BOX	"	20	1 PIECE CENT. 6CELL 40%SPAR,4CL OUTER 2CELL	BUILT IN	INSIDE FUSE. BEHIND REAR SPAR
6	BAe(HS)-TRIDENT	"	5 AT ROOT		"	35	1 PIECE CENT. 6CELL 40%SPAR,4CL OUTER 2CELL	WING CENTRE SECTION CONTINUOUS THROUGH BODY	"
7	BOEING-707	PASSENGER/ CARGO TRANSPORT	2		"	35		WING CENTRE SECTION CONTINUOUS THROUGH BODY	INSIDE OF WING ROOT AND FUSE.
8	BOEING-747	HEAVY COMMERCIAL TRANSPORT			"	37.5		"	2 INSIDE OF WING 2 INSIDE OF BODY
9	LOCKHEED-L1011 TRISTAR	WIDE BODIED MEDIUM RANGE TRANSPORT	2	TORSION BOX	"	35	3(1 CENTRE, 2 OUTER)	"	INSIDE FUSE. (REAR OF WING CENTRE BOX)
10	McDONELL-DOUGLA - DOUGLAS ;IC 9	SHORT/MEDIUM RANGE TRANSPORT	3 INBORD 2OUTBORD		"	24			"

Table A.1 (continue)

I. LARGE CIVIL JET TRANSPORT

	NAME	TYPE	WING STRUCTURE					FUSELAGE	MAIN
			No. OF SPAR	TYPE	POSITION	¼ CHORD SWEEP	MAJOR SUBSECTION	TYPE, CROSS SECTION & WING ATTACHMENT	UNDER CARRAGE
11	McDONELL -DOUGLAS DC 10	HIGH CAPACITY COMMERCIAL TRANSPORT			LOW	35		SEMI MONOCOQUE	INSIDE FUSE. (BEHIND WING CENTRE BOX)
12	ILYUSHIN: IL-62 CLASSIC	LONG RANGE TRANSPORT	3		"	35		"	INSIDE WING ROOT
13	ILYUSHIN IL-76 CANDID	FOUR TURBOFAN MEDIUM/LONG RANGE FREIGHT TRANSPORT			EXTREME HIGH	25		'	
14	TUBOLEV TU-154	THREE ENGINED MEDIUM/LONG RANGE TRANSPORT A/C	3		LOW	35		"	FAIRING ON WING T.E

Table A.1 (continue)

II. SMALL/MEDIUM CIVIL JET AIRCRAFT

	NAME	TYPE	WING STRUCTURE: No. OF SPAR	WING STRUCTURE: TYPE	WING STRUCTURE: POSITION	WING STRUCTURE: ¼ CHORD SWEEP	WING STRUCTURE: MAJOR SUBSECTION	FUSELAGE: TYPE, CROSS SECTION & WING ATTACHMENT	MAIN UNDER CARRAGE
1	CANALAIR CL-600 Challenger	Civil Transport	2	Torsion Box	Low	25^{o}	1 piece wing	semimonocoque, 6 points joint	Inside of Fuse, Back of Rear Spar
2	DASSAULT Mystere 20	Excutive Transport		"	"	30^{o}		"	"
3	VFW-FOKKER (Germany) VFW 614	Short Haul Transport	2	"	"	15^{o}	Centre sect & 2 outer wing	Integrated Centre Wing & Fuselage	"
4	VFW-FOKKER (Dutch) F-28 Fellowship	"	"	" (single cell)	Low/Mid	16^{o}	"	"	"
5	CESSNA Citation500	Executive Transport	2 primary 1 aux.	"	"	0^{o}		3 Points	Inside of Wing
6	GRUMANN Gulf Stream	"			"	25^{o}		"	Inside of Fuselage, Back of Rear Spar
7	LOCKHEED Jet Star II	"			"	30^{o}		"	"
8	ROCKWELL Sabre liner 75	Business Transport	2		"	$28^{o}33'$		"	Wing Lower Surface
9	TUPOLEV TU-134	Medium Range Transport	"		"	35^{o}		"	Fairing on Wing T.E.
10	YAKOLEV YAK 40	Short Haul Transport	3 (main, FWD & AFT aux.)		"	0^{o}	2 piece	.	Behind Centre Wing

Table A.1 (continue)

III. JET ENGINED MILITARY FIGHTING AIRCRAFT

	NAME	TYPE	WING STRUCTURE					FUSELAGE	MAIN
			No. OF SPAR	TYPE	POSITION	¼ CHORD SWEEP	MAJOR SUBSECTION	TYPE, CROSS SECTION & WING ATTACHMENT	UNDER CARRAGE
1	DASSAULT-BREGUET MIRAGE III	SINGLE SEAT FIGHTER-BOMBER/ INTRUDER		TORSION BOX	LOW	$60^{o}34'$ L.E			INSIDE FUSELAGE
2	DASSAULT-BREGUET MIRAGE 50	SINGLE SEAT MULTI MISSION FIGHTER & ATTACK	2	"	HIGH			SEMI MONOCOQUE	
3	DASSAULT-BREGUET/DONNIER ALPHA-JET	2 SEAT TRAINER, CLOSE SUPPORT, BATTLEFIELD RECONN.			"	28	3 PIECES(2 OUTER WING BOLT JOINT WTH CTR WING)	"	SIDE OF ENGINE INTAKE
4	PANAVIA TORNADO	2 SEAT TWIN ENGINED MULTI-ROLL COMBAT AIRCRAFT VARIABLE GEOMETRY			"	25-60	2 PIECES	" CARRY THROUGH BOX	CENTRE SECT. OF FUSELAGE
5	SPECAT JAGUAR	TACTICAL SUPPORT AND ADVANCED TRAINER	2	TORSION BOX	"	40	3 PIECES	" 2 SIDE INTAKE 3 POINT JOINT/EA	"
6	AERITALIA G91Y	LIGHT WEIGHT SNGL SEAT TACTICAL FIGHT-BOMBER/ RECONN.	2		LOW	$37^{o}40'$ 38"		SEMI MONOCOQUE	
7	AERMACCHI MB326	2 SEAT TRAINER & LIGHT TACTICAL ATTACK	2		LOW/MID	$8^{o}29'$	3 PIECES	" CENTRE WING, INTEGRAL WITH FUSE.	INSIDE BODY
8	MITSUBISHI T2	2 SEAT TRAINER	MULTI	TORSION	HIGH	68^{o} at L.E		SEMI MONOCOQUE	"
9	SAAB 37 VIGGEN	SINGLE SEAT MULTI PURPOSE COMBAT AIRCRAFT			LOW			"	MAIN WING & FUSELAGE
10	SAAB 105	MULTI PURPOSE TWIN JET A/C	2		HIGH	$12^{o}48'$	1 PIECE	"	"

Table A.1 (continue)

III. JET ENGINED MILITARY FIGHTING AIRCRAFT

	NAME	TYPE	WING STRUCTURE: No. OF SPAR	WING STRUCTURE: TYPE	WING STRUCTURE: POSITION	WING STRUCTURE: ¼ CHORD SWEEP	WING STRUCTURE: MAJOR SUBSECTION	FUSELAGE: TYPE, CROSS SECTION & WING ATTACHMENT	MAIN UNDER CARRAGE
11	BAC 167 STRIDEMASTER	2 SEAT TRAIN AND TACTICAL SUPPORT A/C	1 MAIN & 8SUBSI-DARY		LOW			SEMI MONOCOQUE 3 POINT JOINT BUILT IN 3 SPAR	WING
12	HAWKER SIDDELEY HAWK	1 OR 2 SEAT TRAINER AND CLOSE SUPPORT A/C		TORSION BOX	LOW	$21^{o}30'$	1 PIECE	" 6 BOLTS ATTACH TO BODY FRAME	"
13	HAWKER SIDDELEY HARRIER	V/STOL CLOSE SUPPORT & RECONN.	3		HIGH	34	1 PIECE	" 6 POINT ATTACH	INSIDE FUSELAGE
14	HAWKER SIDDELY BUCCANEER	2 SEAT STRIKE & RECONN.	MULTI		MID	40^{o}- $30^{o}12'$	4 PIECES	' 3 POINT/EA.SIDE ATTACH TO BODY FRAME	NACELLE
15	CESSNA A-37 DRAGON FLY	2 SEAT 2JET LIGHT STRIKE	2		LOW	0	2 PIECES	'	WING
16	FAIRCHILD A-10	SINGLE SEAT CLOSE SUPPORT	3		LOW		3 PIECES	" 4 POINT JOINT (FRONT & REAR SPAR) WING BOX CARRY THROUGH	FAIRING BENEATH WING
17	GENERAL GENERAL DYNAMICS F 111	2 SEAT VARIABLE GEOMETRY MULTI PURPOSE FIGHTER	5 (OUTER WING)		VARIABLE GEOMETRY HIGH	L.E SWEEP 16-72.5		"	INTAKE DUCT SIDE OF FUSE.
18	GENERAL DYNAMICS F-16	SINGLE SEAT LIGHT WEIGHT AIR COMBAT A/C	12		MID	40^{o}L.E		" MACHINED WING CENTRE FITTING TO BODY	FUSELAGE
19	GRUMANN A-6 INTRUDER	2 SEAT 2 ENGINE CARRIER BASED ATTACK BOMBER			MID	25		"	FAIRING ON AIR INTAKE
20	GRUMANN F-14 TOMCAT	2 SEAT CARRIER BASED ATTACK BOMBER			VARIABLE GEOMETRY MID	L.E SWEEP 20-68	4 PIECES		INNER WING

Table A.1 (continue)

III. JET ENGINED MILITARY FIGHTING AIRCRAFT

	NAME	TYPE	WING STRUCTURE					FUSELAGE	MAIN
			No. OF SPAR	TYPE	POSITION	¼ CHORD SWEEP	MAJOR SUBSECTION	TYPE, CROSS SECTION & WING ATTACHMENT	UNDER CARRAGE
21	LOCKHEED S-3 VIKING	CARRIER BASED 2 ENGINE. ANTISUBMARINE A/C			HIGH	15	3 PIECES	SEMI MONOCOQUE	FUSELAGE
22	McDONNELL-DOUGLAS F-15 EAGLE	SINGLE SEAT AIRSUPERIORITY FIGHTER AND ATTACK A/C			"	L.E 45^{o}		"	"
23	McDONNELL-DOUGLAS F-4 PHANTOM	2 SEAT 2 ENGINE ALL WEATHER FIGHTER	2	TORSION BOX	LOW	L.E 45	3 PIECES	"	WING
24	McDONNELL-DOUGLAS F-18 V	SINGLE SEAT CARRIER BASED AIR COMBAT FIGHTER A/C	MULTI		MID	20	4 PIECES	"	AIRDUCT INSIDE
25	McDONNELL-DOUGLAS A-4 SKYHAWK	SINGLE SEAT ATTACK BOMBER	3		LOW	33	1 PIECE	"	WING
26	ROCKWELL INTERNATIONAL T-2 BUCKEYE	2 SEAT TRAINER	2		MID	0	2 PIECES	"	"
27	NORTHROP F-5E TIGER II	SINGLE SEAT LIGHT TACTICAL FIGHTER	MULTI		LOW	24	1 PIECE	"	FUSELAGE
28	VOUGHT A-7 CORSAIR II	SINGLE SEAT SUBSONIC TACTICAL FIGHTER	MULTI	MULTI MACHINED STIFFENER	HIGH	35		"	"
29	MIKOYAN MIG 21	SINGLE SEAT MULTI ROLE FIGHTER			MID	53		" " NOSE INTAKE	"
30	MIKOYAN MIG 23	SINGLE SEAT VARIABLE GEO. TACTICAL FIGHTER			VARIABLE GEOMETRY HIGH	L.E 9-72		"	REAR OF AIR INTAKE

Table A.1 (continue)

IV. Large Military Jet Aircraft (Transport)

	NAME	TYPE	WING STRUCTURE No. OF SPAR	TYPE	POSITION	¼ CHORD SWEEP	MAJOR SUBSECTION	FUSELAGE TYPE, CROSS SECTION & WING ATTACHMENT	MAIN UNDER CARRAGE
1	LOCKHEED C-5A GALAXY	LONG RANGE MILITARY HEAVY TRANSPORT		BOX STRUC. BUILD IN SPAR	HIGH	25		SEMI MONOCOQUE	INSIDE OF BODY
2	McDONNELL DOUGL DOUGLAS YC 15	ADVANCED MILITARY ADVANCED MILITARY STOL TRANSPORT			"	5.9		"	SPONSON
3	ROCKWELL INTERNATIONAL B1	SUPERSONIC VARIABLE GEOMETRY STRATEGIC BOMBER			LOW	15; FULLY FWD 67.5; FULL SWPT	CENTRE WING 2 VARIABLE GEOMETRY OUTER	" CENTRE WING-BODY CARRY THROUGH STR. INTERGRATED	INSIDE OF BODY
4	BOEING YC 14	ADVANCED MEDIUM STOL MILITARY TRANS-PORT			HIGH	–		"	SPONSON
5	TUPOLEV TU-16 BADGER	MEDIUM BOMBER & MARITIME RECON-NAISSANCE/ATTACK AIRCRAFT			MID	37		"	HOUSING BEYOND WING TRAIL EDGE
6	BAe(HS)NIMROD	MARITIME PATROL RECONNAISSANCE	2		LOW/MID	20	CENTRE SECTION 2 STUB WING 2 OUT.PANNEL	" (CIRCULAR CABIN & UNDER BAY)	WING CENTRE (BETWEEN SPAR
7	KAWASAKI C-1	MEDIUM RANGE MILITARY TRANSPORT	2		HIGH	20		SEMI MONOCOQUE	FAIRING BUILT ON SIDE OF BODY
8	LOCKHEED S-3 VIKING	CARRIER BORNE ANTI SUBMARINE AIRCRAFT			HIGH (SHOULDER)	15		"	INSIDE BODY (IMMEDIATE AFTER WEAPON BAY)
9	BAe(HS)-748	SHORT/MEDIUM RANGE TRANSPORT	2	SINGLE CELL	LOW	2.9		"	ENGINE NACELLE (FWD OF FRONT SPAR)

Table A.1 (continue)

V. LARGE MILITARY PROPELLER AIRCRAFT

	NAME	TYPE	WING STRUCTURE					FUSELAGE	MAIN
			No. OF SPAR	TYPE	POSITION	¼ CHORD SWEEP	MAJOR SUBSECTION	TYPE, CROSS SECTION & WING ATTACHMENT	UNDER CARRAGE
1	GRUMANN -HAWKEYE E2	AIRBORN EARLY WARNING A/C TURBOPROP			HIGH	0^o		SEMI-MONOCOQUE	NACELLE
2	LOCKHEED P-3F ORION	LONG RANGE MARITIME PATROL TURBOPROP	2	BOX	LOW	0		"	"
3	LOCKHEED C-130 HERCULES	MEDIUM/LONG RANGE COMBAT TRANSPORT	2		HIGH	"		"	FUSELAGE SIDE FAIRING
4	ROCKWELL INTER. OV -10 BRONCO	MULTIPURPOSE COUNTER INSURGENT	"	"	"	"		SEMI-MONOCOQUE (SHORT POD TYPE)	NACELLE
5	TUPOLEV TU95 BEAR	LONG RANGE T/P BOMBER & MARITIME RECONN.	3	"	MID	35^o-37^o		SEMI -MONOCOQUE	NACELLE (BULTIN TO WING)
6	KAWASAKI P-2J	ANTI SUBMARINE AND MARITIME PATROL, T/P	3	"	"	0		BOX WING BEAM CONTINUOUS THRU FUSELAGE	ENGINE NACELLE
7	AEROSPATIALLE N262 FREGATE	LIGHT T/P MIL/CIV. TRANSP.	2	"	HIGH			SEMI-MONOCOQUE (39 FRAMES)	FESELAGE SIDE FAIRING
8	DeHAVILLAND (CANADA) CC115 BUFFALO	TWIN T/P STOL UTILITY TRANSPORT	MULTI	"	"	$1^o40'$		SEMI-MONOCOQUE (CARGO FLOOR SUPP'D BY LONG KEEL MEMBER)	NACELLE

Table A.1 (continue)

VI. MEDIUM PROPELLER TRANSPORT

	NAME	TYPE	WING STRUCTURE					FUSELAGE	MAIN
			No. OF SPAR	TYPE	POSITION	¼ CHORD SWEEP	MAJOR SUBSECTION	TYPE, CROSS SECTION & WING ATTACHMENT	UNDER CARRAGE
1	DE HAVILLAND - CANADA: DASH 7	TURBOPROP SHORT/MEDIUM RANGE STOL TRANSPORT	2	BONDED SKIN/STRING TORSION BOX	HIGH		SINGLE	SEMI-MONOCOQUE FUSEL. 2 FRAME 4 POINTS WING PICK UP	NACCELE
2	EMBRAER EMB-110 (AUSTRALIA)	TWIN TURBOPROP GENERAL PURPOSE TRANSPORT			LOW	$0^{o}32'$		CONVENTIONAL SEMI-MONOCOQUE FUSE.	
3	AIR METAL AM -C111	TWIN TURBOPROP STOL TRANPORT & UTILITY A/C			HIGH	0	RECTANGULAR CENTRE SECTION	"	FAIRING ON SIDE OF FUSE.
4	TRANSVAL C-160 (INTERNATIONAL)	TWIN T/P GENERAL PURPOSE TRANSPORT	2		"		CENTRE & 2 OUTER PANN.		"
5	GENERAL AVIA F600 KANGAGAROO (ITALY)	TWIN T/P FREIGHT, AMBULANCE GENERAL UTILITY TRANSPORT	1 MAIN 2 AUX. 2 OUTER		"			"	INSIDE FUSELAGE
6	PIAGGIO P166-BL2	TWIN ENGINED LIGHT TRANSPORT			SHOULDER GIRDER WING			"	WING
7	MITSUBISHI MU-2	TWIN T/P TRANSPORT	2		HIGH	$0^{o}21'$	SINGLE	"	FAIRING ON FUSELAGE SIDE
8	VFW -FOKKER F27 FRIENDSHIP	TWIN T/P MEDIUM RANGE AIRLINER	2	TORSION BOX	"	0		"	ENGINE NACCELE
9	CASA C.212 AVIOCAR (SPAIN)	TWIN T/P STOL UTILITY TRANSPORT			"	"		FOUR LONGERON, RECT. FUSELAGE	FAIRING ON FUSELAGE
10	BRITTEN-NORMAN BN-2 TRISLANDER	THREE T/P FEEDERLINER	2	TORSION BOX	"	"	ONE PIECE	"	NACCELE

Table A.1 (continue)

VI. MEDIUM PROPELLER TRANSPORT

	NAME	TYPE	WING STRUCTURE: No. OF SPAR	WING STRUCTURE: TYPE	WING STRUCTURE: POSITION	WING STRUCTURE: ¼ CHORD SWEEP	WING STRUCTURE: MAJOR SUBSECTION	FUSELAGE: TYPE, CROSS SECTION & WING ATTACHMENT	MAIN UNDER CARRAGE
11	SCOTTISH AVIATION JET STREAM	TWIN T/P LIGHT TRANSPORT			LOW	$0^{o}34'$		SEMI-MONOCOQUE 4 PONTS WING PICK UP FRAME	WING
12	SHORT - SKYVAN	CIVIL OR MILITARY STOL UTILITY A/C		TWO CELL BOX	BRACED HIGH	O		SEMI-MONOCOQUE	
13	SHORT-SKY LINER	TWIN T/P CIVIL & MILITARY TRANSP.	2	SINGLE CELL	BRACED HIGH	O	3 PIECES	INTEGRATED CENTRE WING WITH FUSELAGE	SPONSON
14	BRITTEN NORMAN BN-2A TRISLANDER	FEEDER LINER 3 ENGINED TRANSPORT	2	TORSION BOX	HIGH	O			
15	AUSTRALIAN GOVERNMENT FACT. NOMAD N22,24	2 TURBOPROP STOL UTILITY TRANPORT	2	"	BRACED HIGH	"	2 PIECES	SEMI-MONOCOQUE (RECT)	FAIRING
16	DeHAVILLAND (CANADA) - DHC-6 TWIN OTTER	TWIN T/P LIGHT TRANSPORT	2	"	"	"		" 2 BOLT (FRONT & REAR SPAR) WING JOINT	FUSELAGE
17	AEROSPATIALLE FRÉGATE	TWIN T/P LIGHT TRANSPORT	"		HIGH	"		SEMI-MONOCOQUE (CIRC.)	FAIRING
18	IAI 201 ARVA (ISRAEL)	TWIN T/P LIGHT TRANSPORT	"	TORSION BOX (TWIN BOOMS)	HIGH	"		"	FUSELAGE
19	BECHCRAFT B99 AIRLINER KING AIR 100, 200	TWIN T/P LIGHT PASSENGER FREIGHTER OR EXECUTIVE TRANSP.			LOW	"		"	NACELLE
20	SWEARINGEN METRO II	TWIN T/P COMMUTER	"		LOW	0.9^{o}		"	"

Table A.1 (continue)

VII. LIGHT PROPELLER AIRCRAFT

	NAME	TYPE	WING STRUCTURE: No. of Spar	WING STRUCTURE: Type	WING STRUCTURE: Position	WING STRUCTURE: Chord Sweep	WING STRUCTURE: Major Subsection	FUSELAGE: Type, Cross Section & Wing Attachment	MAIN: Under Carriage
1	AERO BOERO - 180RV (ARGENTINA)	3 SEAT LIGHT A/C		BOX	BRACED HIGH	0			
2	CERVA CE 43 (FRANCE)	4/5 SEAT LIGHT A/C	3(1 main 2 aux.)	TORSION BOX	LOW	0	2 pieces	BOAT TYPE CABIN SEMI-MONOCOQUE	WING
3	ROBIN AVIONICS -PIERRE ROBIN HR100 (FRANCE)	4 SEAT LIGHT A/C	SINGLE	"	"	"	"	BOX GIRDER LOAD BEARING STRUC. 4 BOLT AT EACH WING	WING RIB
4	ROBIN AVIONICS - ROBIN HR200	2 SEAT LIGHT TRAINER	" (I SHAPE)	"	"	"		STRESSED SKIN RECTANGULAR FUSELAGE	"
5	SOCATA - RALLYE	2/4 SEAT LIGHT A/C	"	"	"	"			"
6	MYLIUS - MY102 TORNADO (GERMANY)	SINGLE SEAT SPORTING & AEROBATIC	"	"	"	$1^{o}24'$	"	SEMI-MONOCOQUE 3 BOLTS FOR FOLDING BACK/EACH WING	FUSELAGE BULKHEAD
7	GENERAL AVIA - F15F (ITALY)	4SEAT LIGHT A/C	3(main, rear for aileron & fwd. U/C)	"	"	0		SEMI-MONOCOQUE	WING
8	PARTENAVIA - P168 VICTOR	6 SEAT LIGHT TRANSPORT & TRANER	SINGLE	"	HIGH	0		SEMI-MONOCOQUE (FRAME & 4 LONG.)	FUSELAGE
9	SIAI - MARCHETTI SF 260	3 SEAT MILITARY TRAINER	2		LOW	0	"	SEMI-MONOCOQUE 6 BOLT JOINT WING ATTACHMENT	FUSELAGE
10	FUJI FA-200	4 SEAT LIGHT MONOPLANE	SINGLE (EXTRUDED)		"	"	"	SEMI-MONOCOQUE	WING

Table A.1 (continue)

VII. LIGHT PROPELLER AIRCRAFT

	NAME	TYPE	WING STRUCTURE					FUSELAGE	MAIN
			No. OF SPAR	TYPE	POSITION	¼ CHORD SWEEP	MAJOR SUBSECTION	TYPE, CROSS SECTION & WING ATTACHMENT	UNDER CARRAGE
11	EQUATOR AIRCRA. P-400 TURBOEQUATOR (GERMANY)	LIGHT WEIGHT STOL, AMPILIBIAN EXECUTIVE A/C	SINGLE		HIGH	0		SEMI-MONOCOQUE	FUSELAGE
12	BRITTEN NORMAN BN-2A ISLANDER	TWIN ENGINED FEEDLIN TRANSPO.	2	TORSION BOX	"			SEMI-MONOCOQUE (4 LONGERON)	REAR WING SPAR
13	AMERICAN JET INDUSTRY - HUSTLER	TWIN TURBOPROP EXECUTIVE TRANSPORT	2		MID	15^{o}		SEMI-MONOCOQUE (CIRCULAR CROSS SEC)	FUSELAGE
14	PIPPER PA-31-310 TURBO NAVAJO	6/9 SEAT COMMUTER TRANS.	3 (HEAVY C)		LOW	0	2 PIECES	"	
15	CESSNA - CONQUEST 441	8/10 SEAT CORPOR. & COMMUTER TRANSPORT TWIN ENGINE	3		LOW	0			WING
16	PIPPER PA -31T CHEYENNE	6/8 SEAT CABIN MONOPLANE	3		"	"		"	"
17	TED SMITH - AEROSTAR	TWIN ENGINED 6 SEAT LIGHT TRANSPORT	"		MID	"		MONOCOQUE	"
18	HELLIO STALLION H-550A	8/10 SEAT GENERAL UTILITY STOL A/C	SINGLE		HIGH	"	2 PIECES	SEMI-MONOCOQUE	
19	LAKE LA -4-200 BUCCANER	4 SEAT LIGHT AMPHILIBIAN	3	TORSION BOX	HIGH	"	"	BOAT HULL FUSELAGE STRUCTURE WING ATTACHED TO HULL	WING
20	INTERCEPTOR 400	4 SEAT LIGHT A/C	2		LOW	1^{o}	3 PIECES	SEMI-MONOCOQUE	"

Table A.1 (continue)

VII. LIGHT PROPELLER AIRCRAFT

	NAME	TYPE	WING STRUCTURE: No. OF SPAR	WING STRUCTURE: TYPE	WING STRUCTURE: POSITION	WING STRUCTURE: ¼ CHORD SWEEP	WING STRUCTURE: MAJOR SUBSECTION	FUSELAGE: TYPE, CROSS SECTION & WING ATTACHMENT	MAIN UNDER CARRAGE
21	MOONEY RAGER	4 SEAT LIGHT A/C	2		LOW	$2^{o}29'$	SINGLE PIECE	SEMI-MONOCOQUE	WING
22	PIPER PA-36 PAUNEE BRAVE	SINGLE SEAT AGRICULTURAL A/C	2		"	0		STEEL TUBE, 2 BOLTS ATTACH WING TO FUSELAGE FRAME	FUSELAGE
23	UTVA - 75 (YUGOSLABIA)	2 SEAT LIGHT A/C			"	"		SEMI-MONOCOQUE	WING
24	AEROSPACE - FLETCHER ; FV -24-950 (NEW ZEALAND)	AGRICULTURAL & GENERAL PURPOSE	2		"	"			
25	BEECH CRAFT TURBO MASTER	2 SEAT PRIMARY MILITARY TRAINER		BOX BEAM	"	"			WING(BETWEEN 2 SPARS)
26	BEECH CRAFT SIERRA 200	4/6 SEAT CABIN LIGHT A/C	SINGLE (EXTRUDED)	HINEYCOMB	"	"		CABIN + REAR SEMI-MONOCOQUE FUSELAGE	"
27	BEECH CRAFT BONANZA	4/6 SEAT LIGHT A/C	2	BOX BEAM	"	"		SEMI-MONOCOQUE	"
28	CESSNA CARDINAL	4 SEAT LIGHT A/C			HIGH	"		"	FUSELAGE
29	CESSNA - SKYWAGON 207	1/7 SEAT UTILITY A/C			BRACED HIGH	"		"	"
30	GRUMAN AMERICAN AA -1B	2 SEAT TRAINER/UTILITY LIGHT A/C	SINGLE (TUBE TYPE)	HONEYCOMB	LOW				WING

Table A.1 (continued)

VIII. UNMANNED SMALL AIRCRAFT

	NAME	TYPE	WING STRUCTURE					FUSELAGE	MAIN
			No. OF SPAR	TYPE	POSITION	¼ CHORD SWEEP	MAJOR SUBSECTION	TYPE, CROSS SECTION & WING ATTACHMENT	UNDER CARRAGE
1	AUSTRALIAN GOVERNMENT FACT. JINDVIK MK3B	TARGET DRONE	MULTI	BOX BEAM	LOW/MID			SEMIMONOCOQUE	
2	CANADAIR C2-89	AIR SURVEILLANCE DRONE	SINGLE	STUB WING	CRUCIFORM			"	
3	AEROSPATIALLE CT-20	TARGET DRONE			MID		SINGLE		
4	BEECHCRAFT AQM-37	SUPERSONIC AIR LAUNCHED EXPANDABLE OR RECOVERABLE DRONE			MID	LEADING EDGE 76^{o}		"	
5	BOEING AEROSPACE COMPASSCOPE-B	EXPERIMENTAL HIGH ALTITUDE LONG ENDURANCE STRATEGIC RPV			HIGH		3 PIECES	CIRCULAR : 2 LONG. STRAIGHT THROUGH CONSTANT CHORD	WING
6	TELEDYNE RYAN MODEL 124 FIREBEE I	TARGET DRONE	3	SEMIMONOC.	"	45^{o}		"	
7	TELEDYNE RYAN MODEL 166 FIREBEE II	SUPERSONIC TARGET DRONE		STEEL SKIN HONEYCOMB	"	LEADING EDGE 53^{o}			
8	NORTHROP CHUKAR II	RECOVERABLE TARGET DRONE	2		"		SINGLE	"	
9	TELEDYNE RYAN MODEL 235 COMPASSCOPE R	HIGH ALTITUDE LONG ENDURANCE STRATEGIC RPV		SEMI-MONOCOQUE	LOW	7^{o}		"	
10	FR -500	DRONE	2				SINGLE		

APPENDIX B

PARTICULARS OF CHOSEN RPV

B.1 General Description

A simple small RPV design has been chosen for the efficient investigation of the wing-body structural design parameter variation effect on the overall structural behaviour. The basic configuration of the chosen RPV, which has a cylindrical cross section of body and a trapezoidal planform of wing with the quater chord sweep back angle of zero degree, is shown in Fig.3.1. The external power plant units, such as an engine and rocket assisted take-off (RATO) systems, are excluded in that figure.

The noncylindrical sections at nose and tail of the body are assumed as a nonstructural member as usual in an RPV, so that primary body structure is the cylindrical shell with two wing pick up loaded frames at the forward and rear spar positions of the wing box. The cylindrical body skin is supported by the four longitudinal members (longerons) and the regulary spaced transverse stiffeners (standard rings), at interval of one diameter length. The wing is attached through the two heavy loaded frames. Material in use for the major structural components is chosen as aluminium alloy.

Since the exact distribution of mass and the performance characteristics are not specified, the external load distribution also not specified. Therefore, the aerodynamic load on the wing has been assumed using informations in Ref.83.

B.2 Dimensions

1) Body

Overall length	204.0 inch
Nose cone	48.0 inch
Body	144.0 inch
Tail cone	18.0 inch
Diameter	12.0 inch
Nose cone shape	$0.925\sqrt{X}$
Tail cone shape	$\sqrt{2X}$

2) Wing

Semispan	38.0 inch
Root chord	25.5 inch
Tip chord	16.0 inch
Area (each)	788.5 $inch^2$
Aspect ratio	1.83
Taper ratio	0.627
Airfoil	NACA 65-006
Leading edge sweep back	5.71 degree
1/4 chord sweep	0. degree
Trailing edge sweep forward	-8.53 degree
1/4 chord position	X=75.0 inch
	Z: subject to change
Incidence angle	0. degree

3) Tail plane and Fin

Mid tail	90 and 270 degree
High fin	0. degree
Semispan-exposed	18.0 inch
Root chord	12.0 inch
Tip chord	7.5 inch
Area (each)	175.5 $inch^2$
Aspect ratio	1.85
Taper ratio	0.627
Airfoil	NACA 65-006
Leading edge sweep back	10.65 degree
3/4 chord sweep	0. degree
Trailing edge sweep forward	-3.56 degree
Position of 3/4 chord line	X=192.0

4) Control surfaces

Aileron	
Span	5.2 inch(Z=32.0-37.2)
Percentage wing chord line	75% and afterward
Area (each)	11.83 $inch^2$
Elevator	
Span	18.0 inch(Z=6.0-24.0)
Percentage tail chord line	75% and afterward
Area (each)	43.93 $inch^2$
Rudder	
Span	12.0 inch(Y=6.0-18.0)
Percentage chord of fin	75% and afterward
Area (each)	31.52 $inch^2$

B.3 Body Structure

1) Main body shell

Circular cylindrical cross section	
Radius	6.0 inch
Thickness of skin	0.06 inch
Stringers	
Number	4
Positions	45,135,225,315,deg.
Basic section properties	
second moment of inertia(Is);	0.001 in^4
cross section area(As);	0.1 in^2
constant throughout	
Rings	
Number	11
Spacing	12.0 inch conatant except X=72 and 84
Basic section properties	
Ir;	0.001 in^4
Ar;	0.1 in^2

2) Loaded frames

Positions	X=72.0 & 84.0 inch
Type or Properties	subject to change

B.4 Wing Structure

Type	2 spar-rib torsion box
Position of spars	X=72.0(1/4 chord line)
	X=84.0(3/4 chord line)
Position of ribs(% of semispan)	
Root rib	15.8%
Closing rib	100%
Intermediate ribs	36.8%, 59.8%
Aileron support rib	79.0%
Skin thickness	0.06 inch
Spars and Ribs	
Type	0.04 inch sheet forming
Inner wing structure	
Position	between Z= -6.0 to +6.0
Inner spars	macined I beams
Inner rib	Z=0.0

B.5 Material Used

1) Aluminium Alloys for Major structures

Young's modulus (E)	10.3×10^6 psi
Poisson's ratio (ν)	0.3
Specific weight (ρ)	0.1 lb/in^3

2) Glass-Fiber Reinforced Plastic

Control surface and nose & tail cone

B.6 Loads on the Wing

1) Distributed wing normal force :

Total normal force per each side ; 164.12 lbf

Pressure distribution ; Fig.B.1-B.2.

2) Concentrated normal force due to aileron :

Inner fitting ; 10 lbf at Z = 30.0 inch

Outer fitting ; 2 lbf at Z = 38.0 inch

Along the rear spar.

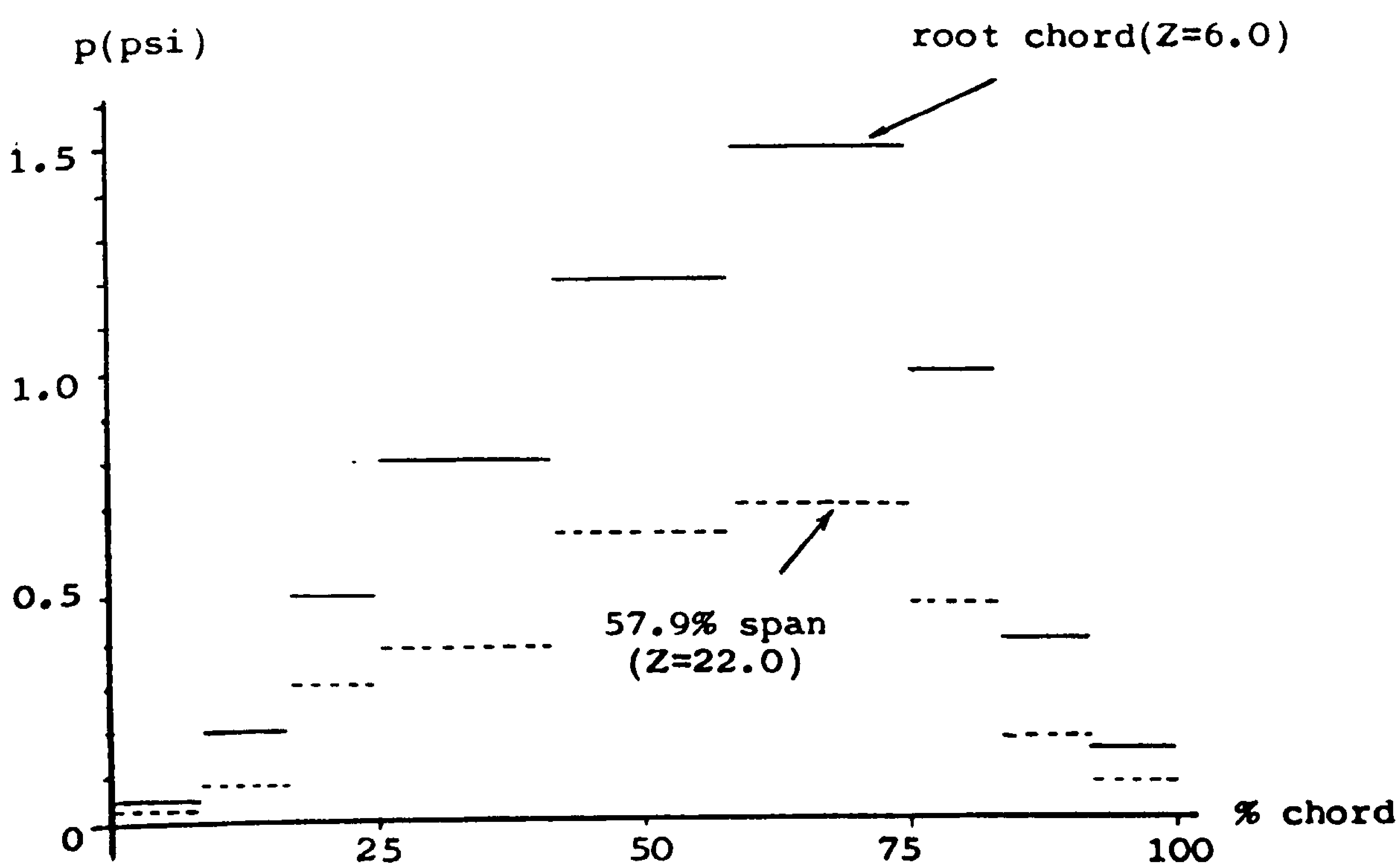

Fig.B.1 Chordwise Pressure Load Distribution on the Wing.

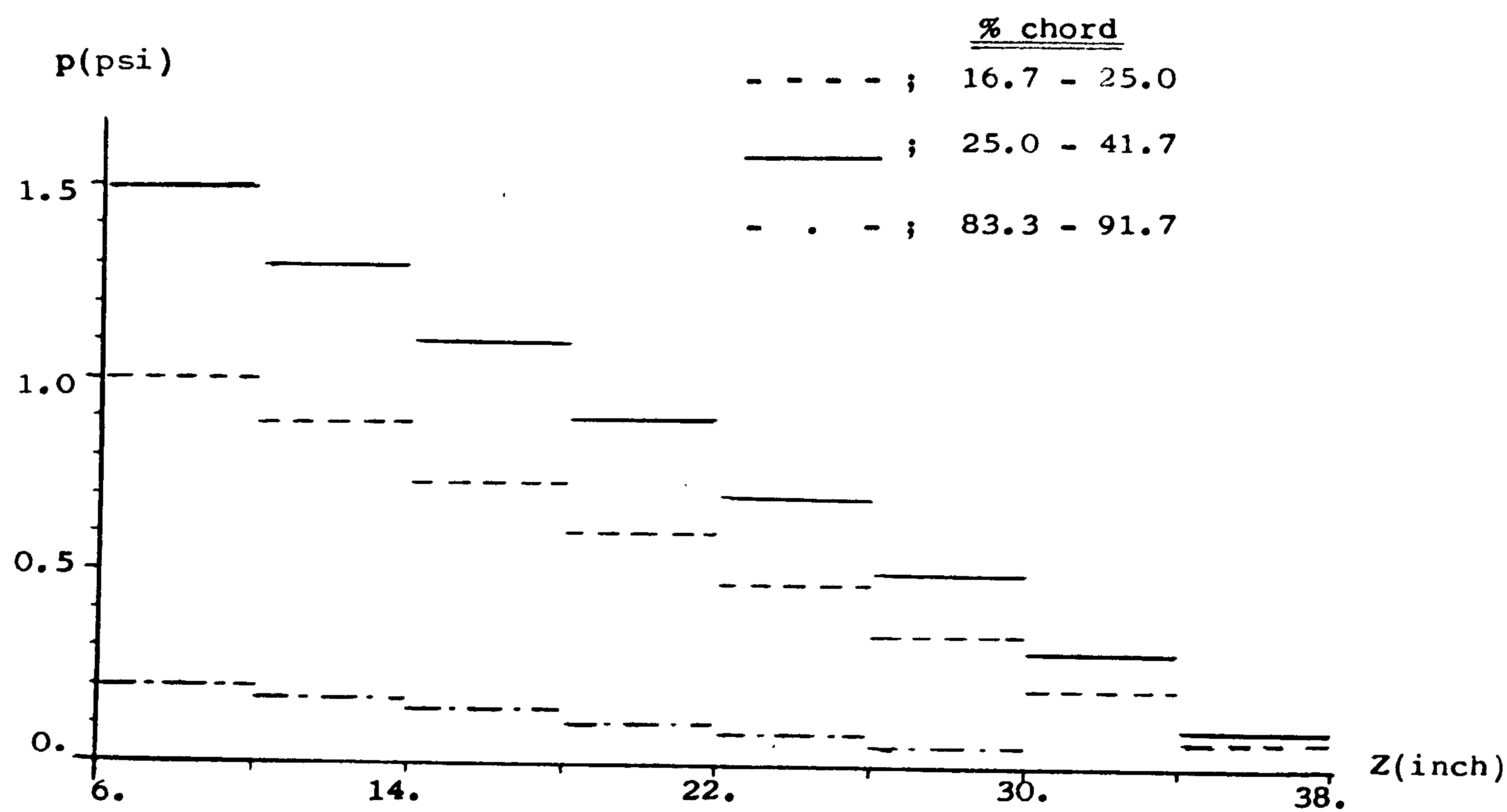

Fig.B.2. Assumed Spanwise Pressure Distribution on the Wing.

APPENDIX C

SHELL ELEMENT USED

C.1 Introduction

The strain element formulation, which is proposed by Sabir and Ashwell (Ref.50, 51), has been used for the finite element idealization of the fuselage shell skin structure. In their finite element formulation, the strains and curvatures are assumed as simple polynomials which satisfy the compatibility equation of the thin shell theory, rather than using the displacement or the stress assumptions.

The merits of this element are that converge rapidly and show reasonable accuracy with small number of degrees of freedom, compare to other types of element for the general thin or moderately thick shell structures. Instead of using Timoshenko's shell equation (Ref.84) in the original, Novozhilov's theory (Ref.75) is used for the element formulation. This includes the coupling between membrane terms and bending terms.

The constant shear strain assumption is chosen from the various possible polynomial assumptions of the shear strain. The accuracy of this element has been compared to other types of shell element or other strain assumptions of the shear strain.

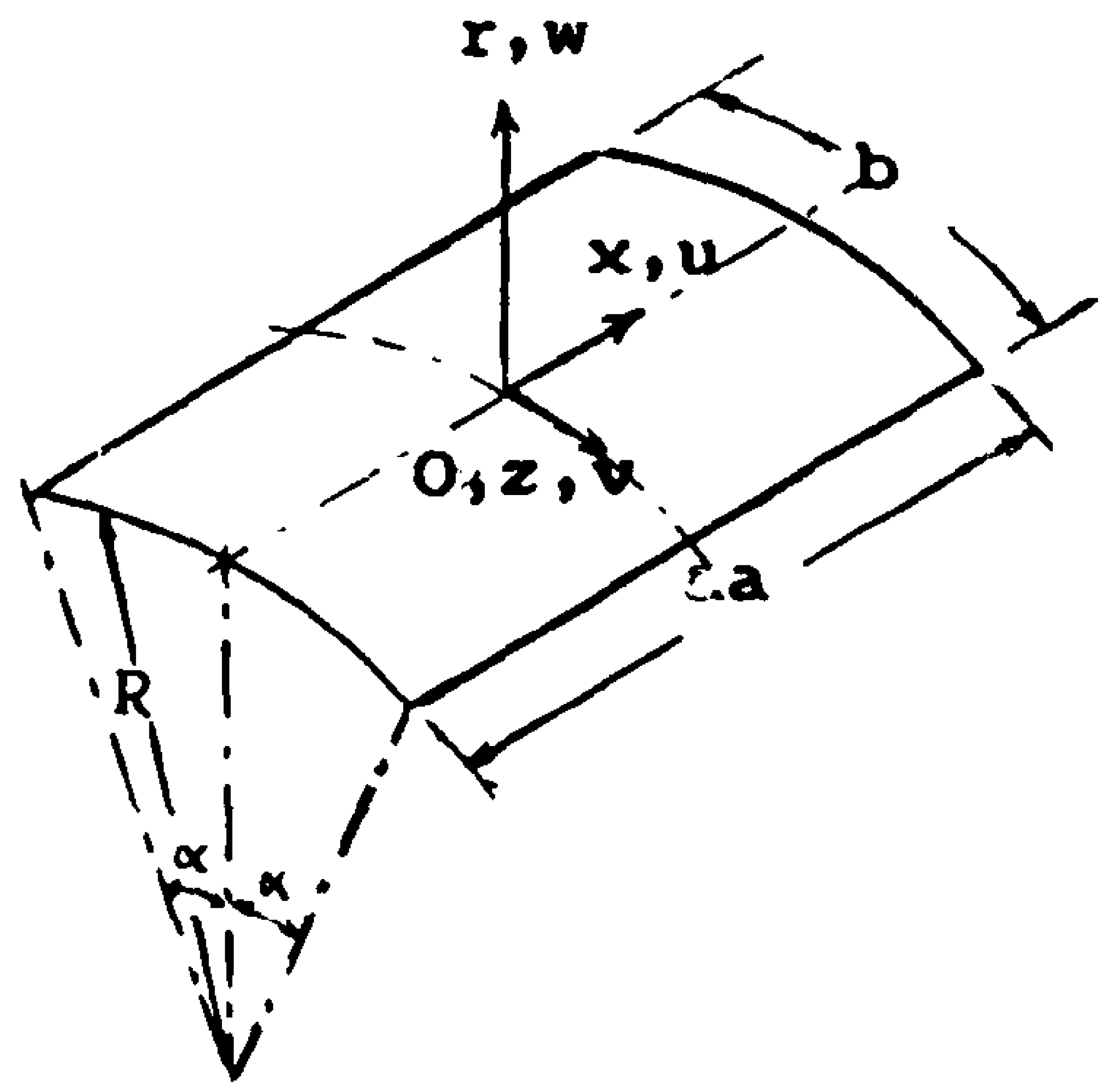

a) Coordinates and Displacements

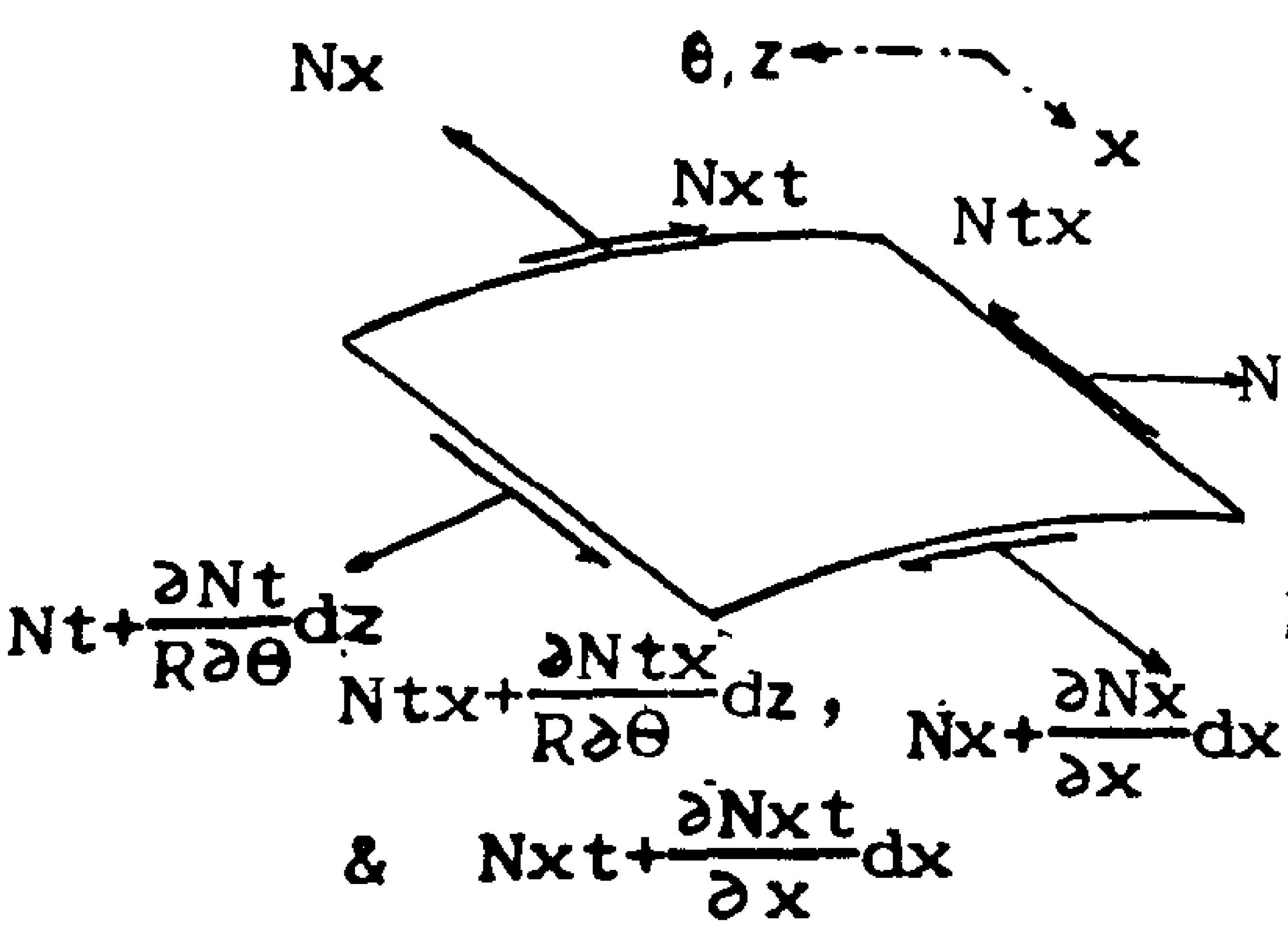

b) Stresses

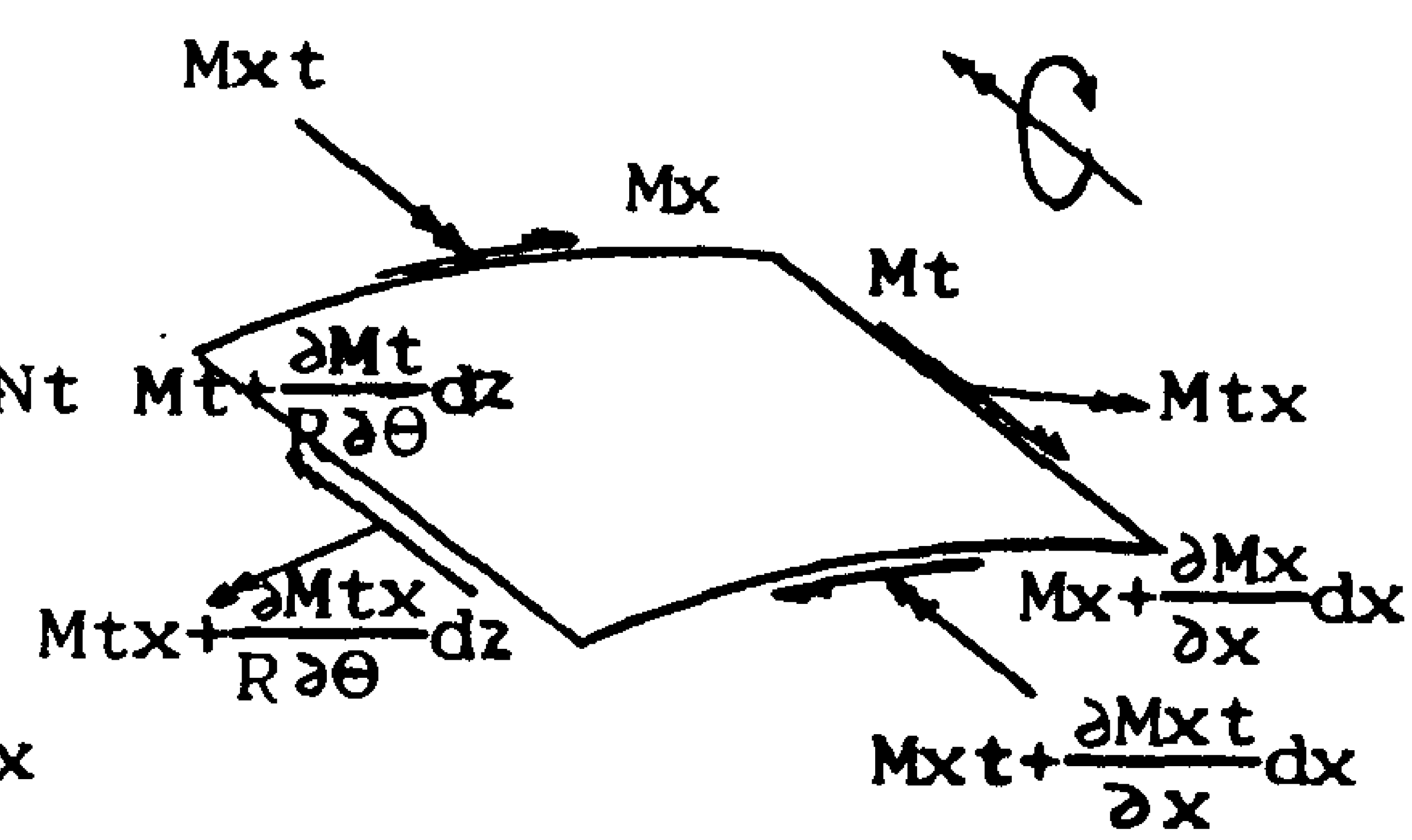

c) Moments

Fig.C.1 Cylindrical Shell Element Coordinates, Displacements and Stress Resultants.

C.2 Strain Functions

The compatibility equation of the thin cylindrical shell theory is

$$\frac{\partial k\theta}{\partial x} - \frac{\partial kx\theta}{\partial z} = 0$$

$$\frac{\partial kx}{\partial z} - \frac{\partial kx\theta}{\partial x} + \frac{1}{R}\left(\frac{\partial \gamma}{\partial x} - \frac{\partial \varepsilon x}{\partial z}\right) = 0$$

$$\frac{kx}{R} + \frac{\partial^2 \varepsilon_\theta}{\partial x^2} + \frac{\partial^2 \varepsilon x}{\partial z^2} - \frac{\partial^2 \gamma}{\partial x \partial z} = 0 \quad \ldots\ldots\ldots\ldots\ldots \quad (C.1)$$

These equation will be satisfied by assuming the relation of strain as follows;

$$\frac{\partial k\theta}{\partial x} = \frac{\partial kx\theta}{\partial z} \quad \ldots\ldots\ldots\ldots\ldots\ldots\ldots\ldots\ldots \quad (C.2.a)$$

$$\frac{\partial kx}{\partial z} = \frac{\partial kx\theta}{\partial x} \quad \ldots\ldots\ldots\ldots\ldots\ldots\ldots\ldots\ldots \quad (C.2.b)$$

$$\frac{\partial \gamma}{\partial x} = \frac{\partial \varepsilon x}{\partial z} \quad \ldots\ldots\ldots\ldots\ldots\ldots\ldots\ldots\ldots \quad (C.2.c)$$

$$\frac{kx}{R} = -\frac{\partial^2 \varepsilon_\theta}{\partial x^2} \quad \ldots\ldots\ldots\ldots\ldots\ldots\ldots\ldots\ldots \quad (C.2.d)$$

Or from the second equation of eq.(C.1), (C.2.b) and (C.2.c) can be altered by following assumption.

$$\frac{\partial kx}{\partial z} - \frac{\partial kx\theta}{\partial x} - \frac{1}{R}\frac{\partial \varepsilon x}{\partial z} = 0 \quad \ldots\ldots\ldots\ldots\ldots\ldots \quad (C.2.e)$$

$$\gamma = \text{constant} \quad \ldots\ldots\ldots\ldots\ldots\ldots\ldots\ldots \quad (C.2.f)$$

The difference between above two assumptions are that the first one produces linearly varying shear strain along the x direction while the second assumption produces the constant strain in the element.

The second assumption is chosen for the present analysis even though it produces the constant shear stress resultants for the all corner nodes, because it gives more satisfactory results than other assumptions from the various tests which were not covered by original paper (see section C.5).

The strian assumptions which is satisfying the eq.(C.2.a), (C.2.d), (C.2.e) and (C.2.f) are chosen as follows:

$$\begin{Bmatrix} \varepsilon_x \\ \varepsilon_\theta \\ \gamma \\ k_x \\ k_\theta \\ k_{x\theta} \end{Bmatrix} = \begin{bmatrix} 1 & \sin\theta & & & & & & & & & & & & \\ & & 1 & x & & \frac{-x^2}{2R} & \frac{-x^3}{6R} & \frac{-x^2\theta}{2R} & \frac{-x^3\theta}{6R} & & & & & \\ & & & & 1 & & & & & & & & & \\ & \frac{\sin\theta}{R} & & & & 1 & x & \theta & x\theta & & & & & \\ & & & & & & & & & 1 & x & \theta & x\theta & \\ & & & & & & & \frac{x}{R} & \frac{x^2}{2R} & & R\theta & & \frac{R\theta^2}{2} & 1 \end{bmatrix} \begin{Bmatrix} a_7 \\ a_8 \\ \cdot \\ \cdot \\ \cdot \\ \cdot \\ \cdot \\ a_{19} \\ a_{20} \end{Bmatrix}$$

$$\qquad \ldots\ldots\ldots\ldots\ldots\ldots\ldots\ldots\ldots \quad (C.3a)$$

or

$$\{\varepsilon\} = [B]\{a\} \qquad \ldots\ldots\ldots\ldots\ldots\ldots \quad (C.3b)$$

in which $\{a\}$ is unknown coefficient vector.

C.3 Displacement Function

Using the strain-displacement relations of the thin shell,

$$
\begin{aligned}
\varepsilon_x &= \frac{\partial u}{\partial x} \\
\varepsilon_\theta &= \frac{\partial v}{\partial z} + \frac{w}{R} \\
\gamma &= \frac{\partial u}{\partial z} + \frac{\partial v}{\partial x} \qquad \text{..............} \quad (C.4) \\
kx &= -\frac{\partial^2 w}{\partial x^2} \\
k\theta &= -\frac{\partial^2 w}{\partial z^2} + \frac{1}{R}\,\frac{v}{z} \\
kx\theta &= -\frac{\partial^2 w}{\partial x \partial z} + \frac{1}{R}\,\frac{\partial v}{\partial x}
\end{aligned}
$$

The polynomial expression of the displacement functions is found using the strain assumptions of eq.(C.3) with coefficient vector $\{a\}$ as;

$$\{u\} = [P]\{a\} \qquad \text{...............} \quad (C.5a)$$

in which

$\{u\} = \lfloor u, w, v, \phi x, \phi z \rceil^T$,

$[P]$ = polynomial matrix of eq.(C.5b) in the next page,

$\phi x = -\frac{\partial w}{\partial z} + \frac{v}{R}$; slope about x axis,

$\phi z = -\frac{\partial w}{\partial x}$; slope about circumferential axis.

The term on column 1 through 6 in the matrix $[P]$ represents the rigid body terms which is found from the eq.(C.4) by the zero strains and curvatures due to rigid body motion.

$$[P] = \begin{array}{cc}
 & \begin{array}{cccccccccccccccccccc} 1 & 2 & 3 & 4 & 5 & 6 & 7 & 8 & 9 & 10 & 11 & 12 & 13 & 14 & 15 & 16 & 17 & 18 & 19 & 20 \end{array} \\
\begin{array}{c} 1 \\ 2 \\ 3 \\ 4 \\ 5 \end{array} &
\begin{bmatrix}
 & R\cos\theta & & R\sin\theta & 1 & & x & x\sin\theta & & & R\cos\theta & & & & & & -\frac{Rz^2}{2} & & -\frac{z^3}{6}+R^2z & -Rz \\
-\cos\theta & -x\cos\theta & -\sin\theta & -x\sin\theta & & & & -\frac{x^2\sin\theta}{2R} & R & Rx & & -\frac{x^2}{2} & -\frac{x^3}{6} & -\frac{x^2\theta}{2} & -\frac{x^3\theta}{6} & -R^2 & -R^2x & -Rz & -Rxz & \\
\sin\theta & x\sin\theta & -\cos\theta & -x\cos\theta & & 1 & & -\frac{x^2\cos\theta}{2R} & & & & & & & & Rz & Rxz & \frac{z^2}{2} & \frac{xz^2}{2}-R^2x & Rx \\
 & & & & & \frac{1}{R} & & & & & & & & \frac{x^2}{2R} & \frac{x^3}{6R} & z & xz & R+\frac{z}{2R} & \frac{xz^2}{2R} & x \\
 & \cos\theta & & \sin\theta & & & & \frac{x\sin\theta}{R} & & -R & & x & \frac{x^2}{2} & x\theta & \frac{x^2\theta}{2} & & R^2 & & -R^2\theta &
\end{bmatrix}
\end{array} \quad \cdots\cdots\cdots\cdots\cdots(C.5b)$$

in which $z=R\theta$

The generalized displacement $\{u_e\}$ is represented by the transformation matrix $[C]$ which is defined by putting appropriate corner node coordinates to the polynomial matrix $[P]$ as follow;

$$\{u_e\} = [C]\{a\} \qquad \ldots\ldots\ldots\ldots\ldots\ldots\ldots \qquad (C.6)$$

From the Novozhilov's theory (Ref.75), the variational change of strain energy is

$$\begin{aligned}\delta U &= \iint [N_x \delta\varepsilon_x + N_\theta \delta\varepsilon_\theta + N_{x\theta}\delta\gamma + M_x \delta k_x + M_\theta \delta k_\theta + 2M_{x\theta}\delta k_{x\theta}]\, dxdz \\ &= \iint [\{N\}^T\{\delta\varepsilon\}]\ dxdz \\ &= \iint [\{\varepsilon\}^T[D]\{\delta\varepsilon\}]\ dxdz \qquad \ldots\ldots\ldots\ldots \qquad (C.7)\end{aligned}$$

in which

$\{N\}$ is stress resultant vector,

$[D]$ is the following constituitive relation matrix of the thin shell;

$$[D] = \begin{bmatrix} C & C\nu & & \frac{D}{R} & & \\ C\nu & C & & & -\frac{D}{R} & \\ & & \frac{1-\nu}{2}C & & & -\frac{1-\nu}{2}\frac{D}{R} \\ \frac{D}{R} & & & D & D\nu & \\ & -\frac{D}{R} & & D\nu & D & \\ & & -\frac{1-\nu}{2}\frac{D}{R} & & & 2(1-\nu)D \end{bmatrix}$$

$$\ldots\ldots\ldots\ldots\ldots\ldots\ldots\ldots\ldots\ldots \qquad (C.7a)$$

$C = Et/(1-\nu^2)$ $\qquad\qquad$ $D = Et^3/12(1-\nu^2)$

C.4 Shell Element Matrices

From the eq.(C.6) and eq.(C.7), the stiffness matrix of shell element which is relating the generalized forces and displacements can be expressed as follow;

$$\{F\} = [K]\{u_e\} \quad \ldots\ldots\ldots\ldots\ldots\ldots\ldots \quad (C.8a)$$

$$[K] = [C]^{-T}\iint[B]^T[D][B]dxdz\,[C]^{-1} \quad \ldots\ldots \quad (C.8b)$$

Integration of $\iint[B]^T[D][B]dxdz$ is given in eq.(C.8c) explicitly, in which only the elastic terms are remaining.

The stress matrix $[S]$ of shell element at node, i, is found from the eq.(C3b) and eq.(C.6), as follow;

$$[S_i] = [D]\left[B(x_i, z_i)\right][C]^{-1}\{u_e\} \quad \ldots\ldots\ldots \quad (C.9)$$

The consistent inertia load matrix $\{F_g\}$ due to 1 g acceleration in the global Y direction can be represented as

$$\{F_g\}=$$

$$\rho t \lfloor aR\cos\varphi\sin\beta,\ 0,\ -aR\sin\varphi\sin\beta,\ 0,\ 0,$$

$$2aR\sin\varphi\sin\frac{\beta}{2},\ 0,\ -\frac{a^3}{24}\sin\varphi\sin\beta,\ -2aR^2\cos\varphi\cos\frac{\beta}{2},\ 0,$$

$$0,\ \frac{Ra^3}{12}\cos\varphi\cos\frac{\beta}{2},\ 0,\ \frac{Ra^3}{24}\sin\frac{\beta}{2}(\beta\cos\varphi-\sin\varphi),\ 0,$$

$$2aR^3\sin\varphi\sin\frac{\beta}{2},\ aR^3\sin\frac{\beta}{2}(\beta\cos\varphi-\sin\varphi),\ 0,\ 0,\ 0\rfloor^T$$

$$\ldots\ldots\ldots\ldots\ldots\ldots\ldots\ldots\ldots\ldots\ldots \quad (C.10)$$

The integration required for stiffness matrix calculation

$$\iint [B]^T[D][B]\,dxdz =$$

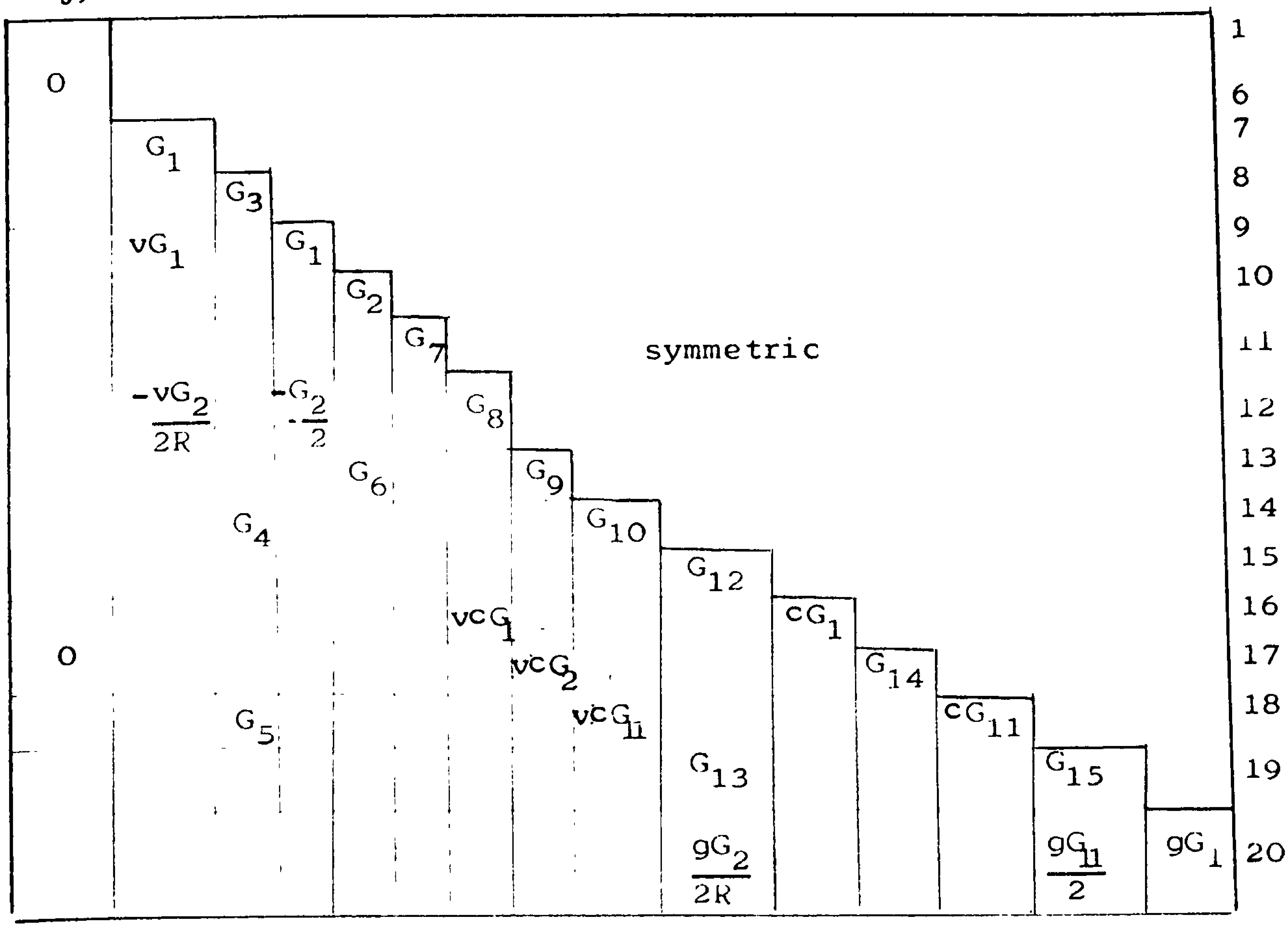

.... (C,8c)

in which

$$G_1 = ab,\quad G_2 = \frac{a^3b}{12},\quad G_3 = \frac{aR}{2}\left(1+\frac{c}{R}\right)(\beta - \sin\beta)$$

$$G_4 = a\left(c - \frac{a^2}{24}\right)\left(2\sin\frac{\beta}{2} - \beta\cos\frac{\beta}{2}\right),\quad G_5 = ac\left(2\sin\frac{\beta}{2} - \beta\cos\frac{\beta}{2}\right)$$

$$G_6 = -\frac{a^5b}{480R},\quad G_7 = \frac{1-\nu}{2}ab,\quad G_8 = \frac{a^5b}{320R} + c\,ab$$

$$G_9 = \frac{a^7b}{16128R} + \frac{ca^3b}{12},\quad G_{10} = \frac{a^5b^3}{3840R} + \frac{cab^3}{12R} + \frac{ca^3b}{12R}$$

$$G_{11} = \frac{ab^3}{12R},\quad G_{12} = \frac{a^7b^3}{193536R} + \frac{ca^3b^3}{144R} + \frac{ga^5b}{320R}$$

$$G_{13} = \frac{ca^3b^3}{144R}\left(\frac{1+\nu}{2}\right),\quad G_{14} = \frac{ab}{12}(ca^2 + gR^2\beta^2),\quad G_{15} = \frac{ca^3b^3}{144R} + \frac{gab^5}{320R}$$

and $g = 2(1-\nu)c^2$, $c = \frac{t^2}{12}$.

in which ρ ; specific weight per unit volume of material (lb/in^3),

φ ; angle measured from global Y axis to the geometric centre of the element, O in Fig.C.1, in the circumferential direction,

β ; arc angle of the element (=2),

a ; the length along the straight line of element.

C.5 Element Test

In References 50 and 51, the convergency and accuracy of the strain element have been demonstrated for the displacement solutions for the free end pinched shell and barrel vault problems. But they do not show the accuracies in the stress distributions. The stress distributions in the pinched shell with the end diaphragms and the simply supported vault structures are examined by comparison with the hybrid element in Ref.47 and the isoparametric facet shell element in PAFEC 75.

The 4 x 4 elements model for the quadrant or octant of shell structure is used. In use of the isoparametric element in PAFEC, eight noded element formulation is used.

C.5.1 Pinched Shell with End Constraints

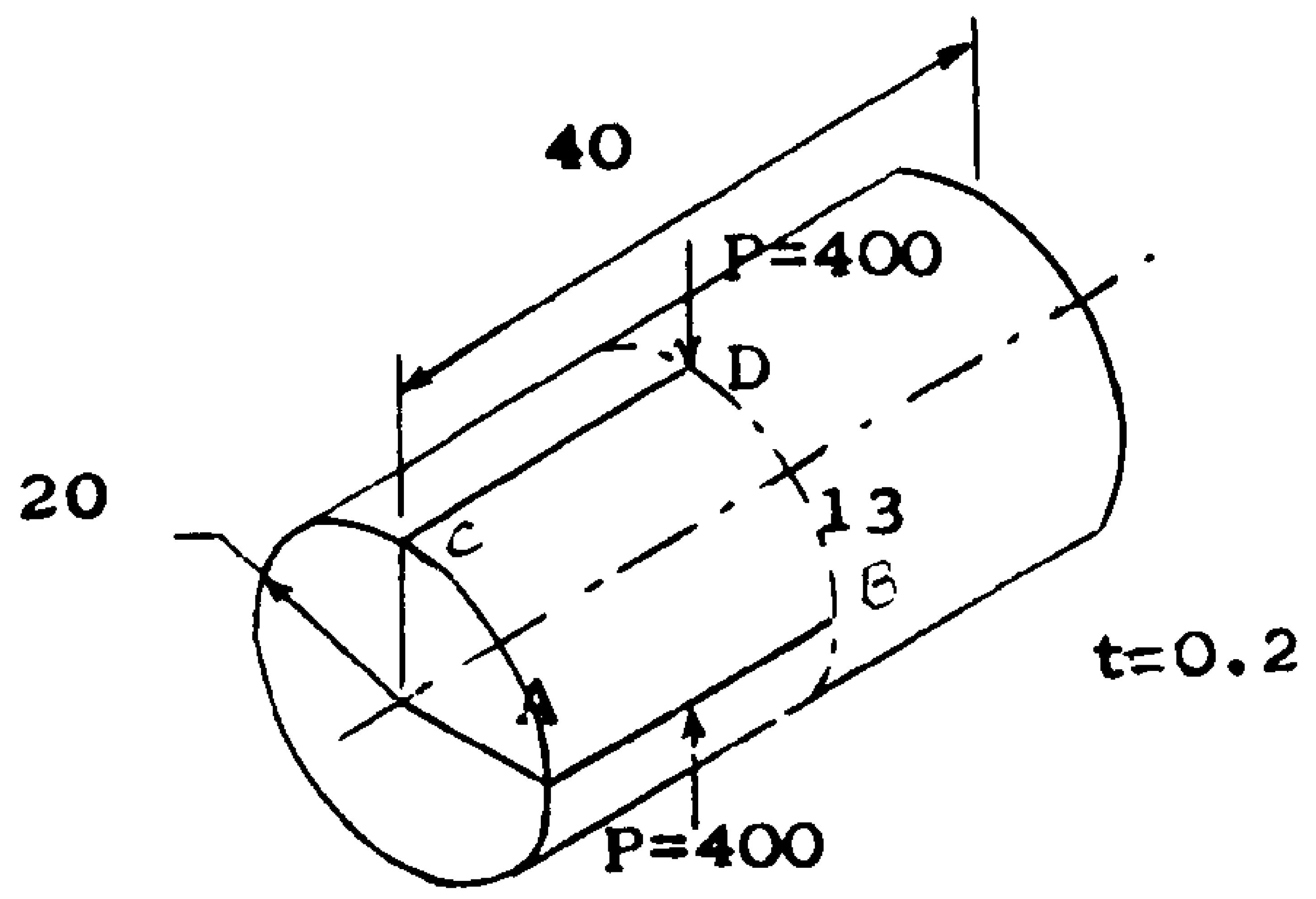

$E=30\times10^6$ psi

$\nu=0.3$

4 x 4 mesh

Exact solution; Ref. 9 & 47

Fig.C.2 Simply Supported Pinched Shell.

1) Radial Displacement along C-D

w x1000 inch

X	0	5.0	10.0	15	20
Exact	0	-1.88	-3.31	-6.90	-10.66
PAFEC 8 Noded	0	-1.91	-3.85	-5.79	-7.22
Strain Element	0	-2.13	-4.46	-7.00	-10.02
Hybrid Element	0	-2.49	-5.0	-6.95	-8.37

2) Axial Stress Resultant Nx

X	0	5.0	10.0	15	20
Exact	0	-12.8	-19.6	-44.3	-126.
PAFEC 8 Noded	0	-12.3	-28.1	-62.7	-144.8
Strain Element	-5.33	-13.6	-36.5	-68.7	-86.4
Hybrid Element	0	-12.3	-22.8	-57.0	-66.4

3) Shear Stress Resultant along C-A Nxt

X	0	5	10.0	15.0	20.0
Exact	0	-11.3	- 2.2	3.0	0
PAFEC 8 Noded	0	-5.83	-2.9	-2.1	0
Strain Element	0	- 9.2	- 5.2	- 3.2	0
Hybrid Element	0	-10.3	- 2.2	3.0	0

C.5.2 Simply-Supported Pannel and Uniform Pressure

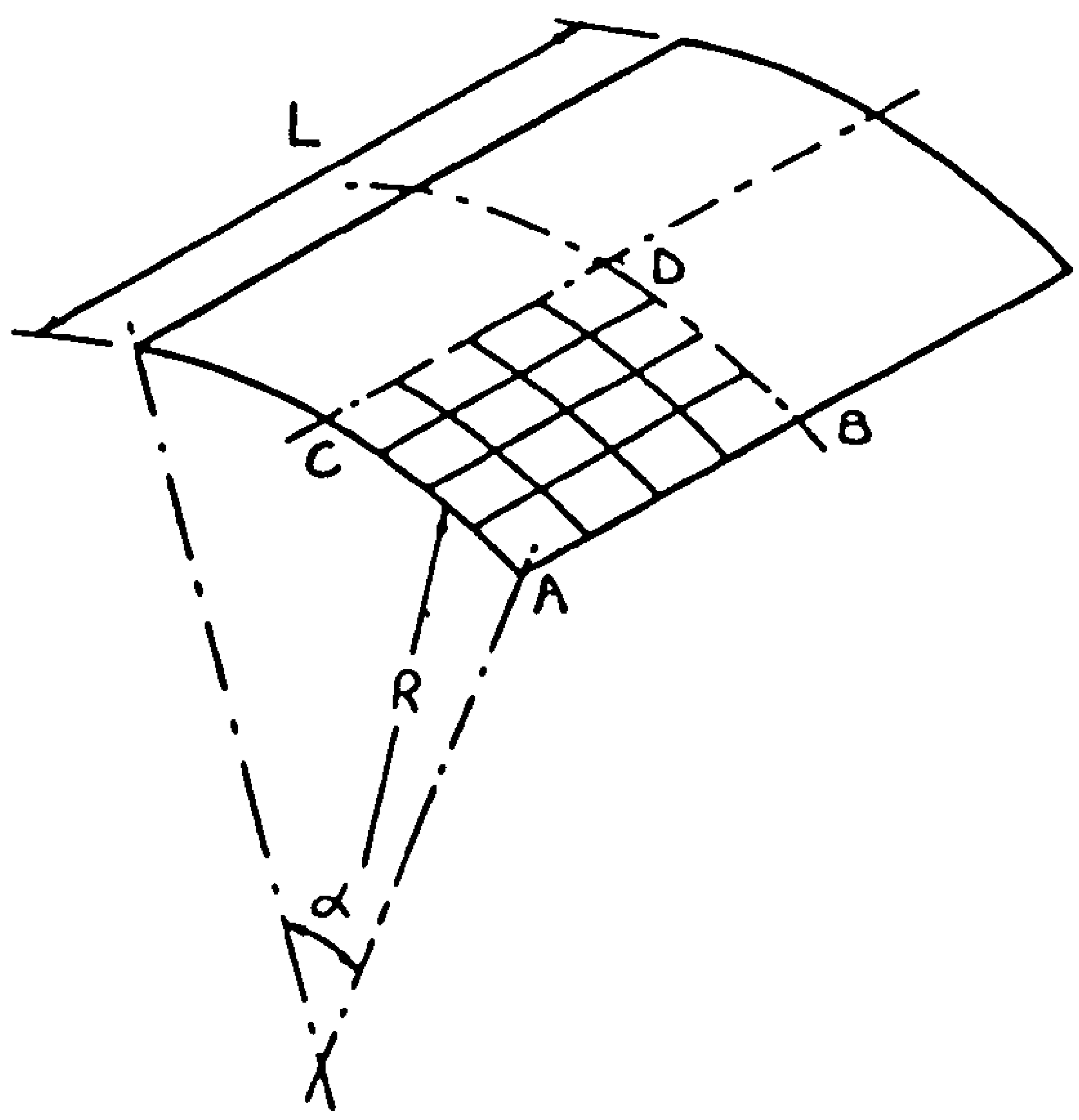

$E=30 \times 10^6$ psi

=0.3

R=20 in

t=0.2 in

4 x 4 mesh

Exact solution; Ref. 9&47

Fig.C.3 Simply supported Vault.

1) Radical Displacement along C-D

w x1000

X	0	5	10	15	20
Exact	0	-1.27	-1.94	-2.29	-2.42
PAFEC 8 Noded	0	-1.23	-2.35	-3.08	-3.35
4 Noded Strain	0	-1.64	-2.55	-3.12	-3.46
Hybrid Element	-	-	-	-	-

2) Axial Stress along C-D

X	0	5	10	15	20
Exact	0	80.	142.1	184	198
PAFEC 8 Noded	0.1	59.	145.	232.	338.
4 Noded Strain	10.8	100.	178.	220.	249.
Hybrid	43.	76.	120.	170.	195.

3) Shear Stress along C-D

X	0	5	10	15	20
Exact	–	–	–	–	–
PAFEC 8 Noded	15.0	16.7	6.5	8.6	9.7
4 Noded Strain	25.7	23.0	16.8	9.2	2.6
Hybrid	–	–	–	–	–

APPENDIX D

THIN-WALLED CURVED BEAM FINITE ELEMENT

D.1 Introduction

For the finite element idealization of the stiffeners, a thin-walled curved beam element is formulated by using Cheney's thin-walled open section ring frame analysis (Ref.85) which solved for the buckling problem of a ring frame by the harmonic analysis.

The exact solution of the governing equations of the thin-walled curved beam is found for the strain components and displacement function as in the formulation of the shell strain element. Since the exact solution of the beam equations has been used for the displacement assumption, the size of the element mesh does not affect the beam's structural behaviour. The effect of shear centre-centroid offset and dislocation of ring-shell connection are allowed to represent discrete stiffener, while the warping of beam cross section is neglected.

It is assumed that the shear deformation and torsion due to the distortion of the cross section of the beam during deformation are negligible. Fig.D.1 shows the coordinates and deformation components used in the formulation. r_s and r_c are the curvature of the beam shear centre and centroid respectively, and x_c and y_c represent the shear centre-centroid offset in the normal and radial direction.

As a special case of the curved beam element, a straight beam element has been derived from the curved element using the infinite curvature. This straight beam element has been used for the representation of the longitudinal stringers.

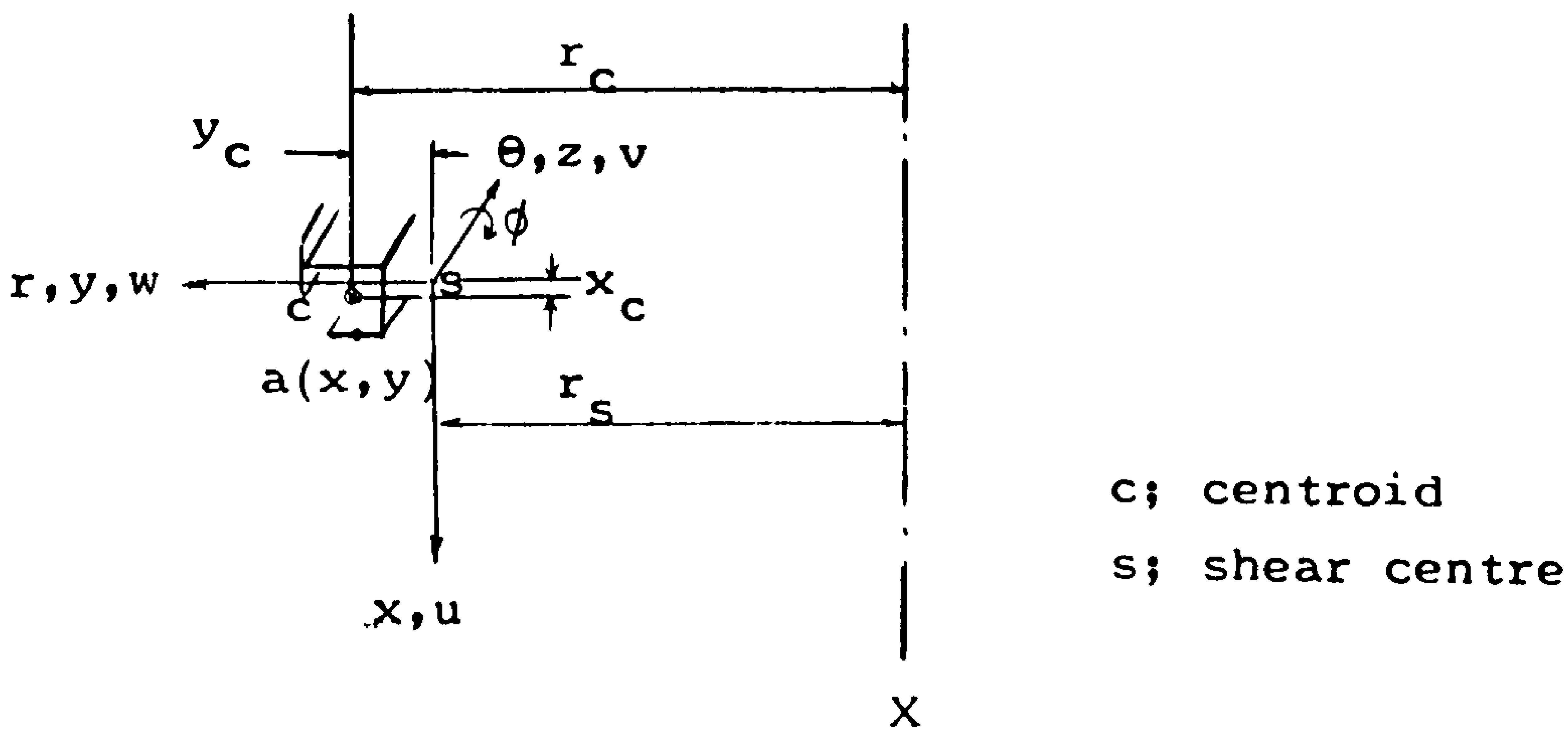

Fig.D.1. Geometry of curved beam cross section.

D.2 Geometric Relations and Displacements

The displacements in the normal, radial and circumferential directions, (u_a, w_a, v_a), of an arbitrary point a(x, y) on the middle surface of the beam cross section, due to shear centre displacements (u, w, v) and a rotation ϕ without warping, become

$$u_a = u - y\phi \qquad \text{(D.1)}$$

$$w_a = w + x\phi \qquad \text{(D.2)}$$

$$v_a = v + y\left(\frac{v}{r_s} - \frac{dw}{dz} \right) - x\,\frac{du}{dz} \qquad \text{(D.3)}$$

in which the second and third terms of the tangential displacement, v_a, represent the effect of the change in the slope of the tangent to the centroidal axis due to the radial and normal displacements respectively.

The normal strain at this point due to the change in the circumferential displacement and the radial displacement is then as it is in the shell:

$$\varepsilon_a = \frac{r_s}{r_s+y}\ \frac{dV_a}{dz} + \frac{w_a}{r_s+y} \quad \ldots\ldots\ldots\ldots\ldots \quad (D.4)$$

Substituting eq.(D.2) and eq.(D.3) into eq.(D.4), ε_a becomes

$$\varepsilon_a = \frac{dv}{dz} - \frac{r_s y}{r_s+y}\ \frac{d^2w}{dz^2} - \frac{r_s x}{r_s+y}\ \frac{d^2u}{dz^2} + \frac{w}{r_s+y} + \frac{x\phi}{r_s+y} \quad \ldots \quad (D.5)$$

From eq.(D.5) with $x=x_c$ and $y=y_c$ the normal strain at the centroid ε_o will be

$$\varepsilon_o = \frac{dv}{dz} - \frac{r_s y_c}{r_c}\ \frac{d^2w}{dz^2} - \frac{r_s x_c}{r_c}\ \frac{d^2u}{dz^2} + \frac{w}{r_c} + \frac{x_c}{r_c} \quad \ldots \quad (D.6)$$

in which $r_c = r_s + y_c$ $\quad \ldots\ldots\ldots\ldots\ldots\ldots \quad$ (D.7)

And expanding $\dfrac{1}{r_s+y}$ in series form and dropping higher order terms, eq.(D.5) becomes

$$\varepsilon_a = \frac{dv}{dz} - y\frac{d^2w}{dz^2} - x\frac{d^2u}{dz^2} + \frac{w}{r_s}\left(1-\frac{y}{r_s}\right) + \frac{x\phi}{r_s} \quad \ldots\ldots \quad (D.8)$$

Substituting eq.(D.6) into eq.(D.8), and expanding

$\dfrac{1}{r_c} = \dfrac{1}{r_s+y_c}$ as a series, gives

$$\varepsilon_a = \varepsilon_o - (y-y_c)\left(\frac{d^2w}{dz^2} + \frac{w}{r_s^2}\right) - (x-x_c)\left(\frac{d^2u}{dz^2} - \frac{\phi}{r_s}\right)$$

$$= \varepsilon_o + (y-y_c)kx - (x-x_c)ky \qquad \text{.........} \qquad (D.9)$$

in which kx and ky represent the curvature of the beam about the normal and radial axes respectively which are defined as follows;

$$kx = -\frac{d^2w}{dz^2} - \frac{w}{r_s^2} \qquad \text{.................} \qquad (D.10)$$

$$ky = \frac{d^2u}{dz^2} - \frac{\phi}{r_s} \qquad \text{..................} \qquad (D.11)$$

The normal strain at a(x, y) is now given in terms of the normal strain at the centroid and the curvatures of the shear centre. The next section will use this result to calculate the normal force and the bending moments.

The angle of twist per unit length along the circumference β due to the torsion of curved beam without warping is found from Ref.85 to be

$$\beta = \frac{d\phi}{dz} + \frac{1}{r_s}\frac{du}{dz} \qquad \text{.....................} \qquad (D.12)$$

D.3 Stress Resultants

From the fundamental elastic law, the normal stress, σ_a at a point a(x,y) is found to be:

$$\sigma_a = E\,\varepsilon_a = E\left[\varepsilon_o + (y-y_c)kx - (x-x_c)k_y\right] \quad \ldots \text{(D.15)}$$

The normal stress resultant N_z on the cross section of the beam element and the bending moments M_x and M_y are obtained by integration of σ_a over the total cross section area;

$$N_z = \iint \sigma_a \, dxdy = E\,\varepsilon_o A \quad \ldots\ldots\ldots\ldots\ldots\ldots \text{(D.16)}$$

$$M_x = \iint \sigma_a (y-y_c) \, dxdy = E(\, I_x k_x - I_{xy} k_y \,) \quad \ldots\ldots \text{(D.17)}$$

$$M_y = \iint \sigma_a (x-x_c) \, dxdy = E(I_{xy} k_x - I_y \, k_y \,) \quad \ldots\ldots \text{(D.18)}$$

in which

A = total cross section area of beam element,
I = second moments of inertia which are defined from the definition of the centroid;

$$I_x = \iint (y-y_c)^2 dxdy,$$

$$I_y = \iint (x-x_c)^2 dxdy,$$

$$I_{xy} = I_{yx} = \iint (x-x_c)(y-y_c)dxdy,$$

and $\iint x \; dxdy = \iint y \; dxdy = 0.$

The Saint-Venant torsion about the shear centre of a curved beam element is:

$$M_z = GJ\beta = GJ\left(\frac{d\phi}{dz} + \frac{1}{r_s}\frac{du}{dz} \right) \quad \ldots\ldots\ldots\ldots\ldots \text{(D.19a)}$$

where J is usual Saint-Venant torsional constant which is given approximately as follow:

$$J = \frac{1}{3}\sum b_i t_i^3 \quad \text{for a thin walled beam,} \quad \text{..... (D.19b)}$$

$$= \iint (x^2 + y^2)\,dxdy \quad \text{for a solid beam,} \quad \text{..... (D.19c)}$$

and shear modulus $G = \frac{E}{2(1+\nu)}$ .... (D.19d)

b ; flange width,

t ; flange thickness of thin walled beam.

The stress resultants-strain relationship of the curved beam element has the following usual type of constituitive equation:

$$\begin{Bmatrix} N_z \\ M_x \\ M_y \\ M_z \end{Bmatrix} = E \begin{bmatrix} A & & & \\ & I_x & -I_{xy} & \\ & -I_{xy} & I_y & \\ & & & \frac{J}{2(1+\nu)} \end{bmatrix} \begin{Bmatrix} \varepsilon_o \\ k_x \\ k_y \\ \beta \end{Bmatrix}$$

.... (D.20)

or

$$\{N\} = E\,[D]\,\{\varepsilon\} \quad \text{.............................. (D.21)}$$

D.4 Governing Equations

As shown on Fig D.2, it is assumed that all internal (or external) loads are applied through the shear centre, while the normal force N_z acts along the centroid.

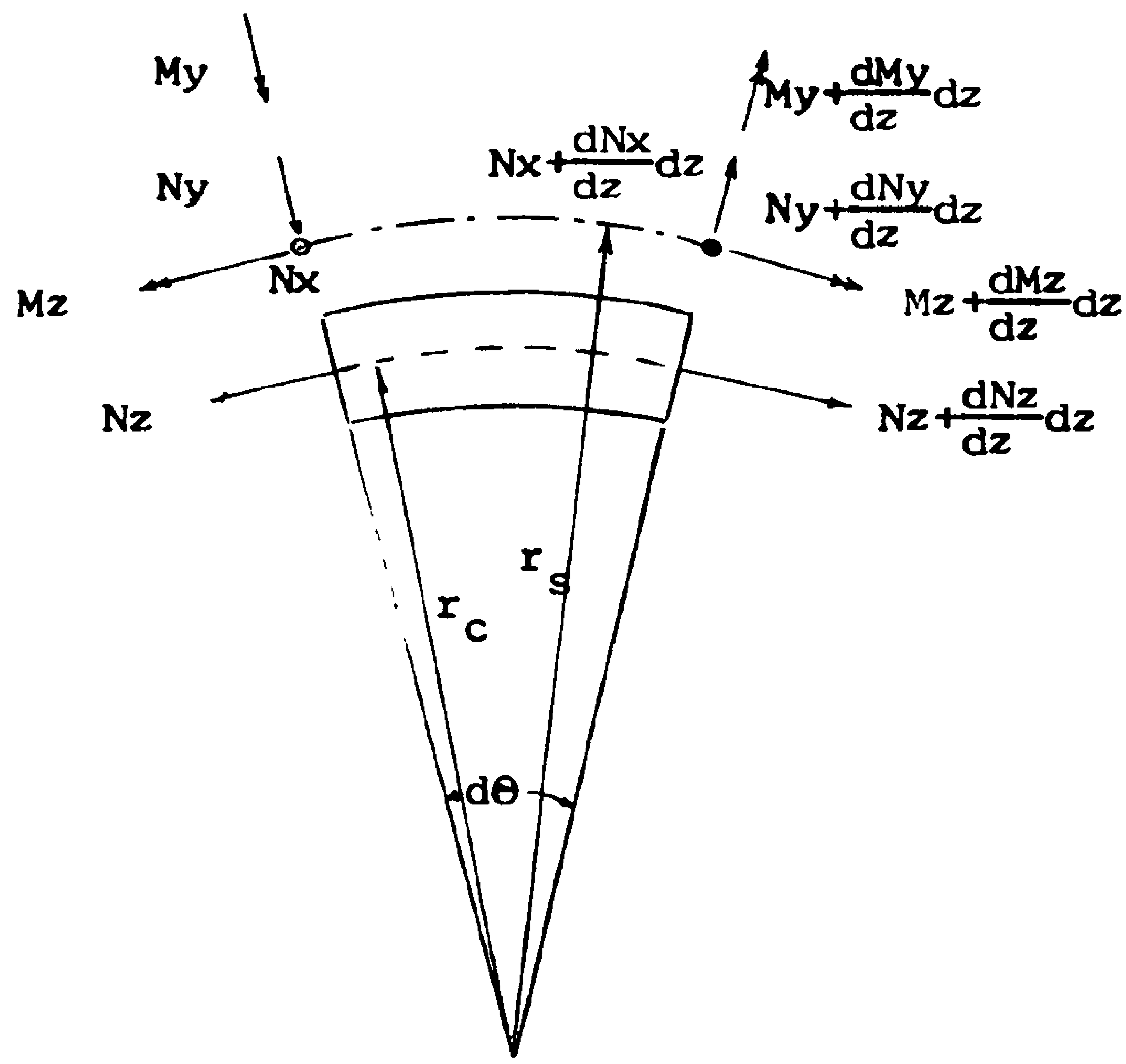

Fig.D.2. Forces in the curved beam element.

The homogeneous governing equilibrium equations of the forces and the moments are

$$\frac{Nz}{r_s} + \frac{d^2Mx}{dz^2} - y_c \frac{d^2Nz}{dz^2} = 0 \quad \ldots\ldots\ldots\ldots\ldots \quad (D.22a)$$

$$\frac{dMz}{dz} - r_s \frac{d^2My}{dz^2} + r_s x_c \frac{d^2Nz}{dz^2} = 0 \quad \ldots\ldots\ldots\ldots \quad (D.22b)$$

$$\frac{dNz}{dz} - \frac{1}{r_c} \frac{dMx}{dz} = 0 \quad \ldots\ldots\ldots\ldots\ldots\ldots\ldots \quad (D.22c)$$

$$\frac{dMz}{dz} + \frac{1}{r_s}(My - x_c Nz) = 0 \quad \ldots\ldots\ldots\ldots\ldots\ldots \quad (D22.d)$$

Substituting eq.(D.22c) into eq.(D.22d) and recalling eq.(D.6) the differential equation of $\mathcal{E}_o$ is found to be

$$\frac{d^2\mathcal{E}_o}{dz^2} + \delta^2\mathcal{E}_o = 0 \quad \ldots\ldots\ldots\ldots\ldots\ldots \quad (D.23)$$

in which $\delta = \frac{1}{r_s}$ .... (D.24)

The general solution of this equation is

$$\mathcal{E}_o = a_1\cos\delta z + a_2\sin\delta z$$

$$= a_1\cos\Theta + a_2\sin\Theta \quad \ldots\ldots\ldots\ldots \quad (D.25)$$

where Θ is the arc angle along the shear centre, relates to the circumferential coordinate z by $z = r_s\Theta$.

From the eq.(D.22b), eq.(D.22d), and eq.(D.19a),

$$\frac{d^3Mz}{dz^3} + \frac{1}{r_s}\frac{dMz}{dz} = 0 \quad \ldots\ldots\ldots\ldots\ldots\ldots \quad (D.26a)$$

$$\frac{d}{dz}\left(\frac{d^2\phi}{dz^2} + \frac{\phi}{r_s^2}\right) = 0 \quad \ldots\ldots\ldots\ldots\ldots\ldots \quad (D.26b)$$

eq.(D.26b) has a solution of the form

$$\phi = a_4\cos\Theta + a_5\sin\Theta + a_6 \quad \ldots\ldots\ldots\ldots \quad (D.27)$$

Substituting the solution for $\mathcal{E}_o$ and ϕ into eq.(D.10) and eq.(D.11) gives

$$I_xk_x - I_{xy}k_y = r_cA(a_1\cos\Theta + a_2\sin\Theta) + a_3 \quad (D.28a)$$

$$-I_{xy}k_x + I_yk_y = x_cA(a_1\cos\Theta + a_2\sin\Theta)$$

$$+ J'(a_4\sin\Theta - a_5\cos\Theta) \quad \ldots\ldots \quad (D.28b)$$

in which $J' = \frac{J}{2(1+\nu)}$

Then the solutions for k_x and k_y are

$$kx = G_1(a_1\cos\theta + a_2\sin\theta) + G_2a_3 + G_3(a_4\sin\theta - a_5\cos\theta) \quad \text{.............. (D.29)}$$

$$ky = G_4(a_1\cos\theta + a_2\sin\theta) + G_5a_3 + G_6(a_4\sin\theta - a_5\cos\theta) \quad \text{.............. (D.30)}$$

where

$G_1 = Go(r_cIy + x_cIxy)A$

$G_2 = Go\ Iy$

$G_3 = Go\ J'\ Ixy$

$G_4 = Go(r_cIxy + x_cIx)\ A$

$G_5 = Go\ Ixy$

$G_6 = Go\ J'\ Ix$

and $$Go = \frac{1}{Ix\ Iy - Ixy^2} \quad \text{..................... (D.31)}$$

The solutions for the normal strain and the curvatures can now be written in the form of

$$\begin{Bmatrix} \varepsilon_o \\ kx \\ ky \\ \phi \end{Bmatrix} = \begin{bmatrix} \cos\theta & \sin\theta & & & & \\ G_1\cos\theta & G_1\sin\theta & G_2 & G_3\sin\theta & -G_3\cos\theta & \\ G_4\cos\theta & G_4\sin\theta & G_5 & G_6\sin\theta & -G_6\cos\theta & \\ & & & \cos\theta & \sin\theta & 1 \end{bmatrix} \begin{Bmatrix} a_1 \\ a_2 \\ a_3 \\ a_4 \\ a_5 \\ a_6 \end{Bmatrix}$$

$$\text{..................... (D.32a)}$$

or

$$\{\varepsilon\} = [B]\{a\} \quad \text{................................... (D.32b)}$$

The displacement solution will be found from these strain and curvature solutions using the strain-displacement relation of eq.(D.6) and eq.(D.10) to eq.(D.12).

D.5 Displacement Solutions.

Substituting eq.(D.32) into eq.(D.10) - eq.(D.12), and rearranging the differential equations of radial displacement, rotation about shear centre and normal displacement becom

$$\frac{d^2w}{d\theta^2} + w = - r_s^2\, kx$$
$$= - r_s^2 \left\{ G_1(a_1\cos\theta + a_2\sin\theta) + G_2a_3 + G_3(a_4\sin\theta - a_5\cos\theta)\right\} \quad \text{.......(D.33a)}$$

$$\frac{d^2\phi}{d\theta^2} + \phi = r_s\left(\frac{d\beta}{d\theta} - ky \right)$$
$$= - r_s \left\{ G_4(a_1\cos\theta + a_2\sin\theta) + G_5a_3 + (G_6 + 1)(a_4\sin\theta - a_5\cos\theta)\right\} \quad \text{..(D.33b)}$$

$$u = r_s^2\int\beta d\theta - r_s\,\phi + \text{constant} \quad \text{...............(D.33c)}$$

The general solutions of these differential equations are

$$w = -\frac{1}{2} r_s^2 \left\{ G_1\theta (a_1\sin\theta - a_2\cos\theta) + 2G_2a_3 - G_3\theta (a_4\cos\theta + a_5\sin\theta)\right\} + a_7\cos\theta + a_8\sin\theta \quad \text{...............(D.34a)}$$

$$\phi = -\frac{1}{2} r_s^2 \left\{ G_4\theta (a_1\sin\theta - a_2\cos\theta) + 2G_5a_3 - (G_6+1)\theta (a_4\cos\theta + a_5\sin\theta)\right\} + a_{10}\cos\theta + a_{11}\sin\theta \quad \text{................(D.34b)}$$

$$u = \frac{1}{2} r_s^2 G_4\theta(a_1\sin\theta - a_2\cos\theta) + r_s^2 G_5a_3 + r_s^2 \left\{ a_4(\sin\theta - G_7\theta \cos\theta) - a_5(\cos\theta - G_7\theta \sin\theta)\right\} + r_s^2\, \theta\, a_6 - r_s(a_{10}\cos\theta + a_{11}\sin\theta) + a_{12} \quad \text{................(D.34c)}$$

in which $G_7 = \dfrac{G_6 + 1}{2}$.

Now from eq.(D.6), eq.(D.10) and eq.(D.11), the differential equation of tangential displacement ,v, can be found to be

$$\frac{dv}{d\theta} = r_s\,\mathcal{E}_o + \frac{d^2w}{d\theta^2} + \frac{1}{r_c}r_s^3\,kx + \frac{1}{r_c}r_s^2\,x_c\,ky \qquad \text{.........(D.35)}$$

The general solution for which is

$$\begin{aligned} v = {} & (G_8\sin\theta - \tfrac{1}{2}\,G_1r_s^2\,\theta\cos\theta)a_1 - (G_8\cos\theta + \tfrac{1}{2}\,G_1r_s^2\,\theta\sin\theta)a_2 \\ & + G_9\theta a_3 - (G_{10}\cos\theta - \tfrac{1}{2}\,G_3r_s^2\,\theta\sin\theta)a_4 \\ & - (G_{10}\sin\theta + \tfrac{1}{2}\,G_3r_s^2\,\theta\cos\theta)a_5 - a_7\sin\theta + a_8\cos\theta \\ & + a_9 \qquad \text{..............................(D.36)} \end{aligned}$$

where

$$\begin{aligned} G_8 &= r_s - \left(\tfrac{1}{2}\,G1 - \frac{r_s^2}{r_c}G_1 + \frac{x_c}{r_c}G_4\right)r_s^2 \\ G_9 &= \frac{1}{r_c}\left(r_sG_2 + x_cG_5\right)r_s^2 \\ G_{10} &= \frac{1}{r_c}\left(\tfrac{1}{2}r_cG_3 + r_sG_3 + x_cG_6\right)r_s^2 \qquad \text{...............(D.37)} \end{aligned}$$

From these displacement solutions, the rotations about the normal axis ϕ_x and the radial axis ϕ_y become

$$\begin{aligned} \phi_x &= -\frac{dw}{dz} + \frac{v}{r_s} \\ &= G_{11}(a_1\sin\theta - a_2\cos\theta) + \frac{1}{r_s}G_8\theta a_3 \\ &\quad -G_{12}(a_5\cos\theta + a_6\sin\theta) + \frac{1}{r_s}a_9 \qquad \text{.............(D.38)} \end{aligned}$$

$$\begin{aligned} \phi_y &= \frac{du}{dz} \\ &= \tfrac{1}{2}\,r_sG_4\left\{(\theta\cos\theta + \sin\theta)a_1 + (\theta\sin\theta - \cos\theta)a_2\right\} \\ &\quad +(r_sG_7\theta\sin\theta - G_{13}\cos\theta)a_4 - (r_sG_7\theta\cos\theta + G_{13}\sin\theta)a_5 \\ &\quad + r_s\theta a_6 + a_{10}\sin\theta - a_{11}\cos\theta \qquad \text{.............(D.39)} \end{aligned}$$

in which new constants are defined as

$$G_{11} = 1. + \frac{1}{r_c} r_s (r_s G_1 + x_c G_4)$$

$$G_{12} = \frac{1}{r_c} r_s (r_s G_3 + x_c G_6)$$

$$G_{13} = \frac{1}{2} r_s (G_6 - 1) \qquad \text{(D.40)}$$

Collecting the solutions, the matrix equation which relates the displacements to their unknown coefficients is

$$\{u\} = [P]\{a\} \qquad \text{(D.41)}$$

where matrix $[P]$ is given in Table.D.1.

Then generalized displacements equation can be written as

$$\{u_e\} = [C]\{a\} \qquad \text{(D.42)}$$

in which

$$\{u_e\} = \lfloor u_1, w_1, v_1, \phi_{x1}, \phi_{y1}, u_2, w_2, v_2, \phi_{x2}, \phi_{y2} \rceil^T \qquad \text{(D.42a)}$$

$[C]$; shape function matrix which is obtained by substituting the appropriate nodal coordinates of the end nodes into matrix $[P]$. Suffices 1 and 2 represent the end nodes.

The unknown coefficients $\{a\}$ and displacements $\{u\}$, can now be defined by the generalized displacements $\{u_e\}$ in the usual manner.

$$\{a\} = [C]^{-1}\{u_e\} \qquad \text{(D.43)}$$

$$\{u\} = [P][C]^{-1}\{u_e\} \qquad \text{(D.44)}$$

$$[P] =$$

$$
\begin{array}{cccccccccccc}
1 & 22 & 3 & 4 & 5 & 6 & 7 & 8 & 9 & 10 & 11 & 12 \\
\end{array}
$$

$$
\left[
\begin{array}{c|c|c|c|c|c|c|c|c|c|c|c}
G_{14}\theta\sin\theta & -G_{14}\theta\sin\theta & r_s^2 G_5 & r_s^2(\sin\theta - G_{17}\theta\cos\theta) & -r_s^2(\cos\theta + G_{17}\theta\sin\theta) & r_s^2 & & & & -r_s\cos\theta & -r_s\sin\theta & 1 \\
\hline
-G_{15}\theta\sin\theta & G_{15}\theta\cos\theta & r_s^2 G_2 & G_{16}\theta\cos\theta & G_{16}\theta\sin\theta & & \cos\theta & \sin\theta & & & & \\
\hline
G_8\sin\theta - G_{15}\theta\cos\theta & -G_8\cos\theta - G_{15}\theta\sin\theta & G_9\theta & -G_{10}\cos\theta + G_{16}\theta\sin\theta & -G_{10}\sin\theta - G_{16}\theta\cos\theta & & -\sin\theta & \cos\theta & 1 & & & \\
\hline
-G_{17}\theta\sin\theta & G_{17}\theta\cos\theta & -r_s G_5 & r_s G_7\theta\cos\theta & r_s G_7\theta\sin\theta & & & & & \cos\theta & \sin\theta & \\
\hline
G_{11}\sin\theta & -G_{11}\cos\theta & \frac{G_8}{r_s}\cdot\theta & -G_{12}\cos\theta & -G_{12}\sin\theta & & & & \frac{1}{r_s} & & & \\
\hline
G_{17}(\theta\cos\theta + \sin\theta) & G_{17}(\theta\sin\theta - \cos\theta) & & r_s G_7\theta\sin\theta - G_{13}\cos\theta & -r_s G_7\theta\cos\theta - G_{13}\sin\theta & r_s & & & & \sin\theta & \cos\theta &
\end{array}
\right]
\quad \ldots\ldots\ldots\ldots\ldots\ldots (D.41a)
$$

where $G_{14} = \frac{1}{2} r_s^2 G_4$, $G_{15} = \frac{1}{2} r_s^2 G_1$, $G_{16} = \frac{1}{2} r_s^2 G_3$, $G_{17} = \frac{1}{r_s} G_{14}$

Table.D.1. Polynomial Coefficients Matrix of Curved Beam Element.

D.6 Formulation of Element Matrices.

The strain energy of the curved beam element is

$$U = \frac{1}{2}\int_{-\alpha}^{\alpha}[N]^T\{\varepsilon\}\, r_c d\theta$$
$$= \frac{1}{2}\int_{-\alpha}^{\alpha}\{\varepsilon\}^T[D]\{\varepsilon\}\, r_c d\theta$$
$$= \frac{1}{2}\{u_e\}^T[C]^{-T}\int_{-\alpha}^{\alpha}[B]^T[D][B]\, r_c d\theta\, [C]^{-1}\{u_e\} \quad \ldots\ldots (D.45)$$

in which

α = half angle of circumference of element

$[\ ]^T$ = transpose of matrix or vector

Minimizing strain energy, the element stiffness matrix becomes

$$[K_e] = r_c\,[C]^{-T}\int_{-\alpha}^{\alpha}[B]^T[D][B]\,d\theta\,[C]^{-1} \quad \ldots\ldots\ldots\ldots\ldots (D.46)$$

The integration of above equation is given explicitly by

$$\int_{-\alpha}^{\alpha}[B]^T[D][B]\,d\theta = \begin{bmatrix} H_1 & & & & & \\ 0 & H_2 & & & & \\ H_3 & 0 & H_4 & & & \\ 0 & H_5 & 0 & H_6 & & \\ H_7 & 0 & H_8 & 0 & H_9 & \\ 0 & 0 & 0 & H_{10} & 0 & H_{11} \end{bmatrix} \quad \ldots\ldots (D.47a)$$

where

$$H_1 = \frac{1}{2}(A+G_1^2Ix - 2G_1G_4Ixy + G_4^2Ixy)(2\alpha + \sin 2\alpha)$$

$$H_2 = \frac{1}{2}(A + G_1^2Ix - 2\,G_1G_4Ixy + G_4^2Ixy)(2\alpha - \sin 2\alpha)$$

$$H_3 = 2(G_1G_2Ix - G_2G_4\,Ixy - G_1G_5Ixy + G_4G_5Iy)\sin\alpha$$

$$H_4 = 2(G_2^2Ix - 2G_2G_5Ixy + G_5^2Iy)\alpha$$

$$H_5 = \frac{1}{2}(G_1G_3Ix - G_1G_6Ixy - G_3G_4Ixy + G_4G_6Iy)(2\alpha - \sin 2\alpha)$$

$$H_6 = \frac{1}{2}(G_3^2Ix - 2\,G_3G_6Ixy + G_6^2Iy)(2\alpha - \sin 2\alpha) + \frac{1}{2}J'(2\alpha + \sin 2\alpha)$$

$$H_7 = \frac{1}{2}(G_1G_3Ix - G_1G_6Ixy - G_3G_4Ixy + G_4G_6Iy)(2\alpha + \sin 2\alpha)$$

$$H_8 = -2(G_2G_3Ix - G_3G_5Ixy - G_2G_6Ixy + G_5G_6Iy)\sin\alpha$$

$$H_9 = \frac{1}{2}(G^2Ix - 2G\ G\ Ixy + G^2Iy)(2\alpha + \sin 2\alpha)$$

$$+ \frac{1}{2}J'(2\alpha - \sin 2\alpha)$$

$$H_{10} = 2J'\sin\alpha$$

$$H_{11} = 2J'$$

$$J' = \frac{J}{2(1+\nu)} \qquad \text{.......................(D.47b)}$$

The transformation matrix $[T]$ which relates the generalized displacements in element coordinates to those in shell - ring connection coordinates via

$$\{u_e\} = [T']\{u_o\} \qquad \text{..............................(D.48)}$$

is found from eq.(D.1), eq.(D.2), and eq.(D.3) by substituting the shell-stiffener interation coordinate, $(\bar{x},\bar{y})$, into (x,y)

$$[T'] = \begin{bmatrix} 1 & & & \bar{y} & & \\ & 1 & & -\bar{x} & & \\ & & 1 & & -\bar{y} & \bar{x} \\ & & & 1 & & \\ & & & & 1 & \\ & & & & & 1 \end{bmatrix} \qquad \text{..........(D.49)}$$

The final form of the stiffness matrix in the cylindrical coordinate becomes

$$[K] = [T]^T[K_e][T] \qquad \text{.............................(D.50)}$$

where the transformation matrix $[T]$ is

$$[T] = \begin{bmatrix} [T'] & [0] \\ [0] & [T'] \end{bmatrix} \qquad \text{..............................(D.51)}$$

The work done by the gravity loading on the beam element is

$$W = -\int \{q(\Theta)\}^T \{u\}\, dv$$

$$= -r_c \int_{-\alpha}^{\alpha} \{q(\Theta)\}^T [P]\, d\Theta\, [C]^{-1} \{u_e\}$$

$$= -\left[F_d\right]^T \{u_e\} \quad \text{..........................(D.52)}$$

where the distributed gravity load vector per unit length, $\{q(\Theta)\}$, is

$$\{q(\Theta)\}^T = A \lfloor 0,\ -\cos\Theta,\ \sin\Theta,\ 0,\ 0,\ 0 \rceil \quad \text{..........(D.53)}$$

The consistent load matrix due to a unit gravity load on the beam element $\{F_{de}\}$ is then

$$\{F_{de}\} = \rho\, r_c A\, [C]^{-T} \int_{-\alpha}^{\alpha} [P]^T \{q(\Theta)\}\, d\Theta \quad \text{..........(D.54)}$$

in which ρ is the specific weight of the material (lb/in^3), and the integration can be shown to be

$$\int_{-\alpha}^{\alpha} [P]^T \{q(\Theta)\}\, d\Theta = \left\{ \begin{array}{l} G_7(\alpha - \tfrac{1}{2}\sin 2\alpha) \\ 0 \\ 2(G_8 \sin\alpha - r_s^2(\sin\alpha - \alpha\cos\alpha)) \\ -G_{18}\sin 2\alpha \\ G_9 - \tfrac{1}{2}\sin 2\alpha(G_9 + G_{18}) - G_{18}\cos 2\alpha \\ 0 \\ -2\alpha \\ 0 \\ 0 \\ 0 \\ 0 \\ 0 \end{array} \right\} \quad \text{(D.55)}$$

The generalized load matrix due to a unit pitching moment of the body structure has been assumed to be the product of the element consistent load matrix with the longitudinal distance from the centre of gravity of total structure.

D.7 Straight Thin-Walled Beam for the stringer Members

Putting the radii r_s and r_c be infinite and substituting the differentiation against arc length $r_s d\theta$ with beam element length dz, the element stiffness matrix of the previous curved beam element becomes the thin-walled straight beam element matrix without shear deformation.

The strain-displacement relations are;

$$\varepsilon_o = \frac{dv}{dz} - y_c \frac{d^2w}{dz^2} - x_c \frac{d^2u}{dz^2}$$

$$\varepsilon_a = \varepsilon_o - (y-y_c)\frac{d^2w}{dz^2} - (x-x_c)\frac{d^2u}{dz^2}$$

$$k_x = -\frac{d^2w}{dz^2}$$

$$k_y = \frac{d^2u}{dz^2}$$

$$\beta = \frac{d\phi}{dz}$$

$$\ldots\ldots\ldots\ldots\ldots\ldots \quad (D.55)$$

Using equilibrium equations (D.22) and above equations, the displacement functions of the thin-walled straight beam element are found as follow;

$$u = a_1 z^3 + a_2 z^2 + a_3 z + a_4$$

$$w = a_5 z^3 + a_6 z^2 + a_7 z + a_8$$

$$v = \frac{3}{2}(a_1 x_c + a_5 y_c) z^2 + 2(a_2 x_c + a_6 y_c + a_9) z + a_{10}$$

$$\phi = a_{11} z + a_{12}$$

$$\ldots\ldots\ldots\ldots\ldots\ldots \quad (D.56)$$

The procedure for finding the element matrices is same with previous section, so that it is not included here.

And it is transformed to the shell middle surface coordinate using eq.(D.49). When the eccentricity x_c and y_c are neglected, eq.(D.56) becomes exactly same as the elementary beam functions.

APPENDIX E

REVIEW OF THE CLASSICAL DESIGN PARAMETERS FOR THE CYLINDRICAL FUSELAGE

E.1 General Assumptions used in the Classical Analyses

The earlier analytical approaches (Ref.14-21) have the following common assumptions to solve the wing-fuselage interaction problem of a transport type aircraft:

i) The fuselage has many stiffeners in longitudinal direction and these stringers are smeared out over the circumference giving an equivalent shell skin thickness including skin, for axial load.

ii) The skin and stringers have no bending stiffness, while bending stiffnesses of the ring stiffeners are smeared out in axial direction for circumferential bending load. The frame has inplane stiffness only.

iii) There is single loaded frame to carry the concentrated radial or tangential load and the inplane bending moment. Multiple loads or inclined loads on the frame are resolved into the concentrated loads and effects of each resolved load have been super imposed.

iv) The structural discontinuity has not been considered in analytical form but has been used emperical data.

v) No eccentricity of the loaded frame or stiffeners has been taken account. Practically no local reinforcement or adjacent loaded frame effect has been included.

E.2 Selection of important Design Parameter

The typical parameters in Ref.21 are GtR^4/EI_fL' for the shell with single loaded frame. In this parameter, the loaded frame has equal properties with the ring stiffeners. The ring spacing is assumed basically to be constant. In the References 18 to 20, the loaded frame has been assumed to have different properties from the rings. The parameters used in those analyses are basically the characteristic lengths of $R\ t'R^2L_{rsp}/I_r\ ^{\frac{1}{4}}/\ 6$ and $R\ Et'/Gt\ ^{\frac{1}{2}}$. They were defined as the distance required for the exponential envelope of the lowest order, self-equilibrating stress systems to decay to 1/e of its value at the loaded frame, provided that the skin panels are rigid in shear for the first one and that the frames are rigid in bending respectively.

It is unlikely to use those closed form of design parameters for the present finite element method investigation of the stiffened shell behaviour. As a preliminary parametric investigations, those collective form of design parameters are resolved into the individual variable to find out the important parameters. Using the formulae in the References 18 to 20, the effect of individual design parameter to the body has been examined in qualitative manner.

The stresses and displacements are basically represented by the shear flow on the loaded frames with above parameters and the loaded frame bending stiffness. They are varying harmonically around the circumference and exponentially along the axial axis. The magnitude of stresses and displacements are entirely dependent upon the shear flow at the frame station which is represented as follows:

$$q_m = \frac{m}{2\pi R} \frac{P_o}{1+\gamma K_m} \quad ; \quad \text{for symmetric loading,}$$

$$q_m = \frac{1}{2\pi R(1+\gamma K_m)} \left(T_o + \frac{(1-m^2)}{R} M_o\right)$$

; for antisymmetric loading.

The parameters γ and K_n in above equations are defined as follows using present notations:

$$\gamma = \frac{\sqrt{6}}{2} \frac{I_f L_{rsp}}{I_r R} \left(\frac{I_r}{t' L_{rsp} R^2}\right)^{1/4}$$

$$K_m = \frac{m\sqrt{m^2-1}}{2\sqrt{3}} \frac{1+2a_m}{(1+a_m)^{1/2}}$$

$$a_m = \frac{m^2-1}{\sqrt{3}} \frac{Et'}{GtR} \left(\frac{I_r}{t' L_{rsp}}\right)^{1/2}$$

$$t' = \text{equivalent shell thickness} = t_s + \frac{A_s N_{str}}{2\pi R}$$

The major difference of above shear flow representation from the engineering beam theory arises from the product of γ and K_m. For higher harmonic number, q_m will be negligible because K_m is increasing in order of m^3. Therefore considering small m and small magnitude of a_m, K_m can be expanded in following series form:

$$\gamma K_m = \frac{m\sqrt{m^2-1}}{2\sqrt{3}} \left(1+\frac{3}{2} a_m\right)$$

$$= \frac{m\sqrt{m^2-1}}{2\sqrt{3}} \quad 1+\frac{(m^2-1)}{2} \frac{Et'}{GtR} \left(\frac{I_r}{t' L_{rsp}}\right)^{1/2}$$

Then the product γK_m becomes as follow:

$$\gamma K_m = \frac{m\sqrt{m^2-1}}{2\sqrt{2}} \frac{I_f L_{rsp}}{I_r R} \left(\frac{I_r}{t' R L_{rsp}}\right)^{\frac{1}{4}} \left(1+ \frac{m^2-1}{2} \frac{Et'}{GtR}\left(\frac{I_r}{t' L_{rsp}}\right)^{\frac{1}{2}}\right)$$

or

$$\gamma K_m = \frac{m\sqrt{m^2-1}}{2\sqrt{2}} I_f L_{rsp}^{\frac{3}{4}} I_r^{-\frac{3}{4}} R^{-\frac{3}{4}} t'^{-\frac{1}{4}} \left(1+ \frac{m^2-1}{2} \frac{Et'}{GtR}\left(\frac{I_r}{t' L_{rsp}}\right)^{\frac{1}{2}}\right)$$

$$= \frac{m\sqrt{m^2-1}}{2\sqrt{2}} \left(\frac{L_{rsp}}{R} \frac{I_f}{I_r}\right)^{\frac{3}{4}} \left(\frac{I_f}{R^3 t'}\right)^{\frac{1}{4}} \left(1+ \frac{m^2-1}{2} \left(\frac{I_r}{t' L_{rsp}}\right)^{\frac{1}{2}}\right)$$

From the above dimensional expression of parameter, the most important design vaiable is the second moment of inertia of frame which is affecting the shell behaviour by the order of one. The secondary parameters are the ring stiffness per unit length, I_r/L_{rsp} , and the area of stringer which are affecting on the shell with the order of 3/4 and 1/4 respectively.

E.3 Decay Length of the Body Structure in App.B

In the appendix C of Ref.18, the decay length has been defined as the distance from the loaded frame to the shell where the displacement solution can be predicted from elementary theory. Using the formula in Ref.18, this length is obtained for the body structure of Appendix B. The harmonic terms considered in this calulation is m=2 which is most predominant term in that formula.

The basic dimensions for the body structure are:

R=6.0 inch, t=0.06 inch, A_s=0.1 in^{2}x 4 stringers,

I_r=0.01 in^4, I_f=0.1 in^4, L_{rsp}=12.0 inch.

the equivalent thickness;

$$t' = 0.06 + \frac{4\times0.1}{2 \quad R} = 0.0706 \text{ (in)}$$

the characteristic lengths in Ref.18;

$$L_{cm} = R(t'R^2L_{rsp}/36I_r)^{\frac{1}{4}}$$

$$= 18.203\text{(in)}$$

$$L_{rm} = R(Et'/Gt)^{\frac{1}{2}}/2$$

$$= 5.247 \text{ (in)}$$

the other parameters;

$$a_m = (m^2-1)(L_{rm}/L_{cm})^2/3$$

$$= 0.083 \text{ for } m=2$$

$$K_m = m(m^2-1)^{\frac{1}{2}}(1 + 2a_m)/(12 + 12a_m)^{\frac{1}{2}}$$

$$= 1.1206 \quad \text{for } m=2$$

$$\gamma = I_fL_{rsp}/I_rL_{cm}$$

$$= 6.593$$

Finally the decay length with m=2 becomes:

$$L_d = L_{cm}(L_{cm}/L_{rm})^2 \quad \frac{4.5\ K_m}{(m^3 - m)^2}$$

$$= \underline{30.68 \text{ (inch)}}$$

E.4 Stress Concentration Around Cutout

The direct stress around the cut out of the body shell structure with R=12.0 is predicted using the formula in Ref.22. The stresses at he middle of two loaded frames is calculated for the two different stringer area cases of the four boom shell under the end tail loading. The stringer area used are 1.125 in^2 and 0.2 in^2. The other basic dimensions are as foloows:

Skin thickness; t = 0.06 inch,

Bending moment at the middle of two frames; M

$$M_b = -24000 \text{ lbf-in},$$

Opening angle; $\phi = \pi/2$,

Undisturbed angle; $\beta_o = \pi/2 - \phi/4 = 3\pi/8$,

The stress is found by the formula in Ref.22 as follow:

Maximum disturbed stress;

$$\sigma_1' = \frac{4MR}{I_{sh}} \frac{\phi}{2_o} \cos\frac{\phi}{4} = 2.436 \frac{MR}{I_{sh}}$$

Distribution of the disturbed stress around the circumference;

$$\sigma' = \sigma_1' (\beta/\beta_o)^3 = \frac{2MR\phi}{I_{sh}} \frac{\beta^3}{\beta_o} \cos(\phi/4)$$

$$= 1.50675 \; MR\,^3/I_{sh}$$

The undisturbed stress under the bending moment without cut out;

$$\bar{\sigma} = MR/I \cos\theta$$

NB. is measured from β_o to the opening.

Assuming negligible deficiency moment which is defined as a difference of the moment produced by the imaginary stress carrying door and that produced by the peturbation stress σ', the direct stress distribution around the circumference has the following formula:

$$\sigma = \sigma' + \bar{\sigma}$$

$$= MR/I_{sh}(1.50675 [\theta - \beta]^3 + \cos\theta)$$

Defining the direct stress coefficient C_n as follow:

$$C_n = \sigma t R^2/M_b$$

C_n can be now defined by the opening angle as follow:

$$C_n = -R^3 t/I_{sh}(1.50675 [\theta - \beta]^3 + \cos\theta).$$

Finally using the second moments of inertia of two shell structures

$$I_{0.2} = 383 \text{ in}^4 , \text{ and } \quad I_{1.125} = 650 \text{ in}^4,$$

the direct stresses around the circumference of cut out at the middle of two frames are found as following table.

A_s \ deg	0	22.5	45	67.5	90	112.5	135
0.2	-0.270	-0.250	-0.192	-0.104	0.018	0.302	0.858
1.125	-0.160	-0.148	-0.112	-0.061	0.014	0.150	0.429

APPENDIX F

USE OF PAFEC 75 TO EVALUATE WING STRUCTURE AND TO OBTAIN CONDENSED WING MATRICES FOR BODY ANALYSIS

The program for automatic finite element calculation (PAFEC) has been used for the analysis of wing structure and obtaining the condensed wing stiffness matrix for the evaluation of wing structure influence on the body. Details of this program package are in Ref.9. Unlikely other big finite element package, e.g., NASTRAN, substructuring method is not implemented in PAFEC 75. Because of its frontal solution scheme, PAFEC never assembles total stiffness matrix for the static analysis.

However its eigenvalue economization scheme enables to condense wing stiffness matrix to the wing-body intersection degrees of freedom, in which mass and stiffness matrix of slave degrees of freedom are condensed to master degrees of freedom before calculating eigenvalue to minimize computing costs. The connecting nodes with the body have been defined as master nodes and the others as slave nodes. Before sloving eigenvalue problem, the master mass and stiffness matrices Mmm and Kmm are assembled respectively from the element matrices. This extracted stiffness matrix Kmm has been stored to the backing storage by modification of one subroutine (R52201) in phase 7. This will be assembled to the centre body matrix with other reduced body structure matrices.

When the wing-body intersection displacements are found from the body analysis with the wing stiffnesses (see Chapter 5), this boundary displacements are applied to the wing model as prescribed displacement boundary conditions to examine the body structure effect on the wing structural behaviour.

The wing structure finite element idealization is described in section 5.3, and PAFEC 75 wing model is shown in Fig.5.5. The schematic flow chart concerning above procedure is given in Fig.F.1. The overall flow diagram is shown in Appendix H.

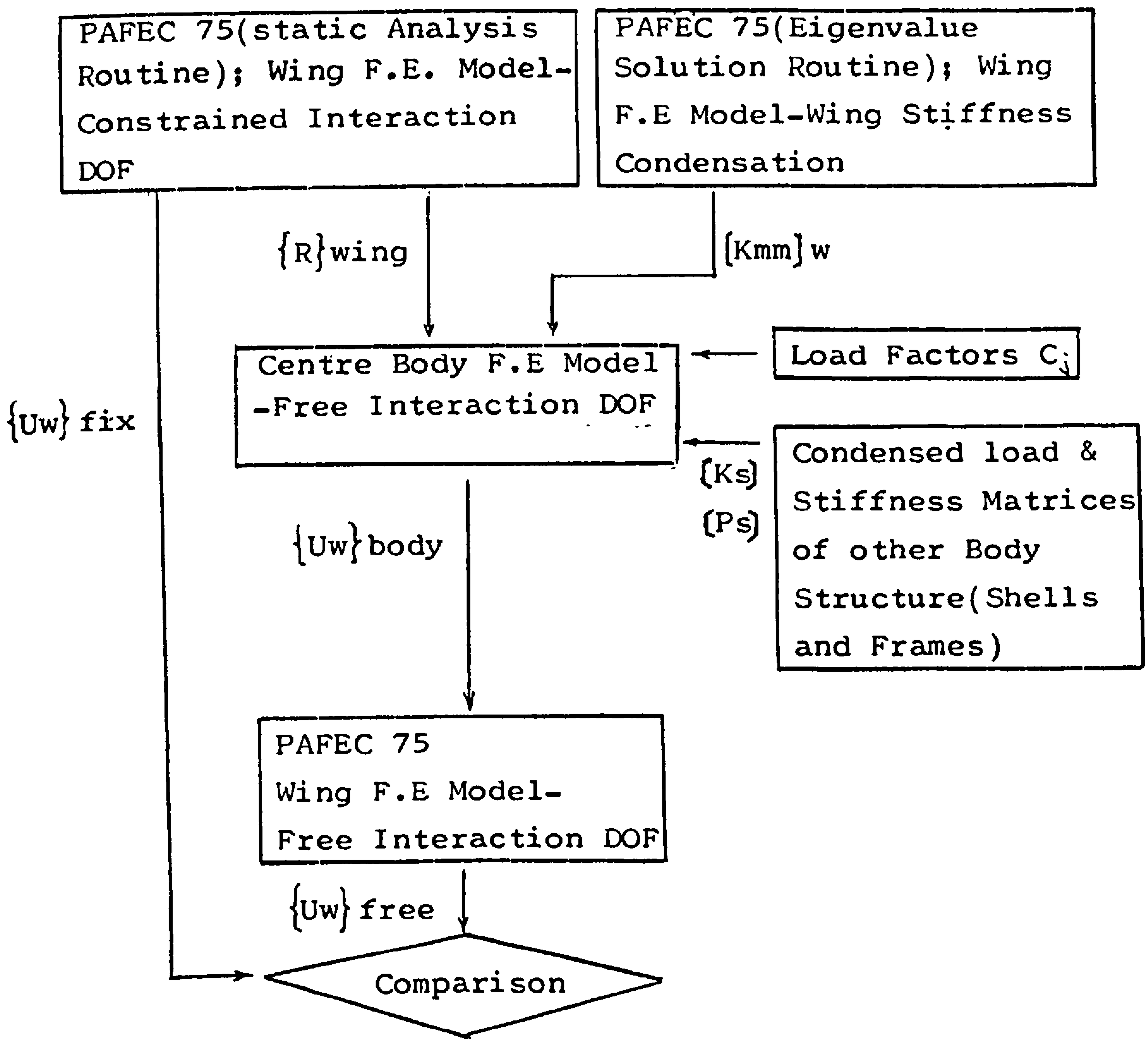

Fig. F.1 Schematic flow of Wing-Body Interference Analysis Using PAFEC 75

Example Input of PAFEC 75

```
TITLE CONDENSED MID WING STIFFNESS
--------------------------------------------------------------
CONTROL
PHASE=1,4,6,7
SEMI.R52201
BASE=50000
CONTROL.END
NODES
NODENO  AXIS X Y Z
1  1  0  0.6  6.0
R3  1  0  4.0  -0.03  0.
5  1  0.  0.6  9.0
R3  1  0  4.  -0.03  0.
9  1  0.  0.6  12.0
R8  4  0  0.  -0.0375  4.0
10  1  4.0  0.57  12.0
R8  4  0  -0.125  -0.03635  4.
11  1  8.  0.54  12.
R8  4  0  -0.25  -0.03521  4.
12  1  12.  0.51  12.
R8  4  0 -0.375  -0.03406  4.
47  1  0.  -0.6  6.
R3  1  0  4.0  0.03  0.
51  1  0.  -0.6  9.
R3  1  0  4.  0.03  0.
55  1  0.  -0.6  12.
R8  4  0  0.  0.0375  4.
56  1  4.  -0.57  12.
R8  4  0  -0.125  0.03635  4.
57  1  8.  -0.54  12.
R8  4  0  -0.25  0.03521  4.
58  1  12.  -0.51  12.
R8  4  0  -0.375  0.03406  4.
ELEMENTS
GROUP.NUMBER  ELEMENT.TYPE  PROPERTIES  TOPOLOGY
1  44200  1  1  2  5  6
R9  0  0  0  4  4  4  4
1  44200  1  2  3  6  7
R9  0  0  0  4  4  4  4
1  44200  1  3  4  7  8
R9  0  0  0  4  4  4  4
2  44200  2  1  5  47  51
R9  0  0  0  4  4  4  4
2  44200  2  4  8  50  54
R9  0  0  0  4  4  4  4
2  44200  2  1  2  47  48
R5  0  0  0  8  8  8  8
2  44200  2  2  3  48  49
R5  0  0  0  8  8  8  8
2  44200  2  3  4  49  50
R5  0  0  0  8  8  8  8
```

```
(    51)   3   34100   3   1   5
(    52)   3   34100   3   5   9
(    53)   R8    0   0   1   4   4
(    54)   3   34100   12   4   8
(    55)   3    34100   12   8   12
(    56)   R8   0   0   1   4   4
(    57)   3   34100   3   1   2
(    58)   R2   0   0   1   1   1
(    59)   3   34100   3   9   10
(    60)   R4   0   0   1   8   8
(    61)   3   34100   4   10   11
(    62)   R4   0   0   1   8   8
(    63)   3   34100   5   11   12
(    64)   R4   0   0   1   8   8
(    65)   GROUP.OF.SIMILAR.ELEMENTS
(    66)   OLD   NEW NUMBER   TOPOLOGY.INCREMENTS
(    67)   1   107   30   46
(    68)   69   137   38   46
(    69)   BEAMS
(    70)   SECTION.NUMBER   MATERIAL.NUMBER   IYY   IZZ   A
(    71)   3   11   0.04   0.04   0.12
(    72)   R8   1   0   -0.002 -0.002   -0.005
(    73)   12   11   0.03   0.03   0.1
(    74)   R8   1   0   -0.002 -0.002   -0.005
(    75)   PLATES.AND.SHELLS
(    76)   PLATE.NUMBER   MATERIAL   THICKNESS
(    77)   1   11   0.06
(    78)   2   11   0.05
(    79)   MATERIAL
(    80)   MATERIAL.NUMBER   E   NU   RO
(    81)   11   10.3E6   0.3   0.1
(    82)   RESTRAINTS
(    83)   NODENO   PLANE   DIRECTION
(    84)   1   3   345
(    85)   MASTERS
(    86)   9
(    87)   12
(    88)   MODES.AND.FREQUENCIES
(    89)   0   1   1
(    90)   IN.DRAW
(    91)   DRAWING.NUMBER   ORIENTATION
(    92)     ,4
(    93)   END.OF.DATA

END OF DATA          0 ERRORS
```

Example Condensed Wing Stiffness

PAFEC Output

```
                                                                 777777  555555
                                                                 77    7  55
SYSTEM LEVEL 3.4          PPPPP  AAAAA FFFFF EEEEE CCCCC  77    7  55
JUNE  1981                P   P  A   A FF    E     C  CC  77    7  55
                          P   P  A   A FF    E     C             7  55
                          PPPPP  AAAAA FFF   EEE   C           777 555555
PHASE NO.  7              PP     AA    A F   EE    C             7      5
STARTS HERE               PP     AA    A F   EE    C             7      5
                          PP     AA    A F   EE    C             7      5
                          PP     AA    A F   EEEEE CCCCC         7      5
                                                                 7  5   5
                                                                 7  555555


REDUCED STIFF. MATRIX

IDF= 12 =
ORDER OF STIFF. MATRIX
  35   36   37   38   39   40   53   54   55   56        57   58

REDUCED STIFFNESS MATRIX BY PAFEC
 0.4337742500000000D+06-0.2969339794921875D+04 0.2050963671875000D+05 0.2906431884765630D+04-0.6508320800781250D+04-0.4337725937500000D+06
 0.2972755371093750D+04 0.2369393164062500D+05 0.1559767211914060D+04 0.7629339843750000D+04-0.4334696875000000D+05 0.3995312890625000D+05
-0.2969339794921875D+04 0.4246459984375000D+04 0.7613139343261720D+02-0.7926643066406250D+03-0.1319160003662110D+03 0.2969422119140630D+04
-0.4243464355468750D+04 0.1006711044311520D+03 0.2400816535949710D+02-0.2736729125976560D+03-0.2646756835937500D+05-0.2420105078125000D+05
 0.2050963671875000D+05 0.7613139343261720D+02 0.7332543750000000D+05-0.1113322031250000D+06 0.7485974218750000D+05-0.2051301367187500D+05
-0.9627683258056640D+02 0.5338684492187500D+05-0.4841373437500000D+05 0.3078952148437500D+05 0.5825248413085940D+03-0.3570129394531250D+04
 0.2906431884765630D+04-0.7926643066406250D+03-0.1113322031250000D+06 0.3117463437500000D+06-0.3545688232421880D+04-0.2906435302734380D+04
 0.7764450683593750D+03-0.4511984375000000D+05-0.5288147265625000D+05-0.4636431640625000D+04 0.1387589233398440D+04 0.7678106445312500D+04
-0.6508320800781250D+04-0.1319160003662110D+03 0.7485974218750000D+05-0.3545688232421880D+04 0.6557487687500000D+06 0.6508225097656250D+04
 0.1298884582519530D+03-0.2444418750000000D+05 0.3019064453125000D+04-0.9896187133789060D+03 0.9327576293945310D+03 0.1203205200195310D+04
-0.4337725937500000D+06 0.2969422119140630D+04-0.2051301367187500D+05-0.2906435302734380D+04 0.6508225097656250D+04 0.4337741250000000D+06
-0.2972748779296880D+04-0.2369140234375000D+05-0.1560607788085940D+04-0.7629039062500000D+04 0.4334697656250000D+05-0.3995307421875000D+05
 0.2972755371093750D+04-0.4243464355468750D+04-0.9627683258056640D+02 0.7764450683593750D+03 0.1298884582519530D+03-0.2972748779296880D+04
 0.4244338427734375D+04-0.1195606460571290D+03-0.3767202758789060D+02 0.2746625671386720D+03 0.2647024414062500D+05 0.2419952734375000D+05
 0.2369393164062500D+05 0.1006711044311520D+03 0.5338684492187500D+05-0.4511984375000000D+05-0.2444418750000000D+05-0.2369140234375000D+05
-0.1195606460571290D+03 0.7659660000000000D+06-0.1411173640625000D+06-0.8254175781250000D+05-0.9388214111328130D+03-0.2594830078125000D+04
 0.1559767211914060D+04 0.2400816535949710D+02-0.4841373437500000D+05-0.5288147265625000D+05 0.3019064453125000D+04-0.1560607788085940D+04
-0.3767202758789060D+02-0.1411173640625000D+06 0.3912024375000000D+06 0.1144591894531250D+05 0.1782420043945310D+04-0.2356378417968750D+04
 0.7629339843750000D+04-0.2736729125976560D+03 0.3078952148437500D+05-0.4636431640625000D+04-0.9896187133789060D+03-0.7629039062500000D+04
 0.2746625671386720D+03-0.8254175781250000D+05 0.1144591894531250D+05 0.8038578750000000D+06 0.1989865112304690D+04 0.6282526245117190D+03
-0.4334696875000000D+05-0.2646756835937500D+05 0.5825248413085940D+03 0.1387589233398440D+04 0.9327576293945310D+03 0.4334697656250000D+05
 0.2647024414062500D+05-0.9388214111328130D+03 0.1782420043945310D+04 0.1989865112304690D+04 0.2960628750000000D+06 0.2546772656250000D+05
 0.3995312890625000D+05-0.2420105078125000D+05-0.3570129394531250D+04 0.7678106445312500D+04 0.1203205200195310D+04-0.3995307421875000D+05
 0.2419952734375000D+05-0.2594830078125000D+04-0.2356378417968750D+04 0.6282526245117190D+03 0.2546772656250000D+05 0.2613420312500000D+06
```

APPENDIX G

STATIC CONDENSATION AND SOLUTION ROUTINE

G.1 Introduction

The accuracy and the efficiency of the finite element method structural analysis are dependent on the finite element used and the solution process to solve large number of simultaneous algebraic equations encountered. Although the VAX/VMS 780 computer in CIT has nearly unlimited virtual memory system, the computing time and the use of central processing unit of the computer are the major factors to be considered for the effective solution routine.

The details of the solution routine and substructuring technique used in the body analysis are explained here, and the descriptions of the developed programs are given in Appendix H.

Using the structural symmetry of the present body of shell structure about the plane of symmetry and the regular mesh model, the band width of the system stiffness matrix become constant. Therefore the effective Gaussian elimination method can be utilized with the constant band width. Since the system equations to be solved have still large number of degrees of freedom and multiple load vectors, the use of the slower backing storage system is neccessary.

The band width of the present body shell model is the degrees of freedom in one constant X coordinate plus the degrees of freedom in two nodes at the next bay in

X direction, because the shell element stiffness matrix has the largest size of the element matrix to determine the band width of system equations to be solved. The element along the radial axis, such as a deep loaded frame, can be assembled without affecting the system band width by prior elimination of the internal nodal degrees of freedom.

G.2 Solution Process

The system equation can be represented, using the bays along the longitudinal direction (Fig.G.1), as follow:

$$\begin{bmatrix} K_{11} & K_{12} & & & & & & \\ & K_{22} & K_{23} & & [0] & & & \\ & & K_{33} & K_{34} & & & & \\ & & & \ddots & & & & \\ & \text{Symmetric} & & & K_{jj} & K_{j,j+1} & & \\ & & & & & \ddots & K_{n-1,n-1} & K_{n-1,n} \\ & & & & & & & K_{nn} \end{bmatrix} \begin{Bmatrix} U_1 \\ U_2 \\ U_3 \\ \vdots \\ U_j \\ \vdots \\ U_{n-1} \\ U_n \end{Bmatrix} = \begin{Bmatrix} P_1 \\ P_2 \\ P_3 \\ \vdots \\ P_j \\ \vdots \\ P_{n-1} \\ P_n \end{Bmatrix} \quad \text{.........(G.2.1)}$$

The degrees of freedom in j th position are always related only to j-1 and j+1 with band width of n+2 nodes (Fig.G.2). Therefore the elimination and the back substitution are involving in those band width range, while the other bays are not affected at all. It is not needed to keep all stiffness terms in the central memory.

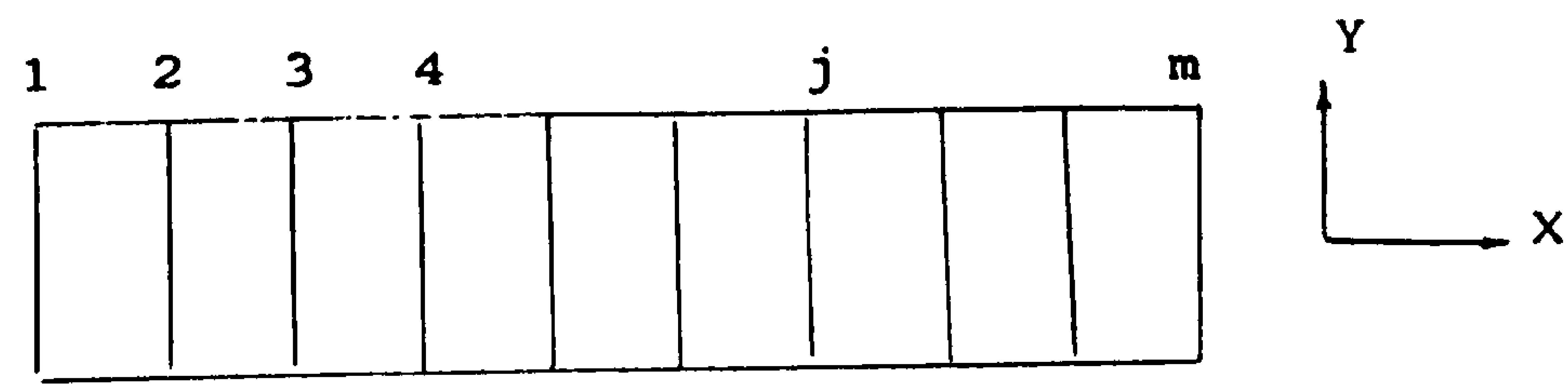

Fig.G.1 A structure divided into bays

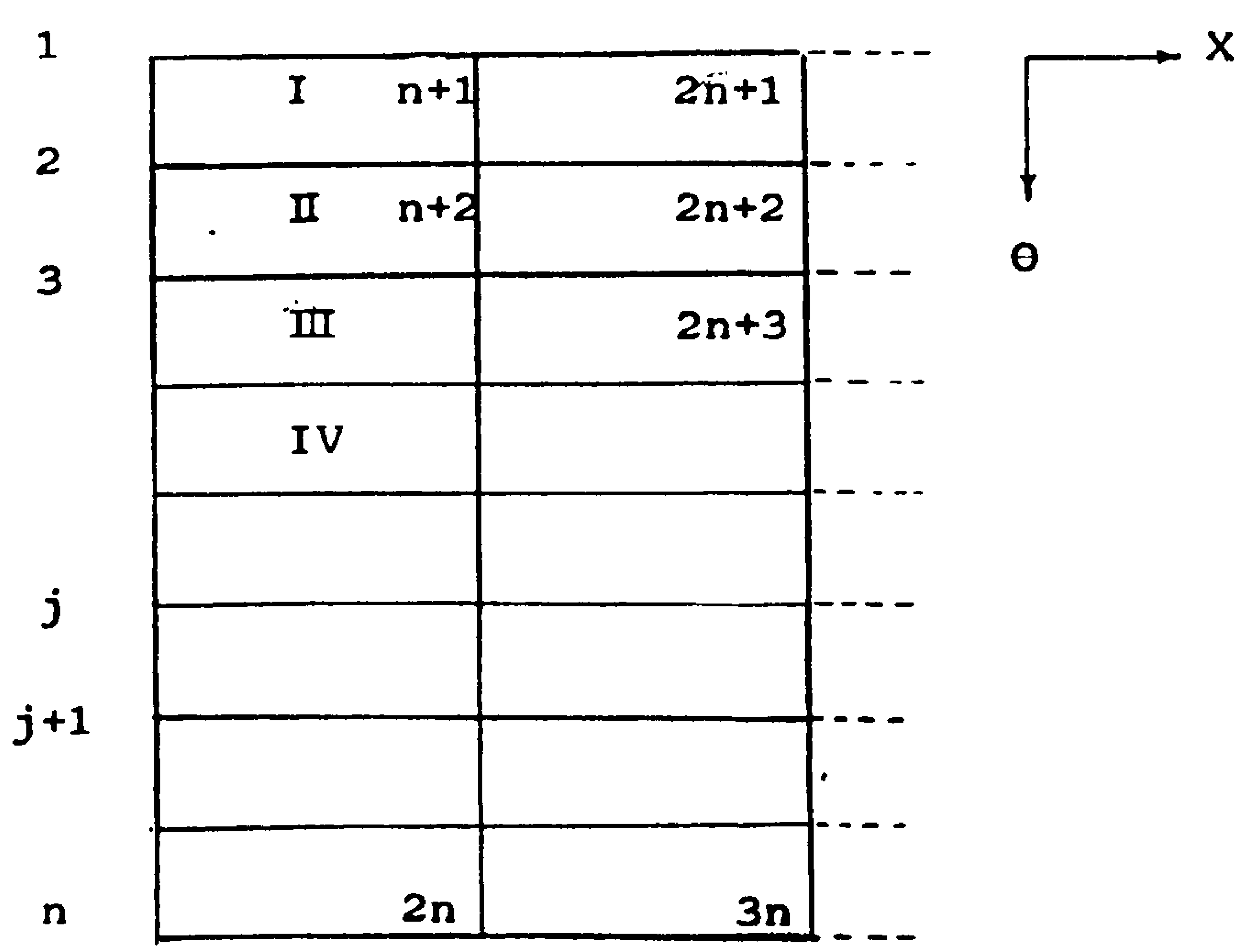

Fig.G.2 Nodes in shell segment

In the beginning of the elimination process, only three nodal stiffnesses in element I are affected by the elimination of node number 1. The equation for the this elimination can be represented as following equation:

$$\begin{bmatrix} K_{11} & K_{12} & 0 & K_{1,n+1} & K_{1,n+2} \\ & K_{22} & 0 & K_{2,n+1} & K_{2,n+2} \\ & & 0 & 0 & 0 \\ & & & K_{n+1,n+1} & K_{n+1,n+2} \\ & & & & K_{n+2,n+2} \end{bmatrix} \begin{Bmatrix} U_1 \\ U_2 \\ \vdots \\ U_{n+1} \\ U_n \end{Bmatrix} = \begin{Bmatrix} P_1 \\ P_2 \\ \vdots \\ P_{n+1} \\ P_{n+2} \end{Bmatrix}$$

..............................(G.2.2)

in which n represents the number of nodes per station. Upper diagonal terms of the stiffness matrix of this equation are the actual size of dimension to be used in the solution procedure.

Eliminating the degrees of freedom on the first node and storing them into the backing storage, the remaining equations become as follow:

$$\begin{bmatrix} K'_{22} & 0 & K'_{2,n+1} & K'_{2,n+2} \\ & 0 & 0 & 0 \\ & & K'_{n+1,n+1} & K'_{n+1,n+2} \\ & & & K'_{n+2,n+2} \end{bmatrix} \begin{Bmatrix} U_2 \\ \vdots \\ U_{n+1} \\ U_{n+2} \end{Bmatrix} = \begin{Bmatrix} P'_2 \\ \vdots \\ P'_{n+1} \\ P'_{n+2} \end{Bmatrix}$$

.... (G.2.3)

in which

$$K'_{ik} = K_{ik} - K^{T}_{1i} \; K^{-1}_{11} \; K_{1k}$$

$$P'_{i} = P_{i} - K^{T}_{1i} \; K^{-1}_{11} \; K_{1k}$$

$$i,k = 2, n+1, n+2.$$

Then the second element is assembled and node 2 has been eliminated. After storing the eliminated degrees of freedom, the remaining terms are shifted to the first row. Therefore total degrees of freedom for this process is those for n+2 nodes.

When the last node is eliminated and shifted, the equation becomes,

$$\begin{bmatrix} K'_{n+1,n+1} & K'_{n+1,n+2} & & & K'_{n+1,2n} \\ & K'_{n+2,n+2} & & & K'_{n+2,2n} \\ & & \ddots & & \vdots \\ & & & K'_{2n-1,2n-1} & K'_{2n-1,2n} \\ & & & & K'_{2n,2n} \end{bmatrix} \begin{Bmatrix} U_{n+1} \\ U_{n+2} \\ \vdots \\ U_{2n-1} \\ U_{2n} \end{Bmatrix} = \begin{Bmatrix} P'_{n+1} \\ P'_{n+2} \\ \vdots \\ P'_{2n-1} \\ P'_{2n} \end{Bmatrix} \qquad \text{.................................(G.2.4)}$$

The stiffness matrix is now fully populated. Assembling the first element in second bay to this condensed matrix equation, the elimination procedure for the next body is carried out. This bay by bay elimination is performed until the nodes in m-1 station are eliminated. At the final position of m, elimination is proceeded until the final nodal displacements are found.

The backing substitutions are performed in reverse procedure of above elimination by recalling the eliminated stiffness terms from the backing storage.

G.3 Static Condensation

The equilibrium equation for usual substructuring is,

$$\begin{bmatrix} K_{ii} & K_{ib} \\ K_{bi} & K_{bb} \end{bmatrix} \begin{Bmatrix} U_i \\ U_b \end{Bmatrix} = \begin{Bmatrix} P_i \\ P_b \end{Bmatrix} \qquad \ldots\ldots\ldots\ldots \quad (G.3.1)$$

and the equivalent boundary stiffness are found by eliminating the internal displacement U_i. The condensed equilibrium equation becomes as follow:

$$\bar{K}_b \; U_b = \bar{P}_b \qquad \ldots\ldots\ldots\ldots \quad (G.3.2)$$

in which

$$\bar{K}_b = K_{bb} - K_{bi} \, K_{ii}^{-1} \, K_{ib} \qquad \ldots\ldots\ldots\ldots \quad (G.3.3a)$$

$$\bar{P}_b = P_b - K_{bi} \, K_{ii}^{-1} \, P_i \qquad \ldots\ldots\ldots\ldots \quad (G.3.3b)$$

Usually the matrix inversion in eq.(G.3.4) is not done explicitly but by finding the following products:

$$K_{ii}^{-1} \; K_{ib} = Q_1 \, , \qquad \ldots\ldots\ldots\ldots \quad (G.3.4a)$$

$$K_{ii}^{-1} \; P_i = Q_2 \qquad \ldots\ldots\ldots\ldots \quad (G.3.4b)$$

These Q matrices are obtained by solving the equation:

$$\left[K_{ii}\right]\left[Q_1, Q_2\right] = \left[K_{ib}, P_i\right] \qquad \text{.........} \quad (G.3.5)$$

via decomposition, forward elimination and back substitution. The reduced stiffness matrix $\overline{K}_b$ can also be obtained by partial triangulation technique. The procedure is applying Gaussian elimination process to the upper triangle of stiffness matrix in eq.(G.3.1), and terminating the elimination when the final row of the triangular matrix K_{ii}, K_{ib} has been reduced. Then the matrix K_{bb} is replaced by the reduced matrix $\overline{K}_b$.

In the present analysis, this condensed matrices for the outer body or the loaded frame have been found from the elimination process in the previous solution routine. The stiffness matrix and the load matrix in eq.(G.2.4) is an example of the reduced stiffness and load matrices of the one bay shell structure. The reduction process for the boom-web-boom type loaded frames is also exactly same as that for the outer shells.

The reduced matrices of the outer shells and the loaded frames are assembled to the centre body system equation. The assemblages to the centre body matrices are performed before starting the elimination procedure for the appropriate longitudinal position of substructures. Therefore the forward body matrices are assembled at the beginning of the main solution routine, while the rear body matrices are assembled at the final stage elimination of the centre body equation.

APPENDIX H

DESCRIPTION OF DEVELOPED PROGRAMS

H.1 Introduction

The set of finite element cylindrical body analysis programs, developed during the procedure of this investigation, are divided into four major subprograms. They are programmed to be able to interface each other. Many of subroutines of those programs can be used for the other finite element program development. The matrix operation subroutines are taken from the PAFEC 75 package, and they are common for all programs.

These four programs accomplish the following tasks, and their junctions are described in section 3.7:

i) The generation of stiffness and inertia load matrices of the shell element, the curved beam element and the stringer element.
ii) The condensation of outer shell matrices, and solving for the equations of those structures, if neccessary, by back-substitution.
iii) The condensation of boom-web-boom type loaded frame matrices, including generation of the membrane element matrices for the idealization of the web.
iv) To solve the main system equations of the centre body.

Those programs are designed to have constant mesh size in the circumferential direction and in longitudinal direction, but the longitudinal mesh size can be altered for the individual program.

The cylindrical coordinate system is used throughout, because the basic structure is the shell skin which can be more conveniently represented by this polar coordinate than the cartesian system.

The double precision real variables (REAL*16 in VAX) are used in these programs.

H.2 Overall Program Interfacing

The program for the element matrix generation (ELMAT) provides input element matrices to the outer shell analysis program (CONSH) and to the main solution routine (CENSOL). After the condensation of outer shell matrices, the reduced outer body matrices are provided to the CENSOL. The loaded frame matrices also assembled in the CENSOL after the condensation by LOADFR. The simple ring type of loaded frame matrices are generated in the CENSOL using ELMAT, so that LOADFR is not used for the ring type of loaded frames. When the influence of wing stiffness to the body structure is considered (Chapter 5), the condensed wing stiffness matrix is also provided to the main solution routine CENSOL.

When the solutions for the main system equation are found , the boundary displacements on the intersections with the outer shells and wing structures are substituted into the CONSH and PAFEC 75 to get the internal displacements and stresses of these substructures.

The overall flow diagram for the interfaces of subprograms are given in Fig.H.1.

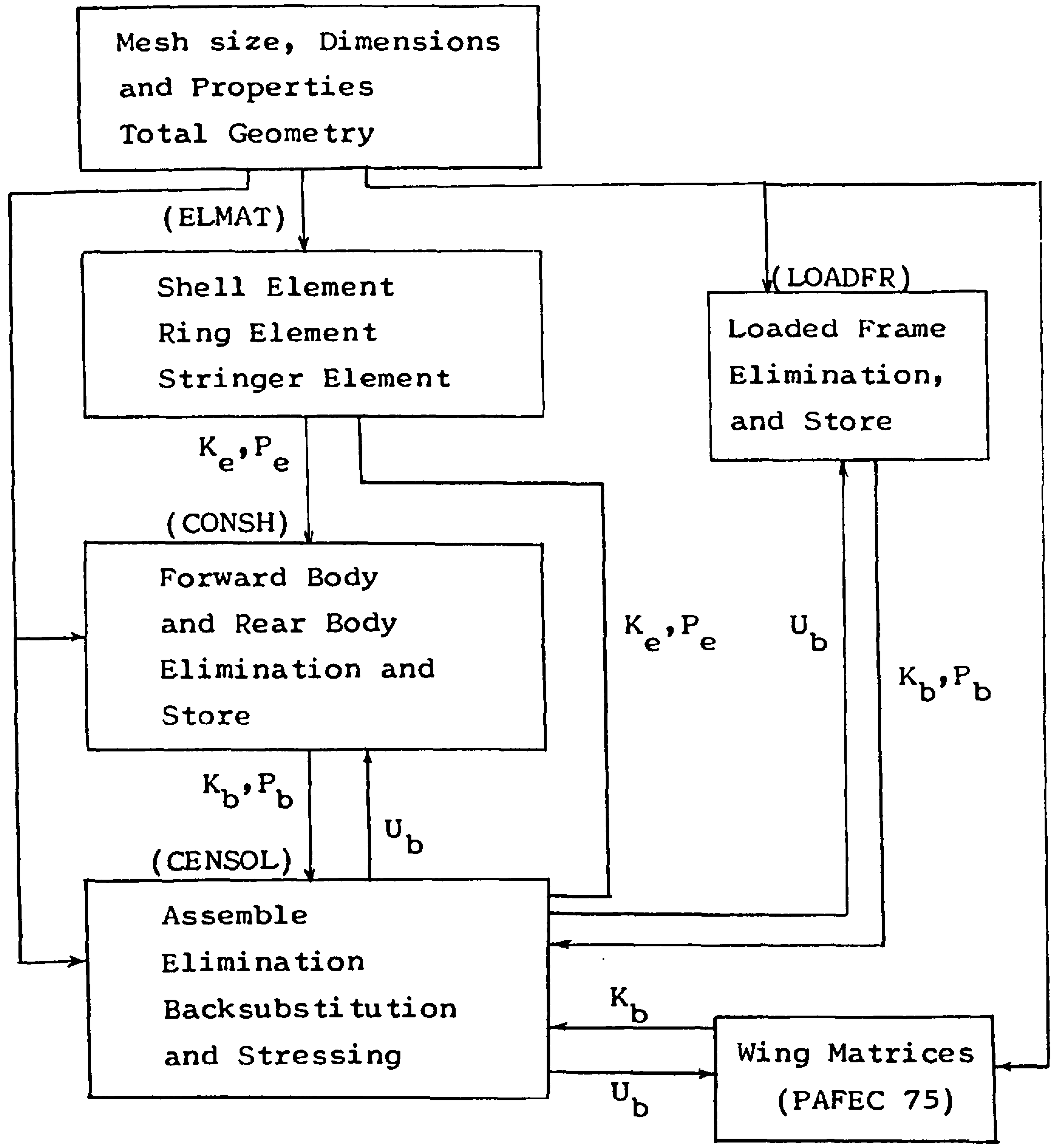

K_e ; element stiffness matrices,

P_e ; element load vector,

K_b ; boundary stiffness matrices,

P_b ; boundary load vector,

U_b ; boundary displacement vector,

Fig.H.1 General Flow Chart and Program Interfacing.

H.3 Description of the Element Matrices Generation Program(ELMAT)

Depending upon the number of elements in the circumference and in the longitude of body shell, the shell and stiffener element matrices are generated and stored to the backing storage disc file by this program. The elements are based on the strain element formulation for the shell and the thin walled curved and/or straight beam formulation in Appendices C and D.

This program is kept outside of the main solution program and the condensation program, because in the most cases of analysis, the elemet matrices are generated only-once and they have been used repeatedly.

The shell element has five degrees of freedom per node which is due to the absence of the rotational degree of freedom about the radial axis as it is in usual thin shell element or plate element. However the beam element for the stringers or rings has six degrees of freedom. The assembly of these two different types of element can be treated either by neglecting the sixth degree of freedom in beam element or by adding additional term to the shell element. It has been found that the second type assumption gives more reasonable results than the five degrees of freedom per node assumption, although the second assumption increases the size of system equation, for the analysis of stiffened shell structure.

Therefore the fictitious sixth degree of freedom has been added to shell element. This additional terms do not have any coupling with the other degrees of freedom in the shell element except between themselves. Thus the rotations of the shell about radial axis are totally governed by the stiffening elements in the system equations.

H.4 Description of the Condensation and Solution Program for the Outer Shells (CONSH)

This program eliminates the internal displacement terms in the outer body alone and condenses the load and stiffness matrices using the procedure described in Appendix G. The eliminated terms are stored into the backing storage for the future internal displacement and stress calculations.

Using the regular mesh and stiffening member positions, the element matrices are not generated for each element by ELMAT, but the types of possible element assembly are used. As shown in Fig.H.2, the types of structural segments are defined by the reltaive positions of the rings and stringers. The number of typical segment types are six for the shell having small number of stringers and four types for the shell with the same number of stringers as the number of shell elements per semi-circumference.

The shell structures are divided by these segments at the beginning of this program and the inertia load and stiffness matrices of the segment are determined from the element matrices. The matrices of each type of segment structure are stored into the auxiliary scratch file.

During the forward elimination procedure, the stored segment matrices are recalled from the backing storage in accordance with the segment definitions for the body structre. This procedure is similar to the element matrix generation procedure in the usual finite element program. The use of this segment generation which is similar to the third level substructuring, enables reduction of computing time.

The general flow chart for this program is given in Fig.H.3.

S; shell element, R; ring element, L; stringer element

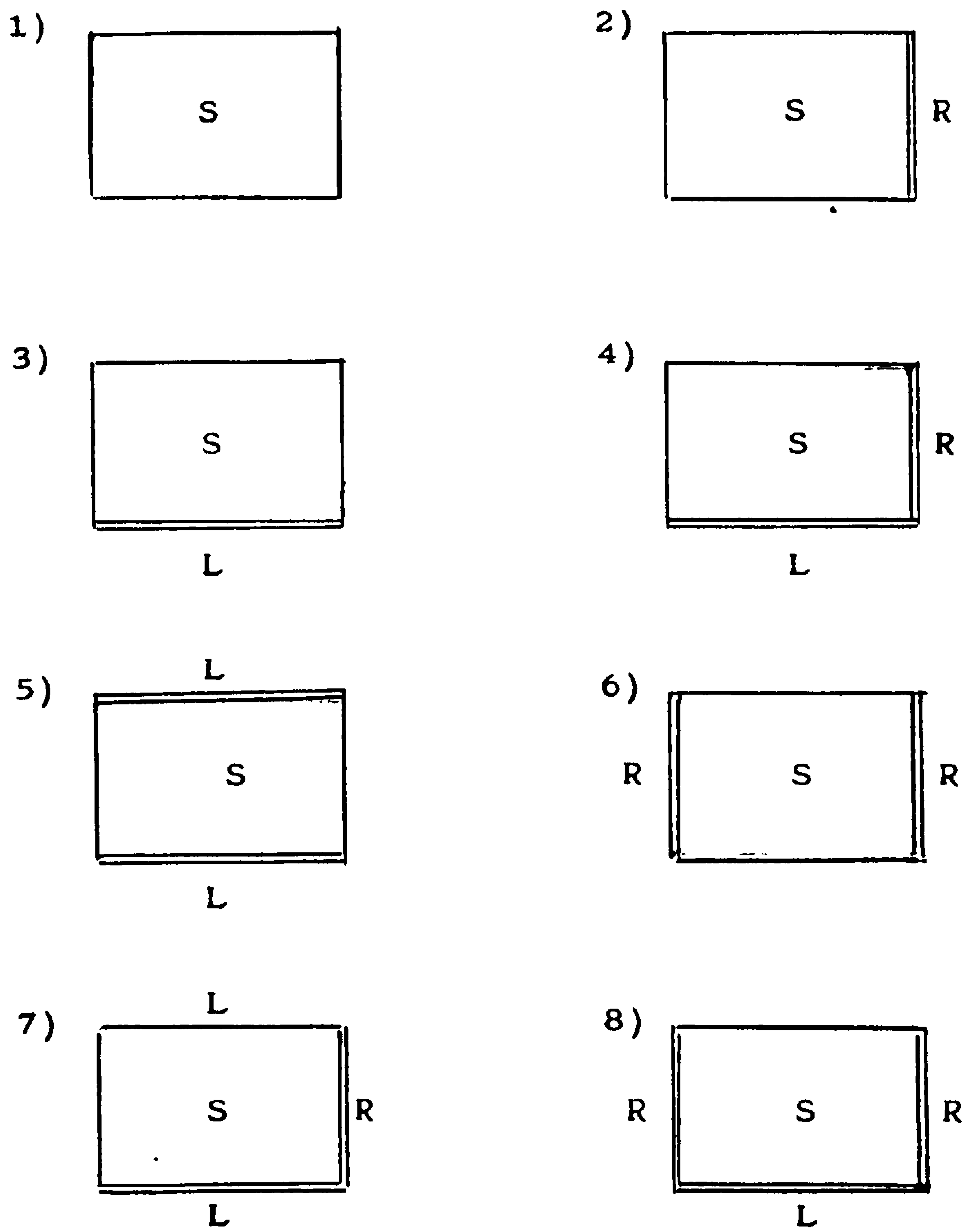

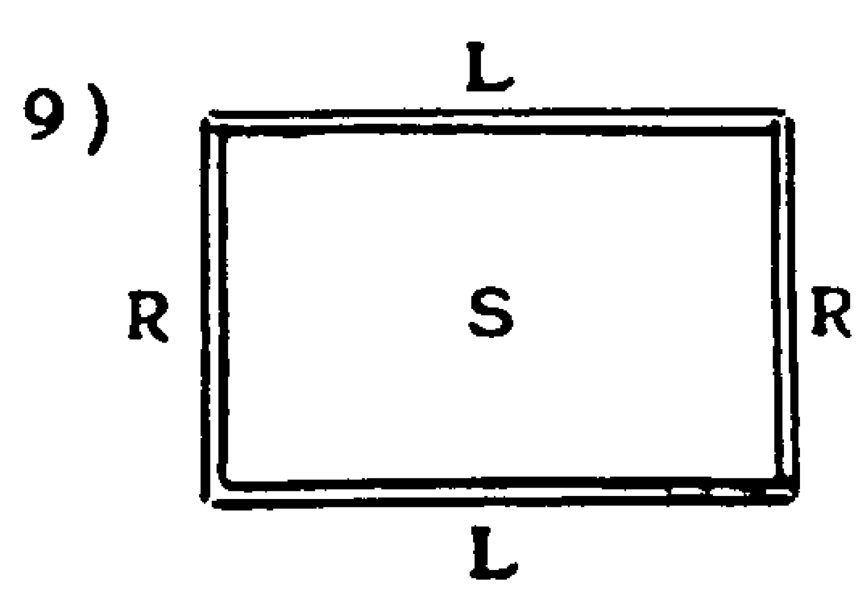

i) Shell with small number of stringer
= 1, 2, 3, 4, 6, 8.

ii) Shell with many stringers
= 5, 7, 8, 9.

*) Cutout; blank element 10

Fig.H.2 Types of Structural Segment in the Body

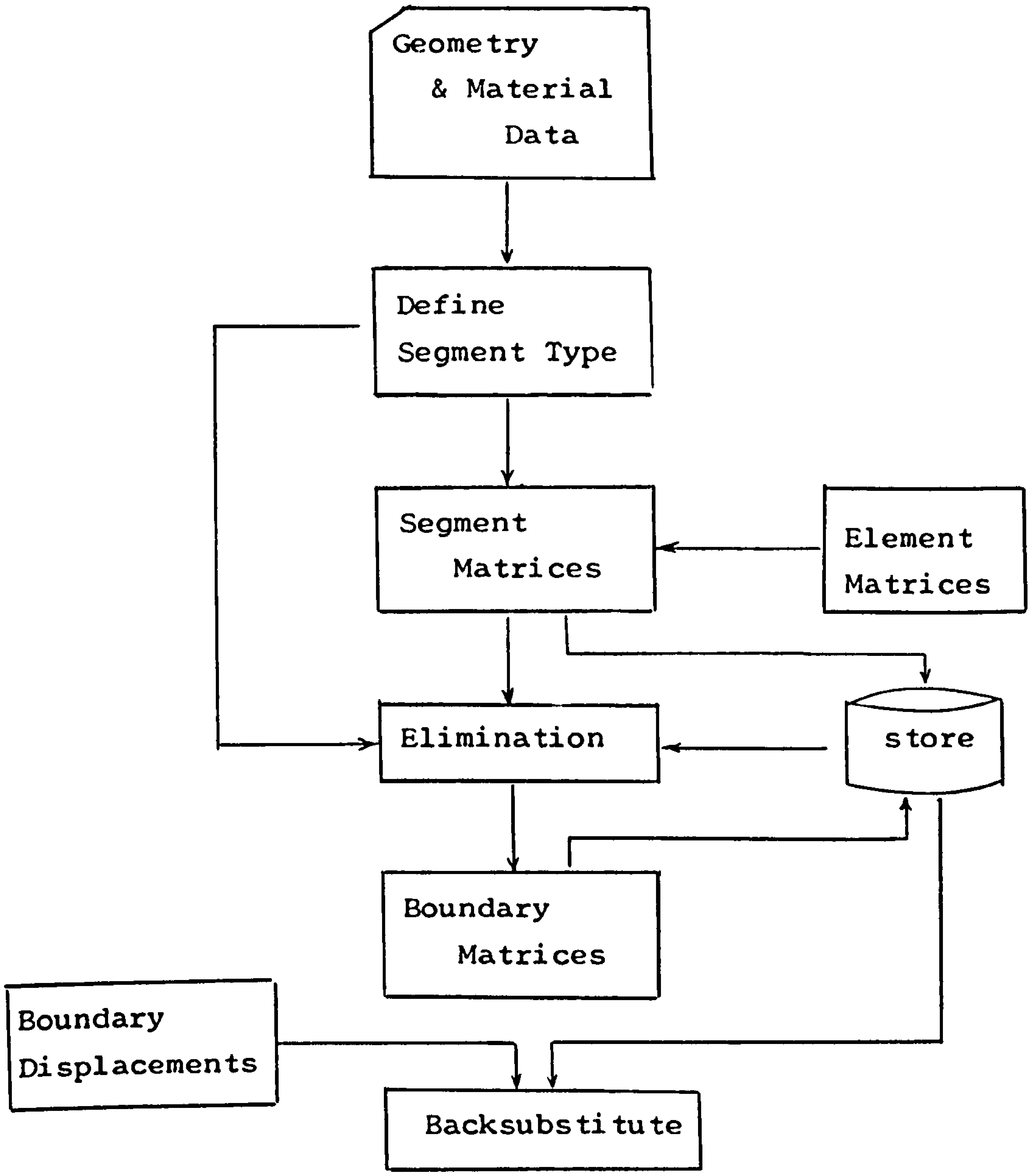

Fig.H.3 Brief Flow Diagram of CONSH

H.5 Description of the Loaded Frame Condensation Program (LOADFR)

This program is mainly used for the generation of condensed loaded frame matrices,especially for the boom-web-boom type deep frames. The element matrices generation routines are included in this program, such as the curved and straight beam elements and the isoparametric membrane element.

The booms are idealized by the beam elements, while the web is idealized by the membrane elements, as described in Chapter 3.

The all internal nodes are condensed to the outer nodes which is attached to the shell nodes. The condensation procedure is the same as previous section.

The brief flow chart for this sub-program is shown in Fig.H.4, and the generated matrices of loaded frame are used as input data for the main solution program.

H.6 Program for the Centre Body Solution (CENSOL)

As shown in the main texts, the major design variables are related to the centre body shell including the loaded frames. Therefore this main solution program needs more flexibility than the other programs, to cope with the change of various design parameters, such as the position of wing or properties of the loaded frames.

The centre body shell is also idealized as the assembly of shell segments which is described in Fig.H.2. The elements in cutout are represented by the fictitious shell elements so that the advantage of constant band width has been kept.

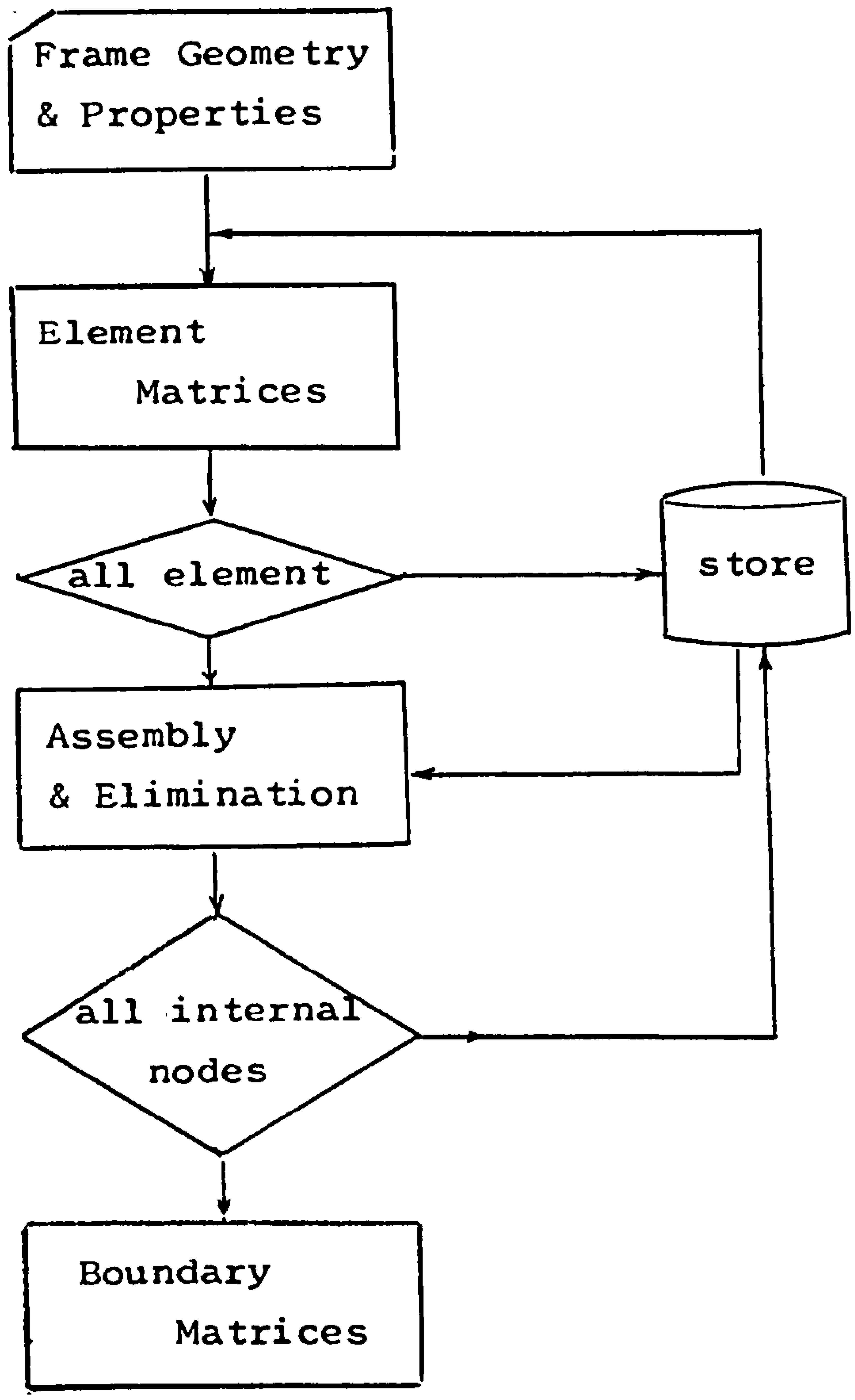

Fig.H.4 Flow Diagram of Loaded Frame Condensation

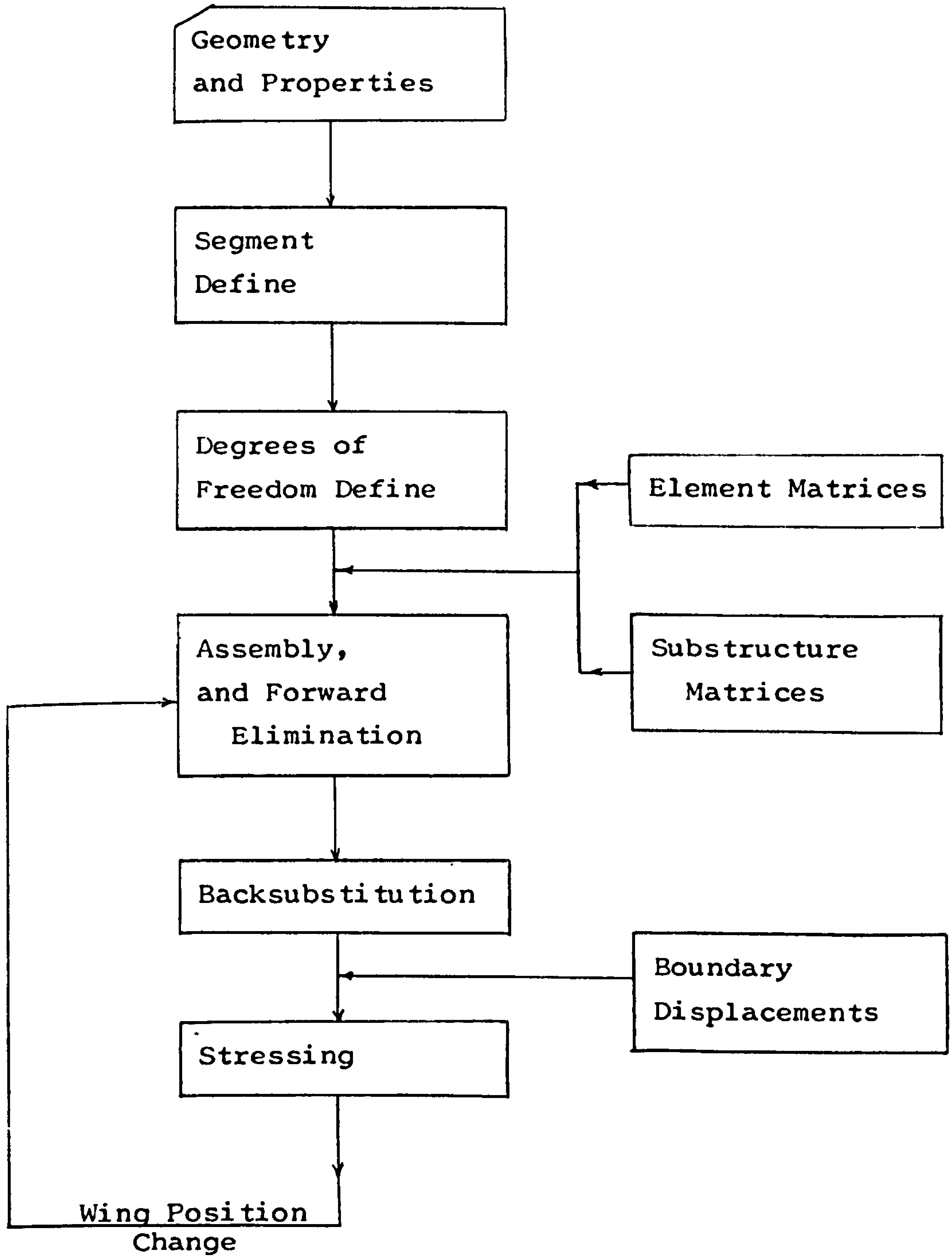

Fig.H.5 Brief Flow Diagram of CENSOL

The nodal degrees of freedom are also defined by the two different types. The one is ordinary active degrees of freedom, and the other is the constrained degrees of freedom. The constrained degrees of freedom do not couple with the active degrees of freedom, so that those are not involved in the elimination or back-substitution process. The stiffness terms of wing-body interaction is replaced by the usual large spring type of stiffnesses for the calculation of reaction forces at the wing pick up points. These degrees of freedom are defined as the third kind.

The degrees of freedom in the fictitious members for the elements in the cutout are also not involved in the elimination or back-substitution process by defining them as the constrained degrees of freedom. Therefore the additional fictitious members for the cut out do not increase the computing time.

The wing pick up points are defined internally at the interval of 11.25 degrees. This program is designed to analyse the all pick up positions in a run of computing.

Three types of the loaded frame are considered in the present investigation as described in the Chapter 3. The structural matrices for the boom-web-boom type deep frames are supplied by the previous LOADFR, while the ring type or rigid diaphragm frames are generated internally in this program. The simple ring frame is modeled by the curved beam element and the diaphragm type frame is idealized by the rigid springs for the appropriate inplane degrees of freedom.

The substructure matrices are assembled before eliminating the degrees of freedom at each longitudinal station where the substructure is attached to.

When the wing stiffness are assembled to the centre body stiffness matrix, the band width is increased by the degrees of freedom between the two loaded frames. Therefore it is no longer possible to use the advantage of constant band width in the solution routine, so that the ordinary Gaussian elimination procedure has been used as described in Chapter 5.

As shown in Fig.H.5, this program is divided into the major three parts. The first one is a preparation process defining the nodes and elements. The second one is the solution process reading in the segment and condensed substructure matrices, and the final procedure is the stressing routine for the centre body. This program is designed to start from or to finish at any above three procedures.

H.7 Input-Output Description

The interfacings of developed programs are basically through the backing storage disc files. The programs are using the unformatted input and the formatted output. To cope with the various parameter variations, each program has been designed to be used for a partial analysis as well as a complete reanalysis.

The condensation program for the outer shells and the main solution program for the centre body require the temporary backing storage scratch files as described in the previous sections.

H.7.1 ELMAT(STDSTF)

A. Function; Generation of the element matrices of shell, ring and stringer elements.

B. Input (channel 1); Free format.

1) Data set 1 : Basic input data and the control variable.

- NC; Number of shell elements in the semi-circle of the body.
- AL; The longitudinal length of element.
- E; Young's modulus of the material used,
- RNU; Poisson's ratio " .
- RHO; Specific weight " .
- R; Radius of the cylindrical body.
- THICK; Thickness of the body skin.
- IANTY; Control variable.
  - =0 for the all three elements,
  - =1 for the ring element only,
  - =2 for the stringer element only,
  - =3 for the shell element only.

2) Data set 2 : i) Data for the thin-walled curved and/ or straight beam element (s).

ii) For IANTY=0, ring data first and stringer data next.

RS; Radius of element shear centre.

RC; " centroid.

PX,PY,PXY; Second moment of inertia and product of inertia about normal axis and radial axis respectively.

PJ; Torsional constant of element.

S ; Cross sectional area.

XC,YC; Shear centre-centroid dislocation in element normal and radial direction respectively.

GA: Warping factor for stand-alone beam analysis otherwise zero.

XB,YB; Shear centre-shell middle surface offset in element coordinates.

C. Output

1) Format : 1X, 6D22.15

2) Channel 3 : Shell element stiffness matrix (24x24) and inertia load matrix (20x1).

3) Channel 4 : Ring element stiffness matrix (12x12) and inertia load matrix (12x1).

4) Channel 5 : Stringer element stiffness matrix (12x12) and inertia load matrix (12x1).

5) Channel 6 : Shell element stress matrix (12x12).

6) Backing Storage Disc Block Size in VAX/VMA per Channel.

Channel	3	4	5	6
Size	27	7	7	25

D. Brief description of subroutines in order of appearance

1) STDBF : Formulation of the stringer element matrices.

2) RSTF : Formulation of the ring element matrices.

3) RINGTR : Transform the ring element matrices to the shell middle surface coordinate.

4) STRSHP : Stringer element displacement assumptions.

5) RNGSHP : Ring element displacement assumptions.

6) CYLSH : Main routine for the formulation of cylindrical shell element stiffness and load matrix calculation.

7) NODAL : Shell element displacement assumption.

8) SHD : Stress-strain relation matrix formulation based on Novzhilov-Lur'e shell theory.

9) SHB : Strain-displacement relation of shell element.

10) SSS : Explicit integral for the shell element stiffness matrix.

11) Matrix manipulation routines : See H.8.

H.7.2 CONSH (SHCOND)

A. Function : Condensation and solution routine for outer body shells.

B. Element Matrices Data and Channels used:

1) Same as out-put of ELMAT (H.7.2.c) for condensation.

2) Boundary displacements for back substitution;

Channel 7 for forward body,

Channel 8 for rear body.

C. General In-put data (Channel 1) :

1) DATA 1 : Title

2) DATA 2 : General input

E; Young's modulus

RNU; Poisson's ratio

T; Thickness of skin

DX; Element length

NC; Number of shell elements in semicircle

NSTR; Number of stringers in the body

IANTY ; Control variable for condensation

=0 for both of forward and rear body.

=1 for forward body only.

=2 for rear body only.

ILDTY; Type of load

=1 for symmetric load with three load conditions.

=2 for antisymmetric loading on the body.

IDIS; Control variable for solution routine

=0 for condensation only.

=1 for condensation and storing the eliminated internal displacements and loads.

=2 for back substitution after having bounary displacements.

3) DATA 3 : Input of outer shells.
Tail load input for rear body only.

(3-1) Definition of shell length, number of rings.

NR; No. of rings

NDELR; No. of elements per ring spacing.

LDC; for arbitrary single load condition

=0 for the present investigation.

=1 for one arbitrary load condition.

(3-2) Load input for LDC=1, otherwise not neccessary.

(3-3) Tail load input for the rear body only.

LN; No. of end tail or fin loading points per semicircle.

NDP; Node number where the tail or fin is attached.

P(1,2,3,4,5,6); Magnitudes of end loading in global cylindrical coordinates.

D. Output and Backing Storage Disc Size Required

1) Format : 1X, 6D22.15

2) Output channels

9; Structural weight, condensed load and stiffness matrices for the forward body.

10; for the rear body.

16; Eliminated stiffnesses of the forward body.

17; Eliminated stiffnesses of the rear body.

18; Eliminated load properties of the forward body.

19; Eliminated load properties of the rear body.

3) Storage Disc Block Size for 8x10 element for the forward body or the rear body;

Channel	9,10	16,17	18,19
Block Size	69	750	180

E. Temporary Backing Storage for the stiffness and the load matrices of the structural segment in Fig.H.2;

	Channel	Blocks
Stiff.	31	175
Load	32	50

F. Brief Description of Subroutines in order of Appearance.

1) REDUCT; Condensation.
2) ELDEF; Definition of structure by the segments in Fig.H.2, and constraints on the degrees of freedom in accordance with the loading conditions.
3) ELFOR; Load matrix define for the segments.
4) BACSUB; Solution routine with given boundary displacement matrices.
5) Matrix manipulation routines; see H.8)

H.7.3 LOADFR

A. Function : Generation of condensed matrices for the boom-web-boom type loaded frames.

B. Input (Channel 1)

1) Data 1 : Control variable and general input
NC, E, RNU, RHO, R; same as previous.
JST, JND; type of frame to be condensed
=1,1 for the forward frame,
=2,2 for the rear frame,
=1,2 for both frames.

IFTY; identity of two loaded frames

=0 for the identical frames at forward and rear.

=1 for the different types of two frames.

ILDTY; loading type as before.

2) Data 2 : Frame properties for each frame

IFR; type of frame

=0 for the boom-web-boom type.

=1 for the ring type.

ISY; Symmetry of the frame around the circumference.

=0 for radially symmetric,

=1 for radially unsymmetric.

RI; basic internal radius.

TW; web thickness.

RPP; element properties as described in H.7.1.B.2. input data set 2. for the outer and inner beams.

3) Data 3 : for ISY=1.

RI; radial coordinate of internal boom nodes in radially unsymmetric boom-web-boom type frame.

C. Output : Condensed stiffnesses and load matrices.

1) Channel 11 : for the forward frame.

2) Channel 12 : for the rear frame.

3) Disc block size required : 69 per frame.

D. Scratch files for the elimination

1) Channel 46 : for temporary storage of the segment stiffness matrix of the boom-web-boom type in circumference.

2) Channel 47 : for segment load matrix.

3) Disc block size required for 8×1 element;

250 blocks for channel 46.

50 blocks for channel 47.

E. Subroutines

1) SSTF; Main routine for the element matrix generation.

2) DPLM; Stress-strain relation of the membrane element for the web.

3) STM; Membrane element matrices formulation main routine.

4) ISOMSH; Isoparametric membrane element shape function.

5) STCR; Curved boom element formulation main routine.
6) STB; Straight boom element formulation routine for the inner boom of radially unsymmetric frame.
7) RSTF; Ring element stiffness matrix formulation.
8) TRNS; Transformation matrix generation.
9) BEAMTR; Coordinate transformation of the outer boom or ring type frame to the shell middle surface coordinate.
10) REDUCT; Condensation to the shell coordinate.
11) RSMB; For the simple ring type frame stiffness and load matrix generation.
12) Matrix Manipulation Routines; see H.8.

H.7.4 CENSOL (SOLUT)

A. Function : Centre body solution routine.

B. Input Matrices and Channels.

Channel No.		
3	;	shell element matrices
4	;	ring element matrices
5	;	stringer element matrices
6	;	shell stress matrices
9	;	forward body
10	;	rear body
11	;	forward loaded frame
12	;	rear loaded frame

C. Input for centre body analysis (Channel 1)

1) TITLE
2) E, RNU, RHO, R, T, DX: As described before.
3) NC; No. of elements in semicircle.
   NSTR; No. of stringers.
   NDXND; No. of element in longitudinal direction per NDRC, NDRF, NDRR.
4) NRC, NRF, NRR; No. of standard rings between two frames, in the forward body and in the rear body respectively.
   NDRC, NDRF, NDRR; No. of elements in NRC, NRF and NRR respectively.

5) ILDTY; Symmetric (=1) and antisymmetric (=2) loading on the body.

LDC ; =0 for the present investigation.
=1 for LDC=1 in CONSH.

6) IIWP, ILWP, IDWP; Initial (IIWP) and final (ILWP) wing pick up position to be investigated with interval of IDWP.

<u>N.B.</u> =1 for 180°
=5 for 90°
=6 for cutout at 135-180 degree
IDWP=1; interval of 22.5 degree

7) ISTRSS; =0 for displacement and stressing of centre body.
=1 for displacement solution only.
=2 for stressing with given displacement by ISTRSS=1.
=1 for displacement only. The results are not stored for ISTRSS=2.

IF1, IF2; Type of the forward and the rear frame respectively.
=0 for diaphragm.
=1 for non-rigid frame.

8) Print out Control Variables.

IDISPR; =0 for print out displacement results.
=1 for no displacement output.

IPRST, LPRST, MPRST; Stressing output from IPRST to LPRST with interval of MPRST.

<u>N.B.</u> 1 to 6; for Nx, Nθ, Nxθ, Mx, Mθ, Mxθ of shell element.

9) STFNPR; Ring and stringer properties as described in H.7.1.B.2

10) LN, NDP, PRAIL; Tail load input as described in H.7.2.C.3.3.

11) IFRTY; Type of frame for nonzero IF1 or IF2

=1 for use of LOADFR output.

=2 for the simple ring frame which can be obtained from the ring stiffener by simple multiplications.

12) FRFCT1, FRFCT2; Multiplication factor to the stand ring stiffener for the forward and for the rear frames with IFRTY=2.

13) IFRSY, FRINTR, FRWEBT, FRMPRP; Frame properties as described in H.7.3.B.2.

14) FRINTR; Frame internal radius of the boom-web-boom type as in H.7.3.B.3.

D. Output.

1) Channel 2; General informations and displacement and/or stress output in the centre body.

2) Channel 25; Average stress output for the graphic program.

E. Scratch Files

1) Channel 50; Temporary storage for the load matrices of segment types in Fig.H.2.

2) Channel 51; for segment stiffness matrix.

3) Channel 52; Backing storage of the eliminated stiffness properties of the centre body.

4) Channel 53; Backing storage of the partial eliminated stiffness properties for different ILWP with IIWP.

5) Disc block sizes to be required.

Channel	50	51	52	53
Blocks	50	135	NISZ	NISZ

* NISZ = No. of element (band width×24-132)/244

F. Subroutines

1) ELDEF; Define the structural element types as segments in Fig.H.2 and define the constraining conditions for each degree of freedom including cutout.

2) ELFOR; Formulation of the load matrices for each segment in Fig.H.2.

3) TLOMT; Assemble load matrices.

4) SOLV; Read in condensed other substructure stiffness matrices and solve the final system equations.

5) AUSRD; Substructure stiffness matrix read in routine for SOLV.

6) STRS; Main stressing routine for the shell element.

7) SAVF; Stress averaging routine at nodal points.

8) RNGSTS; Loaded frames and rings main stress recovery routine.

9) RNF; Internal force calculation routine for RNGTS.

10) STRSTS; Stringer element stress recovery routine.

11) Matrix Manipulation Routines.

H.8 Description of Matrix Manipulation Subroutines

All matrix manipulation routines are quoted from PAFEC 75 (Ref.9). Brief description of subroutines used are as follows:

1) DMATIN; Matrix inversion.
2) DNULL ; Null matrix generation or initialization.
3) DMATMU; Matrix multiplication.
4) DMATRA; Transpose of matrix A times another matrix B.
5) DMULSY; A^T B A

H.8 Listings of Programs

```
      PROGRAM STDSTF
      IMPLICIT DOUBLE PRECISION (A-H,P-Z)
      EXTERNAL DMATIN,DNULL,DMATRA,DMATMU,DMULSY
      DIMENSION RPRO(12,2),W1(576),W2(576),W3(600),W4(576),W5(576)
      COMMON/PROP/E,RNU,RHO,R,THICK,AX,AL,CL,BETA
      COMMON/BPRO/RS,RC,PX,PY,PXY,PJ,S,XC,YC,GA,XB,YB,ES,EX,EY,EXY,GJ
      COMMON/WARP/ D,DI,KG
      COMMON/INER/ACC(24)
      COMMON/GAUS/GW(5),GP(5),GM(7)
      DATA GW/0.236926885056189,0.478628670499366,0.568888888888889,
     +        0.478628670499366,0.236926885056189/
      DATA GP/-0.906179845938664,-0.538469310105683, 0.0 ,
     +        0.538469310105683,0.906179845938664/
CCCCCCCCCCCCCCCCCCCCCCCCCCCCCCCCCCCCCCCCCCCCCCCCCCCCCCCCCCCCCCCCCCCCCCCC
C     CH 1; CONTROL VARIABLES
C     CH 4; OUTPUT OF STD RING  STIFFNESS  MATRIX
C     CH 3; OUTPUT OF STD STRINGER  STIFFNESS  MATRIX
C     CH 2; OUTPUT OF CYL. SHELL ELEMENT STRESS,STIFF   MATRICES
C     CH 5; STRESS MATRIX OF CYL. SHELL ELEMENT
C     OUTPUT ORDER; X,Y,Z,PHIX,PHIZ,PHIY (X: LONGITUDINAL DIRECTION)
C     IANTY=0; FOR CALC. OF  MATRICES OF SHELL,RING AND STRINGER
C     IANTY=1; FOR RING ONLY.    IANTY=2; FOR STRINGER ONLY
C     IANTY=3; FOR SHELL THICKNESS CHANGE ONLY
C     IANTY=4; FOR RING AND STRINGER
CCCCCCCCCCCCCCCCCCCCCCCCCCCCCCCCCCCCCCCCCCCCCCCCCCCCCCCCCCCCCCCCCCCCCCCC
      READ(1,*) NC,AL,E,RNU,RHO,R,THICK,IANTY
      AX=0.5*AL
      PHI=3.1415926541631
      BETA=PHI/2./NC
      CL=2.*R*BETA
      ACC(2)=-1.
      ACC(8)=-1.
      ACC(14)=-1.
      ACC(20)=-1.
C
      IF((IANTY.EQ.0).OR.(IANTY.EQ.3)) CALL CYLSH(W1,W2,W3,W4,W5)
      IF(IANTY.EQ.3) STOP
C
C C C C C C C C C C C C C C C C C C C C C C C C C C C C C C C C C C C C C
C     CURVED AND/OR STRAIGHT THIN-WALLED BEAMM ELEMENT
      JST=1
      JEND=2
      IF(IANTY.EQ.1) JEND=1
      IF(IANTY.EQ.2) JST=2
      IF(IANTY.NE.0) GOTO 150
      CALL DNULL(W1,14,14)
      CALL DNULL(W2,14,14)
150   CONTINUE
C
      READ(1,*)((RPRO(I,J),I=1,12),J=JST,JEND)
C
      DO 500 I=JST,JEND
      RS=RPRO(1,I)
      RC=RPRO(2,I)
      PX=RPRO(3,I)
      PY=RPRO(4,I)
      PXY=RPRO(5,I)
      PJ=RPRO(6,I)
      S=RPRO(7,I)
      XC=RPRO(8,I)
      YC=RPRO(9,I)
```

```
      GA=RPRO(10,I)
      XB=RPRO(11,I)
      YB=RPRO(12,I)
      ES=E*S
      EX=E*PX
      EY=E*PY
      EXY=E*PXY
      GJ=E*PJ/(2.*(1.+RNU))
      D=0.
      DI=0.
      KG=-2
      ND=6
      IF(GA.EQ.0.) GOTO 200
      ND=7
      D=SQRT(GJ/(E*GA))
      DI=1./D
      KG=0
200   CONTINUE
      ND2=2*ND
      NDT=ND2*ND2
      IF(I.EQ.1) CALL RSTF(W1,W2,W3,W4,ND,ND2,NDT)
      IF(JST.EQ.JEND) GOTO 300
      CALL DNULL(W1,ND2,ND2)
      CALL DNULL(W2,ND2,ND2)
300   CONTINUE
      IF(I.EQ.2) CALL STBF(W1,W2,W3,W4,ND,ND2,NDT)
500   CONTINUE
      STOP
      END
CCCCCCCCCCCCCCCCCCCCCCCCCCCCCCCCCCCCCCCCCCCCCCCCCCCCCCCCCCCCCCCCCCCCCCC
      SUBROUTINE STBF(C,B,CINV,TR,ND,ND2,NDT)
C     THIN-WALLED STRAIGHT BEAM ELEMENT FOR ATRINGER
      IMPLICIT DOUBLE PRECISION (A-H,P-Z)
      DIMENSION B(ND2,ND2),C(NDT),CINV(ND2,ND2),TR(NDT)
      COMMON/PROP/E,RNU,RHO,R,T,AX,AL,CTH,BETA
      COMMON/BPRO/RS,RC,PX,PY,PXY,PJ,S,XC,YC,GA,XB,YB,ES,EX,EY,EXY,GJ
      COMMON/WARP/D,DI,KG
      COMMON/INER/ACC(24)
      COMMON/GAUS/GW(5),GP(5),GM(7)
C
      CALL STRSHP(C,Z,AL,XC,YC,GA,ND,ND2,ND2)
      CALL DMATIN(DET,CINV,C,ND2)
C
      DO 150 I=1,2
      J=(I-1)*ND
      B(1+J,J+2)=-1
      B(1+J,J+4)=YB
      B(2+J,J+1)=1.
      B(2+J,J+5)=-XB
      B(2+J,J+6)=YB
      B(3+J,J+3)=-1.
      B(3+J,J+4)=-XB
      B(4+J,J+4)=1.
      B(5+J,J+5)=-1.
      B(6+J,J+6)=-1.
150   CONTINUE
C
      CALL DMATMU(TR,CINV,B,ND2,ND2,ND2)
C
C     STIFFNESS-MATRIX GENERATION
      CALL DNULL(B,ND2,ND2)
```

```
      B(1,1)=ES*AL
      B(2,2)=3.*EY*AL**3
      B(3,3)=4.*EY*AL
      B(4,4)=GJ*AL
      B(5,2)=3.*EXY*AL**3
      B(5,5)=3.*EX*AL**3
      B(6,3)=4.*EXY*AL
      B(6,6)=4.*EX*AL
      IF(GA.EQ.0.) GOTO 200
      B(7,4)=2.*GJ*SINH(0.5*D*AL)/D
      B(7,7)=GJ*SINH(D*AL)/D
      B(8,8)=B(7,7)
200   CONTINUE
C
      DO 300 I=1,ND
      DO 300 J=I+1,ND+1
300   B(I,J)=B(J,I)
      CALL DMULSY(CINV,TR,B,C,ND2,ND2)
      WRITE(5,1)((CINV(I,J),J=1,12),I=1,12)
C
      CALL DNULL(C,12,1)
      WM=RHO*S*AL/2.
      C(2)=-WM
      C(8)=-WM
      WRITE(5,1)(C(I),I=1,12)
C
1     FORMAT(1X,6D22.15)
      RETURN
      END
CCCCCCCCCCCCCCCCCCCCCCCCCCCCCCCCCCCCCCCCCCCCCCCCCCCCCCCCCCCCCCCCCCCCCCCC
      SUBROUTINE RSTF(C,B,CINV,TR,ND,ND2,NDT)
C     THIN-WALLED CURVED BEAM ELEMENT FOR RING
      IMPLICIT DOUBLE PRECISION (A-H,P-Z)
     .DIMENSION C(NDT),B(ND2,ND2),CINV(ND2,ND2),TR(NDT)
      COMMON/PROP/E,RNU,RHO,R,T,AX,AL,CL,BETA
      COMMON/BPRO/RS,RC,PX,PY,PXY,PJ,S,XC,YC,GA,XB,YB,ES,EX,EY,EXY,GJ
      COMMON/RNG/A,RJ,ADI2,C1,C2,G1,G2,G3,G4,G5,G6,B1,B2,B3,B4,B5
      COMMON/WARP/D,DI,KG
      COMMON/INER/ACC(24)
      COMMON/GAUS/GW(5),GP(5),GM(7)
C
      A=1./RS
      RJ=0.5*PJ/(1.+RNU)
      ADI2=0.
      IF(A.NE.0.0.OR.D.NE.0.0) ADI2=1./(A*A+D*D)
      C2=PX*PY-PXY**2
      C1=1./C2
      G1=C1*S*(RC*PXY+YC*PY)
      G2=C1*PXY
      G3=C1*PY*(RJ+GA*A*A)
      G4=C1*S*(RC*PX+YC*PXY)
      G5=C1*PX
      G6=G3*PXY/PY
      B1=0.5*RC*A*(RC*G4+YC*G1)
      B2=0.5*RC*A*(RC*G6+YC*G3)
      B3=RS-RS*RC*G4+B1/A
      B4=RS*RC*G6-B2/A
      B5=0.5*(RS+RC*G3)
C
      CALL RNGSHP(C,Z,ND,ND2,ND2)
      CALL DMATIN(DET,CINV,C,ND2)
```

```
      CALL RINGTR(B,ND2,GA,XB,YB)
      CALL DMATMU(TR,CINV,B,ND2,ND2,ND2)
      CALL DNULL(B,ND2,ND2)
C
      F1=S+PX*G1**2-2.*PXY*G1*G4+PY*G4**2
      F2=-G1*G2*PX+(G2*G4+G1*G5)*PXY-G4*G5*PY
      F3=-G1*G3*PX+(G3*G4+G1*G6)*PXY-G4*G6*PY
      F4=G2*G2*PX-2*G2*G5*PXY+G5*G5*PY
      F5=G2*G3*PX-(G3*G5+G2*G6)*PXY+G5*G6*PY
      F6= -RJ+ A*A*GA+ G3*G3*PX-2.*G3*G6*PXY+G6*G6*PY
      SB=SIN(BETA)
      CB=COS(BETA)
      SB2=SIN(2.*BETA)
      CB2=COS(2.*BETA)
      SH=SINH(D*CL/2.)
      IF(RS.NE.RC) E=E*RC/RS
      CH=COSH(D*CL/2.)
      SH2=SINH(D*CL)
      CH2=COSH(D*CL)
C
      B(1,1)=0.5*E*F1*(RS*SB2+CL)
      B(2,2)=0.5*E*F1*(CL-RS*SB2)
      B(3,1)=2.*E*F2*RS*SB
      B(3,3)=E*F4*CL
      B(4,4)=E*RJ*CL
      B(5,2)=-0.5*E*F3*(CL-RS*SB2)
      B(5,4)=2.*E*RJ*RS*SB
      B(5,5)=0.5*E*F6*(CL-RS*SB2)+E*RJ*CL
      B(6,1)=0.5*E*F3*(CL+RS*SB2)
      B(6,3)=2.*E*RS*F5*SB
      B(6,6)=0.5*E*F6*(CL+RS*SB2)+E*RJ*CL
      IF(GA.EQ.0.) GOTO 150
      B(7,4)=2.*E*RJ*SH*DI
      B(7,5)=2.*E*D*GA*SH*CB
      B(7,7)=E*RJ*DI*SH2
      B(8,6)=2.*E*D*GA*CH*SB
      B(8,8)=B(7,7)
150   CONTINUE
      IF(RS.NE.RC)E=E*RS/RC
      DO 200 I=1,ND
      DO 200 J=I+1,ND+1
      B(I,J)=B(J,I)
200   CONTINUE
C
      CALL DMULSY(CINV,TR,B,C,ND2,ND2)
      WRITE(4,1)((CINV(I,J),J=1,12),I=1,12)
C
      WM=RHO*S*R*BETA
      CALL DNULL(C,12,1)
      C(2)=-WM
      C(8)=-WM
      WRITE(4,1)(C(I),I=1,12)
C
1     FORMAT(1X,6D22.15)
      RETURN
      END
CCCCCCCCCCCCCCCCCCCCCCCCCCCCCCCCCCCCCCCCCCCCCCCCCCCCCCCCCCCCCCCCCCCCCCCC
      SUBROUTINE RINGTR(B,ND2,GA,XB,YB)
C     RING TRANSFORMATION OF COORD. TO GLOBAL CYL. COORD.
      DOUBLE PRECISION B(ND2,ND2),XB,YB,GA
      DO 100 I=1,2
```

```
      J=(I-1)*ND2/2
      B(1+J,J+2)=-1.
      B(1+J,J+5)=YB
      B(2+J,J+3)=1.
      B(2+J,J+4)=XB
      B(2+J,J+6)=YB
      B(3+J,J+1)=1.
      B(3+J,J+5)=-XB
      B(4+J,J+5)=1.
      B(5+J,J+4)=1.
      B(6+J,J+6)=-1.
      IF(GA.EQ.0.) GOTO 100
      B(7+J,J+7)=1.
100   CONTINUE
      RETURN
      END
CCCCCCCCCCCCCCCCCCCCCCCCCCCCCCCCCCCCCCCCCCCCCCCCCCCCCCCCCCCCCCCCCC
      SUBROUTINE STRSHP(C,Z,AL,XC,YC,GA,ND,ND2,M)
      IMPLICIT DOUBLE PRECISION (A-H,P-Z)
      DIMENSION C(M,ND2)
      COMMON/WARP/D,DI,K
C
      DO 200 I=1,2
      J=(I-1)*ND
      Z=0.5*AL*(-1.)**I
      C(J+1,2)=Z**3
      C(1+J,3)=Z**2
      C(J+1,K+9)=Z
      C(J+1,K+10)=1.
      C(2+J,1)=Z
      C(2+J,2)=3.*XC*Z**3
      C(2+J,3)=2.*XC*Z*Z
      C(2+J,5)=3.*YC*Z**3
      C(2+J,6)=2.*YC*Z*Z
      C(J+2,K+14)=1.
      C(3+J,5)=Z**3
      C(3+J,6)=Z**2
      C(J+3,K+11)=Z
      C(J+3,K+12)=1.
      C(4+J,4)=Z
      C(J+4,K+13)=1.
      C(5+J,2)=3.*Z*Z
      C(5+J,3)=2.*Z
      C(J+5,K+9)=1.
      C(6+J,5)=-3.*Z*Z
      C(6+J,6)=-2.*Z
      C(6+J,K+11)=-1.
      IF(GA.EQ.0.) GOTO 200
      C(4+J,7)=SINH(D*Z)/D
      C(4+J,8)=COSH(D*Z)/D
      C(7+J,4)=-1.
      C(7+J,7)=-COSH(D*Z)
      C(7+J,8)=-SINH(D*Z)
200   CONTINUE
      RETURN
      END
CCCCCCCCCCCCCCCCCCCCCCCCCCCCCCCCCCCCCCCCCCCCCCCCCCCCCCCCCCCCCCCCCC
      SUBROUTINE RNGSHP(C,Z,ND,ND2,M)
      IMPLICIT DOUBLE PRECISION (A-H,P-Z)
      DIMENSION C(M,ND2)
      COMMON/PROP/E,RNU,RHO,R,T,AX,AL,CL,BETA
```

```
      COMMON/BPRO/RS,RC,PX,PY,PXY,PJ,S,XC,YC,GA,XB,YB,ES,EX,EY,EXY,GJ
      COMMON/RNG/A,RJ,ADI2,C1,C2,G1,G2,G3,G4,G5,G6,B1,B2,B3,B4,B5
      COMMON/WARP/D,DI,K
C
      DO 100 I=1,2
      J=(I-1)*ND
      Z=0.5*CL*(-1.)**I
      CB=COS(A*Z)
      SB=SIN(A*Z)
      CH=COSH(D*Z)
      SH=SINH(D*Z)
      SBZ=Z*SB
      CBZ=Z*CB
      C(J+1,1)=-B1*SBZ
      C(J+1,2)=B1*CBZ
      C(J+1,3)=RC*(RC*G5+YC*G2)
      C(J+1,5)=B2*CBZ
      C(J+1,6)=B2*SBZ
      C(J+1,K+9)=CB
      C(J+1,K+10)=SB
      C(J+2,1)=B3*SB+B1*Z*CB
      C(J+2,2)=-B3*CB+B1*Z*SB
      C(J+2,3)=G5*RC*Z
      C(J+2,5)=B4*CB+B2*Z*SB
      C(J+2,6)=B4*SB-B2*Z*CB
      C(J+2,K+9)=SB
      C(J+2,K+10)=-CB
      C(J+2,K+11)=1.
      C(J+3,1)=0.5*RC*G1*SBZ
      C(J+3,2)=-0.5*RC*G1*CBZ
      C(J+3,3)=-RC*RS*G2
      C(J+3,4)=RS*Z
      C(J+3,5)=RS*RS*SB-B5*CBZ
      C(J+3,6)=-RS*RS*CB-B5*SBZ
      C(J+3,K+12)=1.
      C(J+3,K+13)=-RS*CB
      C(J+3,K+14)=-RS*SB
      C(J+4,1)=-0.5*RC*A*G1*SBZ
      C(J+4,2)=0.5*RC*A*G1*CBZ
      C(J+4,3)=RC*G2
      C(J+4,5)=B5*A*CBZ
      C(J+4,6)=B5*A*SBZ
      C(J+4,K+13)=CB
      C(J+4,K+14)=SB
      C(J+5,1)=(1.-RC*G4)*SB
      C(J+5,2)=-(1.-RC*G4)*CB
      C(J+5,3)=G5*RC*A*Z
      C(J+5,5)=RC*G6*CB
      C(J+5,6)=RC*G6*SB
      C(J+5,K+11)=A
      C(J+6,1)=-0.5*RC*G1*(A*Z*CB+SB)
      C(J+6,2)=-0.5*RC*G1*(A*Z*SB-CB)
      C(J+6,4)=-RS
      C(J+6,5)=-RS*CB-B5*(A*Z*SB-CB)
      C(J+6,6)=-RS*SB+B5*(A*Z*CB+SB)
      C(J+6,K+13)=-SB
      C(J+6,K+14)=CB
      IF(GA.EQ.0.) GOTO 100
      C(J+3,7)=A*DI*ADI2*SH
      C(J+3,8)=A*DI*ADI2*CH
      C(J+4,7)=D*ADI2*SH
```

```
      C(J+4,8)=D*ADI2*CH
      C(J+6,7)=-A*ADI2*CH
      C(J+6,8)=-A*ADI2*SH
      C(J+7,4)=-1.
      C(J+7,5)=-CB
      C(J+7,6)=-SB
      C(J+7,7)=-CH
      C(J+7,8)=-SH
100   CONTINUE
      RETURN
      END
CCCCCCCCCCCCCCCCCCCCCCCCCCCCCCCCCCCCCCCCCCCCCCCCCCCCCCCCCCCCCCCCCCCCCCCC
      SUBROUTINE CYLSH(C,CINV,W,S,TR)
C     CYLINDRICAL SHELL ELEMENT
      IMPLICIT DOUBLE PRECISION (A-H,P-Z)
      DIMENSION DD(6,6),C(576),CINV(576),W(600),S(576),TR(576)
      COMMON/PROP/E,RNU,RHO,R,T,AX,AL,CL,BETA
      COMMON/GAUS/GW(5),GP(5),GM(7)
      COMMON/INER/ACC(24)
CCCCCCCCCCCCCCCCCCCCCCCCCCCCCCCCCCCCCCCCCCCCCCCCCCCCCCCCCCCCCCCCCCCCCCCC
C     E;YOUNG'S MODULUS   RNU;POISSION'S RATIO  RHO;MASS DENSITY       C
C     R; RADIUS  T; THICKNESS   AX;HALF OF ELEMENT LENGTH IN           C
C     STRAIGHT LINE   BETA; HALF OF ELEMENT CIRCUMFERENTIAL ANGLE      C
CCCCCCCCCCCCCCCCCCCCCCCCCCCCCCCCCCCCCCCCCCCCCCCCCCCCCCCCCCCCCCCCCCCCCCCC
C
      CALL SHD(DD)
      CALL NODAL(R,AX,BETA,C,CINV,W,S,DD,4)
C     CALCULATION  AND WRITING OF STRESS MATRXI IN CYL. COORD.
      CALL DNULL(C,20,24)
      DO 150 I1=1,4
      J=(I1-1)*125
      DO 150 I=1,5
      K=J+21*I-20
      C(K)=1.
150   CONTINUE
      CALL DMATMU(TR,CINV,C,20,20,24)
      CALL DMATMU(S,W,TR,24,20,24)
      WRITE(6,1)(S(I),I=1,576)
C
C     CALCULATION AND STORAGE TO DISC OF STIFFNESS MATRIX
      CALL DNULL(S,24,24)
      CALL SSS(S)
      CALL DMULSY(CINV,TR,S,C,20,24)
C
      FS=-0.05*E*(T**3)/(12.*(1.-RNU*RNU))
      DO 200 I=6,24,6
      DO 200 J=6,24,6
      K=(J-1)*24+I
      CINV(K)=FS
      IF(I.EQ.J) CINV(K)=-2.*FS
200   CONTINUE
      WRITE(3,1)(CINV(I),I=1,576)
C
      CALL DNULL(W,24,1)
      WM=RHO*CL*AL*T/4.
      W(2)=-WM
      W(8)=-WM
      W(14)=-WM
      W(20)=-WM
      WRITE(3,1)(W(I),I=1,24)
C
```

```
1         FORMAT(1X,6D22.15)
          RETURN
          END
CCCCCCCCCCCCCCCCCCCCCCCCCCCCCCCCCCCCCCCCCCCCCCCCCCCCCCCCCCCCCCCCCC
          SUBROUTINE NODAL(R,X,BETA,C,CINV,W,B,D,IN)
C         SHELL ELEMENT SHPAE FUNCTION
          IMPLICIT DOUBLE PRECISION (A-H,P-Z)
          DIMENSION C(576),CINV(576),W(600),B(576),D(6,6)
C
          KN=IN*5
          DO 200 I=1,IN
          I1=(I-1)*5
          Z=-X
          PI=BETA
          IF((I.EQ.3).OR.(I.EQ.4)) Z=X
          IF((I.EQ.1).OR.(I.EQ.3)) PI=-BETA
          IF(IN.EQ.4) GOTO 100
          Z=X
          PI=BETA
100       CONTINUE
          RC=R*COS(PI)
          RS=R*SIN(PI)
          R2=R*R
          R3=R**3
          C(I1+1+KN)=RC
          C(I1+1+3*KN)=RS
          C(I1+1+4*KN)=1.
          C(I1+6*KN+1)=Z
          C(I1+7*KN+1)=Z*PI
          C(I1+10*KN+1)=R*PI
          C(I1+16*KN+1)=-0.5*R3*PI**2
          C(I1+18*KN+1)=R3*PI*(1.-PI*PI/6.)
          C(I1+19*KN+1)=-R2*PI
          C(I1+3)=SIN(PI)
          C(I1+KN+3)=Z*SIN(PI)
          C(I1+2*KN+3)=-COS(PI)
          C(I1+3*KN+3)=-Z*COS(PI)
          C(I1+5*KN+3)=1.
          C(I1+15*KN+3)=R2*PI
          C(I1+16*KN+3)=R2*Z*PI
          C(I1+17*KN+3)=R2*PI**2*0.5
          C(I1+18*KN+3)=R2*Z*(PI**2*0.5-1.)
          C(I1+19*KN+3)=R*Z
          C(I1+2)=-COS(PI)
          C(I1+KN+2)=-Z*COS(PI)
          C(I1+2*KN+2)=-SIN(PI)
          C(I1+3*KN+2)=-Z*SIN(PI)
          C(I1+8*KN+2)=R
          C(I1+9*KN+2)=R*Z
          C(I1+11*KN+2)=-0.5*Z*Z
          C(I1+12*KN+2)=-Z**3/6.
          C(I1+13*KN+2)=-0.5*Z**2*PI
          C(I1+14*KN+2)=-PI*Z**3/6.
          C(I1+15*KN+2)=-R2
          C(I1+16*KN+2)=-R2*Z
          C(I1+17*KN+2)=-R2*PI
          C(I1+18*KN+2)=-R2*Z*PI
          C(I1+KN+5)=-COS(PI)
          C(I1+3*KN+5)=-SIN(PI)
          C(I1+9*KN+5)=R
          C(I1+11*KN+5)=-Z
```

```
      C(I1+12*KN+5)=-Z**2/2.
      C(I1+13*KN+5)=-Z*PI
      C(I1+14*KN+5)=-0.5*Z**2*PI
      C(I1+16*KN+5)=-R2
      C(I1+18*KN+5)=-R2*PI
      C(I1+5*KN+4)=-1./R
      C(I1+13*KN+4)=-0.5*Z**2/R
      C(I1+14*KN+4)=-Z**3/R/6.
      C(I1+15*KN+4)=-R*PI
      C(I1+16*KN+4)=-R*Z*PI
      C(I1+17*KN+4)=-R*(1.+PI*PI*0.5)
      C(I1+18*KN+4)=-0.5*R*Z*PI*PI
      C(I1+19*KN+4)=-Z
C
      IF(IN.EQ.1) GOTO 200
      Y=PI*R
      CALL SHB(B,Z,Y)
      CALL DMATMU(CINV,D,B,6,6,20)
      DO 150 J=1,6
      DO 150 K=1,20
      L=(K-1)*24+J+(I-1)*6
      M=(K-1)*6+J
      W(L)=W(L)+CINV(M)
150   CONTINUE
200   CONTINUE
      IF(IN.EQ.1) RETURN
      CALL DMATIN(DET,CINV,C,20)
      RETURN
      END
CCCCCCCCCCCCCCCCCCCCCCCCCCCCCCCCCCCCCCCCCCCCCCCCCCCCCCCCCCCCCCCCCCCCCCCCCC
      SUBROUTINE SHD(DD)
C     STRESS STRAIN RELATION OF NOVOZHILOV-LUR'E SHELL THEORY
      IMPLICIT DOUBLE PRECISION (A-H,P-Z)
      DIMENSION DD(6,6)
      COMMON/PROP/E,RNU,RHO,R,T,AX,AL,CL,BETA
C
      C=E*T/(1.-RNU**2)
      D=C*T*T/12
      H=(1.-RNU)/2.
      DD(1,1)=C
      DD(1,2)=C*RNU
      DD(1,4)=-D/R
      DD(2,2)=C
      DD(2,5)=-D/R
      DD(3,3)=H*(C+D)
      DD(3,6)=-H*D/R
      DD(4,4)=D
      DD(4,5)=D*RNU
      DD(5,5)=D
      DD(6,6)=4.*H*D
      DO 100 I=1,5
      DO 100 J=I+1,6
      DD(J,I)=DD(I,J)
100   CONTINUE
      RETURN
      END
CCCCCCCCCCCCCCCCCCCCCCCCCCCCCCCCCCCCCCCCCCCCCCCCCCCCCCCCCCCCCCCCCCCCCCCCCC
      SUBROUTINE SHB(B,X,Y)
C     STRAIN DISPLACEMENT RELATION OF NOVOZHILOV THEORY
      IMPLICIT DOUBLE PRECISION (A-H,P-Z)
      DIMENSION B(6,20)
```

```
      COMMON/PRCP/E,RNU,RHO,R,T,AX,AL,CL,BETA
C
      B(1,7)=1.
      B(1,8)=SIN(Y/R)
      B(2,9)=1.
      B(2,10)=X
      B(2,12)=-0.5*X*X/R
      B(2,13)=-X**3/(6.*R)
      B(2,14)=-X*X*Y/(2.*R*R)
      B(2,15)=-X**3 *Y/(6.*R*R)
      B(3,11)=1.
      B(4,8)=SIN(Y/R)/R
      B(4,12)=1.
      B(4,13)=X
      B(4,14)=Y/R
      B(4,15)=X*Y/R
      B(5,16)=1.
      B(5,17)=X
      B(5,18)=Y/R
      B(5,19)=X*Y/R
      B(6,14)=X/R
      B(6,15)=X*X/(2.*R)
      B(6,17)=Y
      B(6,19)=Y*Y/(2.*R)
      B(6,20)=1.
      RETURN
      END
CCCCCCCCCCCCCCCCCCCCCCCCCCCCCCCCCCCCCCCCCCCCCCCCCCCCCCCCCCCCCCCCCCCCCCCC
      SUBROUTINE SSS(B)
      IMPLICIT DOUBLE PRECISION (A-H,P-Z)
      DIMENSION B(20,20)
      COMMON/PRCP/E,RNU,RHO,R,T,AHALF,A,BL,BETA
      CALL DNULL(B,20,20)
      D1=E*T/(1.-RNU*RNU)
      D2=RNU*D1
      D3=(1.-RNU)*D1/2.
      G1=E*T**3/12./(1.-RNU**2)
      G2=RNU*G1
      G3=(1.-RNU)*0.5*G1
      C1=A*BL
      C3=A*BL**3/12.
      C2=A**3*BL/12.
      C4=(A*BL/12)**3*12.
      C5=A**5*BL/80.
      C6=A**5*BL**3/960.
      C7=A*BL**5/80.
      C8=A**7*BL**3/5376
      C9=A**7*BL/448
      B(7,7)=D1*C1
      B(7,9)=D2*C1
      B(7,12)=G1*C1/R-D2*C2/R*0.5
      B(8,8)=D1*C3/R/R+(D3+G3)*C2/R/R
      B(8,14)=G1*C3/R**3-G3*C2/R**3-D2*C4/R**3*0.5
      B(9,9)=D1*C1
      B(9,12)=-D1*C2*0.5/R
      B(9,16)=-G1*C1/R
      B(14,14)=G1*C3/R**2+G3*C2*4./R**2+D1*C6*0.25/R**4
      B(14,18)=G1*C4*0.5/R**4+G2*C3/R/R
      B(11,11)=(D3+G3)*C1
      B(11,15)=-G3*C2*0.5/R**2
      B(11,19)=-G3*C3*0.5/R**2
```

```
      B(11,20)=-G3*C1/R
      B(15,15)=G1*C4/R**2+D1*C8/36./R**4 + G3*C5/R/R
      B(15,19)=G1*(1.+RNU)*0.5*C4/R**2+G3*A**5*BL**3/5760./R**4
      B(15,20)=G3*C2/R*2.
      B(10,10)=D1*C2
      B(10,13)=-D1*C5/6./R
      B(10,17)=-G1*C2/R
      B(12,12)=D1*C5*0.25/R**2+G1*C1
      B(12,16)=C2*0.5*G1/R**2+G2*C1
      B(13,13)=G1*C2+D1*C9/36/R**2
      B(13,17)=G1*C5/6./R**2+G2*C2
      B(16,16)=G1*C1
      B(17,17)=G1*C2+4.*G3*C3
      B(18,18)=G1*C3/R**2
      B(19,19)=G3*C7/R**2 +G1*C4/R/R
      B(19,20)=G3*C3*2./R
      B(20,20)=4.*G3*C1
      DO 100 I=7,19
      DO 100 J=I+1,20
      B(J,I)=B(I,J)
100   CONTINUE
      RETURN
      END
```

```
      PROGRAM SHCONC
      IMPLICIT DOUBLE PRECISION (A-H,P-Z)
      DIMENSION SL(24),RL(12),TL(12),SSH(24,24),SRI(12,12),STR(12,12)
     + ,SE(24,24),P(4000),EP(24),LDEF(240),IB(1340),TITLE(80),AA(2300)
      COMMON/GEOM/NC,NSTR,NAX,NEL,NOD,NYD,NXD,NDT,NX,NY,NV,ILDTY
CCCCCCCCCCCCCCCCCCCCCCCCCCCCCCCCCCCCCCCCCCCCCCCCCCCCCCCCCCCCCCCCCCCCCCCC
C     %1; FCR CONTROL VARIABLES ,RING SPACING AND INERTIA LOAD DATA C
C     %3; SHELL ELEMENT STRESS, STIFFNESS AND INERTIA MATRIX        C
C     %4; STD RING ELEMENT STIFFNESS AND INERTIA MATRIX             C
C     %5; STD STRING. ELEM. STIFFNESS AND INERTIA MATRIX            C
C     %6; CONDENSED STIFF. AND LOAD MATRIX OUTPUT OF FWD SHELL      C
C     %7; CONDENSED STOFF. AND LOAD MATRIX OF REAR SHELL            C
C     %11 ; TEMPORARY STORAGE OF ELEM. STFF. OF 6 TYPE OF COMB.     C
C     NLO : NO. OF LOAD CASE                                        C
C     NDELRC : NO. OF DX IN RING SPACE    NR: TOTAL NO. OF RING     C
C     NSTR : NO. OF STANDARD STRINGERS IN SHELL(0,4,8,12,16,24)     C
C     IN CENTRE SHELL (C: NO STD RING BETWEEN FRAME)                C
C     ILDTY : =1; SYMMETRIC, =2; ANTISYM. LOADING                   C
C     IANTY : =1; FOR FWD SHELL =2; FOR REAR SHELL ONLY & =0; BOTH  C
C     IENDC : =0;FRAMED END      =1;DIAPHRAM END                    C
C     LDC :CONTROL PARAMETER FOR SINGLE LOADING CASE =1             C
C     IDIS : DISPLACEMENT CALCULATICN ID. =1 FOR STORING OF ELIMINA-C
C           =2 FOR BACKSUBSTITUTE   =0 FOR CONDENSATION ONLY        C
CCCCCCCCCCCCCCCCCCCCCCCCCCCCCCCCCCCCCCCCCCCCCCCCCCCCCCCCCCCCCCCCCCCCCCCC
C
      READ(1,51)(TITLE(I),I=1,80)
      IF(IDIS.NE.1) WRITE(2,52)(TITLE(I),I=1,80)
      READ(1,*) E,RNU,R,T,DX,NC,NSTR,IANTY,ILDTY,IDIS
C C C C C C C C C C C C C C C C C C C C C C C C C C C C C C C C C C C C
      NV=6
      NY=NC+1
      NYD=NY*NV
      JST=1
      JND=2
      IF(IANTY.EQ.1) JNC=1
      IF(IANTY.EQ.2) JST=2
      BETA=3.1415926541631/NC
      IF(IDIS.EQ.2) GOTC 135
C
C C C C C C C C C C C C C C C C C C C C C C C C C C C C C C C C C C C C
C
      READ(3,1)((SSH(I,J),I=1,24),J=1,24)
      READ(4,1)((SRI(I,J),I=1,12),J=1,12)
      READ(5,1)((STR(I,J),I=1,12),J=1,12)
      IF(ILDTY.NE.1) GOTO 200
      READ(3,1)(SL(I),I=1,24)
      READ(4,1)(RL(I),I=1,12)
      READ(5,1)(TL(I),I=1,12)
C
C C C C C C C C C C C C C C C C C C C C C C C C C C C C C C C C C C C C
C
200   CONTINUE
      OPEN(UNIT=31,STATUS='SCRATCH',ACCESS='DIRECT',
     + INITIALSIZE=175,RECORDSIZE=1152)
      IF(ILDTY.EQ.1) OPEN(UNIT=32,STATUS='SCRATCH',ACCESS='DIRECT',
     + INITIALSIZE=50,RECORDSIZE=48)
135   CONTINUE
C
      ICHS=16
      IF(IANTY.EQ.2) ICHS=17
      ICHP=18
```

```
      IF(IANTY.EQ.2) ICHP=19
      IF(IDIS.EQ.1) OPEN(UNIT=ICHS,STATUS='NEW',ACCESS='DIRECT',
     + INITIALSIZE=1000,RECORDSIZE=1452)
      IF(IDIS.EQ.2) OPEN(UNIT=ICHS,STATUS='OLD',ACCESS='DIRECT',
     + INITIALSIZE=1000,RECORDSIZE=1452)
      IF(IDIS.EQ.1) OPEN(UNIT=ICHP,STATUS='NEW',ACCESS='DIRECT',
     + INITIALSIZE=500,RECORDSIZE=1500)
      IF(IDIS.EQ.2) OPEN(UNIT=ICHP,STATUS='OLD',ACCESS='DIRECT',
     + INITIALSIZE=500,RECORDSIZE=1500)
C
C C C C C C C C C C C C C C C C C C C C C C C C C C C C C C C C C C C C
C
      DO 800 JSH=JST,JND
      READ(1,*)NR,NDELR,LDC
      IF(IDIS.EQ.2) READ(1,*) X0
C
C C C C C C C C C C C C C C C C C C C C C C C C C C C C C C C C C C C C
C
      NAX=(NR-1)*NDELR
      NX=NAX+1
      XT=NAX*DX
      NXD=NX*NV
      NOD=NX*NY
      NEL=NAX*NC
      NDT=NOD*NV
      NLO=3
      IF(LDC.EQ.1.OR.ILDTY.EQ.2) NLO=1
      IF(IDIS.EQ.2) GOTO 500
C C C C C C C C C C C C C C C C C C C C C C C C C C C C C C C C C C C C
      IF(JSH.EQ.1) GOTO 350
      DO 250 J=1,12
      DO 250 I=1,24
      SE(I,J)=SSH(I,J+12)
      SE(I,J+12)=SSH(I,J)
250   CONTINUE
      DO 280 J=1,24
      DO 280 I=1,12
      SSH(I,J)=SE(I+12,J)
      SSH(I+12,J)=SE(I,J)
280   CONTINUE
      DO 300 J=1,12
      DO 300 I=1,6
      SE(I,J)=STR(I+6,J)
      SE(I+6,J)=STR(I,J)
300   CONTINUE
      DO 330 J=1,6
      DO 330 I=1,12
      STR(I,J)=SE(I,J+6)
      STR(I,J+6)=SE(I,J)
330   CONTINUE
350   CONTINUE
C C C C C C C C C C C C C C C C C C C C C C C C C C C C C C C C C C C C
      IDT=4
      IF(NSTR.GE.16) IDT=2
C
      DO 500 IDEL=1,IDT
      DO 400 J=1,24
      EP(J)=SL(J)
      DO 400 I=1,24
      SE(I,J)=SSH(I,J)
400   CONTINUE
```

```
      GOTO (450,410,430,410),IDEL
410   CONTINUE
      DO 420 J=1,12
      EP(J)=EP(J)+RL(J)
      DO 420 I=1,12
420   SE(I,J)=SE(I,J)+SRI(I,J)
      IF(IDEL.EQ.2) GOTO 450
      IF(NSTR.EQ.0) GOTO 450
430   CONTINUE
      DO 440 J=1,12
      K=NV
      IF(J.GT.NV) K=2*NV
      EP(J+K)=EP(J+K)+TL(J)
      DO 440 I=1,12
      L=NV
      IF(I.GT.NV) L=2*NV
      SE(I+L,J+K)=SE(I+L,J+K)+STR(I,J)
440   CONTINUE
450   CONTINUE
C
      IF(NSTR.LT.16) GOTO 480
      DO 470 I1=1,2
      M=(I1-1)*NV
      DO 460 J=1,12
      L=0
      IF(J.GT.NV) L=NV
      EP(J+L+M)=EP(J+L+M)+0.5*TL(J)
      DO 460 I=1,12
      K=0
      IF(I.GT.NV) K=NV
      SE(I+K+M,J+L+M)=SE(I+K+M,J+L+M)+0.5*STR(I,J)
460   CONTINUE
470   CONTINUE
480   CONTINUE
      WRITE(UNIT=31,REC=IDEL)((SE(I,J),I=1,NV*4),J=1,NV*4)
      IF(ILDTY.EQ.1) WRITE(UNIT=32,REC=IDEL)(EP(I),I=1,NV*4)
500   CONTINUE
C     DEFINE ELEMENTS ,LOADS ,ELEMENT TYPE AND CONSTRAINTS
      CALL ELDEF(LDEF,IB,NR,NDELR,ILDTY,IDIS)
      IF(IDIS.EQ.2) GOTO 700
      IF(LDC.EQ.1) GOTO 550
C
      IF(ILDTY.EQ.1) CALL ELFOR(LDEF,P,EP,XM,DX,NDELR,NLO,JSH)
C
550   CONTINUE
      IF(JSH.EQ.1) GOTO 700
      LL=(NLO-1)*NDT
      READ(1,*) LN,(NDP,(P((NDP-1)*NV+I+LL),I=1,NV),J=1,LN)
600   CONTINUE
700   CONTINUE
C
C     REDUCTION  OR  BACKSUBSTITUTION
C
      IF(ILDTY.EQ.1.AND.IDIS.EQ.1) WRITE(JSH+8,*) XM
      ICH=JSH+8
      n2=(nyd+2*nv+1)*(nyd+2*nv)/2
      IF(IDIS.EQ.1) CALL REDUCT(LDEF,IB,P,SE,AA,ICH,NLO,JSH,ICHS,ICHP
     + ,N2)
      IF(IDIS.EQ.2) CALL BACSUB(AA,IB,P,SE,ICHS,ICHP,NLO,DX,N2,X0)
      IF((JSH.EQ.1).AND.(IANTY.EQ.0)) CALL DNULL(P,NLO,NDT)
800   CONTINUE
```

```
1       FORMAT(1X,6D22.15)
10      FORMAT(/,3X,'IDEL=2',/,(1X,12D10.3))
51      FORMAT(80A1)
52      FORMAT(5X,80A1)
        STOP
        END
CCCCCCCCCCCCCCCCCCCCCCCCCCCCCCCCCCCCCCCCCCCCCCCCCCCCCCCCCCCCCCCCCCCCCCCC
C
        SUBROUTINE REDUCT(LDEF,IB,P,SE,AA,ICH,NLO,JSH,ICHS,ICHP,N2)
        IMPLICIT DOUBLE PRECISION (A-H,P-Z)
        DIMENSION AA(N2),SE(24,24),P(NDT,NLO),LDEF(NEL),IB(NDT)
        COMMON/GEOM/NC,NSTR,NAX,NEL,NOD,NYD,NXD,NDT,NX,NY,NV,ILDTY
C C C C C C C C C C C C C C C C C C C C C C C C C C C C C C C C C C C C
        NLOC=NLO
        IF(JSH.EQ.1) NLOC=NLO-1
        L=1
        IADR=0
        M=12
        N1=NYD + M
        IF(JSH.EQ.2) CALL DNULL(AA,N2,1)
C C C C C C C C C C C C C C C C C C C C C C C C C C C C C C C C C C C C
        DO 1100 NEX=1,NAX
        DO 1050 NEY=1,NC
        NUMEL=(NEX-1)*NC+NEY
        IDEL=LDEF(NUMEL)
C
        READ(UNIT=31,REC=IDEL)((SE(I,J),I=1,24),J=1,24)
2       FORMAT(/,3X,'SE FOR ELE. 1',/,(1X,12D10.3))
C
        KA=0
        KB=N2-(M+1)*M/2
C C C C C C C C C C C C C C C C C C C C C C C C C C C C C C C C C C C C
        DO 300 I=1,M
        IM=I+M
        DO 100 J=I,M
        JM=J+M
        KAJ=KA+J
        AA(KAJ)=AA(KAJ)+SE(I,J)
        KBJ=KB+J
        AA(KBJ)=AA(KBJ)+SE(IM,JM)
100     CONTINUE
        DO 200 J=1,M
        JM=J+M
        KAJ=KA+J+NYD
        AA(KAJ)=AA(KAJ)+SE(I,JM)
200     CONTINUE
        KA=KA+N1-I
        KB=KB+M-I
300     CONTINUE
C C C C C C C C C C C C C C C C C C C C C C C C C C C C C C C C C C C C
C
        LEND=NV
        IF(NEY.EQ.NC) LEND=M
        DO 600 IL=1,LEND
        IF(IB(L).EQ.1) GOTO 600
        ID=(2*N1-IL)*(IL-1)/2+IL
        LSTI=N1-IL
        LSTJ=ID+LSTI
        ICON=N1-IL
        DO 500 I=1,LSTI
        IPL=I+L
```

```
      IF(IB(IPL).EQ.1) GOTO 500
      IDPI=ID+I
      IF(AA(IDPI).EC.0.) GOTO 500
      FACT=AA(IDPI)/AA(ID)
      DO 350 IP=1,NLOC
350   P(IPL,IP)=P(IPL,IP)-P(L,IP)*FACT
      DO 400 J=IDPI,LSTJ
      IPJ=ICON+J
      IF(AA(J).EQ.0.0) GOTO 400
      AA(IPJ)=AA(IPJ)-AA(J)*FACT
400   CONTINUE
500   ICON=ICON+N1-I-IL
600   L=L+1
C C C C C C C C C C C C C C C C C C C C C C C C C C C C C C C C C C C
      IF(NEX.EQ.NAX.AND.NEY.EQ.NC) GOTO 1200
      NEND=(2*N1-LEND+1)*LEND/2
      IADR=IADR+1
      WRITE(UNIT=ICHS,REC=IADR)(AA(I),I=1,NEND)
650   CONTINUE
      LSTI=N1-LEND
      NEND=NEND+1
      DO 900 I=1,LSTI
      KA=(2*N1-I)*(I-1)/2+I
      LSTJ=KA+LSTI-I
      DO 700 J=KA,LSTJ
      AA(J)=AA(NEND)
      NEND=NEND+1
700   CONTINUE
      JST=LSTJ+1
      JEND=LSTJ+LEND
      DO 800 J=JST,JEND
      AA(J)=0.
800   CONTINUE
900   CONTINUE
C
      NEND=N2-(LEND+1)*LEND/2+1
      DO 1000 I=NEND,N2
      AA(I)=0.
1000  CONTINUE
1050  CONTINUE
1100  CONTINUE
C C C C C C C C C C C C C C C C C C C C C C C C C C C C C C C C C C C C
1200  CONTINUE
1     FORMAT(1X,6D22.15)
      JST=(N1+NYD+1)*NV
      IF(JSH.EQ.1.AND.ILDTY.EQ.2) GCTO 1500
      IF(NLCC.NE.0) WRITE(ICH,1)((P(I,J),I=NDT-NYD+1,NDT),J=1,NLOC)
1500  WRITE(ICH,1)(AA(I),I=JST+1,N2)
C
      IADR=IADR+1
      NEND=(2*N1-2*NV+1)*NV
      WRITE(UNIT=ICHS,REC=IADR)(AA(I),I=1,NEND)
      WRITE(UNIT=ICHP,REC=1) IADR,L
      IF(NLOC.EQ.0) RETURN
      DO 1550 J=1,NLO
1550  WRITE(UNIT=ICHP,REC=J+1) (P(I,J),I=1,NDT-NYD)
      RETURN
      END
CCCCCCCCCCCCCCCCCCCCCCCCCCCCCCCCCCCCCCCCCCCCCCCCCCCCCCCCCCCCCCCCCCCCCC
      SUBROUTINE ELCEF(LDEF,IB,NR,NCELR,ILDTY,IDIS)
      IMPLICIT DOUBLE PRECISION (A-H,P-Z)
```

```
      DIMENSION LDEF(NEL),IB(NDT),NLD(3),ISTRPS(12)
      COMMON/GEOM/NC,NSTR,NAX,NEL,NOD,NYD,NXD,NDT,NX,NY,NV
C
      IF(IDIS.EQ.2) GOTO 310
      DO 120 I=1,NC
120   ISTRPS(I)=1
      IF(NSTR.GE.16) GOTO 200
      IF(NSTR.EQ.0) GOTO 200
      M=NC/NSTR
      N=2*M
      DO 150 I=M,NC,N
150   ISTRPS(I)=3
200   CONTINUE
C
      N=0
      if(nr.le.1) goto 310
      DO 300 I=1,NR-1
      DO 300 J=1,NDELR
      M=0
      IF(J.EQ.1) M=1
      DO 300 K=1,NC
      N=N+1
      LDEF(N)=ISTRPS(K)+M
300   CONTINUE
310   continue
C     RESTRAINT FOR LOAD CONDITION ON THE LINE OF SYMMETRY
      IF(ILDTY.EQ.2) GOTO 320
      NLD(1)=3
      NLD(2)=4
      NLD(3)=6
      GOTO 330
320   CONTINUE
      NLD(1)=1
      NLD(2)=2
      NLD(3)=5
330   CONTINUE
      DO 500 I=1,NX
      M=(I-1)*NYD
      N=I*NYD-NV
      DO 500 J=1,3
      K=NLD(J)
      IB(M+K)=1
      IB(N+K)=1
500   CONTINUE
      RETURN
      END
CCCCCCCCCCCCCCCCCCCCCCCCCCCCCCCCCCCCCCCCCCCCCCCCCCCCCCCCCCCCCCCCCCCCCCCCCC
      SUBROUTINE ELFOR(LDEF,P,EP,XM,DX,NDELR,NLO,JSH)
      IMPLICIT DOUBLE PRECISION(A-H,P-Z)
      DIMENSION LDEF(NEL),P(NDT,NLO),EP(24)
      COMMON/GEOM/NC,NSTR,NAX,NEL,NOD,NYD,NXD,NDT,NX,NY,NV
      NLOC=NLO
      IF(JSH.EQ.1) NLOC=NLO-1
C
      N=0
      XM=0.
      BETA=3.1415926541631/NC
      DO 200 IX=1,NAX
      C1=(NAX-IX+NDELR+1)*DX*((-1.)**(JSH-1))
      C2=(NAX-IX+NDELR)*DX*((-1.)**(JSH-1))
      KK=(IX-1)*NYD
```

```
      DO 200 IY=1,NC
      B1=BETA*(IY-1)
      B2=BETA*IY
      K=KK+(IY-1)*NV
      N=N+1
      ID=LDEF(N)
      READ(UNIT=32,REC=ID) (EP(I),I=1,4*NV)
      DO 100 I=2,2*NV,NV
      XM=XM+EP(I)+EP(I+2*NV)
      J=I+NYD
      B=B1
      IF(I.GT.NV) B=B2
      P(K+I,1)=P(K+I,1)+COS(B)*EP(I)
      P(K+I+1,1)=P(K+I+1,1)-SIN(B)*EP(I)
      P(K+J,1)=P(K+J,1)+COS(B)*EP(I+2*NV)
      P(K+J+1,1)=P(K+J+1,1)-SIN(B)*EP(I+2*NV)
      P(K+I,2)=P(K+I,2)+COS(B)*C1*EP(I)
      P(K+I+1,2)=P(K+I+1,2)-SIN(B)*C1*EP(I)
      P(K+J,2)=P(K+J,2)+COS(B)*C2*EP(I+2*NV)
      P(K+J+1,2)=P(K+J+1,2)-SIN(B)*C2*EP(I+2*NV)
100   CONTINUE
200   CONTINUE
      RETURN
      END
CCCCCCCCCCCCCCCCCCCCCCCCCCCCCCCCCCCCCCCCCCCCCCCCCCCCCCCCCCCCCCCCCCCCCCCC
CCCCCCCCCCCCCCCCCCCCCCCCCCCCCCCCCCCCCCCCCCCCCCCCCCCCCCCCCCCCCCCCCCCCCCCC
      SUBROUTINE BACSUB(AA,IB,P,SE,ICHS,ICHP,NLO,DX,N2,X0)
      IMPLICIT DOUBLE PRECISION(A-H,P-Z)
      DIMENSION AA(N2),SE(100),P(NDT,NLO),IB(NDT)
      COMMON/GEOM/NC,NSTR,NAX,NEL,NOD,NYD,NXD,NDT,NX,NY,NV,ILDTY
      DY=180./NC
      N1=NYD+12
      NEND=(2*N1-2*NV+1)*NV
      N2=(N1+1)*N1/2
      M=2*NV
      INIT=NDT-NYD+1
      N=0
      DO 150 I=1,N1
      DO 150 J=I,N1
      N=N+1
      AA(N)=0.
      IF(I.NE.J) GOTO 150
      AA(N)=1.
150   CONTINUE
      CALL CNULL(P,NDT,NLO)
      READ(UNIT=ICHP,REC=1) IADR,L
      L=NDT
      DO 117 J=1,NLO
117   READ(UNIT=ICHP,REC=J+1)(P(I,J),I=1,NDT-NYD)
      READ(ICHS-9,1)((P(I,J),I=INIT,NDT),J=1,NLO)
      READ(UNIT=ICHS,REC=IADR)(AA(I),I=1,NEND)
C
      N=0
      I1=0
      DO 180 I=1,N1
      DO 180 J=I,N1
      N=N+1
      IF(I.NE.J) GOTO 180
      I1=I1+1
      SE(I1)=AA(N)
180   CONTINUE
```

```
C
C         BACK SUBSTITUTION
          DO 1800 NEX=1,NAX
          DO 1800 NEY=1,NC
          LEND=NV
          IF(NEY.EQ.NC) LEND=M
          IF((NEX.EQ.NAX).AND.(NEY.EQ.NC)) LEND=N1-1
C C C C C C C C C C C C C C C C C C C C C C C C C C C C C C C C C C C C
          DO 1500 IL=1,LEND
          IF(IB(L).NE.1) GOTO 1300
          DO 1250 IP=1,NLO
1250      P(L,IP)=0.
          GOTO 1500
1300      CONTINUE
          ID=N2-(IL+1)*IL/2+1
          LSTI=N1-IL
          ICON=IL
          DO 1320 IP=1,NLO
1320      P(L,IP)=P(L,IP)/AA(ID)
          DO 1400 I=1,LSTI
          LMI=L-I
          IF(IB(LMI).EQ.1) GOTO 1400
          IDMI=ID-ICON
          DO 1350 IP=1,NLO
          P(LMI,IP)=P(LMI,IP)-P(L,IP)*AA(IDMI)
1350      CONTINUE
1400      ICON=ICON+IL+I
1500      L=L-1
C C C C C C C C C C C C C C C C C C C C C C C C C C C C C C C C C C C C
          IF(LEND.EQ.(N1-1)) GOTO 1900
          KA=N2-(LEND+1)*LEND/2-LEND
          LSTI=N1-LEND
          LSTJ=KA
          DO 1700 I=1,LSTI
          NEND=N2-(I+1)*I/2+1
          DO 1600 J=KA,LSTJ
          AA(NEND)=AA(J)
          NEND=NEND+1
1600      CONTINUE
          KA=KA-LEND-I-1
          LSTJ=KA+I
1700      CONTINUE
C C C C C C C C C C C C C C C C C C C C C C C C C C C C C C C C C C C C
          NEND=(2*N1-LEND+1)*LEND/2
          IADR=IADR-1
          READ(UNIT=ICHS,REC=IADR)(AA(I),I=1,NEND)
1800      CONTINUE
C C C C C C C C C C C C C C C C C C C C C C C C C C C C C C C C C C C C
1900      CONTINUE
          DO 2000 IP=1,NLO
          IF(IB(1).EQ.1) P(1,IP)=0.
          P(1,IP)=P(1,IP)/AA(1)
2000      CONTINUE
          DO 300 IP=1,NLO
          WRITE(2,2) IP
          N=0
          DO 250 IX=1,NX
          X=(IX-1)*DX+X0
          II=(IX-1)*NY
          DO 250 IY=1,NY
          Y=DY*(IY-1) -
```

```
      N=II+IY
      N1=(N-1)*NV
      IF(X0.NE.0.) N1=(NOD-II-NY+IY-1)*NV
      DO 200 ND=1,NV
      N2=N1+ND
      SE(ND)=P(N2,IP)
200   CONTINUE
      WRITE(2,3) N,X,Y,(SE(I),I=1,NV)
250   CONTINUE
300   CONTINUE
1     FORMAT(1X,6D22.15)
2     FORMAT(3X,'LOAD CONDITION=',I3)
3     FORMAT(1X,I5,2F10.2,6E14.5)
4     FORMAT(1X,125('-'))
5     FORMAT(1H1)
      RETURN
      END
```

```
      PROGRAM LOADFR
      IMPLICIT DOUBLE PRECISION (A-H,P-Z)
      EXTERNAL DNULL,DMATIN,DMATMU,DMULSY
      DIMENSION IB(2,12),P(240),IFR(2),ISY(2)
      COMMON/MATGEO/E,RNU,RHO,R,RI(2,20),TW(2),DPM(3,3)
      COMMON/BEAM/RPP(2,12,2)
      COMMON/STFE/STRO(12,12),STBI(12,12),SM(8,8),SSE(24,24)
      COMMON/COOR/CON(2,40,2),NC,NY,PHI,DELTA,NYD
CCCCCCCCCCCCCCCCCCCCCCCCCCCCCCCCCCCCCCCCCCCCCCCCCCCCCCCCCCCCCCCCCCCCCCCC
C     %1: CONTROL VARIABLES                                              C
C     %2: OUTPUT OF VARIABLES FOR INPUT CHECK PURPORSE                   C
C     %11;CONDENSED FWD. LOADED FRAME STIFF. & INER. LOAD OUTPUT        C
C     %12;CONDENSED REAR FRAME STIFFNESS AND INER. LOAD OUTPUT           C
C     %6; TEMPORARY STORAGE FOR REDUCTION                                C
C     %7; TEMPORARY STORAGE OF INERTIA LOAD REDUCTION                    C
C     * RPP(12); RS,RC,IX,IY,IXY,J,AREA,XC,YC,GAMMA,XBAR,YBAR            C
C     *JST=1,JND=1 FOR FWD FRAME ONLY  JST=2 JND=2 FOR REAR ONLY         C
C     *IFTY=0, SAME FWD & REAR FR.(JST=JND=1)   ,=1 FOR DIFF.            C
C     *IFR=0, FOR BOOM-WEB-BOOM FRAME    =1, FOR RING FRAME              C
C     *ILDTY; TYPE OF LOAD (1; FOR SYM. 2; FOR ANTI-SYM.)                C
CCCCCCCCCCCCCCCCCCCCCCCCCCCCCCCCCCCCCCCCCCCCCCCCCCCCCCCCCCCCCCCCCCCCCCCC
      READ(1,*) NC, E,RNU,RHO,R, IFTY,JST,JND,  ILDTY
      NY=NC+1
      DO 150 I=JST,JND
      READ(1,*)IFR(I),ISY(I),RI(I,1),TW(I),((RPP(I,J,K),J=1,12),K=1,2)
      IF(ISY(I).NE.0) READ(1,*) (RI(I,L),L=2,NY)
150   CONTINUE
      PHI=3.1415926541631
      DELTA=PHI/NC
      NYD=NY*6
      NDT=2*NYD
      BETA=DELTA/2.
      DO 200 L=JST,JND
      R1=RI(L,1)
      DO 200 I=1,NY
      IF(ISY(L).NE.0) R1=RI(L,I)
      ALP=(I-1)*DELTA
      J=I+NY
      CON(L,I,1)=R1*COS(ALP)
      CON(L,I,2)=R1*SIN(ALP)
      CON(L,J,1)=R  *COS(ALP)
      CON(L,J,2)=R  *SIN(ALP)
200   CONTINUE
      WRITE(2,1) E,RNU,RHO,R,NC,JST,JND
      DO 230 I=JST,JND
      WRITE(2,2) ISY(I),RI(I,1),TW(I)
      WRITE(2,3) (K,(RPP(I,J,K),J=1,12),K=1,2)
      WRITE(2,4) I,(J,(CON(I,J,K),K=1,2),J=1,2*NY)
230   CONTINUE
1     FORMAT(//,3X,'E=',D12.4,5X,'NU=',F5.2,5X,'RHO=',F5.2,5X,'R=',
     + F7.3,5X,'NC=',I2,5X,'JST=',I2,5X,'JND=',I2)
2     FORMAT(//,3X,'ISY=',I2,5X,'RI(1)=',D12.5,5X,'TW=',F7.4)
3     FORMAT(//,3X,'BOOM PROPERTIES',/,(1X,I2,5X,12D10.3))
4     FORMAT(//,3X,'LOADED FRAME COORD. DATA FOR NO.',I2,
     +        /,3X,'NODE NO.',14X,'Y',14X,'Z',/,(1X,I7,7X,2F15.4))
C
      OPEN(UNIT=46,STATUS='SCRATCH',ACCESS='DIRECT',
     + INITIALSIZE=300,RECORDSIZE=1200)
      OPEN(UNIT=47,STATUS='SCRATCH',ACCESS='DIRECT',INITIALSIZE=50,
     + RECORDSIZE=50)
C
```

```
      DO 300 IF=JST,JND
      IF(IFR(IF).EQ.1) GOTO 290
      CALL DPLM(IF)
      CALL STCR(STRO,R,0,1,1,IF)
      CALL SSTF(ISY(IF),P,NDT,IF,IFTY,ILDTY)
      IF(ILDTY.EQ.2) GOTO 260
      IB(1,3)=1
      IB(1,4)=1
      IB(1,5)=1
      IB(2,9)=1
      IB(2,10)=1
      IB(2,11)=1
      GOTO 280
260   CONTINUE
      IB(1,1)=1
      IB(1,2)=1
      IB(1,6)=1
      IB(2,7)=1
      IB(2,8)=1
      IB(2,12)=1
280   CONTINUE
      CALL REDUCT(SSE,IB,P,2,NY,12,6,NYD,NY*12,IF,IF+10,ILDTY,IFTY)
290   CONTINUE
      IF(IFR(IF).EQ.1) CALL RSMB(IF,P,STRO,NC,DELTA,NYD,IFTY)
300   CONTINUE
      STOP
      END
CCCCCCCCCCCCCCCCCCCCCCCCCCCCCCCCCCCCCCCCCCCCCCCCCCCCCCCCCCCCCCCCCCCCCCCC
C
      SUBROUTINE  SSTF(ISY,P,NDT,IFP,IFTY,ILDTY)
C     BOOM-WEB-BOOM SEGMENT STIFFNESS CALCULATION AND STORE
      IMPLICIT DOUBLE PRECISION (A-H,P-Z)
      DIMENSION P(NDT),W1(12,12),W2(12,12),W3(144),W4(8,8)
     + ,W5(8,8),TR(12,12)
      COMMON/MATGEO/E,RNU,RHO,R,RI(2,20),TW(2),DPM(3,3)
      COMMON/STFE/STRO(144),STBI(144),SM(8,8),SSE(24,24)
      COMMON/COOR/CON(2,40,2),NC,NY,PHI,DELTA,NYD
C
      WM=0.
C
      DO 500 L=1,NC
      ALPHA=DELTA*(L-1)
      BETA =DELTA*L
      CALL TRNS(TR,ALPHA,BETA)
      CALL DMULSY(W1,TR,STRO,W3,12,12)
      IF(ISY.EQ.0.AND.L.GT.1) GOTO 100
      CALL DNULL(SM,8,8)
      CALL STM  (SM,L,IFP,0)
      CALL STCR(STBI,RI(IFP,L),ISY,L,2,IFP)
100   CONTINUE
      CALL DMULSY(W2,TR,STBI,W3,12,12)
C
      DO 200 I=1,12
      DO 200 J=1,12
      SSE(I,J)=W2(I,J)
      SSE(I+12,J+12)=W1(I,J)
200   CONTINUE
C
      IF(ISY.NE.0) GOTO 250
      DO 220 I=1,4
      J=(I-1)*2
```

```
      W5(J+1,J+1)=COS(BETA)
      W5(J+1,J+2)=SIN(BETA)
      W5(J+2,J+1)=-SIN(BETA)
      W5(J+2,J+2)=COS(BETA)
220   CONTINUE
      CALL DMULSY(W4,W5,SM,W3,8,8)
C
250   CONTINUE
C
      DO 300 I=1,4
      DO 300 II=1,2
      IS=(I-1)*6+1+II
      IE=(I-1)*2+II
      DO 300 J=1,4
      DO 300 JJ=1,2
      JS=(J-1)*6+1+JJ
      JE=(J-1)*2+JJ
      SSE(IS,JS)=SSE(IS,JS)+W4(IE,JE)
300   CONTINUE
      IF(ILDTY.EQ.2) GOTO 480
C
      LL=L*6-6
      DO 400 I=1,2
      II=(I-2)*NYD
      READ(UNIT=47,REC=1)(W3(J),J=1,12)
      DO 400 J=2,12,6
      K=LL+J-II
      P(K)=W3(J)+P(K)
      WM=WM+W3(J)
400   CONTINUE
      READ(UNIT=47,REC=3)(W3(J),J=1,24)
      DO 450 I=2,24,6
      J=LL+I
      IF(I.GT.12) J=J+NYD-12
      P(J)=P(J)+W3(I)
      WM=WM+W3(I)
450   CONTINUE
480   CONTINUE
      WRITE(2,*) L,SSE(1,1),SSE(24,24)
      WRITE(UNIT=46,REC=L)((SSE(I,J),J=1,24),I=1,24)
500   CONTINUE
      WRITE(IFP+10,*) WM
      IF(IFTY.EQ.0) WRITE(12,*) WM
      RETURN
      END
CCCCCCCCCCCCCCCCCCCCCCCCCCCCCCCCCCCCCCCCCCCCCCCCCCCCCCCCCCCCCCCCCCCCCC
      SUBROUTINE DPLM(I)
C
      IMPLICIT DOUBLE PRECISION (A-H,P-Z)
      COMMON/MATGEO/E,RNU,RHO,R,RI(2,20),TW(2),D(3,3)
      T=TW(I)
      C=E*T/(1.-RNU*RNU)
      D(1,1)=C
      D(1,2)=RNU*C
      D(2,1)=RNU*C
      D(2,2)=C
      D(3,3)=C*(1.-RNU)/2.
      RETURN
      END
CCCCCCCCCCCCCCCCCCCCCCCCCCCCCCCCCCCCCCCCCCCCCCCCCCCCCCCCCCCCCCCCCCCCCC
      SUBROUTINE STF(B,L,IFP,IM)
```

```
C
      IMPLICIT DOUBLE PRECISION (A-H,P-Z)
      DIMENSION S(8,8),W1(64),W2(8,8),W3(24),B(64),GP(3),GW(3),XI(4,2)
      COMMON/MATGEO/E,RNU,RHO,R,RI(2,20),TW(2),D(3,3)
      COMMON/COOR/CON(2,40,2),NC,NY,PHI,DELTA,NYD
      DATA GP(1),GP(2),GP(3),GW(1),GW(2),GW(3)/-0.774596669,0.0,
     + 0.774596669,0.5555555556,0.88888889,0.55555556/
      DO 120 I=1,4
      J=L+I-1
      IF(I.GT.2) J=L+NY+I-3
      XI(I,1)=CON(IFP,J,1)
      XI(I,2)=CON(IFP,J,2)
120   CONTINUE
      DO 150 I=1,3
      XG=GP(I)
      WX=GW(I)
      DO 140 J=1,3
      YG=GP(J)
      WY=GW(J)
      CALL ISOMSH(B,XG,YG,XI,DETJ,L)
      CALL DMATMU(W1,D,B,3,3,8)
      CALL DMATRA(W2,B,W1,8,8,3)
      DO 130 I1=1,8
      DO 130 J1=1,8
      S(I1,J1)=S(I1,J1)+WX*WY*DETJ*W2(I1,J1)
130   CONTINUE
      IF(IM.EQ.0) GOTO 140
      DO 135 I1=2,24,6
      J1=I1/6+1
      YD=(-1.)**J1
      XD=-1.
      IF(I1.GT.12) XD=1.
      W3(I1)=-0.25*(1.+XG*XD)*(1.+YG*YD)*RHO*TW(L)*WX*WY*DETJ
135   CONTINUE
      WRITE(UNIT=47,REC=3)(W3(I1),I1=1,24)
140   CONTINUE
150   CONTINUE
C
      IF(IM.NE.0) RETURN
      WX=0.
      DO 200 I=1,4
      J=2
      IF(I.EQ.2) J=4
      IF(I.EQ.3) J=1
      IF(I.EQ.4) J=3
      YD=ABS(XI(J,1)-XI(I,1))
      XD=ABS(XI(J,2)-XI(I,2))
      WX=WX+0.5*XD*YD
200   CONTINUE
      WX=WX+ABS(XI(1,1)-XI(4,1))*ABS(XI(2,2)-XI(3,2))
      CALL DNULL(W3,24,1)
      DO 250 I=1,4
      J=(I-1)*6+2
      W3(J)=-0.25*WX
250   CONTINUE
      WRITE(UNIT=47,REC=3)(W3(I),I=1,24)
      RETURN
      END
CCCCCCCCCCCCCCCCCCCCCCCCCCCCCCCCCCCCCCCCCCCCCCCCCCCCCCCCCCCCCCCCCCCCCCCCCC
      SUBROUTINE ISOMSH(B,XG,YG,XI,DETJ,IE)
      IMPLICIT DOUBLE PRECISION (A-H,P-Z)
```

```
      DIMENSION XD(4),YD(4),XI(4,2),B(3,8),DN(2,4),DJ(2,4),DD(2,2)
      DATA XD(1),XD(2),XD(3),XD(4),YD(1),YD(2),YD(3),YD(4)/-1.,-1.,1.,
     + 1.,-1.,1.,-1.,1./
      DO 100 I=1,4
      DN(1,I)=0.25*XD(I)*(1.+YG*YD(I))
      DN(2,I)=0.25*YD(I)*(1.+XG*XD(I))
100   CONTINUE
      CALL DMATMU(DJ,DN,XI,2,4,2)
      DETJ=DJ(1,1)*DJ(2,2)-DJ(2,1)*DJ(1,2)
      IF(DETJ.GT.0.) GOTO 120
      WRITE(2,1) IE,DETJ,((DJ(I,J),J=1,2),I=1,2)
1     FORMAT(/,3X,'ELEMENT',I3,' HAS LE ZERO DETM. OF',E12.4,/,
     + (1X,2E12.4))
      STOP
120   CONTINUE
      DD(1,1)=DJ(2,2)/DETJ
      DD(1,2)=-DJ(1,2)/DETJ
      DD(2,1)=-DJ(2,1)/DETJ
      DD(2,2)=DJ(1,1)/DETJ
      CALL DMATMU(DJ,DD,DN,2,2,4)
      DO 140 I1=1,4
      I=(I1-1)*2
      B(1,I+1)=DJ(1,I1)
      B(2,I+2)=DJ(2,I1)
      B(3,I+1)=DJ(2,I1)
      B(3,I+2)=DJ(1,I1)
140   CONTINUE
      RETURN
      END
C
CCCCCCCCCCCCCCCCCCCCCCCCCCCCCCCCCCCCCCCCCCCCCCCCCCCCCCCCCCCCCCCCCCCCCCC
      SUBROUTINE STCR(SE,R1,ISY,L,IB,IFP)
      IMPLICIT DOUBLE PRECISION (A-H,P-Z)
      COMMON/MATGEO/E,RNU,RHO,R,RI(2,20),TW(2),DPM(3,3)
      COMMON/BEAM/RPP(2,12,2)
      COMMON/COOR/CON(2,40,2),NC,NY,PHI,DELTA,NYD
      COMMON/BPRO/RS,RC,PX,PY,PXY,PJ,S,XC,YC,GA,XB,YB
      DIMENSION SE(144),W1(144),W2(144),W3(144)
      IF(L.GT.2) GOTO 100
      RS=RPP(IFP,1,IB)
      RC=RPP(IFP,2,IB)
      PX=RPP(IFP,3,IB)
      PY=RPP(IFP,4,IB)
      PXY=RPP(IFP,5,IB)
      PJ=RPP(IFP,6,IB)
      S=RPP(IFP,7,IB)
      XC=RPP(IFP,8,IB)
      YC=RPP(IFP,9,IB)
      GA=RPP(IFP,10,IB)
      XB=RPP(IFP,11,IB)
      YB=RPP(IFP,12,IB)
100   CONTINUE
      IS=1
      IF(ISY.NE.0.AND.IB.EQ.2) IS=2
      GOTO (150,200),IS
150   CONTINUE
      CL=RS*DELTA
      CALL RSTF(SE,W1,W2,W3,E,RNU,R1,CL,DELTA,6,12,144,IB,RHO)
      RETURN
200   CONTINUE
C     FOR UNSYM.-INNER BOOM
```

```
      CL=SQRT((CON(IFP,L,1)-CON(IFP,L+1,1))**2+(CON(IFP,L,2)
     +           -CON(IFP,L+1,2))**2)
      ALPHA=PHI/2.+DELTA-ASIN(R1*SIN(DELTA)/CL)
      BETA=THETA1-DELTA
      CALL STB(SE,W1,W2,W3,E,RNU,CL,ALPHA,BETA,6,12,144,RNO)
      RETURN
      END
CCCCCCCCCCCCCCCCCCCCCCCCCCCCCCCCCCCCCCCCCCCCCCCCCCCCCCCCCCCCCCCCCCCCCCCCC
      SUBROUTINE STB(C,B,CINV,W,E,RNU,CL,THETA1,THETA2,ND,ND2,NDT,RHO)
      IMPLICIT DOUBLE PRECISION (A-H,P-Z)
      DIMENSION B(ND2,ND2),C(ND2,ND2),CINV(NDT),W(NDT)
      COMMON/BPRO/RS,RC,PX,PY,PXY,PJ,S,XC,YC,GA,XB,YB
      CALL DNULL(B,ND2,ND2)
      CALL DNULL(C,ND2,ND2)
      RJ=PJ/(2.+2.*RNU)
      D=0.
      IF(GA.NE.0.) D=SQRT(RJ/GA)
      B(1,1)=E*S*CL
      B(2,2)=3.*E*PY*CL**3
      B(3,3)=4.*E*PY*CL
      B(4,4)=E*RJ*CL
      B(5,2)=3.*E*PXY*CL**3
      B(5,5)=3.*E*PX*CL**3
      B(6,3)=4.*E*PXY*CL
      B(6,6)=4.*E*PX*CL
      IF(GA.EQ.0.) GOTO 50
      B(7,4)=2.*E*RJ/D*SINH(0.5*D*CL)
      B(7,7)=E*RJ/D*SINH(D*CL)
      B(8,8)=B(7,7)
50    CONTINUE
      DO 100 I=1,ND
      DO 100 J=I+1,ND+1
100   B(I,J)=B(J,I)
C
      DO 200 I=1,2
      J=(I-1)*ND
      Z=0.5*CL*(-1.)**I
      K=0
      IF(GA.EQ.0.) K=-2
      C(J+1,2)=Z**3
      C(1+J,3)=Z**2
      C(2+J,1)=Z
      C(2+J,2)=3.*XC*Z**3
      C(2+J,3)=2.*XC*Z*Z
      C(2+J,5)=3.*YC*Z**3
      C(2+J,6)=2.*YC*Z*Z
      C(3+J,5)=Z**3
      C(3+J,6)=Z**2
      C(4+J,4)=Z
      C(5+J,2)=3.*Z*Z
      C(5+J,3)=2.*Z
      C(6+J,5)=-3.*Z*Z
      C(6+J,6)=-2.*Z
      C(1+J,K+9)=Z
      C(1+J,K+10)=1.
      C(2+J,K+14)=1.
      C(3+J,K+11)=Z
      C(3+J,K+12)=1.
      C(4+J,K+13)=1.
      C(5+J,K+9)=1.
      C(6+J,K+11)=-1.
```

```
      IF(GA.EQ.0.) GOTO 200
      C(4+J,7)=SINH(D*Z)/D
      C(4+J,8)=COSH(D*Z)/D
      C(7+J,4)=-1.
      C(7+J,7)=-COSH(D*Z)
      C(7+J,8)=-SINH(D*Z)
200   CONTINUE
C
      CALL DMATIN(DET,CINV,C,ND2)
      CALL DMULSY(C,CINV,B,W,ND2,ND2)
      CALL DNULL(B,ND2,ND2)
      CALL BEAMTR(B,ND2,GA,XB,YB)
      CALL DMULSY(W,B,C,CINV,ND2,ND2)
      CALL DNULL(B,ND2,ND2)
C
      K=0
      DO 300 I=1,2
      BETA=THETA1
      IF(I.EQ.2) BETA=THETA2
      DO 300 J=1,2
      B(K+1,K+1)=1.
      B(K+2,K+2)=COS(BETA)
      B(K+2,K+3)=SIN(BETA)
      B(K+3,K+2)=-SIN(BETA)
      B(K+3,K+3)=COS(BETA)
      K=K+ND
300   CONTINUE
      CALL DMULSY(C,B,W,CINV,ND2,ND2)
C
      CALL DNULL(W,12,1)
      CM=-0.5*RHO*CL*S
      W(2)=CM
      W(8)=CM
      WRITE(UNIT=47,REC=2)(W(I),I=1,12)
      RETURN
      END
CCCCCCCCCCCCCCCCCCCCCCCCCCCCCCCCCCCCCCCCCCCCCCCCCCCCCCCCCCCCCCCCCCCCCCCCC
      SUBROUTINE RSTF(C,B,CINV,W,E,RNU,R,CL,BETA,ND,ND2,NDT,IB,RHO)
      IMPLICIT DOUBLE PRECISION (A-H,P-Z)
      DIMENSION C(ND2,ND2),B(ND2,ND2),CINV(NDT),W(NDT)
      COMMON/BPRO/RS,RC,PX,PY,PXY,PJ,S,XC,YC,GA,XB,YB
      CALL DNULL(B,ND2,ND2)
      CALL DNULL(C,ND2,ND2)
      A=1./RS
      RJ=0.5*PJ/(1.+RNU)
      D=0.
      DI=0.
      IF(GA.NE.0.) D=SQRT(RJ/GA)
      IF(D.NE.0.) DI=1./D
      ADI2=0.
      IF(A.NE.0.0.OR.D.NE.0.0) ADI2=1./(A*A+D*D)
      C2=PX*PY-PXY**2
      C1=1./C2
      G1=C1*S*(RC*PXY+YC*PY)
      G2=C1*PXY
      G3=C1*PY*(RJ+GA*A*A)
      G4=C1*S*(RC*PX+YC*PXY)
      G5=C1*PX
      G6=G3*PXY/PY
      B1=0.5*RC*A*(RC*G4+YC*G1)
      B2=0.5*RC*A*(RC*G6+YC*G3)
```

```
      B3=RS-RS*RC*G4+0.5*RC*(RC*G4+YC*G1)
      B4=RS*RC*G6-0.5*RC*(RC*G6+YC*G3)
      B5=0.5*(RS+RC*G3)
C
      DO 100 I=1,2
      J=(I-1)*ND
      K=0
      IF(GA.EQ.0.) K=-2
      Z=-CL/2.
      IF(I.EQ.2) Z=-Z
      CB=COS(A*Z)
      SB=SIN(A*Z)
      CH=COSH(D*Z)
      SH=SINH(D*Z)
      SBZ=Z*SB
      CBZ=Z*CB
      C(J+1,1)=-B1*SBZ
      C(J+1,2)=B1*CBZ
      C(J+1,3)=RC*(RC*G5+YC*G2)
      C(J+1,5)=B2*CBZ
      C(J+1,6)=B2*SBZ
      C(J+1,K+9)=CB
      C(J+1,K+10)=SB
      C(J+2,1)=B3*SB+B1*Z*CB
      C(J+2,2)=-B3*CB+B1*Z*SB
      C(J+2,3)=G5*RC*Z
      C(J+2,5)=B4*CB+B2*Z*SB
      C(J+2,6)=B4*SB-B2*Z*CB
      C(J+2,K+9)=SB
      C(J+2,K+10)=-CB
      C(J+2,K+11)=1.
      C(J+3,1)=0.5*RC*G1*SBZ
      C(J+3,2)=-0.5*RC*G1*CBZ
      C(J+3,3)=-RC*RS*G2
      C(J+3,4)=RS*Z
      C(J+3,5)=RS*RS*SB-B5*CBZ
      C(J+3,6)=-RS*RS*CB-B5*SBZ
      C(J+3,K+12)=1.
      C(J+3,K+13)=-RS*CB
      C(J+3,K+14)=-RS*SB
      C(J+4,1)=-0.5*RC*A*G1*SBZ
      C(J+4,2)=0.5*RC*A*G1*CBZ
      C(J+4,3)=RC*G2
      C(J+4,5)=B5*A*CBZ
      C(J+4,6)=B5*A*SBZ
      C(J+4,K+13)=CB
      C(J+4,K+14)=SB
      C(J+5,1)=(1.-RC*G4)*SB
      C(J+5,2)=-(1.-RC*G4)*CB
      C(J+5,3)=G5*RC*A*Z
      C(J+5,5)=RC*G6*CB
      C(J+5,6)=RC*G6*SB
      C(J+5,K+11)=A
      C(J+6,1)=-0.5*RC*G1*(A*Z*CB+SB)
      C(J+6,2)=-0.5*RC*G1*(A*Z*SB-CB)
      C(J+6,4)=-RS
      C(J+6,5)=-RS*CB-B5*(A*Z*SB-CB)
      C(J+6,6)=-RS*SB+B5*(A*Z*CB+SB)
      C(J+6,K+13)=-SB
      C(J+6,K+14)=CB
      IF(GA.EQ.0.) GOTO 100
```

```
      C(J+3,7)=A*DI*ADI2*SH
      C(J+3,8)=A*DI*ADI2*CH
      C(J+4,7)=D*ADI2*SH
      C(J+4,8)=D*ADI2*CH
      C(J+6,7)=-A*ADI2*CH
      C(J+6,8)=-A*ADI2*SH
      C(J+7,4)=-1.
      C(J+7,5)=-CB
      C(J+7,6)=-SB
      C(J+7,7)=-CH
      C(J+7,8)=-SH
100   CONTINUE
C
      F1=S+PX*G1**2-2.*PXY*G1*G4+PY*G4**2
      F2=-G1*G2*PX+(G2*G4+G1*G5)*PXY-G4*G5*PY
      F3=-G1*G3*PX+(G3*G4+G1*G6)*PXY-G4*G6*PY
      F4=G2*G2*PX-2*G2*G5*PXY+G5*G5*PY
      F5=G2*G3*PX-(G3*G5+G2*G6)*PXY+G5*G6*PY
      F6= -RJ+ A*A*GA+ G3*G3*PX-2.*G3*G6*PXY+G6*G6*PY
      BET=CL*0.5/RS
      SB=SIN(BET)
      CB=COS(BET)
      SB2=SIN(2.*BET)
      CB2=COS(2.*BET)
      SH=SINH(D*CL/2.)
      IF(RS.NE.RC) E=E*RC/RS
      CH=COSH(D*CL/2.)
      SH2=SINH(D*CL)
      CH2=COSH(D*CL)
      B(1,1)=0.5*E*F1*(RS*SB2+CL)
      B(2,2)=0.5*E*F1*(CL-RS*SB2)
      B(3,1)=2.*E*F2*RS*SB
      B(3,3)=E*F4*CL
      B(4,4)=E*RJ*CL
      B(5,2)=-0.5*E*F3*(CL-RS*SB2)
      B(5,4)=2.*E*RJ*RS*SB
      B(5,5)=0.5*E*F6*(CL-RS*SB2)+E*RJ*CL
      B(6,1)=0.5*E*F3*(CL+RS*SB2)
      B(6,3)=2.*E*RS*F5*SB
      B(6,6)=0.5*E*F6*(CL+RS*SB2)+E*RJ*CL
      IF(GA.EQ.0.) GOTO 50
      B(7,4)=2.*E*RJ*SH*DI
      B(7,5)=2.*E*D*GA*SH*CB
      B(7,7)=E*RJ*DI*SH2
      B(8,6)=2.*E*D*GA*CH*SB
      B(8,8)=B(7,7)
50    CONTINUE
      IF(RS.NE.RC)E=E*RS/RC
C
      DO 200 I=1,ND
      DO 200 J=I+1,ND+1
      B(I,J)=B(J,I)
200   CONTINUE
C
      CALL DMATIN(DET,CINV,C,ND2)
      CALL DMULSY(W,CINV,B,C,ND2,ND2)
      CALL DNULL(B,ND2,ND2)
      CALL BEAMTR(B,ND2,GA,XB,YB)
      CALL DMULSY(C,B,W,CINV,ND2,ND2)
C
      CALL DNULL(W,12,1)
```

```
      CM=-0.5*RHO*CL*S
      W(2)=CM
      W(8)=CM
      WRITE(UNIT=47,REC=IB)(W(I),I=1,12)
      RETURN
      END
CCCCCCCCCCCCCCCCCCCCCCCCCCCCCCCCCCCCCCCCCCCCCCCCCCCCCCCCCCCCCCCCCCCCCCCC
      SUBROUTINE TRNS(T,A1,A2)
      IMPLICIT DOUBLE PRECISION(A-H,P-Z)
      DIMENSION T(12,12)
      DO 100 I=1,2
      J=(I-1)*6
      A=A1
      IF(I.EQ.2) A=A2
      C=COS(A)
      S=SIN(A)
      T(J+1,J+1)=1.
      T(J+2,J+2)=C
      T(J+2,J+3)=S
      T(J+3,J+2)=-S
      T(J+3,J+3)=C
      T(J+4,J+4)=1.
      T(J+5,J+5)=S
      T(J+5,J+6)= C
      T(J+6,J+5)= C
      T(J+6,J+6)=-S
100   CONTINUE
      RETURN
      END
CCCCCCCCCCCCCCCCCCCCCCCCCCCCCCCCCCCCCCCCCCCCCCCCCCCCCCCCCCCCCCCCCCCCCCCC
      SUBROUTINE BEAMTR(B,ND2,GA,XB,YB)
      IMPLICIT DOUBLE PRECISION (A-H,P-Z)
      DIMENSION B(ND2,ND2)
      DO 100 I=1,2
      J=(I-1)*ND2/2
      B(1+J,J+2)=-1.
      B(1+J,J+5)=YB
      B(2+J,J+3)=1.
      B(2+J,J+4)=XB
      B(2+J,J+6)=YB
      B(3+J,J+1)=1.
      B(3+J,J+5)=-XB
      B(4+J,J+5)=1.
      B(5+J,J+4)=1.
      B(6+J,J+6)=-1.
      IF(GA.EQ.0.) GOTO 100
      B(7+J,J+7)=1.
100   CONTINUE
      RETURN
      END
CCCCCCCCCCCCCCCCCCCCCCCCCCCCCCCCCCCCCCCCCCCCCCCCCCCCCCCCCCCCCCCCCCCCCCCC
      SUBROUTINE REDUCT(SE,IB,P,NX,NY,M,NV,LA,NDT,IF,ICH,ILDTY,IFTY)
      IMPLICIT DOUBLE PRECISION (A-H,P-Z)
      DIMENSION AA(2400),SE(24,24),P(NDT),IB(2,12)
C
      L=1
      N1=LA+M
      N2=(N1+1)*N1/2
      NX1=NX-1
      NY1=NY-1
      DO 1100 NEX=1,NX1
```

```
      DO 1100 NEY=1,NY1
      READ(UNIT=46,REC=NEY)((SE(I,J),J=1,24),I=1,24)
      KA=0
      KB=N2-(M+1)*M/2
C
      DO 300 I=1,M
      IM=I+M
      DO 100 J=I,M
      JM=J+M
      KAJ=KA+J
      AA(KAJ)=AA(KAJ)+SE(I,J)
      KBJ=KB+J
      AA(KBJ)=AA(KBJ)+SE(IM,JM)
C
      IF(NEY.GT.1.AND.NEY.LT.NY1) GOTO 100
      IF(I.NE.J) GOTO 100
      K=1
      IF(NEY.EQ.NY1) K=2
      K2=IB(K,I)
      IF(K2.EQ.0) GOTO 100
      AA(KAJ)=-1.0D25
C
100   CONTINUE
      DO 200 J=1,M
      JM=J+M
      KAJ=KA+J+LA
      AA(KAJ)=AA(KAJ)+SE(I,JM)
200   CONTINUE
      KA=KA+N1-I
      KB=KB+M-I
300   CONTINUE
C
      LEND=NV
      IF(NEY.EQ.NY1) LEND=M
      DO 600 IL=1,LEND
      ID=(2*N1-IL)*(IL-1)/2+IL
      LSTI=N1-IL
      LSTJ=ID+LSTI
      ICON=N1-IL
      DO 500 I=1,LSTI
      IPL=I+L
      IDPI=ID+I
      IF(AA(IDPI).EQ.0.0) GOTO 500
      FACT=AA(IDPI)/AA(ID)
      IF(ILDTY.EQ.2) GOTO 350
      P(IPL)=P(IPL)-P(L)*FACT
350   CONTINUE
      DO 400 J=IDPI,LSTJ
      IPJ=ICON+J
      AA(IPJ)=AA(IPJ)-AA(J)*FACT
400   CONTINUE
500   ICON=ICON+N1-I-IL
600   L=L+1
C
      IF(LEND.EQ.M) GOTO1200
      NEND=(2*N1-LEND+1)*LEND/2
      LSTI=N1-LEND
      NEND=NEND+1
      DO 900 I=1,LSTI
      KA=(2*N1-I)*(I-1)/2+I
      LSTJ=KA+LSTI-I
```

```
      DO 700 J=KA,LSTJ
      AA(J)=AA(NEND)
      NEND=NEND+1
700   CONTINUE
      JST=LSTJ+1
      JEND=LSTJ+LENC
      DO 800 J=JST,JEND
      AA(J)=0.
800   CONTINUE
900   CONTINUE
C
      NEND=N2-(LEND+1)*LEND/2+1
      DO 1000 I=NEND,N2
      AA(I)=0.
1000  CONTINUE
1100  CONTINUE
1200  CONTINUE
C
      IST=(2*N1-M+1)*M/2+1
      IF(ILDTY.NE.2) WRITE(ICH,1)(P(I),I=LA+1,NDT)
      WRITE(ICH,1)(AA(I),I=IST,N2)
      IF(IFTY.NE.0) RETURN
C
      IF(ILDTY.NE.2) WRITE(12,1)(P(I),I=LA+1,NDT)
      WRITE(12,1)(AA(I),I=IST,N2)
C
      RETURN
1     FORMAT(1X,6D22.15)
      END
CCCCCCCCCCCCCCCCCCCCCCCCCCCCCCCCCCCCCCCCCCCCCCCCCCCCCCCCCCCCCCCCCCCCCC
      SUBROUTINE RSMB(IF,P,SE,NC,DELTA,NYD,IFTY,ILDTY)
C
      IMPLICIT DOUBLE PRECISION(A-H,P-Z)
      DIMENSION AA(60,60),P(NYD),W1(12,12),W3(144),TR(144),SE(12,12)
      CALL STCR(SE,R,0,1,1,IF)
      IF(ILDTY.EQ.2) GOTO 150
      READ(UNIT=47,REC=1)(W3(I),I=1,12)
      DO 100 L=1,NC
      LL=(L-1)*6
      DO 100 I=1,12
      K=LL+I
      P(K)=P(K)+W3(I)
100   CONTINUE
      WM=NC*(W3(2)+W3(8))
      WRITE(IF+10,*) WM
      WRITE(IF+10,1)(P(I),I=1,NYD)
      IF(IFTY.NE.0) GOTO 150
      WRITE(12,*) WM
      WRITE(12,1)(P(I),I=1,NYD)
150   CONTINUE
C
      DO 300 L=1,NC
      LL=(L-1)*6
      ALPHA=DELTA*(L-1)
      BETA =DELTA*L
      CALL TRNS(TR,ALPHA,BETA)
      CALL DMULSY(W1,TR,SE,W3,12,12)
      DO 200 I=1,12
      II=I+LL
      DO 200 J=I,12
      JJ=LL+J
```

```
      AA(II,JJ)=AA(II,JJ)+W1(I,J)
200   CONTINUE
300   CONTINUE
      WRITE(IF+10,1)((AA(I,J),J=I,NYD),I=1,NYD)
      IF(IFTY.EQ.0) WRITE(12,1) ((AA(I,J),J=I,NYD),I=1,NYD)
1     FORMAT(1X,6D22.15)
      RETURN
      END
```

```
      PROGRAM SOLUT
      IMPLICIT DOUBLE PRECISION (A-H,P-Z)
      EXTERNAL DMATMU,DNULL,DMATRA
      DIMENSION LDEF(240),IB(1333),SE(24,24),AA(14000),AFL(11000)
     + ,SL(24),RL(12),TL(12),SSH(24,24),SRI(12,12),STR(12,12),IFRSY(2)
     + ,STFNPR(12,2),FRMPRP(12,2,2),FRWEBT(2),PTAIL(100),FRINTR(2,17)
     + ,TITLE(50),W1(2500),P(4000)
      COMMON/STRC/IFRTY(2),IPRST,LPRST,MPRST,IPRSTF,LPRSTF,NDRF,
     ;        NRF,NDRR,NRR,FRFCT1,FRFCT2,WPANG
      COMMON/GEOM/NC,NSTR,NAX,NDXND,NRC,NDRC,NEL,NOD,NYD,NXD,NDT,
     +        NX,NY,NV,NLO,ILDTY,IF1,IF2,IIWP,ILWP,IDWP
      COMMON/MATR/E,RNU,RHO,R,T,DX
C
CCCCCCCCCCCCCCCCCCCCCCCCCCCCCCCCCCCCCCCCCCCCCCCCCCCCCCCCCCCCCCCCCCCCCCCC
C     %1; FOR CONTROL VARIABLES                                         C
C     %2; FOR DISPL. AND  STRESS OUTPUT                                 C
C     %3; SHELL ELEMENT  STIFFNESS AND LOAD MATRIX                      C
C     %4; STD RING ELEMENT STIFFNESS AND LOAD MATRIX                    C
C     %5; STD STRING. ELEM. STIFFNESS AND LOAD MATRIX                   C
C     %6; SHELL ELEMENT STRESS MATRIX                                   C
C     %7; FRAME SHEAR FLOW                                              C
C     %7; STORAGE OF CONDENSED STIFF. &LOAD FOR IANTY=2                 C
C     %8; CODENSED FWD SHELL &FRAME AND CENTER SHELL STIFF. & LOAD      C
C         INPUT FOR IANTY=2                                             C
C     %9; CONDENSED FWD. SHELL STIFF. INPUT                             C
C     %10;CONDENSED REAR SHELL STIFF. INPUT                             C
C     %11,12; CONDENSED FWD.& REAR FRAME PROPERTIES                     C
C     %22,24; ELEMENT DEFINITION & DISPLACEMENT MATRIX FOR ISTRSS=1     C
C     %25; GRAFIC STRESS DATA  FOR GRAS.F PROGRAM                       C
C     %26; DISPLACEMENT DATA FOR GRAFIC PROGRAM GRA.F                   C
C     %50 ; TEMPORARY STORAGE OF ELEMENT INERTIA LOAD MATRIX TYPES      C
C     %51 ; TEMPORARY STORAGE OF ELEM. STFF. OF 6 TYPE OF COMB.         C
C     %52;TEMPORARY STORAGE FOR  DISPL. CALCULATION                     C
C     %53;TRANSFORMATION MATRICES STORAGE                               C
C     NLO : NO. OF LOAD CASES                                           C
C     NDELRC : NO. OF DX IN RING SPACE    NR: TOTAL NO. OF RING IN      C
C     CENTRE SHELL (0: NO STD RING BETWEEN FRAME)                       C
C     F1: F2:  EQ.0 RIGID DIAPHRAM AT FWD. OR REAR FRAME                C
C     ILDTY : =1; SYMMETRIC  =2; ANTISYM. LOADING                       C
C     IANTY : =1; TOTAL ANALYS     ,=2; REAR FRAME ONLY CHANGE          C
C     LDCX: FOR SINGLE EXT. LOADING CASE =1                             C
C     ISTRSS: =0; DISPL-STRESS  =1;DISPL. ONLY  =2;STRESS ONLY          C
C             =3; DISPLACEMENT ONLY- NO FURTHER STRESSING               C
C     IPRST,LPRST,MPRST; SHELL STRESS RESULTANT PRINT OUT CONTROL       C
C             1,2,3,4,5,&6 FOR NX,NT,NXT,MX,MT,MR                       C
C     IPRSTF,LPRSTF; STRINGER INT. FORCES PRINT OUT CONTROL             C
C             1,2 FOR RING AND STRINGER                                 C
C     IDISPR; DISPLACEMENT PRINT OUT CONTROL 0;PRINT 1;NOPRINT          C
CCCCCCCCCCCCCCCCCCCCCCCCCCCCCCCCCCCCCCCCCCCCCCCCCCCCCCCCCCCCCCCCCCCCCCCC
C
      READ(1,31) (TITLE(I),I=1,50)
      WRITE(2,32)(TITLE(I),I=1,50)
      READ(1,*) E,RNU,RHO,R,T,DX
      READ(1,*) NC,NSTR,NDXND
      READ(1,*) NRC,NDRC,NRF,NDRF,NRR,NDRR
      READ(1,*) ILDTY,LDC
      READ(1,*) IIWP,ILWP,IDWP
      READ(1,*) ISTRSS,IF1,IF2
      READ(1,*) IDISPR,IPRST,LPRST,MPRST,IPRSTF,LPRSTF
      READ(1,*) ((STFNPR(I,J),I=1,12),J=1,2)
      READ(1,*) LN,NDP,(PTAIL(I),I=1,6)
```

```
      IF(IF1.EQ.0.AND.IF2.EQ.0) GOTO 150
      READ(1,*) (IFRTY(I),I=1,2)
      IF(IFRTY(1).EQ.2.AND.IFRTY(2).EQ.2) READ(1,*) FRFCT1,FRFCT2
      IF(IFRTY(1).EQ.2.AND.IFRTY(2).EQ.2) GOTO 150
      READ(1,*) (IFRSY(I),FRINTR(I,1),FRWEBT(I),((FRMPRP(I,J,K),
     +          J=1,12),K=1,2),I=1,2)
      IF(IFRSY(1).NE.0) READ(1,*) (FRINTR(1,I),I=2,NC+1)
      IF(IFRSY(2).NE.0) READ(1,*) (FRINTR(2,I),I=2,NC+1)
150   CONTINUE
C
C C C C C C C C C C C C C C C C C C C C C C C C C C C C C C C C C C C C
C     NAX= NO. OF ELEMENT IN CENTRE SHELL WITH ONE STD. RING SPACE
C           AT EACH SIDE
      NAX=(NRC+1)*NDRC*NDXND+(NDRF+NDRR)*NDXND
      NY=NC+1
      NV=6
      NYD=NY*6
      NX=NAX+1
      NXD=NX*6
      NOD=NX*NY
      NDT=NOD*6
      NEL=NAX*NC
      XT=NAX*DX
      ALPHA=180./NC
      NLO=3
      IF(ILDTY.EQ.2) NLO=1
      IF(LDC.EQ.1) NLO=1
      N1=NYD+2*NV
      N2=(N1+1)*N1/2
      IAA=(NYD+1)*NYD/2
C
      IF(ISTRSS.EQ.2) READ(22,21)(LDEF(II),II=1,NEL),(IB(I),I=1,NDT)
C
C C C C C C C C C C C C C C C C C C C C C C C C C C C C C C C C C C C C
      ELEMENT PROPETIES READ IN
C
      READ(3,1)((SSH(I,J),J=1,24),I=1,24)
      READ(4,1)((SRI(I,J),J=1,12),I=1,12)
      READ(5,1)((STR(I,J),J=1,12),I=1,12)
      IF(ILDTY.NE.1) GOTO 180
      READ(3,1)(SL(I),I=1,24)
      READ(4,1)(RL(I),I=1,12)
      READ(5,1)(TL(I),I=1,12)
180   CONTINUE
C C C C C C C C C C C C C C C C C C C C C C C C C C C C C C C C C C C C
      IF(ISTRSS.EQ.2) GOTO 380
C
      IF(ILDTY.EQ.1.AND.LDC.NE.1) OPEN(UNIT=50,STATUS='SCRATCH',
     + ACCESS='DIRECT',INITIALSIZE=50,RECORDSIZE=48)
190   CONTINUE
      OPEN(UNIT=51,STATUS='SCRATCH',ACCESS='DIRECT',
     + INITIALSIZE=135,RECORDSIZE=600)
      NRSZ=24*N1-132
      NISZ=NRSZ*NC*NAX/244
      OPEN(UNIT=52,STATUS='SCRATCH',ACCESS='DIRECT',
     + INITIALSIZE=NISZ,RECORDSIZE=NRSZ)
      IF(IIWP.NE.ILWP) OPEN(UNIT=54,STATUS='SCRATCH',ACCESS='DIRECT',
     + INITIALSIZE=200,RECORDSIZE=6*NDT)
      NISZ=60+(IF1+IF2)*30
      IF(IIWP.NE.ILWP) OPEN(UNIT=55,STATUS='SCRATCH',ACCESS='DIRECT',
     + INITIALSIZE=NISZ,RECORDSIZE=IAA*2)
C
```

```
      IDT=6
      DO 350 IDEL=1,IDT
      DO 200 I=1,24
      P(I)=SL(I)
      DO 200 J=1,24
      SE(I,J)=SSH(I,J)
200   CONTINUE
      GOTO (300,220,260,220,220,220),IDEL
220   CONTINUE
      K=0
      IF(IDEL.GE.5) K=12
      DO 230 I=1,12
      P(I+K)=P(I+K)+RL(I)
      DO 230 J=1,12
230   SE(I+K,J+K)=SE(I+K,J+K)+SRI(I,J)
      IF(IDEL.EQ.2.OR.IDEL.EQ.5) GOTO 300
      IF(NSTR.EQ.0) GOTO 300
260   CONTINUE
      DO 280 I=1,12
      K=6
      IF(I.GT.6) K=12
      P(I+K)=P(I+K)+TL(I)
      DO 280 J=1,12
      L=6
      IF(J.GT.6) L=12
      SE(I+K,J+L)=SE(I+K,J+L)+STR(I,J)
280   CONTINUE
300   CONTINUE
C
      IF(NSTR.LT.16) GOTO 330
      DO 320 I1=1,2
      M=(I1-1)*6
      DO 320 I=1,12
      K=0
      IF(I.GT.6) K=6
      P(I+K+M)=P(I+K+M)+0.5*TL(I)
      DO 320 J=1,12
      L=0
      IF(J.GT.6) L=6
      SE(I+K+M,J+L+M)=SE(I+K+M,J+L+M)+0.5*STR(I,J)
320   CONTINUE
330   CONTINUE
C
      IF(ILDTY.EQ.1.AND.LDC.NE.1) WRITE(UNIT=50,REC=IDEL)(P(I),I=1,24)
      WRITE(UNIT=51,REC=IDEL)((SE(I,J),I=J,24),J=1,24)
350   CONTINUE
C
C C C C C C C C C C C C C C C C C C C C C C C C C C C C C C C C C C C
380   CONTINUE
C
      XTF=NRF*NDRF*NDXND*DX
      XTR=NRR*NDRR*NDXND*DX
      XTC=XT-NDXND*(NDRR+NDRF)*DX
      XTT=XTF+XTC+XTR
      WRITE(2,2) R,T,XTT,XTF,XTC,XTR,E,RNU,RHO,ALPHA,DX,
     +         ((STFNPR(I,J),I=1,12),J=1,2)
      AWP1=180.-(IIWP-1)*22.5
      AWPL=180.-(ILWP-1)*22.5
      IF(IIWP.EQ.6) AWP1=135.
      IF(IIWP.EQ.6) AWPL=135.
      AWIN=22.5*IDWP
```

```
      IF(IDWP.EQ.1) AWIN=0.
      WRITE(2,19) AWP1,AWPL,AWIN
      IF(ILDTY.EQ.1) WRITE(2,12)
      IF(ILDTY.EQ.2) WRITE(2,13)
      TANG=ALPHA*(NDP-1)
      WRITE(2,14) TANG,(PTAIL(I),I=1,6)
      WRITE(2,15)
      IF(IF1.EQ.0) WRITE(2,17)
      IF(IF2.EQ.0) WRITE(2,18)
      IF(IF1.EQ.0.AND.IF2.EQ.0) GOTO 390
      IF(IFRTY(1).EQ.2.AND.IFRTY(2).EQ.2) WRITE(2,10) FRFCT1,FRFCT2
      IF(IFRTY(1).EQ.2.AND.IFRTY(2).EQ.2) GOTO 390
385   CONTINUE
C     WRITE(2,24)(IFRSY(I),I=1,2)
C     WRITE(2,25)(IFRTY(I),FRINTR(I,1),FRWEBT(I),((FRMPRP(I,J,K),
C    +        J=1,12),K=1,2),I=1,2)
C     IF(IFRSY(1).NE.0) WRITE(2,26)(FRINTR(1,I),I=1,NY)
C     IF(IFRSY(2).NE.0) WRITE(2,27)(FRINTR(2,I),I=1,NY)
390   CONTINUE
C
C C C C C C C C C C C C C C C C C C C C C C C C C C C C C C C C C C C
C
C
      call dnull(p,576,1)
      DO 500 IWP=IIWP,ILWP,IDWP
      WPANG=202.5-IWP*22.5
      IF(IWP.EQ.6) WPANG=135.
      WRITE(2,11)
      IF(IWP.EQ.1) WRITE(2,6)
      IF(IWP.GE.2.AND.IWP.LE.4) WRITE(2,7) WPANG
      IF(IWP.EQ.5) WRITE(2,8)
      IF(IWP.EQ.6) WRITE(2,9)
C
      IF(ISTRSS.EQ.2) GOTO 460
C
C     ELEMENT DEFINE AND RESTRAIN
      IF(LDC.NE.2) GOTO 400
      READ(1,*)(LDEF(I),I=1,NEL)
400   CONTINUE
      CALL ELDEF(NRF,NRR,NDRF,NDRR,IWP,LDEF,IB,LDC)
      IF(ISTRSS.EQ.1) WRITE(22,21)(LDEF(I),I=1,NEL),(IB(I),I=1,NDT)
C
      IF(IWP.EQ.IIWP) GOTO 410
      CALL DNULL(P,NDT,NLO)
410   CONTINUE
      IF(ILDTY.EQ.2.OR.IWP.GT.IIWP) GOTO 420
      IF(LDC.EQ.1) GOTO 420
C
      CALL ELFOR(LDEF,NDRF,NDRR,P,SL,XM)
C
420   CONTINUE
C
      CALL TLOMT(XM,XMT,P,SE,NDRF,NDRR,IWP,LDC,NRF,NRR,NDP,PTAIL
     + ,IFRTY,FRFCT1,FRFCT2,RL)
C
C     SOLUTION ROUTINE
C
      CALL SOLV(P,SE,SL,IWP,LDEF,IB,NDRF,NDRR,N1,N2,IAA,AA,AFL,NRF
     +  ,NRR,IFRTY,FRFCT1,FRFCT2,SRI)
      IF(ISTRSS.EQ.1) WRITE(24,22)(P(I),I=1,NLO*NDT)
C
```

```
      IF(IDISPR.EQ.1.AND.ISTRSS.EQ.0) GOTO 455
C
C C C C C C C C C C C C C C C C C C C C C C C C C C C C C C C C C C C
C
      DO 450 IL=1,NLO
      NLV=NDT*(IL-1)
      IF(IL.GT.1) WRITE(2,11)
      WRITE(2,5) IL
      WRITE(2,16)
      WRITE(2,3)
      WRITE(2,16)
      N=0
      DO 450 IX=1,NX
      WRITE(2,16)
      X=XTF-NDRF*NDXND*DX+(IX-1)*DX
      DO 450 IY=1,NY
      Y=(IY-1)*ALPHA
      N=N+1
      J=(N-1)*NV+NLV
      WRITE(2,4) N,X,Y,(P(K),K=J+1,J+NV)
450   CONTINUE
C
455   CONTINUE
C C C C C C C C C C C C C C C C C C C C C C C C C C C C C C C C C C C
C
C     STRESSING
C
460   CONTINUE
      IF(ISTRSS.EQ.1.OR.ISTRSS.EQ.3) GOTO 500
      IF(ISTRSS.EQ.2) READ(24,22)(P(I),I=1,NLO*NDT)
C     READ IN  ELEMENT STRESS MATRIX
      IF(IWP.EQ.IIWP) READ(6,1)((SSH(I,J),I=1,24),J=1,24)
      IF((IWP.GT.IIWP.AND.IWP.NE.4).AND.(IF1.EQ.0.AND.IF2.EQ.0))
     +                                GOTO 480
      N4=4*NEL
      N5=N4*NLO*6
      CALL DNULL(AA,N5,1)
      CALL DNULL(AFL,N4,4)
      CALL DNULL(SE,24,24)
      AFL(1)=XTF-NDRF*NDXND*DX
      CALL STRS(P,SSH,LDEF,SRI,STR,AA,AFL,W1,SE,N4,XTF,XTC,IB,IWP)
C
      GOTO 500
480   CONTINUE
      WRITE(2,23)
500   CONTINUE
C
      STOP
C
1     FORMAT(1X,6D22.15)
2     FORMAT(//,3X,16('*'),/,3X,'*  INPUT DATA  *',/,3X,16('*'),///,
     + 5X,'$ STRUCTURE DIMENSION',/,16X,'RADIUS=',F15.3,/,16X,'SKIN ',
     + 'THICKNESS=',F7.3,/,16X,'TOTAL LENGTH=',F9.3,/,40X,'FWD SHELL ',
     + 'LENGTH=',F12.3,/,40X,'CENTRE SHELL LENGTH=',F7.3,/,40X,'REAR',
     + 'SHELL LENGTH=',F10.3,//,5X,'$ MATERIAL PROPERTIES',/,40X,'E=',
     + E12.3,/,40X,'NU=',F7.3,/,40X,'RHO=',F6.3,//,5X,'$ STANDARD ',
     + 'ELEMENT PROP. OF FEM MODEL',/,16X,'ELEMENT ARC ANGLE=',F6.2,
     + 'deg',/,16X,'ELEMENT LENGTH=',F9.2,/,16X,'STANDARD STIFFENER',/,
     + 31X,'Rs',5X,'Rc',5x,'Ix',5x,'Iy',5X,'Ixy',4x,'J',6x,'As',5x,
     + 'Xc',5x,'Yc',5X,'Gam',3x,'Xb',5x,'Yb',/,16X,'STD RING',5x,
     + 12F7.3,/,16X,'STD STRINGER',1X,12F7.3)
```

```
3       FORMAT(/,3X,'DISPLACEMENTS',/,3X,'NODE',7X,'X',7X,'THETA',
     +  10X,'UX',12X,'UR',12X,'UT',10X,'PHIX',10X,'PHIT',10X,'PHIR')
4       FORMAT(1X,I5,2F10.2,5X,6E14.5)
5       FORMAT(/,5X,'LOAD CONDITION=',I1,/,5X,16('*'))
6       FORMAT(//,3X,' LOW/HIGH WING',/,3X,'**************',//)
7       FORMAT(//,3X,' MODERATE LOW/HIGH WING',5X,' PICK UP AT',
     +  F7.2,' deg',/,3X,52('*'),//)
8       FORMAT(//,3X,' MID WING',/,3X,'*********',//)
9       FORMAT(//,3X,' MODR. LOW/HIGH WING WITH CUTOUT',/,3X,35('*'),//)
10      FORMAT(16X,'STIFFNESS RATIO OF FWD FRAME TO STD. RING STIFFENER'
     +  ,'=',F5.2,/,16X,'STIFFNESS RATIO OF REAR FRAME TO STD. RING ',
     +  'STIFFENER=',F5.2)
11      FORMAT(1H1)
12      FORMAT(//,5X,'$ SYMMETRIC LOADING',/,16X,'CONDITION 1= 1G ',
     +  ' NORMAL ACC.',/,16X,'CONDITION 2= 1RAD/SEC PITCHINGACC.',/,16X,
     +  'CONDITION 3= UNIT TAIL LOAD AT END OF STRUCTURE')
13      FORMAT(//,5X,'$ ANTI-SYMM. LOADING',/,16X,'CONDITION 1= UNIT',
     +  'FIN LOAD AT END OF STRUCTURE',/,16X,'CONDITION 2= UNIT TAIL',
     +  'TAIL TORQUE LOAD(SPIN)')
14      FORMAT(16X,'TAIL (OR FIN) LOAD AT',F10.2,' deg',/,40x,'Fx=',
     +  F8.2,5X,'Fr=',F8.2,5X,'Ft=',F8.2,5X,/,40x,'Mx=',F8.2,5X,
     +  'Mt=',F8.2,5X,'Mr=',F8.2)
15      FORMAT(/,5X,'$ FRAME PROPERTIES')
16      FORMAT(1X,120('-'))
17      FORMAT(16X,'FORWARD FRAME IS RIGID DIAPHRAM')
18      FORMAT(16X,'REAR FRAME IS RIGID DIAPHRAM')
19      FORMAT(//,5X,'$ PICK UP POSITION AND VARIATION',/,16X,'1 st',
     +  ' PICK UP POSITION',F8.2,/,16X,'LAST PICK UP POSITION',F8.2,
     +  /,16X,'WITH INTERVAL OF',F12.2,' deg')
21      FORMAT(16I2)
22      FORMAT(1X,6D22.15)
23      FORMAT(/////,5X,'STRESS RESULTANTS ARE SAME WITH PREVIOUS CASE'
     +  ,/,5X,45('*'))
31      FORMAT(50A1)
32      FORMAT(///,5X,'***',3X,50A1,//)
C
        END
C
CCCCCCCCCCCCCCCCCCCCCCCCCCCCCCCCCCCCCCCCCCCCCCCCCCCCCCCCCCCCCCCCCCCCCCC
C
```

```
      SUBROUTINE ELDEF(NRF,NRR,NDRF,NDRR,IWP,LDEF,IB,LDC)
      IMPLICIT DOUBLE PRECISION (A-H,O-Z)
      DIMENSION LDEF(NEL),IB(NDT),NFRC(6),NLD(3),NWP(6),IST(17)
      COMMON/GEOM/NC,NSTR,NAX,NDXND,NRC,NDRC,NEL,NOD,NYD,NXD,NDT,
     +        NX,NY,NV,NLD,ILDTY,IF1,IF2,IIWP,ILWP,IDWP
C
      IF(IWP.GT.IIWP) GOTO 620
      NELC=NDRC*(NRC+1)*NDXND
      IF(LDC.EQ.2) GOTO 305
C
C     STRINGER POSITION DEFINE FOR NSTR=0,4,8,12,24,AND MORE(SMEARED)
C     IST=0 FOR NO STRNGER, =1; FOR STRINGER AT 2-4, 2; AT 1-4 LINE
      DO 110 I1=1,NC
110   IST(I1)=1
      IF(NSTR.GE.16.OR.NSTR.EQ.0) GOTO 180
      M=NC/NSTR
      N=2*M
      DO 150 I=M,NC,N
150   IST(I)=3
180   CONTINUE
C C C C C C C C C C C C C C C C C C C C C C C C C C C C C C C C C C C
      N=0
C     FWD SHELL AND ELEMENT TYPE DEFINE
      DO 200 I1=1,NDXND*NDRF
      L=0
      IF(I1.EQ.1) L=1
      DO 200 I=1,NC
      N=N+1
      LDEF(N)=IST(I)+L
200   CONTINUE
C     CENTRE SHELL
      DO 250 I=1,NRC+1
      DO 250 J=1,NDRC*NDXND
      M=0
      IF(I.GT.1.AND.J.EC.1) M=1
      DO 250 K=1,NC
      N=N+1
      LDEF(N)=IST(K)+M
250   CONTINUE
C     REAR SHELL
      L=NDXND*NDRR
      DO 300 I1=1,L
      M=0
      IF(I1.EQ.L) M=4
      DO 300 I=1,NC
      N=N+1
      LDEF(N)=IST(I)+M
      IF(LDEF(N).GT.6) LDEF(N)=6
300   CONTINUE
C
C     CONSTRAINTS
305   CONTINUE
C
C     RESTRAINT FOR LOAD CONDITION
      DO 310 I=1,3
310   NFRC(I)=I+1
      IF(ILDTY.EQ.2) GOTO 330
      NLD(1)=3
      NLD(2)=4
      NLD(3)=6
      GOTO 350
```

```
330     CONTINUE
        NLD(1)=1
        NLD(2)=2
        NLD(3)=5
350     CONTINUE
C
        IF(IF1.NE.0) GOTO 400
        IF(LDC.EQ.2) GOTO 400
C       CONSTRAINTS OF FWD. DIAPHRAM
        M=NY*NDXND*NDRF
        DO 380 I=M+1,M+NY
        N=(I-1)*6
        DO 380 J=1,3
        L=NFRC(J)
380     IB(N+L)=1
400     CONTINUE
        IF(IF2.NE.0) GOTO 500
        N=M*NV
        IF(LDC.EQ.2) GOTO 500
C       CONSTRAINTS OF REAR DIAPHRAM
        M=(NDXND*NDRR+1)*NYD
        DO 450 I=1,NY
        N=(I-1)*6+NDT-M
        DO 450 J=1,3
        L=NFRC(J)
450     IB(L+N)=1
500     CONTINUE
C       DEFINE WING PICK UP POSITION D.O.F
        DO 550 I=1,5
        NWP(I)=NYD-NV-(I-1)*NV*NC/8
550     CONTINUE
        NWP(6)=NWP(3)
C       CONSTRAINTS ON LINE OF SYMMETRY
        DO 600 I=1,NX
        M=(I-1)*NYD
        N=I*NYD-6
        DO 600 J=1,3
        K=NLD(J)
        IB(K+M)=1
        IB(K+N)=1
600     CONTINUE
C
C       RESTRAINT ON WING PICK-UP TO PREVENT RIGID BODY MOTION
620     CONTINUE
        N1=NDXND*NDRF*NYD+NWP(IWP)
        N2=NDT-(NDXND*NDRR+1)*NYD+NWP(IWP)
        IF(ILDTY.eq.1) IB(N1+1)=2
        IF(ILDTY.EQ.2.AND.IWP.EQ.1) IB(N1+4)=2
        IF(ILDTY.EQ.2.AND.IWP.EQ.1) IB(N2+4)=2
        IB(N1+2)=2
        IB(N1+3)=2
        IB(N2+2)=2
        IB(N2+3)=2
        IF(IWP.EQ.IIWP.OR.(IWP.EQ.6.AND.(IWP-IDWP).EQ.3)) GOTO 700
        N=NWP(IWP-IDWP)-NWP(IWP)
        IF(ILDTY.EQ.2.AND.IIWP.EQ.1.AND.IWP-IDWP.EQ.1) IB(N1+N+4)=0
        IF(ILDTY.EQ.2.AND.IIWP.EQ.1.AND.IWP-IDWP.EQ.1) IB(N2+N+4)=0
        IB(N1+N+1)=0
        IF(IF1.EQ.0) GOTO 630
        IB(N1+N+2)=0
        IB(N1+N+3)=0
```

```
      IF((IWP-IDWP).EQ.1.AND.ILDTY.EQ.1) IB(N1+N+3)=1
      GOTO 650
630   CONTINUE
      IB(N1+N+2)=1
      IB(N1+N+3)=1
650   IF(IF2.EQ.0) GOTO 680
      IB(N2+N+2)=0
      IB(N2+N+3)=0
      IF((IWP-IDWP).EQ.1.AND.ILDTY.EQ.1) IB(N2+N+3)=1
      GOTO 700
680   CONTINUE
      IB(N2+N+2)=1
      IB(N2+N+3)=1
700   CONTINUE
C
      GOTO (1000,1000,1000,1000,1000,800),IWP
C
C     CONSTRAINT ON CUT-OUT
800   CONTINUE
      M=NWP(6)/NV+1
      M1=NDXND*NDRF
      DO 850 IX=1,NELC
      I1=(IX+M1-1)*NC
      DO 850 IY=M,NC
      N=I1+IY
      LDEF(N)=0
850   CONTINUE
C
      IF(NELC.EQ.1) GOTO 1000
      DO 900 IX=1,(NELC-1)
      I1=(IX+M1)*NYD
      DO 900 IY=M+1,NY
      N=I1+(IY-1)*6
      DO 900 IZ=1,6
      L=N+IZ
      IB(L)=1
900   CONTINUE
C     CONSTRAINTS ON DECK
C     RADIAL AND TANGENTIAL DISPLACEMENTS CONSTRAINED
      M=NWP(6)+2
      DO 950 IX=1,NELC-1
      I1=(IX+M1)*NYD
      N=I1+M
      IB(N)=1
      IB(N+1)=1
950   CONTINUE
C
1000  CONTINUE
      IF(LDC.NE.2) RETURN
      READ(1,*) NCON
      IF(NCON.EQ.0) RETURN
      DO 1010 N=1,NCON
      READ(1,*)J,(IB((J-1)*NV+I),I=1,NV)
1010  CONTINUE
      RETURN
      END
CCCCCCCCCCCCCCCCCCCCCCCCCCCCCCCCCCCCCCCCCCCCCCCCCCCCCCCCCCCCCCCCCCCCCCCC
      SUBROUTINE ELFOR(LDEF,NDRF,NDRR,P,EP,XM)
      IMPLICIT DOUBLE PRECISION(A-H,P-Z)
      DIMENSION LDEF(NEL),P(NDT,NLO),EP(24)
      COMMON/GEOM/NC,NSTR,NAX,NDXND,NRC,NDRC,NEL,NJD,NYD,NXD,NDT,
```

```
     +          NX,NY,NV,NLO,ILDTY,IF1,IF2,IIWP,ILWP,IDWP
        COMMON/MATR/E,RNU,RHO,R,T,DX
        N=0
        BETA=3.1415926541631/NC
        XM=0.
        DO 200 IX=1,NAX
        KK=(IX-1)*NYD
        C1=(NDXND*NDRF-IX+1)*DX
        C2=(NDXND*NDRF-IX)*DX
        DO 200 IY=1,NC
        B1=BETA*(IY-1)
        B2=BETA*IY
        K=KK+(IY-1)*6
        N=N+1
        ID=LDEF(N)
        IF(ID.EQ.0) GOTO 200
        READ(UNIT=50,REC=ID)(EP(I),I=1,24)
        DO 100 I=2,12,6
        XM=XM+EP(I)+EP(I+12)
        B=B1
        IF(I.GT.6) B=B2
        J=I+NYD
        P(K+I,1)=P(K+I,1)+COS(B)*EP(I)
        P(K+I+1,1)=P(K+I+1,1)-SIN(B)*EP(I)
        P(K+J,1)=P(K+J,1)+COS(B)*EP(I+12)
        P(K+J+1,1)=P(K+J+1,1)-SIN(B)*EP(I+12)
        P(K+I,2)=P(K+I,2)+C1*COS(B)*EP(I)
        P(K+I+1,2)=P(K+I+1,2)-C1*SIN(B)*EP(I)
        P(K+J,2)=P(K+J,2)+C2*COS(B)*EP(I+12)
        P(K+J+1,2)=P(K+J+1,2)-C2*SIN(B)*EP(I+12)
100     CONTINUE
200     CONTINUE
        RETURN
        END
CCCCCCCCCCCCCCCCCCCCCCCCCCCCCCCCCCCCCCCCCCCCCCCCCCCCCCCCCCCCCCCCCCCCCCCCC
        SUBROUTINE TLOMT(XM,XC,P,EP,NDRF,NDRR,IWP,LDC,NRF,NRR,NPT,PT
     +  ,IFRTY,FRFCT1,FRFCT2,RL)
        IMPLICIT DOUBLE PRECISION (A-H,P-Z)
        DIMENSION P(NDT,NLO),EP(NYD,NLO),XW(4),XI(4),PT(100)
     +  ,IFRTY(2),RL(12)
        COMMON/GEOM/NC,NSTR,NAX,NDXND,NRC,NDRC,NEL,NOD,NYD,NXD,NDT,
     +          NX,NY,NV,NLO,ILDTY,IF1,IF2,IIWP,ILWP,IDWP
        COMMON/MATR/E,RNU,RHO,R,T,DX
        IF(IWP.GT.IIWP) GOTO 500
        XC=XM
        XI(1)=DX*NDXND*NDRF
        XI(3)=0.
        XI(4)=-(NRC+1)*NDRC*NDXND*DX
        XI(2)=XI(4)-DX*NDRR*NDXND
        IF(LDC.EQ.1) GOTO 110
        GOTO (110,400),ILDTY
110     CONTINUE
        DO 300 I1=1,4
        ICH=I1+8
        N2=1
        IF(I1.EQ.2) N2=0
        IF(I1.GT.2) N2=2
        JJ=NLO-N2
        CALL DNULL(EP,NYD,JJ)
        IF(I1.EQ.1.AND.NRF.EQ.1) GOTO 300
        IF(I1.EQ.2.AND.NRR.EQ.1) GOTO 150
```

```
      IF(I1.EQ.3.AND.IF1.EQ.0) GOTO 150
      IF(I1.EQ.4.AND.IF2.EQ.0) GOTO 150
      IF((I1.EQ.3.AND.IFRTY(1).EQ.2).OR.(I1.EQ.4.AND.IFRTY(2).EQ.2))
     + GOTO 120
      IF(LDC.NE.1) READ(ICH,*) XW(I1)
      IF(JJ.EQ.0) GCTO 115
      READ(ICH,1) ((EP(I,J),I=1,NYD),J=1,JJ)
115   CONTINUE
      GOTO 150
120   CONTINUE
      FRFCT=FRFCT1
      IF(I1.EQ.4) FRFCT=FRFCT2
      XWR=0.
      DO 130 I=1,NC
      DO 130 J=1,12
      IR=(I-1)*6+J
      XWR=XWR+RL(J)*FRFCT
      EP(IR,1)=EP(IR,1)+RL(J)*FRFCT
130   CONTINUE
      XW(I1)=XWR
150   CONTINUE
      ND=0
      IF(I1.EQ.2) ND=NDT-NYD
      IF(I1.EQ.3) ND=NYD*NDRF*NDXND
      IF(I1.EQ.4) ND=NDT-(NDXND*NDRR+1)*NYD
      IF(I1.NE.2) GOTO 180
      IF(NRR.GT.1) GOTO 180
      NI=(NPT-1)*6
      DO 170 I=1,NV
      II=ND+I+NI
      P(II,JJ)=P(II,JJ)+PT(I)
170   CONTINUE
      GOTO 300
180   CONTINUE
      DO 200 J=1,JJ
      DO 200 I=1,NYD
      II=ND+I
      P(II,J)=P(II,J)+EP(I,J)
200   CONTINUE
      XMS=XI(I1)*XW(I1)
      DO 250 I=2,NYD,NV
      CC=1./NC
      IF(I.EQ.2.OR.I.EQ.(NYD-4)) CC=0.5/NC
250   P(ND+I,2)=P(ND+I,2)+CC*XMS
      XC=XW(I1)+XC
300   CONTINUE
      GOTO 480
400   CONTINUE
      ND=NDT-NYD
      IF(NRR.GT.1) READ(10,1)((EP(I,J),I=1,NYD),J=1,NLO)
      IF(NRR.GT.1) GOTO 445
      NI=(NPT-1)*NV
      DO 443 I=1,NV
      N=NI+I
      EP(N,NLO)=PT(I)
443   CONTINUE
445   CONTINUE
      DO 450 I=1,NLO
      DO 450 J=1,NYD
      P(ND+J,I)=EP(J,I)
450   CONTINUE
```

```
480     CONTINUE
        IF(IIWP.NE.ILWP) WRITE(UNIT=54,REC=1)((P(I,J),I=1,NDT),J=1,NLO)
        WRITE(2,2) XC
C
        RETURN
500     CONTINUE
        READ(UNIT=54,REC=1)((P(I,J),I=1,NDT),J=1,NLO)
        RETURN
1       FORMAT(1X,6D22.15)
2       FORMAT(/,5X,'TOTAL STRUCTURAL WEIGHT=',F10.3,'LBS')
        END
```

```
      SUBROUTINE SOLV(P,SE,EP,IWP,LDEF,IB,NDRF,NDRR,N1,N2,IAA,AA,AF
     + ,NRF,NRR,IFRTY,FRFCT1,FRFCT2,SRI)
      IMPLICIT DOUBLE PRECISION (A-H,P-Z)
      DIMENSION AA(N2),SE(24,24),EP(24),P(NDT,NLO),AF(NYD,NYD),
     +          LDEF(NEL),IB(NDT),IFRTY(2),SRI(12,12)
      COMMON/GEOM/NC,NSTR,NAX,NDXND,NRC,NDRC,NEL,NOD,NYD,NXD,NDT,
     +          NX,NY,NV,NLO,ILDTY,IF1,IF2,IIWP,ILWP,IDWP
C C C C C C C C C C C C C C C C C C C C C C C C C C C C C C C C C C C
      IADR=0
      L=1
      M=12
      IF(IWP.GT.IIWP) CALL DNULL(AA,N2,1)
C
      IF(NRF.GT.1) CALL AUXRD(9,AA,AF,1,N1,N2,IAA,1,IWP,
     + IFRTY,FRFCT1,SRI)
C C C C C C C C C C C C C C C C C C C C C C C C C C C C C C C C C C C
      DO 1100 NEX=1,NAX
      IF(IF1.NE.0.AND.NEX.EQ.(NDXND*NDRF+1)) CALL AUXRD(11,AA,AF,NEX,
     +          N1,N2,IAA,1,IWP,IFRTY,FRFCT1,SRI)
      IF(NEX.EQ.(NAX-NDXND*NDRR+1).AND.IF2.NE.0) CALL AUXRD(12,AA,AF,
     +          NEX,N1,N2,IAA,1,IWP,IFRTY,FRFCT2,SRI)
C C C C C C C C C C C C C C C C C C C C C C C C C C C C C C C C C C C
      DO 1100 NEY=1,NC
      NUMEL=(NEX-1)*NC+NEY
      IDEL=LDEF(NUMEL)
      IF(IDEL.EQ.0) GOTO 350
C
      READ(UNIT=51,REC=IDEL)((SE(I,J),J=I,24),I=1,24)
C
      KA=0
      KB=N2-(M+1)*M/2
      DO 300 I=1,M
      IM=I+M
      DO 100 J=I,M
      JM=J+M
      KAJ=KA+J
      AA(KAJ)=AA(KAJ)+SE(I,J)
      KBJ=KB+J
      AA(KBJ)=AA(KBJ)+SE(IM,JM)
100   CONTINUE
      DO 200 J=1,M
      JM=J+M
      KAJ=KA+J+NYD
      AA(KAJ)=AA(KAJ)+SE(I,JM)
200   CONTINUE
      KA=KA+N1-I
      KB=KB+M-I
300   CONTINUE
350   CONTINUE
      LEND=NV
      IF(NEY.EQ.NC) LEND=M
      IF((NEX.EQ.NAX).AND.(NEY.EQ.NC)) LEND=N1-1
C
      IF(LEND.EQ.(N1-1).AND.NRR.GT.1) CALL AUXRD(10,AA,AF,NEX,N1,
     + N2,IAA,2,IWP,IFRTY,FRFCT2,SRI)
C
      DO 600 IL=1,LEND
      IF(IB(L).EQ.1) GOTO 600
      ID=(2*N1-IL)*(IL-1)/2+IL
      IF(IB(L).EQ.2.AND.ABS(AA(ID)).LT.1.0D10) AA(ID)=1.0D25
      LSTI=N1-IL
```

```
      LSTJ=ID+LSTI
      ICON=N1-IL
      DO 500 I=1,LSTI
      IPL=I+L
      IF(IB(IPL).EQ.1) GOTO 500
      IDPI=ID+I
      FACT=AA(IDPI)/AA(ID)
      DO 380 IP=1,NLO
380   P(IPL,IP)=P(IPL,IP)-P(L,IP)*FACT
      DO 400 J=IDPI,LSTJ
      IPJ=ICON+J
      IF(AA(J).EQ.0.0) GOTO 400
      AA(IPJ)=AA(IPJ)-AA(J)*FACT
400   CONTINUE
500   ICON=ICON+N1-I-IL
600   L=L+1
C C C C C C C C C C C C C C C C C C C C C C C C C C C C C C C C C C C C C C
      IF(LEND.EQ.(N1-1)) GOTO 1200
      NEND=(2*N1-LEND+1)*LEND/2
      IADR=IADR+1
      WRITE(UNIT=52,REC=IADR)(AA(I),I=1,NEND)
C C C C C C C C C C C C C C C C C C C C C C C C C C C C C C C C C C C C C C
      LSTI=N1-LEND
      NEND=NEND+1
      DO 900 I=1,LSTI
      KA=(2*N1-I)*(I-1)/2+I
      LSTJ=KA+LSTI-I
      DO 700 J=KA,LSTJ
      AA(J)=AA(NEND)
      NEND=NEND+1
700   CONTINUE
      JST=LSTJ+1
      JEND=LSTJ+LEND
      DO 800 J=JST,JEND
      AA(J)=0.
800   CONTINUE
900   CONTINUE
C
      NEND=N2-(LEND+1)*LEND/2+1
      DO 1000 I=NEND,N2
      AA(I)=0.
1000  CONTINUE
1100  CONTINUE
C C C C C C C C C C C C C C C C C C C C C C C C C C C C C C C C C C C C C C
C
CCCCCCCCCCCCCCCCCCCCCCCCCCCCCCCCCCCCCCCCCCCCCCCCCCCCCCCCCCCCCCCCCCCCCCCCC
C     BACK SUBSTITUTION
1200  CONTINUE
      WRITE(2,*) '    L=',L,'   IADR=',IADR
      DO 1800 NEX=1,NAX
      DO 1800 NEY=1,NC
      LEND=NV
      IF(NEY.EQ.NC) LEND=M
      IF((NEX.EQ.NAX).AND.(NEY.EQ.NC)) LEND=N1-1
C C C C C C C C C C C C C C C C C C C C C C C C C C C C C C C C C C C C C C
      DO 1500 IL=1,LEND
      IF(IB(L).NE.1) GOTO 1300
      DO 1250 IP=1,NLO
1250  P(L,IP)=0.
      GOTO 1500
1300  CONTINUE
```

```
      ID=N2-(IL+1)*IL/2+1
      LSTI=N1-IL
      ICON=IL
      DO 1320 IP=1,NLO
1320  P(L,IP)=P(L,IP)/AA(ID)
      DO 1400 I=1,LSTI
      LMI=L-I
      IF(IB(LMI).EQ.1) GOTO 1400
      IDMI=ID-ICON
      DO 1350 IP=1,NLO
      P(LMI,IP)=P(LMI,IP)-P(L,IP)*AA(IDMI)
1350  CONTINUE
1400  ICON=ICON+IL+I
1500  L=L-1
C C C C C C C C C C C C C C C C C C C C C C C C C C C C C C C C C C C C
      IF(LEND.EQ.(N1-1)) GOTO 1900
      KA=N2-(LEND+1)*LEND/2-LEND
      LSTI=N1-LEND
      LSTJ=KA
      DO 1700 I=1,LSTI
      NEND=N2-(I+1)*I/2+1
      DO 1600 J=KA,LSTJ
      AA(NEND)=AA(J)
      NEND=NEND+1
1600  CONTINUE
      KA=KA-LEND-I-1
      LSTJ=KA+I
1700  CONTINUE
C C C C C C C C C C C C C C C C C C C C C C C C C C C C C C C C C C C C
      NEND=(2*N1-LEND+1)*LEND/2
      READ(UNIT=52,REC=IADR)(AA(I),I=1,NEND)
      IADR=IADR-1
1800  CONTINUE
C C C C C C C C C C C C C C C C C C C C C C C C C C C C C C C C C C C C
1900  CONTINUE
      DO 2000 IP=1,NLO
      IF(IB(1).EQ.1) P(1,IP)=0.
      P(1,IP)=P(1,IP)/AA(1)
2000  CONTINUE
1     FORMAT(1X,6D22.15)
      RETURN
      END
CCCCCCCCCCCCCCCCCCCCCCCCCCCCCCCCCCCCCCCCCCCCCCCCCCCCCCCCCCCCCCCCCCCCCC
C
      SUBROUTINE AUXRD(ICH,AA,AF,NEX,N1,N2,IAA,IP,IWP
     + ,IFRTY,FRFCT,SRI)
      IMPLICIT DOUBLE PRECISION (A-H,P-Z)
      DIMENSION AA(N2),AF(NYD,NYD),IFRTY(2),SRI(12,12)
      COMMON/GEOM/NC,NSTR,NAX,NDXND,NRC,NDRC,NEL,NOD,NYD,NXD,NDT,
     +        NX,NY,NV,NLO,ILDTY,IF1,IF2,IIWP,ILWP,IDWP
C
      IF(IWP.GT.IIWP) GOTO 110
      IF((IFRTY(1).EQ.2.AND.ICH.EQ.11).OR.(IFRTY(2).EQ.2.AND.
     ; ICH.EQ.12)) GOTO 120
      READ(ICH,1)((AF(I,J),J=I,NYD),I=1,NYD)
      GOTO 128
120   CONTINUE
      CALL DNULL (AF,NYD,NYD)
      DO 125 IR=1,NC
      I1=(IR-1)*NV
      DO 125 I=1,2*NV
```

```
        IS=I1+I
        DO 123 J=I,2*NV
        JS=I1+J
        AF(IS,JS)=AF(IS,JS)+SRI(I,J)*FRFCT
123     CONTINUE
125     CONTINUE
128     CONTINUE
        IF(IIWP.NE.ILWP) WRITE(UNIT=55,REC=ICH-8)((AF(I,J),J=I,NYD),
     +  I=1,NYD)
110     CONTINUE
        IF(IWP.GT.IIWP) READ(UNIT=55,REC=ICH-8)
     +  ((AF(I,J),J=I,NYD),I=1,NYD)
C
        IF(IP.EQ.2) GOTO 200
        DO 100 I=1,NYD
        IJ=(2*N1-I)*(I-1)/2+I
        DO 100 J=I,NYD
        K=IJ+J-I
        AA(K)=AA(K)+AF(I,J)
100     CONTINUE
        RETURN
C C C C C C C C C C C C C C C C C C C C C C C C C C C C C C C C C C C C
200     CONTINUE
        L1=N2-IAA
        DO 300 I=1,NYD
        DO 300 J=I,NYD
        L1=L1+1
        AA(L1)=AA(L1)+AF(I,J)
300     CONTINUE
1       FORMAT(1X,6D22.15)
        RETURN
        END
CCCCCCCCCCCCCCCCCCCCCCCCCCCCCCCCCCCCCCCCCCCCCCCCCCCCCCCCCCCCCCCCCCCCC
```

```
      SUBROUTINE STRS(DIS,SST,LDEF,SRI,STR,STBL,XTBL,TTBL,TBL,N4,XTF
     + ,XTC,IB,IWP)
      IMPLICIT DOUBLE PRECISION (A-H,P-Z)
      DIMENSION DIS(NDT,NLO),SST(24,24),RES(24,3),USH(24,3),
     + W(72),LDEF(NEL),SRI(12,12),STR(12,12),ANG(17),
     + TBL(17,4,NLO),STBL(NLO,6,N4),XTBL(N4),TTBL(N4),
     + AVRG(17,3),LST(17),IB(NDT),RCT(10,3)
      COMMON/MATR/E,RNU,RHO,R,T,DX
      COMMON/GEOM/NC,NSTR,NAX,NDXND,NRC,NDRC,NEL,NOD,NYD,NXD,NDT,
     +        NX,NY,NV,NLO,ILDTY,IF1,IF2,IIWP,ILWP,IDWP
      COMMON/STRC/IFRTY(2),IPRST,LPRST,MPRST,IPRSTF,LPRSTF,NDRF,
     +        NRF,NDRR,NRR,FRFCT1,FRFCT2,WPANG
C
C C C C C C C C C C C C C C C C C C C C C C C C C C C C C C C C C C C
      XTFC=XTF+XTC
      DELX=R
      LX1=NDXND*NDRF/2
      DELX1=DX*LX1
      IF(DELX.GT.DELX1) DELX=DELX1
      DEL=180./NC
      NREACT=0
      WRITE(2,23)
      DO 110 I=1,NOD
      I1=(I-1)*NV
      DO 110 J=1,NV
      J1=I1+J
      IF(IB(J1).NE.2) GOTO 110
      NREACT=NREACT+1
      WRITE(2,24) I,J,( -DIS(J1,ILO)*1.0D25,ILO=1,NLO)
110   CONTINUE
      NE=0
      NRNG=0
      X0=XTBL(1)
      XTBL(1)=0.
C
      IF(IFRTY(1).NE.2) GOTO 112
      LFRIX1=NDXND*NDRF
      GOTO 116
112   CONTINUE
      IF(IFRTY(2).NE.2) GOTO 116
      LFRIX2=LFRIX1+NDXND*NDRC*(NRC+1)
116   CONTINUE
C
      DO 118 I=1,NY
      ANG(I)=(I-1)*DEL
118   CONTINUE
      WRITE(2,1)
C C C C C C C C C C C C C C C C C C C C C C C C C C C C C C C C C C C
      DO 500 IX=1,NAX
      X1=(IX-1)*DX+X0
      X2=X1+DX
      DO 500 IY=1,NC
      DEL1=ANG(IY)
      DEL2=ANG(IY+1)
      NE=NE+1
      IDT=LDEF(NE)
      LNE=(NE-1)*4
      N1=(IX-1)*NYD+(IY-1)*NV
      N2=N1+NYD
C
      IF(IDT.NE.0) GOTO 120
```

```
      CALL DNULL(RES,24,NLO)
      GOTO 160
C
120   CONTINUE
      DO 150 I=1,12
      J=N1+I
      DO 150 ILO=1,NLO
      USH(I,ILO)=DIS(J,ILO)
      USH(I+12,ILO)=DIS(J+NYD,ILO)
150   CONTINUE
      CALL CMATMU(RES,SST,USH,24,24,NLO)
160   CONTINUE
      DO 200 IN=1,4
      XX=X1
      IF(IN.GT.2) XX=X2
      YY=DEL1
      IF(IN.EQ.2.OR.IN.EQ.4) YY=DEL2
      J=(IN-1)*6
      JN=LNE+IN
      DO 180 IS=IPRST,LPRST,MPRST
      JI=J+IS
      DO 180 ILO=1,NLO
      STBL(ILO,IS,JN)=RES(JI,ILO)
180   CONTINUE
      XTBL(JN)=XX
      TTBL(JN)=YY
200   CONTINUE
300   CONTINUE
500   CONTINUE
C
      WRITE(2,2)
      WRITE(2,6)
      DO 600 IS=IPRST,LPRST,MPRST
      DO 590 IX=1,NX
      DO 520 I=1,NLO
      DO 520 J=1,4
      DO 520 K=1,NY
520   TBL(K,J,I)=0.
      X=(IX-1)*DX+X0
      DO 550 IN=1,N4
      IF(X.NE.XTBL(IN)) GOTO 550
      NE=(IN-1)/4+1
      M=TTBL(IN)/DEL+1
      N=4*NE-IN+1
      DO 530 ILO=1,NLO
      TBL(M,N,ILO)=STBL(ILO,IS,IN)
530   CONTINUE
550   CONTINUE
      DO 560 IY=1,NY
      DO 560 ILO=1,NLO
560   AVRG(IY,ILO)=0.
      IF((X.EQ.XTF.OR.X.EQ.XTFC).AND.IS.EQ.3) GOTO 573
      COX=0.5
      IF(IX.EQ.1.OR.IX.EQ.NX) COX=1.0
      DO 570 IY=1,NY
      COY=0.5
      IF(IY.EQ.1.OR.IY.EQ.NY) COY=1.0
      COF=COX*COY
      DO 570 ILO=1,NLO
      DO 570 IV=1,4
      AVRG(IY,ILO)=AVRG(IY,ILO)+COF*TBL(IY,IV,ILO)
```

```
      IF(IY.NE.1.AND.IY.NE.NY) GOTO 570
      IF(IS.NE.3) GOTO 570
      IF(IS.EQ.3.AND.ILDTY.EQ.1) AVRG(IY,ILD)=0.
570   CONTINUE
573   CONTINUE
      IF(IS.GT.1.AND.IX.EQ.1) WRITE(2,12)
      WRITE(2,6)
      IF(IX.NE.1) GOTO 575
      IF(IS.EQ.1) WRITE(2,3)
      IF(IS.EQ.2) WRITE(2,14)
      IF(IS.EQ.3) WRITE(2,15)
      WRITE(2,20)
575   CONTINUE
      WRITE(2,19) IS
      WRITE(2,6)
C
      DO 580 ILC=1,NLO
      IF(NY.LT.10) WRITE(2,4) X,ILO,(ANG(I),I=1,NY)
      IF(NY.GE.10) WRITE(2,41) X,ILO,(ANG(I),I=1,NY)
      IF(NY.EQ.9) WRITE(2,5)((TBL(I,J,ILO),I=1,NY),J=1,4)
      IF(NY.GT.9.AND.IS.EQ.1) WRITE(2,51)((TBL(I,J,ILO),I=1,NY),J=1,4)
51    FORMAT(1X,17F7.2)
C
      IF(X.NE.XTF.AND.X.NE.XTFC) GOTO 576
      CALL SAVF(TBL,X,NLO,ILO,NY,ILDTY,IS,XTF,XTFC,IWP)
      GOTO 580
C
576   CONTINUE
      IF(NY.LT.10) WRITE(2,17)(AVRG(I,ILO),I=1,NY)
      IF(NY.GE.10) WRITE(2,42) (AVRG(I,ILO),I=1,NY)
      WRITE(25,18)X,ILO,(AVRG(I,ILO),I=1,NY)
580   CONTINUE
590   CONTINUE
600   CONTINUE
      NV2=2*NV
C    .RING ELEMENT INTERNAL LOAD CALCULATION
      IF(IPRSTF.NE.1) GOTO 650
      WRITE(2,7)
      WRITE(2,6)
      WRITE(2,8)
      WRITE(2,6)
      CALL RNGSTS(DIS,SRI,ANG,W,SST,NV,NV2,NDT,NLO,NC,NY,NYD,
     +           XTF,XTFC,DX,X0,FRFCT1,FRFCT2,IFRTY,IF1,IF2,
     +           NRF,NDRF,NRC,NDRC,NRR,NDRR,NDXND)
C
650   CONTINUE
C     STRINGER ELEMENT INTERNAL LOAD CALCULATION
      IF(LPRSTF.NE.2.OR.NSTR.EQ.0) GOTO 700
      WRITE(2,9)
      WRITE(2,6)
      WRITE(2,8)
      WRITE(2,6)
      CALL STRSTS(DIS,STR,ANG,W,SST,NSTR,NV,NV2,NDT,NLO,NC,NY,NX,
     +           NYD,DX,X0)
700   CONTINUE
C
1     FORMAT(1H1,/,3X,'STRESS RESULTANT',/,3X,20('*'),//,
     + 3X,'SHELL ELEMENT STRESSES',/,16X,'Nx,Ntheta,Nxt, & ',
     + 'Mx,Mt,Mxt at EACH NODE',/,3X,'RING AND STRINGER ELEMENT',
     + ' END FORCES & COUPLES IN GLOBAL COORD.',/,16X,'Fx(LONG.),'
     + 'Fr(RADIAL), Ft(TANGENTIAL), Mx ,Mt & Mr',/,1x,120('-'))
```

```
2       FORMAT(/,3X,'SHELL ELEMENT',/,3X,12('*'))
3       FORMAT(3X,'STRESS RESULTANT OF ---  Nx  ---',/,3x,33('*'))
4       FORMAT(1X,60('- '),/,3X,'X=',F10.3,3X,'ILO=',I2,3X,<NY>F10.3,/)
41      FORMAT(1X,60('- '),/,3X,'X=',F10.3,3X,'ILO=',I2,/,(3X,<NY>F7.2))
5       FORMAT(27X,9F10.3)
6       FORMAT(1X,120('-'))
7       FORMAT(1H1,/,3X,'RING ELEMENT',/,3X,12('*'))
8       FORMAT(5X,'NO',3X,'NODE',3X,'X',6X,'THETA',3X,'ILO',10X,'Fx',
     +  8X,'Fr',8x,'Ft',8X,'Mx',8X,'Mt',8X,'Mr')
9       FORMAT(1H1,/,3X,'STRINGER ELEMENT',/,3X,15('*'))
12      FORMAT(1H1)
14      FORMAT(3X,'STRESS RESULTANT  ---  Ntheta  ---',/,3x,50('*'))
15      FORMAT(3X,'SHEAR STRESS RESULTANT - Nxt -',/,3X,25('*'))
16      FORMAT(1X,50('- '))
17      FORMAT(18X,'AVRG',4X,<NY>F10.3)
42      FORMAT(18X,'AVRG',5X,/,3X,<NY>F7.2)
18      FORMAT(1X,F5.1,I2,<NY>F7.2)
19      FORMAT(5X,'IS=',I2)
20      FORMAT(1X,60('- '))
23      FORMAT(1H1,///,3X,'REACTIONS AT P/U',/,3X,16('*'),//,5X,'NODE',
     +  ' NO',5X,'DIRECTION',10X,'LOAD CASE=',5X,'1',15X,'2',15X,'3',/)
24      FORMAT(5X,I5,10X,I3,15X,<NLO>(F12.3,3X))
        RETURN
        END
CCCCCCCCCCCCCCCCCCCCCCCCCCCCCCCCCCCCCCCCCCCCCCCCCCCCCCCCCCCCCCCCCCCCCCC
        SUBROUTINE SAVF(STR,X,NLO,ILO,NY,ILDTY,IS,XTF,XTFC,IWP)
C       AVERAGE STRESS RESULTANT OF SHELL ELEMENT AT FWD & REAR OF FRAME
        IMPLICIT DOUBLE PRECISION(A-H,P-Z)
        DIMENSION STR(17,4,NLO),AVR(17),B(17)
        DO 200 JS=1,2
        J=(JS-1)*2
        DO 100 I=1,NY
        COF=0.5
        IF((STR(I,J+1,ILO).EQ.0.0).OR.(STR(I,J+2,ILO).EQ.0.0)) COF=1.
        AVR(I)=COF*(STR(I,J+1,ILO)+STR(I,J+2,ILO))
        IF(ILDTY.NE.1) GOTO 100
        IF(IS.EQ.3.AND.(I.EQ.1.OR.I.EQ.NY)) AVR(I)=0.
        IF(JS.EQ.1) B(I)=AVR(I)
        IF(JS.EQ.2.AND.IS.EQ.3) B(I)=B(I)-AVR(I)
        COF=0.5
        IF(B(I).EQ.0.0.OR.AVR(I).EQ.0.0) COF=1.0
        IF(JS.EQ.2.AND.IS.NE.3) B(I)=COF*(B(I)+AVR(I))
100     CONTINUE
        IF(NY.EQ.9.AND.JS.EQ.1) WRITE(2,1)(AVR(I),I=1,NY)
        IF(NY.EQ.9.AND.JS.EQ.2) WRITE(2,2)(AVR(I),I=1,NY)
        IF(NY.EQ.9.AND.JS.EQ.2.AND.IS.EQ.3) WRITE(2,4)(B(I),I=1,NY)
        IF(IS.NE.3.AND.NY.EQ.9.AND.JS.EQ.2) WRITE(2,5)(B(I),I=1,NY)
        WRITE(25,3) X+(JS-1)*0.1,ILO,(AVR(I),I=1,NY)
        IF(NY.EQ.9) GOTO 200
        IF(JS.EQ.1) WRITE(2,11) (AVR(I),I=1,NY)
        IF(JS.EQ.2) WRITE(2,12) (AVR(I),I=1,NY)
        IF(JS.EQ.2.AND.IS.EQ.3) WRITE(2,14) (B(I),I=1,NY)
        IF(JS.EQ.2.AND.IS.NE.3) WRITE(2,13) (B(I),I=1,NY)
200     CONTINUE
        RETURN
1       FORMAT(7X,'FRAME FOWD AVRG.',4X,9F10.3)
2       FORMAT(7X,'FRAME REAR AVRG.',4X,9F10.3)
3       FORMAT(1X,F5.1,I2,<NY>F7.2)
4       FORMAT(7X,'FRAME SHEAR FLOW',3X,9F10.3)
5       FORMAT(17X,'AVRG.',4X,9F10.3)
6       FORMAT(7X,<NY>F7.2)
```

```
11      FORMAT(7X,'FRAME FWD. AVRG.',4X,/,1X,<NY>F7.2)
12      FORMAT(7X,'FRAME REAR AVRG.',4X,/,1X,<NY>F7.2)
13      FORMAT(7X,'AVRG',/,<NY>F7.2)
14      FORMAT(7X,'FRAME SHEAR FLOW',/,1X,<NY>F7.2)
        END
CCCCCCCCCCCCCCCCCCCCCCCCCCCCCCCCCCCCCCCCCCCCCCCCCCCCCCCCCCCCCCCCCCCCCCCC
        SUBROUTINE RNGSTS(DIS,SRI,ANG,RF,UR,NV,NV2,NDT,NLO,NC,NY,NYD,
     +          XTF,XTFC,DX,X0,FRFCT1,FRFCT2,IFRTY,IF1,IF2,NRF,NDRF,NRC,
     +          NDRC,NRR,NDRR,NDXND)
        IMPLICIT DOUBLE PRECISION (A-H,P-Z)
        DIMENSION  DIS(NDT,NLO),SRI(NV2,NV2),RF(NV2,NLO),UR(NV2,NLO),
     +          ANG(NY),IFRTY(2)
C
        NR=0
        IF(NRF.EQ.1) GOTO 120
        NR=NR+1
        X=X0
        ND=0
        II=1
        GOTO 500
100     CONTINUE
120     CONTINUE
        IF(NRC.EQ.0) GOTO 200
        N2=NDXND*NDRC
        N1=NRC*N2
        NDX=NDXND*NDRF+N2
        DO 180 IR=1,N1,N2
        X=X0+DX*N2
        IF(IR.GT.1) X=X+(IR-N2)*DX
        NR=NR+1
        ND=NDX*NYD
        IF(IR.GT.1) ND=ND+(IR-N2)*NYD
        II=2
        GOTO 500
150     CONTINUE
180     CONTINUE
200     CONTINUE
        IF(NRR.EQ.1) GOTO 250
        ND=NDT-NYD
        X=XTFC+NDXND*NDRC*DX
        NR=NR+1
        II=3
        GOTO 500
220     CONTINUE
250     CONTINUE
        IF(IF1.EQ.0.OR.IFRTY(1).NE.2) GOTO 350
        X=XTF
        NR=NR+1
        ND=NDXND*NDRF*NYD
        II=4
        WRITE(2,1)
        GOTO 500
300     CONTINUE
350     CONTINUE
        IF(IF2.EQ.0.OR.IFRTY(2).NE.2) GOTO 600
        X=XTFC
        NR=NR+1
        ND=NDT-(NDXND*NDRR+1)*NYD
        II=5
        WRITE(2,2)
        GOTO 500
```

```
380     CONTINUE
        GOTO 600
C
500     CONTINUE
        C1=1.
        IF(II.EQ.4) C1=FRFCT1
        IF(II.EQ.5) C1=FRFCT2
        CALL RNF(DIS,SRI,RF,UR,ANG,NC,NY,NV,NV2,NDT,NLO,X,ND,NR,C1)
        GOTO (100,150,220,300,380),II
C
600     CONTINUE
        RETURN
1       FORMAT(/,5X,'*** FWD RING FRAME ***')
2       FORMAT(/,5X,'*** REAR RING FRAME ***')
        END
CCCCCCCCCCCCCCCCCCCCCCCCCCCCCCCCCCCCCCCCCCCCCCCCCCCCCCCCCCCCCCCCCCCCC
        SUBROUTINE RNF(U,S,RF,UR,ANG,NC,NY,NV,NV2,NDT,NLO,X,ND,NR,C1)
        IMPLICIT DOUBLE PRECISION (A-H,P-Z)
        DIMENSION U(NDT,NLO),S(NV2,NV2),RF(NV2,NLO),UR(NV2,NLO),ANG(NY)
        DO 200 IR=1,NC
        I1=(IR-1)*NV+ND
        DO 150 L=1,NLO
        DO 150 J=1,NV2
        UR(J,L)=U(J+I1,L)*C1
150     CONTINUE
        CALL DMATMU(RF,S,UR,NV2,NV2,NLO)
        WRITE(2,1) NR,X,ANG(IR),(L,(RF(I,L),I=1,NV),L=1,NLO)
        WRITE(2,2) ANG(IR+1),(L,(RF(I+NV,L),I=1,NV),L=1,NLO)
        WRITE(2,3)
200     CONTINUE
        RETURN
1       FORMAT(5X,I2,5X,2F9.3,/,(30X,I3,5X,<NV>F10.3))
2       FORMAT(21X,F9.3,/,(30X,I3,5X,<NV>F10.3))
3       FORMAT(1X,55('- '))
        END
CCCCCCCCCCCCCCCCCCCCCCCCCCCCCCCCCCCCCCCCCCCCCCCCCCCCCCCCCCCCCCCCCCCCC
        SUBROUTINE STRSTS(U,S,ANG,RS,US,NSTR,NV,NV2,NDT,NLO,NC,NY,NX,
     +          NYD,DX,X0)
        IMPLICIT DOUBLE PRECISION (A-H,P-Z)
        DIMENSION U(NDT,NLO),S(NV2,NV2),ANG(NY),RS(NV2,NLO),US(NV2,NLO)
        NB=0
        NE=NX-1
        M1=NC/NSTR
        N=2*M1
        M=M1+1
        DO 300 IS=M,NC,N
        THETA=ANG(IS)
        MV=(IS-1)*NV
        DO 200 IB=1,NE
        NB=NB+1
        X1=X0+DX*(IB-1)
        X2=X1+DX
        K1=MV+NYD*(IB-1)
        K2=K1+NYD
        DO 100 L=1,NLO
        DO 100 I=1,NV
        US(I,L)=U(K1+I,L)
        US(I+NV,L)=U(K2+I,L)
100     CONTINUE
        CALL DMATMU(RS,S,US,NV2,NV2,NLO)
        WRITE(2,1) NB,X1,THETA,(L,(RS(I,L),I=1,NV),L=1,NLO)
```

```
      WRITE(2,2) X2,(L,(RS(I+NV,L),I=1,NV),L=1,NLO)
      WRITE(2,3)
200   CONTINUE
300   CONTINUE
      RETURN
1     FORMAT(5X,I2,5X,2F9.3,/,(30X,I3,5X,<NV>F10.3))
2     FORMAT(12X,F9.3,/,(30X,I3,5X,<NV>F10.3))
3     FORMAT(1X,55('- '))
      END
```

H.9 Example Output of CENSOL

```
***   SYMM RING  SHORT


****************
*  INPUT DATA  *
****************

 $ STRUCTURE DIMENSION
           RADIUS=              6.000
           SKIN THICKNESS=   0.060
           TOTAL LENGTH=    60.000
                                         FWD SHELL LENGTH=        24.000
                                         CENTRE SHELL LENGTH= 12.000
                                         REARSHELL LENGTH=     24.000

 $ MATERIAL PROPERTIES
                                         E=    0.103E+08
                                         NU=  0.300
                                         RHO= 0.100

 $ STANDARD ELEMENT PROP. OF FEM MODEL
           ELEMENT ARC ANGLE= 22.50deg
           ELEMENT LENGTH=      5.00
           STANDARD STIFFENER
                          Rs       Rc       Ix       Iy       Ixy      j        As       Xc       Yc       Gam      Xb       Yb
           STD RING       6.000    6.000    0.010    0.010    0.000    0.015    0.100    0.000    0.000    0.000    0.000    0.000
           STD STRINGER   6.000    6.000    0.010    0.010    0.000    0.015    0.100    0.000    0.000    0.000    0.000    0.000

 $ PICK UP POSITION AND VARIATION
           1 st PICK UP POSITION   180.00
           LAST PICK UP POSITION   180.00
           WITH INTERVAL OF          0.00 deg

 $ SYMMETRIC LOADING
           CONDITION 1= 1G  NORMAL ACC.
           CONDITION 2= 1RAD/SEC PITCHINGACC.
           CONDITION 3= UNIT TAIL LOAD AT END OF STRUCTURE
           TAIL (OR FIN) LOAD AT       90.00 deg
                                        Fx=     0.00       Fr=      0.00       Ft= -100.00
                                        Mx=     0.00       Mt=      0.00       Mr=     0.00

 $ FRAME PROPERTIES
           STIFFNESS RATIO OF FWD FRAME TO STD. RING STIFFENER=10.00
           STIFFNESS RATIO OF REAR FRAME TO STD. RING STIFFENER=10.00
```

LOW/HIGH WING
****

TOTAL STRUCTURAL WEIGHT=   -12.510LBS

LOAD CONDITION=1
****

DISPLACEMENTS NODE	X	THETA	UX	UR	UT	PHIX	PHIT	PHIR
1	12.00	0.00	-0.13352D-04	-0.12323D-03	0.00000D+00	0.00000D+00	0.48350D-06	0.00000D+00
2	12.00	22.50	-0.18839D-04	-0.11412D-03	0.47874D-04	-0.35474D-05	0.93340D-06	0.79315D-07
3	12.00	45.00	-0.18062D-04	-0.76333D-04	0.35467D-04	-0.53313D-05	0.19823D-05	0.68775D-06
4	12.00	67.50	-0.16141D-04	-0.25053D-04	0.10540D-03	-0.47597D-05	0.24357D-05	0.11071D-05
5	12.00	90.00	-0.12325D-04	0.23969D-04	0.10552D-03	-0.64468D-06	0.24759D-05	0.21794D-05
6	12.00	112.50	-0.61471D-05	0.53587D-04	0.89218D-04	0.37645D-05	0.10150D-05	0.29050D-05
7	12.00	135.00	0.33420D-06	0.76410D-04	0.62632D-04	0.59501D-05	-0.18219D-05	0.30829D-05
8	12.00	157.50	0.70210D-05	0.80571D-04	0.31699D-04	0.50143D-05	-0.41660D-05	0.19623D-05
9	12.00	180.00	0.95145D-05	0.90278D-04	0.00000D+00	0.00000D+00	-0.53729D-05	0.00000D+00
10	18.00	0.00	-0.16529D-04	-0.12590D-03	0.00000D+00	0.00000D+00	-0.18084D-06	0.00000D+00
11	18.00	22.50	-0.16457D-04	-0.10722D-03	0.46773D-04	0.15907D-04	-0.21025D-06	0.42673D-06
12	18.00	45.00	-0.15955D-04	-0.66145D-04	0.78965D-04	-0.51829D-05	0.17400D-05	0.11723D-05
13	18.00	67.50	-0.14520D-04	-0.99275D-05	0.95408D-04	0.19955D-04	0.18387D-05	0.18918D-05
14	18.00	90.00	-0.11899D-04	0.41097D-04	0.87816D-04	0.41032D-05	0.24851D-05	0.29061D-05
15	18.00	112.50	-0.71767D-05	0.65016D-04	0.65241D-04	-0.18258D-04	0.24814D-05	0.37731D-05
16	18.00	135.00	-0.12429D-05	0.68049D-04	0.41458D-04	0.69399D-05	-0.11214D-05	0.41194D-05
17	18.00	157.50	0.43316D-05	0.53074D-04	0.15587D-04	-0.28341D-04	-0.24275D-05	0.23463D-05
18	18.00	180.00	0.66198D-05	0.40173D-04	0.00000D+00	0.00000D+00	-0.53711D-05	0.00000D+00
19	24.00	0.00	-0.12806D-04	-0.11760D-03	0.00000D+00	0.00000D+00	0.38286D-06	0.00000D+00
20	24.00	22.50	-0.12801D-04	-0.10013D-03	0.43608D-04	-0.70626D-05	0.51886D-06	0.27098D-07
21	24.00	45.00	-0.12586D-04	-0.54149D-04	0.74371D-04	-0.11026D-04	0.80929D-06	0.17075D-06
22	24.00	67.50	-0.11953D-04	0.36922D-05	0.84118D-04	-0.99463D-05	0.99767D-06	0.41453D-06
23	24.00	90.00	-0.10442D-04	0.51563D-04	0.72423D-04	-0.31733D-05	0.94652D-06	0.89686D-06
24	24.00	112.50	-0.77575D-05	0.71147D-04	0.47018D-04	0.68981D-05	0.36690D-06	0.13394D-05
25	24.00	135.00	-0.43644D-05	0.57039D-04	0.20537D-04	0.15395D-04	-0.69406D-06	0.14857D-05
26	24.00	157.50	-0.12793D-05	0.22133D-04	0.41719D-05	0.15810D-04	-0.17139D-05	0.10194D-05
27	24.00	180.00	-0.67623D-37	0.43699D-24	0.25557D-24	0.00000D+00	-0.21854D-05	0.00000D+00
28	30.00	0.00	-0.83707D-05	-0.12252D-03	0.00000D+00	0.00000D+00	-0.19930D-17	0.00000D+00
29	30.00	22.50	-0.83707D-05	-0.10169D-03	0.44992D-04	0.21644D-04	-0.19240D-17	-0.75940D-18
30	30.00	45.00	-0.83707D-05	-0.55079D-04	0.72923D-04	-0.69162D-05	-0.78471D-18	-0.10007D-17
31	30.00	67.50	-0.83707D-05	0.50018D-05	0.84681D-04	0.28205D-04	-0.23960D-18	-0.13601D-17
32	30.00	90.00	-0.83707D-05	0.59130D-04	0.70293D-04	0.86308D-05	0.51117D-18	-0.19383D-17
33	30.00	112.50	-0.83707D-05	0.74521D-04	0.41740D-04	-0.24120D-04	0.91935D-18	-0.14308D-17
34	30.00	135.00	-0.83707D-05	0.59061D-04	0.18954D-04	0.99276D-05	0.32361D-18	-0.19547D-18
35	30.00	157.50	-0.83707D-05	0.24050D-04	-0.88334D-07	-0.43055D-04	0.53341D-18	-0.24379D-18
36	30.00	180.00	-0.83707D-05	-0.11390D-05	0.00000D+00	0.00000D+00	0.24049D-18	0.00000D+00
37	36.00	0.00	[illegible]	-0.11760D-03	0.00000D+00	0.00000D+00	-0.38286D-06	0.00000D+00
[illegible]	[illegible]	[illegible]	[illegible]	-0.10013D-03	0.43608D-04	-0.70626D-05	-0.51886D-06	-0.27098D-07
[illegible]	[illegible]	[illegible]	[illegible]	-0.54149D-04	0.74371D-04	-0.11026D-04	-0.80929D-06	-0.17075D-06

40	36.00	67.50	-0.47982D-05	0.26922D-05	0.84118D-04	-0.99463D-05	-0.99767D-06	-0.41453D-06
41	36.00	90.00	-0.62990D-05	0.51563D-04	0.72423D-04	-0.31733D-05	-0.34652D-06	-0.89686D-06
42	36.00	112.50	-0.99839D-05	0.71147D-04	0.47018D-04	0.68981D-05	-0.36690D-06	-0.13394D-05
43	36.00	135.00	-0.12377D-04	0.57038D-04	0.20537D-04	0.15395D-04	0.69406D-06	-0.14857D-05
44	36.00	157.50	-0.15462D-04	0.22133D-04	0.41719D-05	0.15810D-04	0.17189D-05	-0.10194D-05
45	36.00	180.00	-0.16741D-04	0.43699D-24	0.25557D-24	0.00000D+00	0.21854D-05	0.00000D+00
46	42.00	0.00	-0.20214D-06	-0.12590D-03	0.00000D+00	0.00000D+00	0.18084D-05	0.00000D+00
47	42.00	22.50	-0.28453D-06	-0.10722D-03	0.46773D-04	0.15907D-04	0.21025D-06	-0.42673D-06
48	42.00	45.00	-0.73672D-06	-0.66145D-04	0.78865D-04	-0.51829D-05	-0.17400D-05	-0.11723D-05
49	42.00	67.50	-0.19217D-05	-0.99275D-05	0.95408D-04	0.19955D-04	-0.18387D-05	-0.18918D-05
50	42.00	90.00	-0.48420D-05	0.41097D-04	0.87816D-04	0.41032D-05	-0.24851D-05	-0.29061D-05
51	42.00	112.50	-0.96043D-05	0.65016D-04	0.65241D-04	-0.19258D-04	-0.24814D-05	-0.37731D-05
52	42.00	135.00	-0.15499D-04	0.68049D-04	0.41458D-04	0.69399D-05	0.11214D-05	-0.41194D-05
53	42.00	157.50	-0.21073D-04	0.53074D-04	0.15587D-04	-0.28341D-04	0.24275D-05	-0.23463D-05
54	42.00	180.00	-0.23361D-04	0.40178D-04	0.00000D+00	0.00000D+00	0.53711D-05	0.00000D+00
55	48.00	0.00	0.21106D-05	-0.12823D-03	0.00000D+00	0.00000D+00	-0.48350D-06	0.00000D+00
56	48.00	22.50	0.20973D-05	-0.11412D-03	0.47874D-04	-0.35474D-05	-0.98340D-06	-0.78315D-07
57	48.00	45.00	0.13202D-05	-0.75323D-04	0.85467D-04	-0.53313D-05	-0.19823D-05	-0.68775D-06
58	48.00	67.50	-0.60010D-06	-0.25053D-04	0.10540D-03	-0.47597D-05	-0.24357D-05	-0.11071D-05
59	48.00	90.00	-0.44169D-05	0.23989D-04	0.10552D-03	-0.64468D-06	-0.24753D-05	-0.21794D-05
60	48.00	112.50	-0.10594D-04	0.58587D-04	0.89218D-04	0.37645D-05	-0.10150D-05	-0.29050D-05
61	48.00	135.00	-0.17676D-04	0.76410D-04	0.62632D-04	0.59501D-05	0.18219D-05	-0.30829D-05
62	48.00	157.50	-0.23762D-04	0.80671D-04	0.31699D-04	0.50143D-05	0.41660D-05	-0.19623D-05
63	48.00	180.00	-0.26256D-04	0.80278D-04	0.00000D+00	0.00000D+00	0.53729D-05	0.00000D+00

LOAD CONDITION=2
****

DISPLACEMENTS

NODE	X	THETA	UX	UP	UT	PHIX	PHIT	PHIR
1	12.00	0.00	-0.51182D-02	-0.93660D-02	0.00000D+00	0.00000D+00	0.43604D-03	0.00000D+00
2	12.00	22.50	-0.49186D-02	-0.79383D-02	0.33405D-02	-0.20314D-03	0.40666D-03	0.16772D-03
3	12.00	45.00	-0.43463D-02	-0.54526D-02	0.59985D-02	-0.28691D-03	0.32623D-03	0.31217D-03
4	12.00	67.50	-0.34364D-02	-0.20741D-02	0.74828D-02	-0.24904D-03	0.18986D-03	0.40914D-03
5	12.00	90.00	-0.24604D-02	0.13025D-02	0.76205D-02	-0.32332D-04	0.38061D-04	0.45306D-03
6	12.00	112.50	-0.14019D-02	0.28985D-02	0.65764D-02	0.21611D-03	-0.13230D-03	0.43350D-03
7	12.00	135.00	-0.46485D-03	0.54347D-02	0.47186D-02	0.32601D-03	-0.31749D-03	0.35425D-03
8	12.00	157.50	0.19262D-03	0.50785D-02	0.24343D-02	0.26694D-03	-0.45705D-03	0.19698D-03
9	12.00	180.00	0.42195D-03	0.62077D-02	0.00000D+00	0.00000D+00	-0.51745D-03	0.00000D+00
10	18.00	0.00	-0.51481D-02	-0.61521D-02	0.00000D+00	0.00000D+00	0.47530D-03	0.00000D+00
11	18.00	22.50	-0.49279D-02	-0.53956D-02	0.23419D-02	0.52928D-03	0.41973D-03	0.26080D-03
12	18.00	45.00	-0.43077D-02	-0.35139D-02	0.40557D-02	-0.16695D-03	0.31828D-03	0.32946D-03
13	18.00	67.50	-0.34051D-02	-0.10246D-02	0.50114D-02	0.70613D-03	0.13106D-03	0.68735D-03
14	18.00	90.00	-0.23698D-02	0.15358D-02	0.48495D-02	0.23074D-03	-0.31472D-04	0.76995D-03
15	18.00	112.50	-0.13578D-02	0.31096D-02	0.39420D-02	-0.59937D-03	-0.15474D-03	0.56712D-03
16	18.00	135.00	-0.50365D-03	0.36189D-02	0.25711D-02	0.23474D-03	-0.29283D-03	0.35945D-03
17	18.00	157.50	0.90595D-04	0.33368D-02	0.11177D-02	-0.10561D-02	-0.35863D-03	0.24083D-03
18	18.00	180.00	0.39290D-03	0.23901D-02	0.00000D+00	0.00000D+00	-0.45946D-03	0.00000D+00
19	24.00	0.00	-0.52000D-02	-0.39727D-02	0.00000D+00	0.00000D+00	0.50657D-03	0.00000D+00
20	24.00	22.50	-0.49506D-02	-0.26686D-02	0.11543D-02	-0.14242D-03	0.45245D-03	0.20653D-03
21	24.00	45.00	-0.42634D-02	-0.15705D-02	0.20059D-02	-0.23932D-03	0.30908D-03	0.36681D-03
22	24.00	67.50	-0.32901D-02	-0.98756D-04	0.23385D-02	-0.24911D-03	0.11243D-03	0.45278D-03
23	24.00	90.00	-0.22046D-02	0.12573D-02	0.20960D-02	-0.12256D-03	-0.86817D-04	0.44410D-03
24	24.00	112.50	-0.12463D-02	0.19653D-02	0.14275D-02	0.13401D-03	-0.23524D-03	0.36089D-03
25	24.00	135.00	-0.53530D-03	0.17138D-02	0.65937D-03	0.41366D-03	-0.31534D-03	0.23793D-03
26	24.00	157.50	-0.12660D-03	0.71597D-03	0.14503D-03	0.49233D-03	-0.33811D-03	0.11082D-03
27	24.00	180.00	-0.22823D-34	0.18266D-22	0.15919D-22	0.00000D+00	-0.33722D-03	0.00000D+00
28	30.00	0.00	-0.52285D-02	0.43961D-03	0.00000D+00	0.00000D+00	0.55241D-03	0.00000D+00
29	30.00	22.50	-0.49675D-02	0.36347D-03	-0.16218D-03	-0.74305D-04	0.51086D-03	0.29058D-03
30	30.00	45.00	-0.42457D-02	0.20459D-03	-0.26632D-03	0.24546D-04	0.30175D-03	0.38492D-03
31	30.00	67.50	-0.32110D-02	-0.19130D-04	-0.31080D-03	-0.95434D-04	0.10186D-03	0.71095D-03
32	30.00	90.00	-0.21123D-02	-0.20637D-03	-0.25992D-03	-0.25302D-04	-0.15192D-03	0.74309D-03
33	30.00	112.50	-0.11716D-02	-0.26419D-03	-0.15343D-03	0.83933D-04	-0.36549D-03	0.55502D-03
34	30.00	135.00	-0.53922D-03	-0.21837D-03	-0.75184D-04	-0.35220D-04	-0.35772D-03	0.62724D-04
35	30.00	157.50	-0.24724D-03	-0.89148D-04	-0.32340D-05	0.15555D-03	-0.35431D-03	0.13290D-03
36	30.00	180.00	-0.17760D-03	-0.87475D-06	0.00000D+00	0.00000D+00	-0.17981D-03	0.00000D+00
37	36.00	0.00	-0.52061D-02	0.39098D-02	0.00000D+00	0.00000D+00	0.50422D-03	0.00000D+00
38	36.00	22.50	-0.49557D-02	0.33821D-02	-0.14649D-02	0.13215D-03	0.45149D-03	0.20497D-03
39	36.00	45.00	-0.42757D-02	0.19530D-02	-0.25360D-02	0.31729D-03	0.31125D-03	0.36498D-03
40	36.00	67.50	-0.32960D-02	0.75001D-04	-0.29387D-02	0.31962D-03	0.11727D-03	0.45194D-03
41	36.00	90.00	-0.22194D-02	-0.16219D-02	-0.26136D-02	0.14501D-03	-0.80558D-04	0.44622D-03
42	36.00	112.50	-0.12517D-02	-0.24700D-02	-0.17645D-02	-0.19301D-03	-0.23114D-03	0.36554D-03
43	36.00	135.00	-0.52481D-03	-0.21192D-02	-0.80747D-03	-0.52317D-03	-0.31710D-03	0.24543D-03
44	36.00	157.50	[illegible]	-0.27337D-03	-0.17577D-03	-0.60493D-03	-0.34633D-03	0.11637D-03
45	36.00	180.00	[illegible]	-0.21369D-22	-0.17897D-22	0.00000D+00	-0.34357D-03	0.00000D+00
[illegible]	[illegible]	[illegible]	[illegible]	[illegible]	0.00000D+00	0.00000D+00	0.46503D-03	0.00000D+00

47	42.00	22.50	-0.49417D-02	0.60891D-02	-0.26536D-02	-0.63722D-03	0.40829D-03	0.25881D-03
48	42.00	45.00	-0.43233D-02	0.39627D-02	-0.45323D-02	0.20352D-03	0.32281D-03	0.32903D-03
49	42.00	67.50	-0.34331D-02	0.10609D-02	-0.56452D-02	-0.84131D-03	0.13795D-03	0.68876D-03
50	42.00	90.00	-0.23951D-02	-0.18296D-02	-0.54228D-02	-0.24664D-03	-0.16011D-04	0.77761D-03
51	42.00	112.50	-0.13676D-02	-0.35439D-02	-0.42609D-02	0.73544D-03	-0.13853D-03	0.68186D-03
52	42.00	135.00	-0.49646D-03	-0.40725D-02	-0.28322D-02	-0.28420D-03	-0.29320D-03	0.37994D-03
53	42.00	157.50	0.12653D-03	-0.36631D-02	-0.12088D-02	0.12622D-02	-0.38347D-03	0.25249D-03
54	42.00	180.00	0.35139D-03	-0.31202D-02	0.00000D+00	0.00000D+00	-0.49294D-03	0.00000D+00
55	48.00	0.00	-0.51307D-02	0.96574D-02	0.00000D+00	0.00000D+00	0.42974D-03	0.00000D+00
56	48.00	22.50	-0.49356D-02	0.86381D-02	-0.36313D-02	0.22914D-03	0.40403D-03	0.16454D-03
57	48.00	45.00	-0.43717D-02	0.59106D-02	-0.65140D-02	0.32480D-03	0.32885D-03	0.30844D-03
58	48.00	67.50	-0.35193D-02	0.22117D-02	-0.81114D-02	0.28180D-03	0.20388D-03	0.40751D-03
59	48.00	90.00	-0.24897D-02	-0.14607D-02	-0.82398D-02	0.35943D-04	0.55863D-04	0.45829D-03
60	48.00	112.50	-0.14109D-02	-0.42406D-02	-0.70900D-02	-0.24354D-03	-0.12142D-03	0.44462D-03
61	48.00	135.00	-0.44475D-03	-0.58703D-02	-0.50721D-02	-0.36818D-03	-0.31883D-03	0.36751D-03
62	48.00	157.50	0.24200D-03	-0.65174D-02	-0.26104D-02	-0.30190D-03	-0.47660D-03	0.20718D-03
63	48.00	180.00	0.49447D-03	-0.66348D-02	0.00000D+00	0.00000D+00	-0.54538D-03	0.00000D+00

LOAD CONDITION=3
****

DISPLACEMENTS

NODE	X	THETA	UX	UR	UT	PHIX	PHIT	PHIR
1	12.00	0.00	-0.60950D-02	-0.98501D-02	0.00000D+00	0.00000D+00	0.51457D-03	0.00000D+00
2	12.00	22.50	-0.53566D-02	-0.88143D-02	0.37256D-02	-0.23485D-03	0.47506D-03	0.20008D-03
3	12.00	45.00	-0.51799D-02	-0.60242D-02	0.66820D-02	-0.32516D-03	0.36671D-03	0.36513D-03
4	12.00	67.50	-0.41662D-02	-0.22588D-02	0.83237D-02	-0.27743D-03	0.21028D-03	0.48220D-03
5	12.00	90.00	-0.29649D-02	0.14919D-02	0.84642D-02	-0.32617D-04	0.30893D-04	0.52718D-03
6	12.00	112.50	-0.17369D-02	0.43452D-02	0.72929D-02	0.25060D-03	-0.16155D-03	0.50048D-03
7	12.00	135.00	-0.66378D-03	0.60302D-02	0.52259D-02	0.36977D-03	-0.35697D-03	0.40155D-03
8	12.00	157.50	0.93219D-04	0.67303D-02	0.26944D-02	0.29823D-03	-0.51637D-03	0.22384D-03
9	12.00	180.00	0.35450D-03	0.68700D-02	0.00000D+00	0.00000D+00	-0.58305D-03	0.00000D+00
10	18.00	0.00	-0.61989D-02	-0.66897D-02	0.00000D+00	0.00000D+00	0.58444D-03	0.00000D+00
11	18.00	22.50	-0.59218D-02	-0.58659D-02	0.25543D-02	0.55574D-03	0.52164D-03	0.31119D-03
12	18.00	45.00	-0.51830D-02	-0.38441D-02	0.44492D-02	-0.17488D-03	0.36478D-03	0.37798D-03
13	18.00	67.50	-0.40918D-02	-0.11424D-02	0.55020D-02	0.74189D-03	0.15323D-03	0.82115D-03
14	18.00	90.00	-0.28547D-02	0.16498D-02	0.53358D-02	0.24763D-03	-0.53264D-04	0.91699D-03
15	18.00	112.50	-0.16599D-02	0.33835D-02	0.42371D-02	-0.63942D-03	-0.20045D-03	0.78255D-03
16	18.00	135.00	-0.66280D-03	0.39603D-02	0.28363D-02	0.24763D-03	-0.33656D-03	0.39530D-03
17	18.00	157.50	0.52152D-05	0.36509D-02	0.12358D-02	-0.11270D-02	-0.42599D-03	0.27258D-03
18	18.00	180.00	0.24679D-03	0.31660D-02	0.00000D+00	0.00000D+00	-0.51828D-03	0.00000D+00
19	24.00	0.00	-0.63671D-02	-0.30627D-02	0.00000D+00	0.00000D+00	0.62625D-03	0.00000D+00
20	24.00	22.50	-0.60567D-02	-0.26746D-02	0.11563D-02	-0.12992D-03	0.55708D-03	0.25675D-03
21	24.00	45.00	-0.52037D-02	-0.16090D-02	0.20198D-02	-0.22453D-03	0.37455D-03	0.45479D-03
22	24.00	67.50	-0.39843D-02	-0.15345D-03	0.23737D-02	-0.24434D-03	0.13092D-03	0.56087D-03
23	24.00	90.00	-0.26565D-02	0.12255D-02	0.21498D-02	-0.13163D-03	-0.11511D-03	0.54600D-03
24	24.00	112.50	-0.14945D-02	0.19837D-02	0.14824D-02	0.12184D-03	-0.29368D-03	0.43859D-03
25	24.00	135.00	-0.62763D-03	0.17657D-02	0.69542D-03	0.41550D-03	-0.38224D-03	0.28298D-03
26	24.00	157.50	-0.14630D-03	0.74960D-03	0.15730D-03	0.51182D-03	-0.40268D-03	0.12892D-03
27	24.00	180.00	-0.27928D-34	0.20008D-22	0.18597D-22	0.00000D+00	-0.39790D-03	0.00000D+00
28	30.00	0.00	-0.65374D-02	0.13729D-02	0.00000D+00	0.00000D+00	0.70695D-03	0.00000D+00
29	30.00	22.50	-0.62044D-02	0.11458D-02	-0.48925D-03	-0.26373D-03	0.65571D-03	0.36940D-03
30	30.00	45.00	-0.52839D-02	0.57368D-03	-0.77815D-03	0.79205D-04	0.38013D-03	0.48148D-03
31	30.00	67.50	-0.39601D-02	-0.49509D-04	-0.89793D-03	-0.34939D-03	0.13461D-03	0.90900D-03
32	30.00	90.00	-0.25541D-02	-0.66398D-03	-0.73217D-03	-0.13153D-03	-0.19027D-03	0.95350D-03
33	30.00	112.50	-0.13475D-02	-0.95691D-03	-0.40704D-03	0.24921D-03	-0.46261D-03	0.71231D-03
34	30.00	135.00	-0.53143D-03	-0.62616D-03	-0.16179D-03	-0.11352D-03	-0.45064D-03	0.74885D-04
35	30.00	157.50	-0.15332D-03	-0.25395D-03	0.26995D-04	0.47663D-03	-0.45444D-03	0.17034D-03
36	30.00	180.00	-0.61934D-04	0.44826D-04	0.00000D+00	0.00000D+00	-0.23385D-03	0.00000D+00
37	36.00	0.00	-0.66640D-02	0.57408D-02	0.00000D+00	0.00000D+00	0.66957D-03	0.00000D+00
38	36.00	22.50	-0.63373D-02	0.49502D-02	-0.21464D-02	0.29470D-03	0.60051D-03	0.27077D-03
39	36.00	45.00	-0.54345D-02	0.28290D-02	-0.37052D-02	0.47946D-03	0.41675D-03	0.48242D-03
40	36.00	67.50	-0.41379D-02	0.53826D-04	-0.42749D-02	0.47263D-03	0.16603D-03	0.59960D-03
41	36.00	90.00	-0.27033D-02	-0.24119D-02	-0.37806D-02	0.20438D-03	-0.93768D-04	0.59792D-03
42	36.00	112.50	-0.13976D-02	-0.36095D-02	-0.25346D-02	-0.27902D-03	-0.29809D-03	0.49845D-03
43	36.00	135.00	-0.40032D-03	-0.30647D-02	-0.11489D-02	-0.76518D-03	-0.42211D-03	0.34071D-03
44	36.00	157.50	0.19629D-03	-0.12532D-02	-0.24494D-03	-0.87043D-03	-0.47411D-03	0.16569D-03
45	36.00	180.00	0.38807D-03	-0.30008D-22	-0.23723D-22	0.00000D+00	-0.48310D-03	0.00000D+00
46	[illegible]	[illegible]	[illegible]	[illegible]	[illegible]	0.00000D+00	0.63369D-03	0.00000D+00

47	42.00	22.50	-0.64582D-02	0.87139D-02	-0.37777D-02	-0.95964D-03	0.56639D-03	0.35652D-03
48	42.00	45.00	-0.56169D-02	0.55600D-02	-0.64885D-02	0.29150D-03	0.45777D-03	0.46422D-03
49	42.00	67.50	-0.43811D-02	0.15372D-02	-0.79788D-02	-0.12430D-02	0.22056D-03	0.95942D-03
50	42.00	90.00	-0.29244D-02	-0.25892D-02	-0.76665D-02	-0.40030D-03	0.19765D-05	0.10894D-02
51	42.00	112.50	-0.14877D-02	-0.50352D-02	-0.60240D-02	0.10128D-02	-0.17416D-03	0.96386D-03
52	42.00	135.00	-0.23724D-03	-0.57220D-02	-0.40195D-02	-0.40842D-03	-0.41557D-03	0.54899D-03
53	42.00	157.50	0.63949D-03	-0.52560D-02	-0.17351D-02	0.17456D-02	-0.53639D-03	0.36186D-03
54	42.00	180.00	0.96177D-03	-0.45188D-02	0.00000D+00	0.00000D+00	-0.69783D-03	0.00000D+00
55	48.00	0.00	-0.68396D-02	0.13706D-01	0.00000D+00	0.00000D+00	0.60463D-03	0.00000D+00
56	48.00	22.50	-0.65705D-02	0.12273D-01	-0.51621D-02	0.31440D-03	0.58190D-03	0.22830D-03
57	48.00	45.00	-0.57744D-02	0.84298D-02	-0.92687D-02	0.44345D-03	0.50270D-03	0.44314D-03
58	48.00	67.50	-0.45517D-02	0.32029D-02	-0.11561D-01	0.39089D-03	0.32095D-03	0.58773D-03
59	48.00	90.00	-0.30542D-02	-0.20407D-02	-0.11775D-01	0.60934D-04	0.86899D-04	0.66997D-03
60	48.00	112.50	-0.14781D-02	-0.60563D-02	-0.10160D-01	-0.33219D-03	-0.19426D-03	0.64711D-03
61	48.00	135.00	-0.75943D-04	-0.84372D-02	-0.72900D-02	-0.50964D-03	-0.48929D-03	0.53436D-03
62	48.00	157.50	0.91206D-03	-0.94229D-02	-0.37608D-02	-0.41462D-03	-0.69705D-03	0.29522D-03
63	48.00	180.00	0.12709D-02	-0.96183D-02	0.00000D+00	0.00000D+00	-0.78630D-03	0.00000D+00

REACTIONS AT P/U

LOAD CASE	PX1	RR1	RT1	RR2	RT2
1	0.00 Lbs	4.37 Lbs	2.56 Lbs	4.37 Lbs	2.56 Lbs
2	0.00 Lbs	182.66 Lbs	159.19 Lbs	-213.68 Lbs	-178.97 Lbs
3	0.00 Lbs	200.08 Lbs	185.97 Lbs	-300.08 Lbs	-237.23 Lbs

STRESS RESULTANT
****

SHELL ELEMENT STRESSES
Nx,Ntheta,Nxt, & Mx,Mt,Mxt at EACH NODE
RING AND STRINGER ELEMENT END FORCES & COUPLES IN GLOBAL COORD.
Fx(LONG.),Fr(RADIAL), Ft(TANGENTIAL), Mx ,Mt & Mr

SHELL ELEMENT
****

STRESS RESULTANT OF --- Nx ---
****

IS= 1

X=	12.000	ILC= 1	0.000	22.500	45.000	67.500	90.000	112.500	135.000	157.500	180.000
			0.000	0.000	0.000	0.000	0.000	0.000	0.000	0.000	0.000
			0.000	0.000	0.000	0.000	0.000	0.000	0.000	0.000	0.000
			0.000	0.272	0.214	0.136	0.020	-0.139	-0.228	-0.293	-0.289
			0.251	0.268	0.205	0.106	0.037	-0.114	-0.192	-0.222	0.000
		AVRG	0.251	0.270	0.210	0.121	0.028	-0.126	-0.210	-0.258	-0.289
X=	12.000	ILC= 2	0.000	22.500	45.000	67.500	90.000	112.500	135.000	157.500	180.000
			0.000	0.000	0.000	0.000	0.000	0.000	0.000	0.000	0.000
			0.000	0.000	0.000	0.000	0.000	0.000	0.000	0.000	0.000
			0.000	0.192	3.847	7.548	7.859	2.398	-5.060	-12.139	-14.033
			-2.266	-0.273	3.319	6.000	7.551	3.626	-3.151	-9.181	0.000
		AVRG	-2.266	-0.093	3.582	6.774	7.705	3.012	-4.106	-10.660	-14.033
X=	12.000	ILC= 3	0.000	22.500	45.000	67.500	90.000	112.500	135.000	157.500	180.000
			0.000	0.000	0.000	0.000	0.000	0.000	0.000	0.000	0.000
			0.000	0.000	0.000	0.000	0.000	0.000	0.000	0.000	0.000
			0.000	-5.940	0.142	7.041	10.298	6.325	-0.648	-7.991	-10.213
			-9.301	-6.956	-0.615	5.273	9.536	7.582	1.354	-4.976	0.000
		AVRG	-9.301	-6.448	-0.236	6.157	9.917	6.953	0.353	-6.483	-10.213

IS= 1

X=	18.000	ILC= 1	0.000	22.500	45.000	67.500	90.000	112.500	135.000	157.500	180.000
			0.000	0.178	0.211	0.084	0.044	-0.042	-0.214	-0.172	-0.286
			0.210	0.171	0.209	0.128	0.027	-0.023	-0.211	-0.219	0.000
			0.000	[illegible]	0.289	0.281	0.123	-0.064	-0.273	-0.602	-0.650
			0.355	0.379	0.329	0.341	0.207	-0.029	-0.219	-0.608	0.000
		AVRG	[illegible]	0.266	0.260	0.209	0.100	-0.039	-0.229	-0.400	-0.468
X=	18.000	ILC= 2	0.000	22.500	45.000	67.500	90.000	112.500	135.000	157.500	180.000
			0.000	-1.314	4.150	6.759	7.609	4.533	-3.288	-7.998	-12.336
			[illegible]	-1.322	3.997	7.904	7.504	4.258	-3.755	-9.559	0.000
			0.000	[illegible]	4.061	13.147	15.742	10.534	-3.052	-21.834	-28.694
			[illegible]	[illegible]	[illegible]	13.174	17.627	12.474	0.125	-21.395	0.000

AVRG	-3.726	-1.746	3.855	10.245	12.123	7.963	-2.493	-15.194	-20.515

X= 18.000 ILC= 3	0.000	22.500	45.000	67.500	90.000	112.500	135.000	157.500	180.000
	0.000	-7.186	-0.192	6.596	8.996	7.560	0.564	-4.933	-9.218
	-9.105	-6.824	-0.378	7.356	9.060	6.864	-0.057	-6.491	0.000
	0.000	-12.422	-1.521	11.296	19.399	17.075	3.307	-15.937	-24.014
	-16.735	-13.120	-3.315	10.673	20.429	18.899	6.499	-15.754	0.000
AVRG	-12.950	-9.888	-1.351	8.980	14.471	12.599	2.578	-10.779	-16.616

IS= 1

X= 24.000 ILC= 1	0.000	22.500	45.000	67.500	90.000	112.500	135.000	157.500	180.000
	0.000	0.495	0.401	0.291	0.072	-0.218	-0.447	-0.631	-0.596
	0.487	0.460	0.351	0.206	0.008	-0.258	-0.468	-0.537	0.000
	0.000	0.585	0.505	0.378	0.153	-0.220	-0.572	-0.831	-0.823
	0.564	0.539	0.440	0.276	0.080	-0.233	-0.536	-0.676	0.000
FRAME FCWD AVRG.	0.487	0.478	0.376	0.249	0.040	-0.238	-0.458	-0.584	-0.595
FRAME REAR AVRG.	0.564	0.562	0.473	0.327	0.117	-0.226	-0.554	-0.754	-0.823
AVRG.	0.525	0.520	0.424	0.288	0.078	-0.232	-0.506	-0.669	-0.709

X= 24.000 ILC= 2	0.000	22.500	45.000	67.500	90.000	112.500	135.000	157.500	180.000
	0.000	-0.419	5.951	13.565	16.844	8.474	-7.306	-24.100	-28.885
	-4.023	-0.794	5.820	12.254	14.714	6.417	-9.277	-21.578	0.000
	0.000	-0.561	1.567	5.723	7.083	4.916	-2.080	-11.416	-13.614
	-0.554	1.141	4.320	7.428	5.840	0.149	-9.024	-13.992	0.000
FRAME FCWD AVRG.	-4.023	-0.507	5.890	12.910	15.779	7.445	-8.292	-22.839	-28.885
FRAME REAR AVRG.	-0.554	0.280	2.394	6.575	6.462	2.532	-5.552	-12.704	-13.614
AVRG.	-2.288	-0.163	4.442	9.742	11.120	4.989	-6.922	-17.772	-21.249

X= 24.000 ILC= 3	0.000	22.500	45.000	67.500	90.000	112.500	135.000	157.500	180.000
	0.000	-11.913	-1.360	11.625	20.491	15.276	-0.328	-18.469	-23.929
	-16.961	-11.908	-0.961	10.811	18.561	13.211	-2.440	-15.705	0.000
	0.000	-15.414	-9.772	0.463	7.693	11.824	9.596	1.795	0.083
	-16.248	-12.801	-5.979	3.289	6.900	5.856	0.574	-2.413	0.000
FRAME FCWD AVRG.	-16.961	-11.911	-1.161	11.218	19.571	14.244	-1.384	-17.087	-23.929
FRAME REAR AVRG.	-16.248	-14.109	-7.875	1.876	7.297	8.840	5.085	-0.309	0.083
AVRG.	-16.605	-13.009	-4.518	6.547	13.434	11.542	1.850	-8.698	-11.923

IS= 1

X= 30.000 ILC= 1	0.000	22.500	45.000	67.500	90.000	112.500	135.000	157.500	180.000
	0.000	0.376	0.379	0.323	0.187	-0.021	-0.351	-0.661	-0.826
	0.405	0.409	0.414	0.402	0.254	0.019	-0.315	-0.708	0.000
	0.000	0.376	0.379	0.323	0.187	-0.021	-0.351	-0.661	-0.826
	0.405	0.409	0.414	0.402	0.254	0.019	-0.315	-0.708	0.000
AVRG	0.405	0.392	0.396	0.363	0.221	-0.001	-0.333	-0.685	-0.826

X= 30.000 ILC= 2	0.000	22.500	45.000	67.500	90.000	112.500	135.000	157.500	180.000
	0.000	-0.740	2.173	10.065	10.574	5.171	-1.732	-18.672	-19.272
	-3.997	-1.727	0.068	7.791	12.534	9.235	3.354	-14.926	0.000
	0.000	0.353	-3.250	-11.400	-12.012	-7.090	2.444	20.935	22.587
	3.601	1.214	-1.31[illegible]	-9.439	-14.294	-10.331	-3.326	17.608	0.000
AVRG	[illegible]	[illegible]	-0.590	-0.796	-0.799	-0.516	0.310	1.237	1.658

X= 30.000	ILC= 3	0.000	22.500	45.000	67.500	90.000	112.500	135.000	157.500	180.000
		0.000	-12.625	-6.884	5.913	12.325	11.984	7.486	-9.530	-9.489
		-17.926	-14.250	-9.999	3.152	13.884	15.274	14.072	-4.661	0.000
		0.000	-13.383	-14.302	-21.353	-15.901	-3.657	13.981	42.934	45.662
		-10.452	-13.167	-12.606	-19.956	-20.136	-8.461	5.940	38.516	0.000
	AVRG	-14.139	-13.356	-10.946	-7.811	-2.457	3.785	10.370	16.815	19.086

IS= 1

X= 36.000	ILC= 1	0.000	22.500	45.000	67.500	90.000	112.500	135.000	157.500	180.000
		0.000	0.585	0.505	0.378	0.153	-0.220	-0.572	-0.831	-0.823
		0.564	0.539	0.440	0.276	0.080	-0.233	-0.536	-0.676	0.000
		0.000	0.495	0.401	0.291	0.072	-0.218	-0.447	-0.631	-0.596
		0.487	0.460	0.351	0.206	0.009	-0.258	-0.468	-0.537	0.000
FRAME FORD AVRG.		0.564	0.562	0.473	0.327	0.117	-0.226	-0.554	-0.754	-0.823
FRAME REAR AVRG.		0.487	0.478	0.376	0.249	0.040	-0.238	-0.458	-0.584	-0.596
	AVRG.	0.525	0.520	0.424	0.288	0.078	-0.232	-0.506	-0.669	-0.709

X= 36.000	ILC= 2	0.000	22.500	45.000	67.500	90.000	112.500	135.000	157.500	180.000
		0.000	-0.939	-3.132	-7.363	-8.082	-4.354	4.154	14.795	16.636
		-0.559	-2.407	-5.392	-8.338	-6.424	0.495	10.922	16.213	0.000
		0.000	-0.816	-6.995	-14.739	-17.252	-7.776	8.780	26.407	30.695
		3.037	-0.295	-6.522	-12.846	-14.529	-5.472	10.869	23.134	0.000
FRAME FORD AVRG.		-0.559	-1.673	-4.287	-7.850	-7.253	-1.929	7.488	15.504	16.636
FRAME REAR AVRG.		3.037	-0.555	-6.754	-13.792	-15.040	-6.624	9.825	24.771	30.695
	AVRG.	1.239	-1.114	-5.520	-10.821	-11.647	-4.277	8.656	20.137	23.666

X= 36.000	ILC= 3	0.000	22.500	45.000	67.500	90.000	112.500	135.000	157.500	180.000
		0.000	-13.067	-17.346	-17.020	-11.699	0.705	18.490	36.598	40.404
		-18.629	-18.171	-19.456	-17.405	-8.550	7.096	25.901	37.689	0.000
		0.000	-17.716	-22.500	-26.050	-22.649	-2.995	24.506	50.220	56.731
		-13.665	-14.220	-21.360	-23.143	-18.660	0.172	27.496	45.979	0.000
FRAME FORD AVRG.		-18.629	-18.619	-18.411	-17.213	-10.124	3.900	22.695	37.144	40.404
FRAME REAR AVRG.		-13.665	-14.968	-21.930	-24.597	-20.655	-1.412	26.001	43.099	56.731
	AVRG.	-16.147	-17.794	-20.171	-20.905	-15.389	1.244	24.348	42.621	48.568

IS= 1

X= 42.000	ILC= 1	0.000	22.500	45.000	67.500	90.000	112.500	135.000	157.500	180.000
		0.000	0.339	0.293	0.231	0.123	-0.064	-0.273	-0.602	-0.650
		0.355	0.379	0.329	0.341	0.207	-0.029	-0.219	-0.508	0.000
		0.000	0.173	0.211	0.034	0.044	-0.042	-0.214	-0.172	-0.286
		0.000	0.171	0.209	0.128	0.027	-0.023	-0.211	-0.219	0.000
	AVRG	[illegible]	0.266	0.260	0.209	0.100	-0.039	-0.229	-0.400	-0.468

X= 42.000	ILC= 2	0.000	22.500	45.000	67.500	90.000	112.500	135.000	157.500	180.000
		[illegible]	[illegible]	-4.754	-14.324	-16.771	-11.207	3.529	23.706	30.982
		[illegible]	[illegible]	-4.107	-14.715	-19.056	-13.399	0.052	23.496	0.000
		[illegible]	[illegible]	-4.734	-6.967	-8.135	-4.950	3.406	7.750	12.616
		[illegible]	[illegible]	-4.650	-8.397	-7.910	-4.693	3.827	9.542	0.000
	[illegible]	[illegible]	[illegible]	[illegible]	-11.076	-12.348	-8.550	2.703	16.124	21.799

X=	42.000	ILC= 3	0.000	22.500	45.000	67.500	90.000	112.500	135.000	157.500	180.000
			0.000	-11.466	-16.379	-24.698	-21.516	-8.135	15.397	46.906	56.779
			-8.993	-12.739	-16.336	-25.840	-25.619	-11.238	10.131	45.945	0.000
			0.000	-9.772	-15.380	-14.819	-9.593	0.171	15.108	21.926	28.929
			-8.838	-9.964	-15.215	-16.947	-10.039	0.139	15.585	24.515	0.000
		AVRG	-8.915	-10.985	-15.827	-20.576	-16.692	-4.766	14.055	34.823	42.854

IS= 1

X=	48.000	ILC= 1	0.000	22.500	45.000	67.500	90.000	112.500	135.000	157.500	180.000
			0.000	0.272	0.214	0.136	0.020	-0.139	-0.228	-0.293	-0.289
			0.251	0.268	0.205	0.106	0.037	-0.114	-0.192	-0.222	0.000
			0.000	0.000	0.000	0.000	0.000	0.000	0.000	0.000	0.000
			0.000	0.000	0.000	0.000	0.000	0.000	0.000	0.000	0.000
		AVRG	0.251	0.270	0.210	0.121	0.028	-0.125	-0.210	-0.258	-0.289
X=	48.000	ILC= 2	0.000	22.500	45.000	67.500	90.000	112.500	135.000	157.500	180.000
			0.000	-0.295	-3.882	-7.690	-7.719	-1.700	5.739	12.863	14.730
			2.458	0.355	-3.223	-5.874	-7.483	-3.113	3.637	9.522	0.000
			0.000	0.000	0.000	0.000	0.000	0.000	0.000	0.000	0.000
			0.000	0.000	0.000	0.000	0.000	0.000	0.000	0.000	0.000
		AVRG	2.458	0.030	-3.552	-6.782	-7.601	-2.406	4.689	11.195	14.730
X=	48.000	ILC= 3	0.000	22.500	45.000	67.500	90.000	112.500	135.000	157.500	180.000
			0.000	-14.310	-16.801	-16.672	-11.064	3.513	17.970	29.055	31.604
			-11.181	-13.518	-16.172	-14.330	-10.056	1.561	14.797	24.123	0.000
			0.000	0.000	0.000	0.000	0.000	0.000	0.000	0.000	0.000
			0.000	0.000	0.000	0.000	0.000	0.000	0.000	0.000	0.000
		AVRG	-11.181	-13.914	-16.486	-15.501	-10.560	2.537	16.384	26.539	31.604

SHEAR STRESS RESULTANT - Nxt -
****

IS= 3

X=	12.000	ILC= 1	0.000	22.500	45.000	67.500	90.000	112.500	135.000	157.500	180.000
			0.000	0.000	0.000	0.000	0.000	0.000	0.000	0.000	0.000
			0.000	0.000	0.000	0.000	0.000	0.000	0.000	0.000	0.000
			0.000	-0.014	-0.092	-0.172	-0.214	-0.287	-0.251	-0.174	-0.086
			-0.014	-0.092	-0.172	-0.214	-0.287	-0.251	-0.174	-0.087	0.000
		AVRG	0.000	-0.053	-0.132	-0.193	-0.250	-0.269	-0.213	-0.130	0.000

X=	12.000	ILC= 2	0.000	22.500	45.000	67.500	90.000	112.500	135.000	157.500	180.000
			0.000	0.000	0.000	0.000	0.000	0.000	0.000	0.000	0.000
			0.000	0.000	0.000	0.000	0.000	0.000	0.000	0.000	0.000
			0.000	1.036	0.769	0.041	-1.159	-5.828	-7.486	-7.000	-3.802
			1.034	0.770	0.040	-1.157	-5.326	-7.488	-6.998	-3.805	0.000
		AVRG	0.000	0.903	0.404	-0.558	-3.492	-5.658	-7.242	-5.403	0.000

X=	12.000	ILC= 3	0.000	22.500	45.000	67.500	90.000	112.500	135.000	157.500	180.000
			0.000	0.000	0.000	0.000	0.000	0.000	0.000	0.000	0.000
			0.000	0.000	0.000	0.000	0.000	0.000	0.000	0.000	0.000
			0.000	2.021	3.377	4.332	3.677	-1.696	-4.550	-5.921	-3.584
			2.019	3.379	4.330	3.679	-1.694	-4.551	-5.918	-3.587	0.000
		AVRG	0.000	2.700	3.854	4.005	0.992	-3.124	-5.234	-4.754	0.000

IS= 3

X=	18.000	ILC= 1	0.000	22.500	45.000	67.500	90.000	112.500	135.000	157.500	180.000
			0.000	-0.014	-0.092	-0.172	-0.214	-0.287	-0.251	-0.174	-0.086
			-0.014	-0.092	-0.172	-0.213	-0.287	-0.251	-0.174	-0.087	0.000
			0.000	-0.054	-0.100	-0.209	-0.300	-0.302	-0.344	-0.258	-0.073
			-0.054	-0.100	-0.209	-0.301	-0.302	-0.344	-0.258	-0.073	0.000
		AVRG	0.000	-0.065	-0.143	-0.224	-0.276	-0.296	-0.257	-0.148	0.000

X=	18.000	ILC= 2	0.000	22.500	45.000	67.500	90.000	112.500	135.000	157.500	180.000
			0.000	1.036	0.769	0.041	-1.159	-5.828	-7.486	-7.000	-3.802
			1.034	0.770	0.039	-1.157	-5.826	-7.488	-6.998	-3.805	0.000
			0.000	-0.151	0.992	0.616	-2.287	-4.216	-8.061	-8.816	-3.016
			-0.149	0.991	0.618	-2.289	-4.218	-8.060	-8.619	-3.013	0.000
		AVRG	0.000	0.661	0.605	-0.697	-3.372	-6.398	-7.841	-5.659	0.000

X=	18.000	ILC= 3	0.000	22.500	45.000	67.500	90.000	112.500	135.000	157.500	180.000
			0.000	2.020	3.377	4.332	3.677	-1.696	-4.550	-5.921	-3.584
			2.019	3.378	4.320	3.679	-1.693	-4.551	-5.918	-3.587	0.000
			0.000	0.919	3.755	5.201	2.804	0.380	-4.809	-7.525	-2.661
			2.821	3.753	5.203	2.802	0.377	-4.807	-7.528	-2.658	0.000
		AVRG	0.000	2.493	4.166	4.003	1.291	-2.669	-5.701	-4.923	0.000

IS= 3

X= 24.000	ILC= 1	0.000	22.500	45.000	67.500	90.000	112.500	135.000	157.500	180.000
		0.000	-0.054	-0.100	-0.209	-0.300	-0.302	-0.344	-0.258	-0.073
		-0.054	-0.100	-0.209	-0.301	-0.302	-0.344	-0.258	-0.073	0.000
		0.000	0.026	-0.002	0.004	0.042	-0.011	0.046	0.061	-0.008
		0.026	-0.002	0.004	0.042	-0.011	0.046	0.062	-0.008	0.000
FRAME FOWD AVRG.		0.000	-0.077	-0.154	-0.255	-0.301	-0.323	-0.301	-0.165	0.000
FRAME REAR AVRG.		0.000	0.012	0.001	0.023	0.015	0.017	0.054	0.027	0.000
FRAME SHEAR FLOW		0.000	-0.089	-0.156	-0.278	-0.317	-0.341	-0.354	-0.192	0.000

X= 24.000	ILC= 2	0.000	22.500	45.000	67.500	90.000	112.500	135.000	157.500	180.000
		0.000	-0.151	0.992	0.616	-2.288	-4.216	-8.061	-8.816	-3.015
		-0.149	0.991	0.618	-2.289	-4.218	-8.060	-8.819	-3.012	0.000
		0.000	-1.175	-2.037	1.459	8.136	16.915	22.867	20.668	8.505
		-1.175	-2.037	1.459	8.186	16.915	22.868	20.667	8.504	0.000
FRAME FOWD AVRG.		0.000	0.420	0.805	-0.836	-3.253	-6.138	-8.440	-5.914	0.000
FRAME REAR AVRG.		0.000	-1.606	-0.289	4.823	12.551	19.891	21.767	14.586	0.000
FRAME SHEAR FLOW		0.000	2.026	1.094	-5.659	-15.603	-26.029	-30.207	-20.500	0.000

X= 24.000	ILC= 3	0.000	22.500	45.000	67.500	90.000	112.500	135.000	157.500	180.000
		0.000	0.819	3.755	5.201	2.803	0.379	-4.808	-7.525	-2.661
		0.821	3.753	5.203	2.802	0.377	-4.307	-7.528	-2.658	0.000
		0.000	-1.141	-1.089	4.662	13.073	24.459	31.384	27.129	11.305
		-1.141	-1.089	4.662	13.072	24.459	31.385	27.128	11.305	0.000
FRAME FOWD AVRG.		0.000	2.286	4.479	4.001	1.590	-2.214	-6.168	-5.091	0.000
FRAME REAR AVRG.		0.000	-1.115	1.787	8.867	13.766	27.922	29.256	19.217	0.000
FRAME SHEAR FLOW		0.000	3.401	2.692	-4.865	-17.175	-30.136	-35.424	-24.308	0.000

IS= 3

X= 30.000	ILC= 1	0.000	22.500	45.000	67.500	90.000	112.500	135.000	157.500	180.000
		0.000	0.026	-0.002	0.004	0.042	-0.011	0.046	0.061	-0.008
		0.026	-0.002	0.004	0.042	-0.011	0.046	0.062	-0.008	0.000
		0.000	-0.026	0.002	-0.004	-0.042	0.011	-0.046	-0.061	0.008
		-0.026	0.002	-0.004	-0.042	0.011	-0.046	-0.062	0.008	0.000
	AVRG	0.000	0.000	0.000	0.000	0.000	0.000	0.000	0.000	0.000

X= 30.000	ILC= 2	0.000	22.500	45.000	67.500	90.000	112.500	135.000	157.500	180.000
		0.000	-1.175	-2.037	1.459	8.186	16.914	22.868	20.668	8.506
		-1.175	-2.038	1.459	8.185	16.914	22.869	20.668	8.505	0.000
		0.000	-0.969	-1.985	1.739	8.677	17.028	23.430	21.182	8.476
		-0.970	-1.965	1.739	8.673	17.029	23.430	21.182	8.475	0.000
	AVRG	0.000	-1.542	-0.206	5.016	12.702	20.060	22.037	14.707	0.000

X= 30.000	ILC= 3	0.000	22.500	45.000	67.500	90.000	112.500	135.000	157.500	180.000
		0.000	-1.141	-1.089	4.662	13.072	24.459	31.384	27.129	11.306
		-1.141	-1.090	4.662	13.072	24.458	31.385	27.128	11.306	0.000
		0.000	-0.645	-1.439	3.495	13.047	23.235	31.208	28.187	11.023
		-0.647	-1.439	3.494	13.048	23.237	31.208	28.198	11.020	0.000
	AVRG	0.000	-1.079	1.407	8.569	18.453	27.572	29.477	19.411	0.000

IS= 3

X= 36.000	ILC= 1	0.000	22.500	45.000	67.500	90.000	112.500	135.000	157.500	180.000
		0.000	-0.026	0.002	-0.004	-0.042	0.011	-0.046	-0.061	0.008
		-0.026	0.002	-0.004	-0.042	0.011	-0.046	-0.062	0.008	0.000
		0.000	0.054	0.100	0.209	0.300	0.302	0.344	0.258	0.073
		0.054	0.100	0.209	0.301	0.302	0.344	0.258	0.073	0.000
FRAME FORD AVRG.		0.000	-0.012	-0.001	-0.023	-0.015	-0.017	-0.054	-0.027	0.000
FRAME REAR AVRG.		0.000	0.077	0.154	0.255	0.301	0.323	0.301	0.165	0.000
FRAME SHEAR FLOW		0.000	-0.089	-0.156	-0.278	-0.317	-0.341	-0.354	-0.192	0.000

X= 36.000	ILC= 2	0.000	22.500	45.000	67.500	90.000	112.500	135.000	157.500	180.000
		0.000	-0.969	-1.985	1.739	8.678	17.029	23.429	21.182	8.475
		-0.970	-1.985	1.739	8.678	17.030	23.430	21.182	8.474	0.000
		0.000	-0.403	0.630	-0.424	-3.788	-5.723	-10.042	-10.314	-3.408
		-0.402	0.629	-0.422	-3.789	-5.725	-10.041	-10.317	-3.405	0.000
FRAME FORD AVRG.		0.000	-1.477	-0.123	5.209	12.854	20.229	22.306	14.828	0.000
FRAME REAR AVRG.		0.000	0.113	0.104	-2.107	-4.757	-7.882	-10.180	-6.859	0.000
FRAME SHEAR FLOW		0.000	-1.590	-0.227	7.315	17.610	23.111	32.485	21.687	0.000

X= 36.000	ILC= 3	0.000	22.500	45.000	67.500	90.000	112.500	135.000	157.500	180.000
		0.000	-0.646	-1.433	3.495	13.047	23.235	31.207	28.187	11.022
		-0.647	-1.438	3.494	13.048	23.237	31.207	28.188	11.019	0.000
		0.000	-1.215	-0.527	-1.649	-6.631	-9.106	-14.787	-15.376	-5.118
		-1.213	-0.529	-1.546	-6.633	-9.110	-14.785	-15.381	-5.113	0.000
FRAME FORD AVRG.		0.000	-1.042	1.028	8.271	18.142	27.221	29.698	19.603	0.000
FRAME REAR AVRG.		0.000	-0.872	-1.086	-4.141	-7.971	-11.946	-15.084	-10.245	0.000
FRAME SHEAR FLOW		0.000	-0.170	2.114	12.412	26.013	39.167	44.781	29.848	0.000

IS= 3

X= 42.000	ILC= 1	0.000	22.500	45.000	67.500	90.000	112.500	135.000	157.500	180.000
		0.000	0.054	0.100	0.209	0.300	0.302	0.344	0.258	0.073
		0.054	0.100	0.209	0.301	0.302	0.344	0.258	0.073	0.000
		0.000	0.014	0.092	0.172	0.214	0.287	0.251	0.174	0.086
		0.014	0.092	0.172	0.213	0.287	0.251	0.174	0.087	0.000
	AVRG	0.000	0.065	0.143	0.224	0.276	0.296	0.257	0.148	0.000

X= 42.000	ILC= 2	0.000	22.500	45.000	67.500	90.000	112.500	135.000	157.500	180.000
		0.000	-0.403	0.631	-0.424	-3.788	-5.723	-10.042	-10.314	-3.409
		-0.402	0.629	-0.422	-3.789	-5.725	-10.041	-10.317	-3.405	0.000
		0.000	1.102	0.564	-0.244	-1.658	-6.857	-8.391	-7.732	-4.246
		1.100	0.565	-0.246	-1.656	-6.854	-8.393	-7.729	-4.249	0.000
	AVRG	0.000	0.473	0.132	-1.528	-4.506	-7.753	-9.120	-6.425	0.000

X= 42.000	ILC= 3	0.000	22.500	45.000	67.500	90.000	112.500	135.000	157.500	180.000
		0.000	-1.215	-0.526	-1.649	-6.631	-9.106	-14.787	-15.377	-5.119
		-1.213	-0.528	-1.646	-6.633	-9.110	-14.796	-15.381	-5.114	0.000
		0.000	0.698	-1.276	-4.083	-5.663	-12.719	-14.786	-12.454	-6.576
		0.695	-1.274	-4.092	-5.661	-12.715	-14.789	-12.450	-6.590	0.000
	AVRG	0.000	-0.580	-1.685	-4.508	-8.530	-12.850	-14.351	-9.881	0.000

IS= 3

X= 48.000	ILC= 1	0.000	22.500	45.000	67.500	90.000	112.500	135.000	157.500	180.000

			0.000	0.014	0.092	0.172	0.214	0.287	0.251	0.174	0.086
			0.014	0.092	0.172	0.214	0.287	0.251	0.174	0.087	0.000
			0.000	0.000	0.000	0.000	0.000	0.000	0.000	0.000	0.000
			0.000	0.000	0.000	0.000	0.000	0.000	0.000	0.000	0.000
		AVPG	0.000	0.053	0.132	0.193	0.250	0.269	0.213	0.130	0.000
X=	48.000	ILC= 2	0.000	22.500	45.000	67.500	90.000	112.500	135.000	157.500	180.000
			0.000	1.102	0.564	-0.244	-1.658	-6.857	-8.391	-7.733	-4.246
			1.100	0.565	-0.246	-1.656	-6.854	-8.393	-7.730	-4.249	0.000
			0.000	0.000	0.000	0.000	0.000	0.000	0.000	0.000	0.000
			0.000	0.000	0.000	0.000	0.000	0.000	0.000	0.000	0.000
		AVPG	0.000	0.834	0.159	-0.950	-4.256	-7.625	-8.061	-5.991	0.000
X=	46.000	ILC= 3	0.000	22.500	45.000	67.500	90.000	112.500	135.000	157.500	180.000
			0.000	0.698	-1.275	-4.089	-5.663	-12.719	-14.786	-12.455	-6.575
			0.695	-1.274	-4.092	-5.661	-12.716	-14.789	-12.450	-6.580	0.000
			0.000	0.000	0.000	0.000	0.000	0.000	0.000	0.000	0.000
			0.000	0.000	0.000	0.000	0.000	0.000	0.000	0.000	0.000
		AVPG	0.000	-0.288	-2.684	-4.875	-9.139	-13.754	-13.618	-9.517	0.000

CRANFIELD INSTITUTE OF TECHNOLOGY

COLLEGE OF AERONAUTICS

Ph.D. THESIS

D.M. AHN

INVESTIGATION OF THE STRUCTURAL INTERACTION BETWEEN THE WING AND BODY OF A CLASS OF SIMPLE REMOTELY PILOTED AIRCRAFT

VOL. II FIGURES AND TABLES

SUPERVISOR: K.H. GRIFFIN

OCTOBER, 1982

LIST OF FIGURES

4.4.4 Effect of frame bending stiffness change on shell circumferential bending - Tail load.

4.4.5 Effect of frame bending stiffness change on shell twisting stress - Tail load.

4.4.6 Effect of frame bending stiffness on direct stress - Antisymmetric load - Low wing.

4.4.7 Effect of frame bending stiffness on hoop stress - Antisymmetric load - Low wing.

4.4.8 Effect of frame bending stiffness on shear stress - Antisymmetric load - low wing.

4.4.9 Effect of frame bending stiffness on direct stress - Antisymmetric load - Mid wing.

4.4.10 Effect of frame bending stiffness on hoop stress - Antisymmetric load - Mid wing.

4.4.11 Effect of frame bending stiffness on shear stress - Antisymmetric load - Mid wing.

4.4.12 Effect of frame stiffness change on the shear flow from shell to frames - Tail load - Low wing.

4.4.13 Effect of frame stiffness change on shear flow from shell to frames - Antisymmetric load - Mid wing.

4.4.14 Effect of frame stiffness change on the frame displacement - Tail load - Low wing.

4.4.15 Effect of frame stiffness change on the frame internal force distribution - Tail load - Low wing.

4.4.16 Effect of frame depth on direct stress - Tail load - Low wing.

LIST OF TABLES

NOTATION

a	Length of shell element in longitudinal direction.
	Unknown coefficient matrix for finite element displacement assumption.
A	Cross sectional area of beam element.
A_f, A_r, A_s	Cross sectional area of frame element, ring element, and stringer element respectively.
b	Length of shell element in circumferential direction.
B	Strain-displacement relation matrix.
c	Shell element bending figidity to extedsional figidity ratio; $= t^2/12$.
C	Shell element extensional rigidity; $C = Et/(1-\nu^2)$
	Nodal displacement matrix for the shell element formulation.
C_{fx}, C_{fr}, C_{ft}	Frame internal force coefficients in X, R, and θ direction respectively. $C_f=FR/PL_c$
C_{mx}	Frame internal inplane moment coefficient $C_{mx}=M/PR$.
C_{ux}, C_{ur}, C_{ut}	Frame displacement coefficients in X, R θ direction respectively. $C_u=uGtR/PL_c$
C_{px}	Frame internal inplane rotation coefficient. $C_{px}=\phi_x GtR^2/PL_c$
C_g, C_p, C_t, C_f	Load factors for unit normal acceleration, unit pitching acceleration, tail load, and fin load respectively.
C.G.	Centre of gravity of the vehicle.

d	Depth of the deep frame.
D	Shell element bending rigidity.
	$D = Et^3/12(1-\nu^2)$
	Stress-strain relation matrix of finite element formulation.
E	Young's modulus.
F	Load vector for system equations.
	Internal forces of frame or stiffeners.
$F_{b\,fw}$, $F_{b\,rw}$	Interaction load vectors at forward and rear wing attachment respectively.
g	Gravitational acceleration.
G	Shear modulus of rigidity.
I	Second moment of inertia.
I_f, I_r, I_s, I_{sh}	Second moment of inertia of loaded frame, rings, stringers, and body cross section respectively.
I_x, I_y, I_{xy}	Beam element second moment of inertia normal, lateral respectively.
J	Torsional constant of beam element.
K	Shear coefficient of beam element with shear deformation effect.
	Stiffness matrix.
K_b, K_w	Condensed stiffness matrix of total body and wing respectively.
K_e	Element stiffness matrix.
L_c, L_f, L_r	Length of centre body, forward body, and rear body respectively.
L_{rsp}	Standard ring spacing.
m	Harmonic number in analytic formulae.
	Master degree of freedom.
M	Concentrated moment load on loaded frame in harmonic analysis.
	Mass matrix.
	Internal moment of frame or stiffeners.
M_b	Bending moment on the body cross section.

$M_x, M_\theta, M_{x\theta}$	Bending moment in longitudinal direction, in circumferential direction, and twesting moment of shell element. (= M_x, M_t, M_{xt} in graphs)
M_x, M_y, M_z	Bending moment about normal axis, lateral axis, and axis along shear centre of beam element.
N	Stress resultants vector of shell element.
N_{str}	Number of stringers in body cross section.
$N_x, N_\theta, N_{x\theta}$	Direct stress resultant, hoop stress resultant, and shear stress resultant of shell element. (= N_x, N_t, N_{xt} in graphs)
o	Fictitious member.
O	Null matrix or vector.
P	Concentrated radial load on loaded frame or reaction load at wing pick up point,
	Element load vector or matrix.
P_t	Total normal force on the tail plane.
$\bar{P}$	Condensed load matrix.
Q	Shear flow on the frames.
q	Distributed load vector.
R	Radius of body.
	Circumferential curvature of shell element.
R_B, R_W	Resultant reaction load vectors of body and wing respectively.
R_g, R_p, R_t	Reaction load vectors on wing pick up points due to unit normal acceleration, load, unit pitching acceleration load and tail load respectively.
r_c, r_s	Curvature of beam element centroid and shear centre respectively.
t	Thickness of body skin or shell element.
t'	Effective thickness of body skin in extension.
T_o	Concentrated tangential load on frame.
u	Displacement along body longitudinal axis.
u_e	Element displacement vector.

u_e, u_w	Displacement vector of body and wing.
U	Strain energy.
U_b	Interaction displacement vector.
U_g, U_p, U_t	Interaction displacement components by body loads of 1 g inertia, 1 rad/sec^2 pitching, and unit tail load respectively.
v	Circumferential displacement of shell element.
w	Radial displacement of shell element.
$\bar{x}, \bar{y}$	Offset of stiffening element shear centre from shell middle surface.
x_c, y_c	Dislocation between shear centre and centroid.
$Z(L), Z(Lc)$	Parameters in ESDU and Chpater 7; GtR^4/EI_fL .
α	Semiarc angle of shell element or beam element.
β	Twisting angle of beam element.
β_o	Opening angle of cutout.
γ	Shear strain of shell element.
γ_{xz}, γ_{yz}	Shear strain of beam element.
ε	Strain vector.
ε_o	Normal strain of beam element at centroid.
$\varepsilon_x \; \varepsilon_\theta$	Strain along longitudinal axis and circumferential axis respectively.
$k_x, k_\theta, k_{x\theta}$	Change of curvature about longitudinal axis, circumferential axis, and twisting of shell element.
θ	Circumferential angle.
ρ	Specific weight.
σ	Normal stress of beam element.
ϕ	Rotation of beam element about shear centre.
ϕ_x, ϕ_z	Curvature about longitudinal axis and circumferential axis of the shell or beam elementary respectively.
ν	Poisson's ratio.
ζ	$1/(\pi+2A_s/Rt)$

Subscripts and others

c	Centre body.
f	Frame or forward body.
r	Standard ring stiffeners or rear body.
s	Longitudinal stringers or booms.
rsp	Ring spacing.
str	Stringers.
w	Wing structure.
72-12-60	Representation of body substructure length; L_f=72.0 in. L_c=12.0 in. and L_r=60.0 in.
$[\ ]$	Matrix
$[\ ]^T$	Transposed matrix.
$\{\ \}$	Vector.
$\lfloor\ \rceil^T$	Transposed vector.

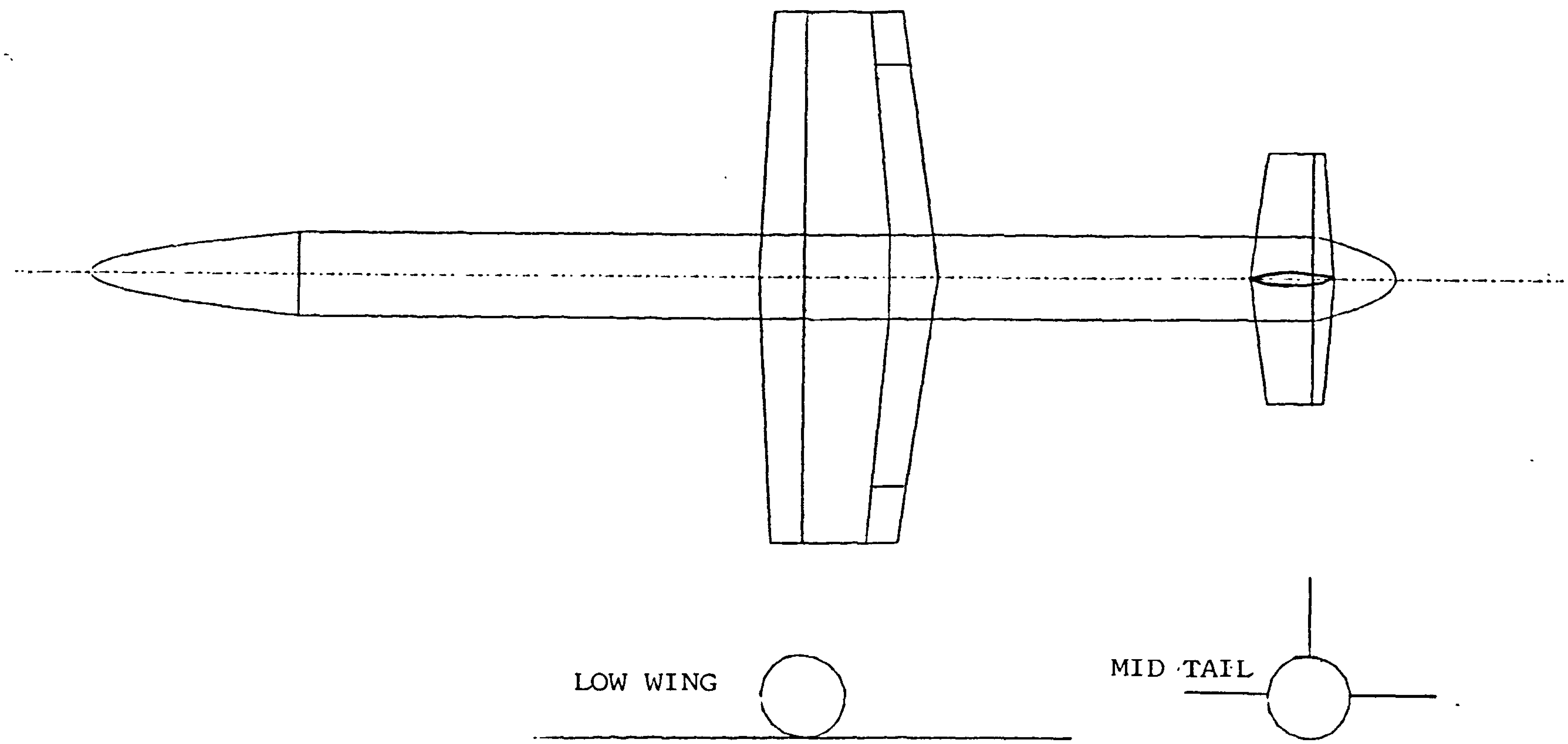

Fig.3.1 BASIC CONFIGURATION OF CHOSEN RPV

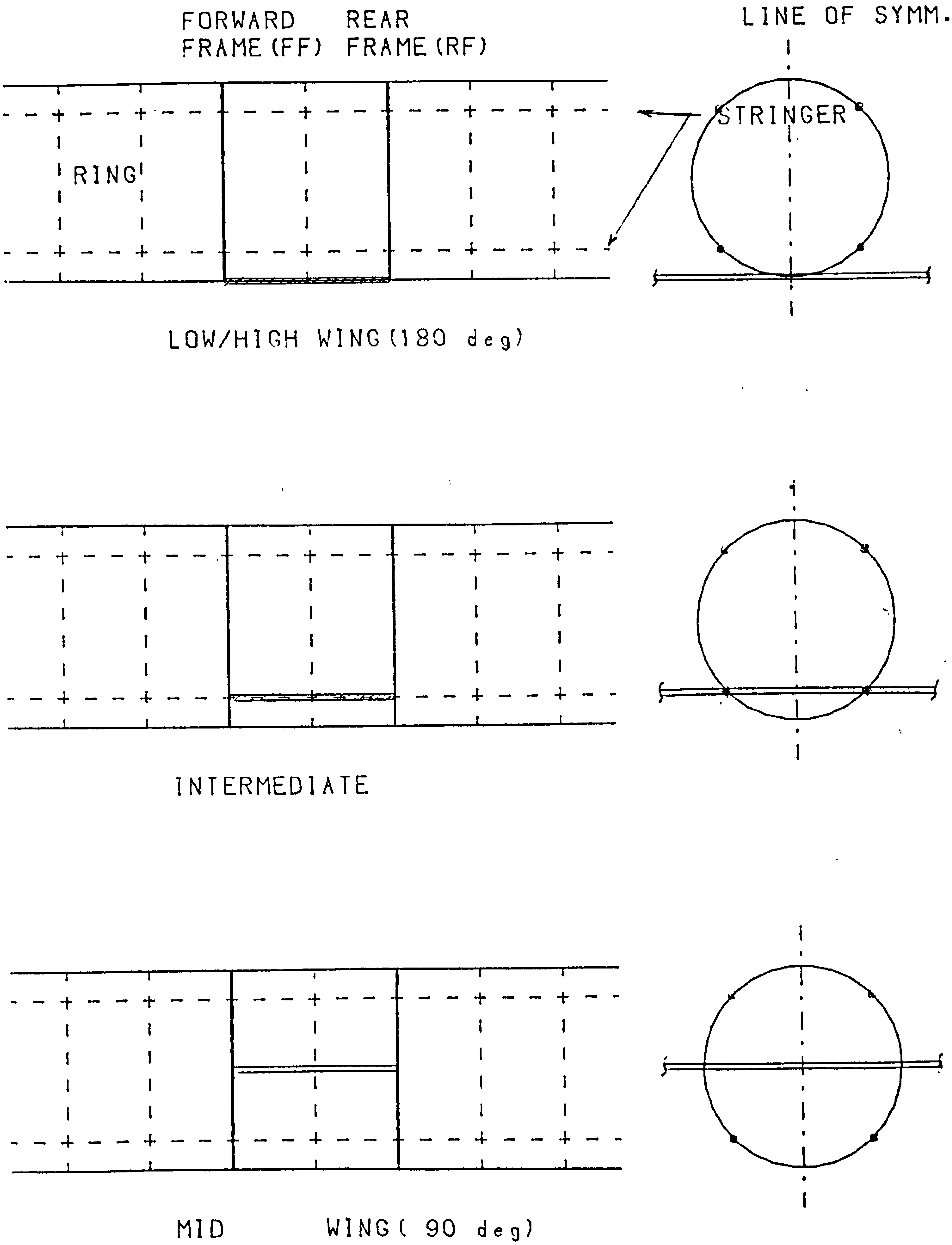

Fig.3.2 POSITIONS OF WING PICK-UP (2 LOADED FRAMES)

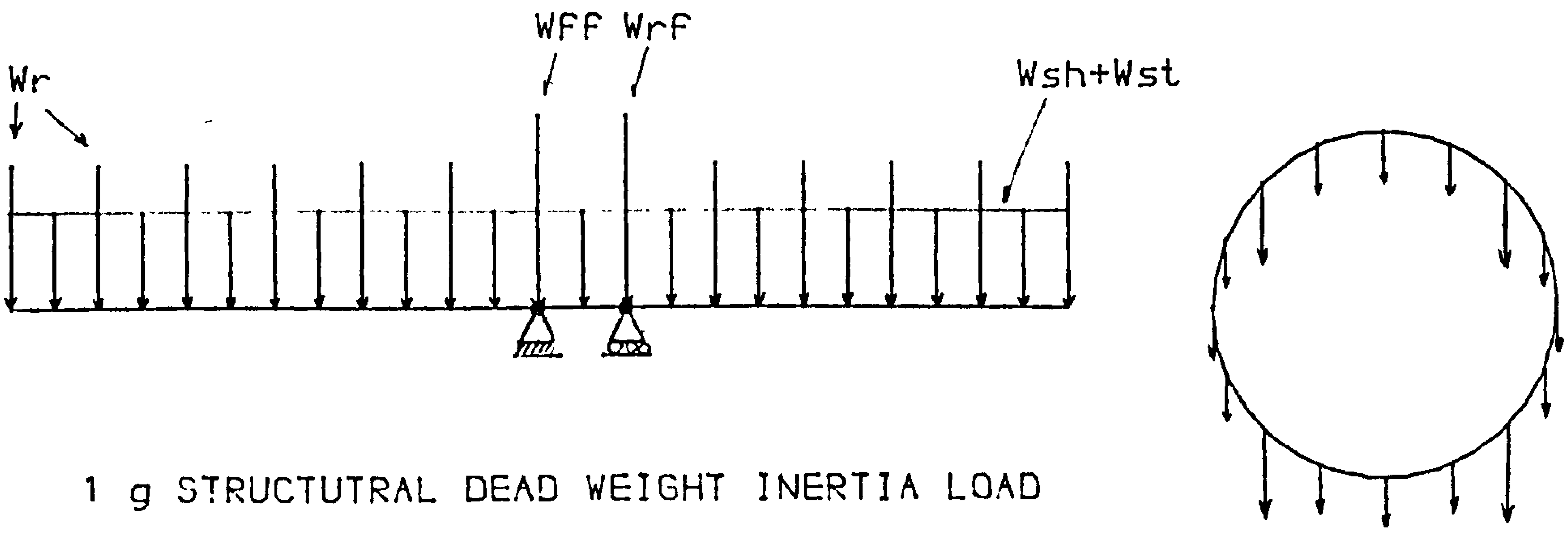

1 g STRUCTUTRAL DEAD WEIGHT INERTIA LOAD

Wsh=DISTRIBUTED SHELL , WFF=FWD FRAME, WrF=REAR FRAME WEIGHT

Wst=DISTRIBUTED STRINGER, Wr=RING WEIGHT, Pt=TAIL LOAD

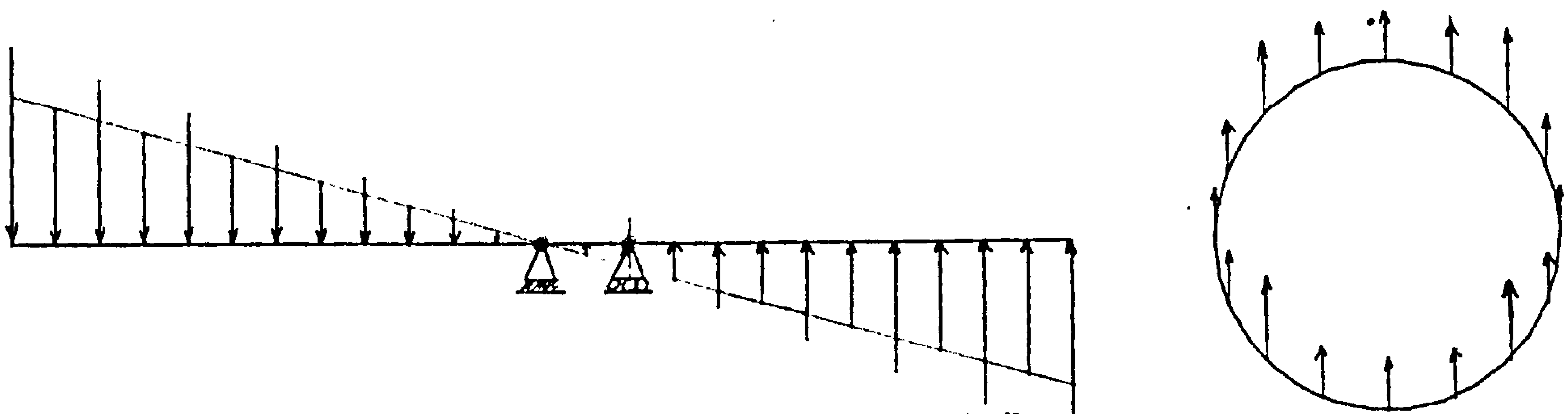

1 rad/sec**2 PITCHING ACCELERATION LOAD OF STRUCT

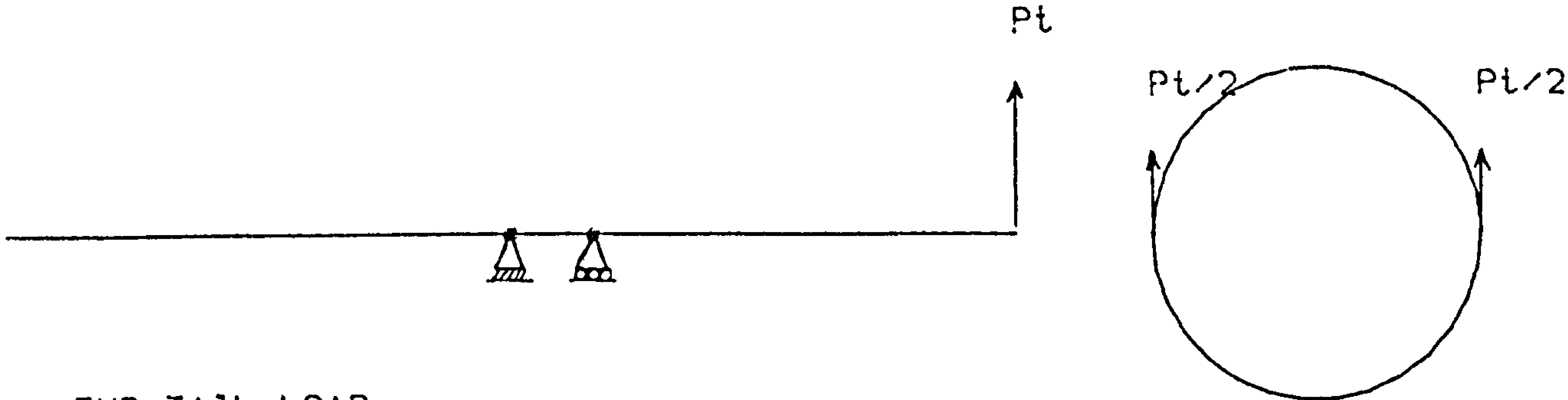

END TAIL LOAD

Fig. 3.3 SYMMETRIC LOAD CONDITIONS CONSIDERED

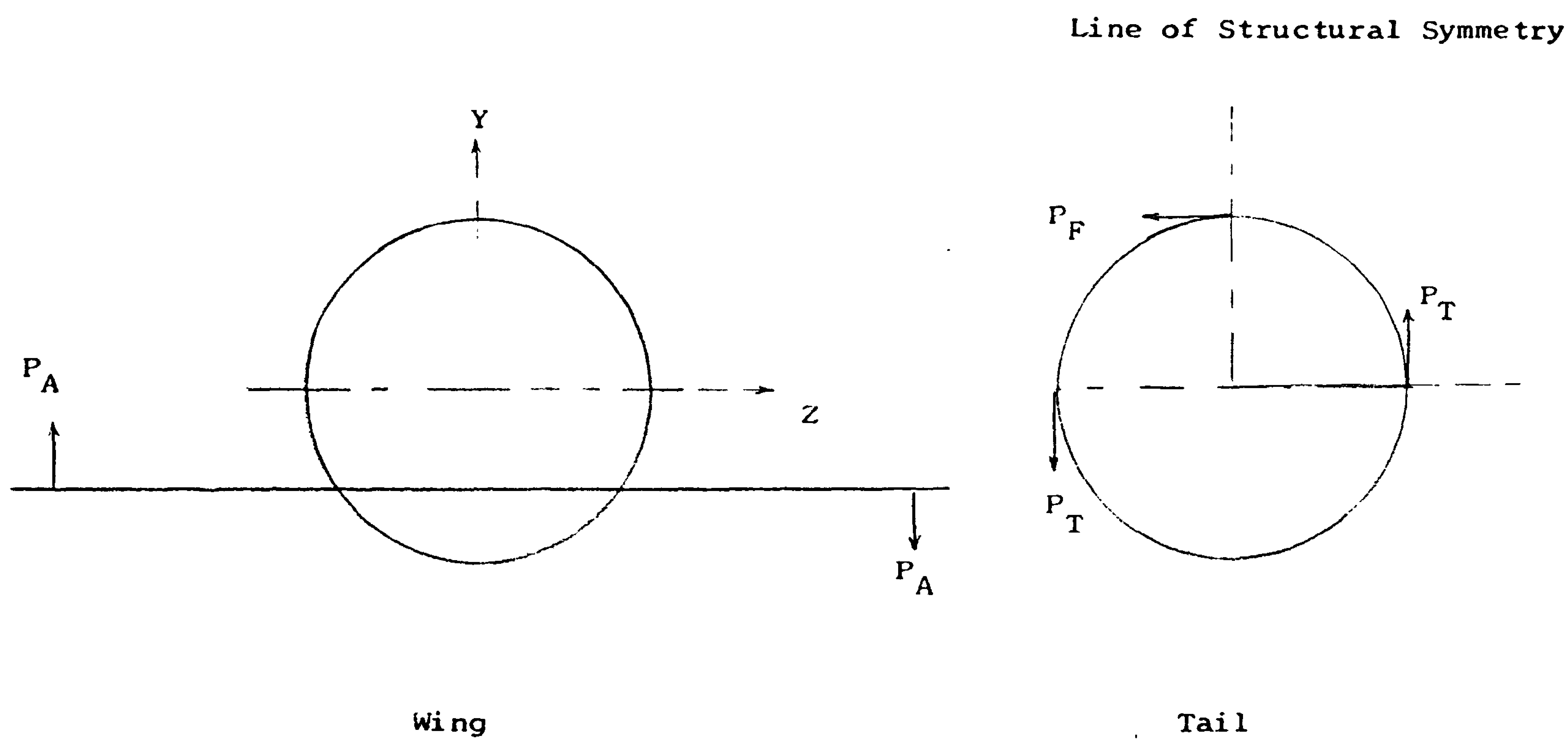

Fig.3.4 Antisymmetric Load Condition Considered

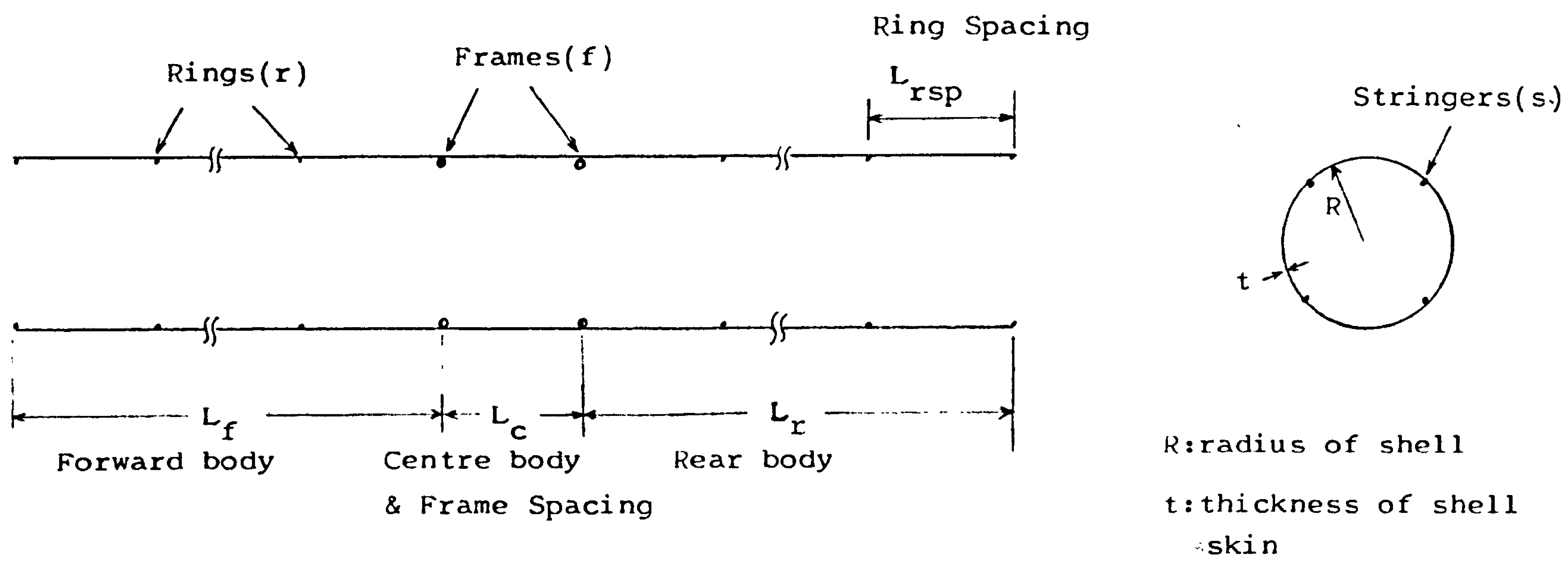

Fig. 3.5 Geometric Notations of Body

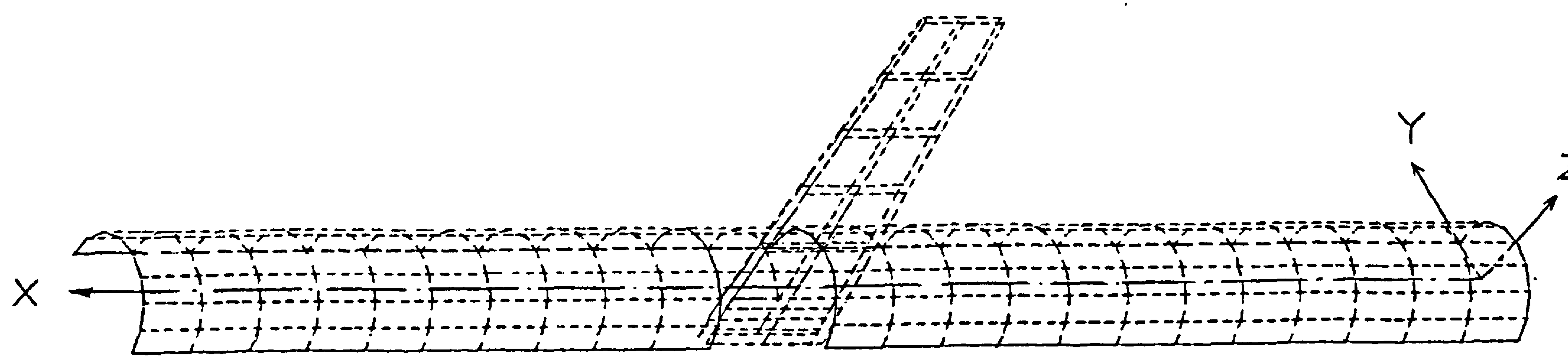

Fig. 3.6 Finite Element Idealization of RPV Structure and Global Coordinate System

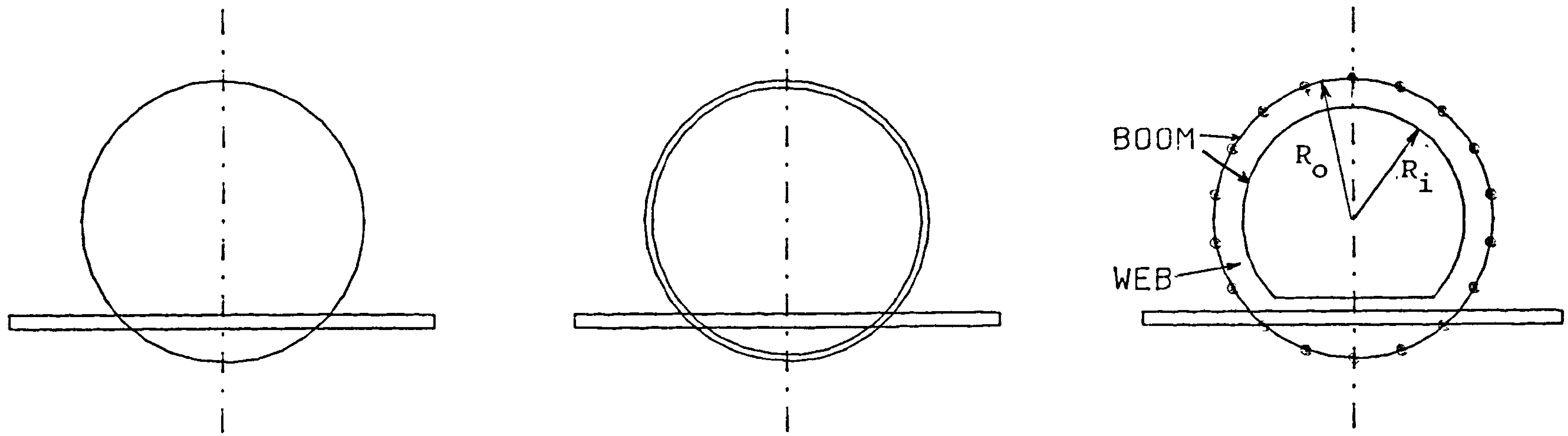

I. RIGID DIAPHRAGM
OR BULKHEAD

II. SIMPLE RING FRAME
OR SYM. DEEP FRAME

III. DEEP UNSYMM. FRAME
OR LOCALLY REINFORCED

Fig.3.7 TYPES OF LOADED FRAMES

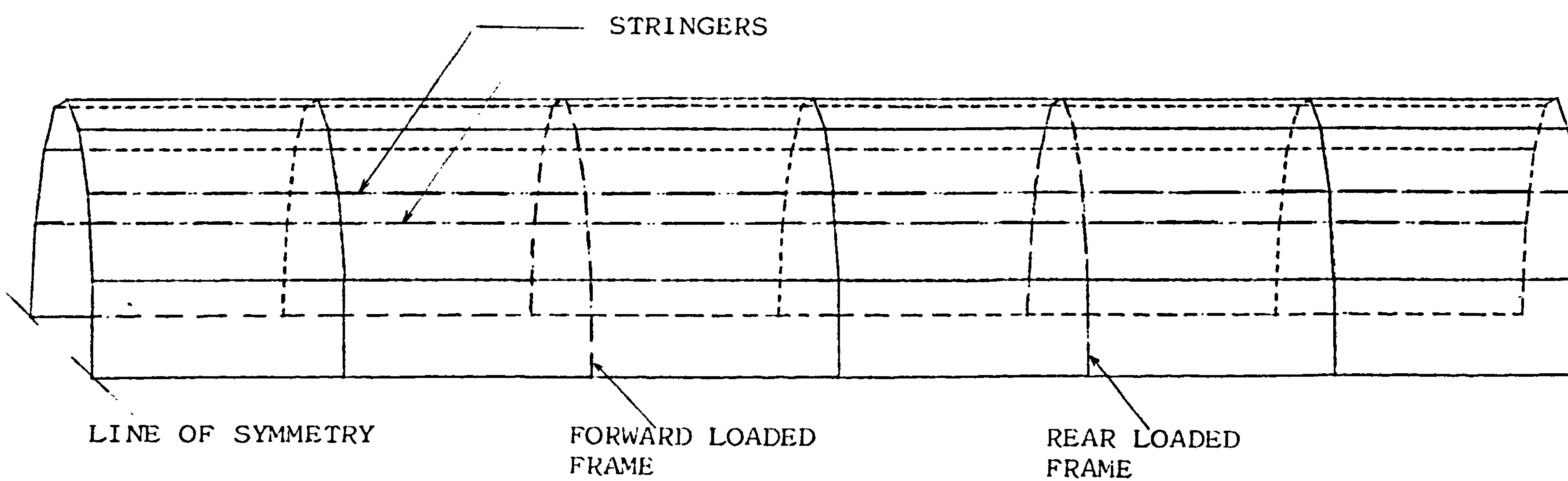

Fig.4.1.2 Centre Body Finite Element Model.

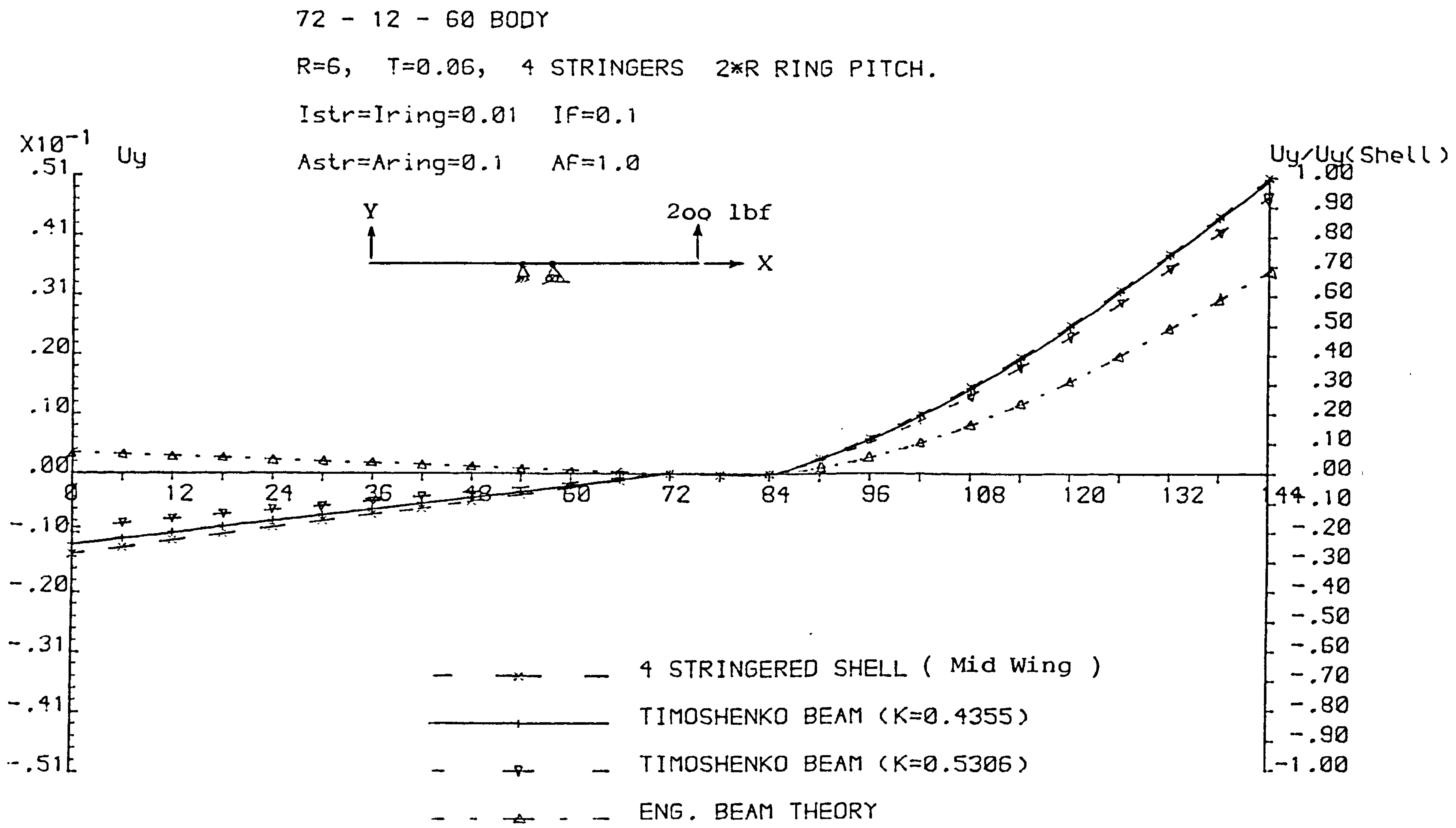

Fig.4.3.1 VERTICAL DISPLACEMENT DISTRIBUTION UNDER SYMM. TAIL LOAD

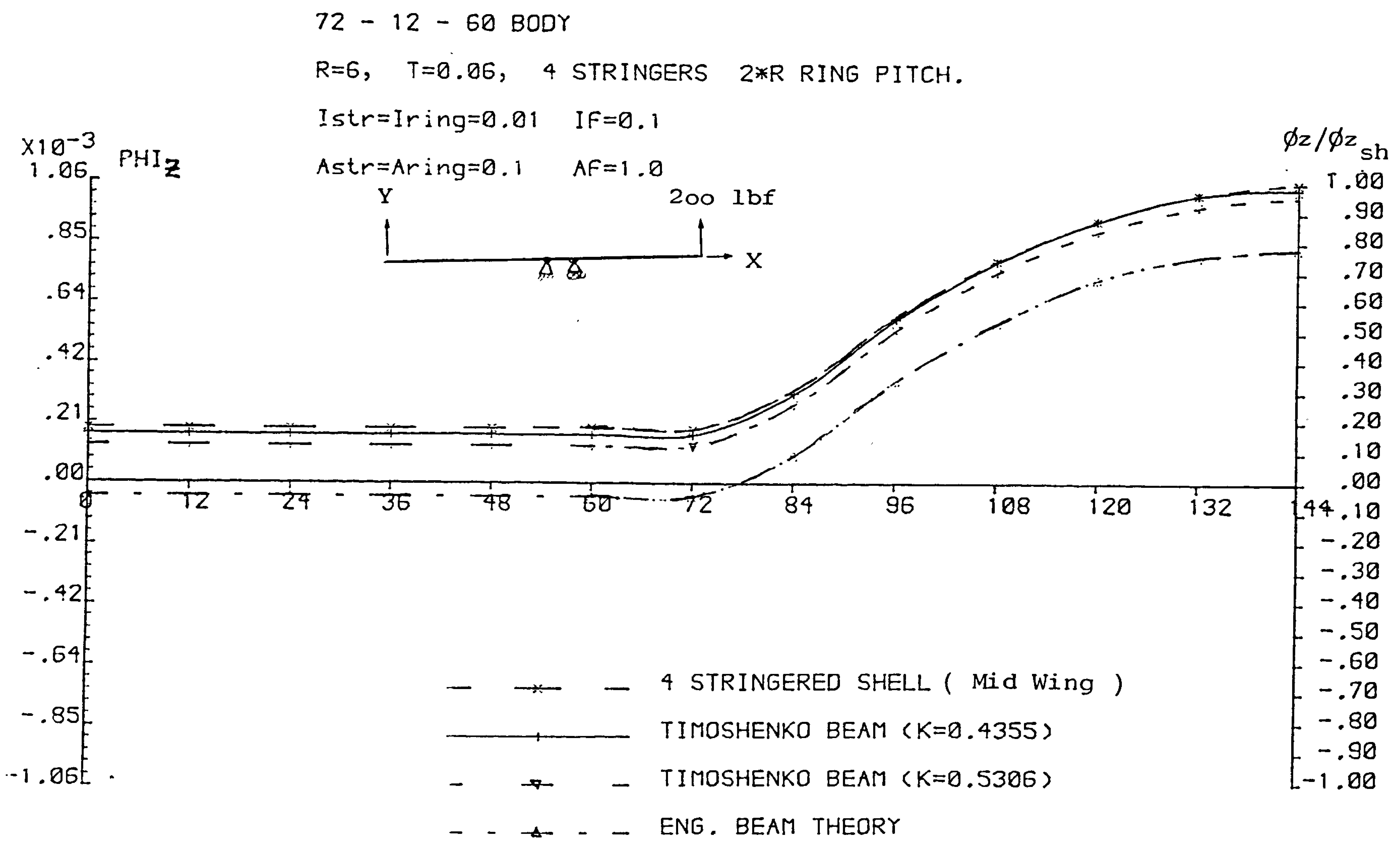

Fig.4.3.2 Rotation of Body Cross Section Under End Tail Load

MID WING PICK UP (72-12-60)

R=6. t=0.06 Nstr=4 Lrsp=12. I_f=0.1

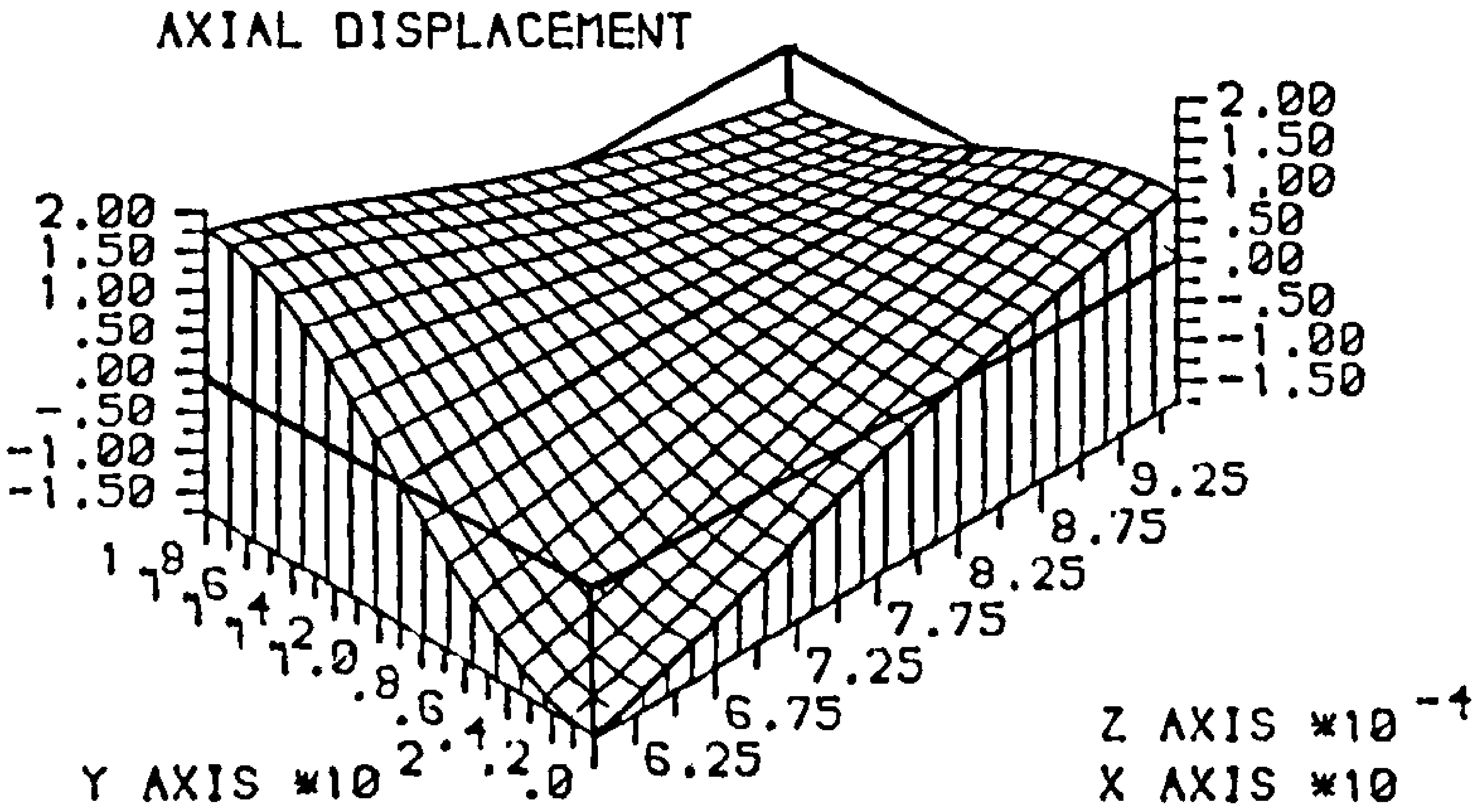

y; circumferential angle

z; displacement(in)

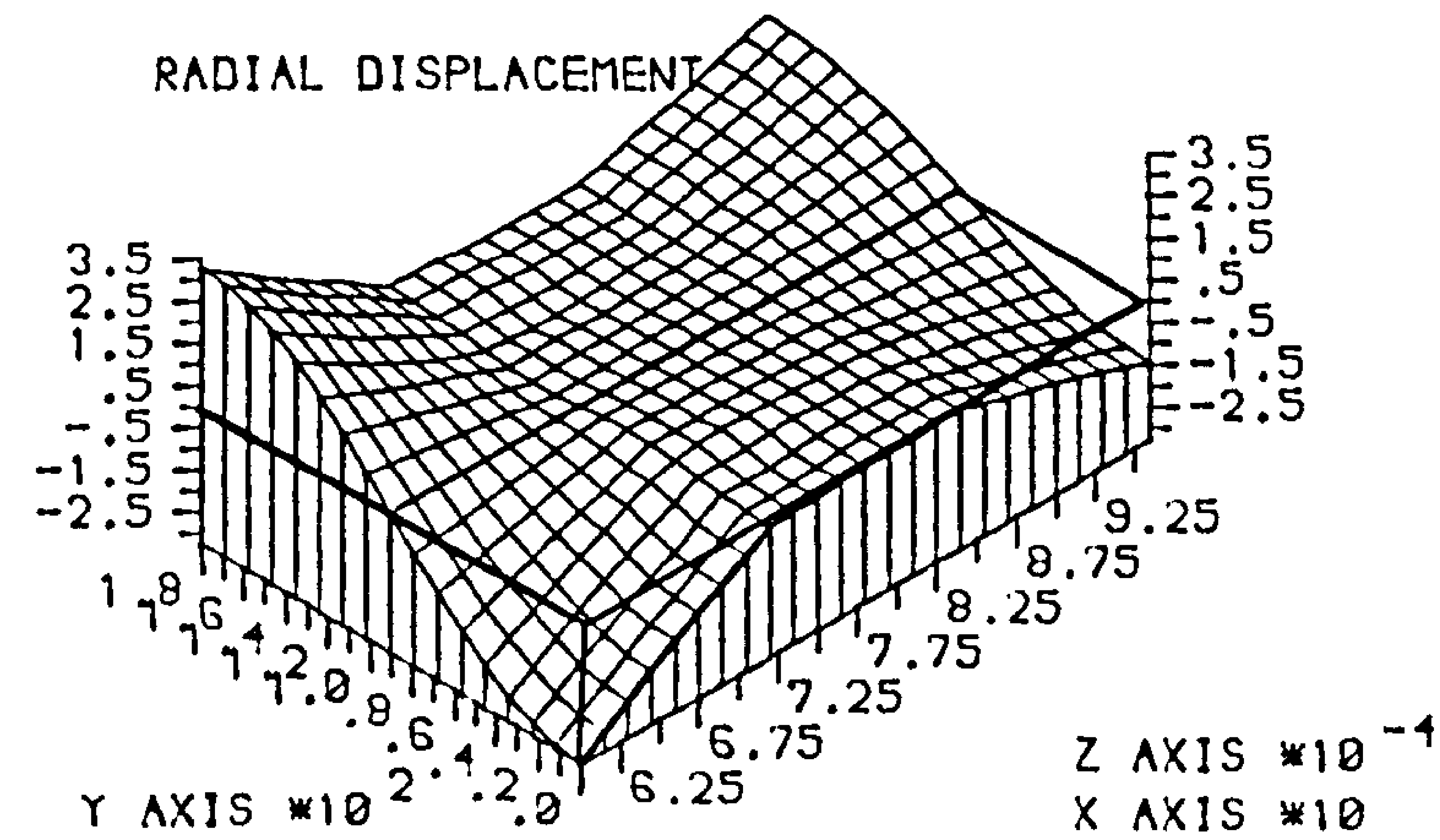

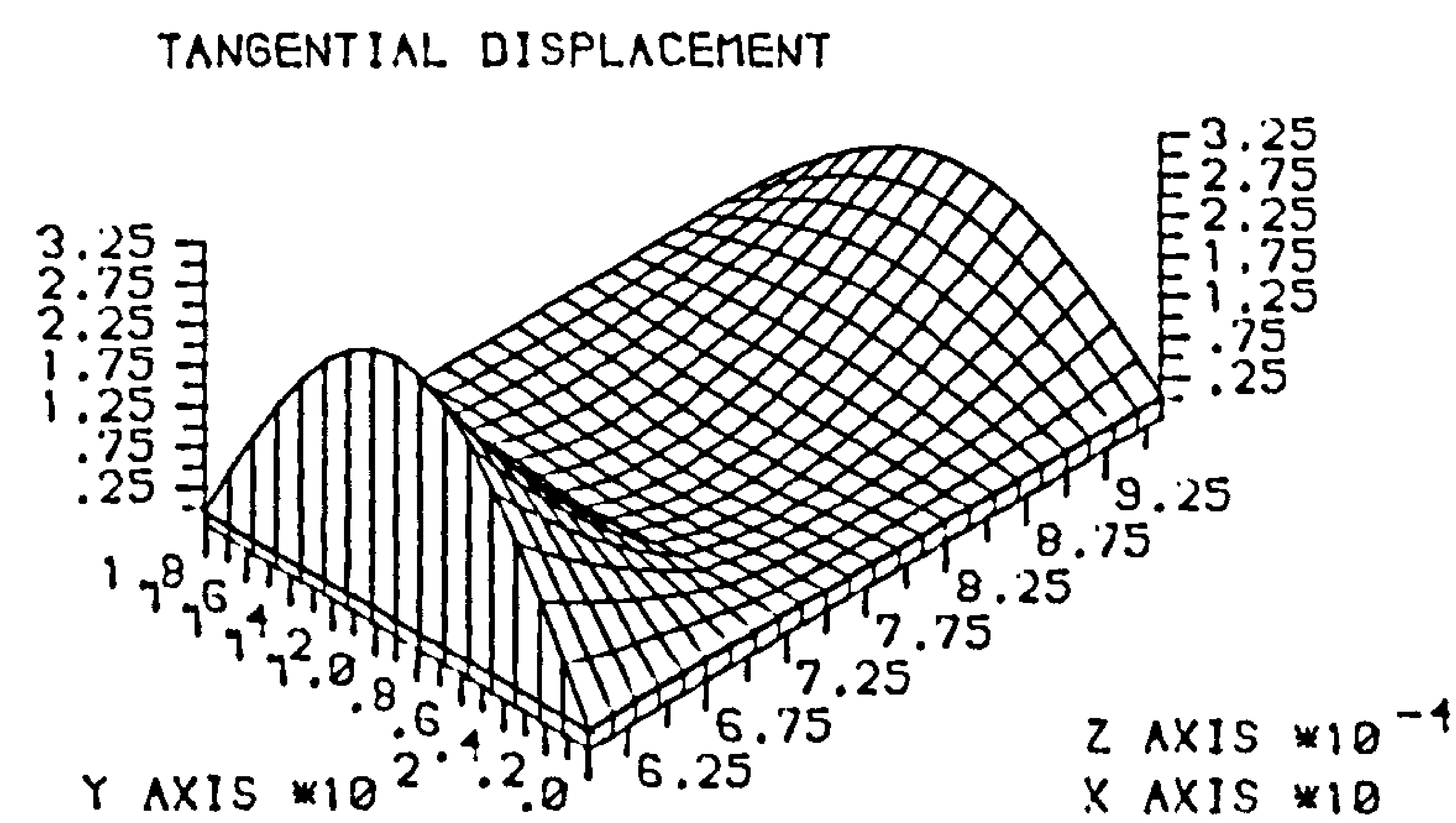

+ clockwise

Fig.4.3.3 DISPL. OF RING FRAMED CENT. SHELL - 1 g INERT.

MID WING PICK UP (72-12-60); 1 rad/sec^2 pitching

R=6. t=0.06 Nstr=4 Lrsp=12. I_f=0.1

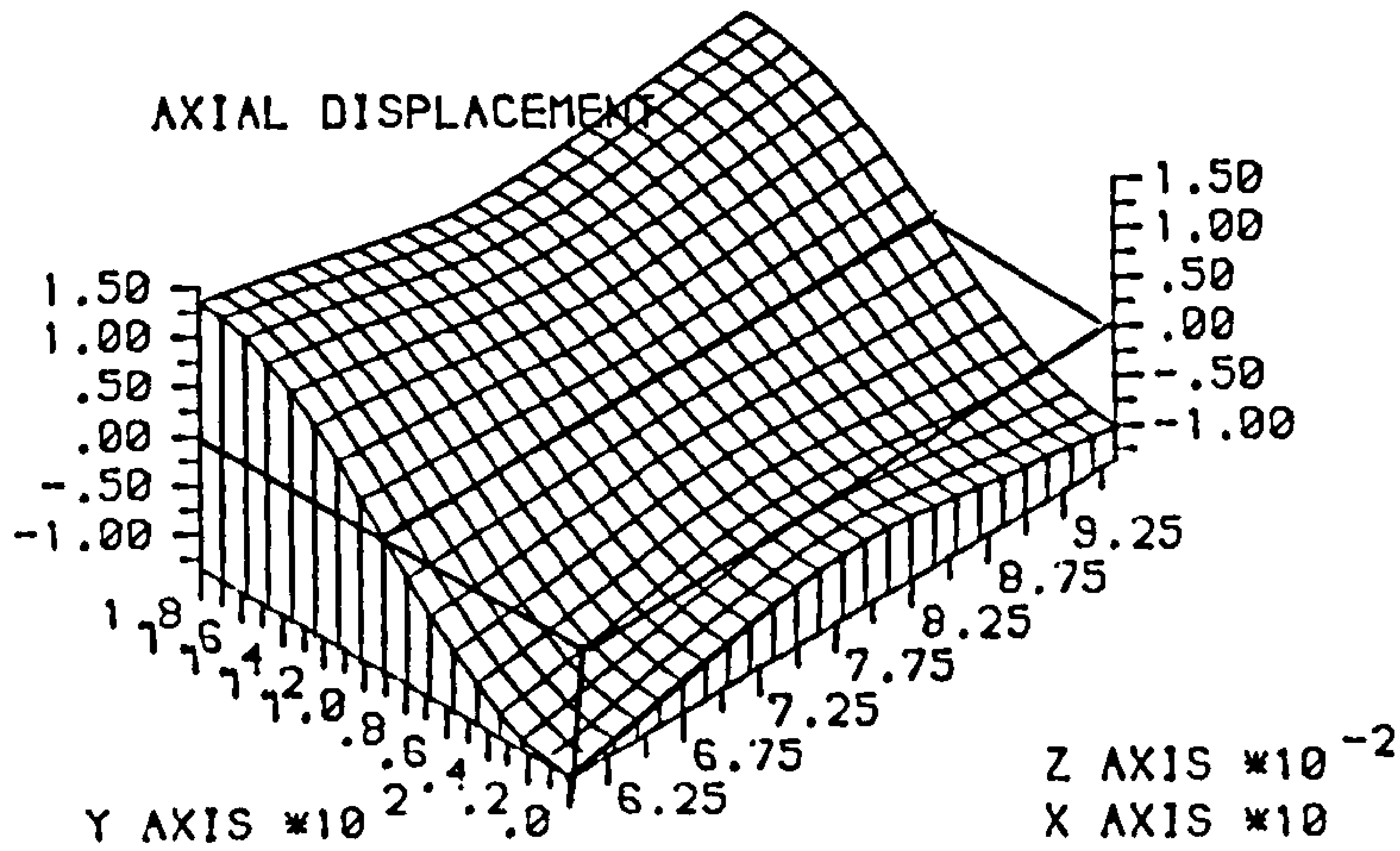

y; circumferential angle (deg)

z ; Displacement(in)

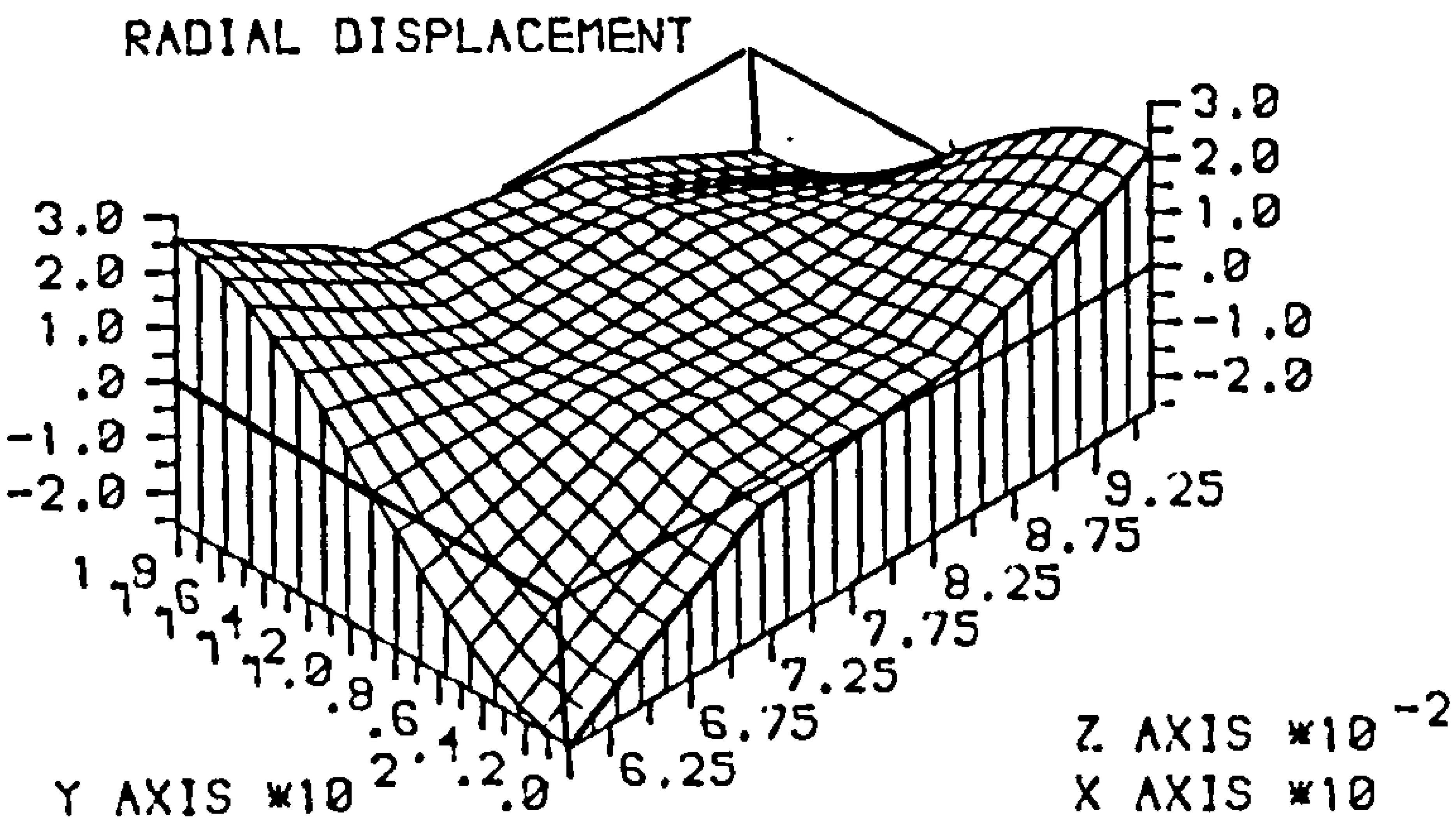

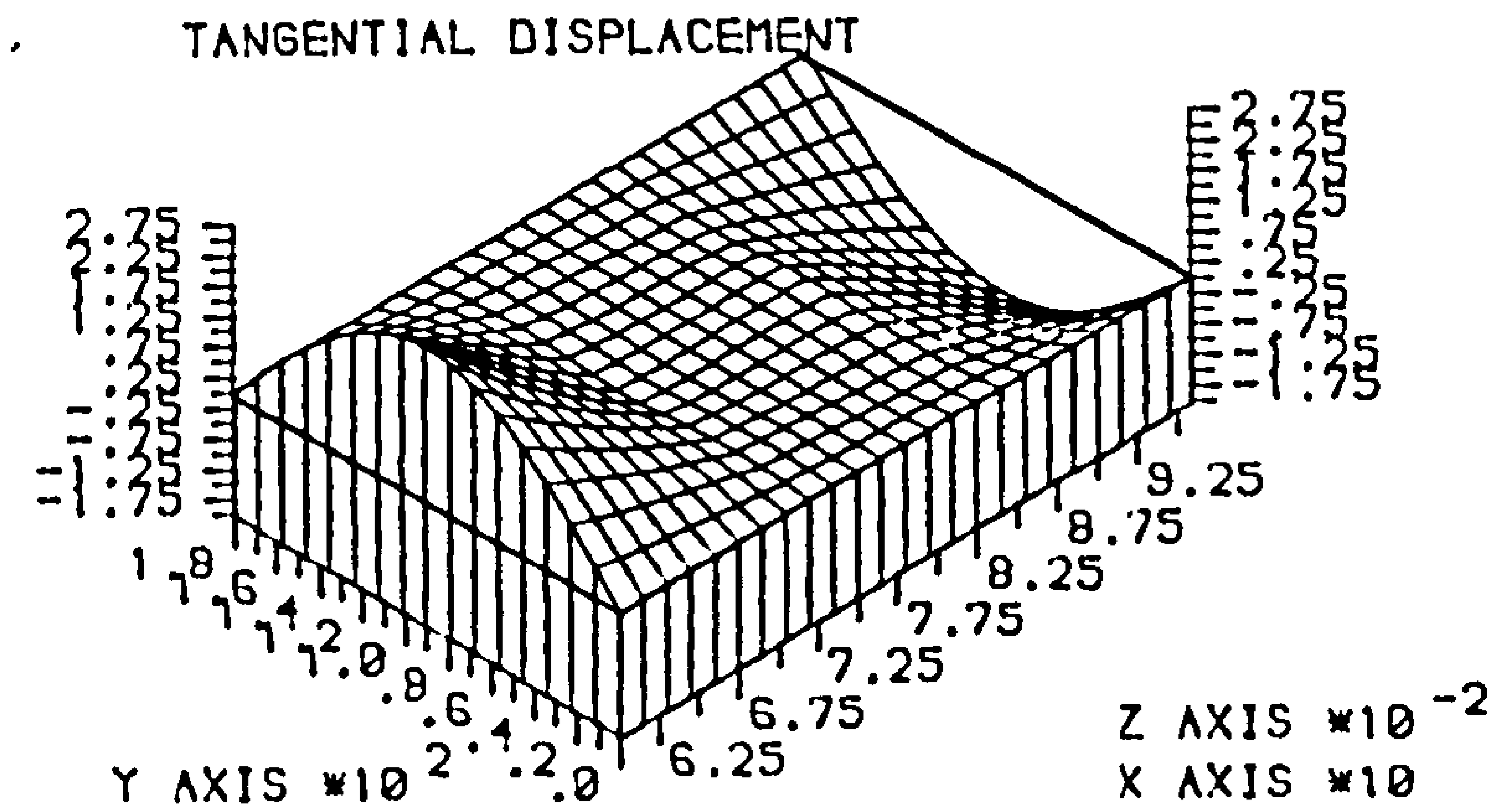

+ clockwise

Fig.4.3.4 DISPL. OF RING FRAMED CENT. SHELL

MID WING PICK UP(72-12-60); TAIL LOAD

R=6. t=0.06 Nstr=4 Lrsp=12. I_f=0.1

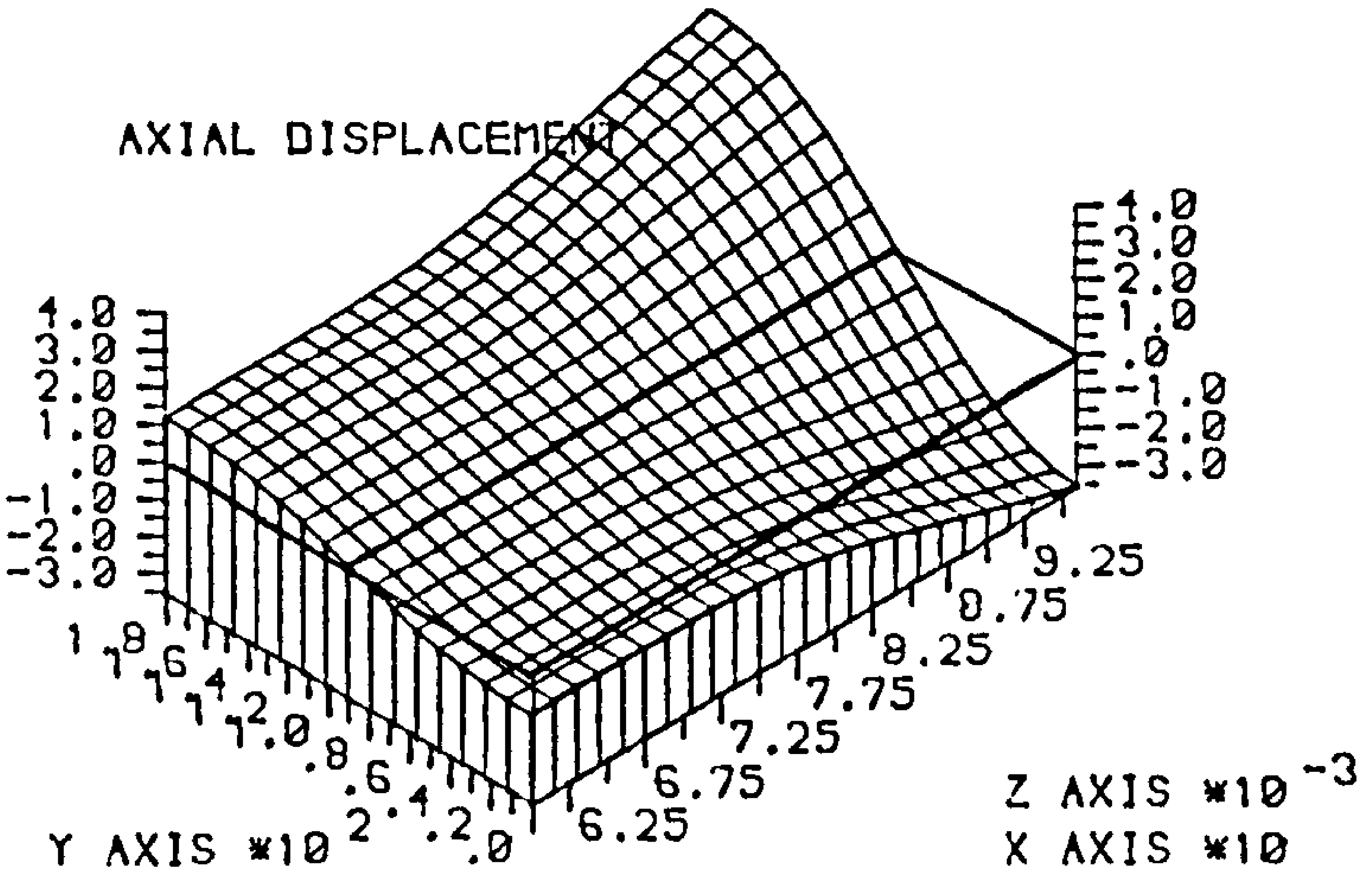

y; circumferential angle(deg)

z; displacement(in)

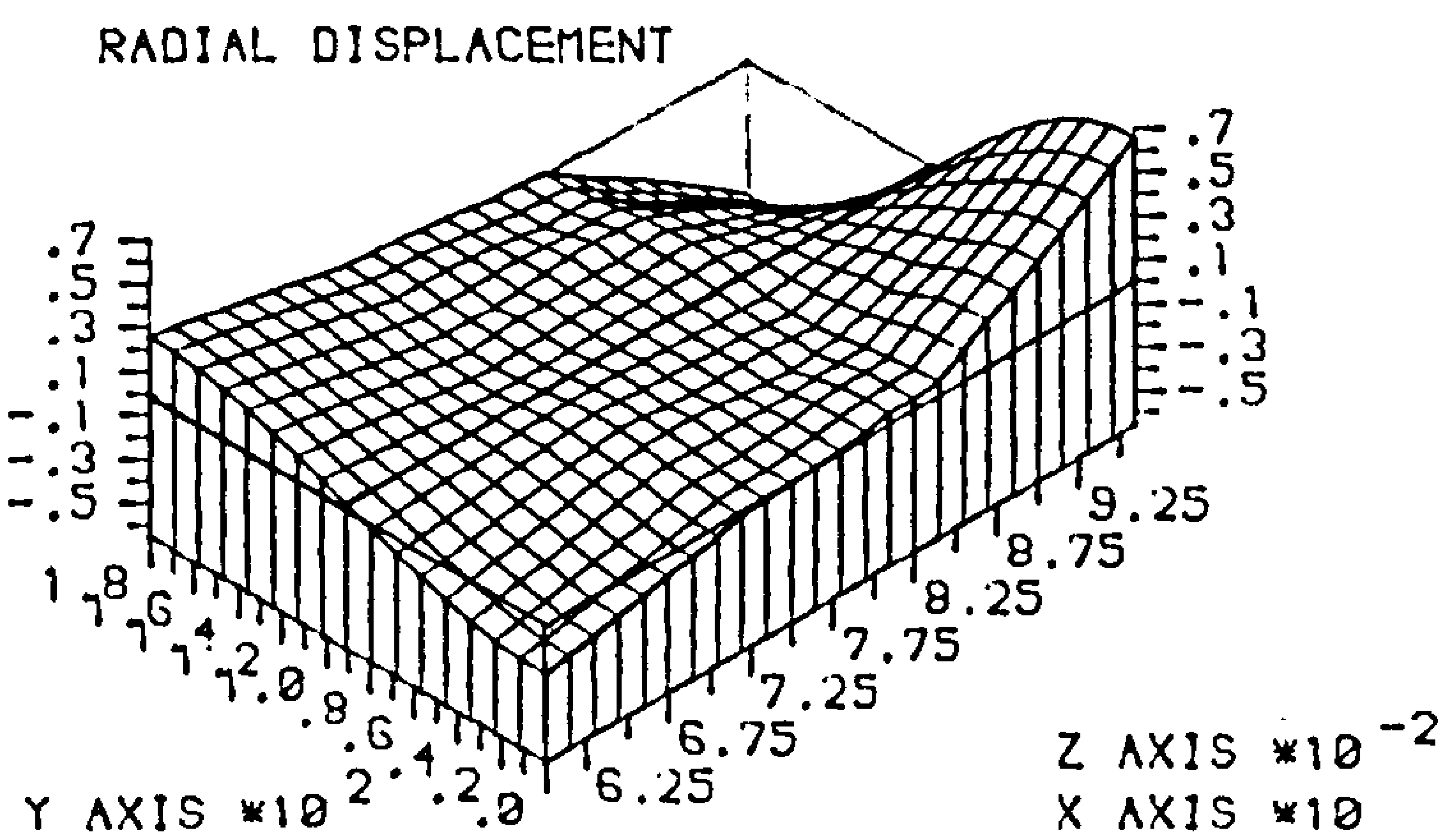

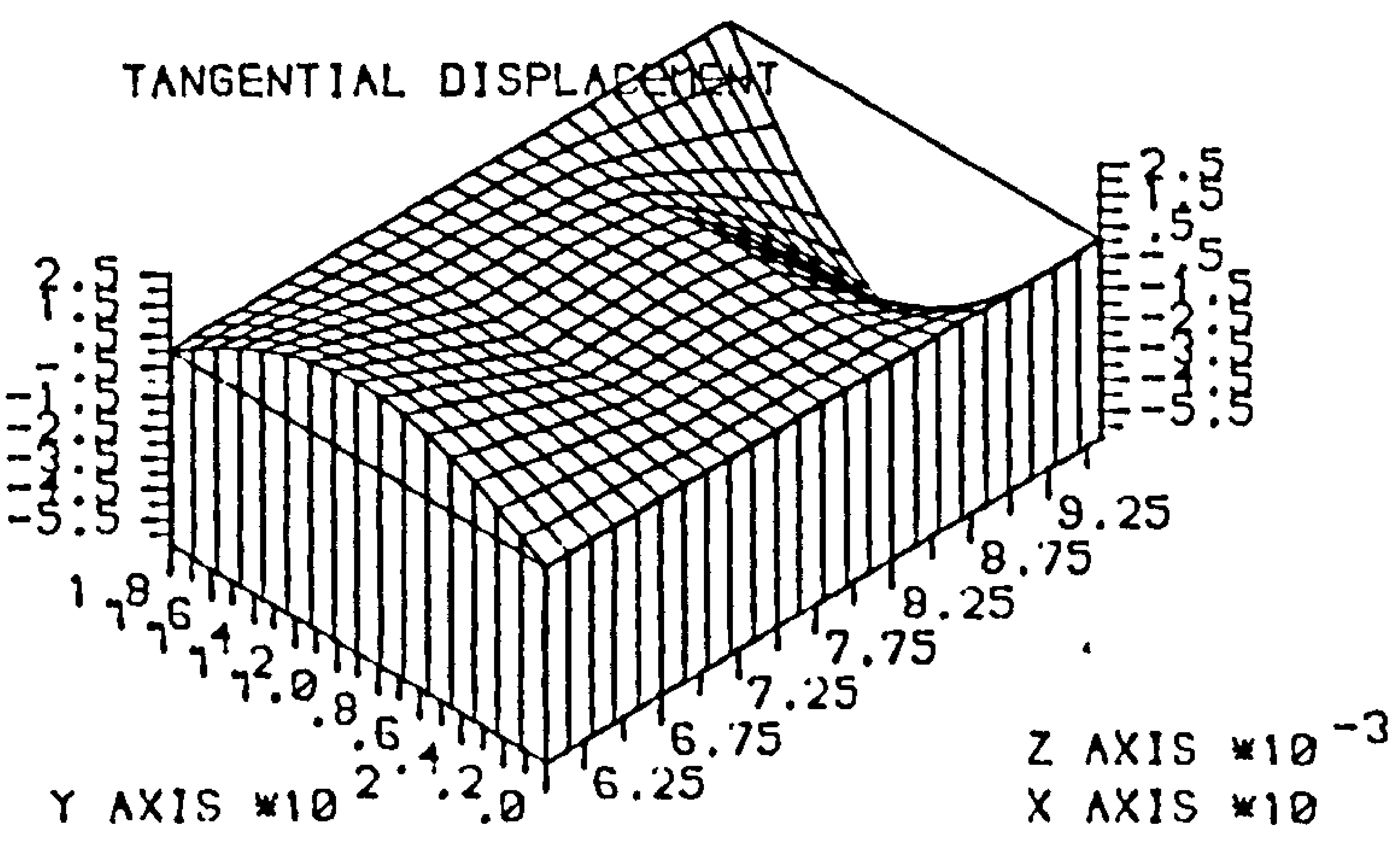

+ clockwise

Fig.4.3.5 Ring Framed Centre Shell Displacement Distribution.

LOW WING PICK UP (72-12-60) ; 1 g INERTIA

R=6. t=0.06 Nstr=4 Lrsp=12. I_f=0.1 in^4

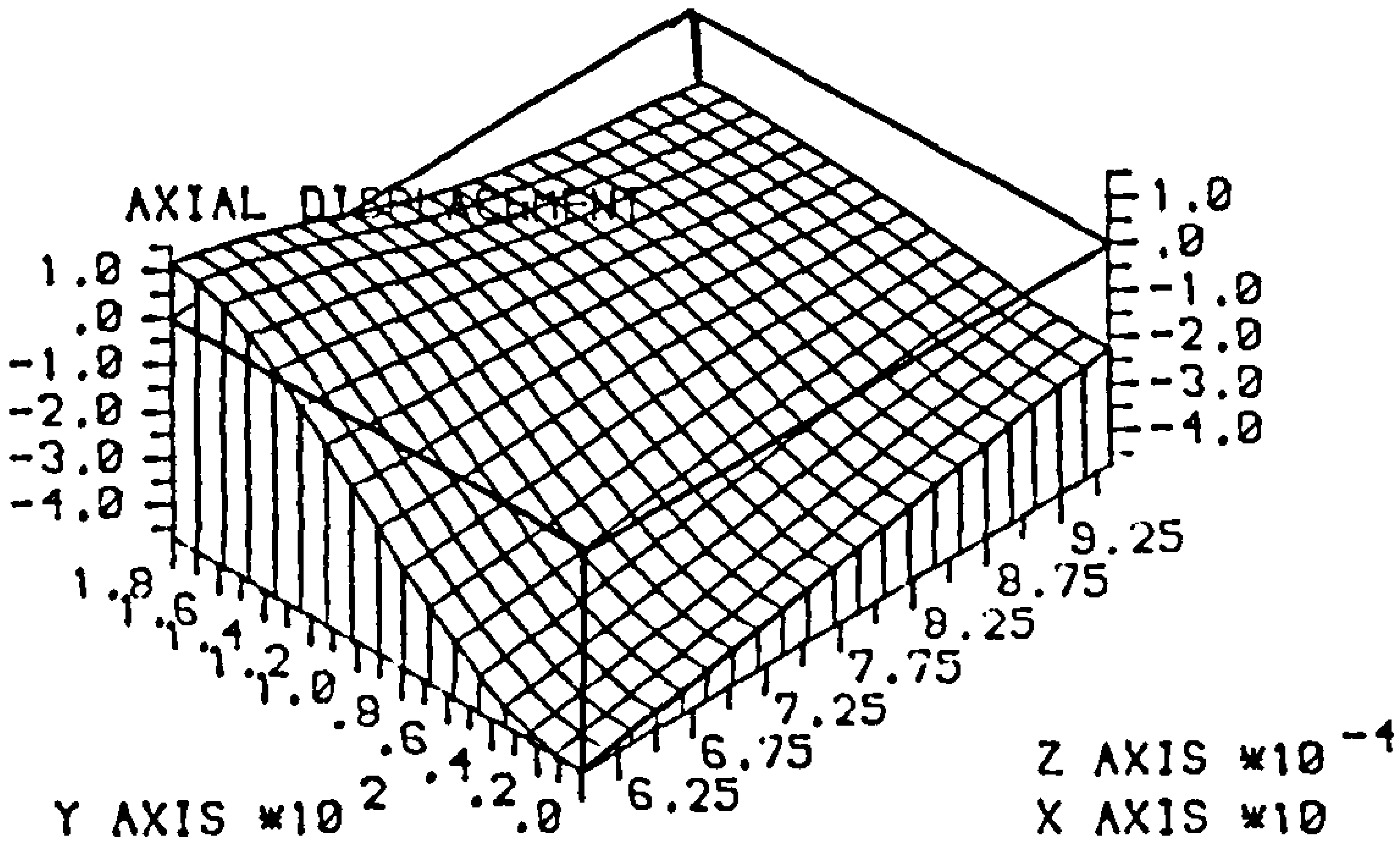

y; circumferential angle(deg)

z; displacement(inch)

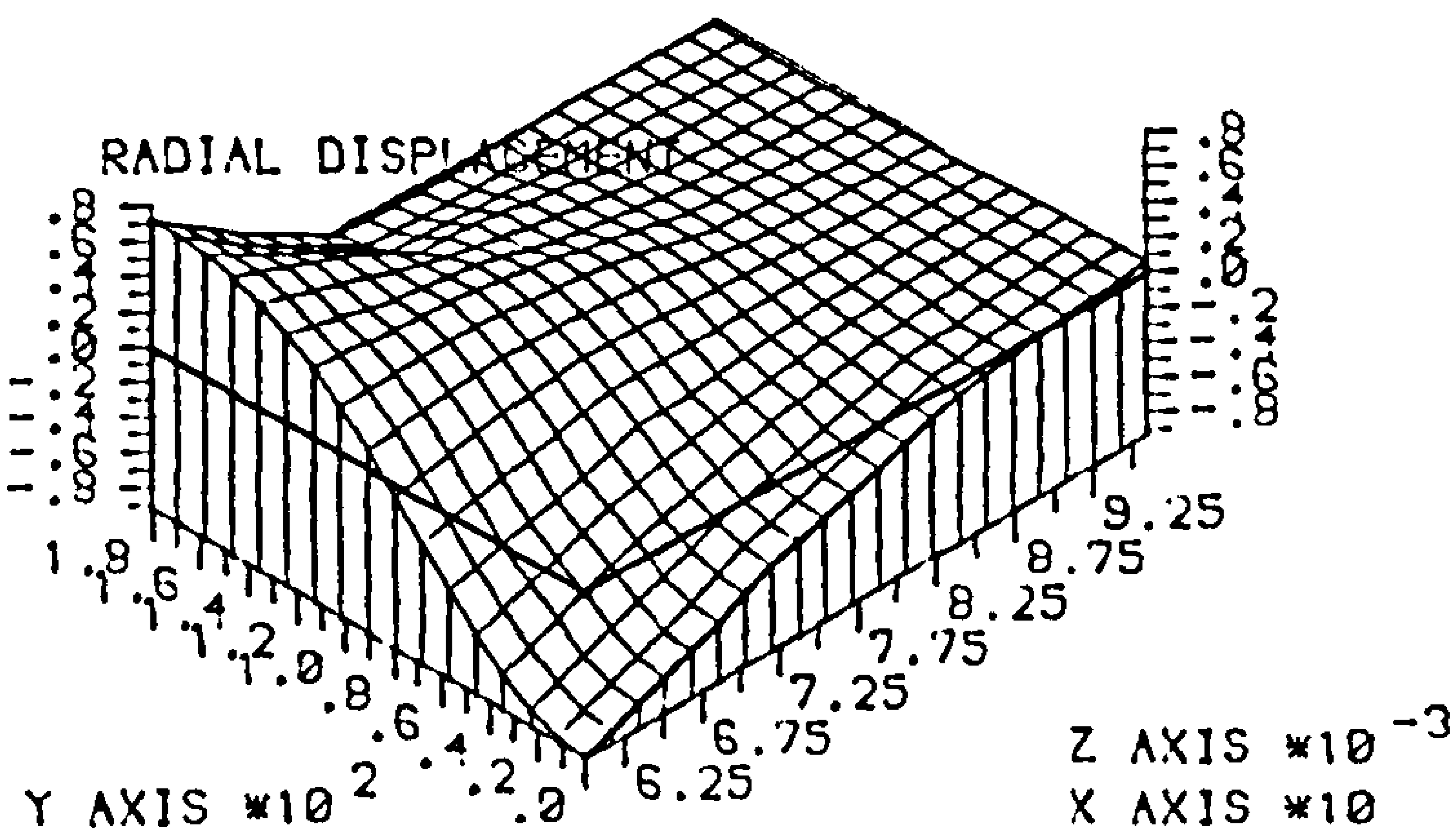

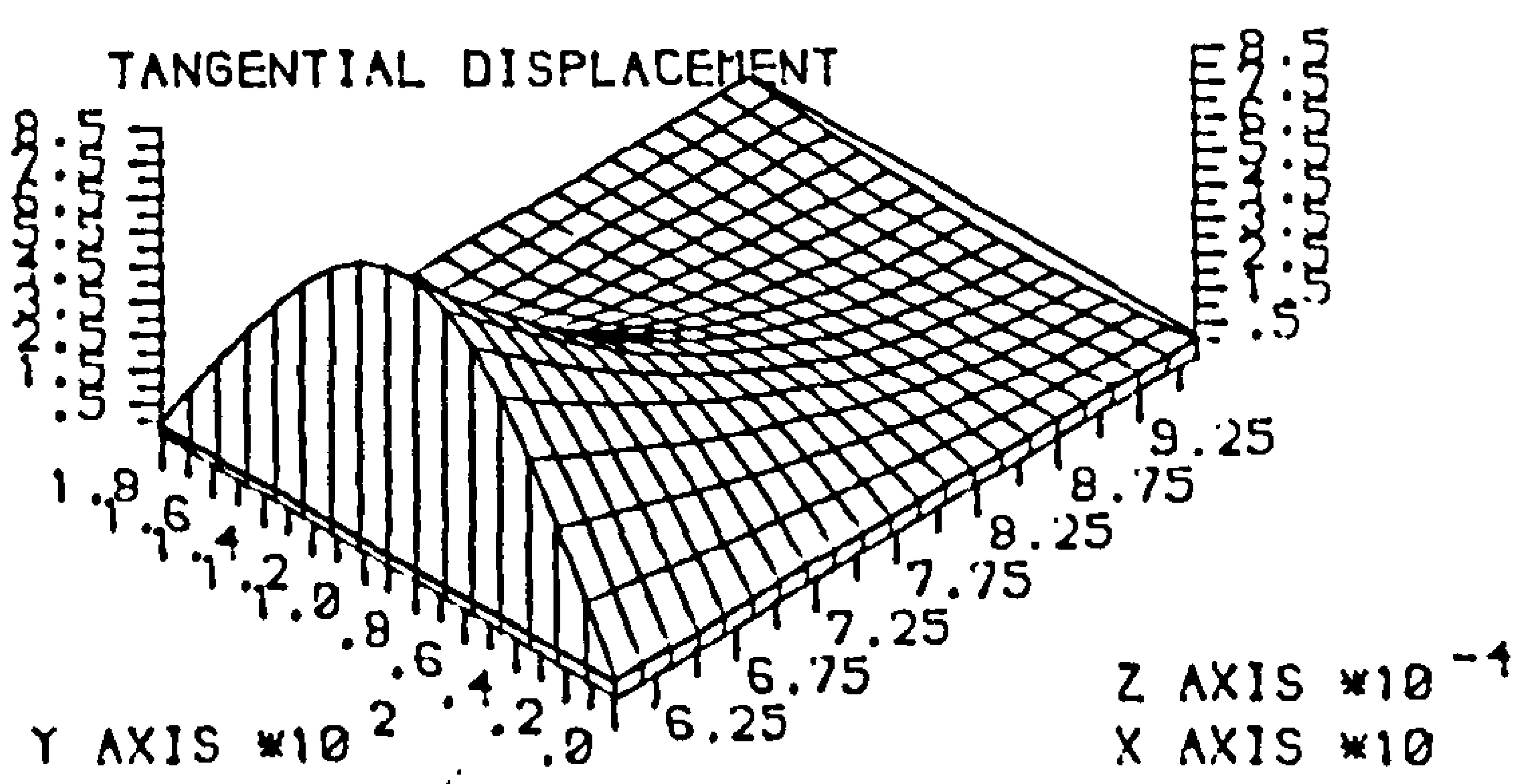

Fig.4.3.6 Ring Framed Centre Body Displacement Distribution

LOW WING PICK UP (72-12-60) ; 1 rad/sec^2 pitcing

R=6. t=0.06 Nstr=4 Lrsp=12. I_f=0.1 in^4

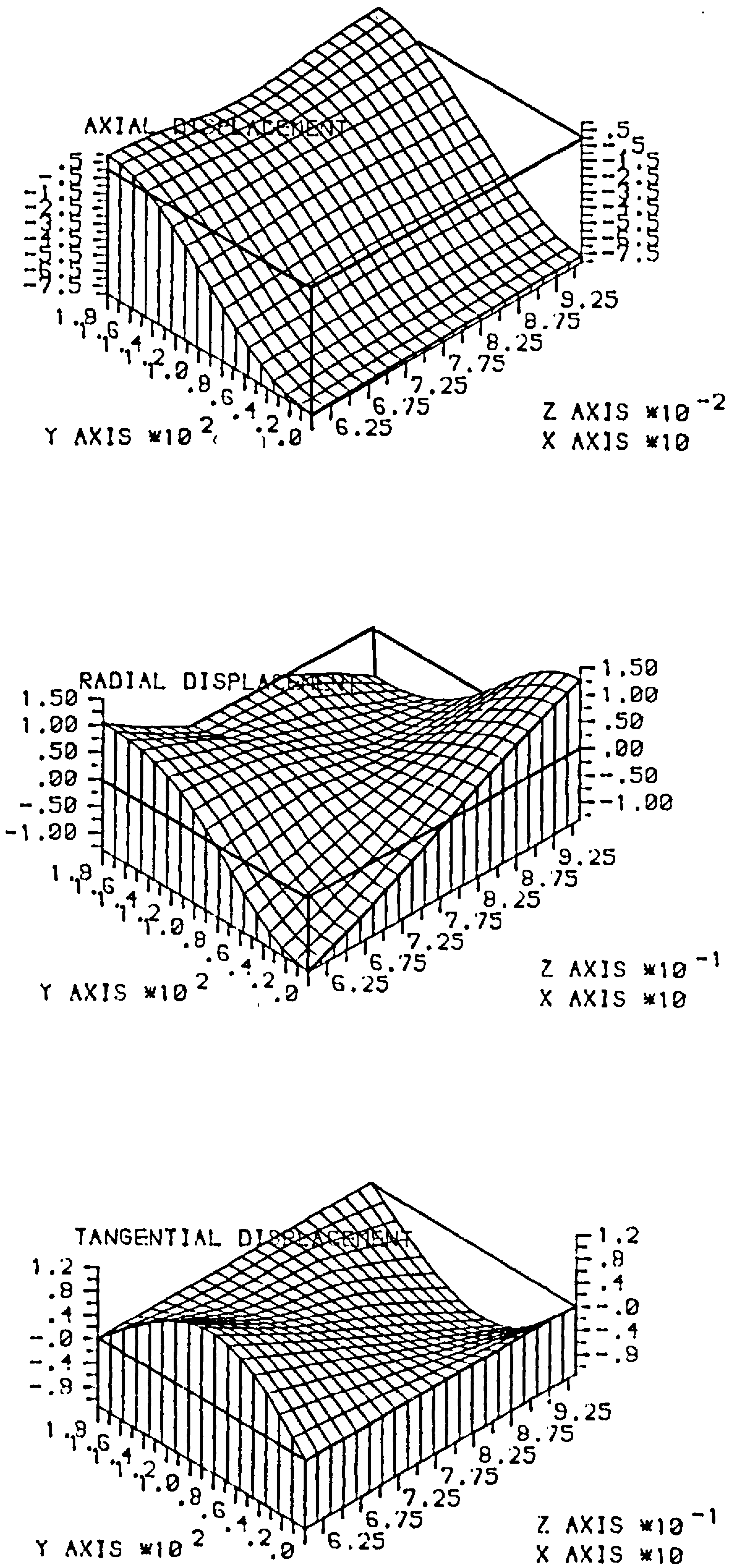

y; circumferential angle (deg)

z; displacement (in)

+ clockwise

Fig.4.3.7 Ring Framed Centre Body Displacement Displacements

LOW WING PICK UP (72-12-60) ; TAIL LOAD

R=6. t=0.06 Nstr=4 Lrsp=12. I_f=0.1 A_s=0.1

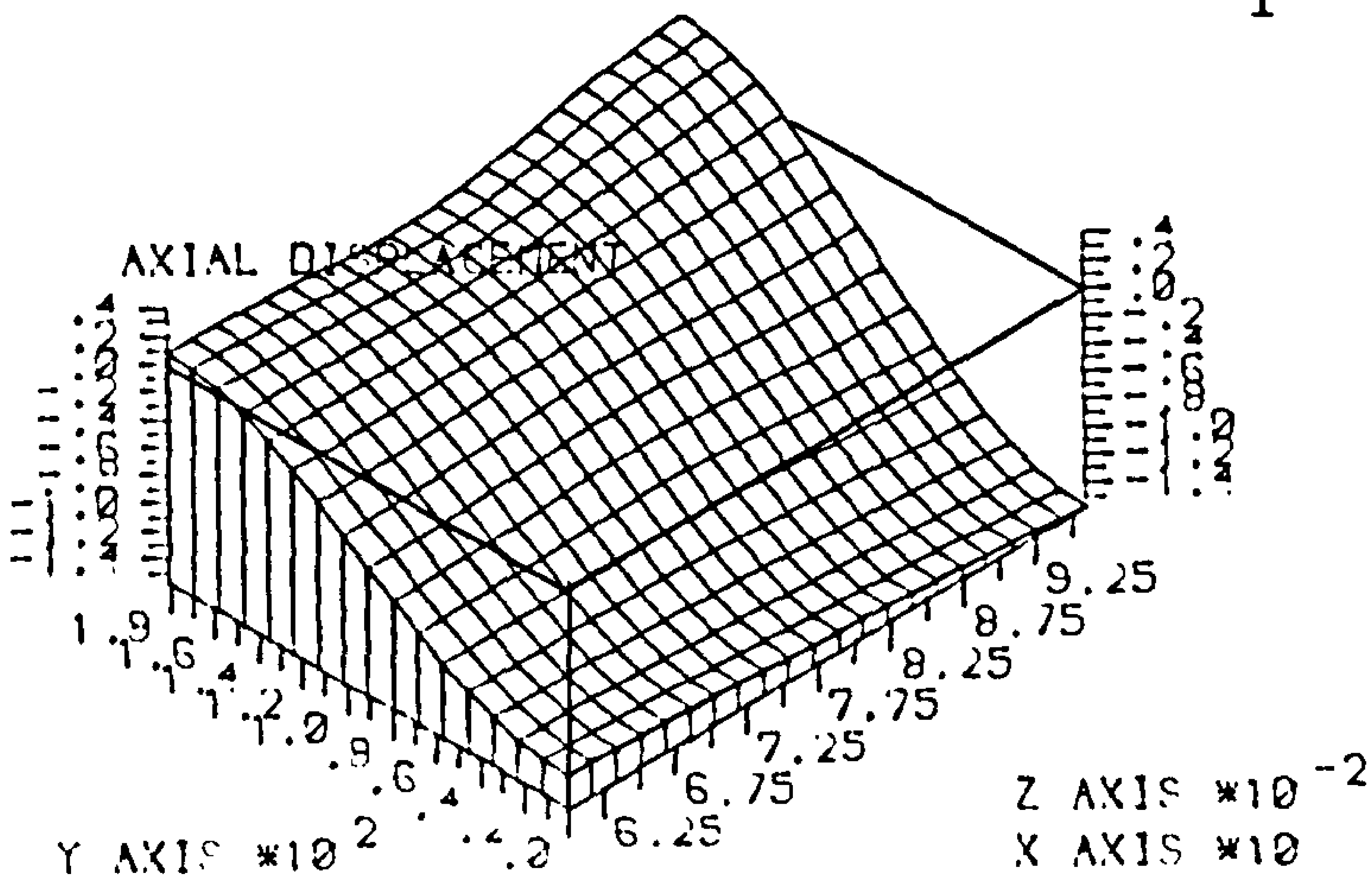

y; circumferential angle (deg)

z; displacement (in)

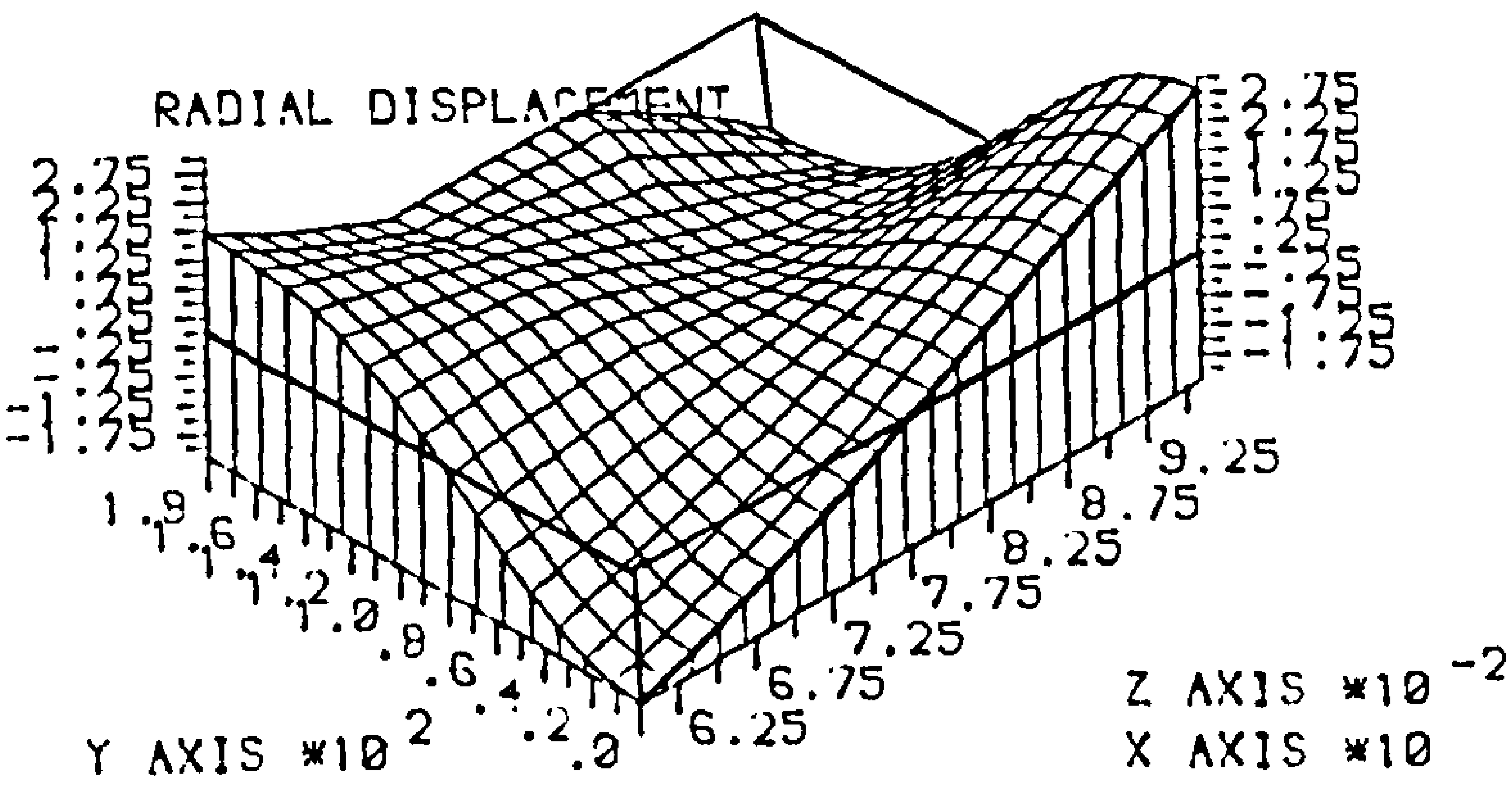

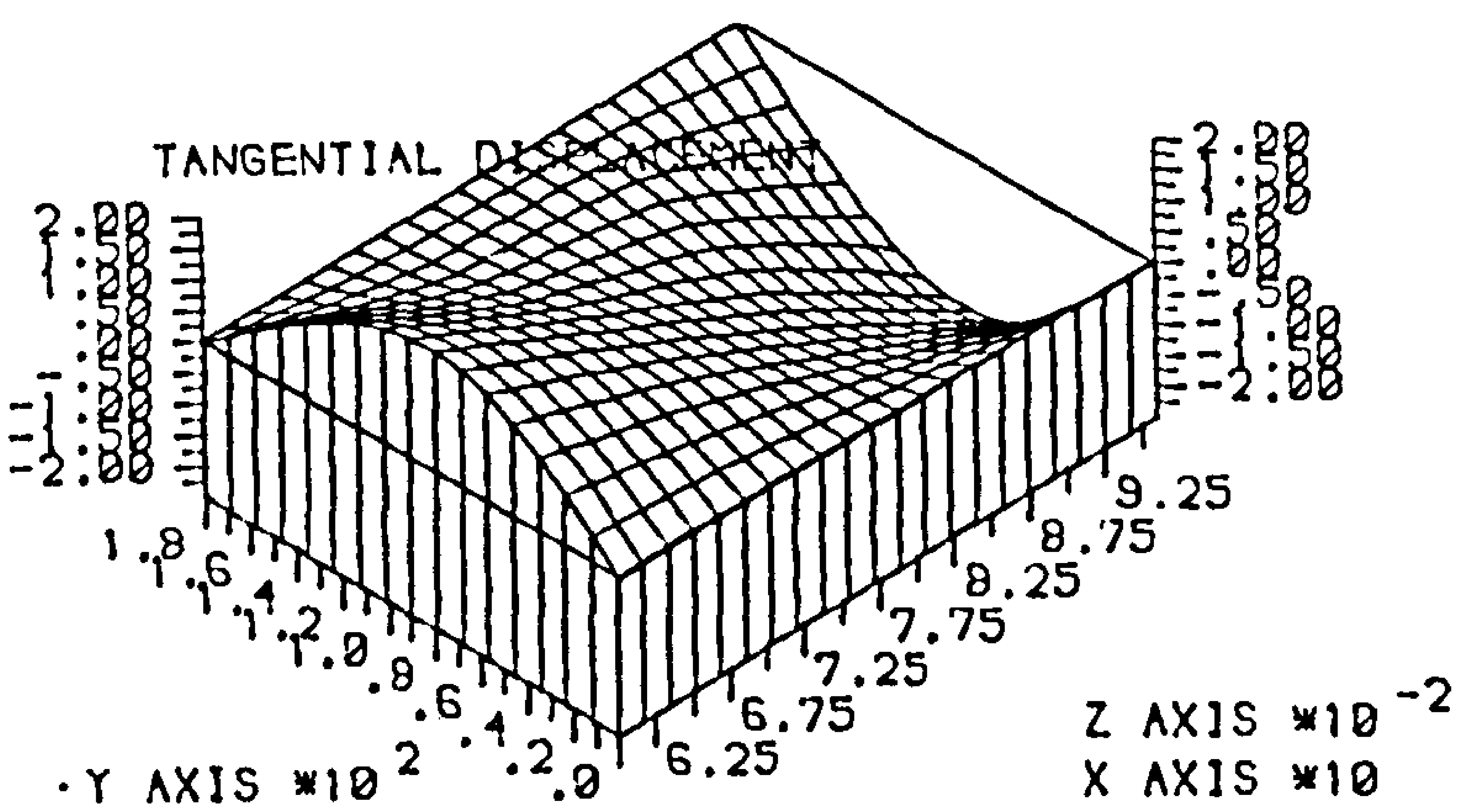

Fig.4.3.8 Ring Framed Centre Body Displacement Distributions

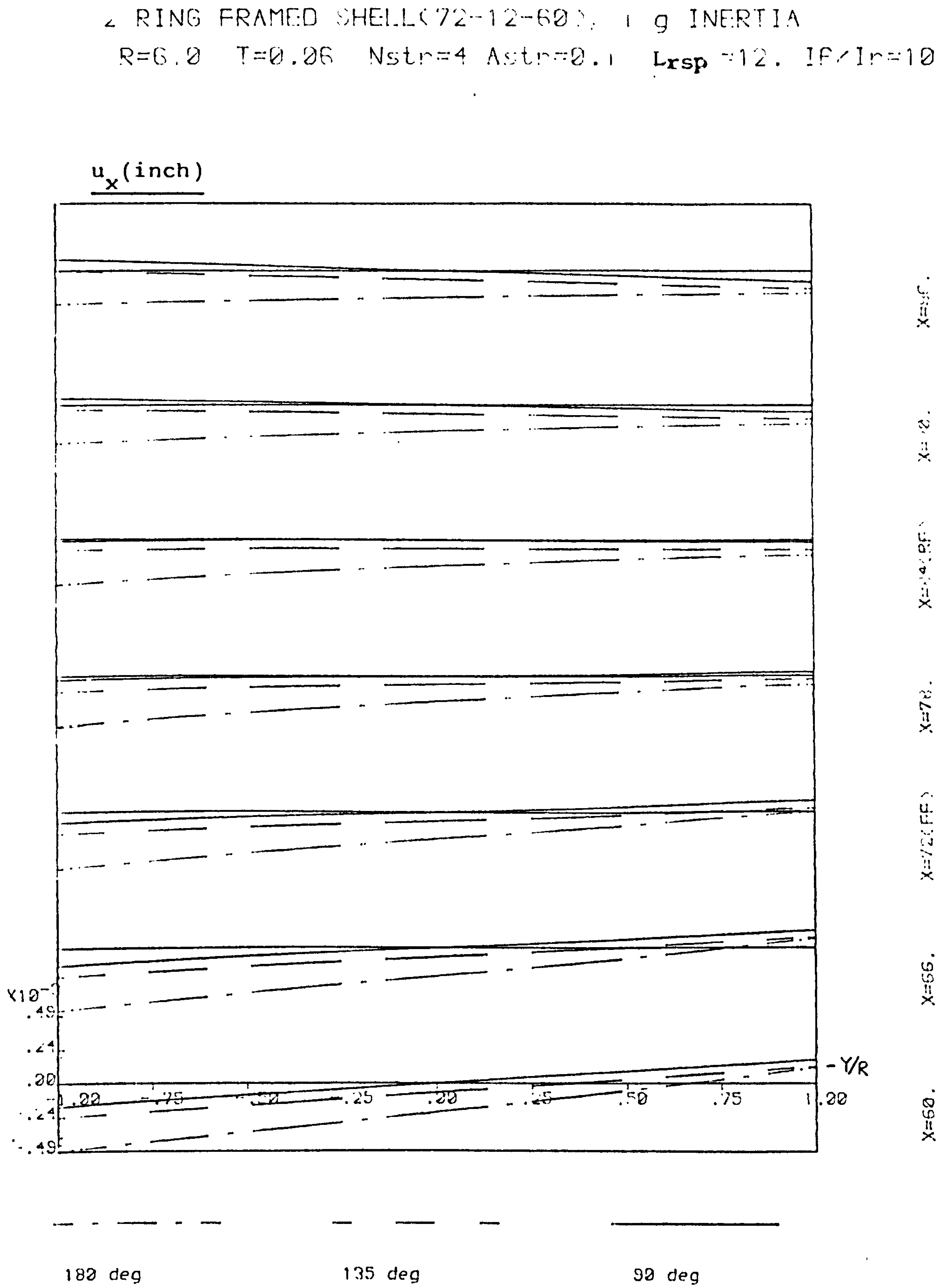

Fig.4.3.9 CENTRE BODY CROSS SECTION WARPING-PICK UP POSITION CHANGE

* refer paragraph (i) of section 3.9.

2 DIAPHRAGM FRAMED SHELL(72-12-60); TAIL LOAD
R=6.0 T=0.06 Nstr=4 Astr=0.1 Rspa=12.

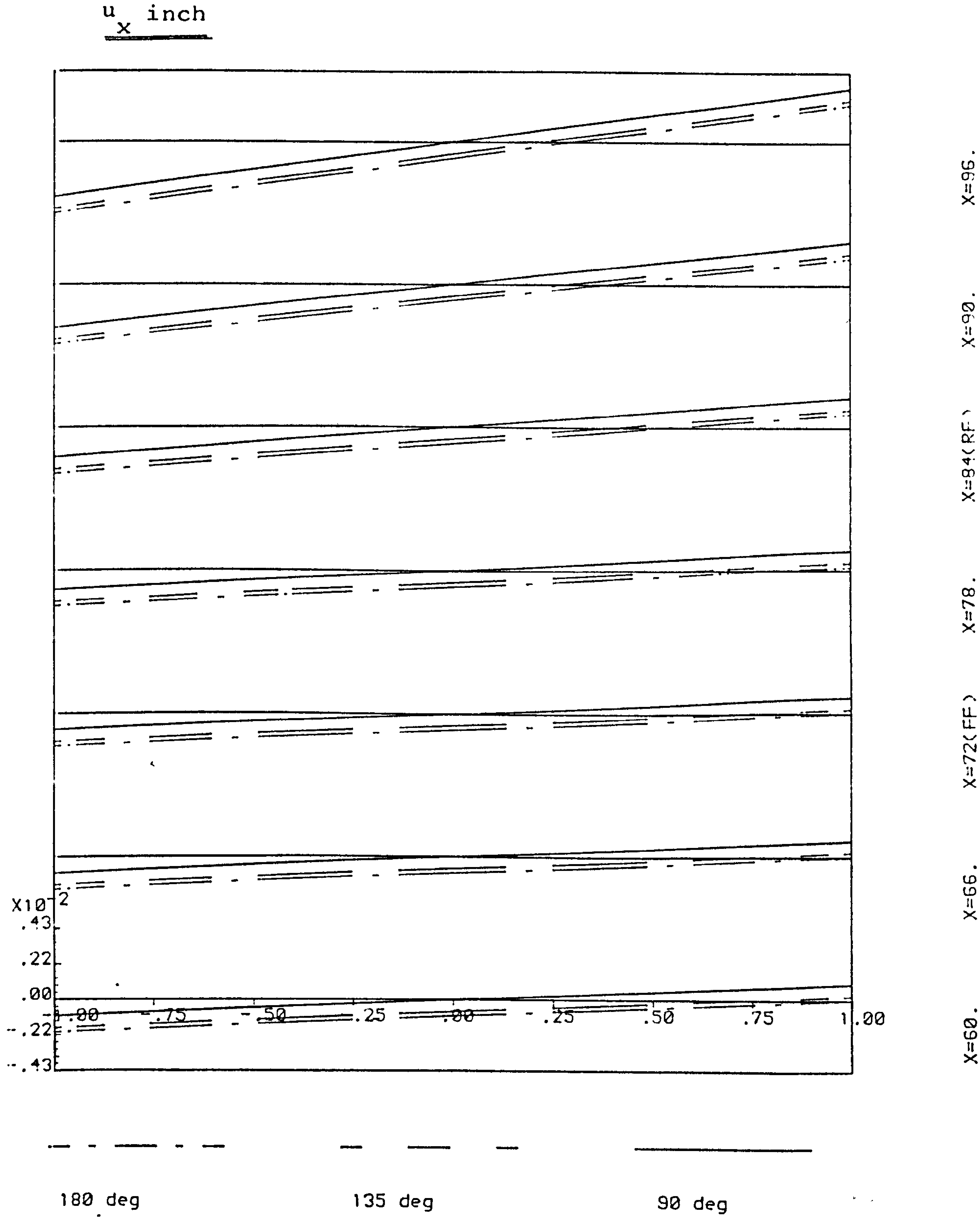

Fig.4.3.10 CENTRE BODY CROSS SECTION WARPING-PICK UP POSITION

* refer paragraph (i) of section 3.9.

2 DIAPHRAGM FRAMED SHELL(72-12-60); TAIL LOAD

R=6.0 T=0.06 Nstr=4 Astr=0.1 Rspa=12.

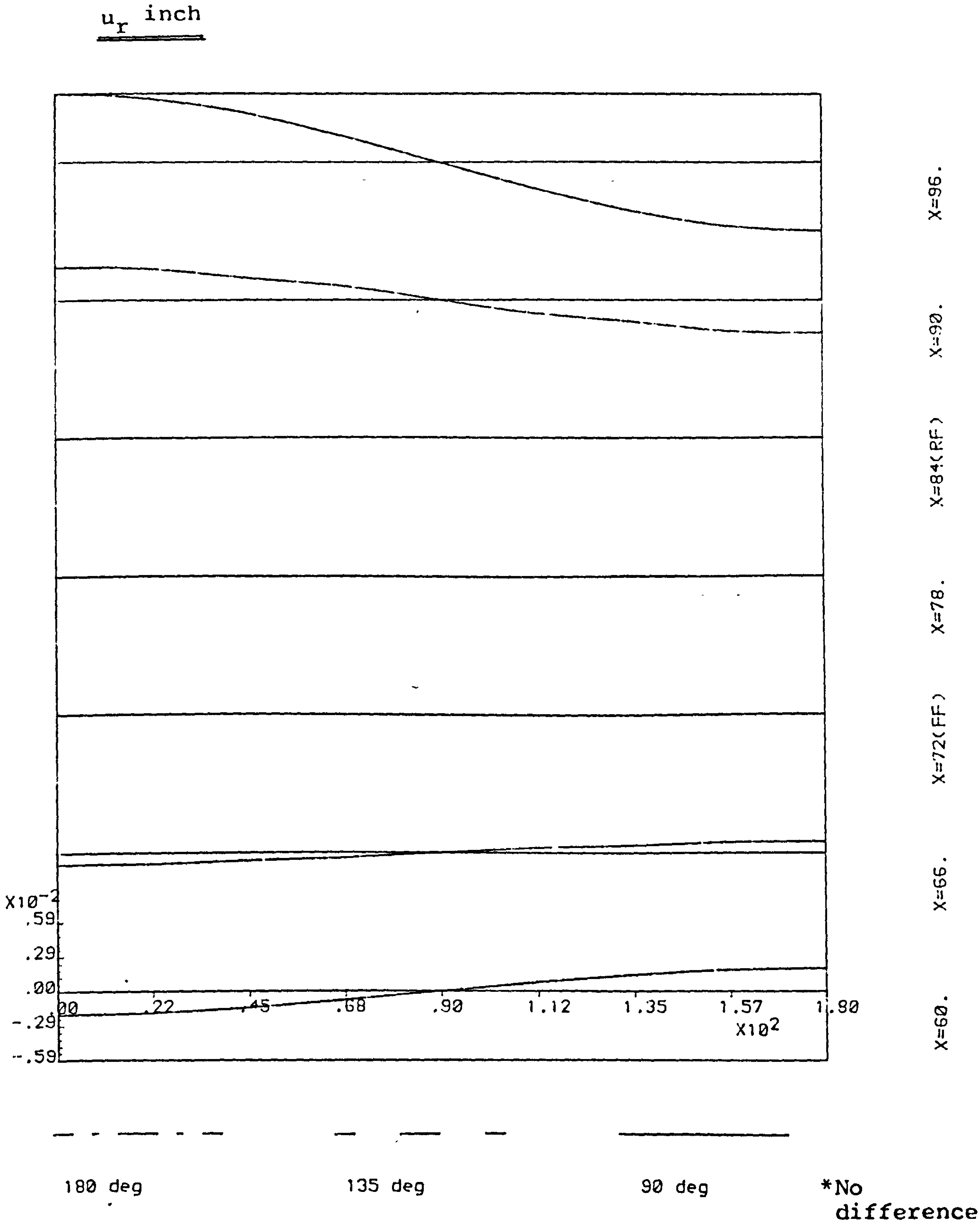

Fig.4.3.11 EFFECT OF PICK UP POSITION CHANGE - RADIAL DISPL.

2 DIAPHRAGM FRAMED SHELL(72-12-60); TAIL LOAD

R=6.0 T=0.06 Nstr=4 Astr=0.1 Rspa=12.

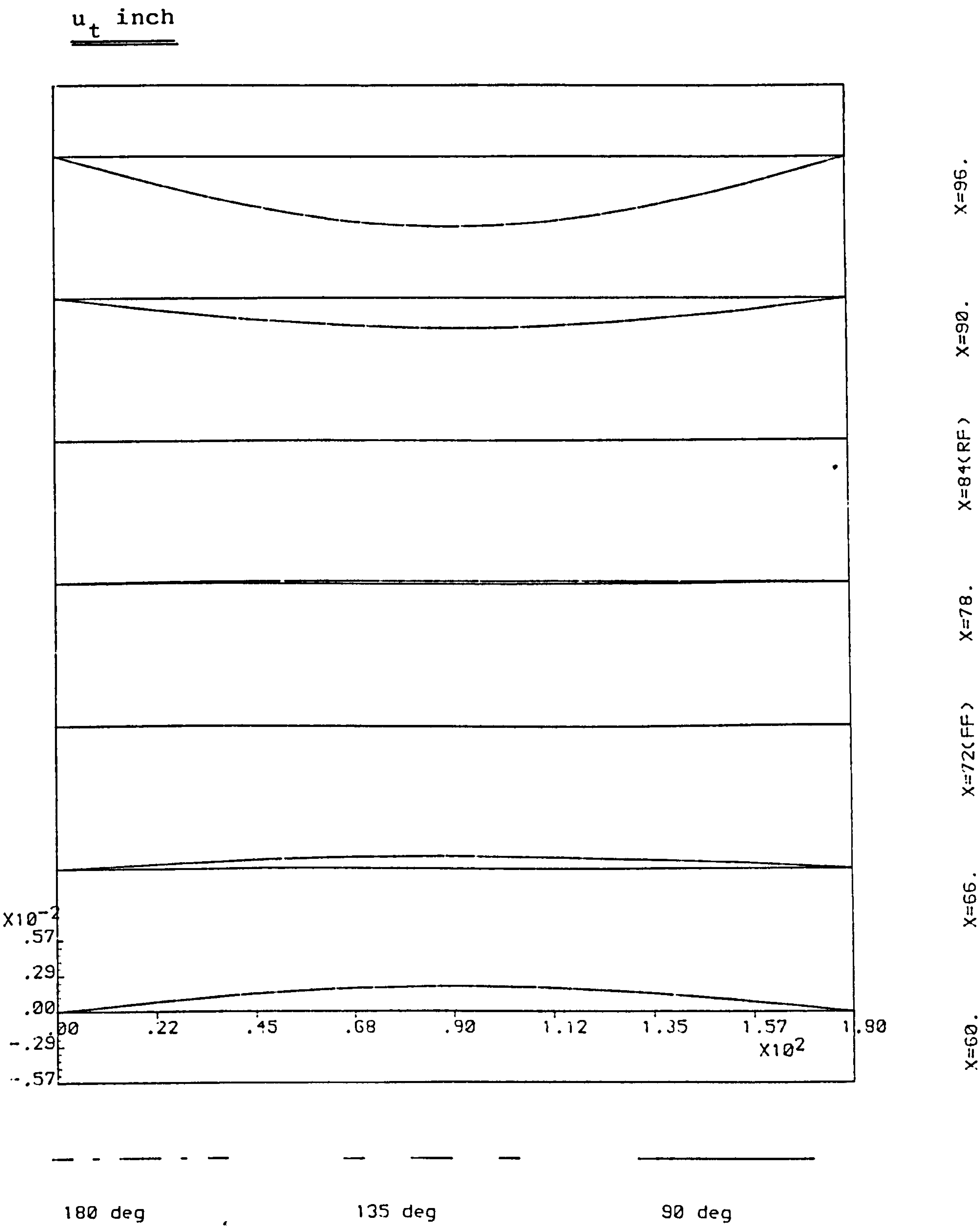

Fig.4.3.12 EFFECT OF PICK UP POSITION CHANGE - TANG. DISPL.

CENTRE BODY (6R t=0.06 72-12-60.1; SYM. TAIL LOAD

If=0.1 Af=1.0 Ir=0.01 Lrsp=12. Nstr=4 As=0.1

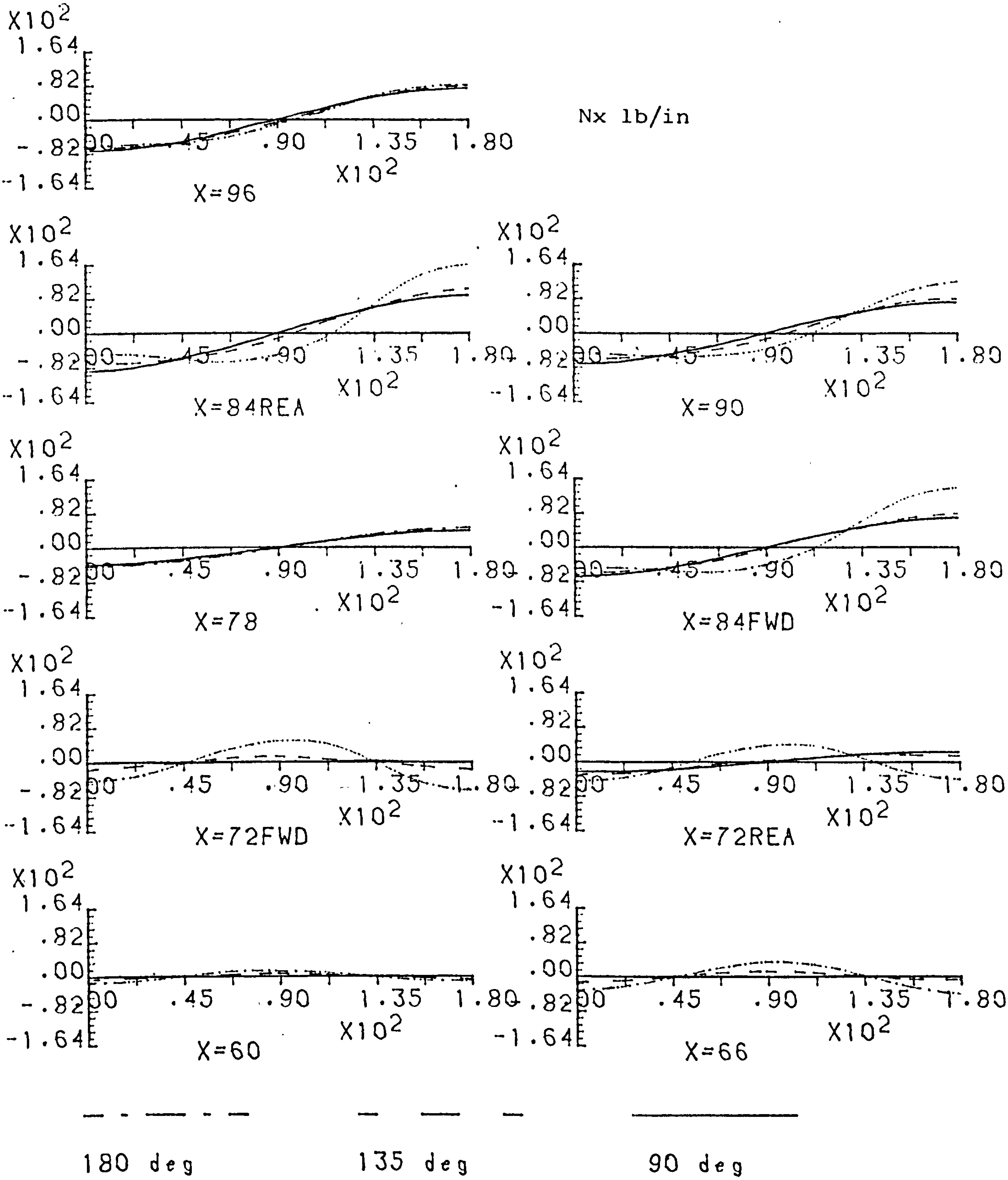

Fig.4.3.13 EFFECT OF PICK UP POSITION CHANGE - <u>DIRECT</u> STRESS

* refer paragraph (ii) of section 3.9.

CENTRE BODY (6R t=0.06 72-12-60.): SYM. TAIL LOAD

If=0.1 Af=1.0 Ir=0.01 Lrsp=12. Nstr=4 As=0.1

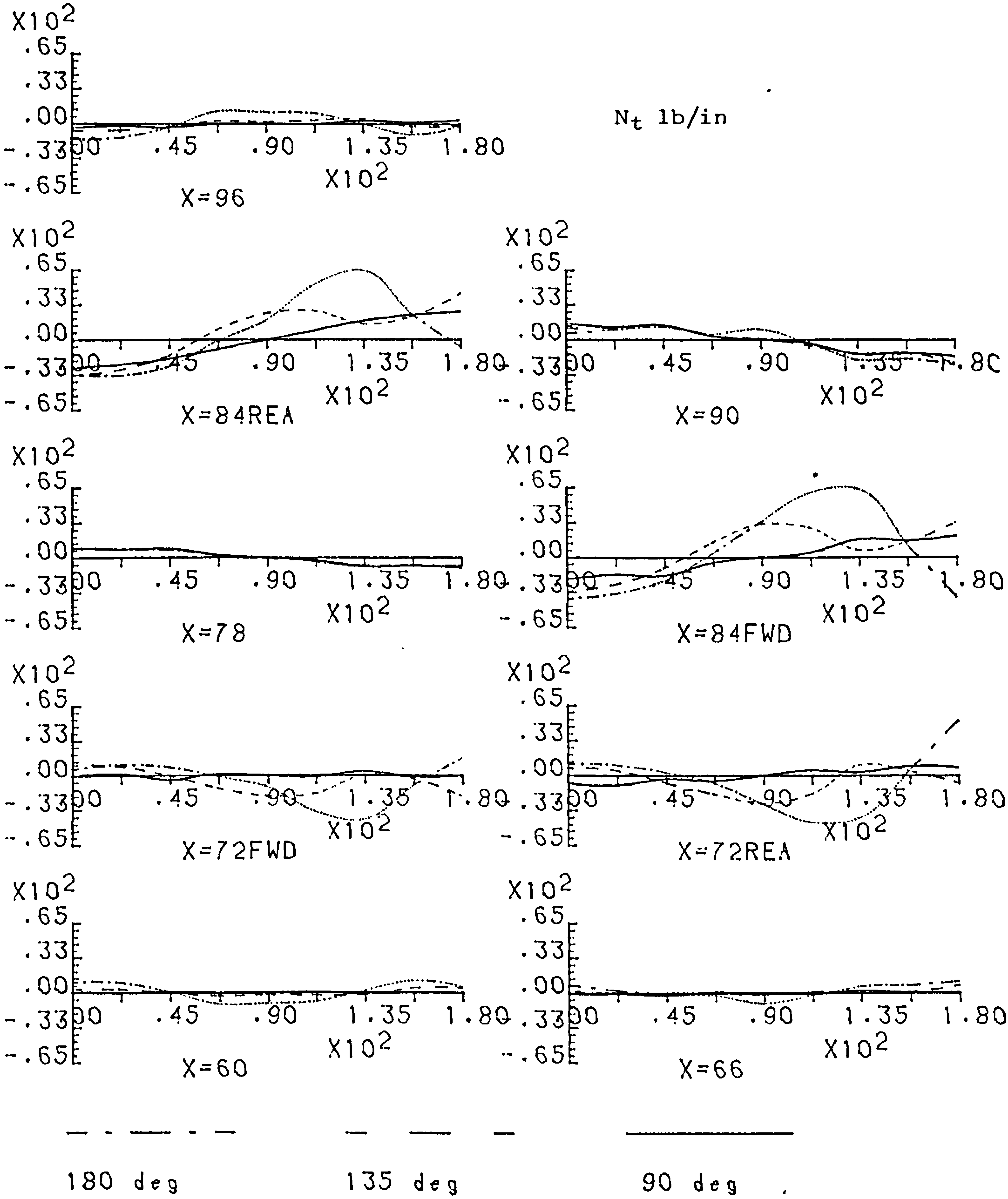

Fig. 4.3.14 EFFECT OF PICK UP POSITION CHANGE - HOOP STRESS

CENTRE BODY (6R t=0.06 72-12-60.): SYM. TAIL LOAD
If=0.1 Af=1.0 Ir=0.01 Lrsp=12. Nstr=4 As=0.1

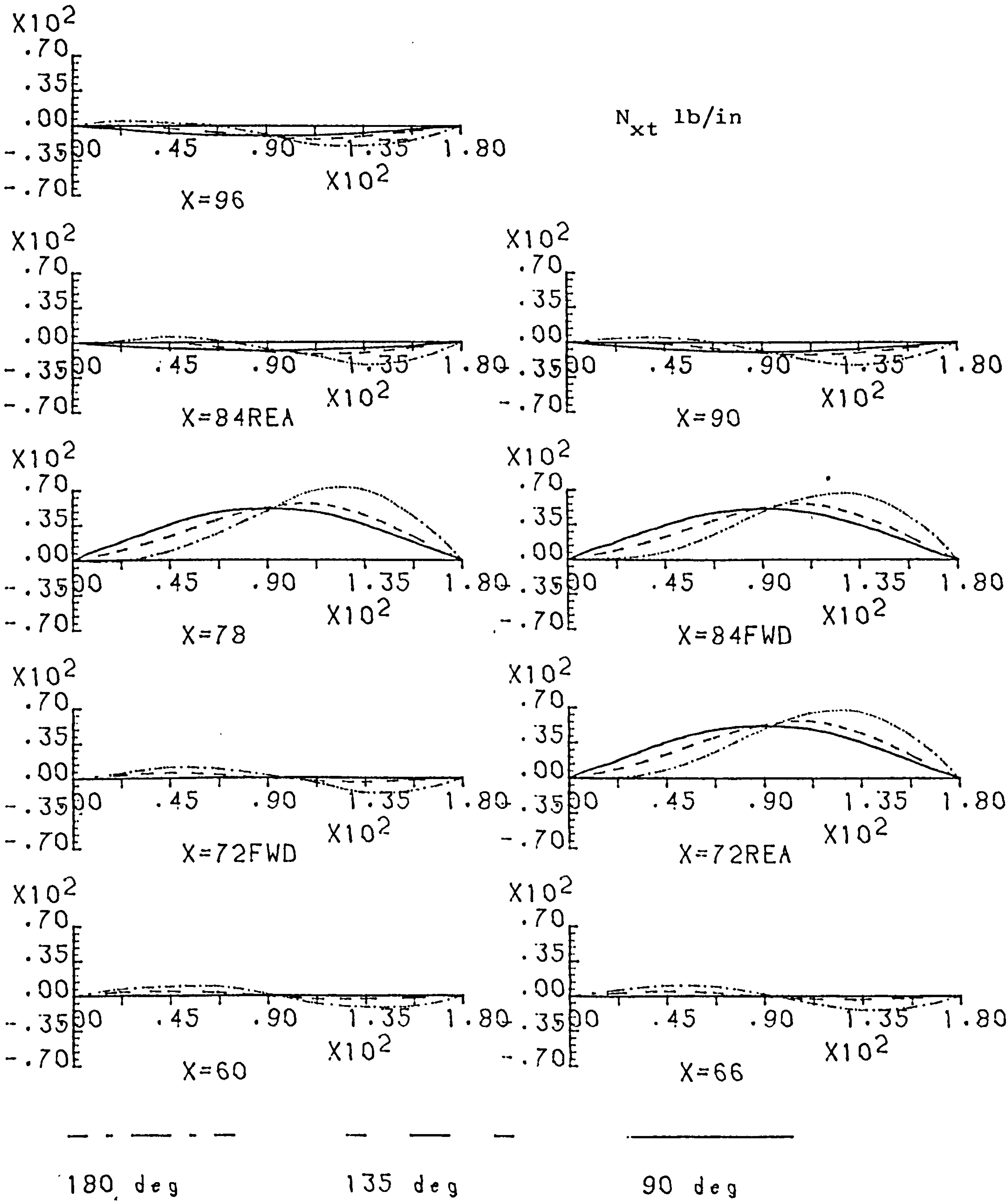

Fig.4.3.15 EFFECT OF PICK UP POSITION CHANGE - SHEAR FLOW

CENTRE BODY (6R t=0.06 72-12-60.); SYM. TAIL LOAD
If=0.1 Af=1.0 Ir=0.01 Lrsp=12. Nstr=4 As=0.1

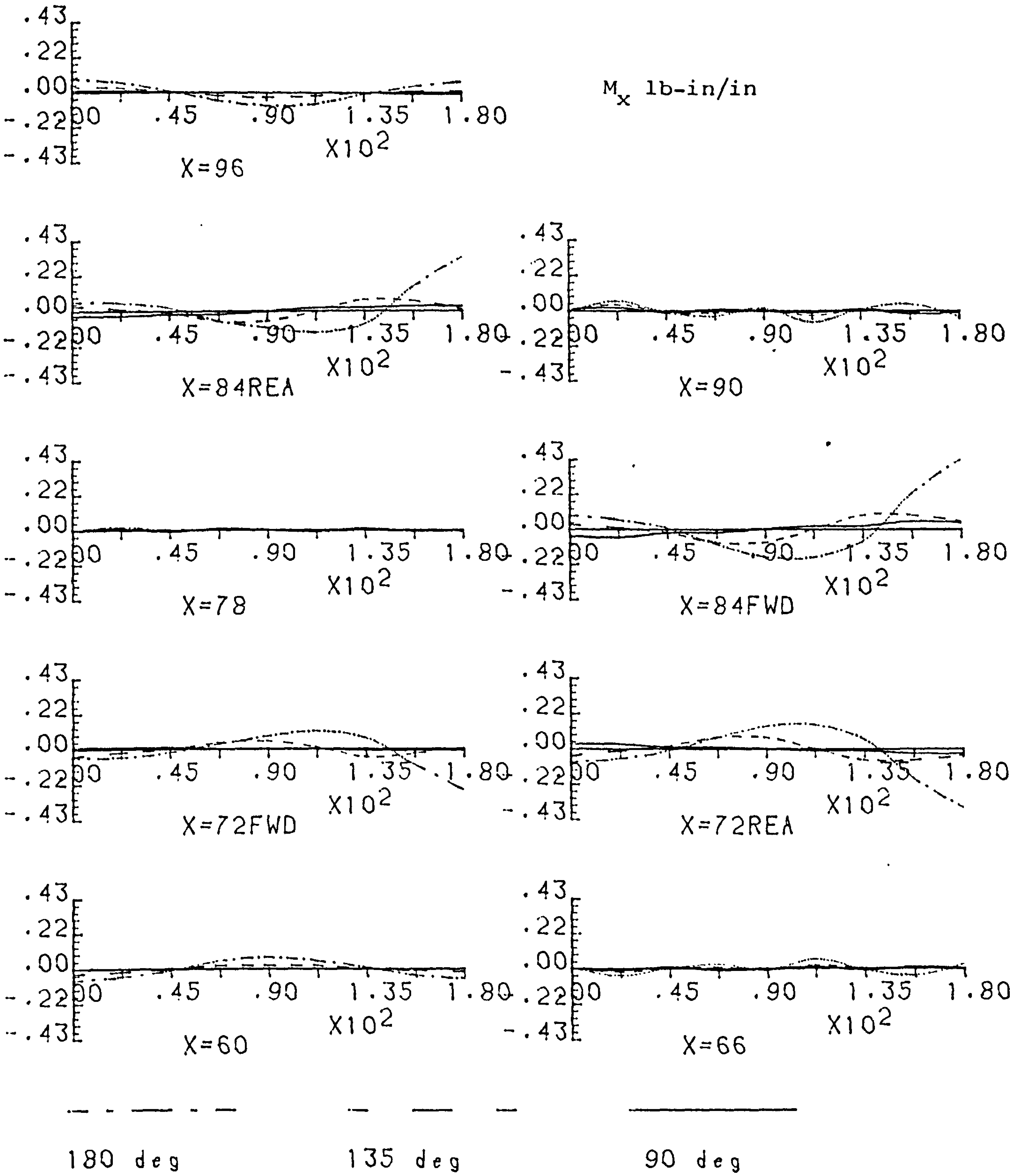

Fig. 4.3.16 EFFECT OF PICK UP POSITION CHANGE - AXIAL BENDING
(Mx)

CENTRE BODY (6R t=0.06 72-12-60.): SYM. TAIL LOAD
If=0.1 Af=1.0 Ir=0.01 Lrsp=12. Nstr=4 As=0.1

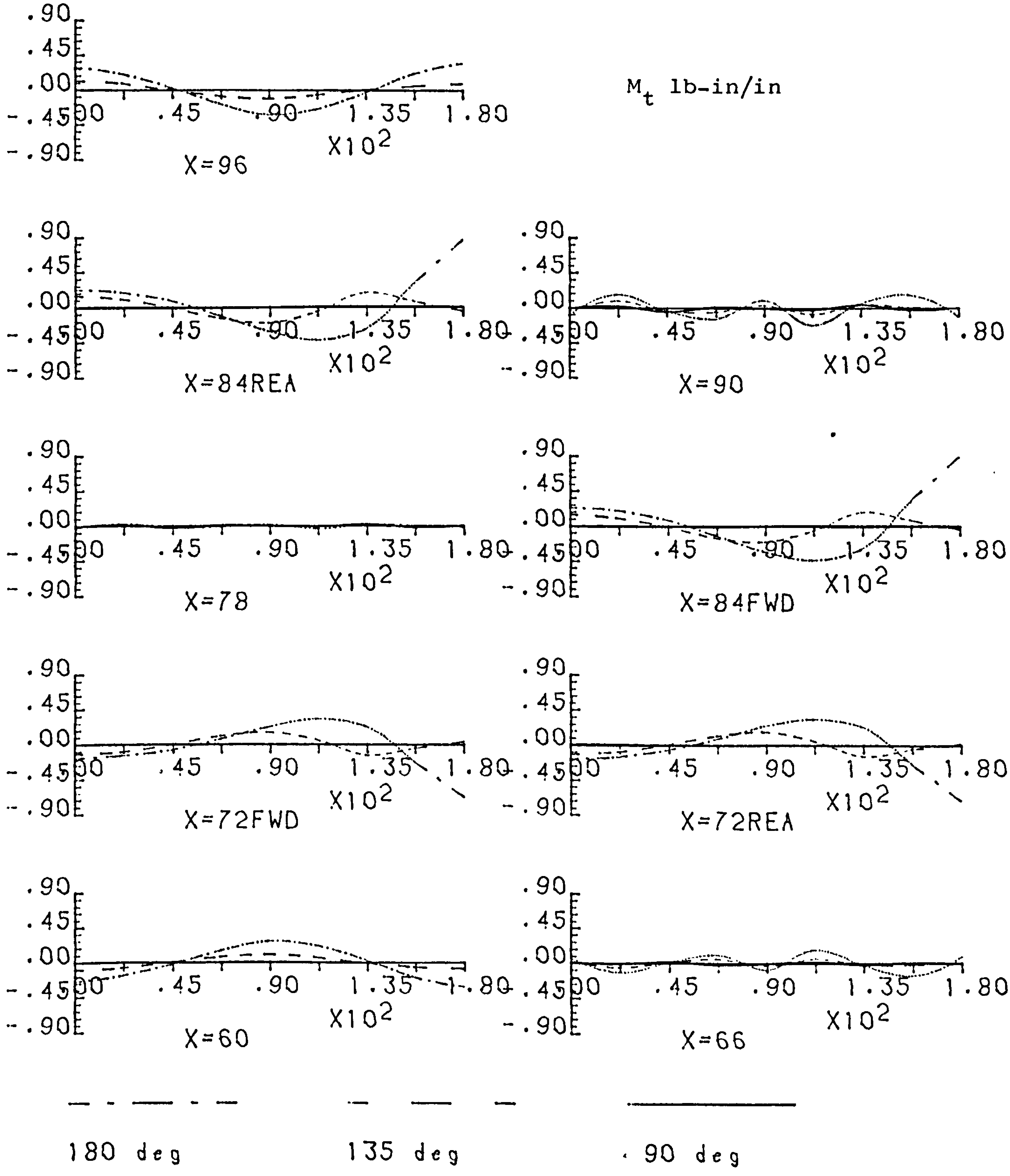

Fig.4.3.17 EFFECT OF PICK UP POSITION CHANGE - CIRC. BENDING (M_t)

CENTRE BODY (6R t=0.06 72-12-60.): SYM. TAIL LOAD
If=0.1 Af=1.0 Ir=0.01 Lrsp=12. Nstr=4 As=0.1

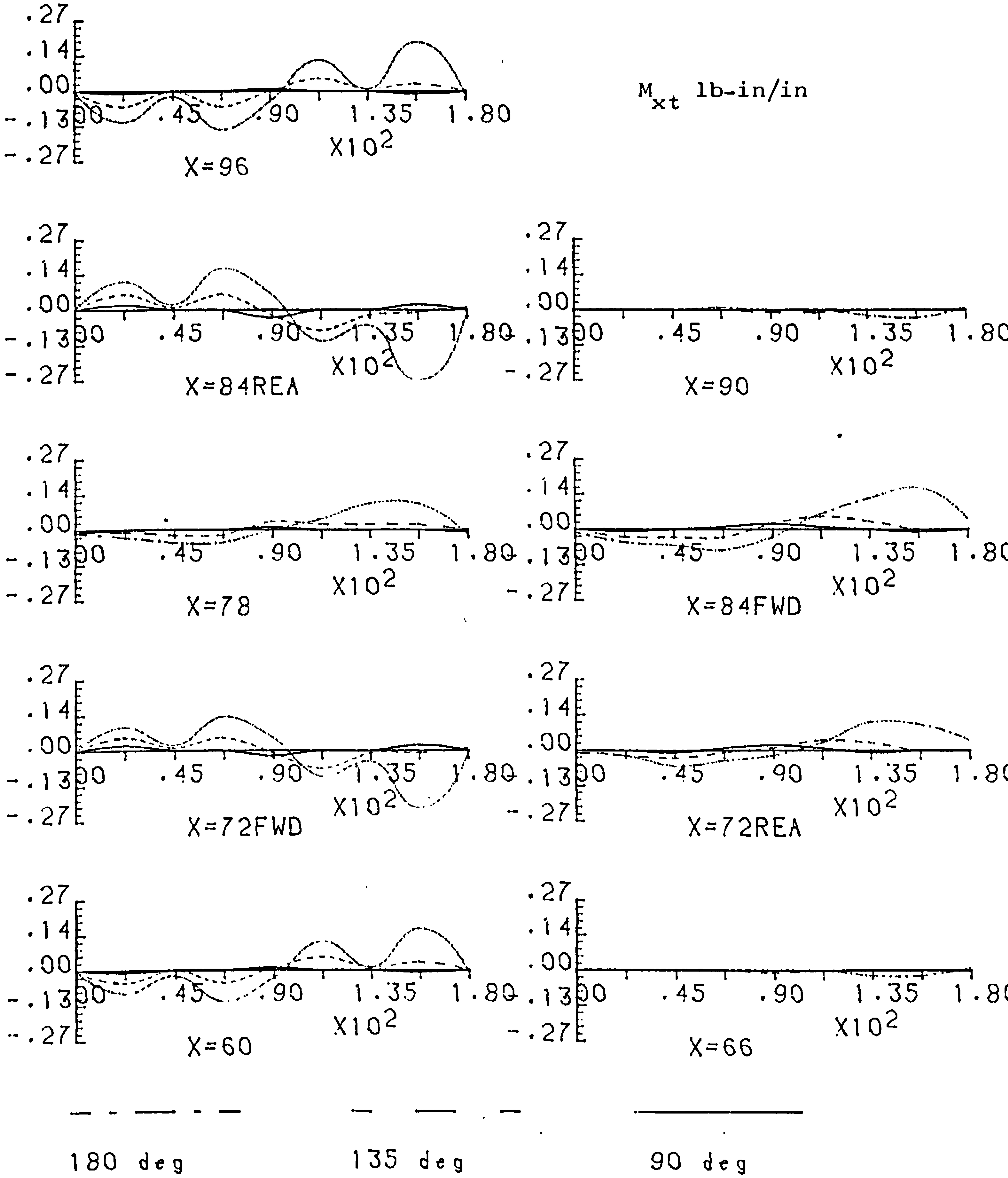

Fig. 4.3.18 EFFECT OF PICK UP POSITION CHANGE - TWISTING
(M_{xt})

Fig.4.3.19 Shear Flow From Shell To Frame - Pick Up Position Change

* refer paragraph (vi) of section 3.9.

RING FRAMED SHELL(LF=72 Lr=60); ANTISYMM TAIL-FIN LOAD

R=6.0 T=0.06 Ir=0.01 Astr=Ar=0.1 Nstr=4 IF=0.1

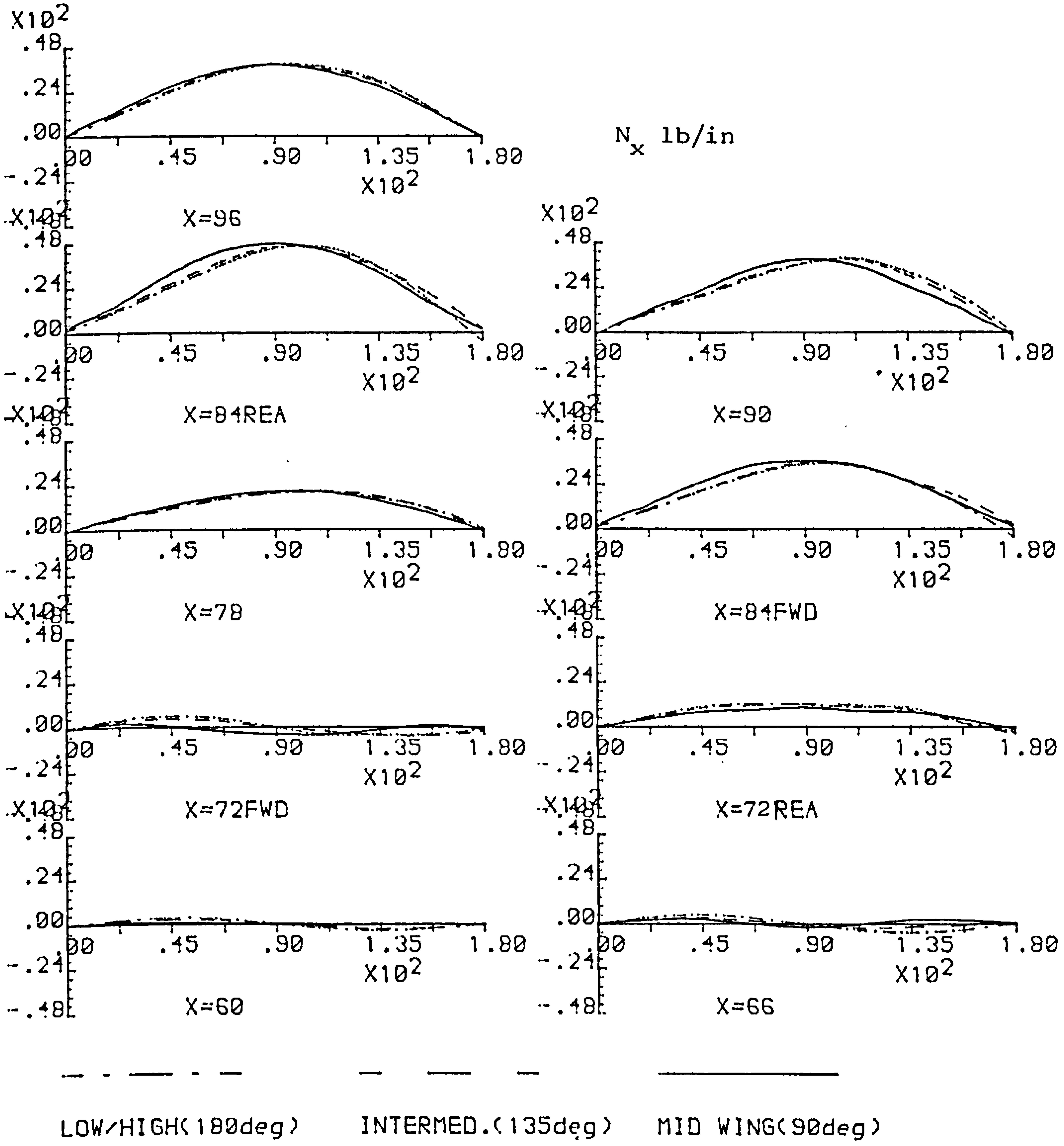

Fig.4.3.20 EFFECT OF PICK UP POSITION CHANGE - DIRECT STRESS

RING FRAMED SHELL(LF=72 Lr=60); ANTISYMM TAIL-FIN LOAD

R=6.0 T=0.06 Ir=0.01 Astr=Ar=0.1 Nstr=4 IF=0.1

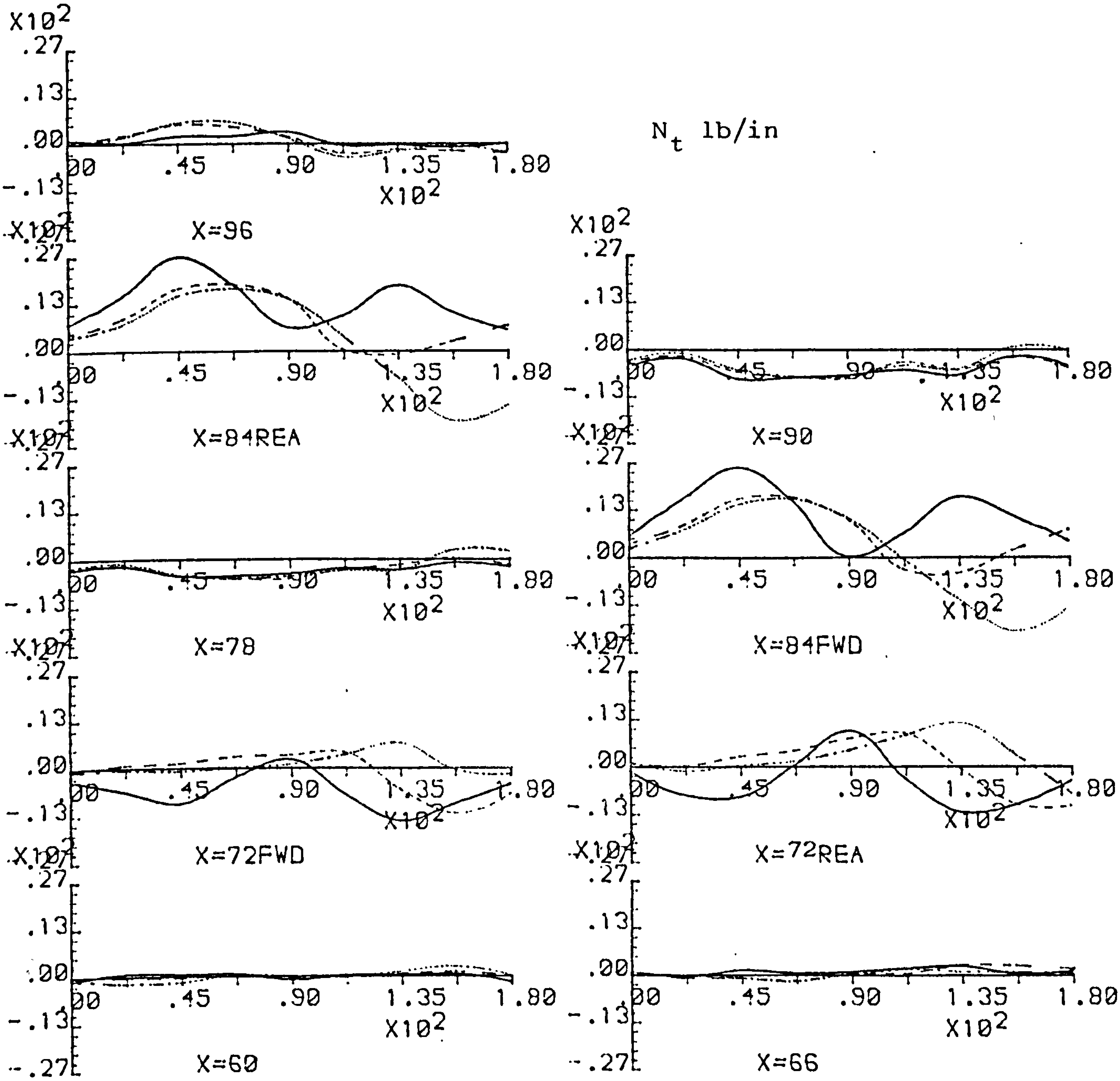

LOW/HIGH(180deg) INTERMED.(135deg) MID WING(90deg)

Fig.4.3.21EFFECT OF PICK UP POSITION CHANGE - <u>HOOP STRESS</u>

RING FRAMED SHELL(LF=72 Lr=60); ANTISYMM. TAIL-FIN LOAD

R=6.0 T=0.06 Ir=0.01 Astr=Ar=0.1 Nstr=4 IF=0.1

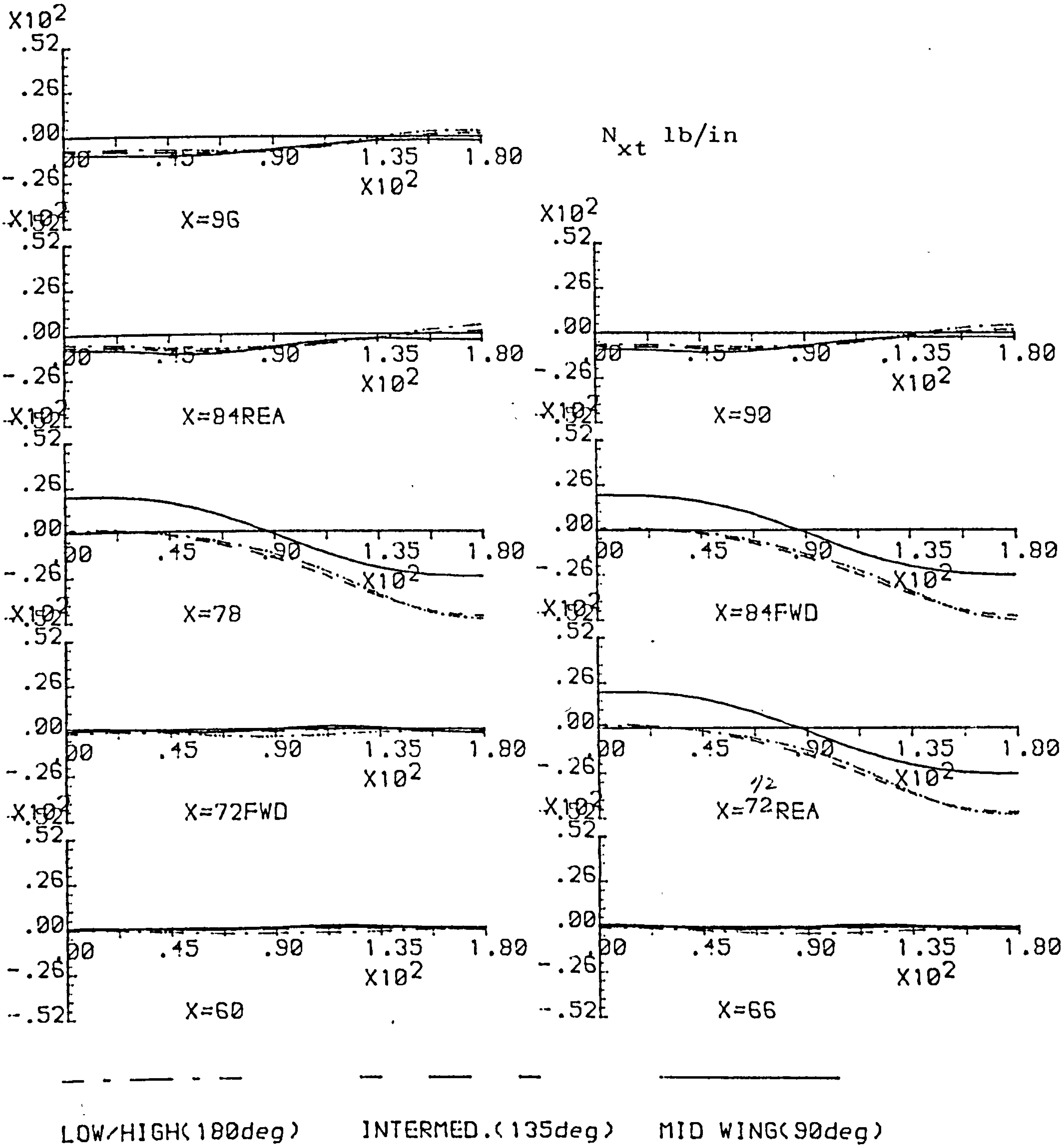

Fig.4.3.22 EFFECT OF PICK UP POSITION CHANGE - SHEAR FLOW

CENTRE BODY STRESS RESULT. (72-12-60) : TAIL LOAD
R=6.0 T=0.06 Rspa=12. Astr=0.1 4 STRING.
Low Wing, I_r=0.01

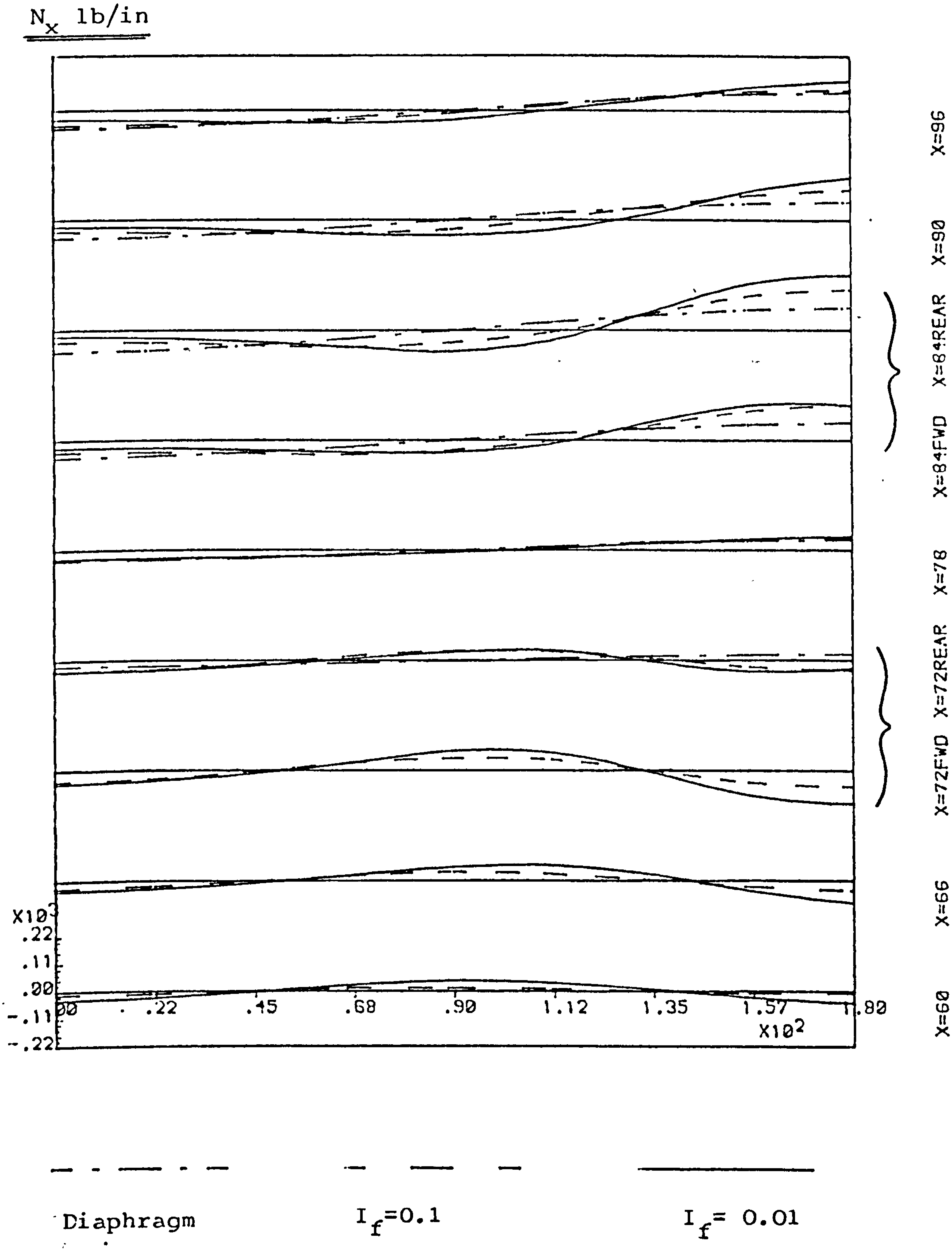

Fig.4.4.1 EFFECTS OF FRAME PROPERTY(I_f) CHANGE - DIRECT

* refer paragraph (iii) of section 3.9.

CENTRE BODY STRESS RESULT. (72-12-60) : TAIL LOAD
R=6.0 T=0.06 Rspa=12. Astr=0.1 4 STRING.
LOW WING PICK UP, I_r=0.01

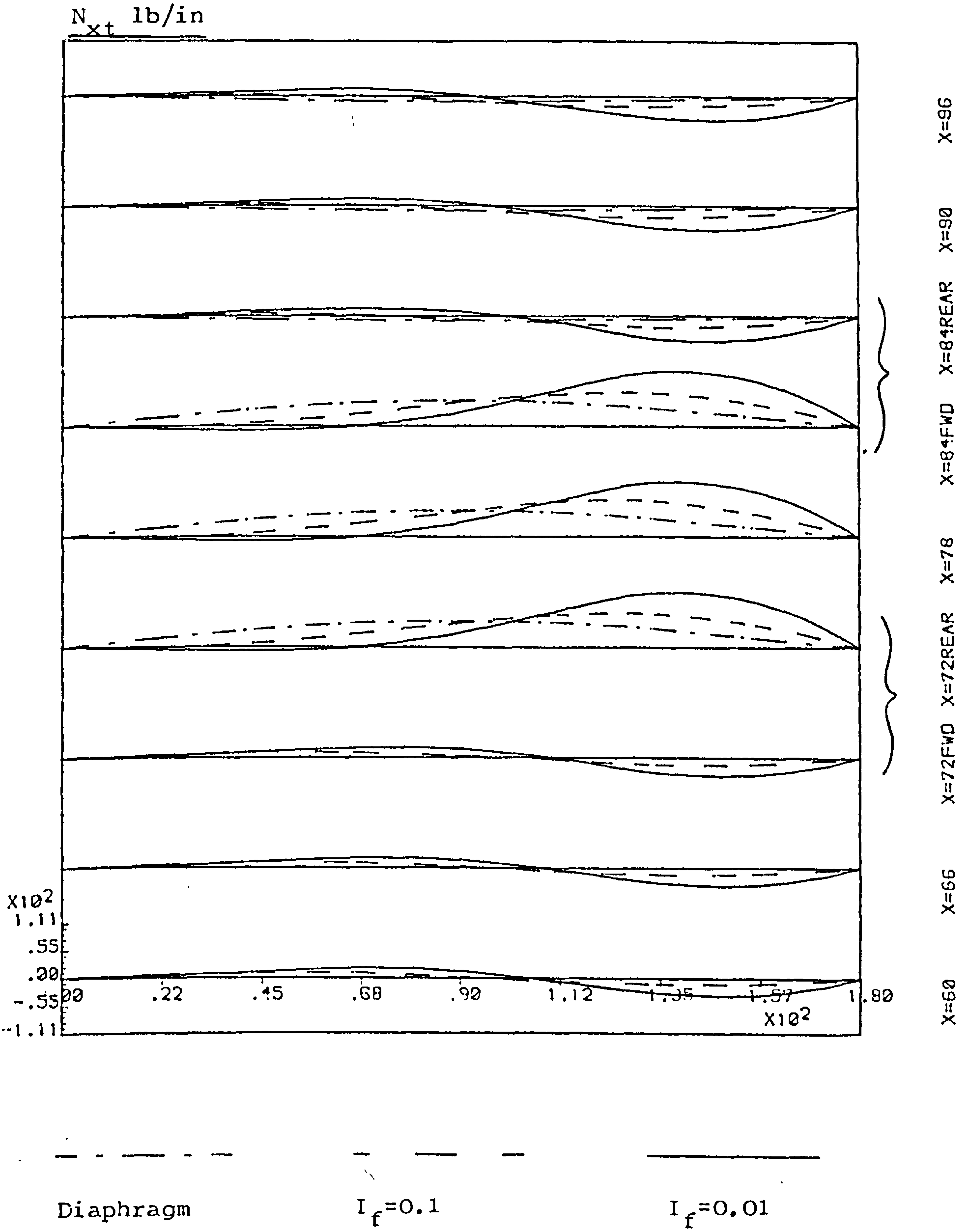

Fig. 4.4.2 EFFECTS OF FRAME PROPERTY(I_f) CHANGE - SHEAR FLOW

BENDING STRESS RESULTANT OF CENTRE BODY(180deg); TAIL
R=6.0 T=0.06 Ir=0.01 Astr=Ar=0.1 Nstr=4, 72-12-60

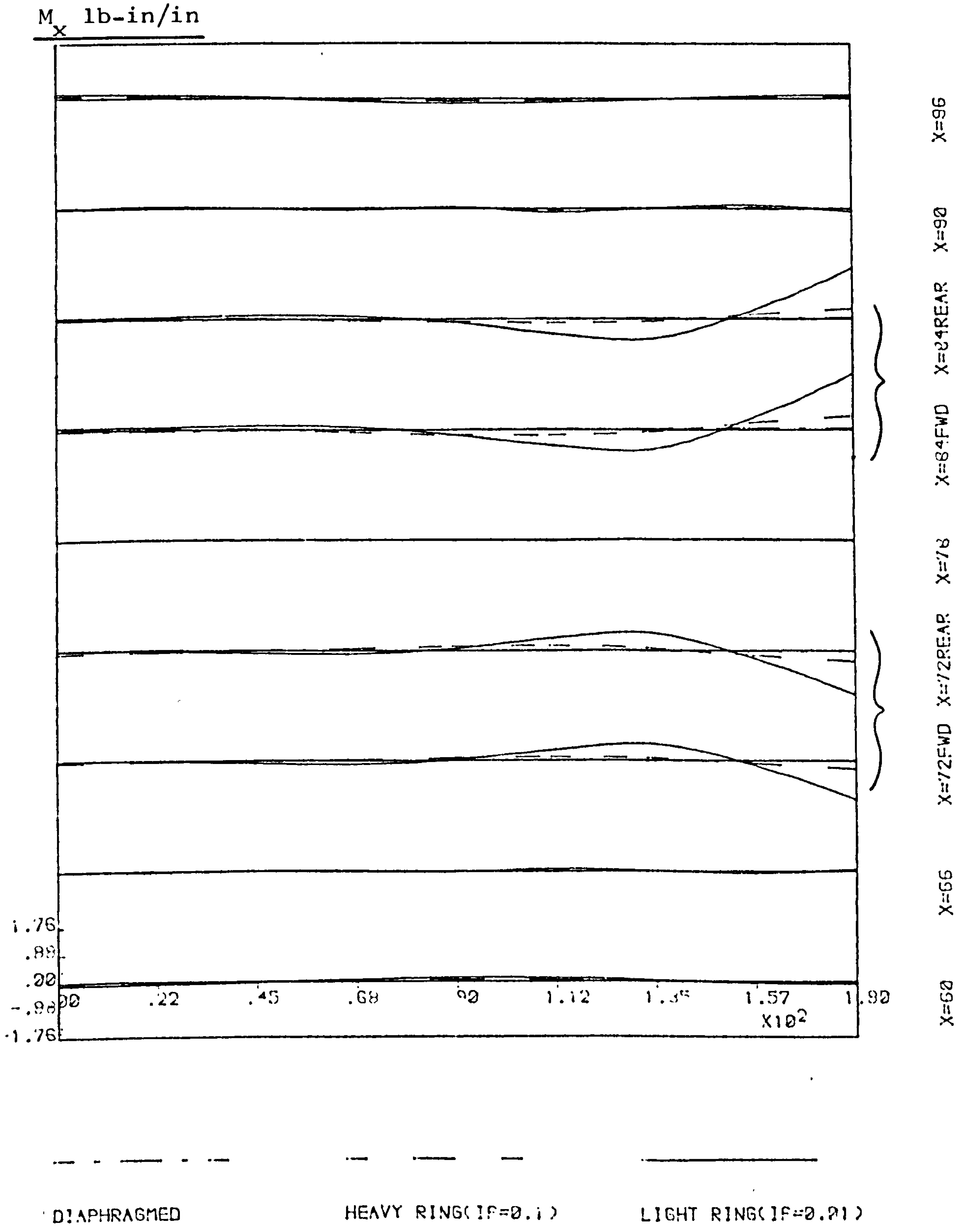

Fig. 4.4.3 EFFECTS OF FRAME STIFF. VARIATION- AXIAL BENDING

BENDING STRESS RESULTANT OF CENTRE BODY(180deg); TAIL
R=6.0 T=0.06 Ir=0.01 Astr=Ar=0.1 Nstr=4, 72-12-60

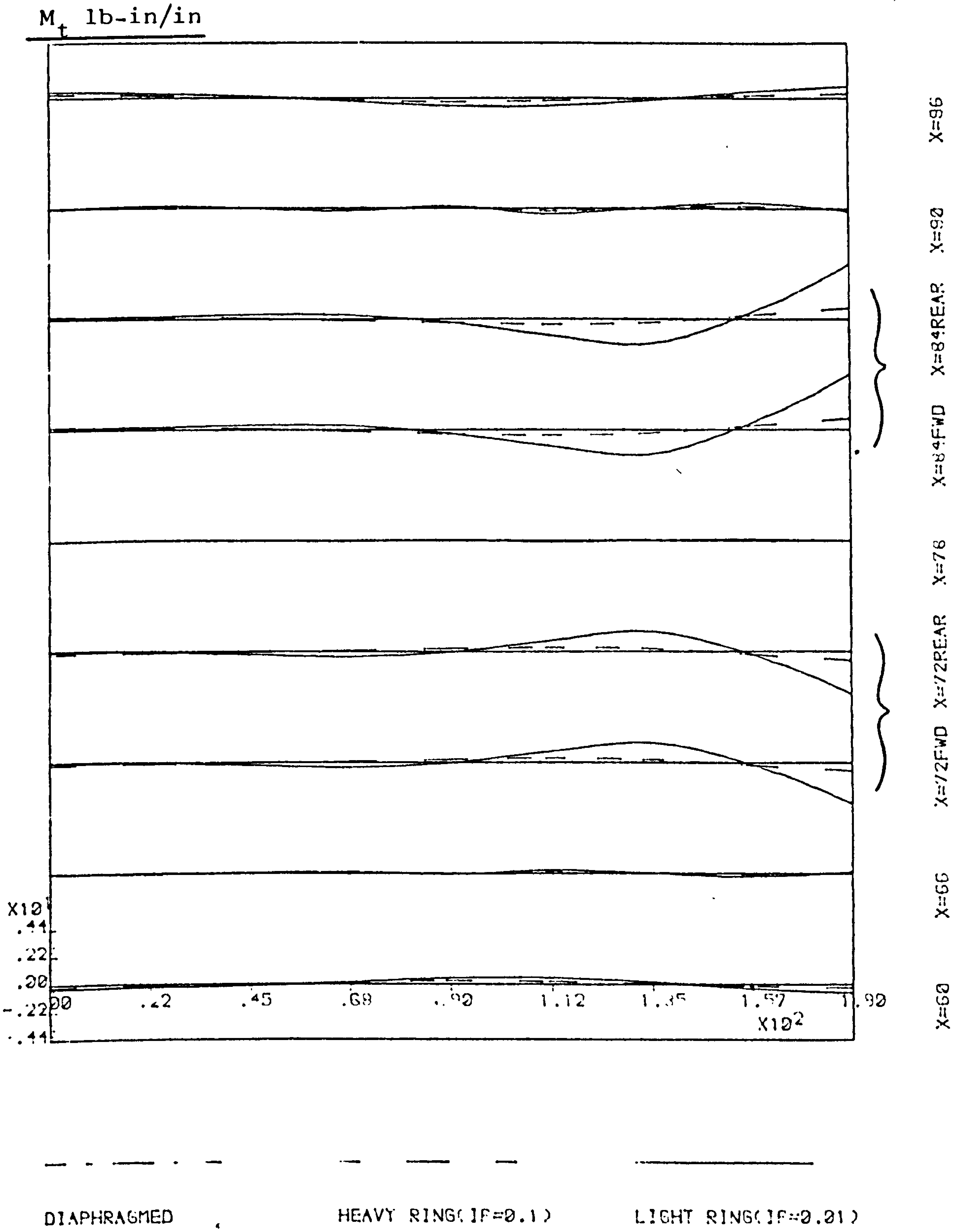

Fig.4.4.4 EFFECTS OF FRAME STIFF. VARIATION - CIRCUMF. BEND

BENDING STRESS RESULTANT OF CENTRE BODY(180deg); TAIL.
R=6.0 T=0.06 Ir=0.01 Astr=Ar=0.1 Nstr=4, 72-12-60

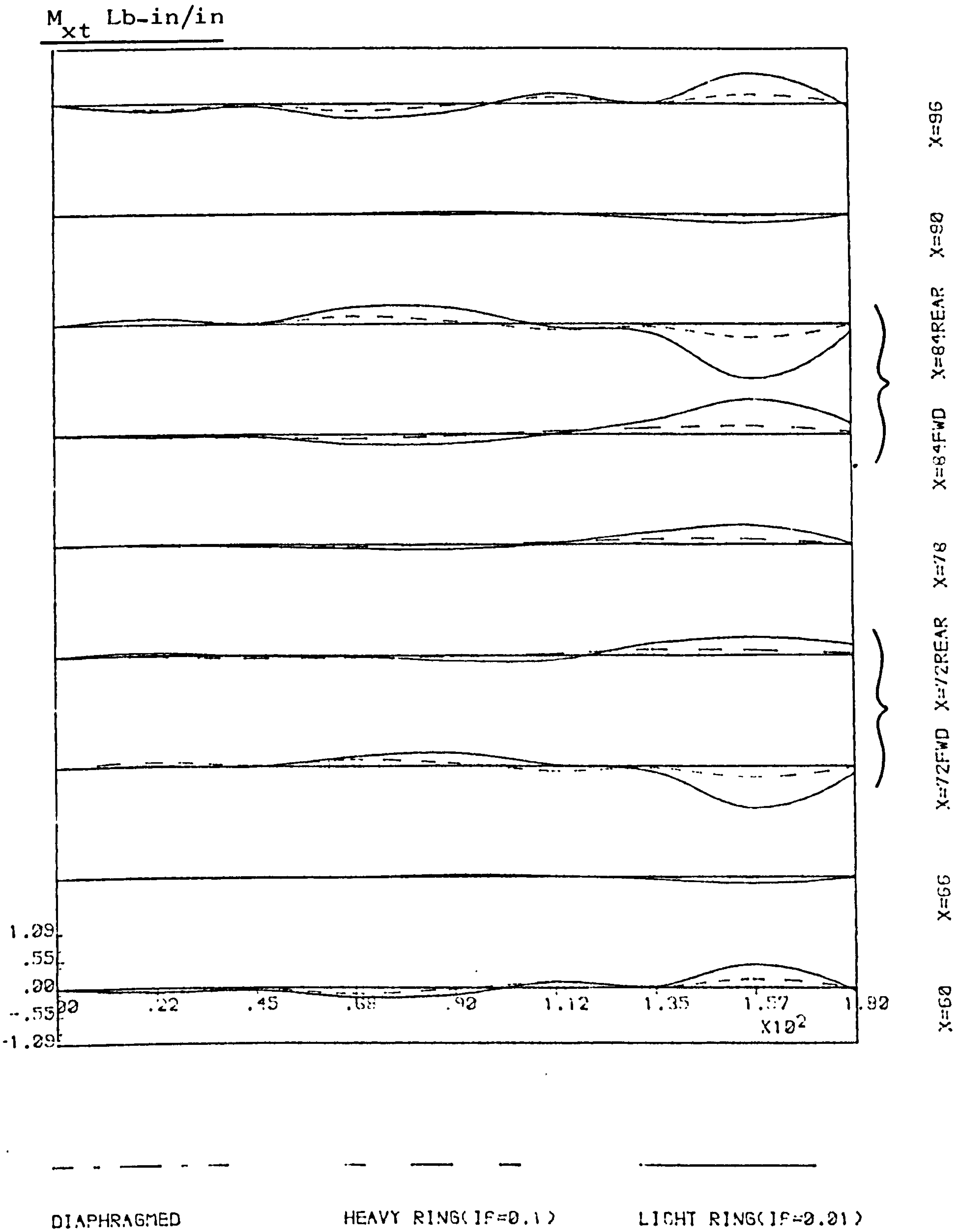

Fig.4.4.5 EFFECTS OF FRAME STIFF. VARIATION - TWISTING

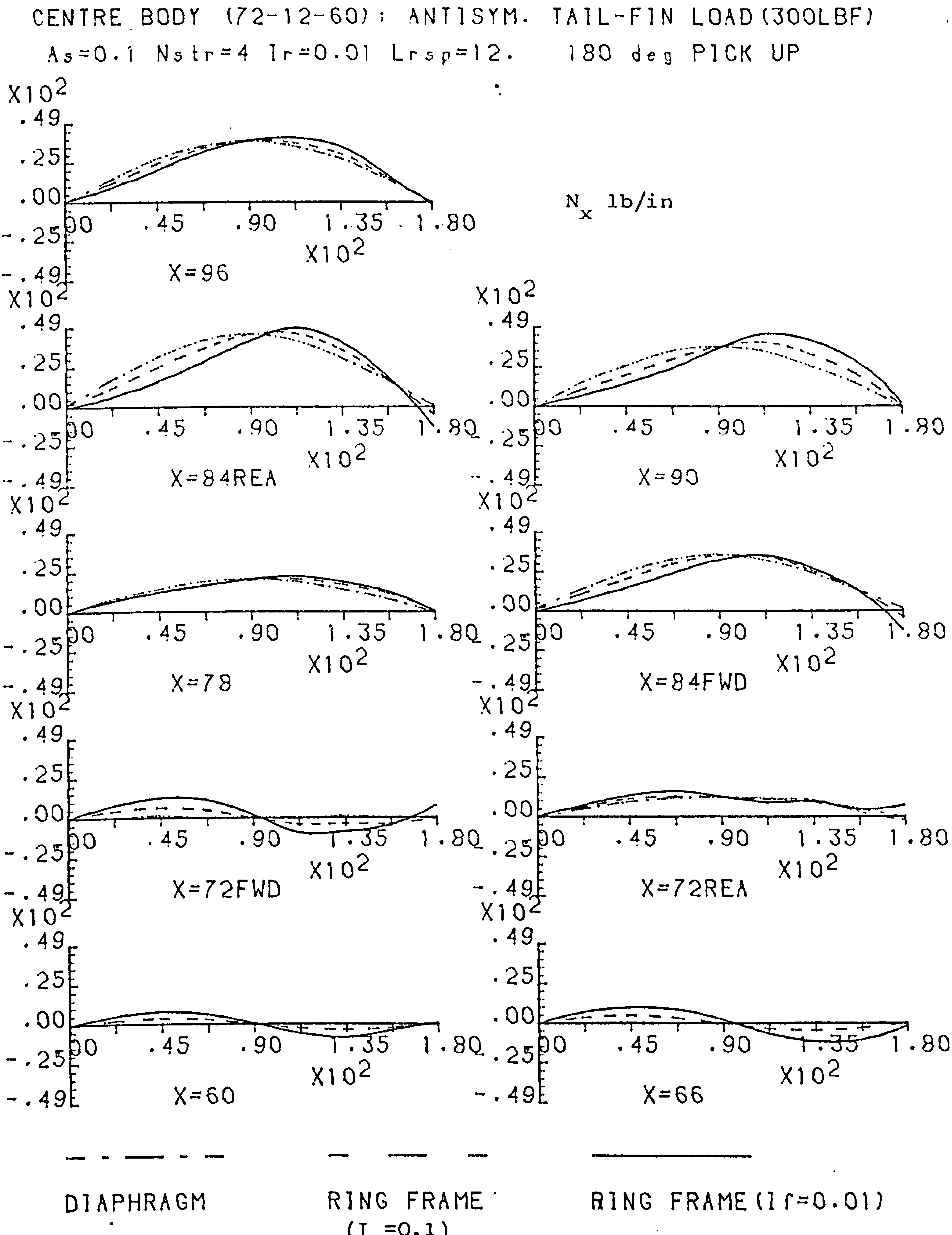

Fig.4.4.6 EFFECT OF FRAME PROPERTY CHANGE - DIRECT STRESS

* refer paragraph (ii) of section 3.9.

CENTRE BODY (72-12-60): ANTISYM. TAIL-FIN LOAD(300LBF)
As=0.1 Nstr=4 Ir=0.01 Lrsp=12. 180 deg PICK UP

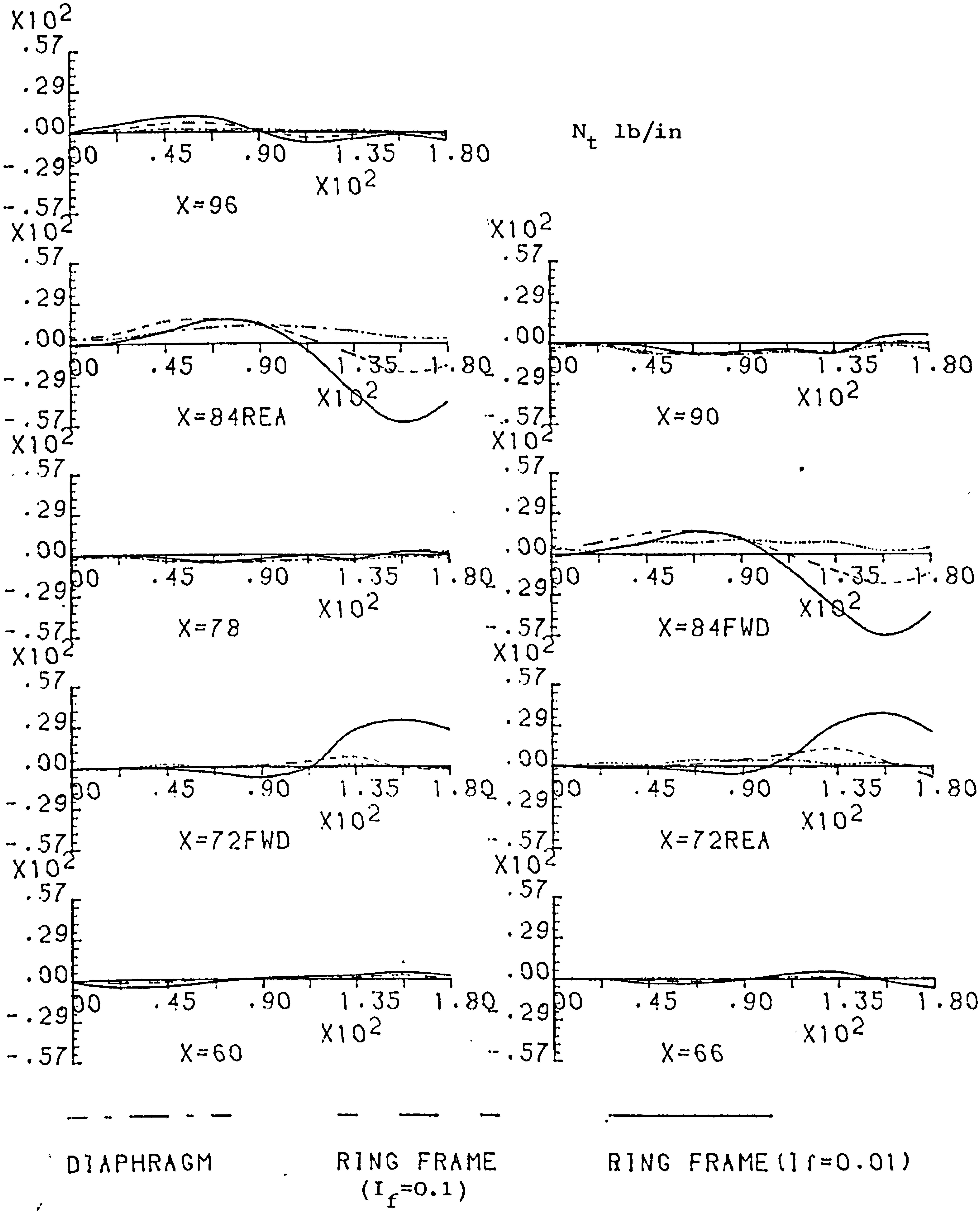

Fig.4.4.7 EFFECT OF FRAME PROPERTY CHANGE - <u>HOOP STRESS</u>

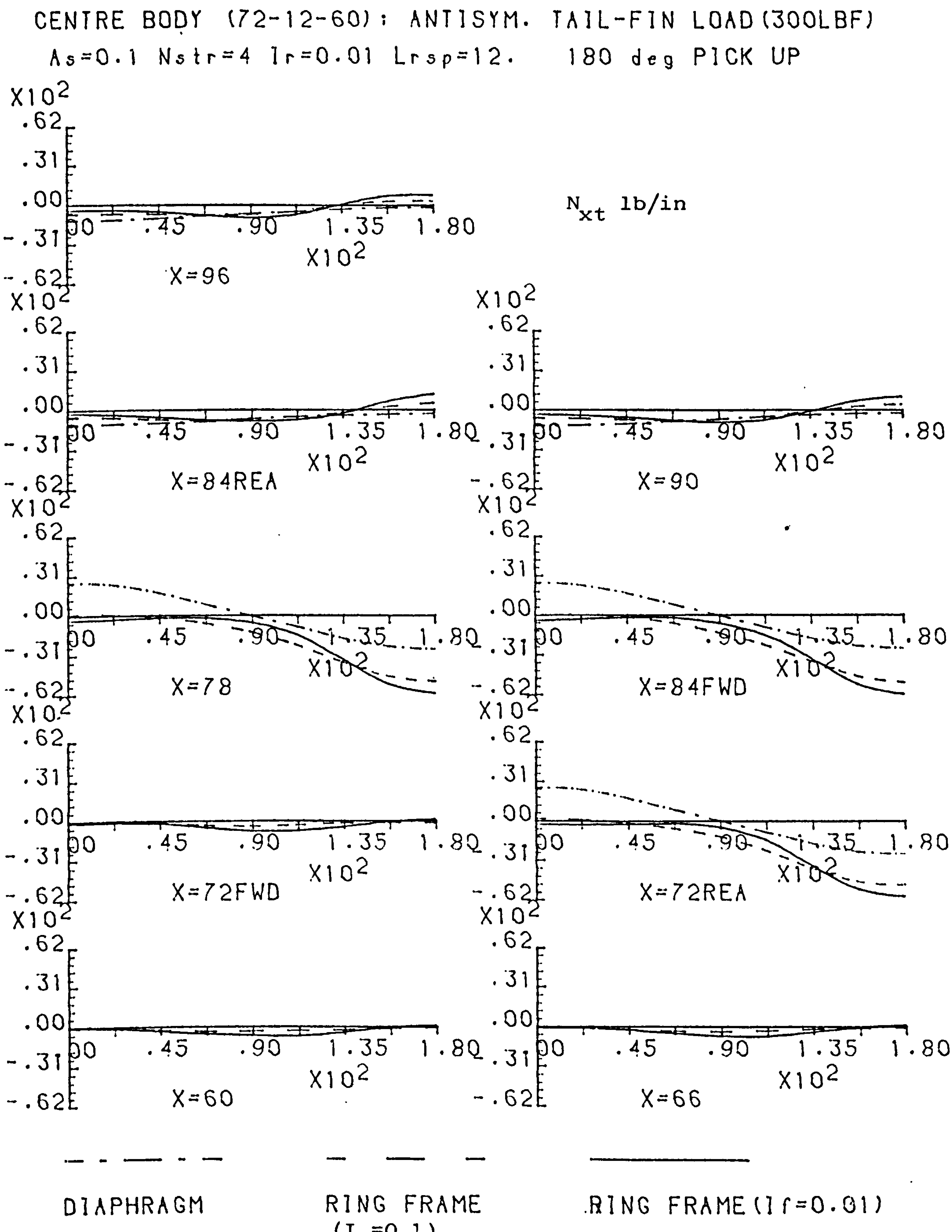

Fig. 4.4.8 EFFECT OF FRAME PROPERTY CHANGE - SHEAR FLOW

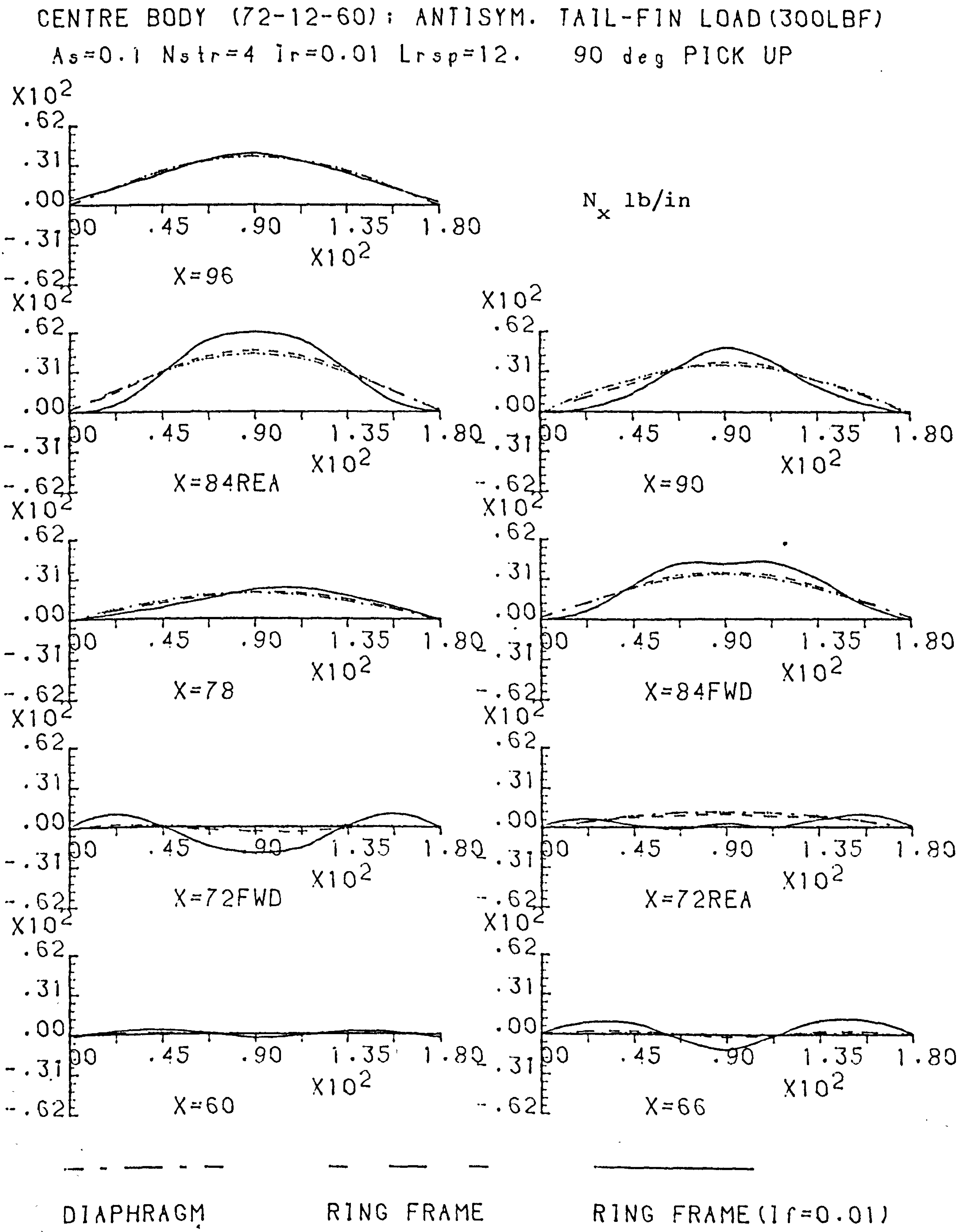

Fig.4.4.9 EFFECT OF FRAME PROPERTY CHANGE - <u>DIRECT STRESS</u>

CENTRE BODY (72-12-60): ANTISYM. TAIL-FIN LOAD(300LBF)

As=0.1 Nstr=4 Ir=0.01 Lrsp=12. 90 deg PICK UP

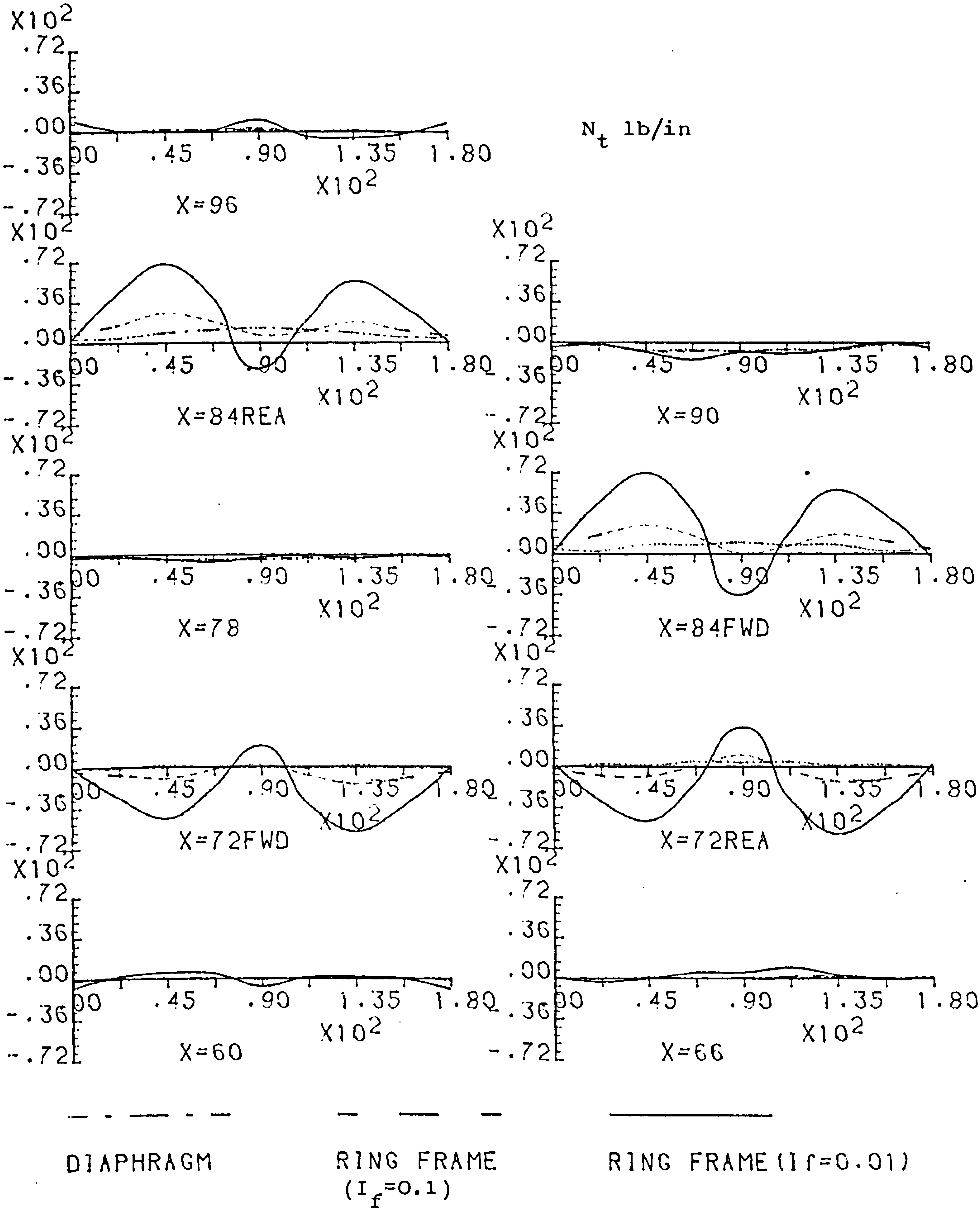

Fig.4.4.10 EFFECT OF FRAME PROPERTY CHANGE - HOOP STRESS

CENTRE BODY (72-12-60): ANTISYM. TAIL-FIN LOAD (300LBF)

As=0.1 Nstr=4 Ir=0.01 Lrsp=12. 90 deg PICK UP

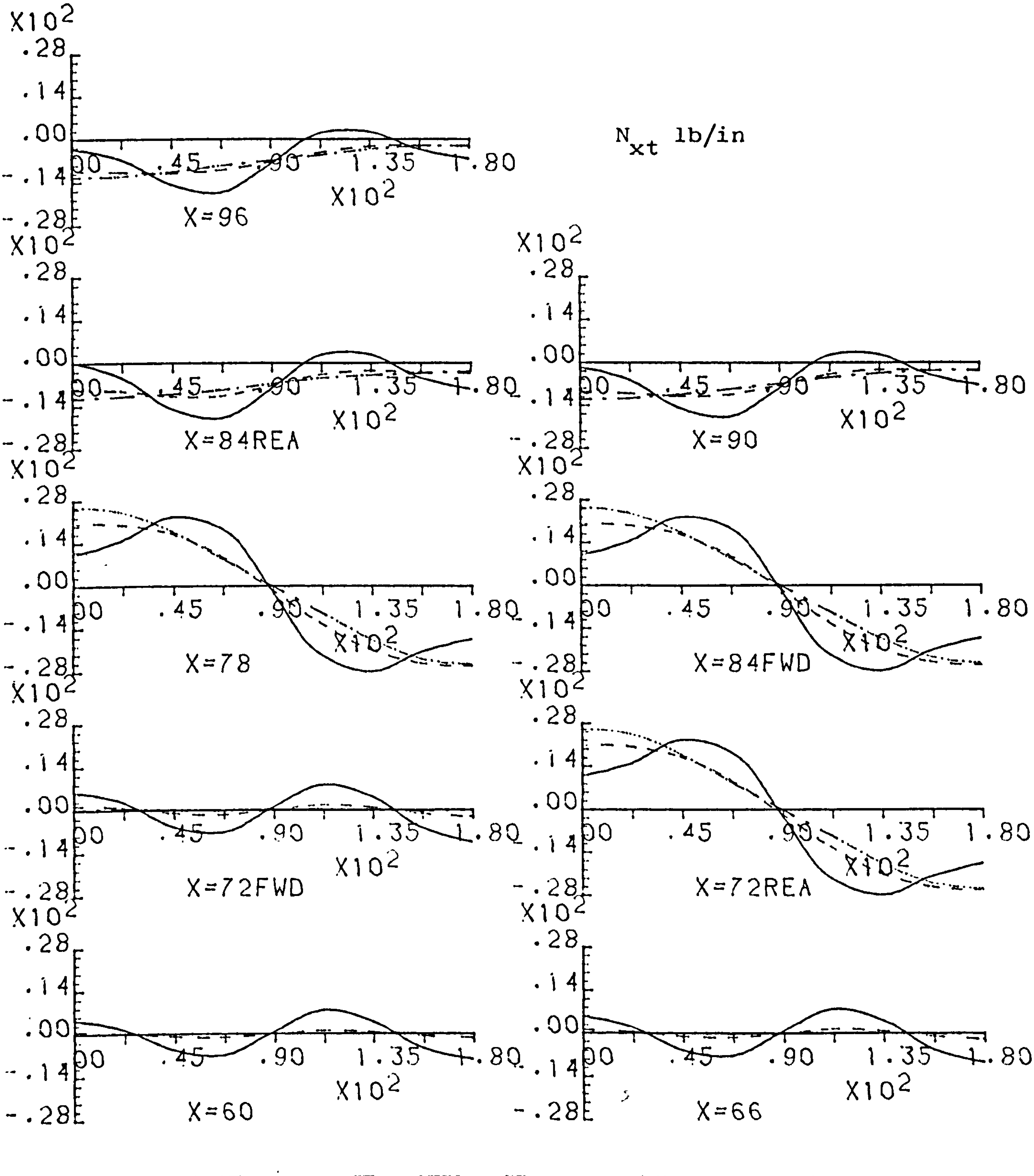

DIAPHRAGM

RING FRAME (I_f=0.1)

RING FRAME (If=0.01)

Fig.4.4.11 EFFECT OF FRAME PROPERTY CHANGE - SHEAR FLOW

Fig.4.4.12 SHEAR FLOW FROM SHELL TO FRAMES - FRAME STIFFNESS VARIATION EFFECT

MID WING PICK UP: ANTISYMM. LOAD(Ptail=200.Pfin=100)

Fig.4.4.13 SHEAR FLOW FROM SHELL TO FRAME - FRAME If CHANGE

FORWARD FRAME , TAIL LOAD, 180deg (72-12-60)
R=6. T=0.06 Nstr=4 Lrsp=12.

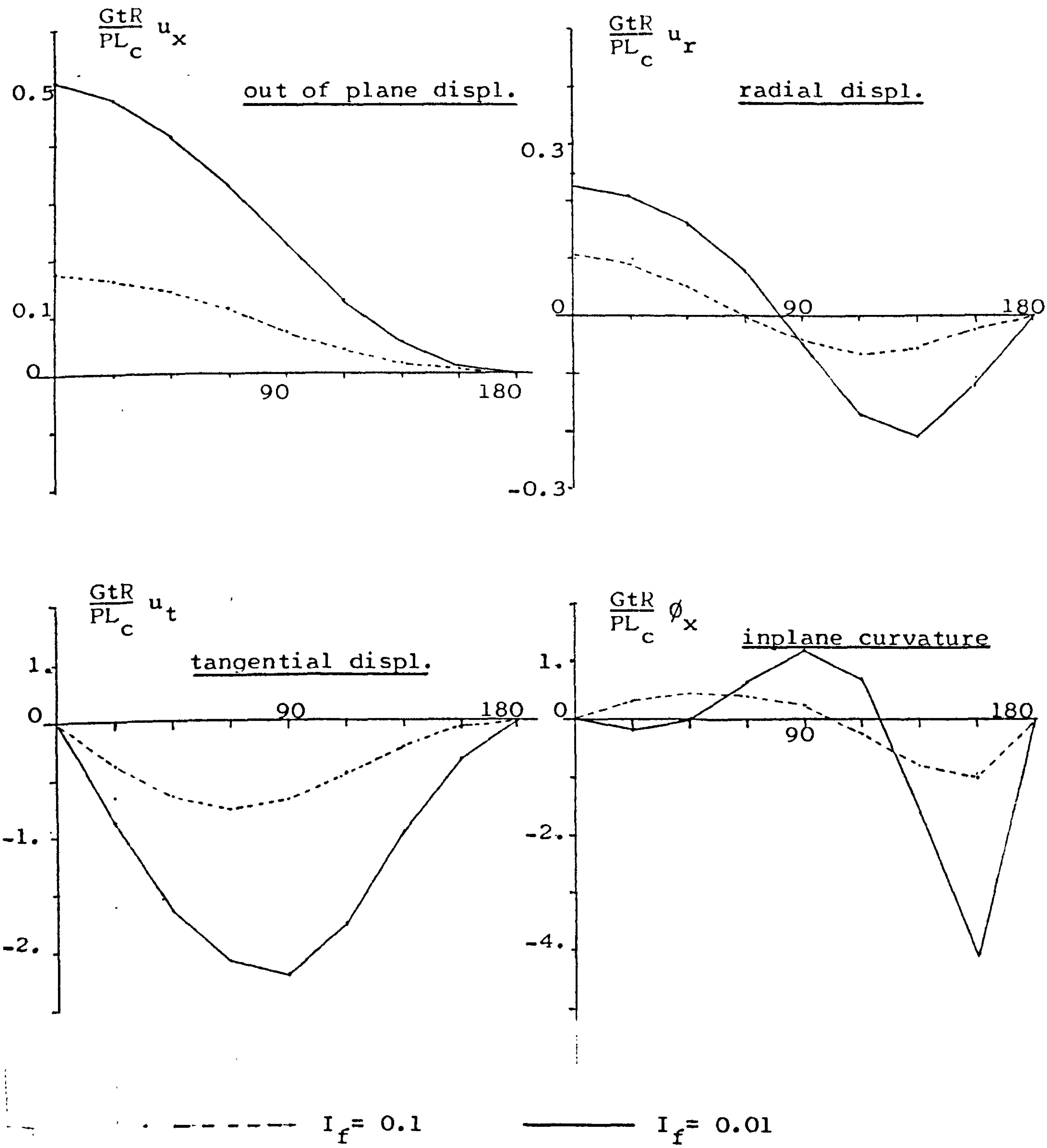

Fig.4.4.14 FRAME DISPLACEMENTS - EFFECT OF STIFF. VARIATION

FORWARD FRAME ; TAIL LOAD,180deg (72-12-60)

R=6. T=0.06 Nstr=4 Lrsp=12.

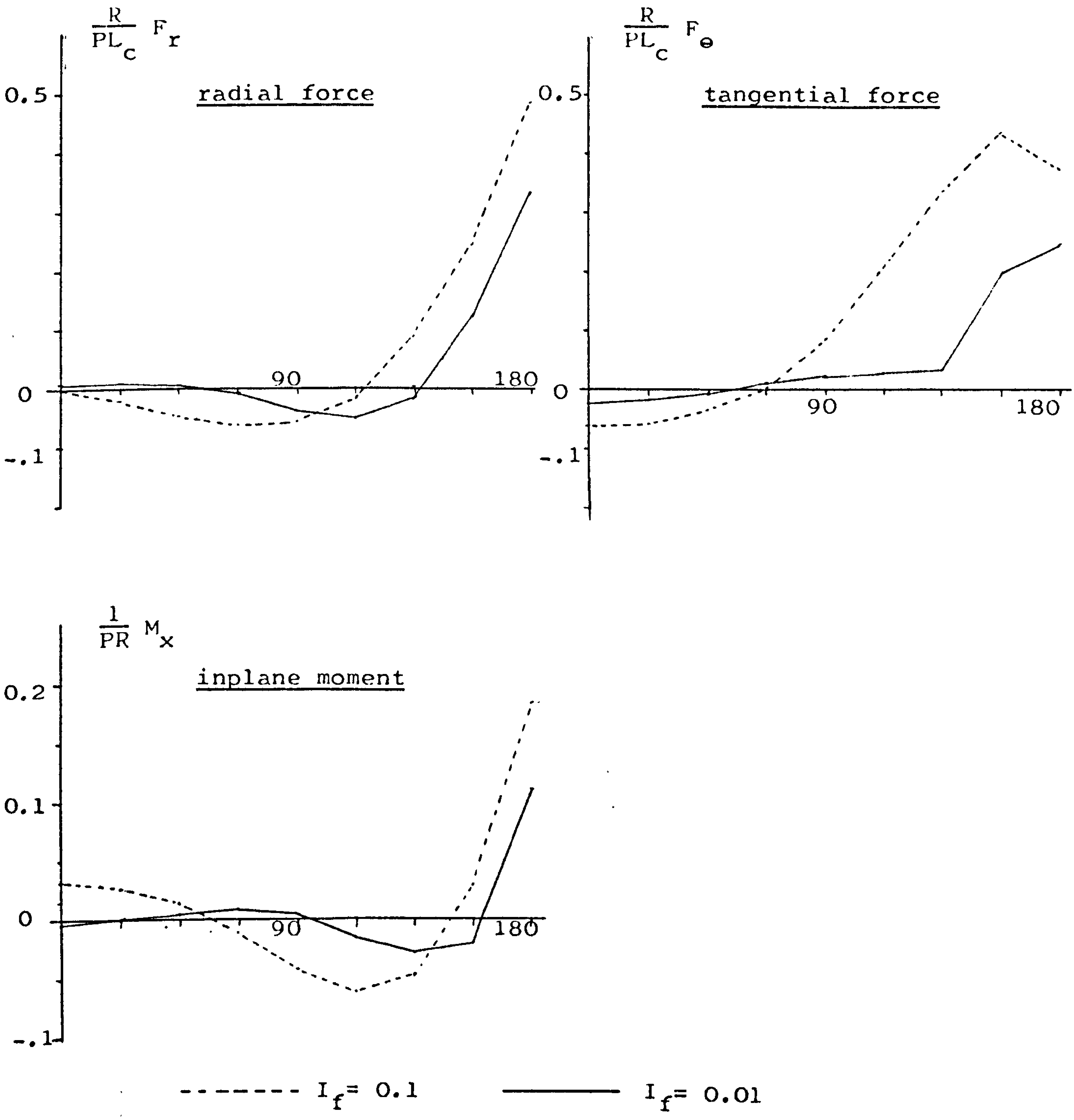

Fig.4.4.15 FRAME INTERNAL FORCES - EFFECT OF STIFF. VARIATION

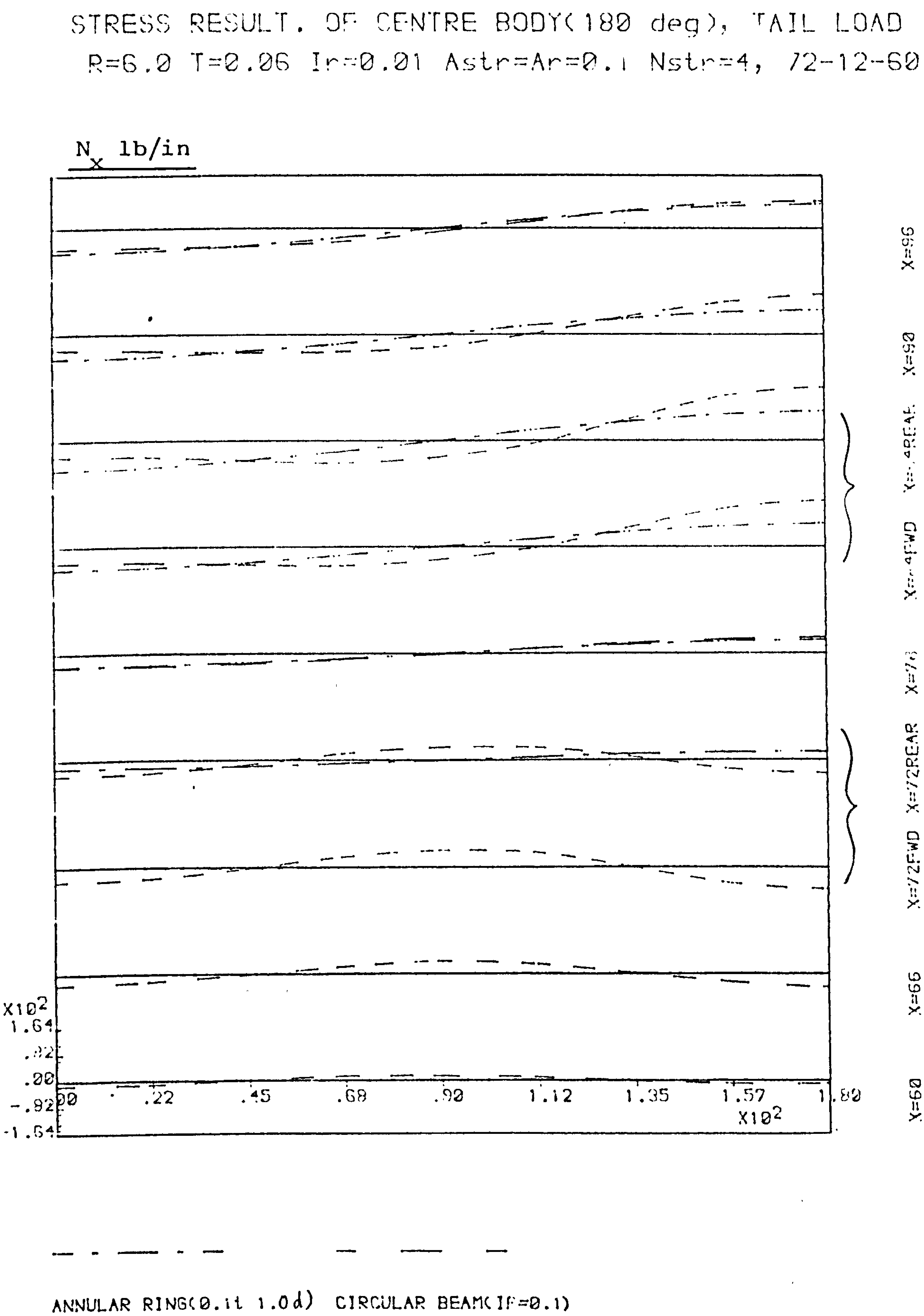

Fig. 4.4.16 EFFECTS OF FRAME DEPTH VARIATION - DIRECT

* refer paragraph (iii) of section 3.9.

STRESS RESULT. OF CENTRE BODY(180 deg); TAIL LOAD
R=6.0 T=0.06 Ir=0.01 Astr=Ar=0.1 Nstr=4, 72-12-60

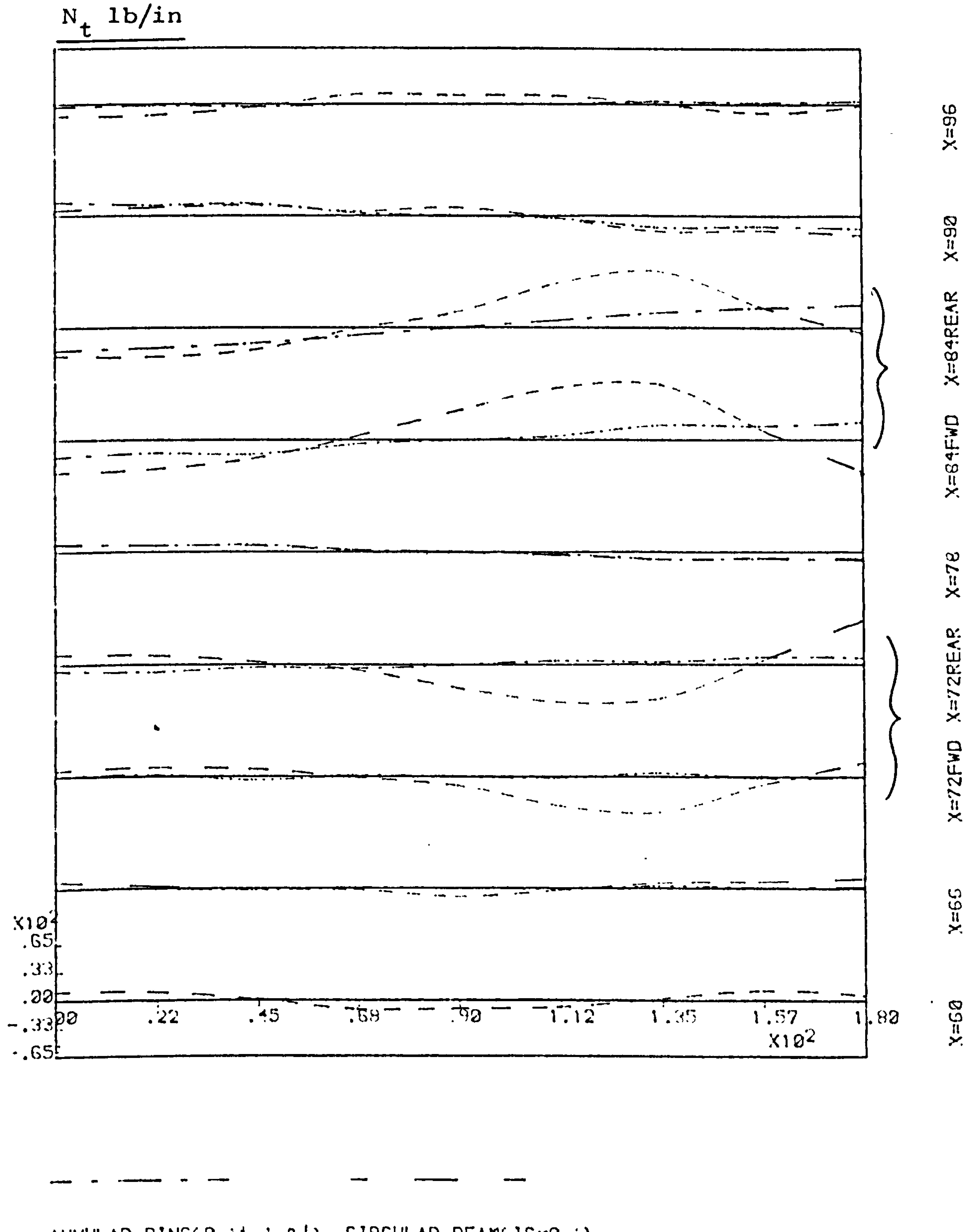

Fig.4.4.17 EFFECTS OF FRAME DEPTH VARIATION - HOOP

STRESS RESULT. OF CENTRE BODY(180 deg); TAIL LOAD
R=6.0 T=0.06 Ir=0.01 Astr=Ar=0.1 Nstr=4, 72-12-60

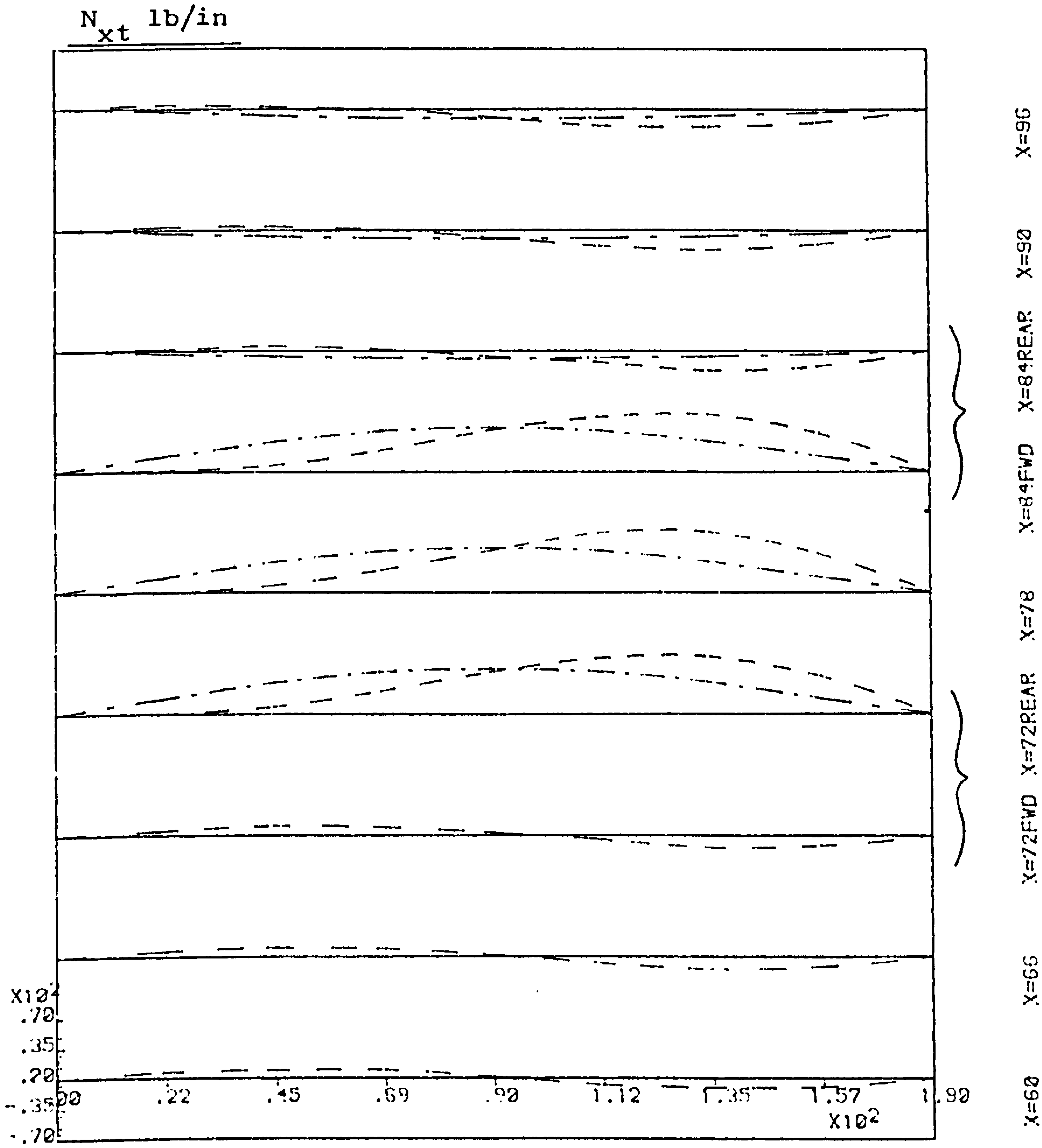

ANNULAR RING(0.1t 1.0d) CIRCULAR BEAM(IF=0.1

FFig.4.4.18 EFFECTS OF FRAME DEPTH VARIATION – SHEAR

BENDING STRESS RESULT. OF CENTRE BODY(180 deg); TAIL
R=6.0 T=0.06 Ir=0.01 Astr=Ar=0.1 Nstr=4, 72-12-60

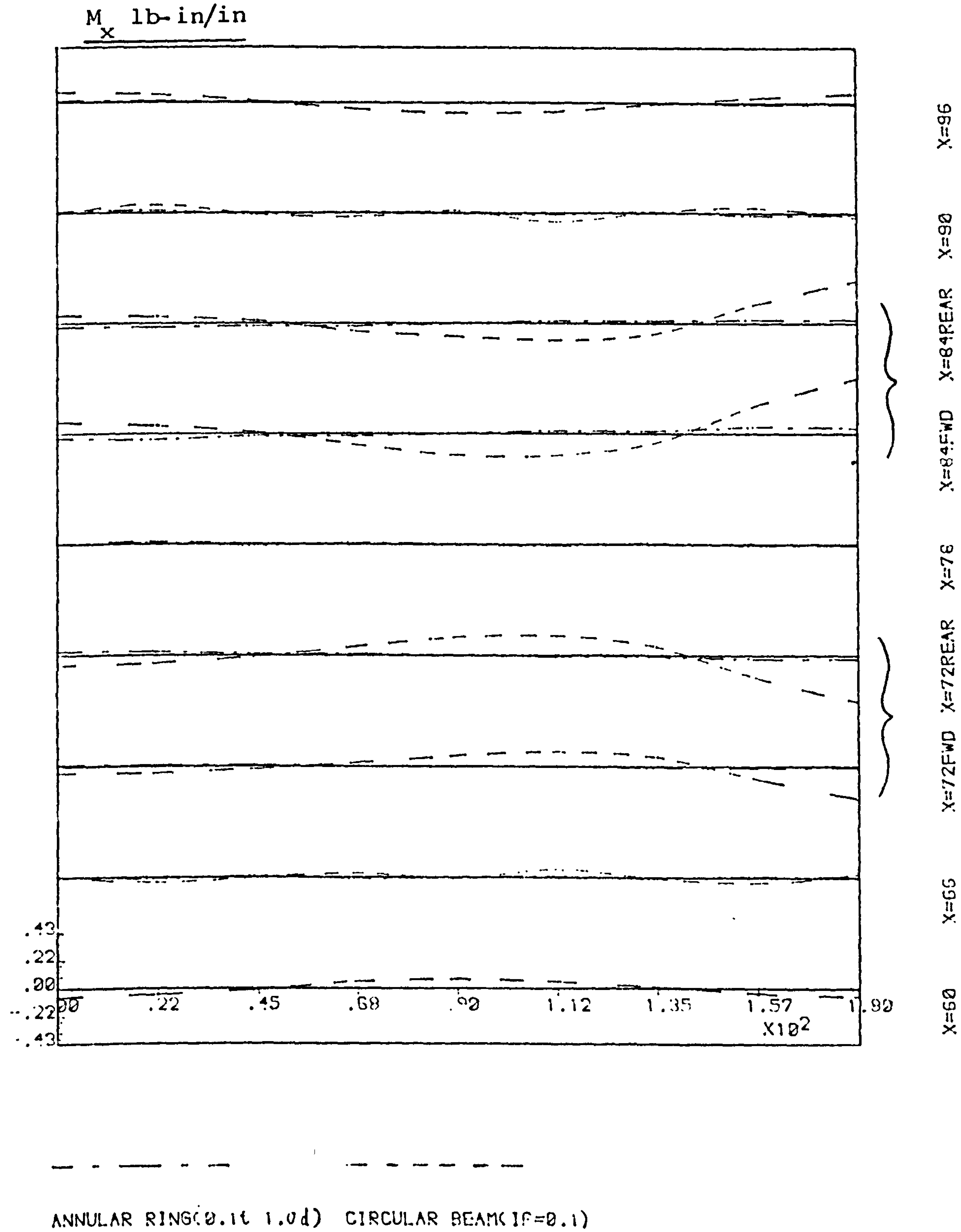

Fig.4.4.19 EFFECTS OF FRAME DEPTH VARIATION - AXIAL BENDING

BENDING STRESS RESULT. OF CENTRE BODY(180 deg); TAIL
R=6.0 T=0.06 Ir=0.01 Astr=Ar=0.1 Nstr=4, 72-12-60

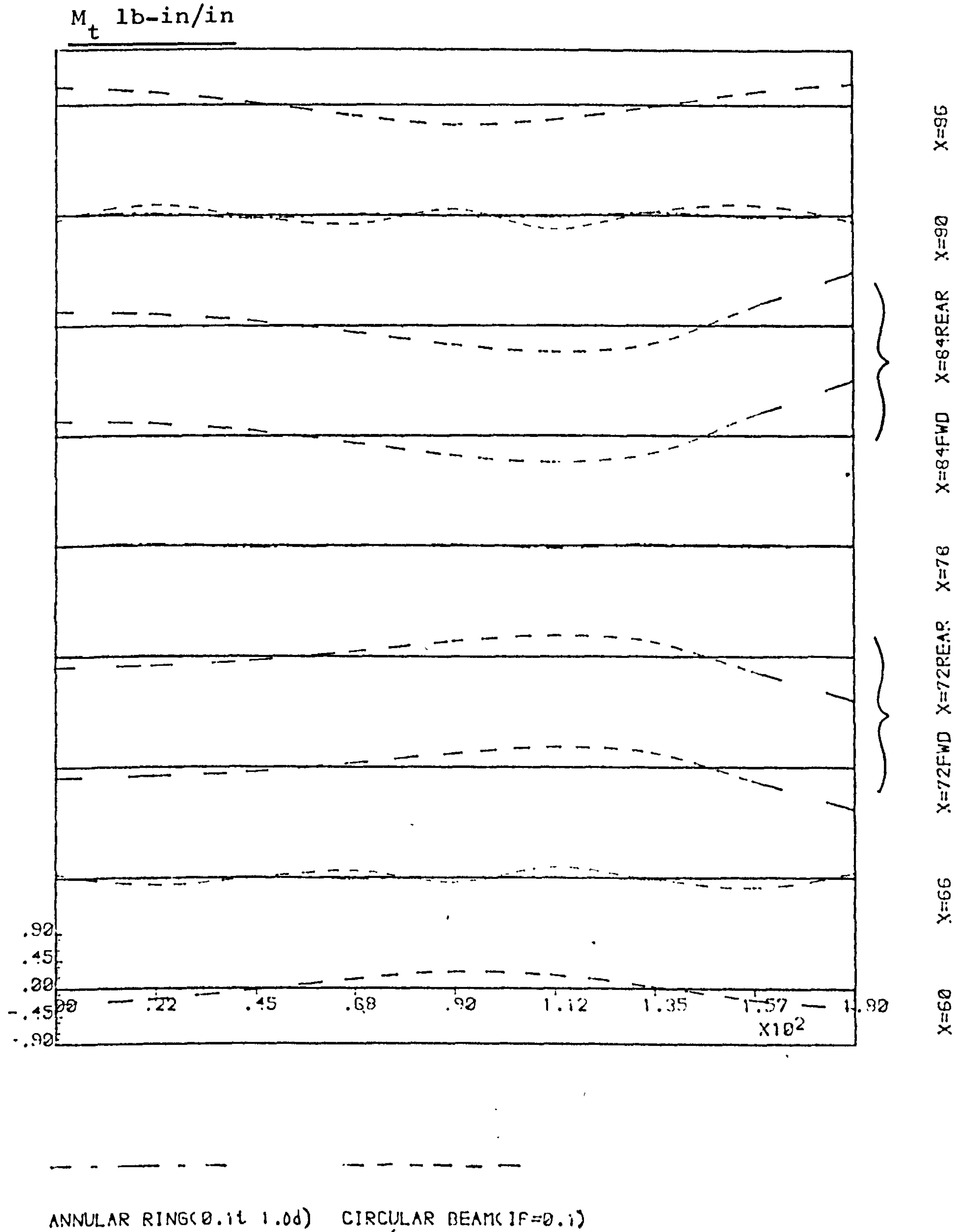

Fig.4.4.20 EFFECTS OF FRAME DEPTH VARIATION - CIRC. BENDING

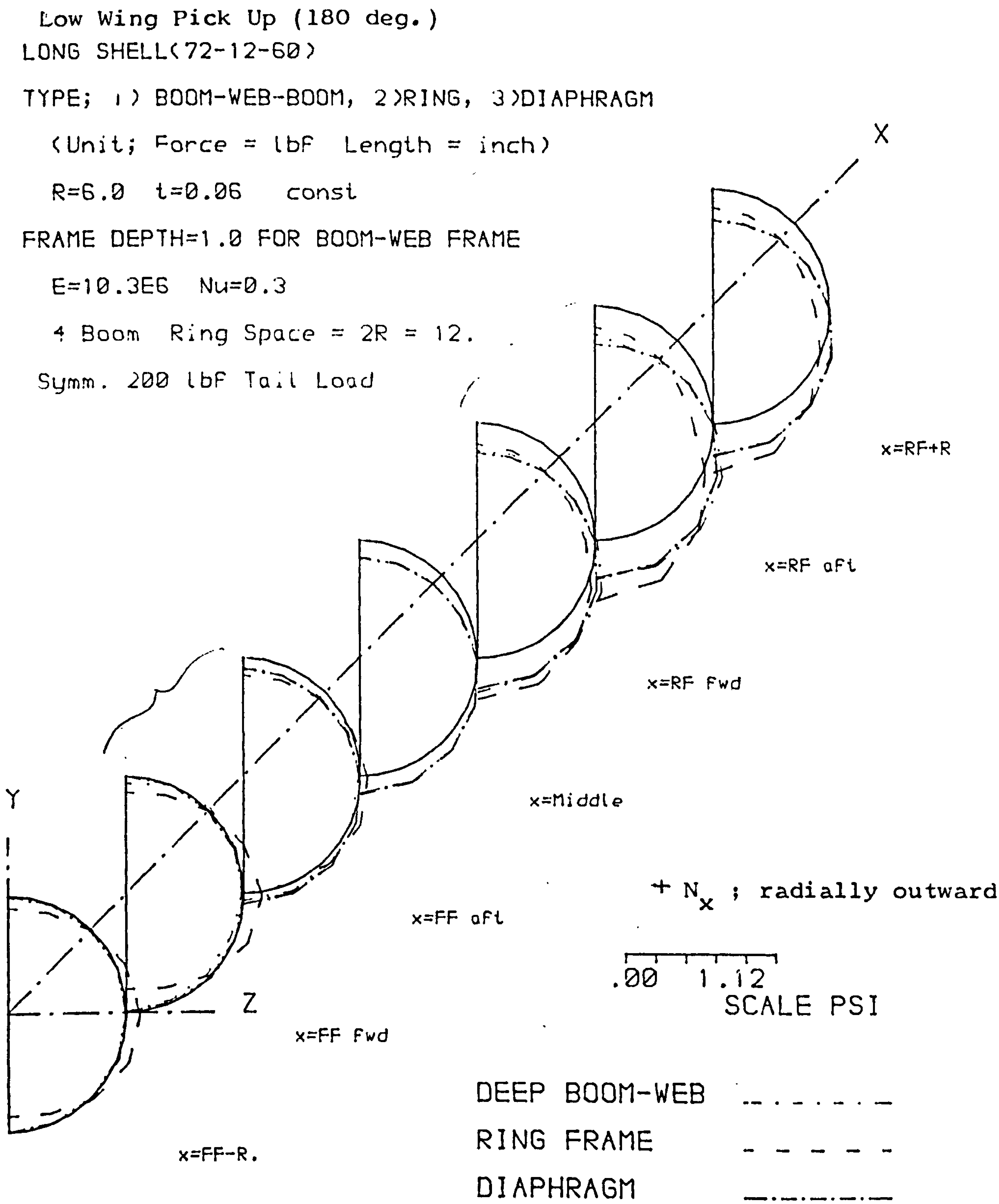

Fig.4.4.21 EFFECT OF PICK-UP FRAME CHANGE ON DIRECT STRESS DISTR.

* refer paragraph (iv) of section 3.9.

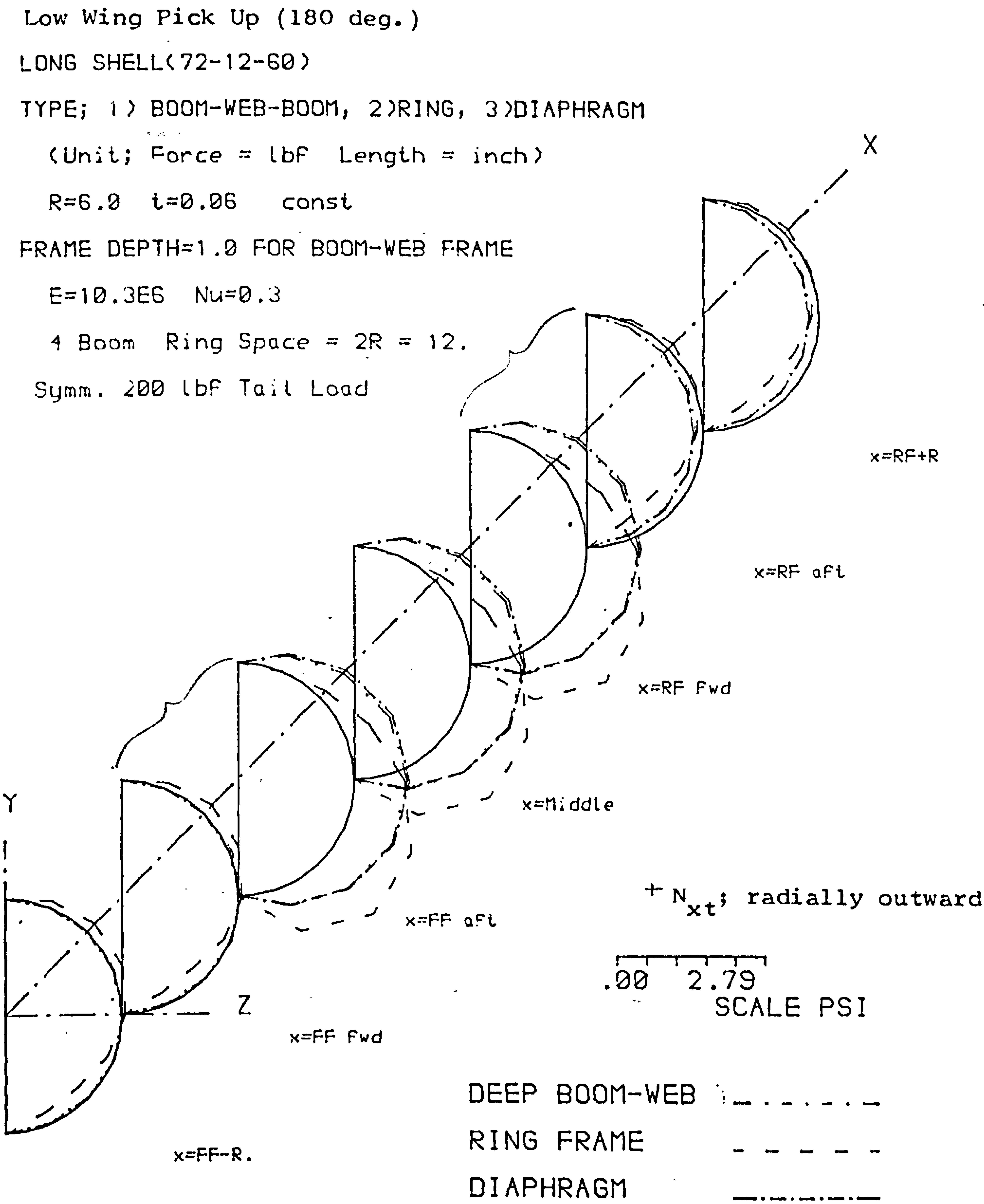

Fig.4.4.22 EFFECT OF PICK-UP FRAME CHANGE ON <u>SHEAR STRESS</u> DISTRI.

CENTRE BODY STRESS RESULT.(180 deg P/U) : TAIL LOAD
R=6.0 T=0.06 Lrs=12. Astr=0.1 Nstr=4, 72-12-60

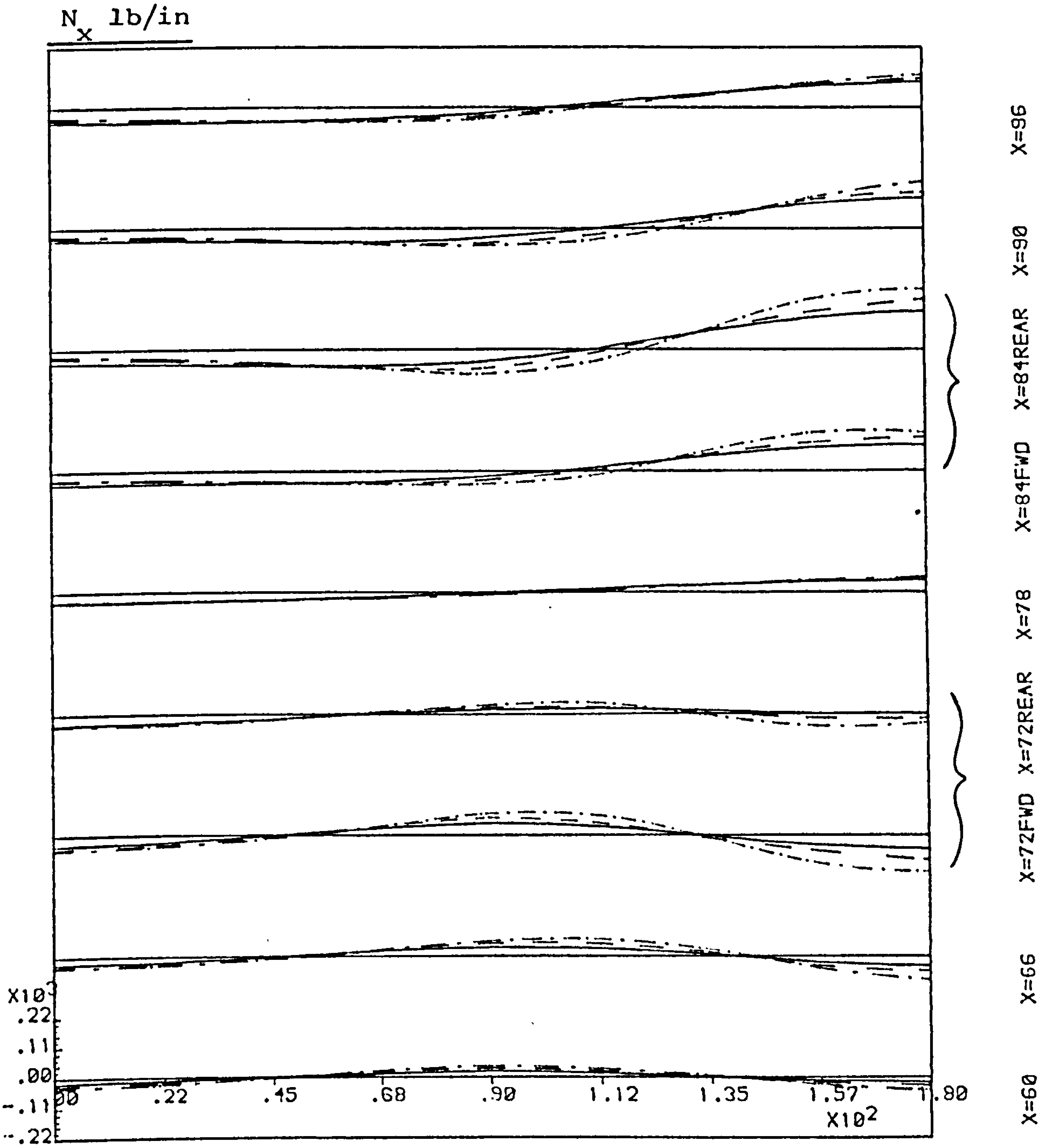

IF=0.01 constant IF=0.1 (157.5-202.5) IF=0.1 (135.0-225.0)

Fig. 4.5.1 EFFECTS OF FRAME LOCAL REINFORCEMENT- DIRECT STR.

CENTRE BODY STRESS RESULT.(180 deg P/U) : TAIL LOAD
R=6.0 T=0.06 Lrs=12. Astr=0.1 Nstr=4, 72-12-60

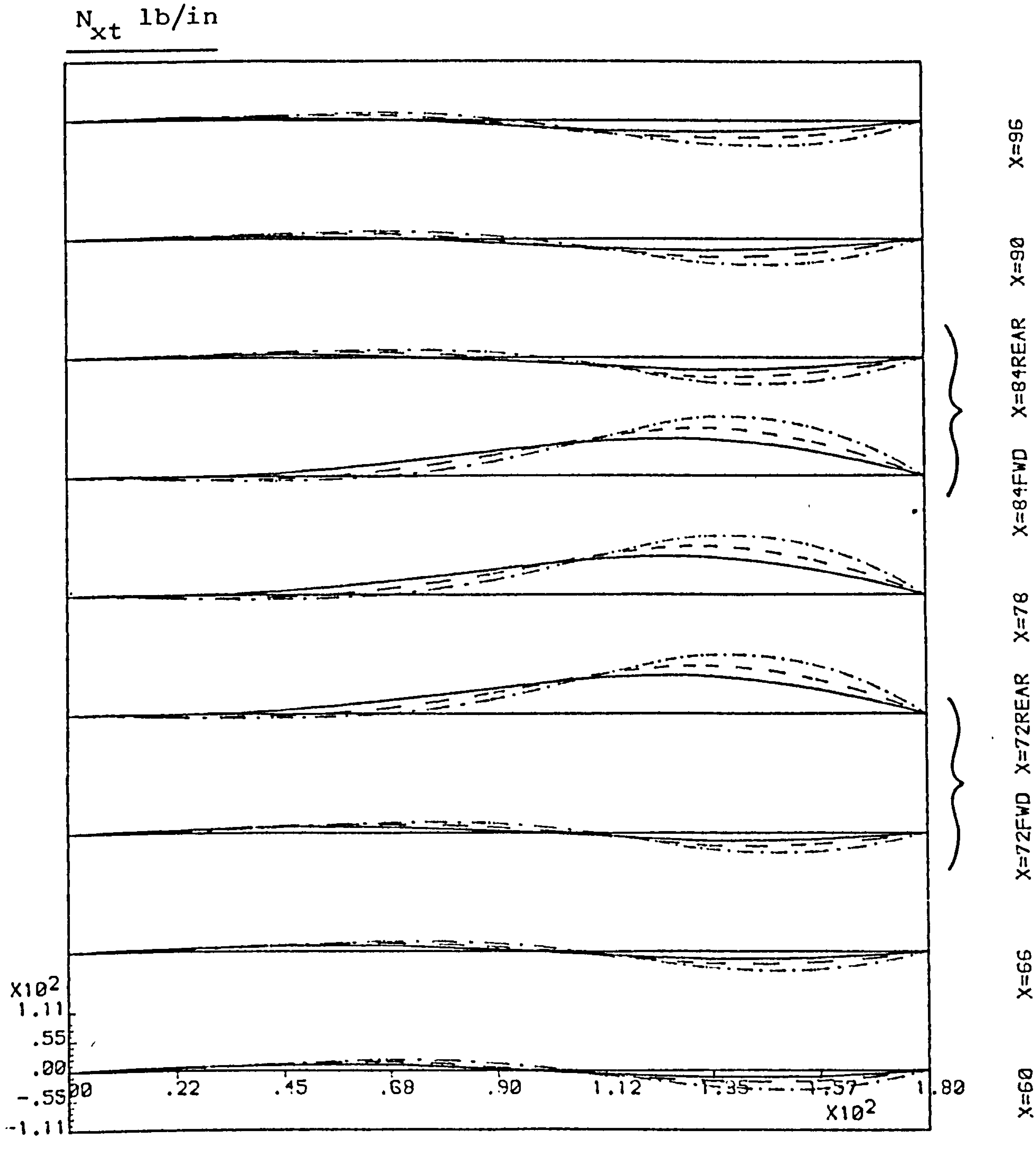

IF=0.01 constant IF=0.1 (157.5-202.5) IF=0.1 (135.0-225.0)

Fig. 4.5.2 EFFECTS OF FRAME LOCAL REINFORCEMENT - SHEAR

Fig.4.5.3 SHEAR FLOW FROM SHELL TO FRAMES- LOCAL REINFORCEMENT EFFECT

FORWARD FRAME ; TAIL LOAD, 180deg (72-12-60)

R=6. T=0.06 Nstr=4 Lrsp=12. ReinForce. at 157.5-202.5

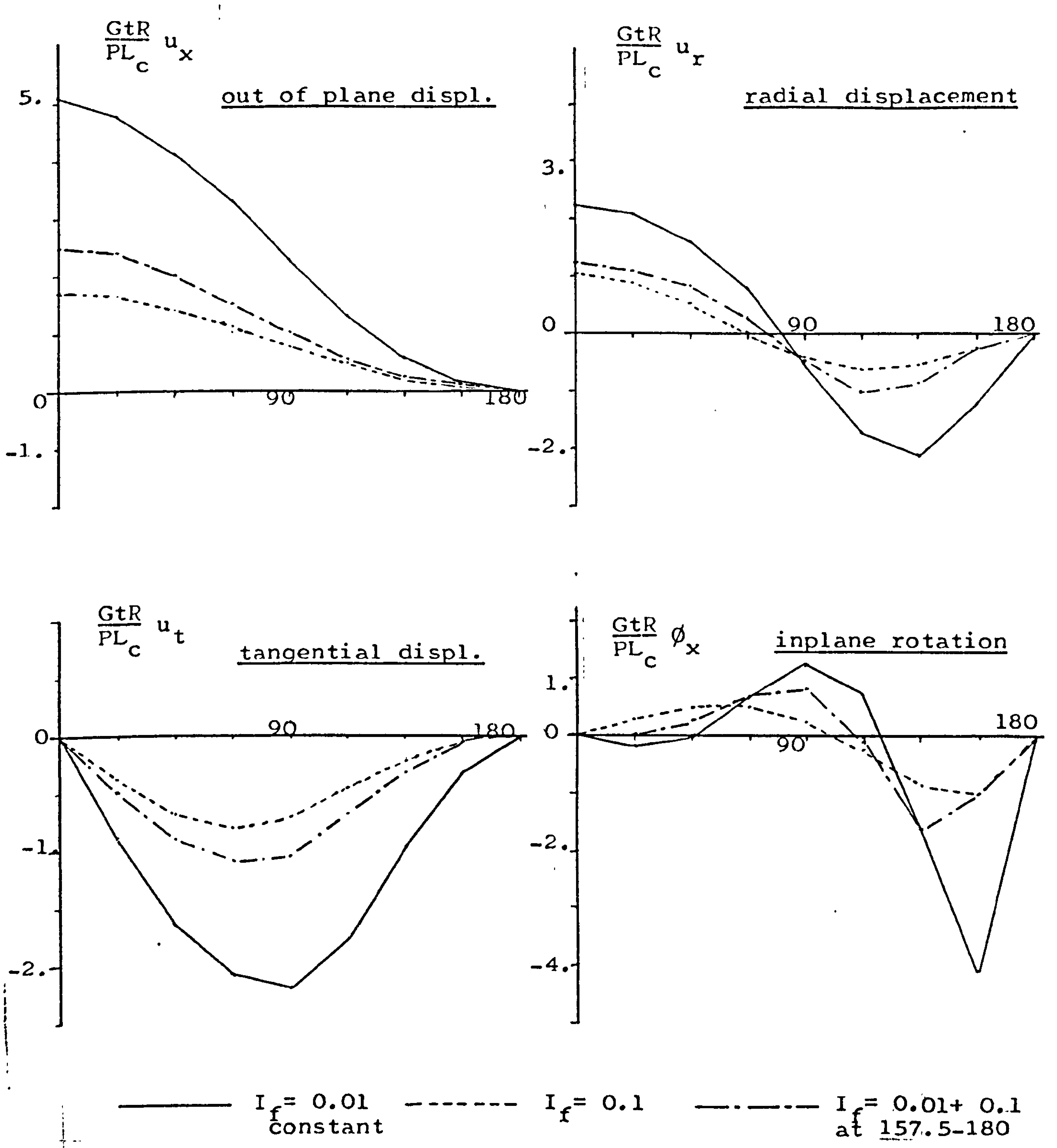

Fig.4.5.4 FRAME DISPLACEMENTS - EFFECT OF LOCAL REINFORCE.

FORWARD FRAME ; TAIL LOAD, 180deg (72-12-60)

R=6. T=0.06 Nstr=4 Lrsp=12.

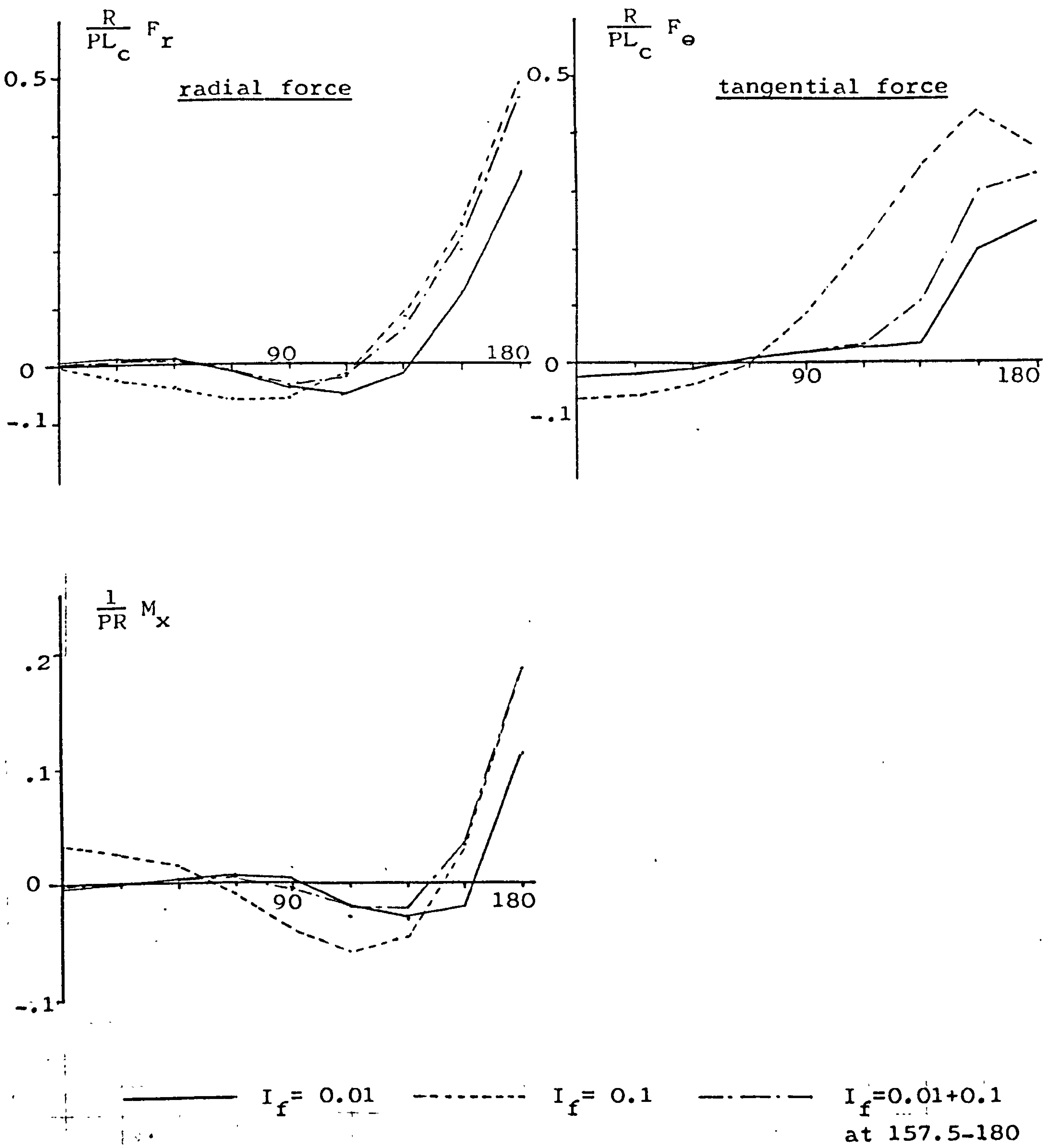

Fig.4.5.5 FRAME INTERNAL FORCES - EFFECT OF LOCAL REINFORCEME

CENTR BODY-DEEP FRAME (180 deg P/U): SYMM. TAIL LOAD

R=6.0 T=0.06 Ir=0.01 Astr=Ar=0.1 Nstr=4 R_i=5.0

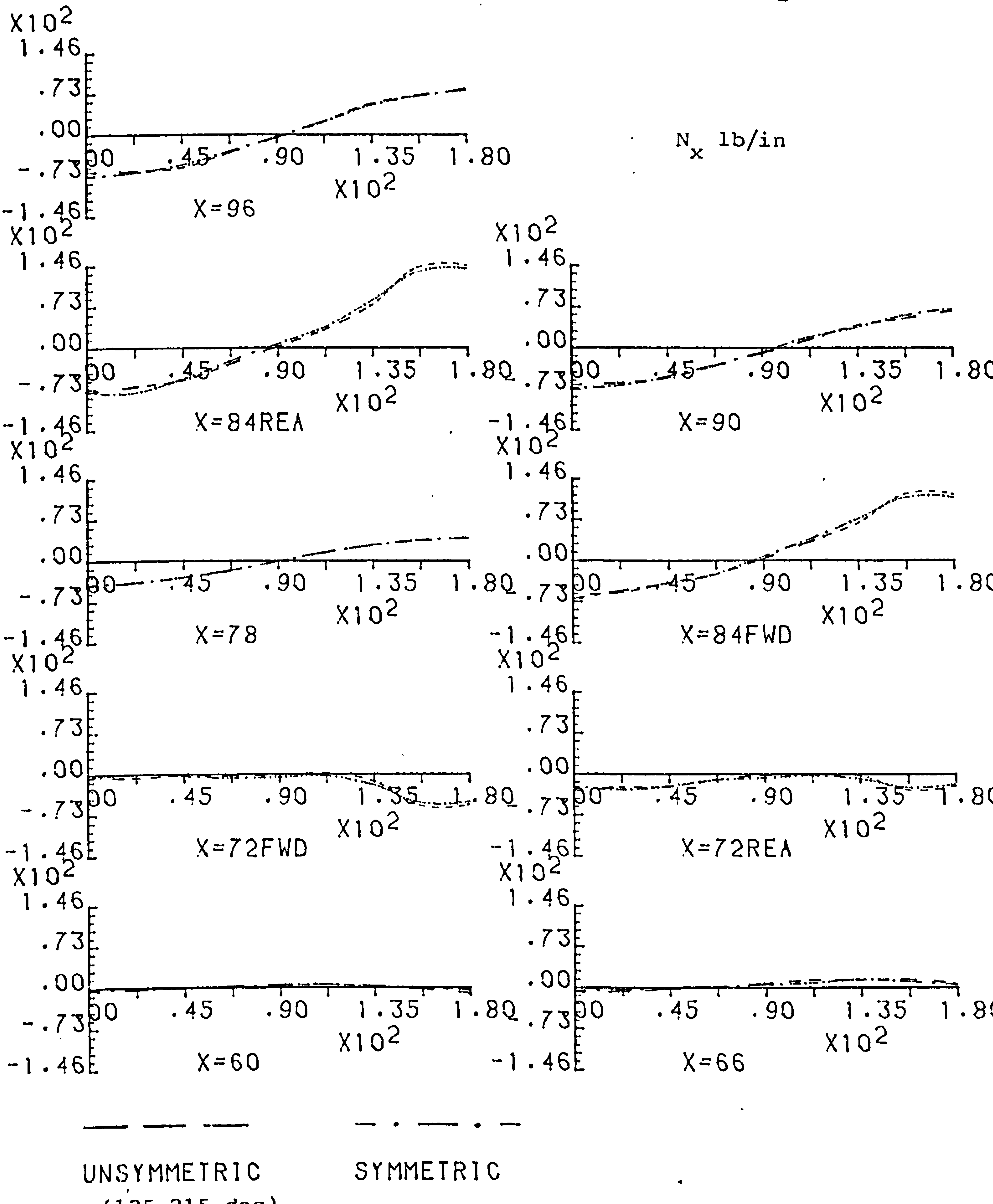

Fig.4.5.6 EFFECT OF FRAME SYMMETRY - DIRECT STRESS

CENTR BODY-DEEP FRAME (180 deg P/U); SYMM. TAIL LOAD

R=6.0 T=0.06 Ir=0.01 Astr=Ar=0.1 Nstr=4 R_i=5.

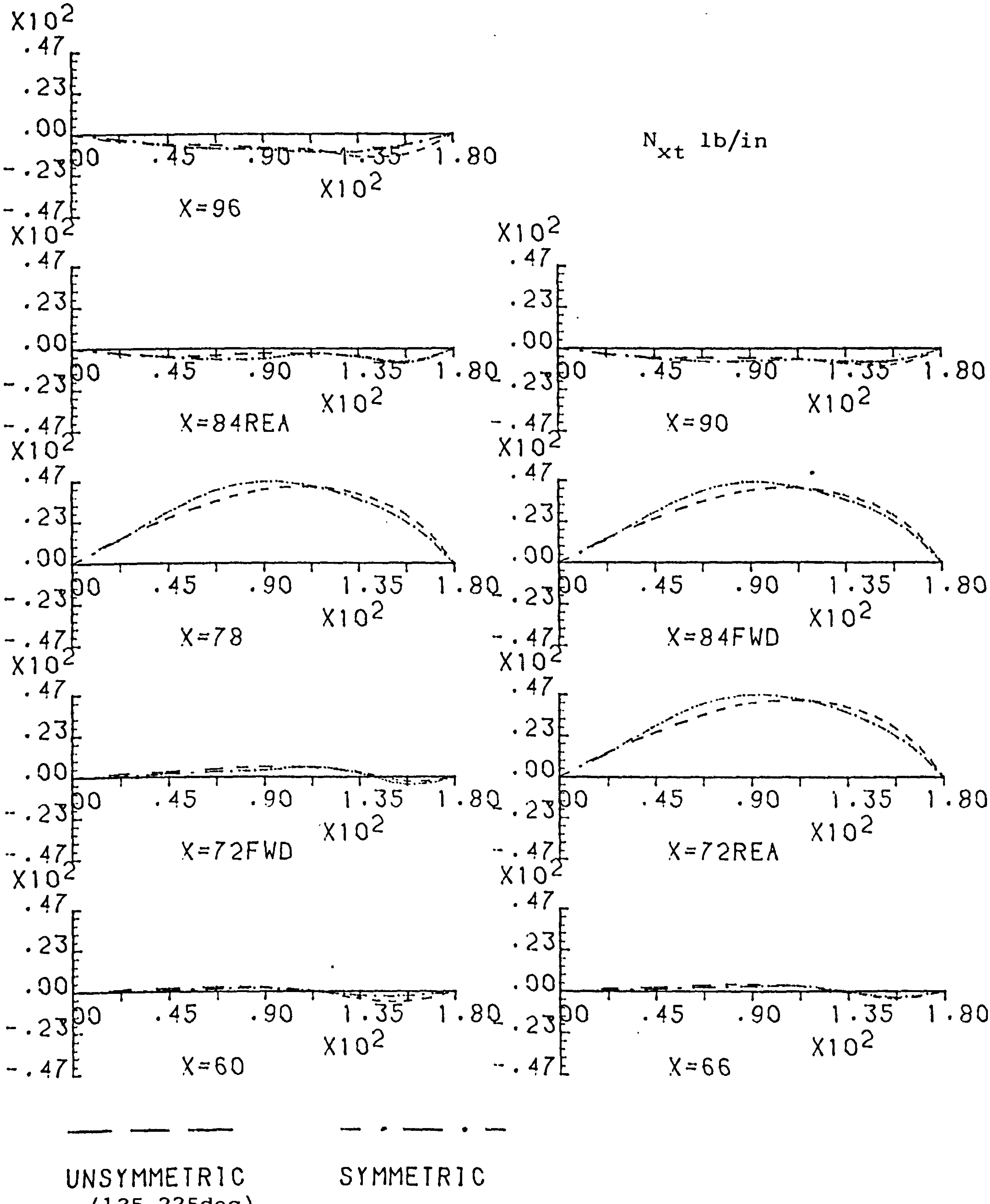

Fig.4.5.7 EFFECT OF FRAME SYMMETRY - SHEAR

CENTRE BODY (6R t=0.06 72-12-60.); SYM. 1 g INERTIA
If =0.1 Af=1.0 Ir=0.01 Lrsp=12. Nstr=4 As=0.1, LOW WING

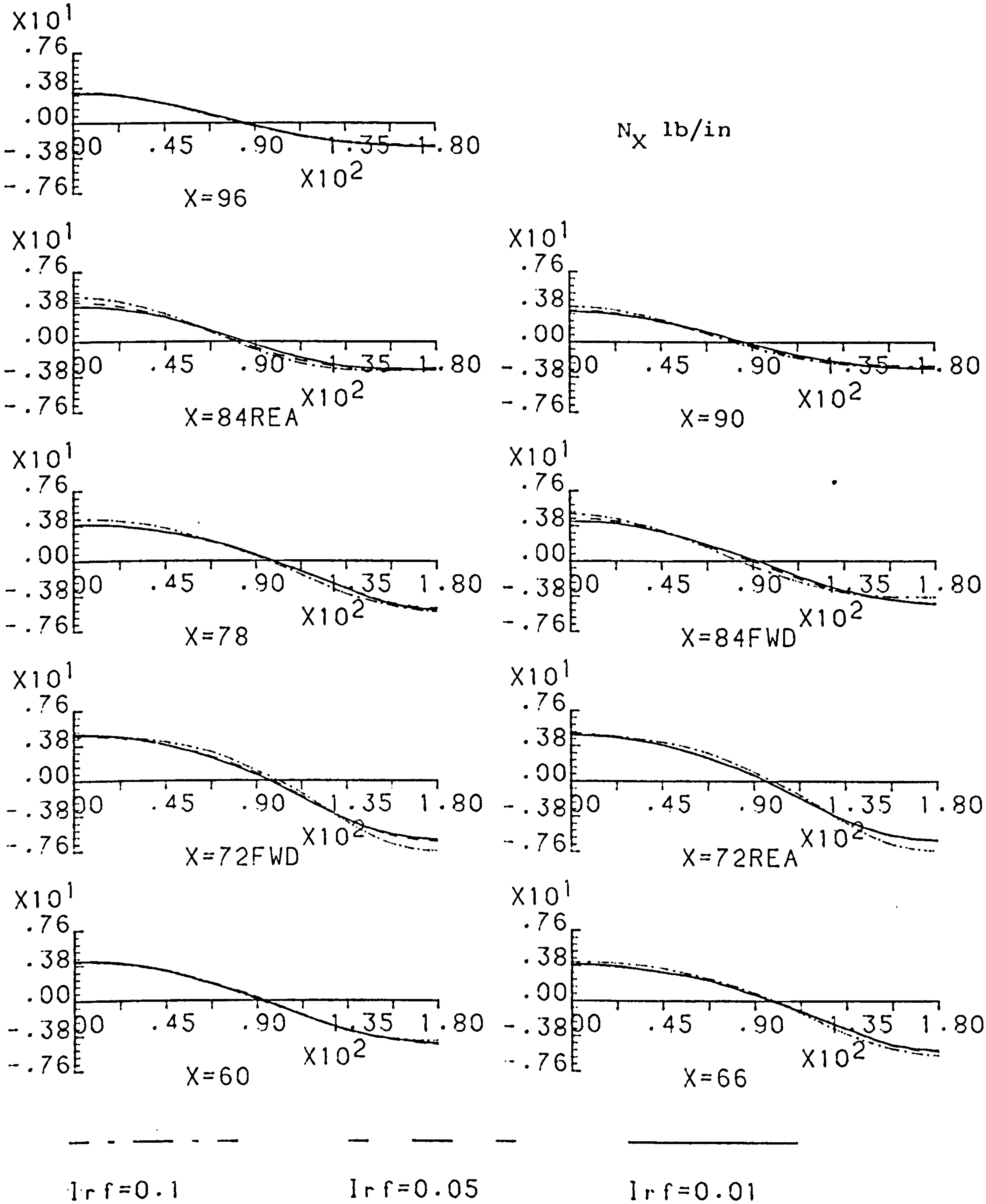

Fig. 4.6.1 EFFECT OF REAR FRAME STIFFNESS CHANGE - DIRECT

CENTRE BODY (6R t=0.06 72-12-60.): SYM. 1 g INERTIA

Iff=0.1 Af=1.0 Ir=0.01 Lrsp=12. Nstr=4 As=0.1, LOW WING

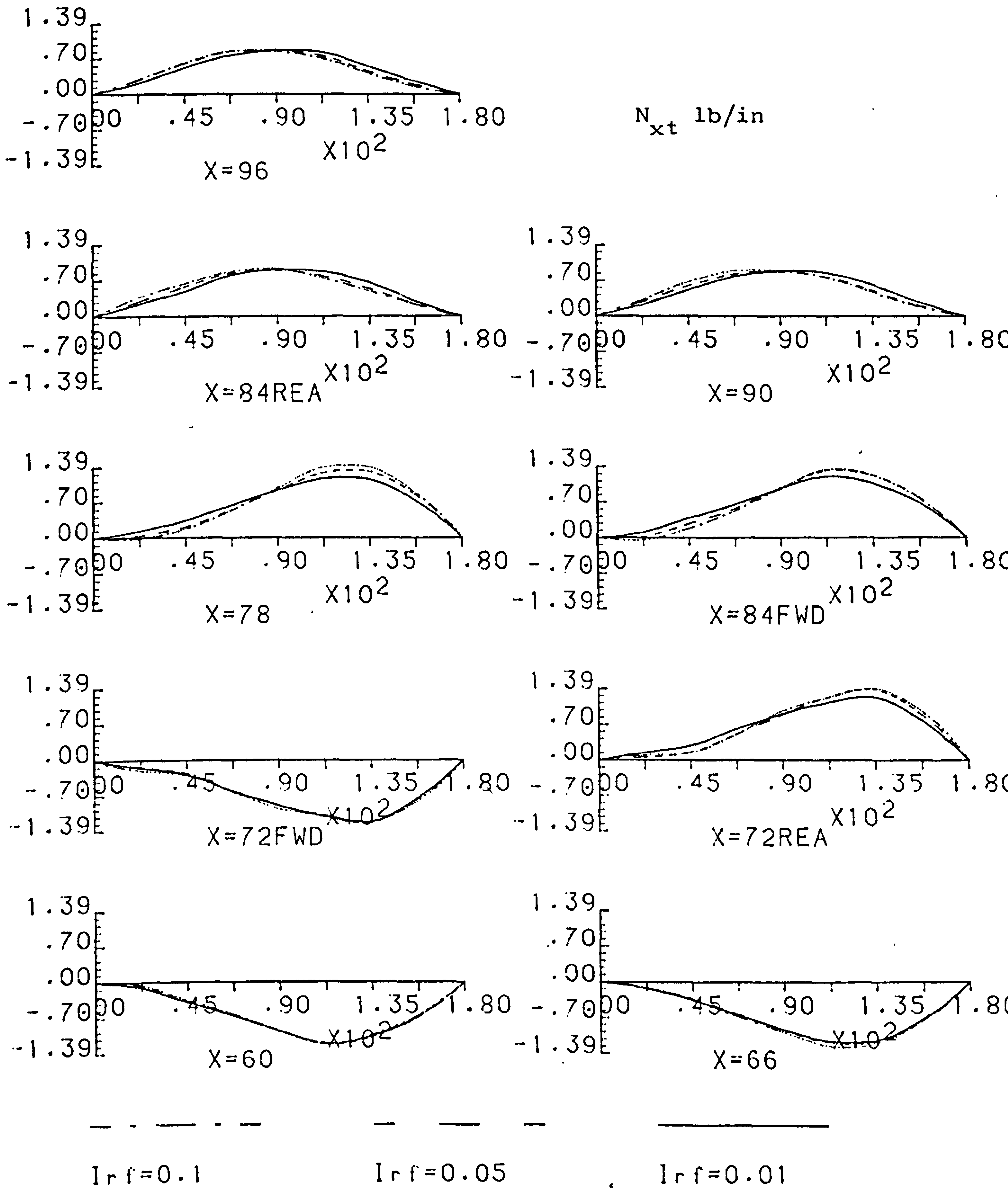

Fig.4.6.2 EFFECT OF REAR FRAME STIFFNESS CHANGE - SHEAR

CENTRE BODY STRESS RESULT.(180 deg P/U) : TAIL LOAD
R=6.0 T=0.06 Lrs=12. Astr=0.1 Nstr=4, 72-12-60

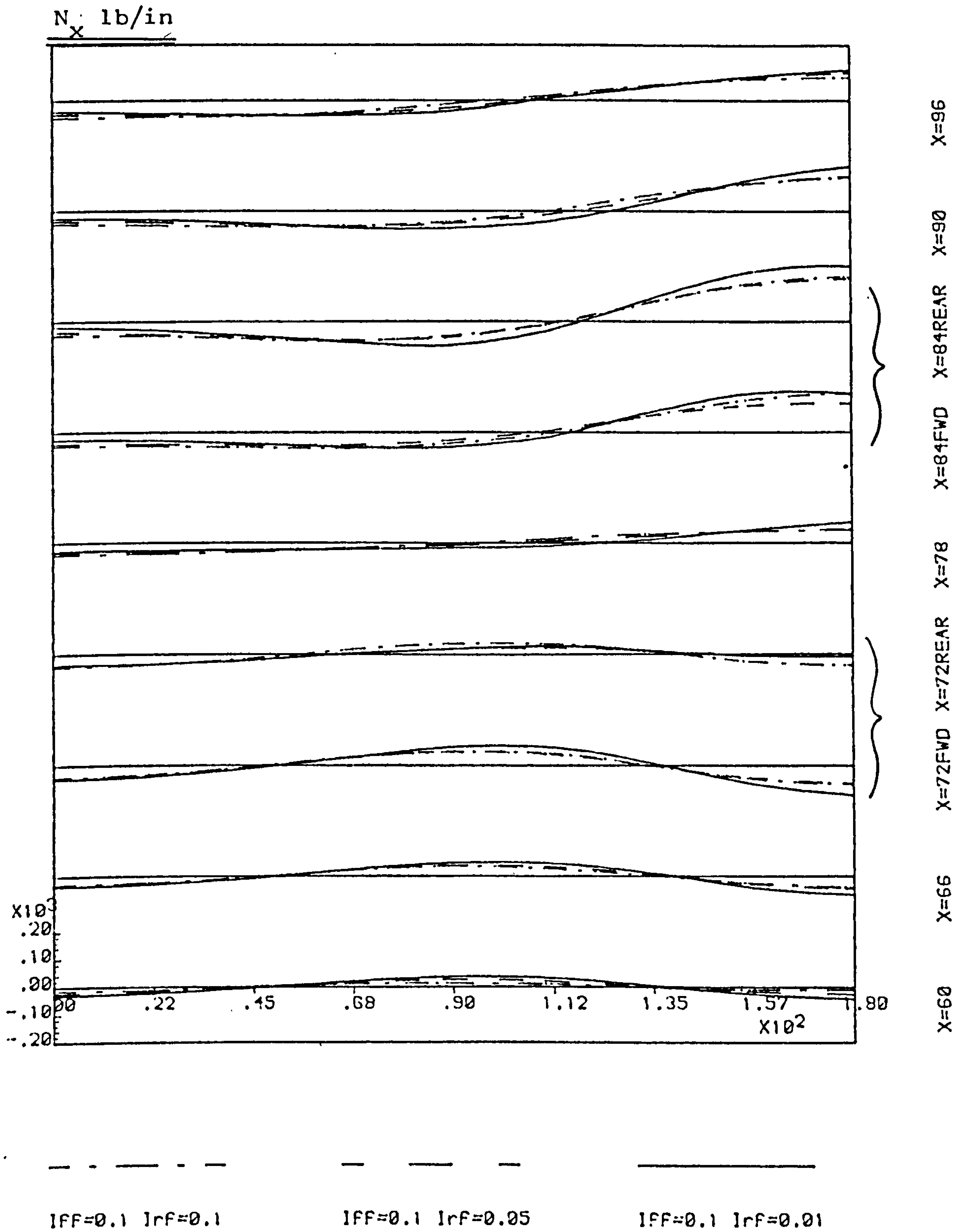

Fig. 4.6.3 EFFECTS OF REAR FRAME STIFFNESS VARI. - <u>DIRECT</u> STR.

CENTRE BODY STRESS RESULT.(180 deg P/U) : TAIL LOAD
R=6.0 T=0.06 Lrs=12. Astr=0.1 Nstr=4, 72-12-60

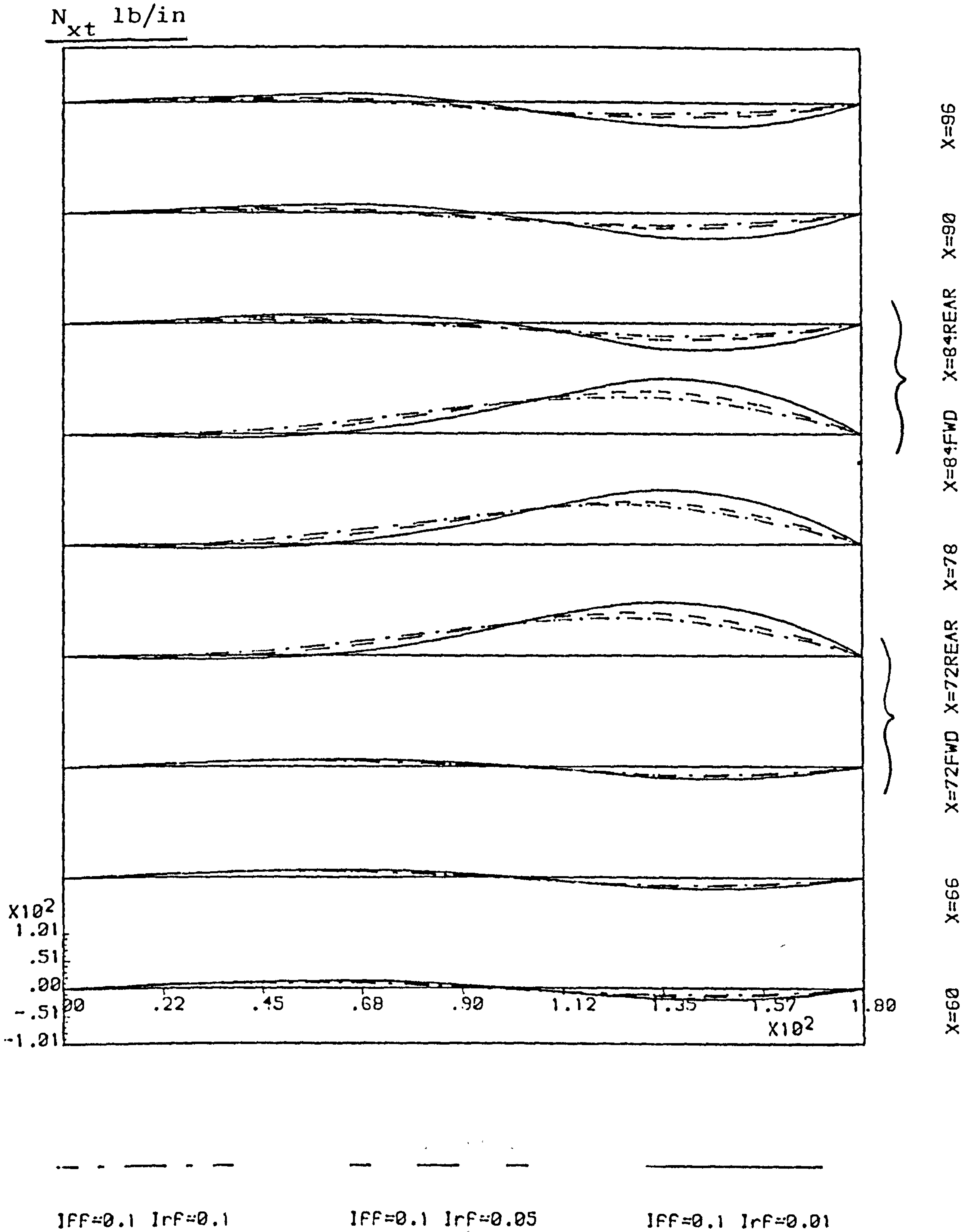

Fig.4.6.4 EFFECTS OF REAR FRAME STIFFNESS VARI. - SHEAR

Fig.4.6.5 SHEAR FLOW FROM SHELL TO FRAME - REAR FRAME STIFFNESS VARIATION

CENTRE BODY (6R t=0.06 72-12-60); 180 P/U-SYM. TAIL LOAD
Ir=0.01 Lrsp=12. Nstr=4 As=0.1 ; FWD. DIAPHRAGM

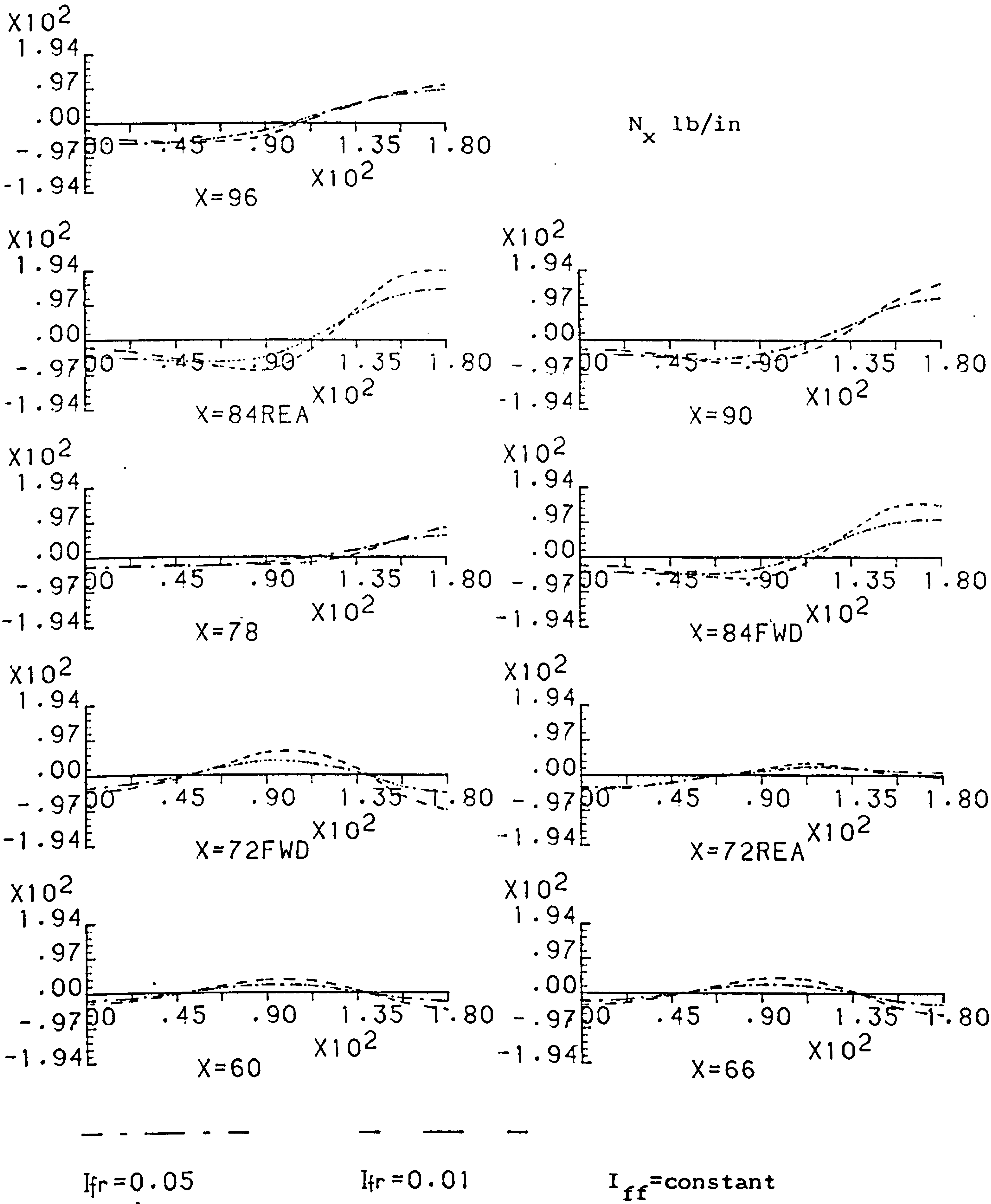

Fig.4.6.6 EFFECT OF REAR FRAME STIFF. CHANGE - <u>AXIAL STRESS</u>

CENTRE BODY (6R t=0.06 72-12-60) ; 180 P/U-SYM. TAIL LOAD
Ir=0.01 Lrsp=12. Nstr=4 As=0.1 ; FWD. DIAPHRAGM

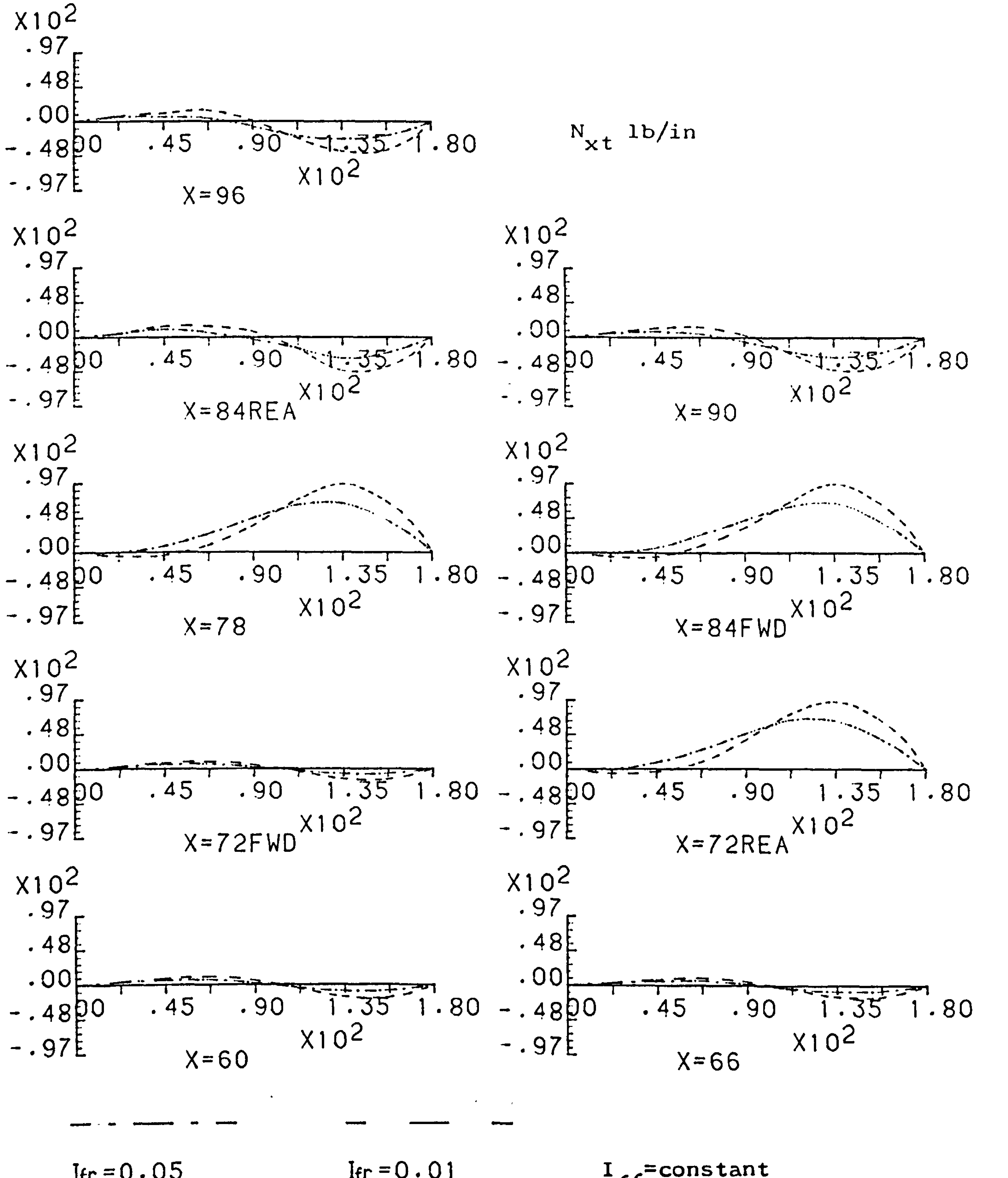

Fig. 4.6.7 EFFECT OF REAR FRAME STIFF. CHANGE - <u>SHEAR STRESS</u>

Fig.4.6.8 SHEAR FLOW FROM SHELL TO FRAME - REAR FRAME STIFF. VAR.

CENTRE BODY (6R t=0.06 72-12-60) ; 180 P/U-SYM. TAIL LOAD
Ir=0.01 Lrsp=12. Nstr=4 As=0.1 ; REAR DIAPHRAGM

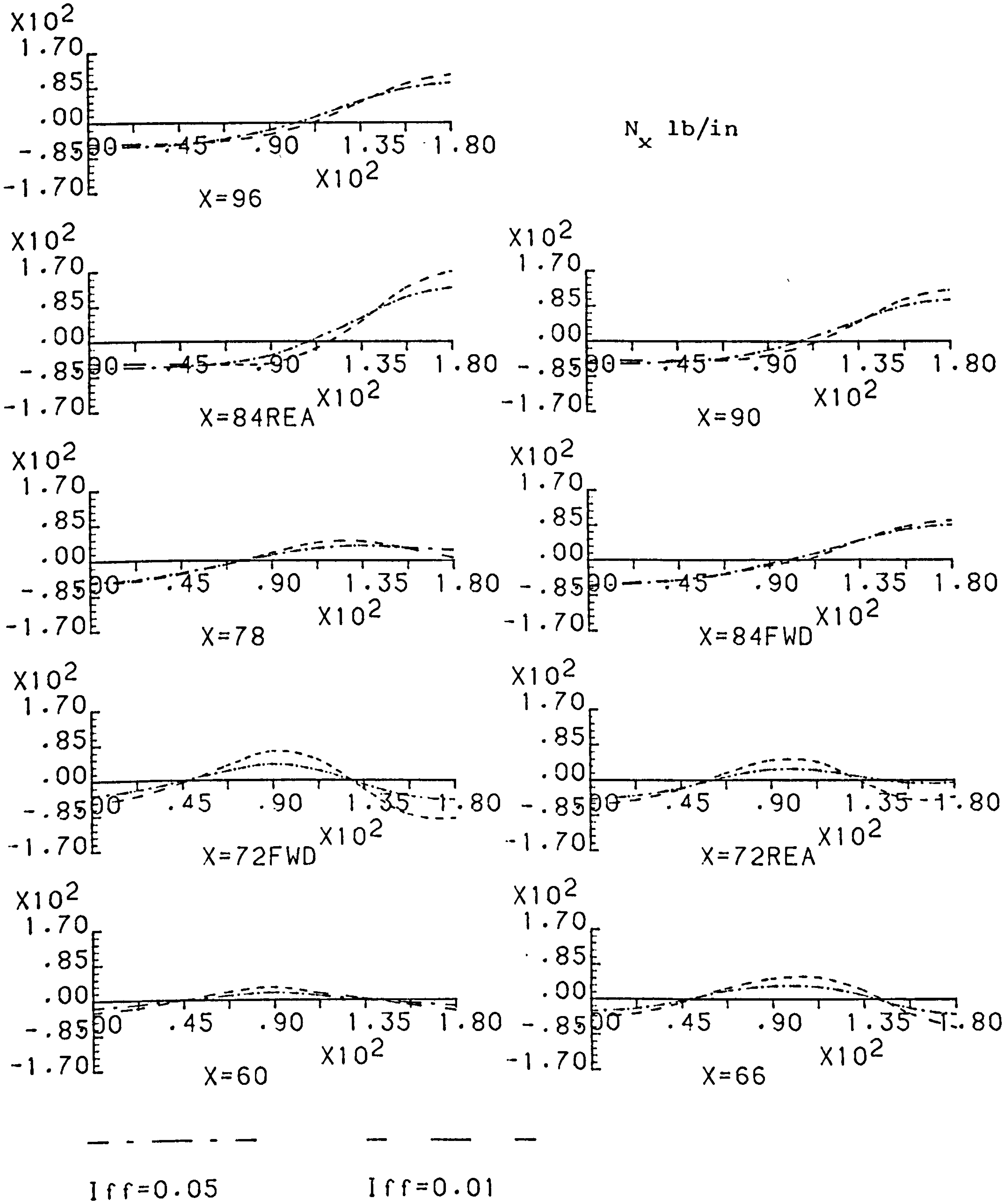

Fig. 4.6.9 EFFECT OF FWD. FRAME STIFF. CHANGE - AXIAL STRESS

CENTRE BODY (6R t=0.06 72-12-60) ; 180 P/U-SYM. TAIL LOAD
Ir=0.01 Lrsp=12. Nstr=4 As=0.1 ; REAR DIAPHRAGM

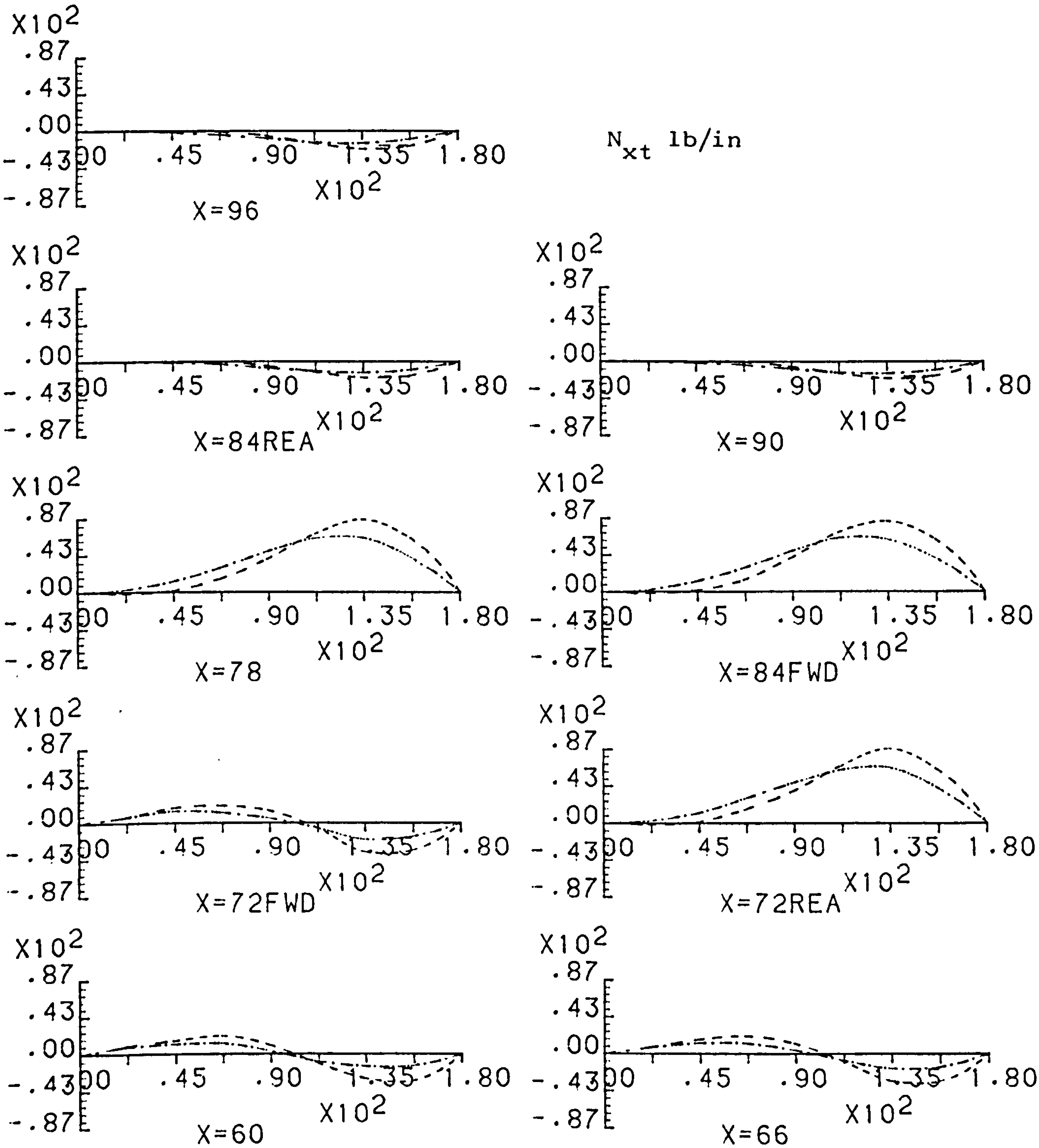

Iff=0.05 Iff=0.01

Fig.4.6.10 EFFECT OF FWD. FRAME STIFF. CHANGE - SHEAR STRESS

FORWARD FRAME , TAIL LOAD 180deg (72-12-60)

R=6. T=0.06 Nstr=4 Lrsp=12.

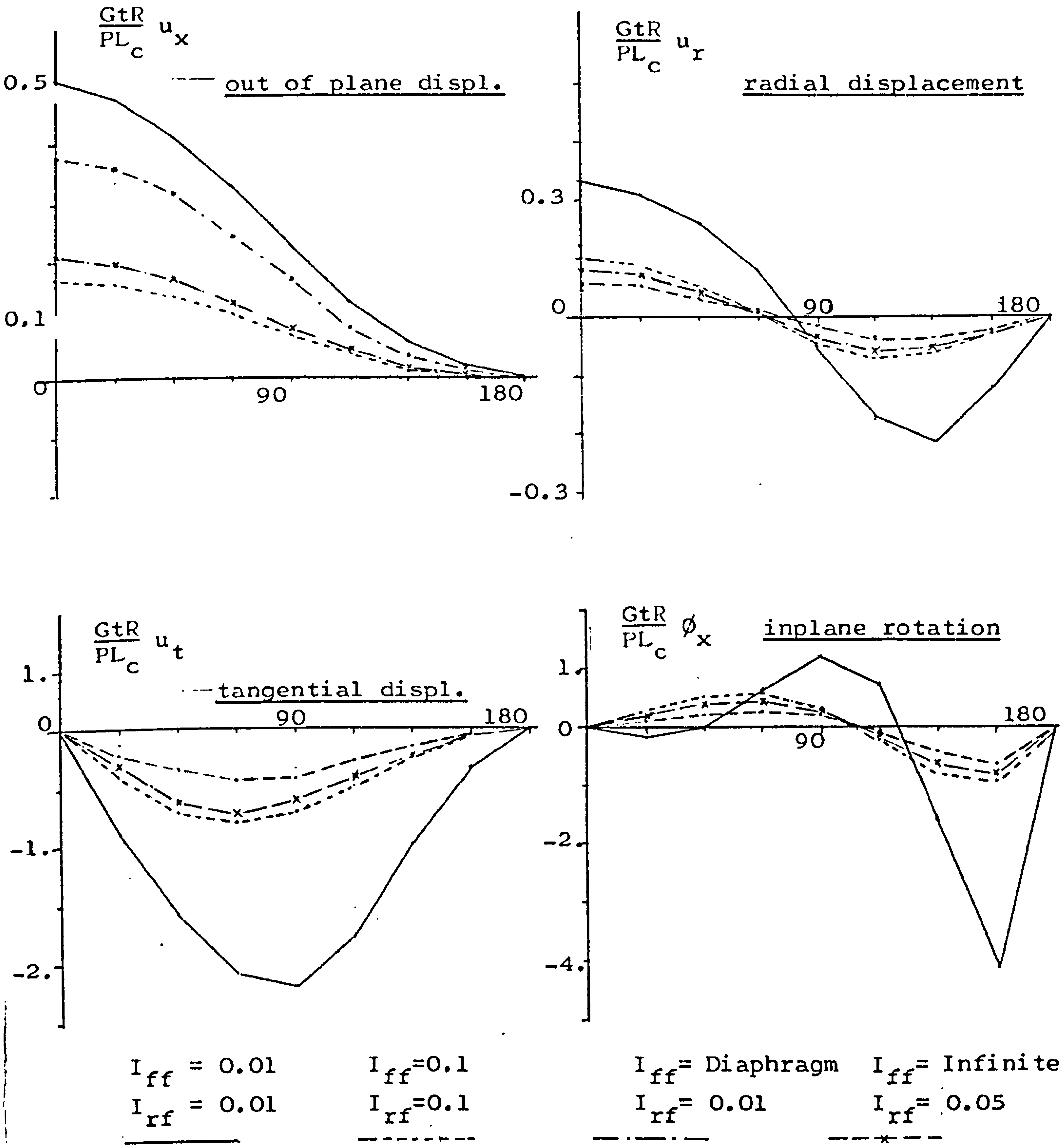

Fig 4.6.11 FRAME DISPLACEMENTS - EFFECT OF FRAME COMBINATION

FORWARD FRAME , TAIL LOAD 180deg (72-12-60)

R=6. T=0.06 Nstr=4 Lrsp=12.

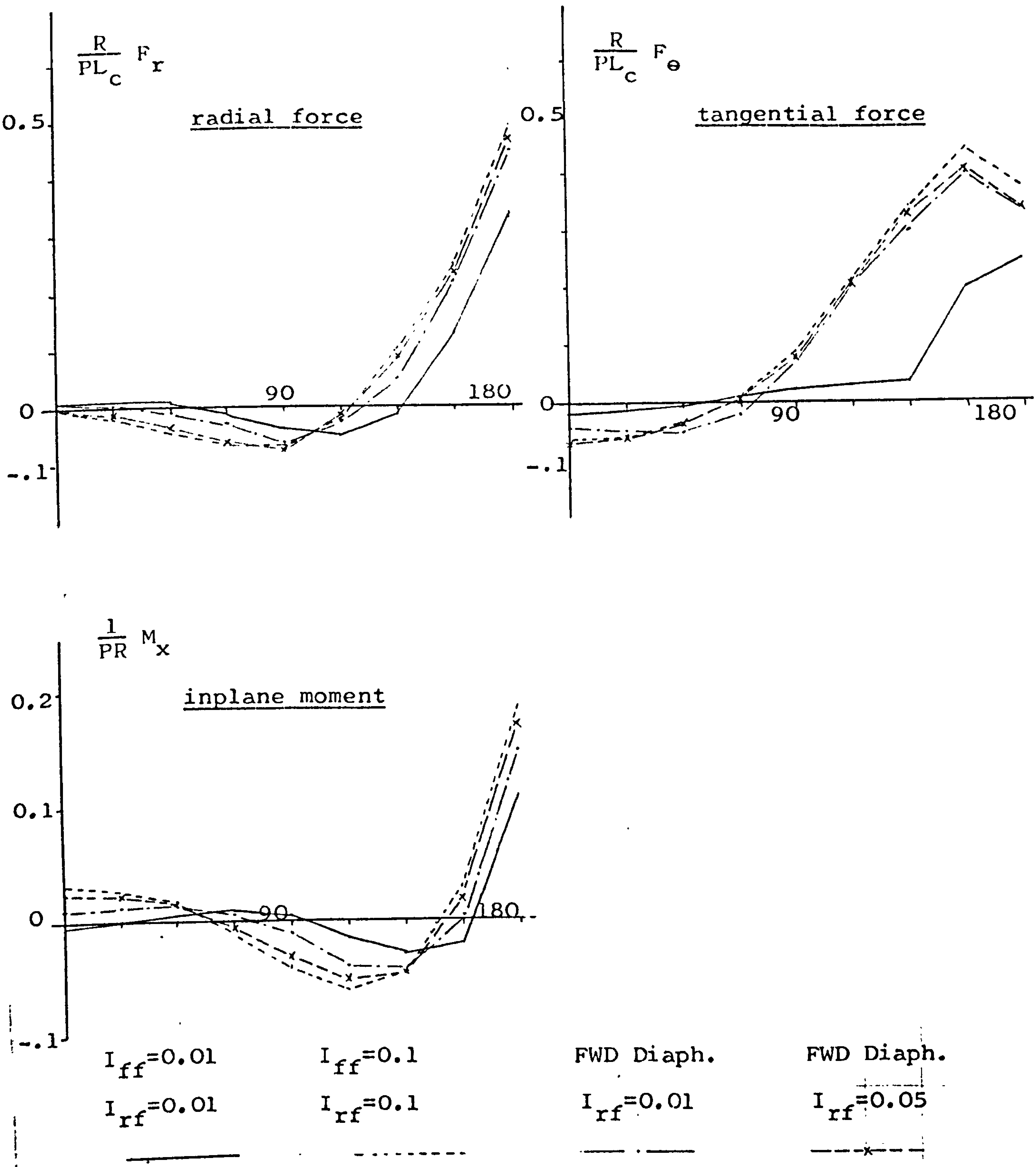

Fig.4.6.12 FRAME INTERNAL FORCES – EFFECT OF FRAME COMBINATION

2 DIAPHRAGM FRAMED SHELL(72-12-60); 1g INERTIA
R=6.0 T=0.06 Nstr=4 Astr=0.1 Rspa=12.

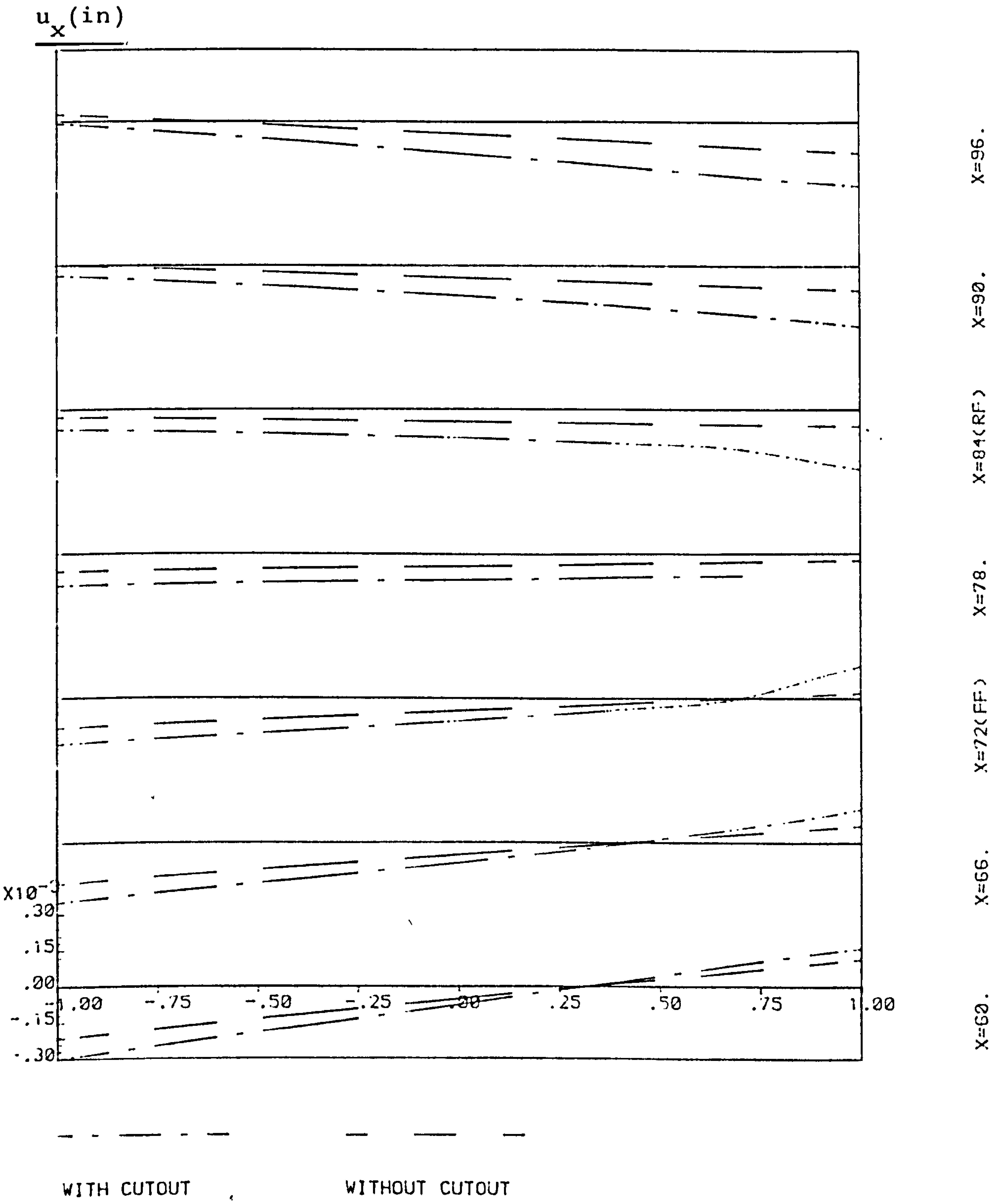

Fig. 4.7.1 CENTRE BODY CROSS SECTION WARPING-CUT OUT EFFECT

2 DIAPHRAGM FRAMED SHELL(72-12-60); TAIL LOAD
R=6.0 T=0.06 Nstr=4 Astr=0.1 Rspa=12.

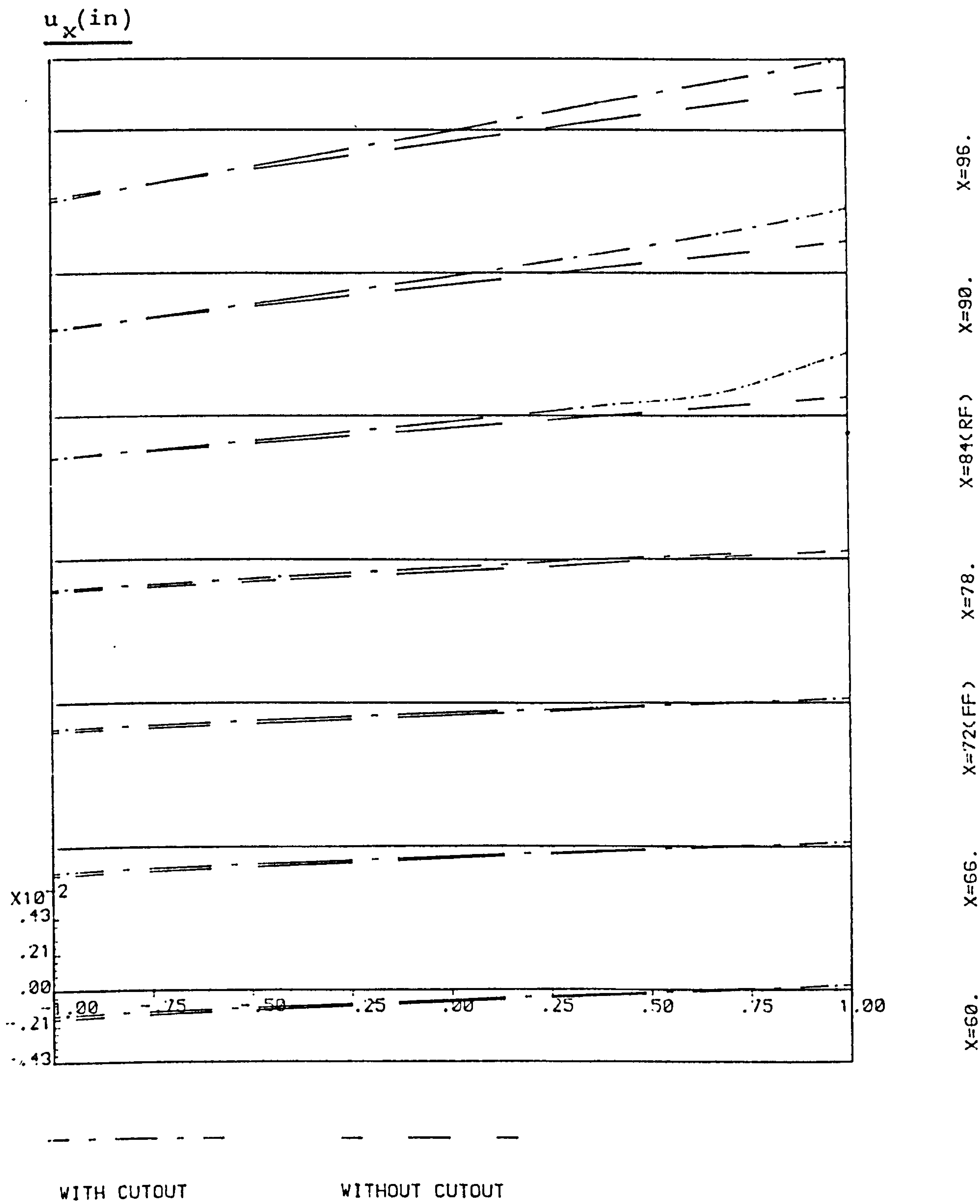

Fig.4.7.2 CENTRE BODY CROSS SECTION WARPING-CUT OUT EFFECT

CENTRE BODY (6R t=0.06 72-12-60.); SYM. 1 g INERTIA

If=0.1 Af=1.0 Ir=0.01 Lrsp=12. Nstr=4 As=0.1

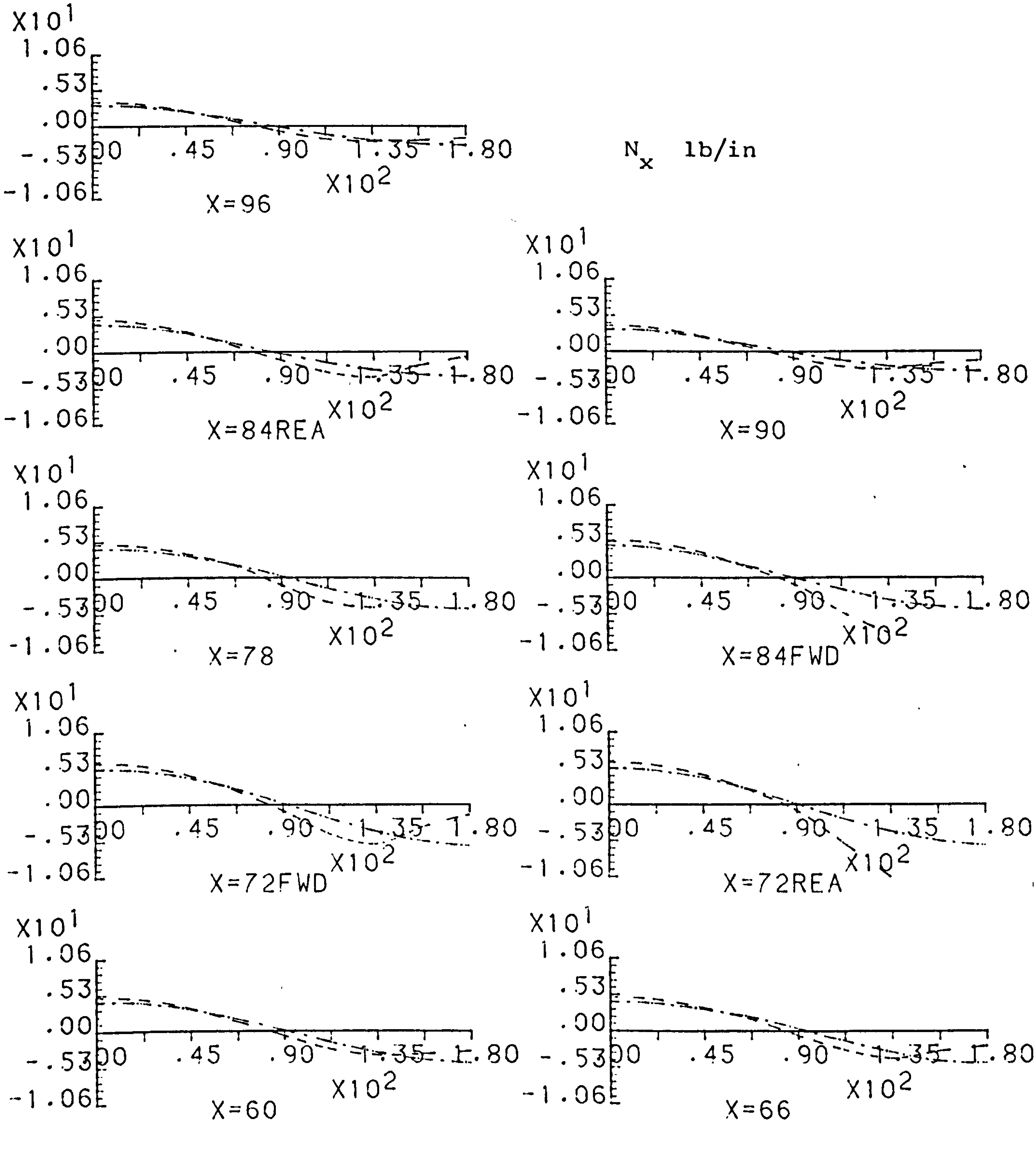

WITHOUT CUTOUT   WITH CUTOUT (135-180)

Fig.4.7.3 EFFECT OF CENTRE BODY CUTOUT - AXIAL STRESS

CENTRE BODY (6R t=0.06 72-12-60.); SYM. 1 g INERTIA

If=0.1 Af=1.0 Ir=0.01 Lrsp=12. Nstr=4 As=0.1

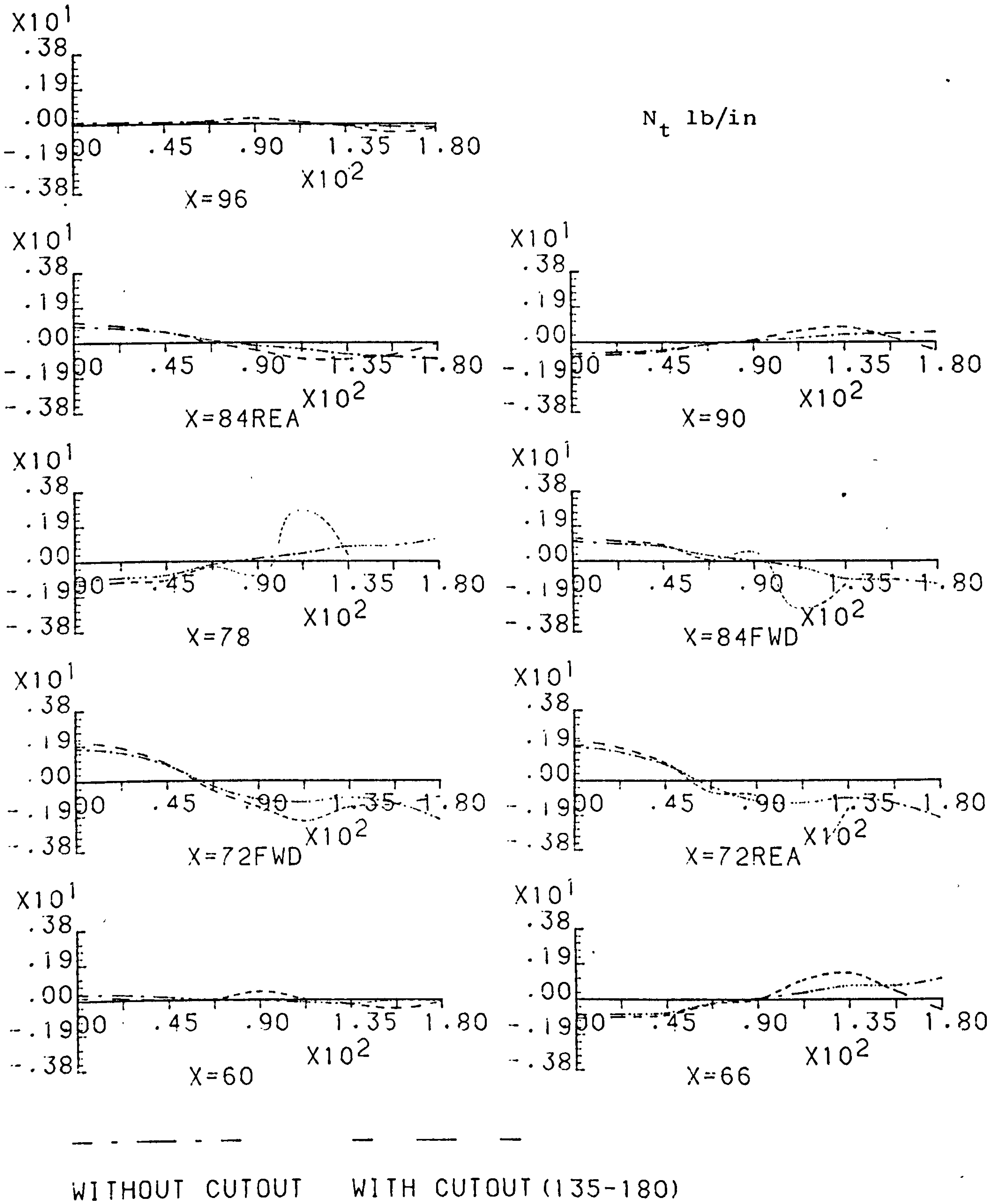

Fig.4.7.4 EFFECT OF CENTRE BODY CUTOUT - HOOP STRESS

CENTRE BODY (6R t=0.06 72-12-60.); SYM. 1 g INERTIA

If=0.1 Af=1.0 Ir=0.01 Lrsp=12. Nstr=4 As=0.1

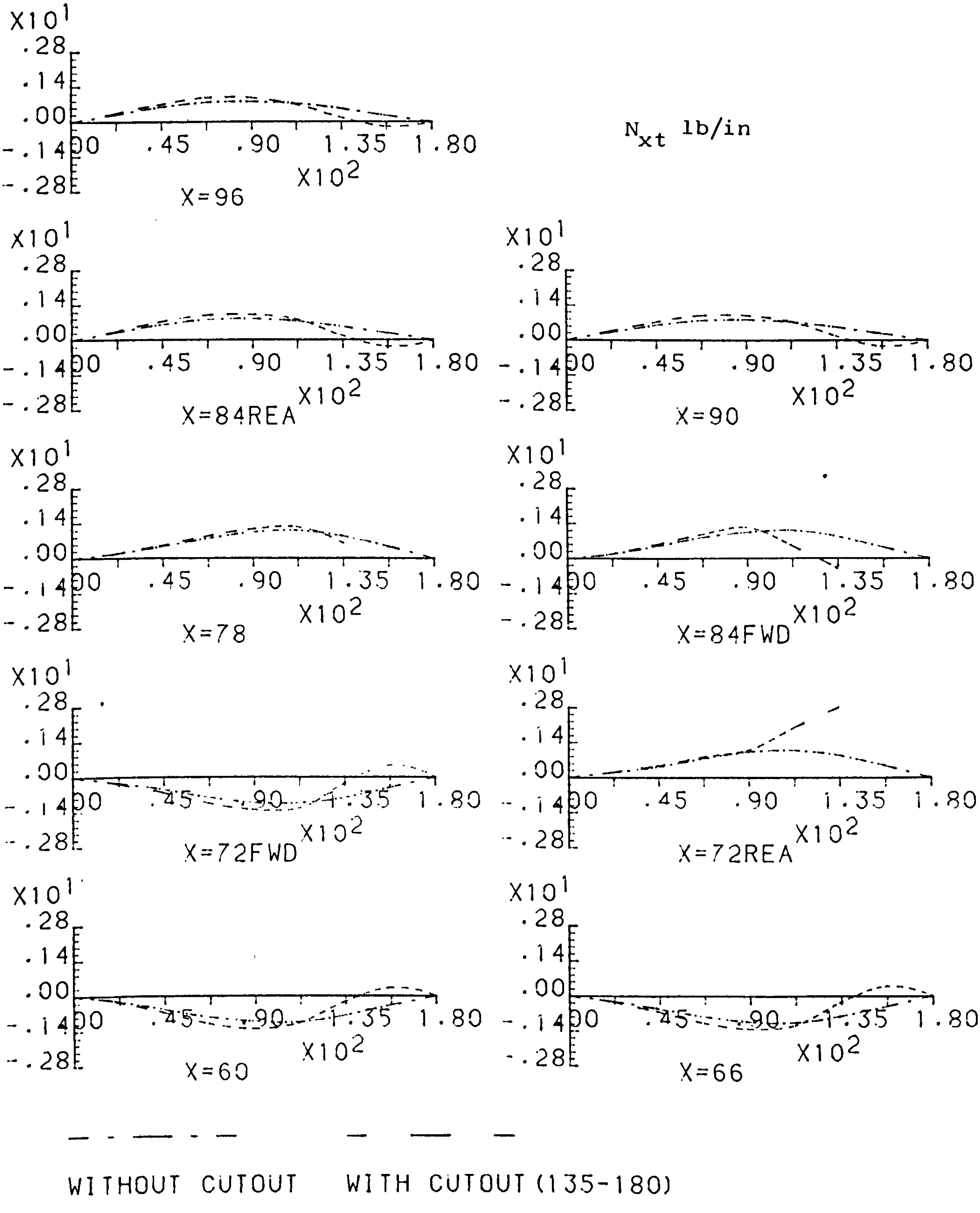

Fig. 4.7.5 EFFECT OF CENTRE BODY CUTOUT - SHEAR STRESS

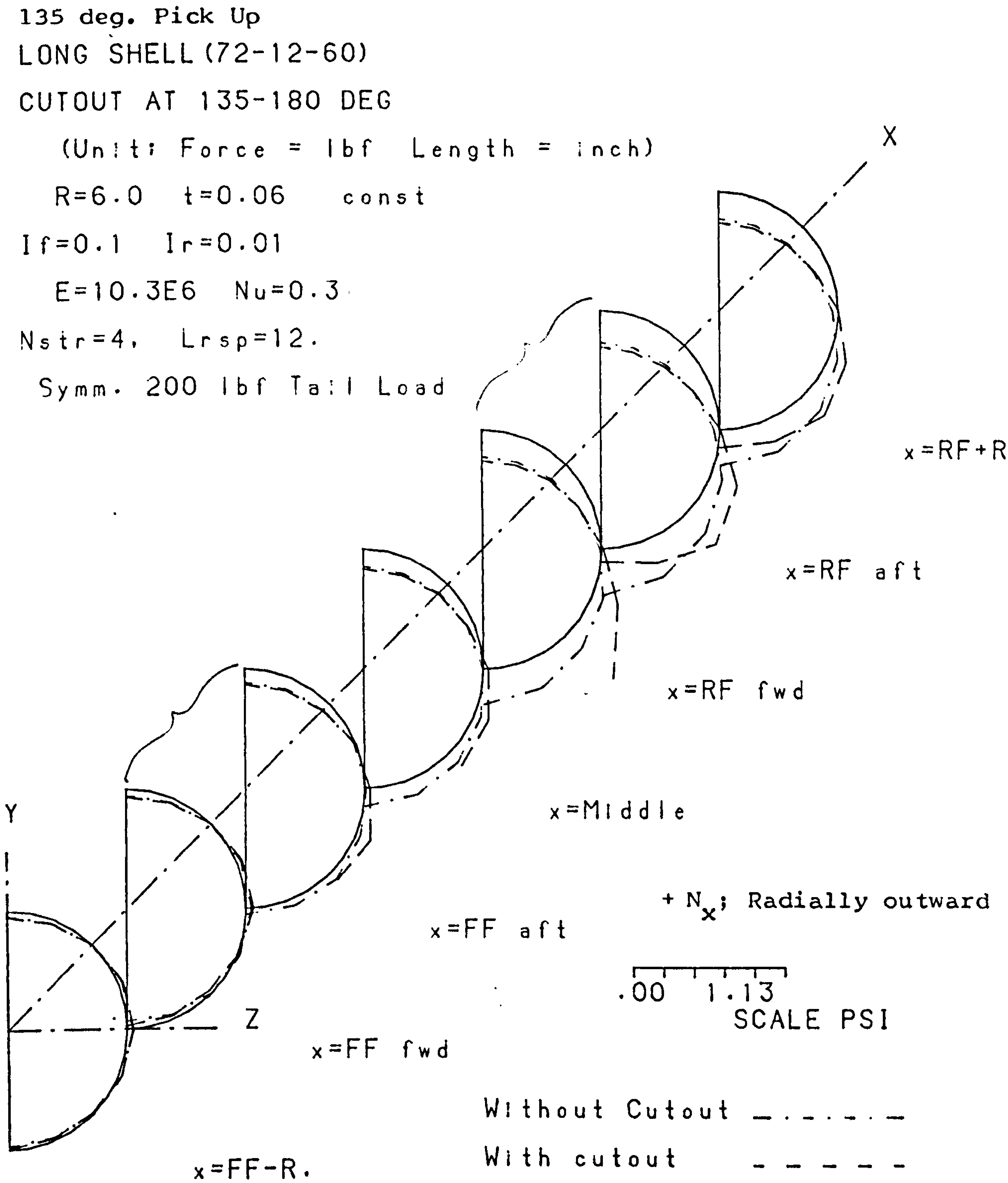

Fig.4.7.6 EFFECT OF CENTRE SHELL CUTOUT ON DIRECT STRESS DISTRI.

* refer paragraph (iv) of section 3.9.

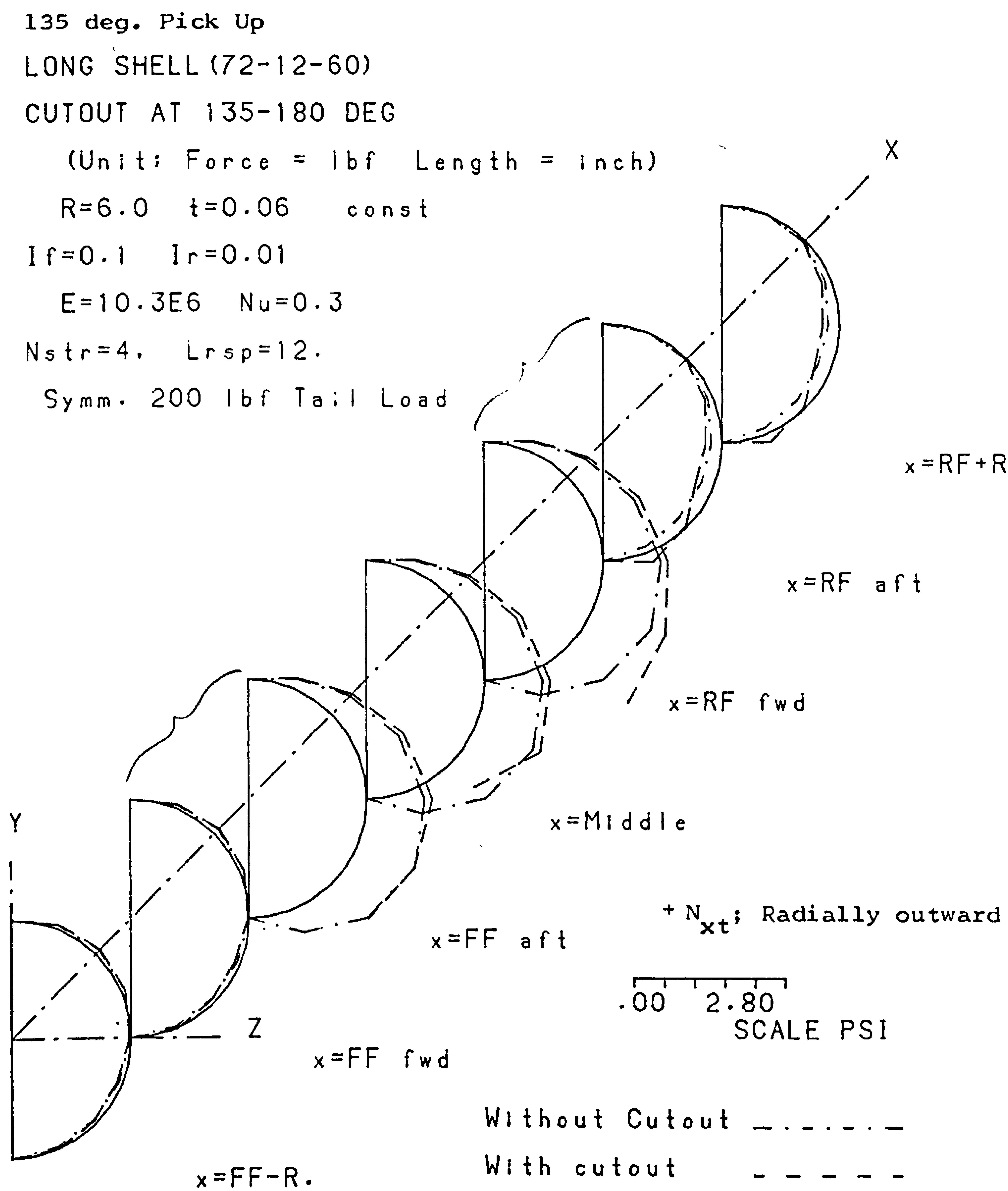

Fig. 4.7.7 EFFECT OF CENTRE SHELL CUTOUT ON <u>SHEAR STRESS</u> DISTRI.

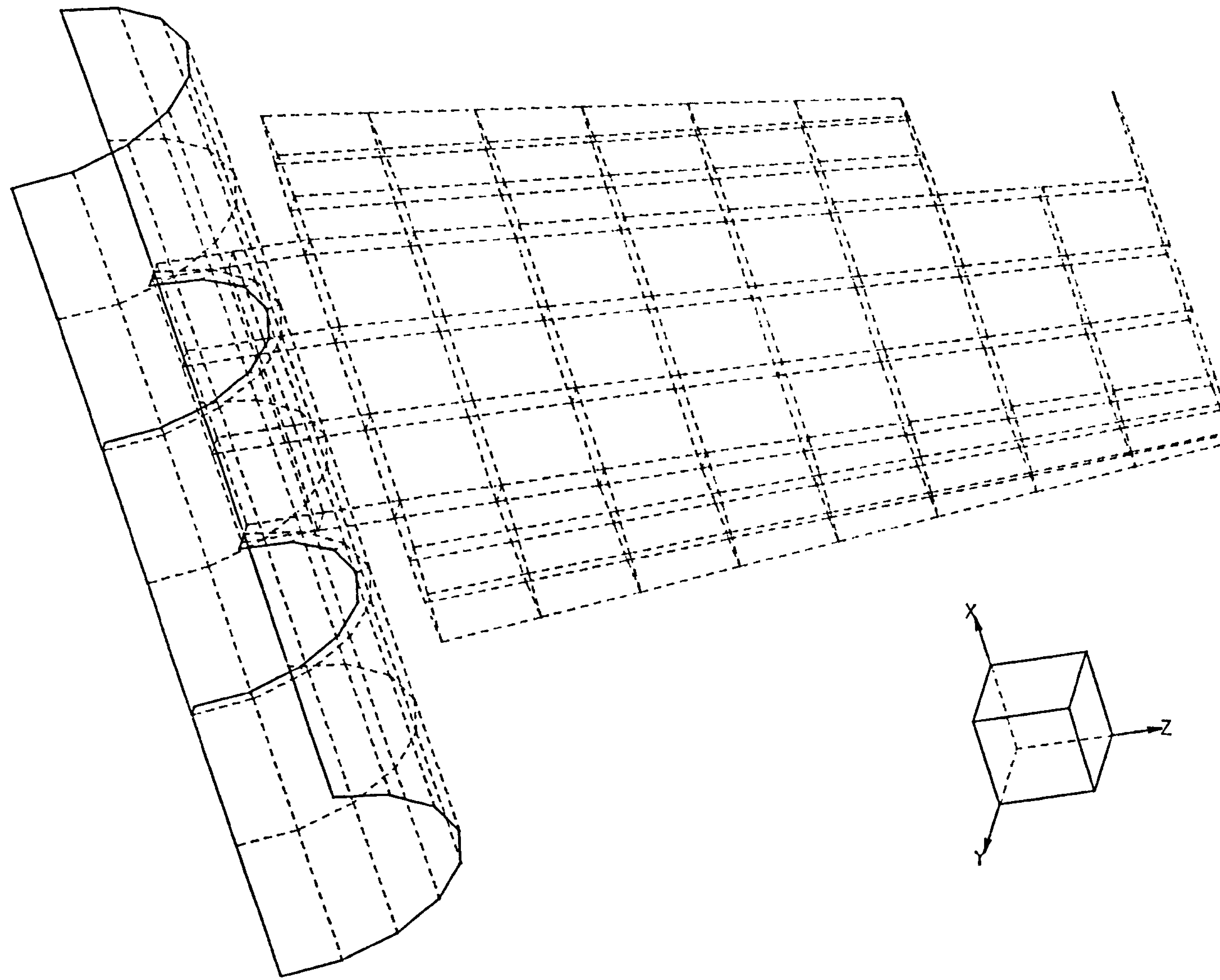

Fig.5.1.1 FEM Model of The Combined Strucure - Low Wing.

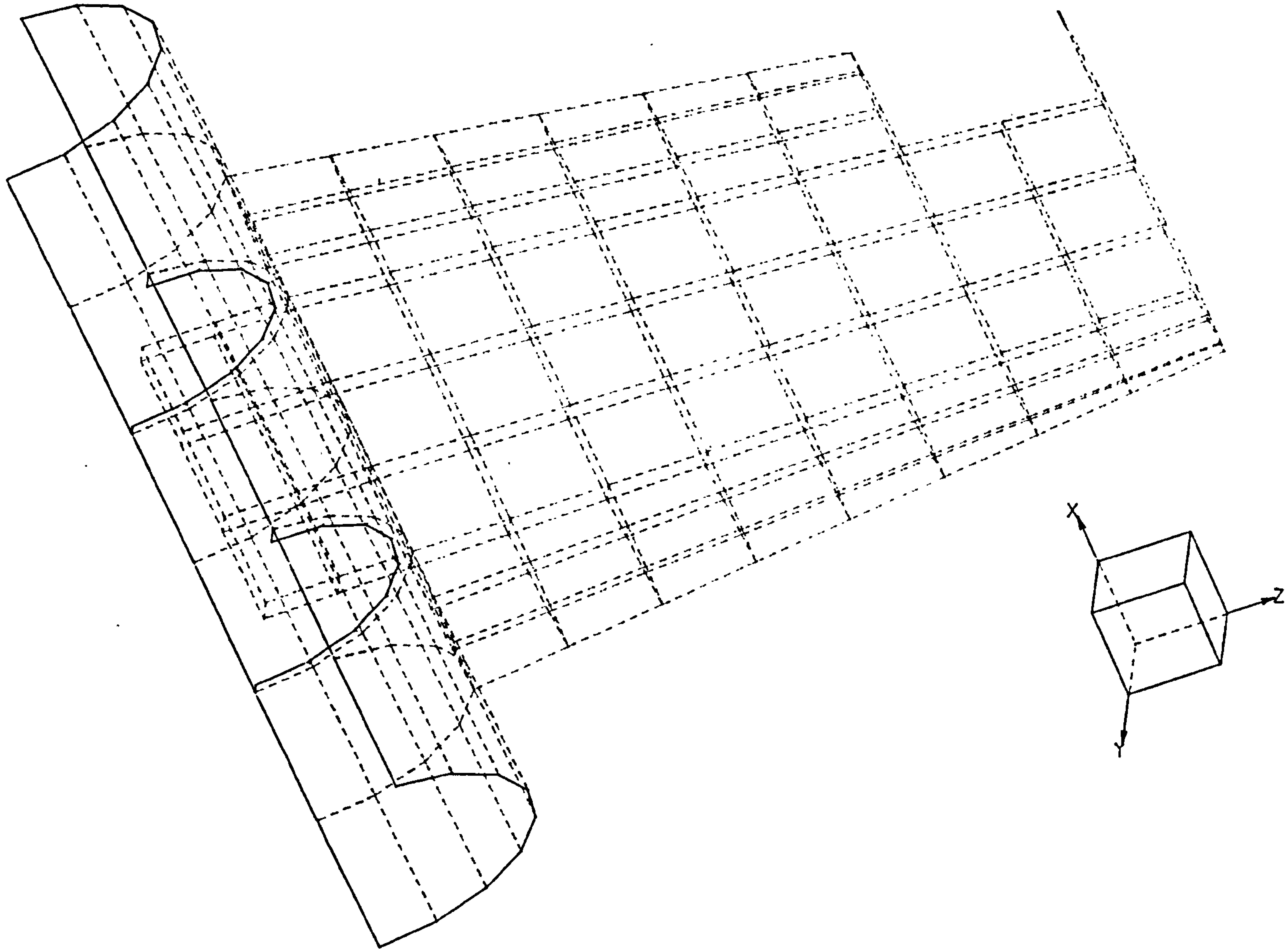

Fig.5.1.2 FEM Model of the Combined Structure - Mid Wing.

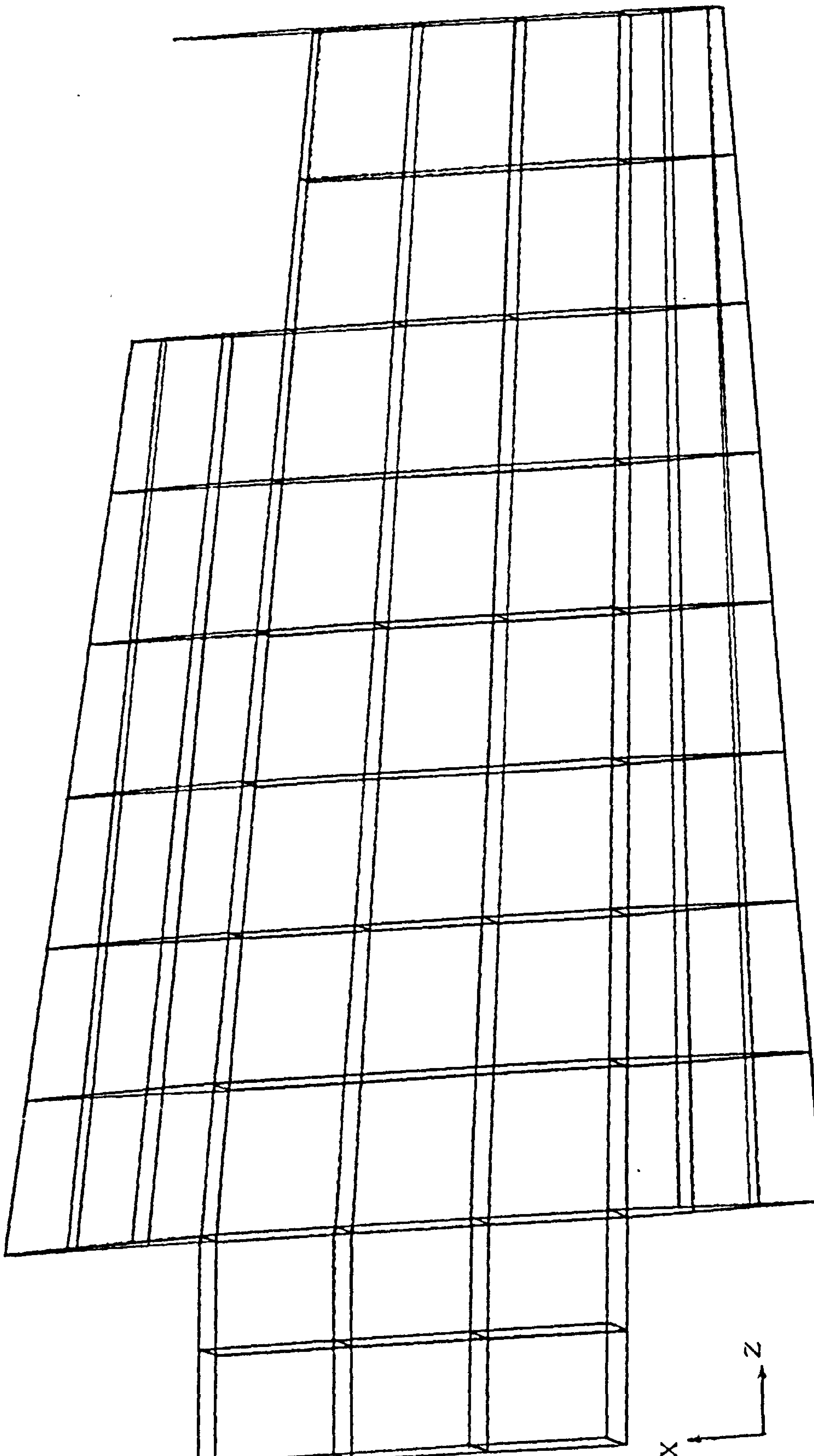

Fig.5.1.3 Finite Element Model of the Wing Structure

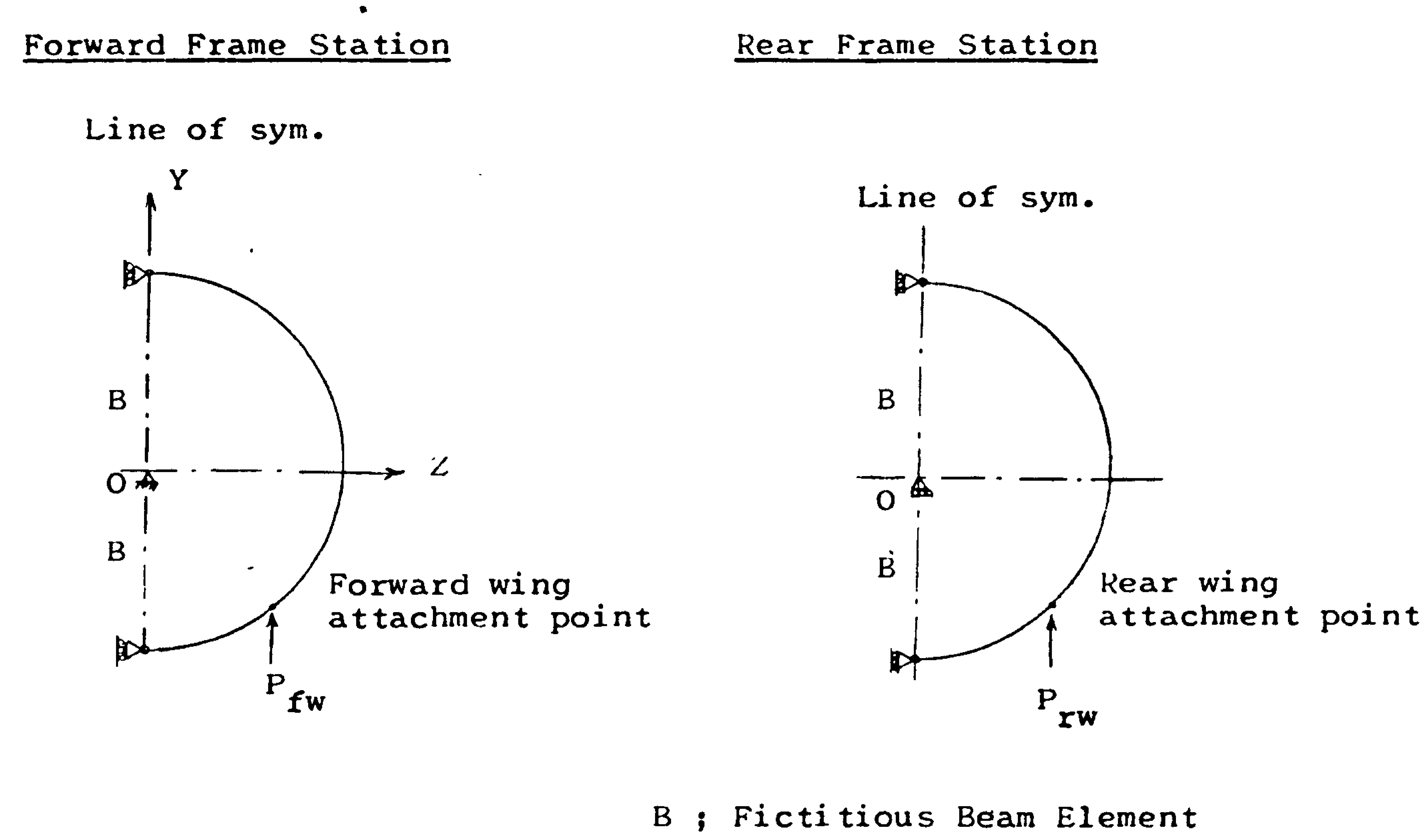

Fig.5.2.1 Restraint of Rigid Body Motion of the Body F.E. Model

Table 5.1 Comparison of the wing interaction matrix.

a) Low Wing

	Y_1	Z_1	Y_2	Z_2
Y_1	5.066E3		Symmetric	
Z_1	2.714E0	9.488E3		
Y_2	-5.063 3	-3.605E0	5.072E3	
Z_2	-2.606E0	-9.479E3	3.533E0	9.490E3

b) Mid Wing

	Y_1	Z_1	Y_2	Z_2
Y_1	1.067E4		Symmetric	
Z_1	4.620E3	7.763E5		
Y_2	4.322E4	9.594E4	4.804E5	
Z_2	-7.161E3	3.789E4	-5.371E3	1.416E6

-cf.-

Diagonal Terms of Shell & Frame Element Stiffnesses

$R = 6 \quad t = 0.06 \quad I_f = 0.1$

	u_x	u_r	u_θ	ϕ_x	ϕ_θ
Shell	2.96E5	1.19E5	2.42E5	2.07E3	1.38E4
Frame	4.71E5	0.54E6	2.13E6	8.80E5	1.37E5

CENTRE BODY (72-12-60): LOW WING PICK UP - TAIL LOAD
R=6. t=0.06 Nstr=4 As=0.1 Ir=0.01 If=0.1

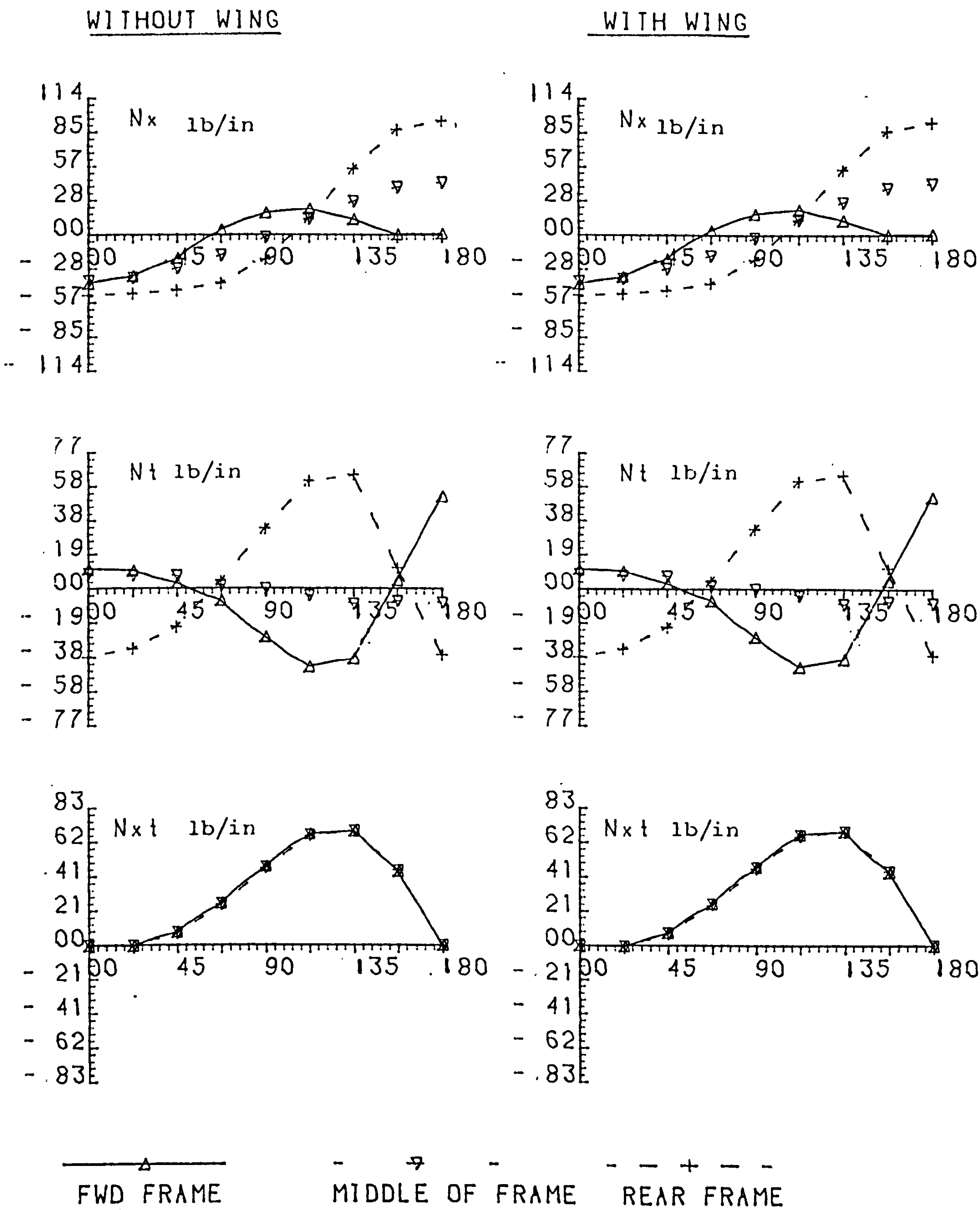

Fig.5.5.1 MEMBRANE STRESS RESULTANTS DIST.-WING STIFFNESS EFFECT

* refer paragraph (v) of section 3.9.

CENTRE BODY (72-12-60) ; LOW WING PICK UP - TAIL LOAD

R=6. t=0.06 Nstr=4 As=0.1 Ir=0.01 If=0.1

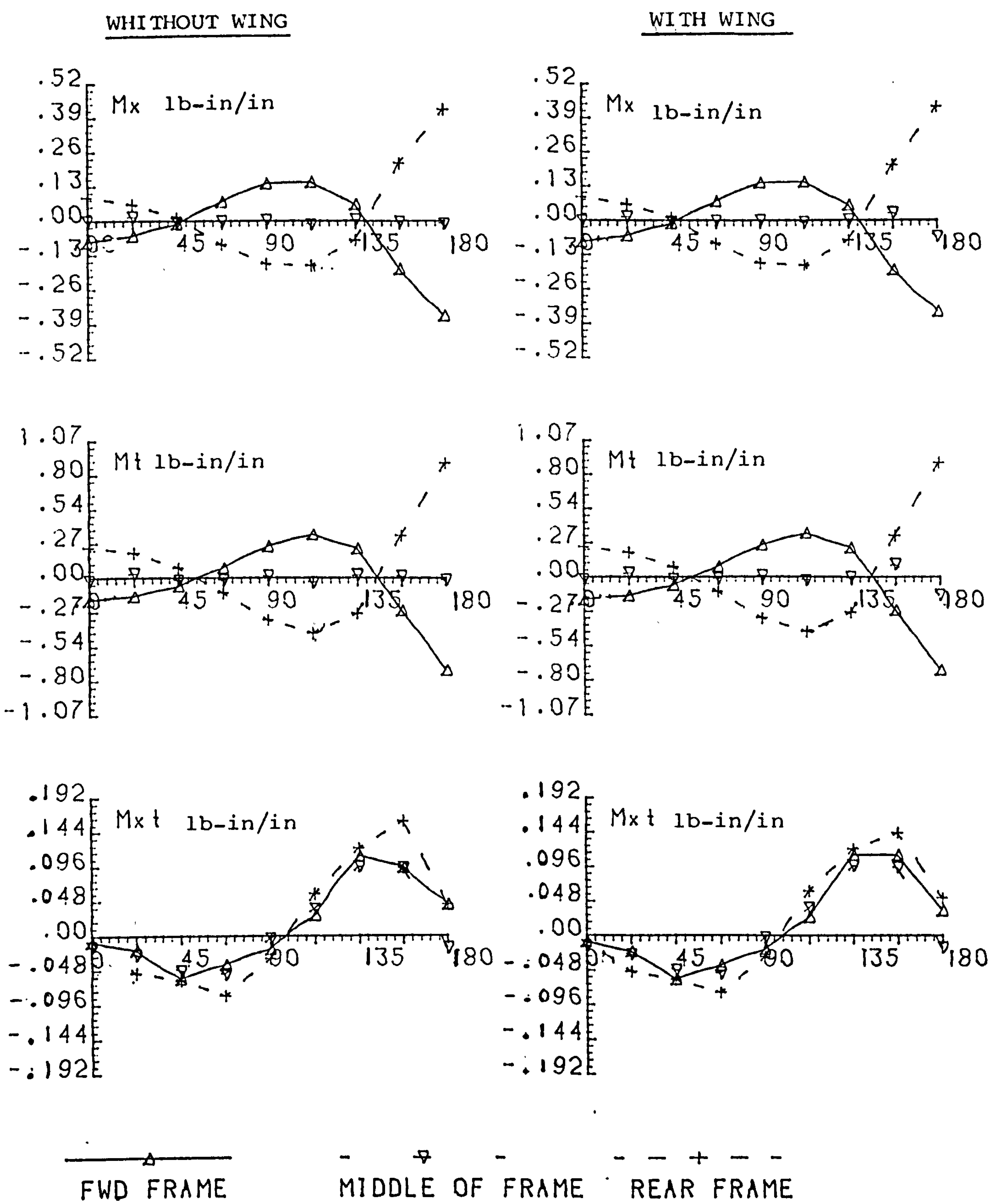

Fig 5.5.2 BENDING STRESS RESULTANTS DIST.-WING STIFFNESS EFFECT

CENTRE BODY (72-12-60) : MID WING PICK UP - TAIL LOAD

R=6. t=0.06 Nstr=4 As=0.1 Ir=0.01 If=0.1

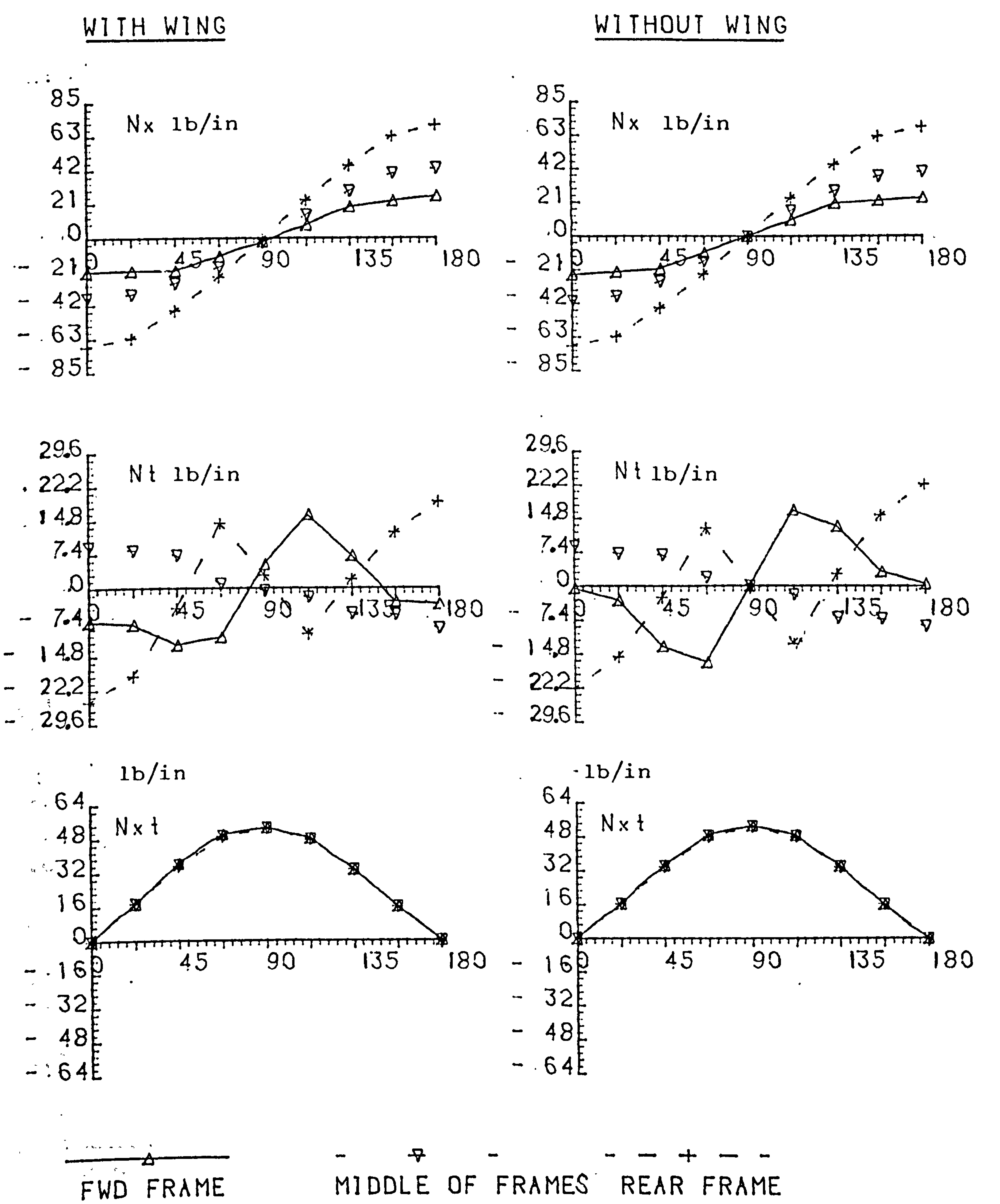

Fig.5.5.3 MEMBRANE STRESS RESULTANTS DISTRIBUTION-WING STIFF EFFECT

CENTRE BODY (72-12-60) : MID WING PICK UP - TAIL LOAD

R=6. t=0.06 Nstr=4 As=0.1 Ir=0.01 If=0.1

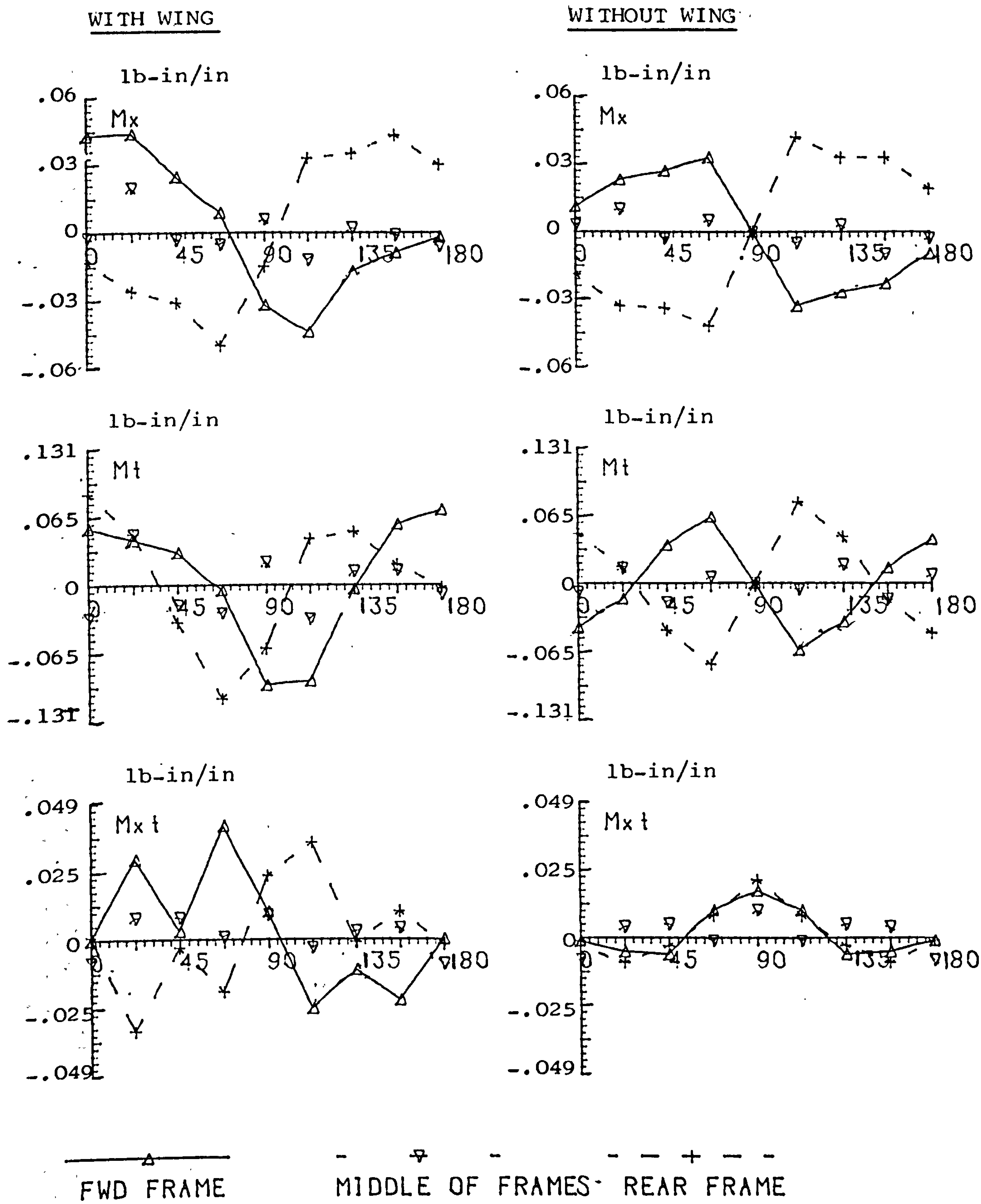

Fig. 5.5.4 BENDING STRESS RESULTANTS DISTRIBUTION-WING STIFF EFFECT.

CENTRE BODY (72-12-60) : MID WING PICK UP - 1 g INERTIA

R=6. t=0.06 Nstr=4 As=0.1 Ir=0.01 If=0.1

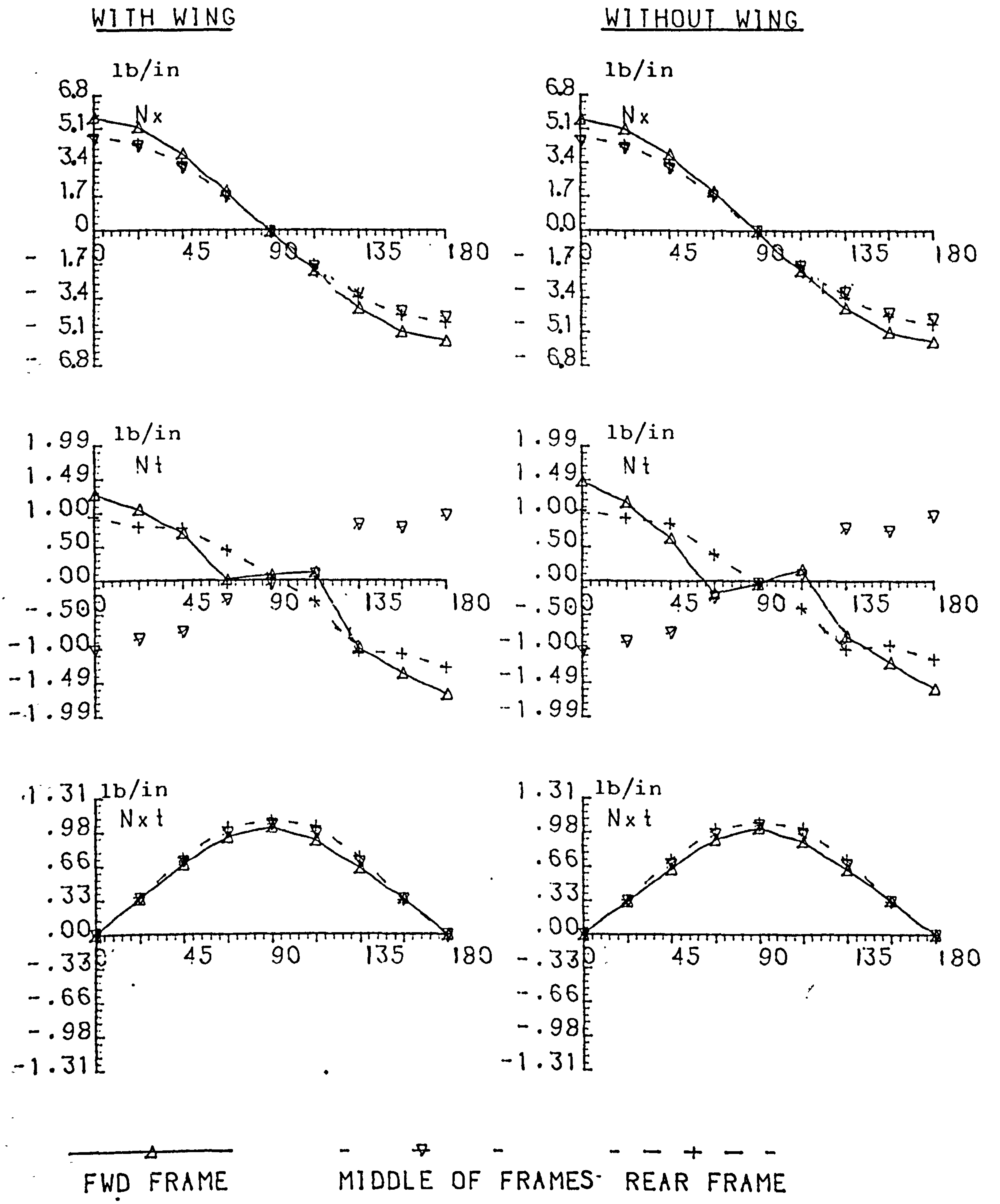

Fig.5.5.5 MEMBRANE STRESS RESULTANTS DISTRIBUTION-WING STIFF EFFECT

CENTRE BODY (72-12-60) : MID WING PICK UP - 1 g INERTIA

R=6. t=0.06 Nstr=4 Ao=0.1 Ir=0.01 If=0.1

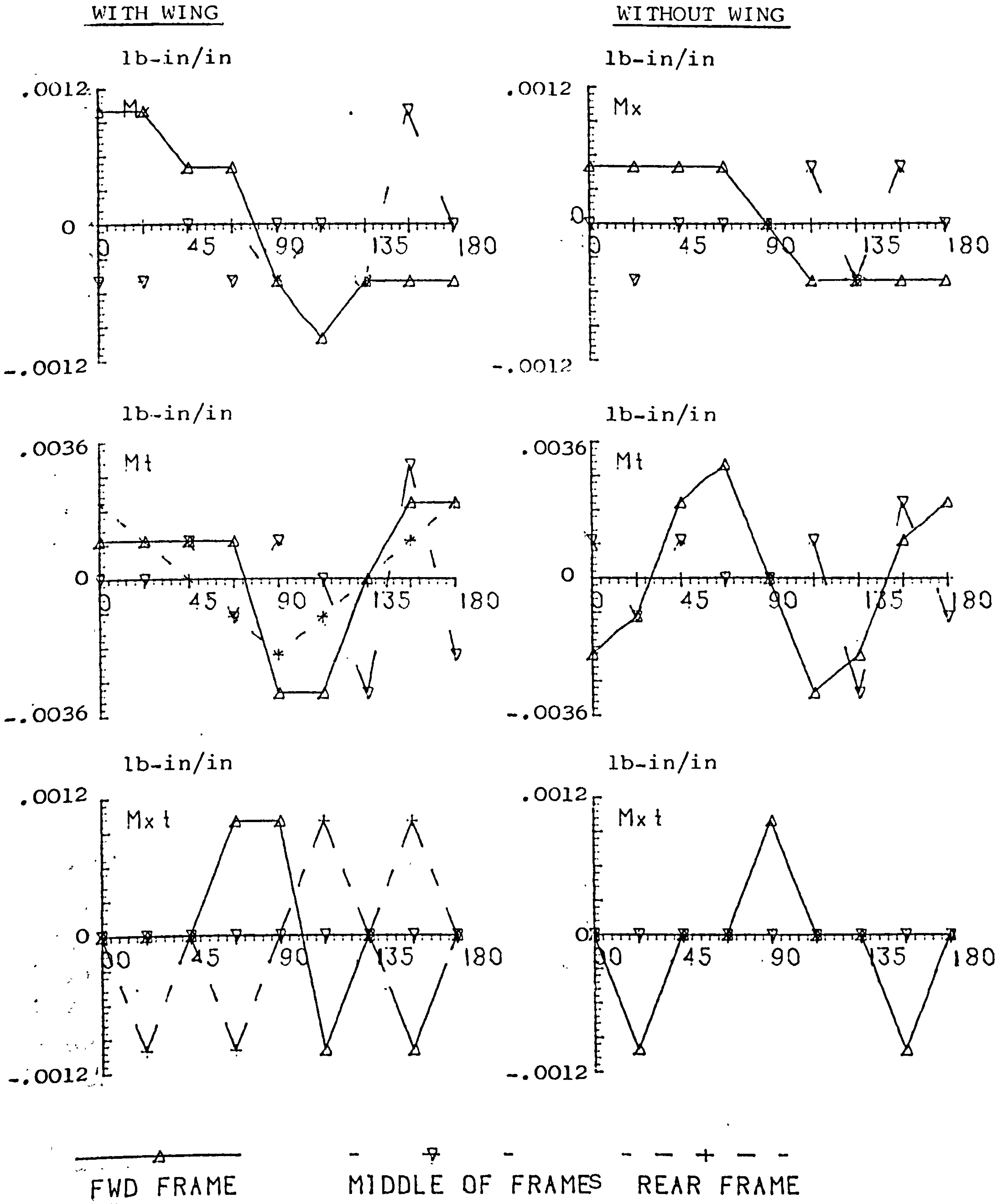

Fig.5.5.6 BENDING STRESS RESULTANTS DISTRIBUTION-WING STIFF. EFFECT.

CENTRE BODY (72-12-60) : WITH WING STIFF. - TAIL LOAD

R=6. t=0.06 Nstr=4 As=0.1 Ir=0.01 If=0.1

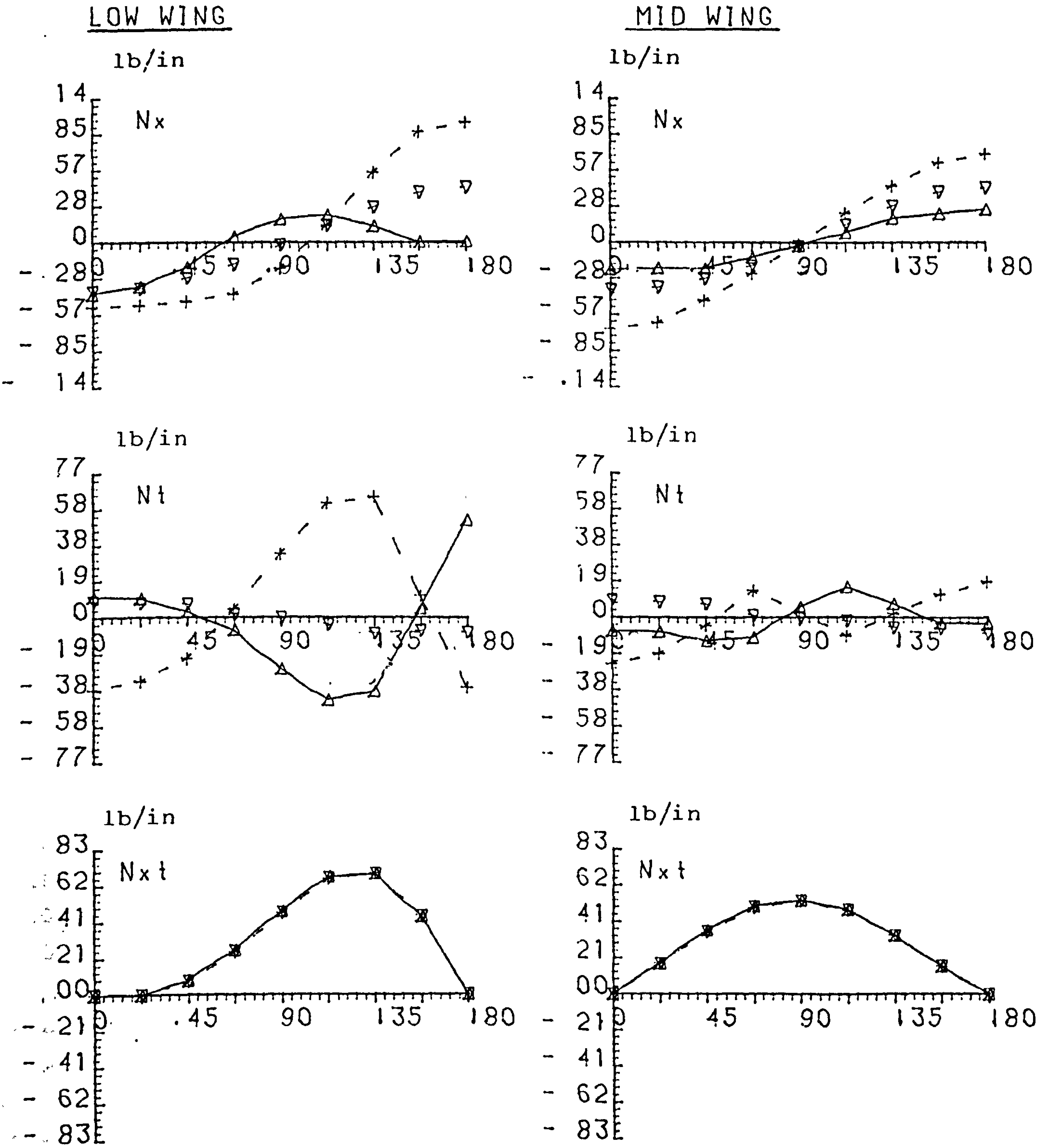

FWD FRAME — MIDDLE OF FRAMEs — REAR FRAME

Fig.5.5.7 MEMBRANE STRESS RESULTANTS DIST.-WING POSITION CHANGE.

CENTRE BODY (72-12-60): WITH WING STIFF. - TAIL LOAD

R=6. t=0.06 Nstr=4 As=0.1 Ir=0.01 If=0.1

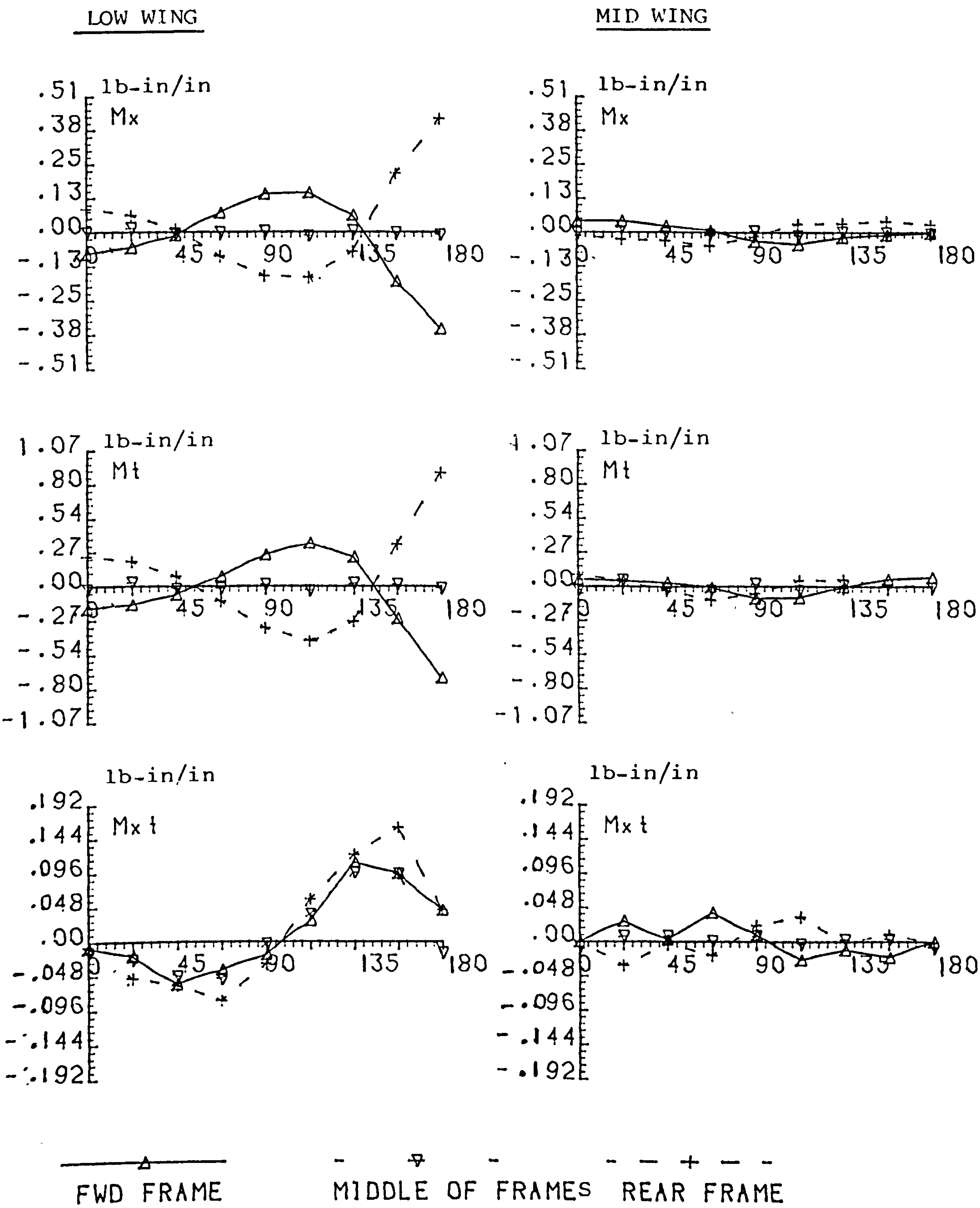

Fig.5.5.8 BENDING STRESS RESULTANTS DIST.-WING POSITION CHANGE EFFECT

Table 5.2 Body Interaction Forces of Chosen RPV under Symmetric Loads

F_y (lbf)

Loads \ Position		Forward Frame	Rear Frame	Total
Wing		93.8	82.8	176.6
Body	1 g	21.4	- 0.2	21.2
	1 rad/sec^2	2920.3	-2834.0	86.3
	Tail Load	500	- 600.0	-100.0

Table 5.3 Body Interaction Displacements of Chosen RPV under Symmetric Body Load Conditions

U_yx100(inch)

Loads \ wing, p/u	Low wing Forward	Low wing Rear	Mid wing Forward	Mid wing Rear
1 g	0.242	0.241	- 6.0	0.055
1 rad/sec^2	-14.70	-0.294	-102.26	10.056
Tail load	- 0.053	-0.076	- 15.74	1.69

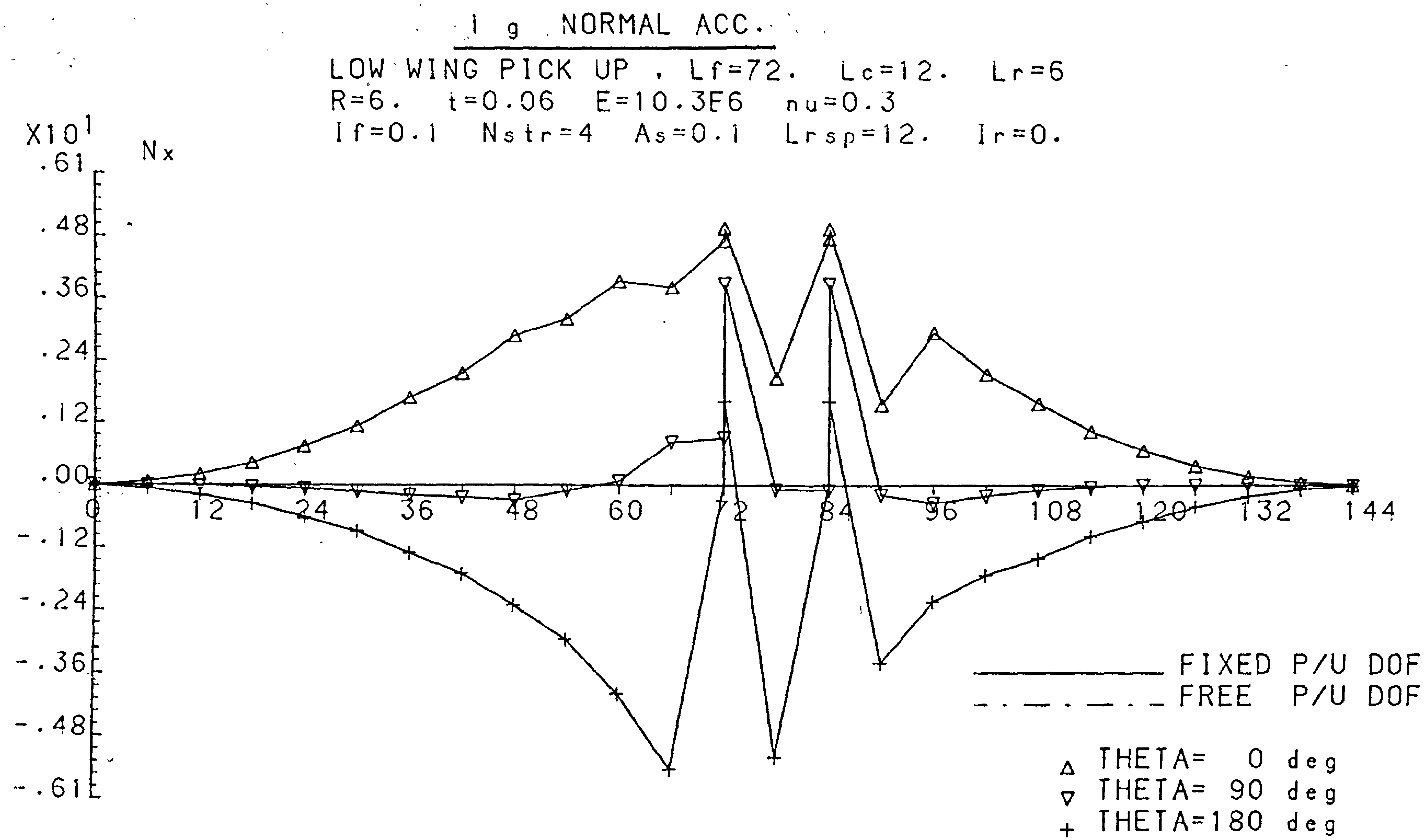

Fig.5.5.9a DIRECT STRESS RESULTANTS ALONG LONGITUDINAL AXIS

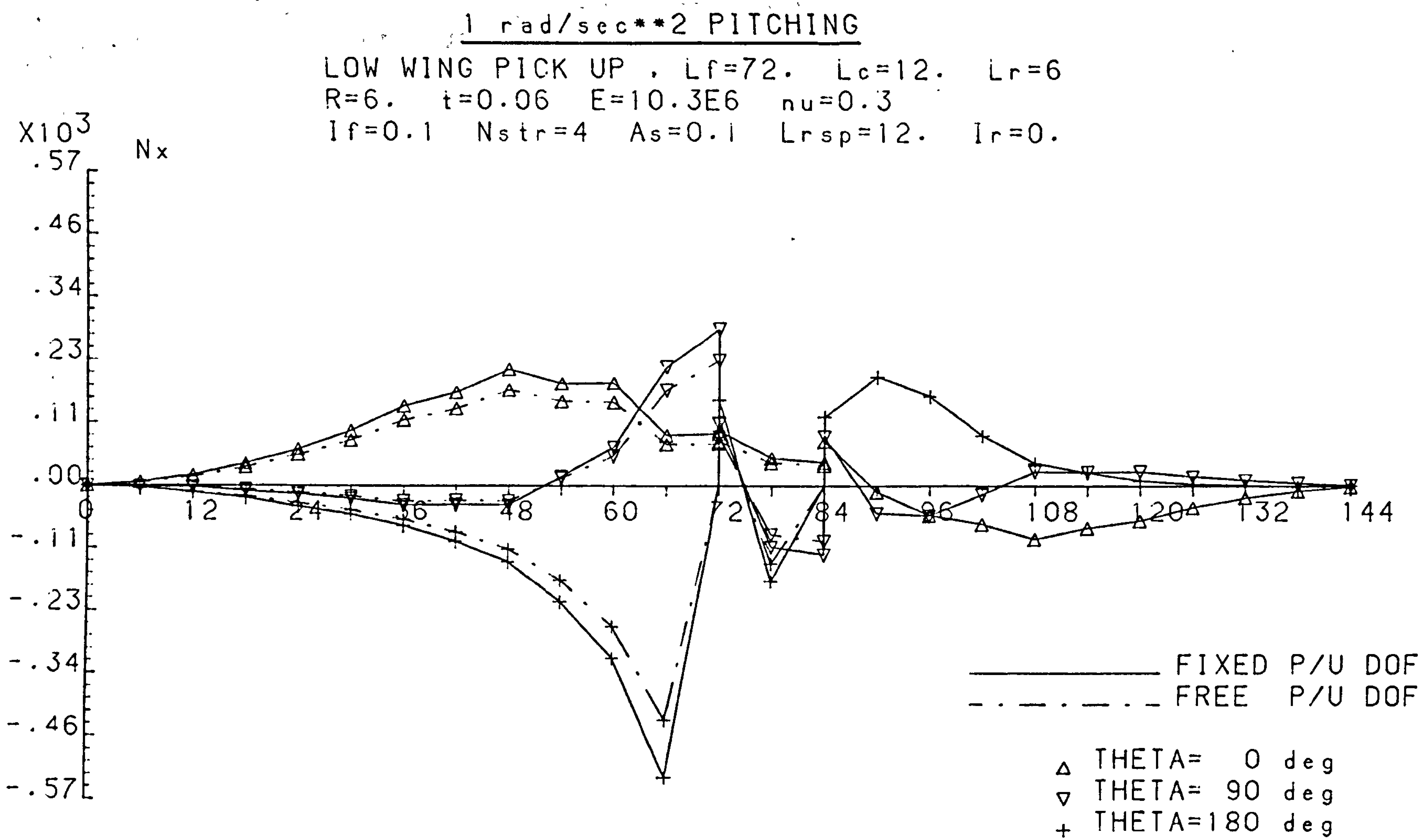

Fig.5.5.9b DIRECT STRESS RESULTANTS ALONG LONGITUDINAL AXIS

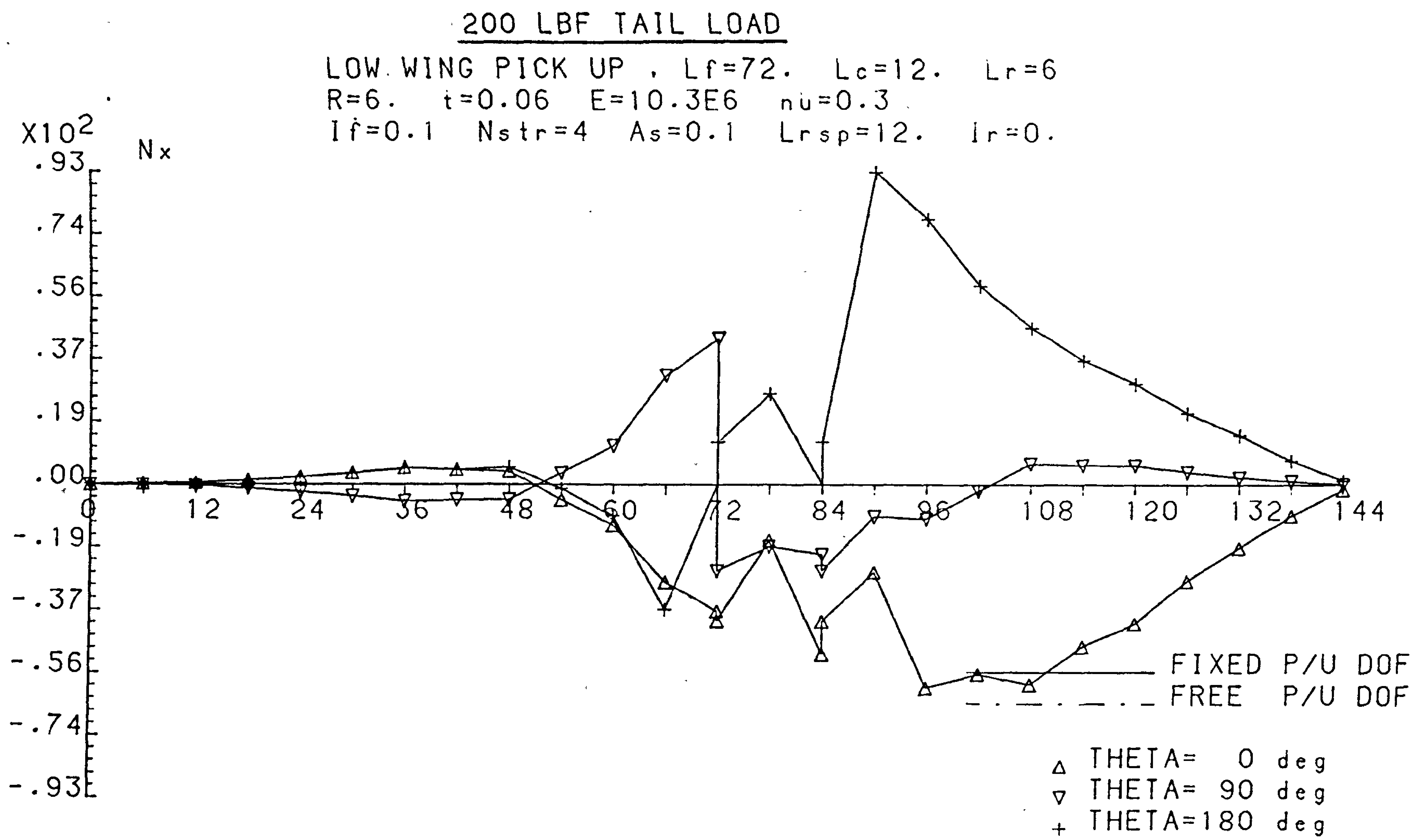

Fig.5.5.9c DIRECTSTRESS RESULTANTS ALONG LONGITUDINAL AXIS

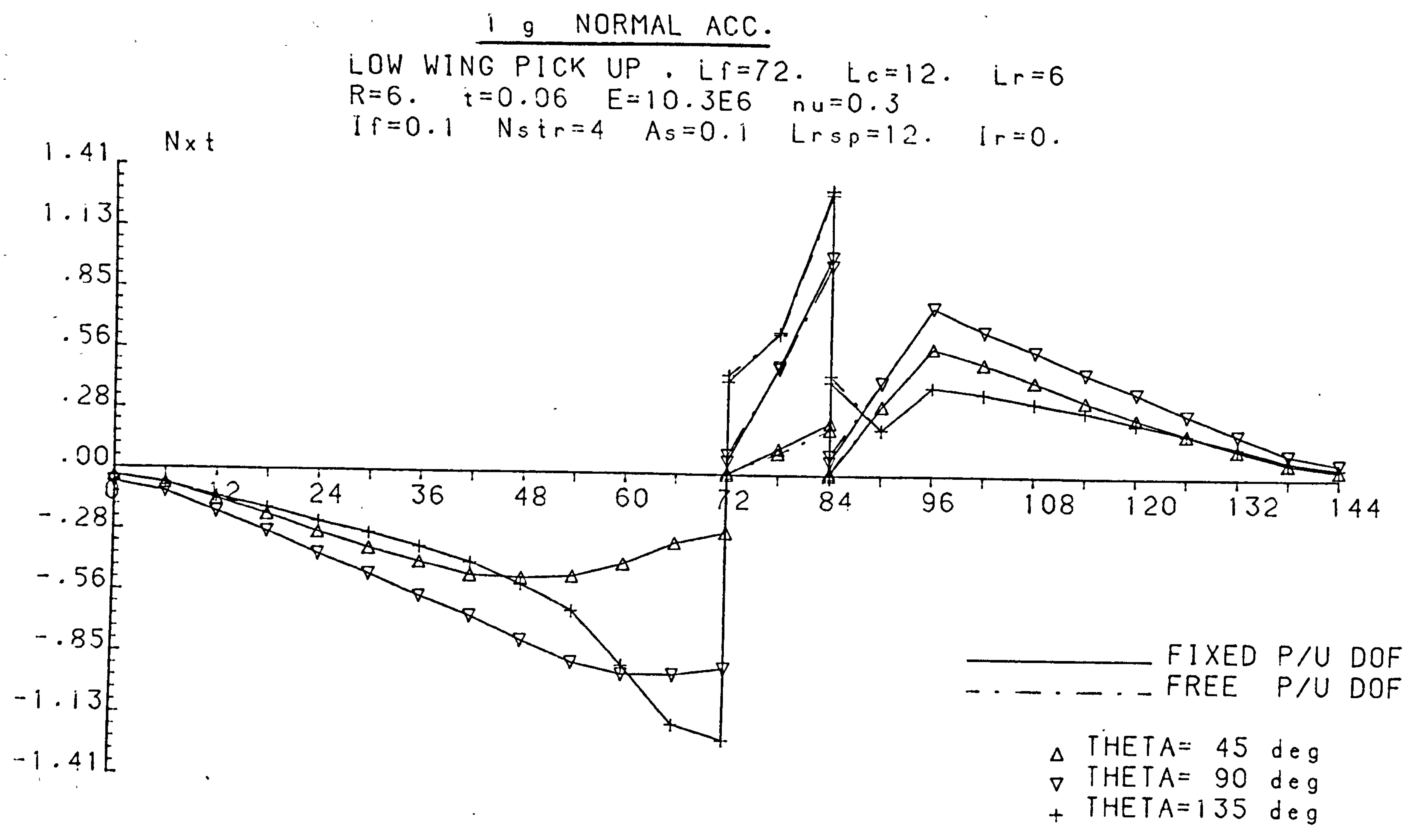

Fig.5.5.10a AVERAGED SHEAR STRESS RESULTANTS ALONG AXIAL AXIS

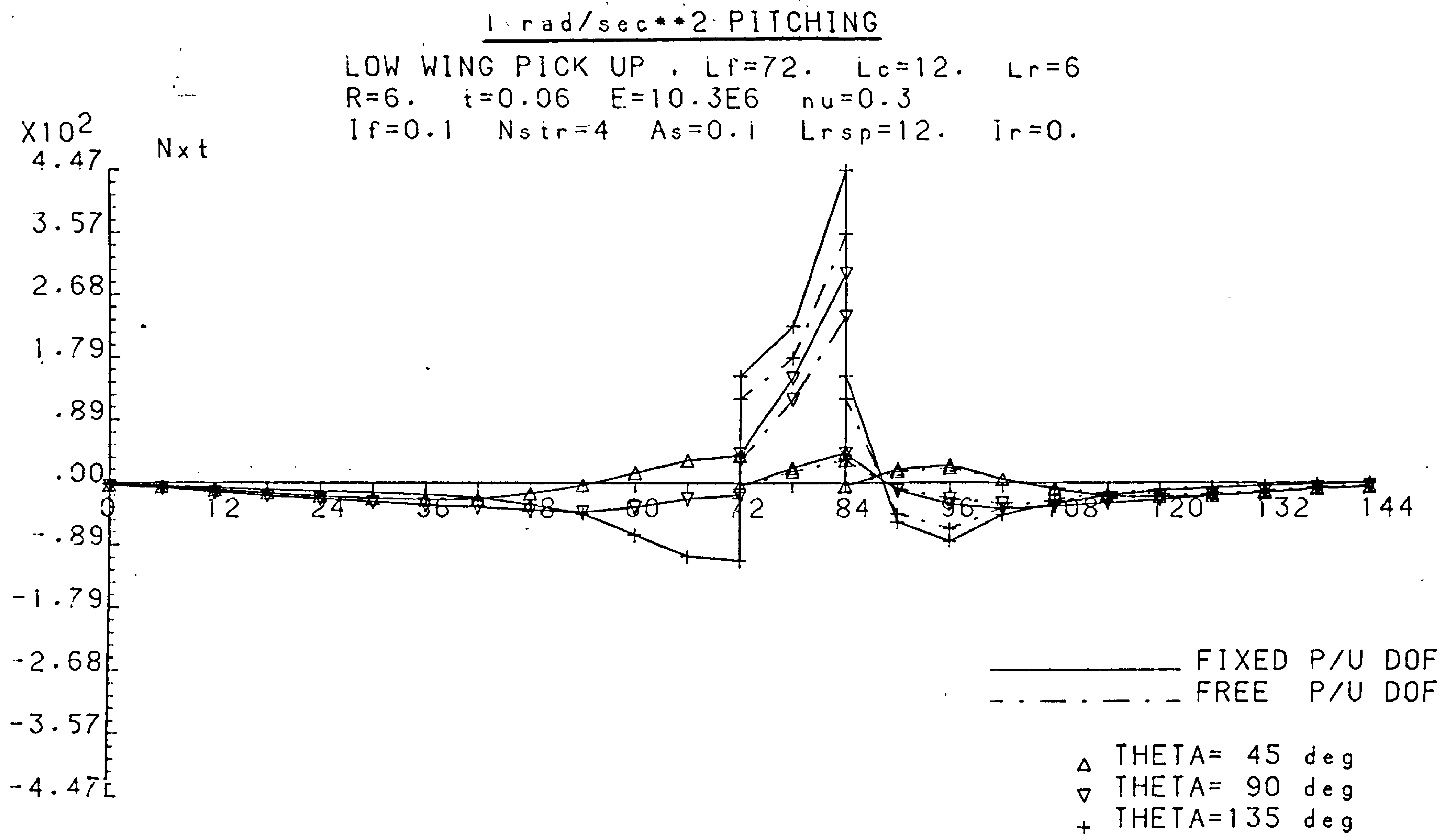

Fig.5.5.10b AVERAGED SHEAR STRESS RESULTANTS ALONG AXIAL AXIS

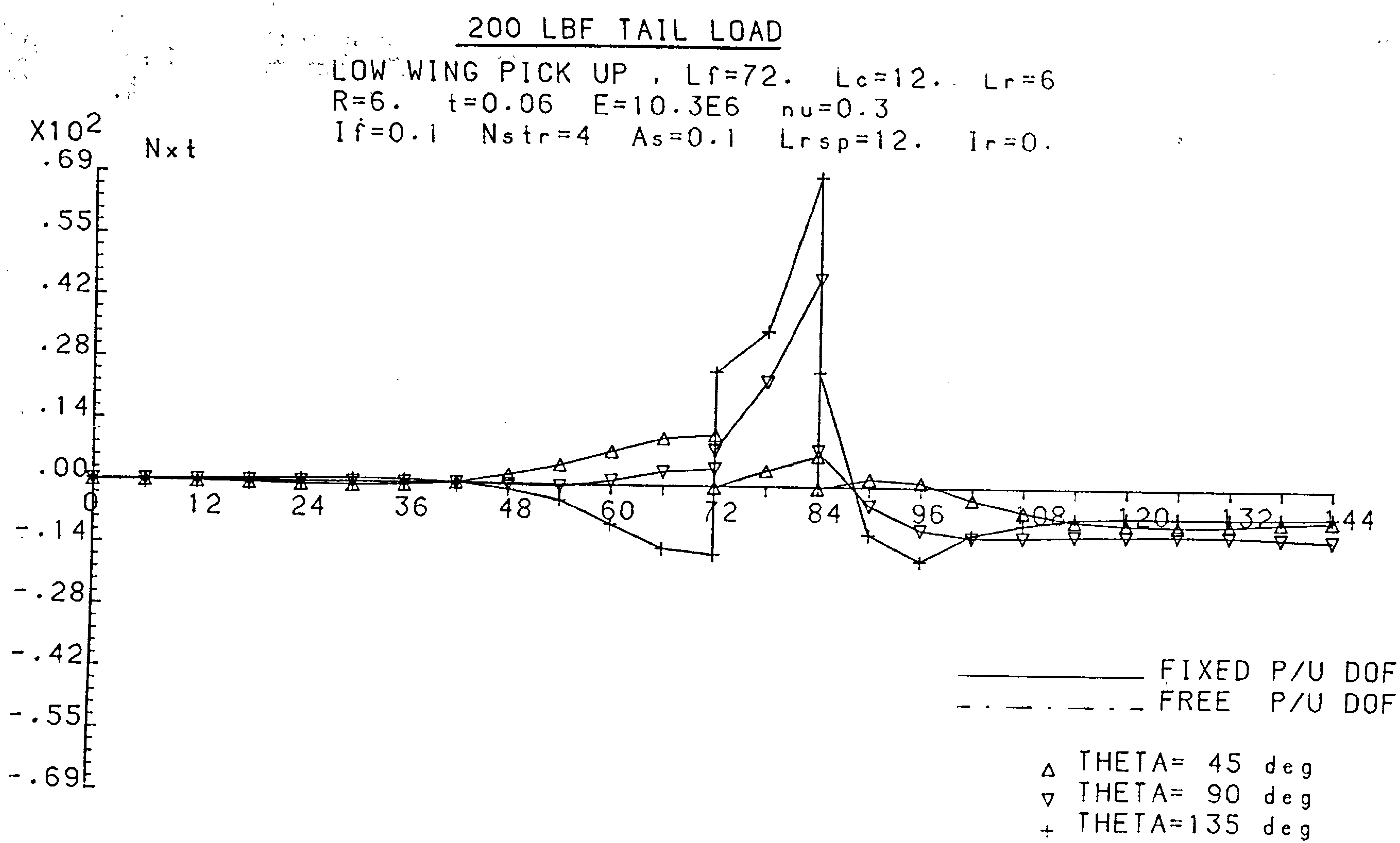

Fig.5.5.10c AVERAGED SHEAR STRESS RESULTANTS ALONG AXIAL AXIS

CENTRE BODY (72-12-60) : LOW WING PICK UP - TAIL LOAD

R=6. t=0.06 Nstr=4 As=0.1 Ir=0.01 If=0.1

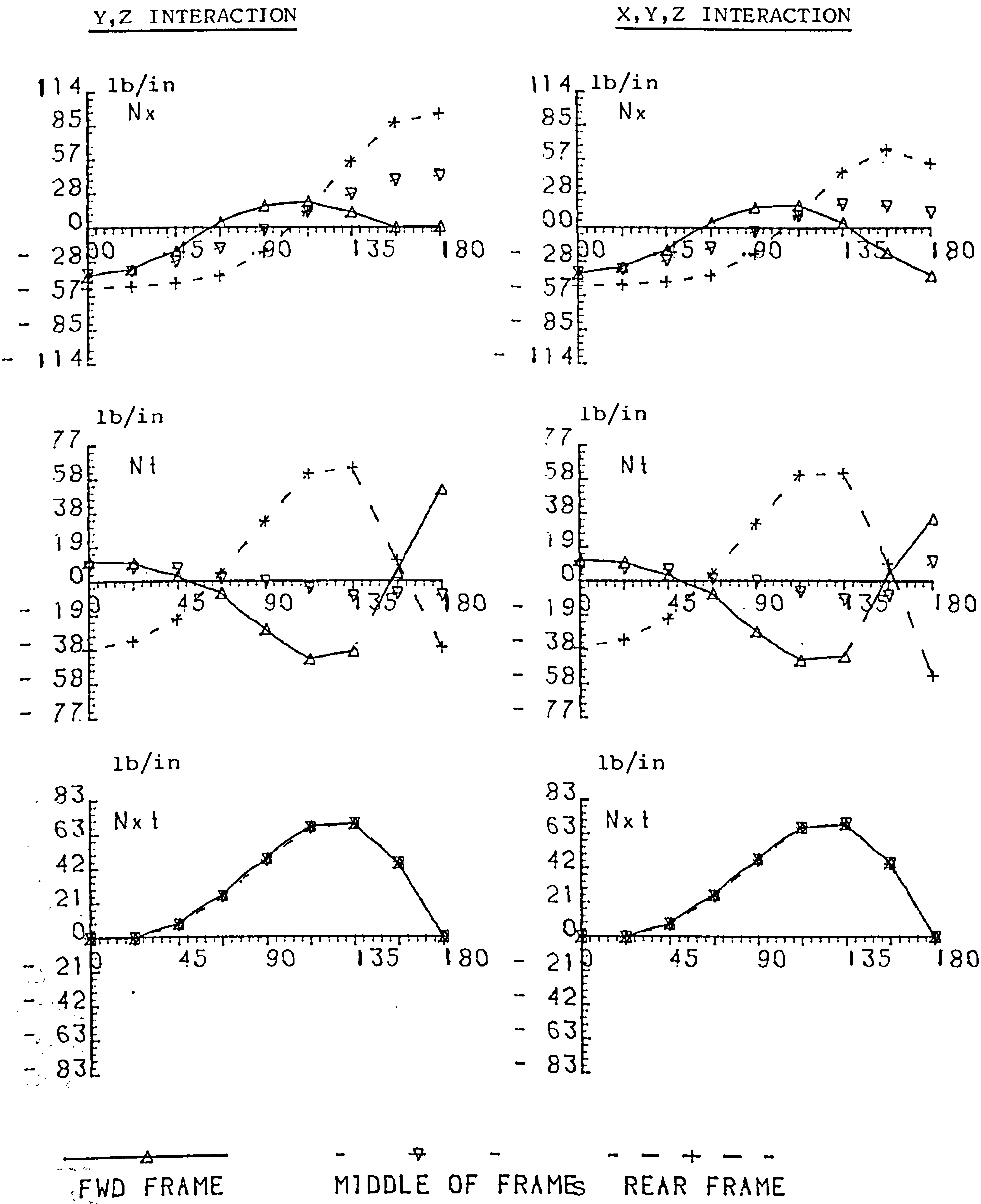

Fig 5.6.1 MEMBRANE STRESS RESULTANTS DIST. - INTERACTION TYPE EFFECT. (1)

* refer paragraph (v) of section 3.9.

CENTRE BODY (72-12-60) : LOW WING PICK UP - TAIL LOAD

R=6. t=0.06 Nstr=4 As=0.1 Ir=0.01 If=0.1

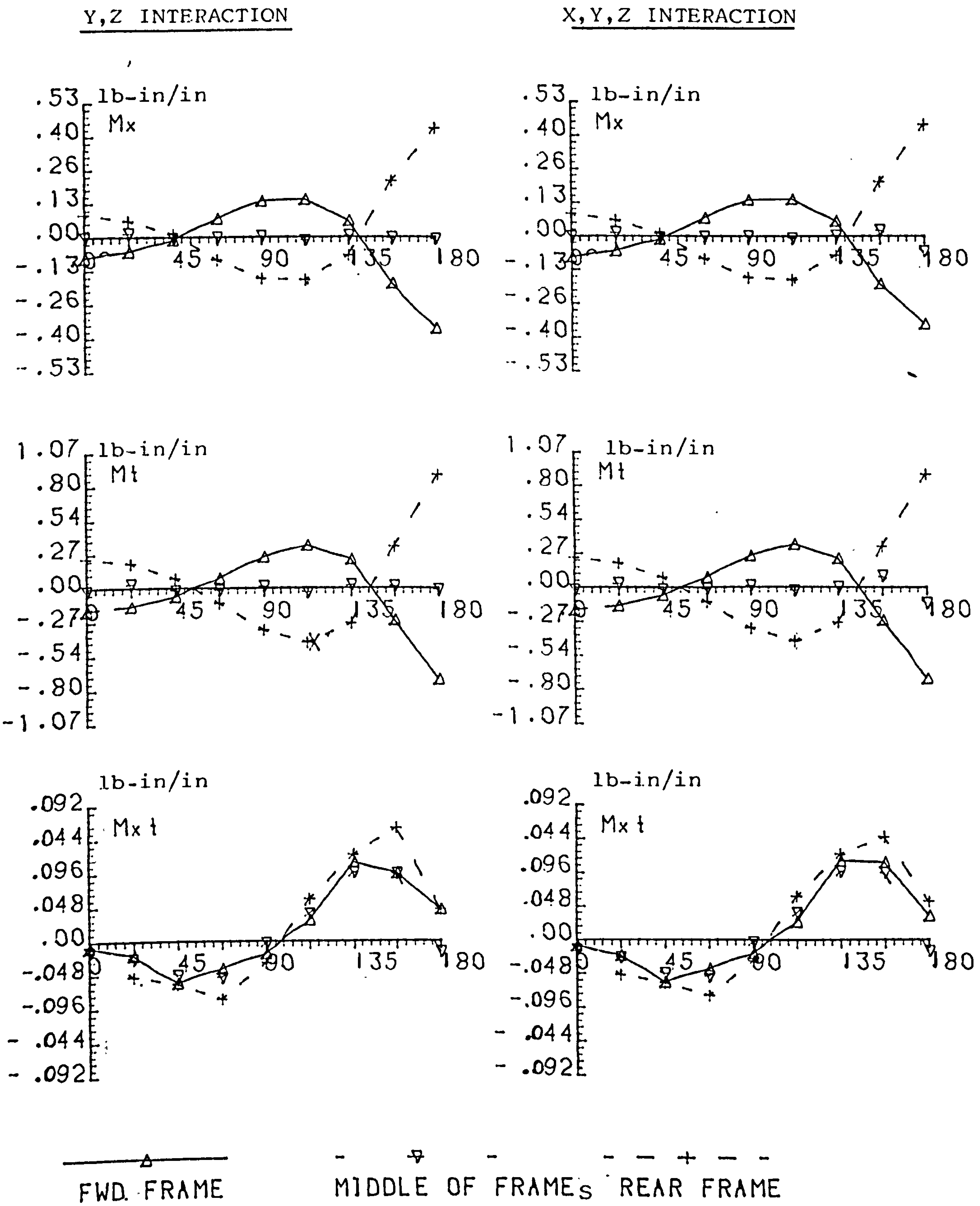

Fig.5.6.2 BENDING STRESS RESULTANTS DIST.-INTERACTION TYPE EFFECT (1)

CENTRE BODY (72-12-60) : MID WING PICK UP - TAIL LOAD

R=6. t=0.06 Nstr=4 As=0.1 Ir=0.01 If=0.1

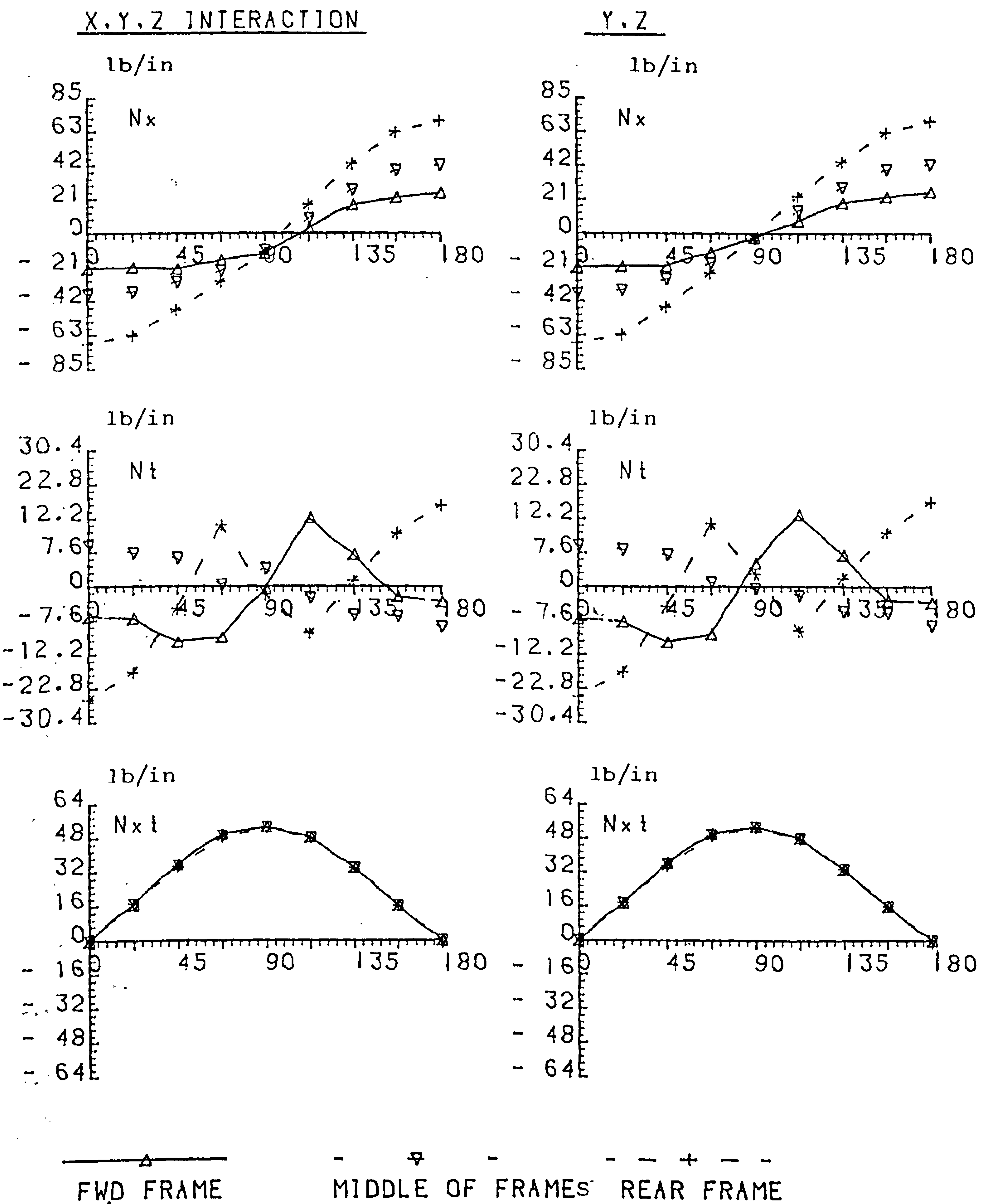

Fig.5.6.3 MEMBRANE STRESS RESULTANTS DIST.-WING PICK UP TYPE CHANGE (2)

CENTRE BODY (72-12-60); MID WING PICK UP - TAIL LOAD

R=6. t=0.06 Nstr=4 As=0.1 Ir=0.01 If=0.1

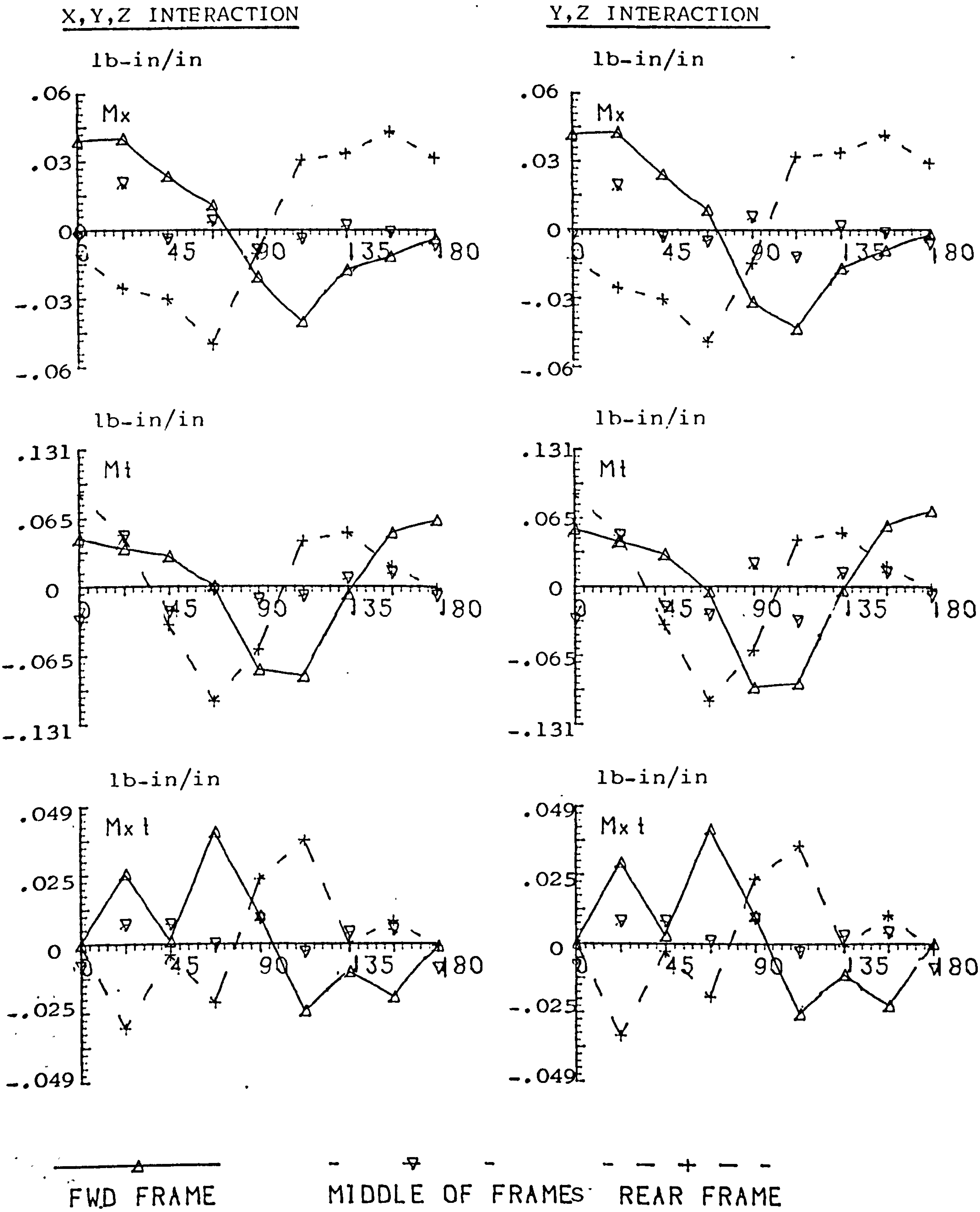

Fig.5.6.4 BENDING STRESS RESULTANTS DIST.-WING PICK UP TYPE CHANGE (2)

CENTRE BODY (72-12-60): MID WING PICK UP - TAIL LOAD

R=6. t=0.06 Nstr=4 As=0.1 Ir=0.01 If=0.1

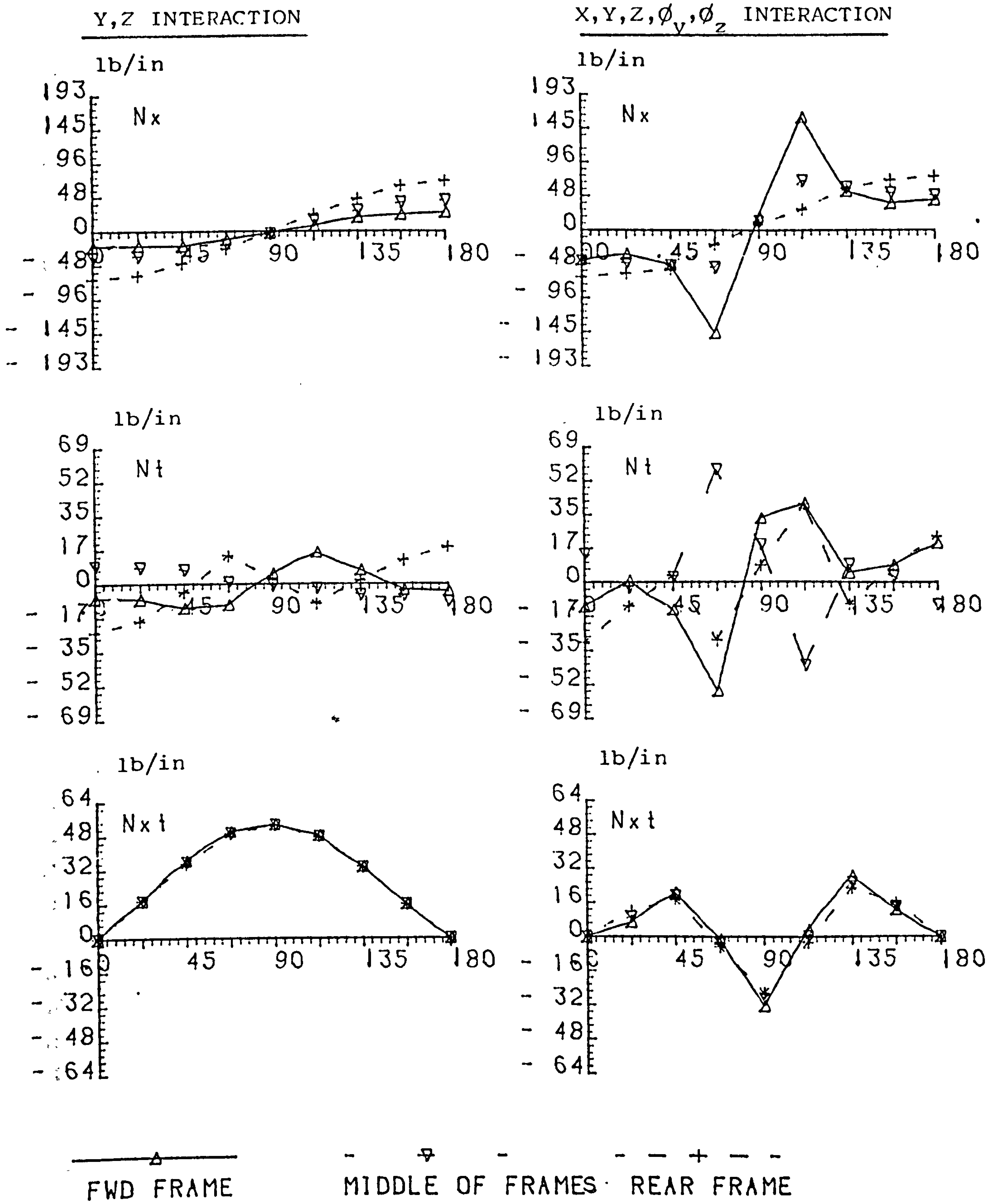

Fig.5.6.5 MEMBRANE STRESS RESULTANTS DIST.-WING PICK UP TYPE CHANGE (3)

CENTRE BODY (72-12-60): MID WING PICK UP - TAIL LOAD

R=6. t=0.06 Nstr=4 As=0.1 Ir=0.01 If=0.1

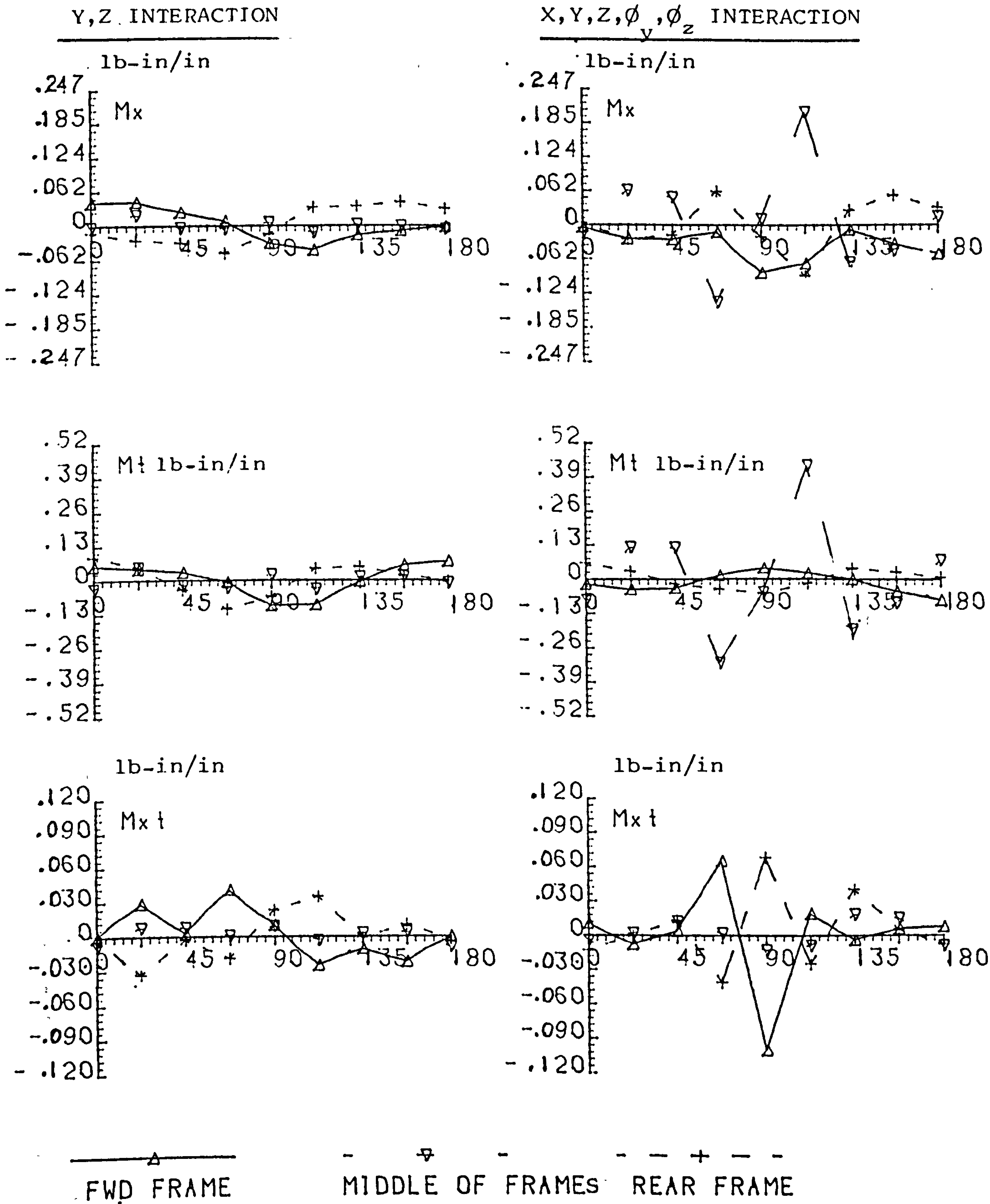

Fig.5.6.6 BENDING STRESS RESULTANTS DIST.-WING PICK UP TYPE CHANGE (2)

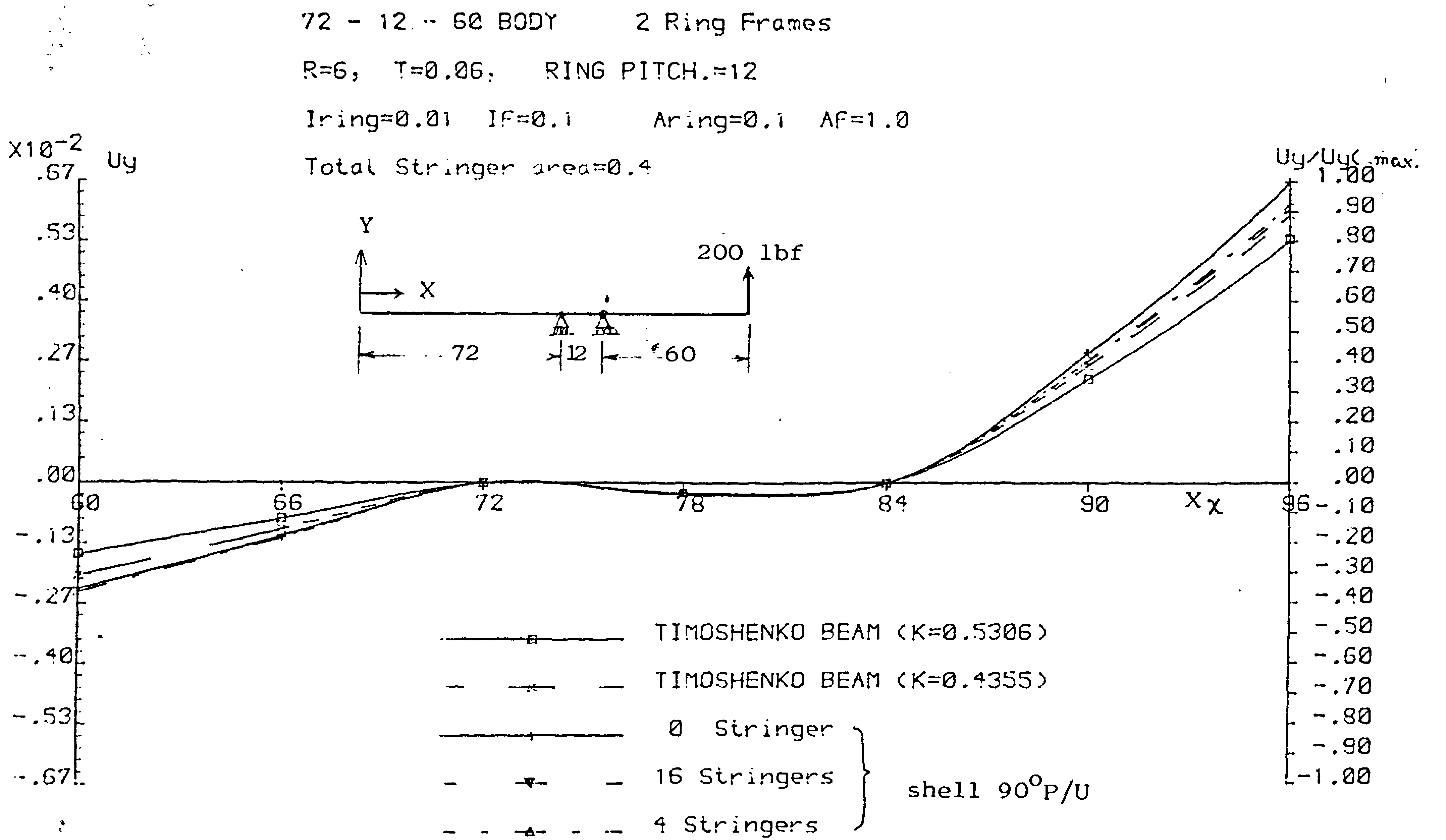

Fig.6.2.1EFFECT OF NO. OF STRINGERS ON THE CENTRE BODY VERTICAL DISPLACEMENT ALONG THE CENTRE LINE

RING FRAMED CENTRE BODY - MID WING ; TAIL LOAD

R=6.0 T=0.06 Rspac=12. IF/Ir=10 Astr=0.4 Const.

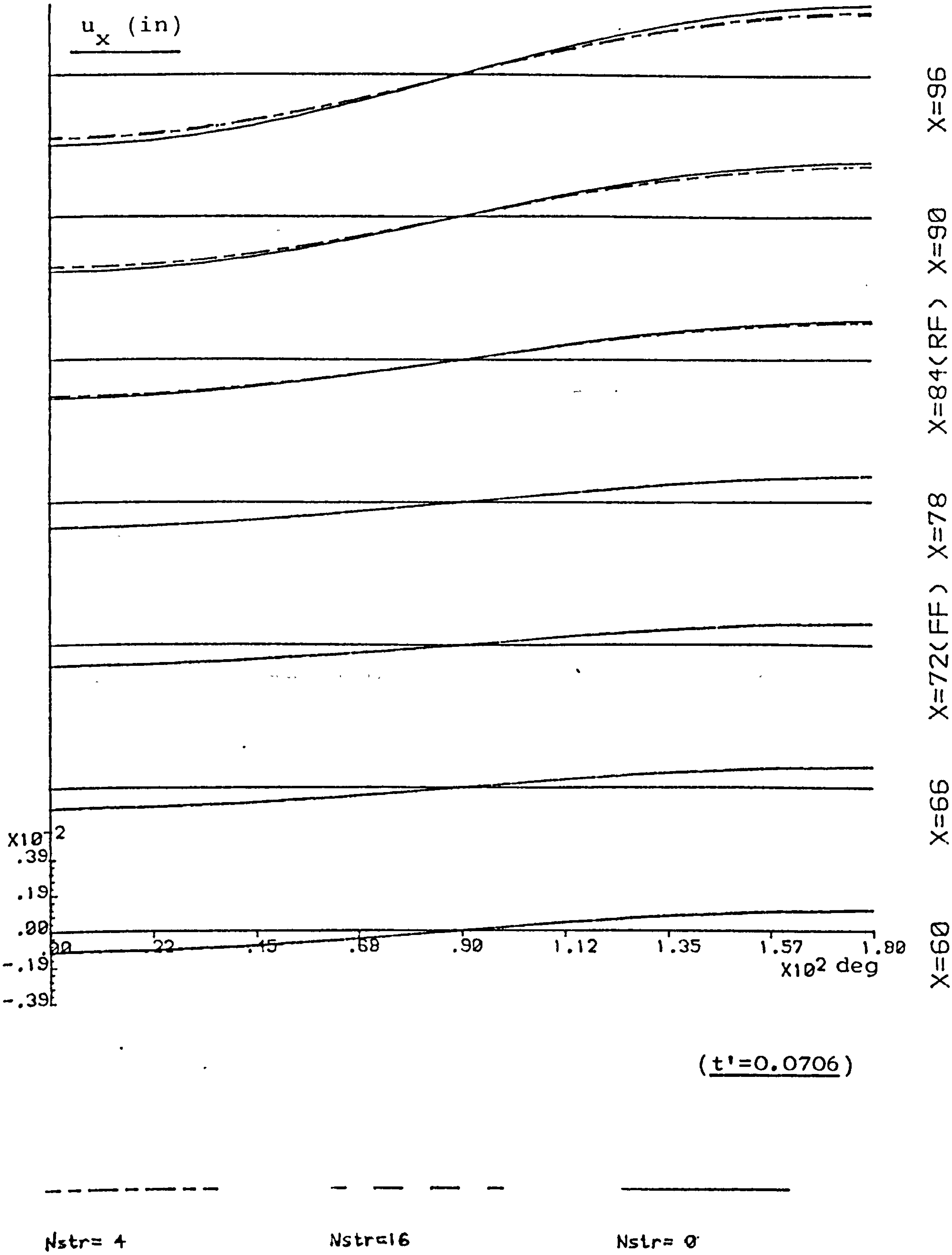

Fig.6.2.2 EFFECTS OF NO. OF STRINGERS CHANGE - AXIAL DISPL.

* refer paragraph (i) of section 3.9.

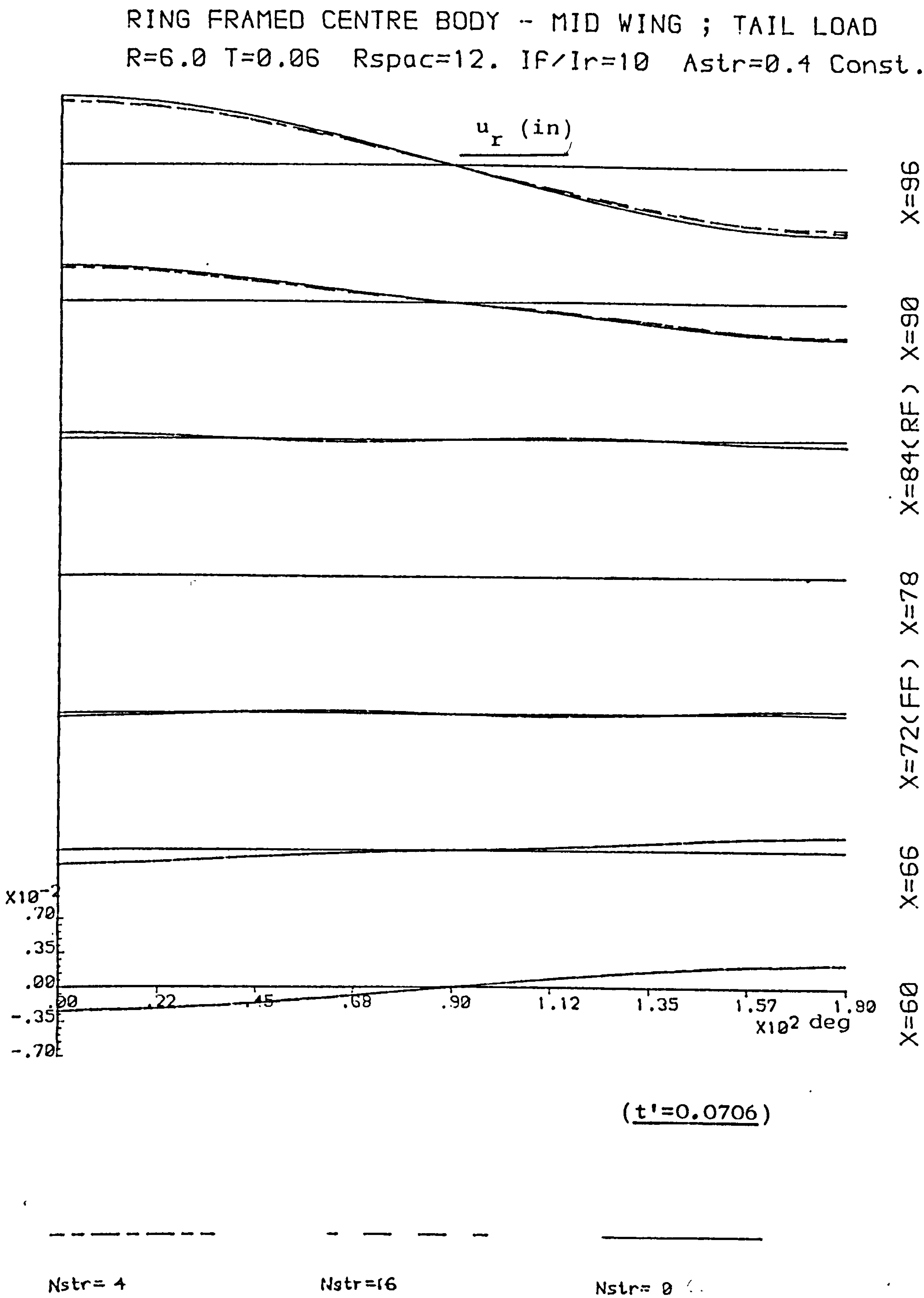

Fig.6.2.3 EFFECTS OF NO. OF STRINGERS CHANGE - RADIAL DISPL.

RING FRAMED CENTRE BODY - MID WING ; TAIL LOAD
R=6.0 T=0.06 Rspac=12. IF/Ir=10 Astr=0.4 Const.

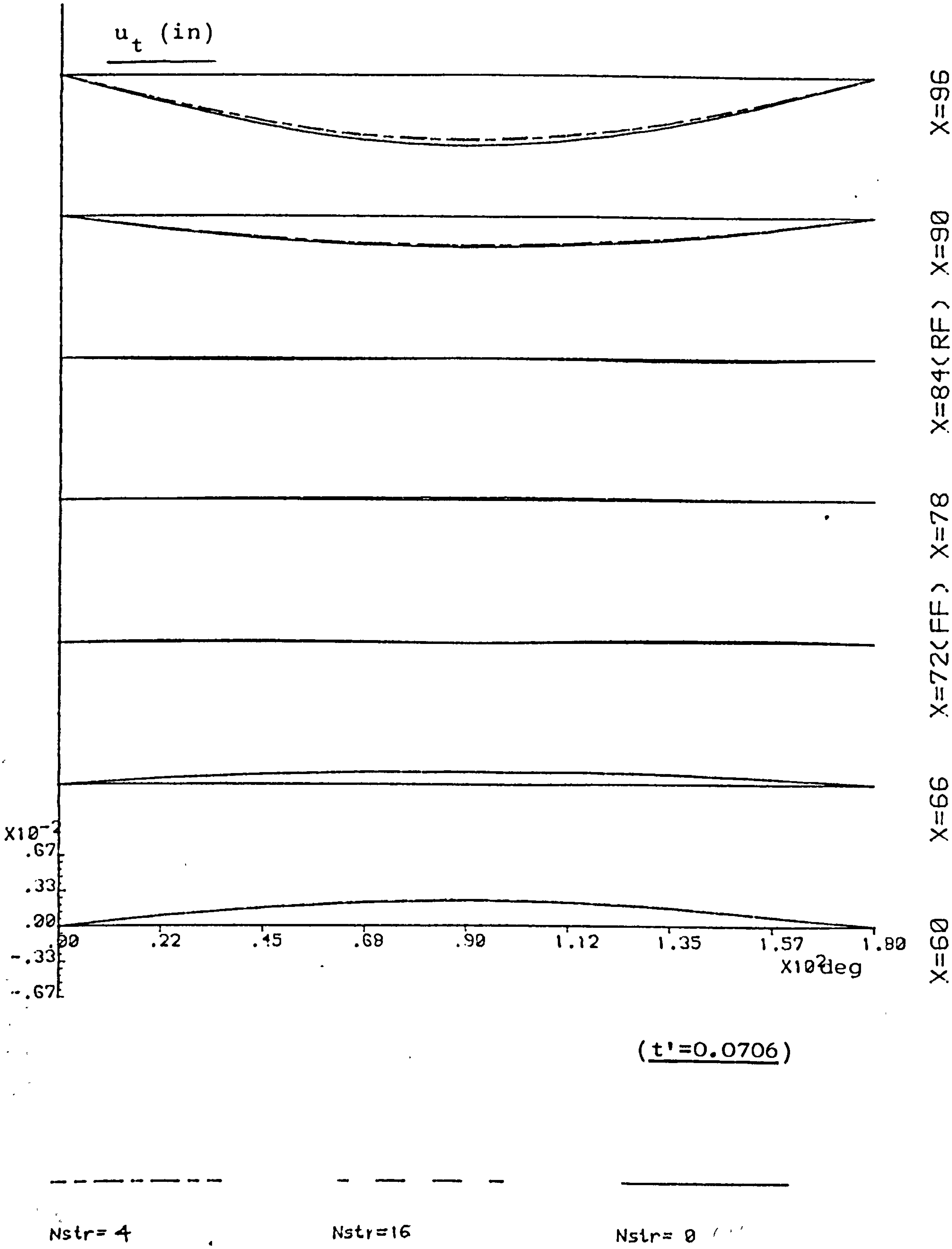

Fig.6.2.4 EFFECTS OF NO. OF STRINGERS CHANGE - TANG. DISPL.

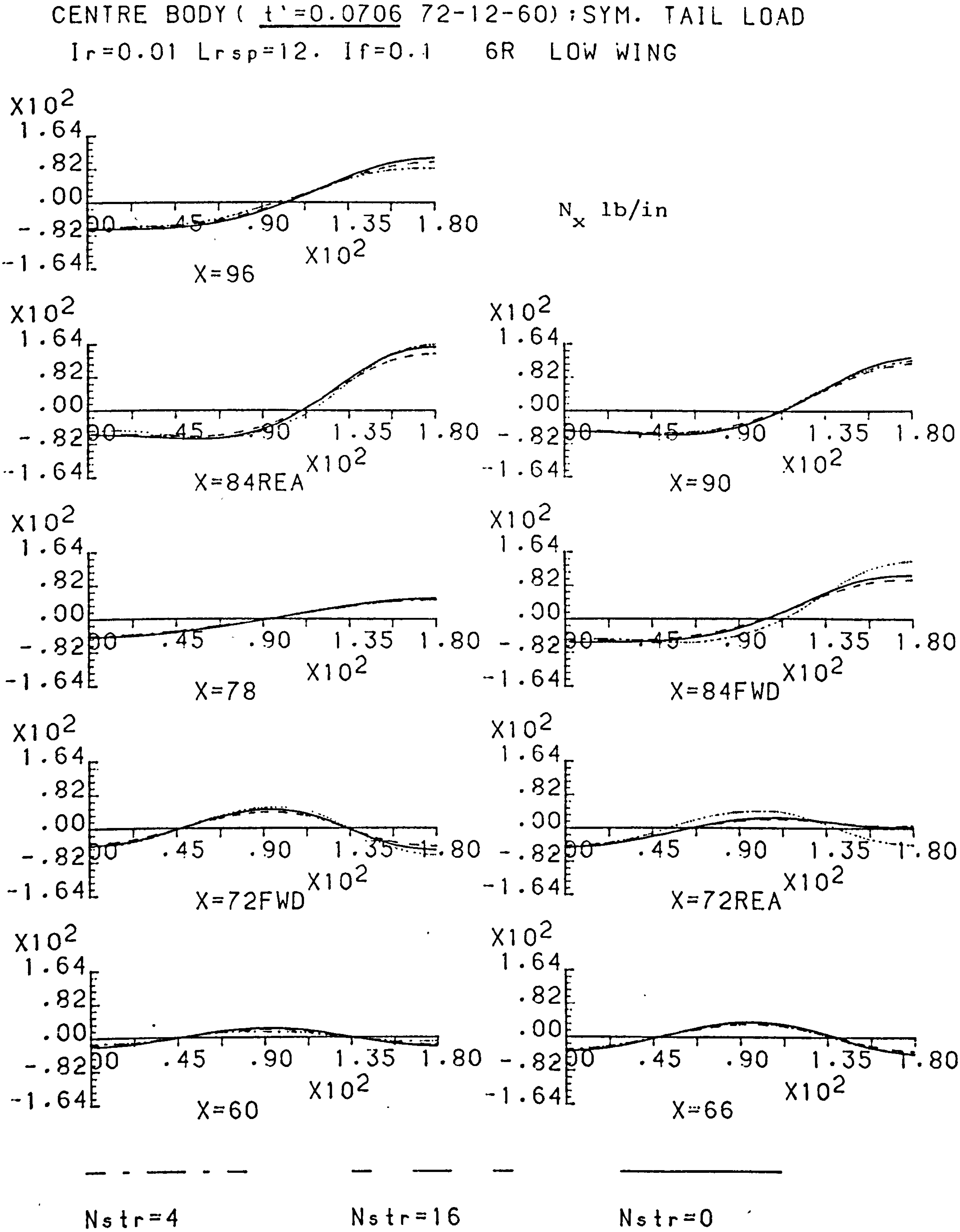

Fig.6.2.5 EFFECT OF NO. OF STRINGERS CHANGE - AXIAL STRESS

* refer paragraph (ii) of section 3.9.

CENTRE BODY (t'=0.0706 72-12-60) ; SYM. TAIL LOAD

Ir=0.01 Lrsp=12. If=0.1 6R LOW WING

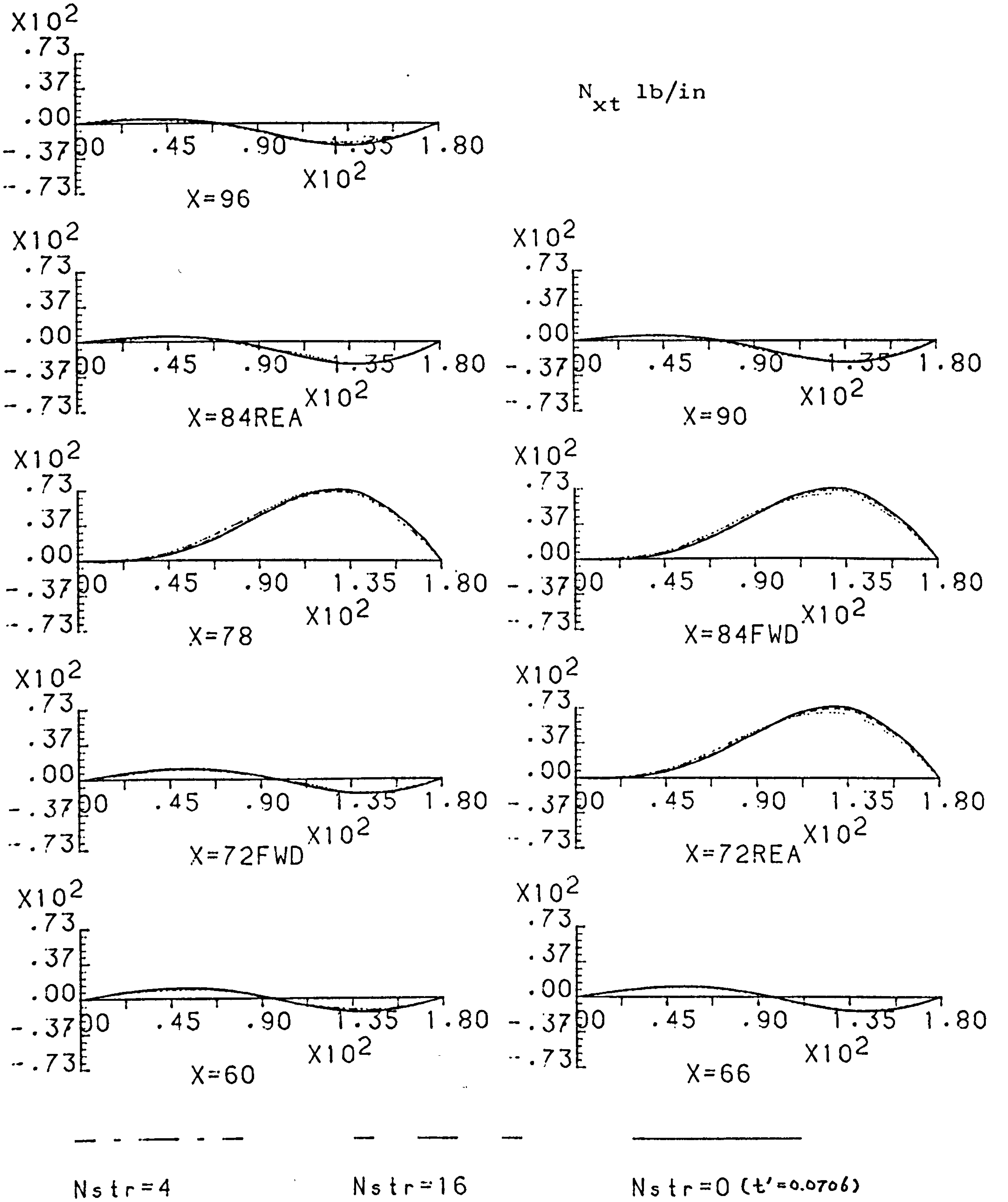

Fig.6.2.6 EFFECT OF NO. OF STRINGERS CHANGE - SHEAR STRESS

TAIL LOADING(PFF=1000, PrF=1200)

SYMMETRIC - LOW/HIGH WING (180 deg)

R=5.0 t=0.06 LF=72 Lc=12 Lr=60

Ar=0.1 Ir=0.01 IF=0.1

TOTAL STRINGER AREA=0.4, t'=0.0706

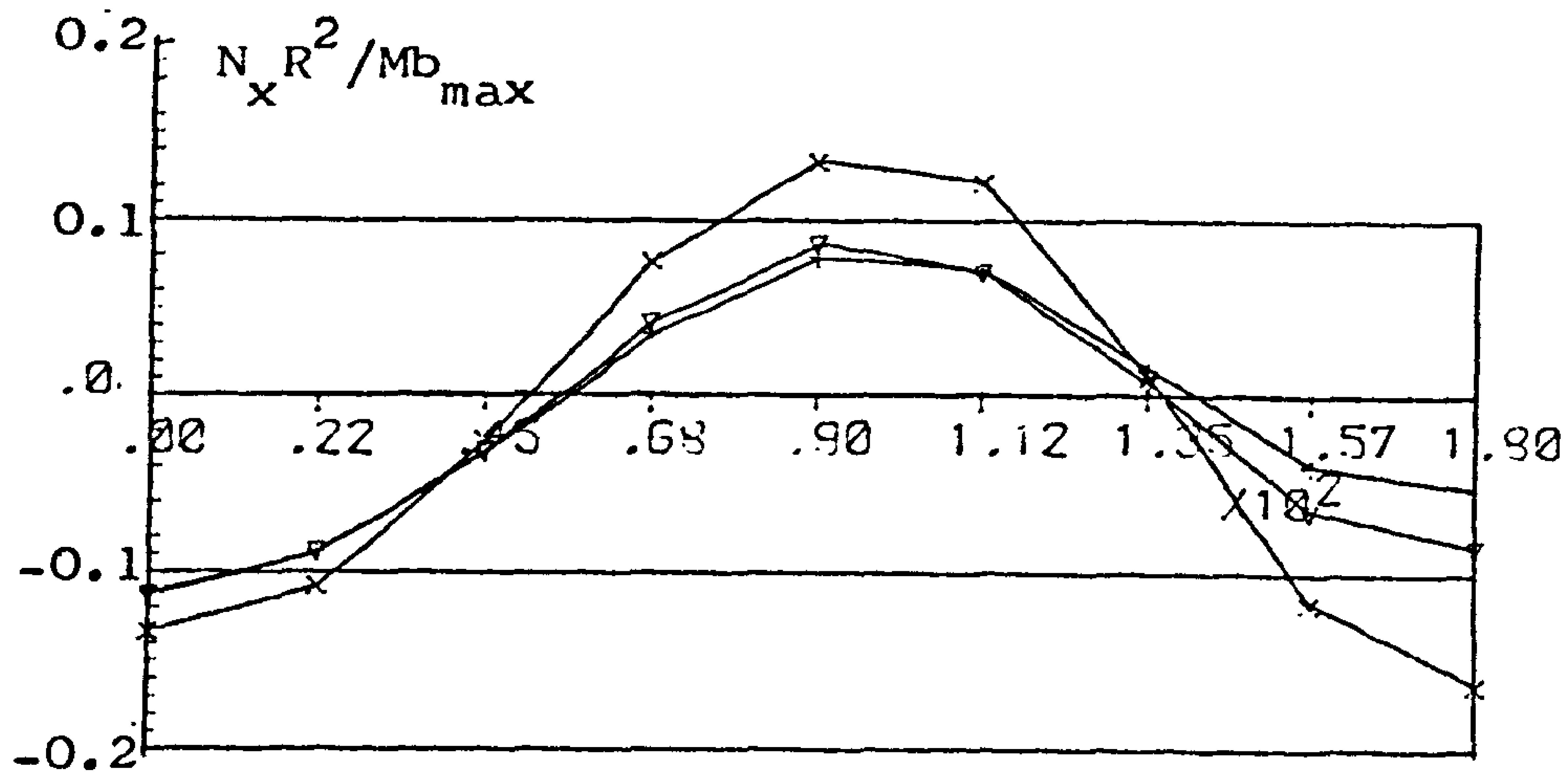

FORWARD FRAME

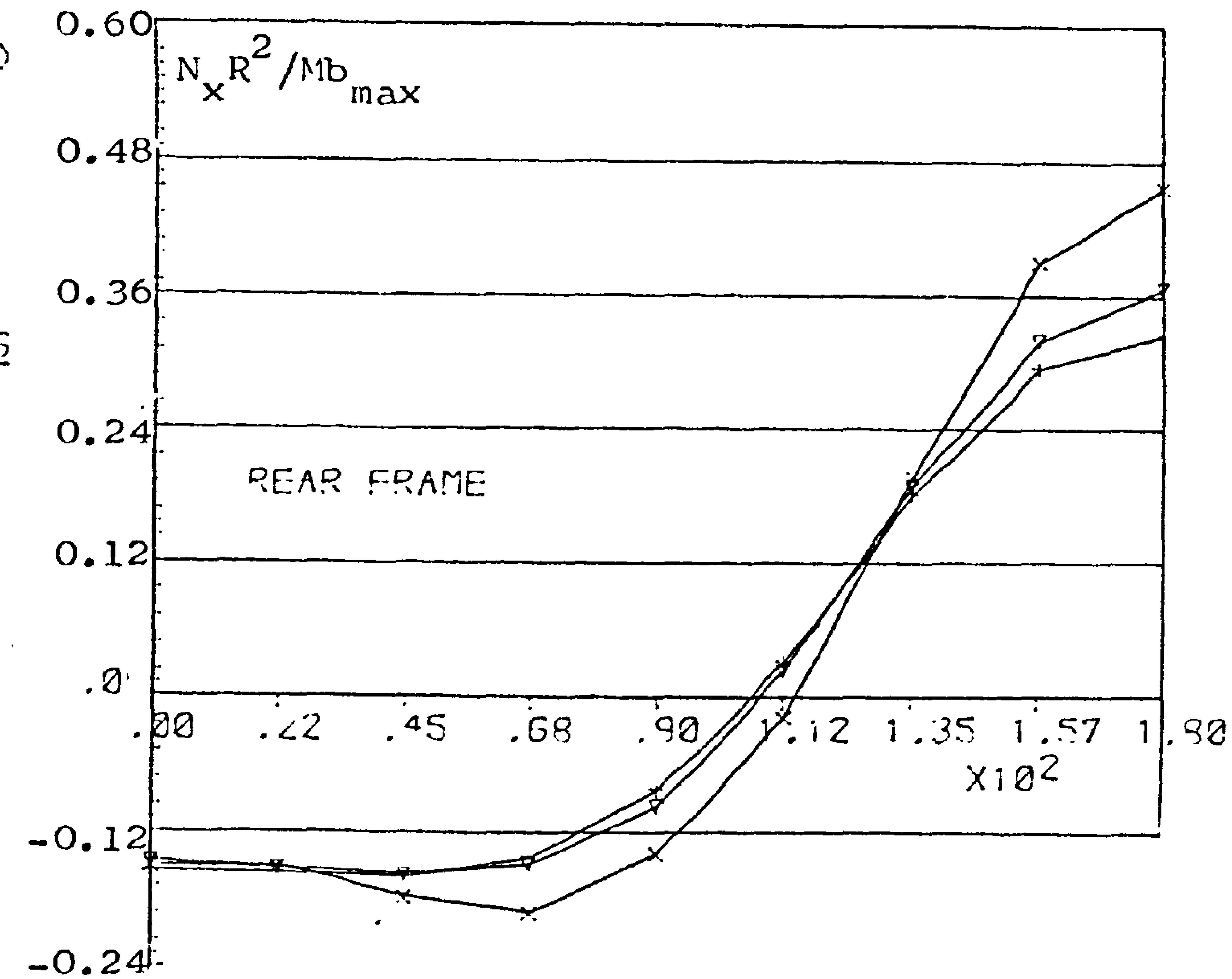

▽ Nstr=0 , t'=0.0706

+ Nstr=16 , t =0.06

× Nstr=4 , t =0.06

* Mb_{max} : Maximum Bending Moment
= 12000 lbf-in

Fig 6.2.7 DIRECT STRESS DISTR. AT FRAME STA. - NO. OF STRINGERS CHANGE

MIDDLE OF 2 FRAMES; TAIL LOAD

LF=72. Lc=12. Lr=60.

R=6.0 Lrsp=12. Ar=0.1 Ir=0.01

2 Ring Frame IF=0.1 AF=1.0

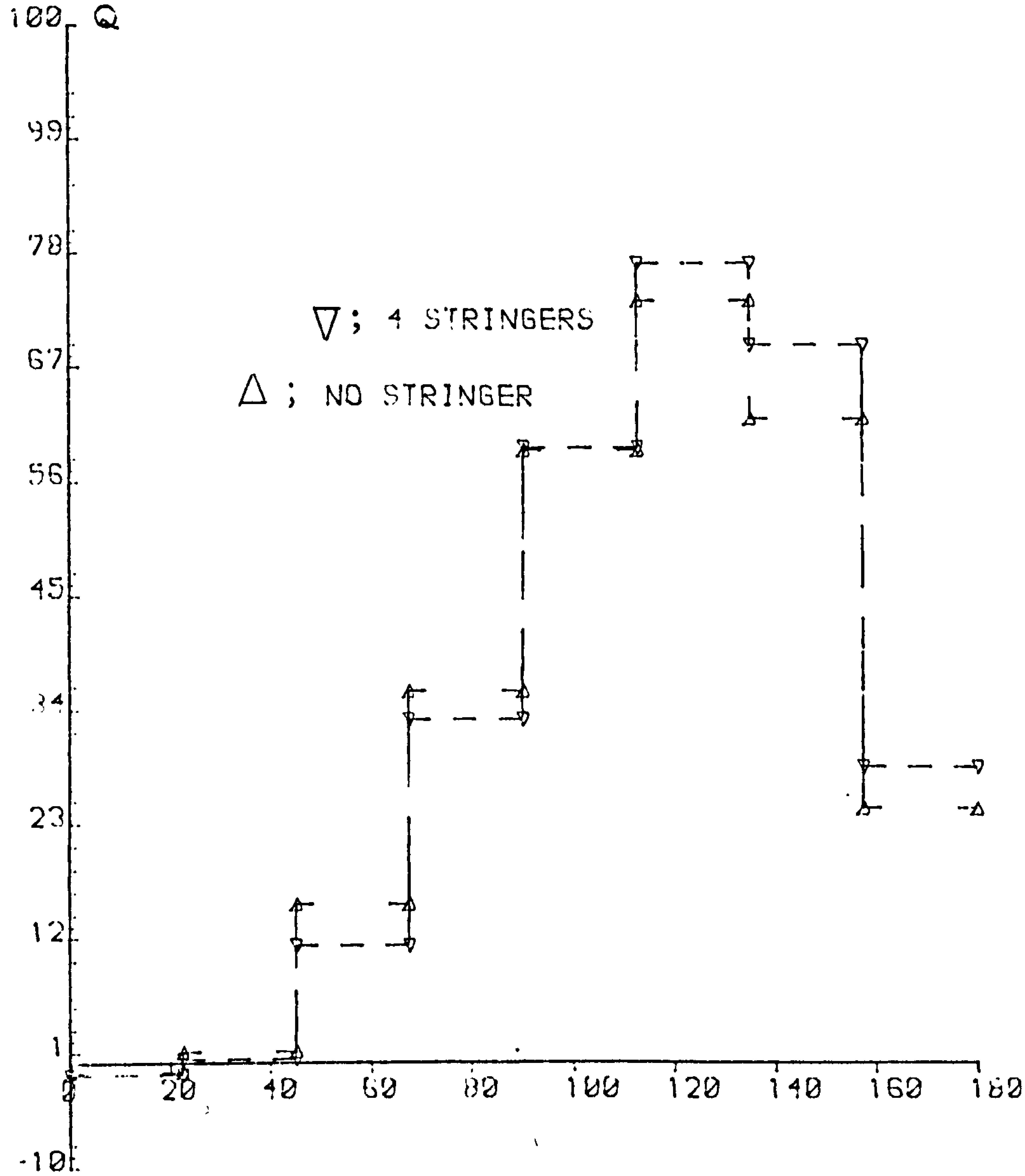

Fig.6.2.8 EFFECT OF 4 STRINGERS TO SHEAR FLOW DISTRIBUTION

Fig.6.2.9 SHEAR FLOW FROM SHELL TO FRAME - NO. OF STRINGERS CHANGE

CENTRE BODY (t'=0.0706 72-12-60) : SYM. TAIL LOAD
Ir=0.01 Lrsp=12. If=0.1 6R LOW WING

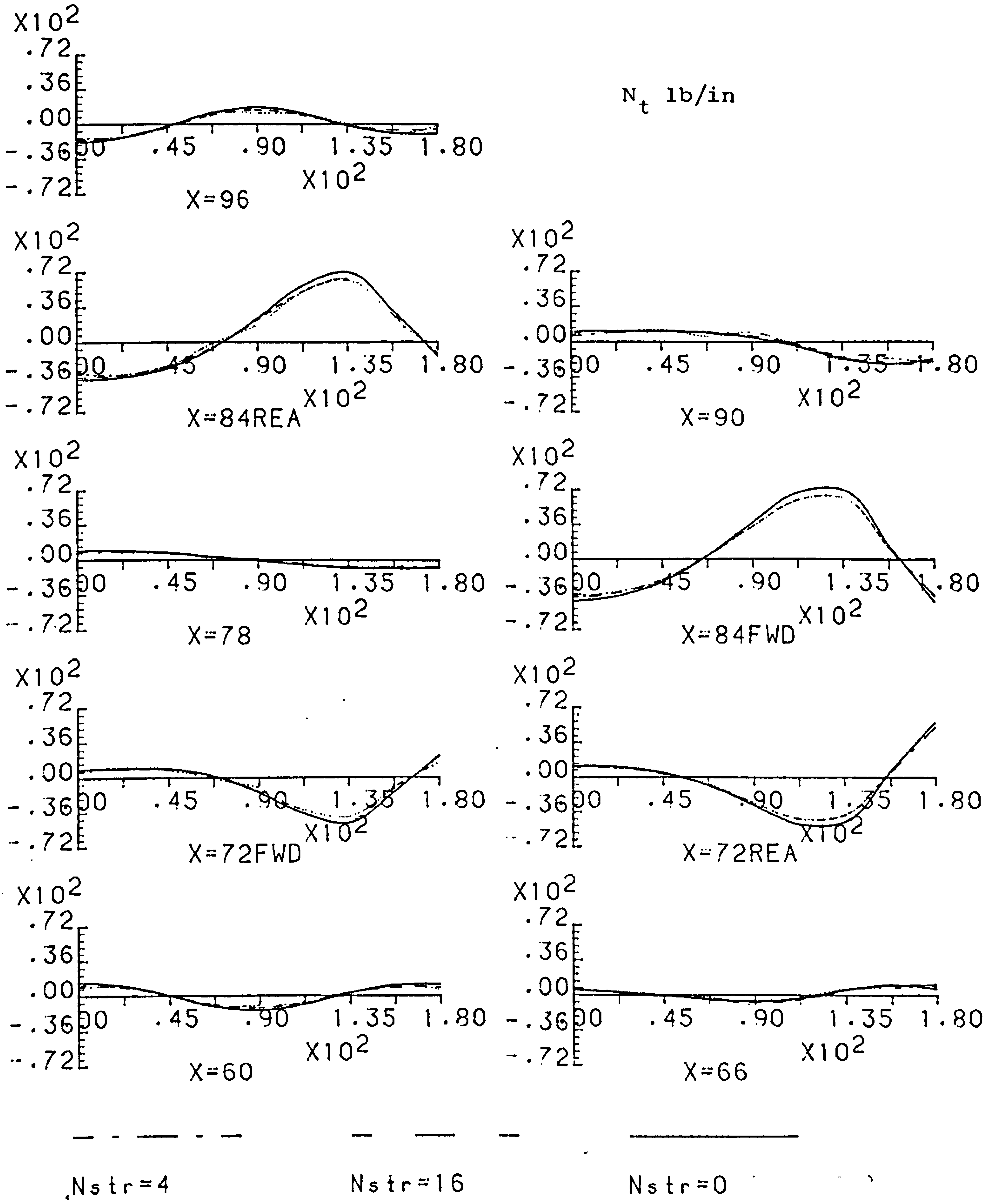

Fig.6.2.10 EFFECT OF NO. OF STRINGERS CHANGE - HOOP STRESS

CENTRE BODY (t'=0.0706 72-12-60) ; SYM. TAIL LOAD

Ir=0.01 Lrsp=12. If=0.1 6R LOW WING

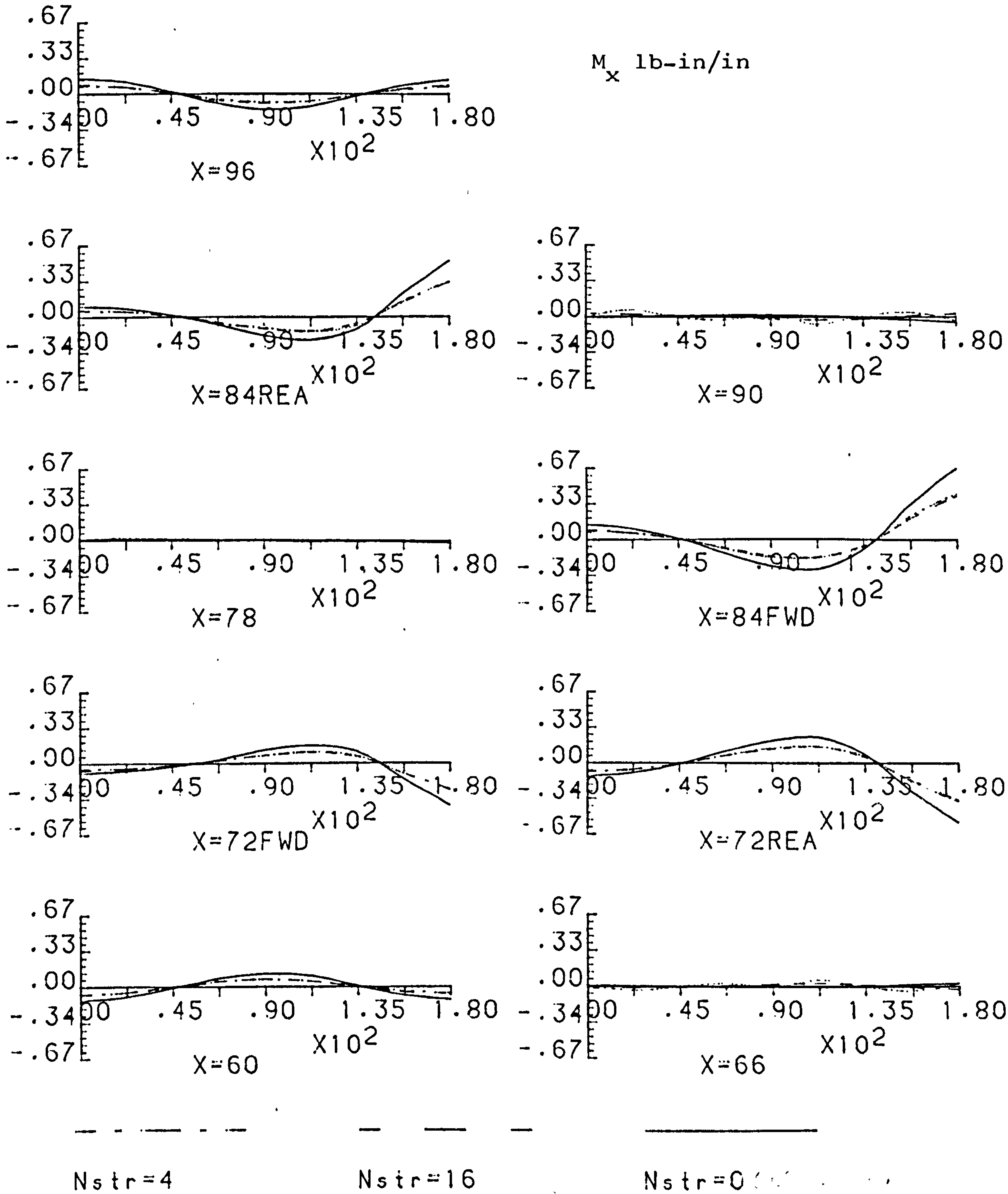

Fig.6.2.11 EFFECT OF NO. OF STRINGERS CHANGE - AXIAL BEND.

CENTRE BODY(t'=0.0706 72-12-60);SYM. TAIL LOAD
Ir=0.01 Lrsp=12. If=0.1 6R LOW WING

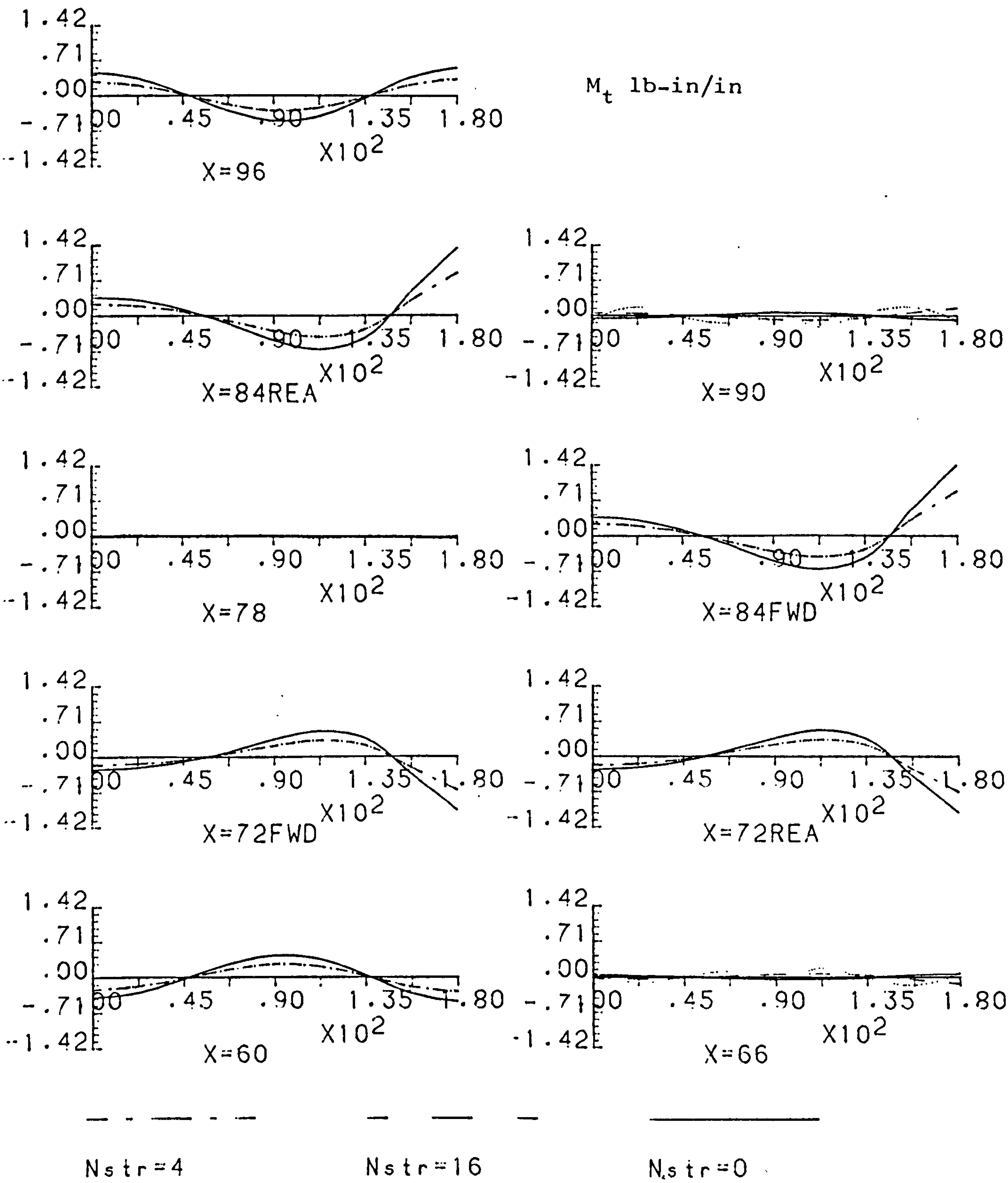

Fig.6.2.12 EFFECT OF NO. OF STRINGERS CHANGE - CIRC. BEND.

CENTRE BODY(t'=0.0706 72-12-60);SYM. TAIL LOAD

Ir=0.01 Lrsp=12. If=0.1 6R LOW WING

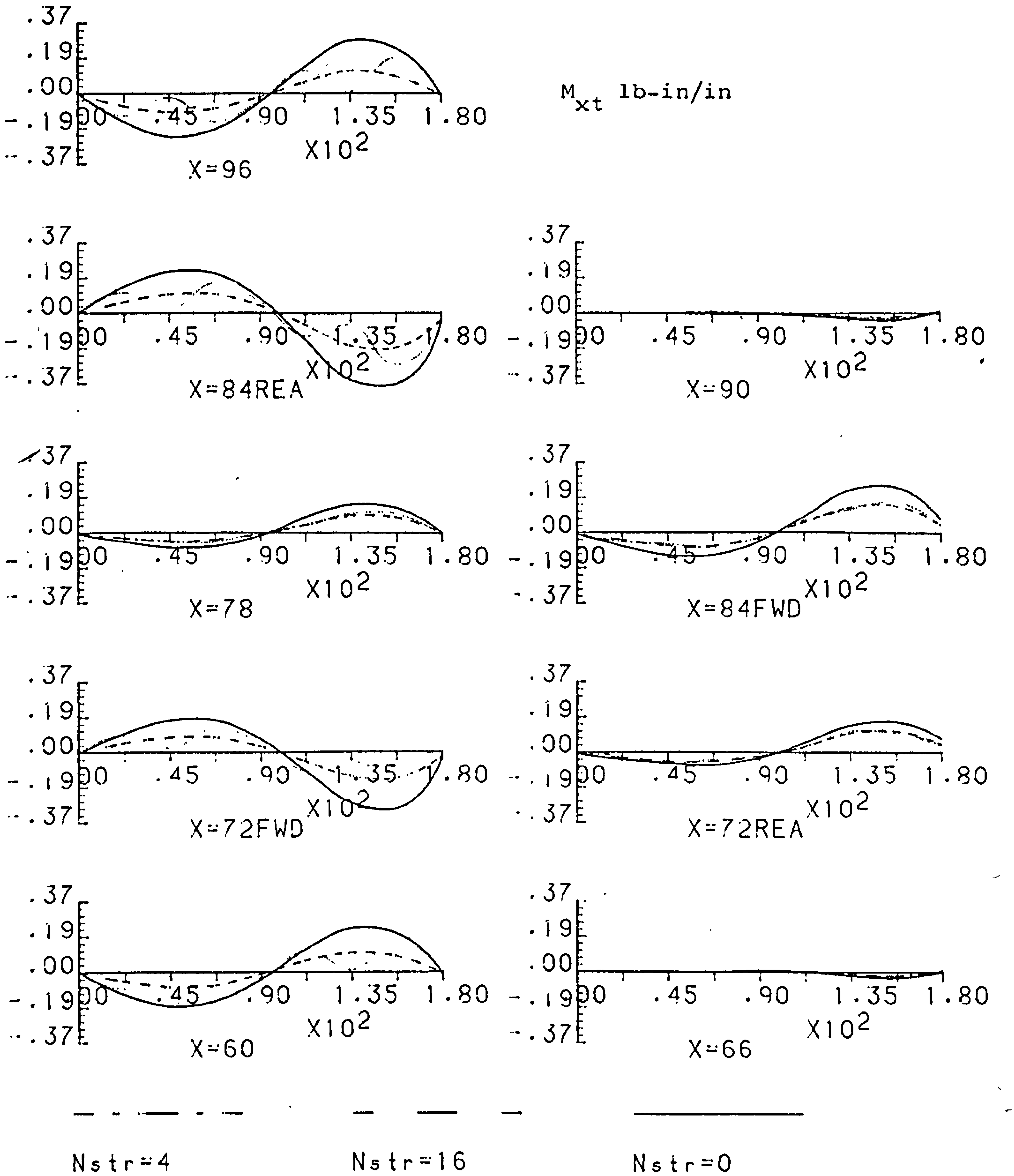

Fig.6.2.13 EFFECT OF NO. OF STRINGERS CHANGE - TWISTING

CENTRE BODY (12R, Nstr = 4, 72-12-60) : SYM. TAIL (F=400LBF)
Ir=0.8 Af=2.0 Ir=0.08 Lrsp=12. 180 deg PICK UP

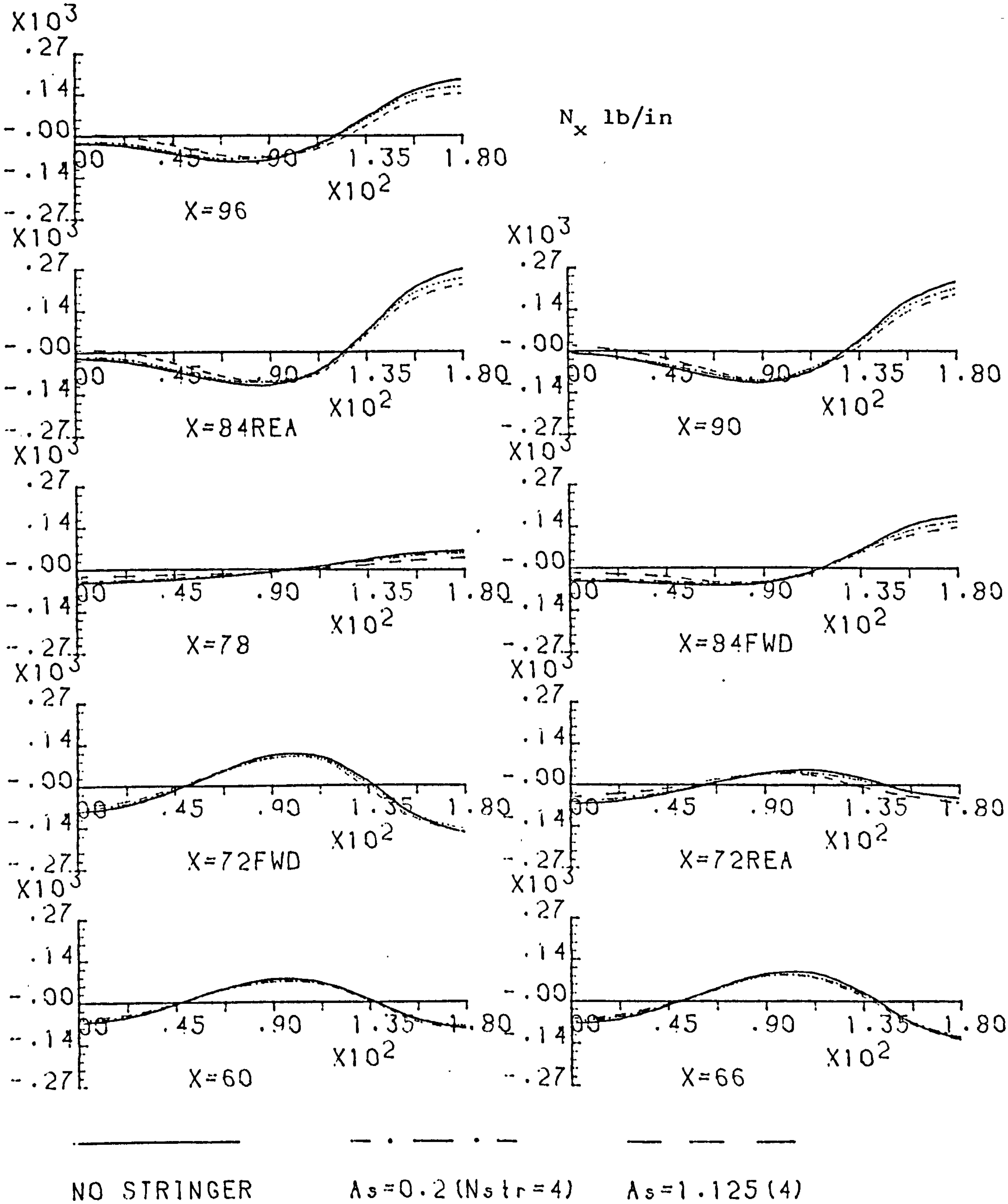

Fig.6.2.14 EFFECT OF STRINGER AREA CHANGE - DIRECT STRESS

CENTRE BODY (12R, Nstr=4, 72-12-60): SYM. TAIL (F=400LBF)
Ir=0.8 Af=2.0 Ir=0.08 Lrsp=12. 180 deg PICK UP

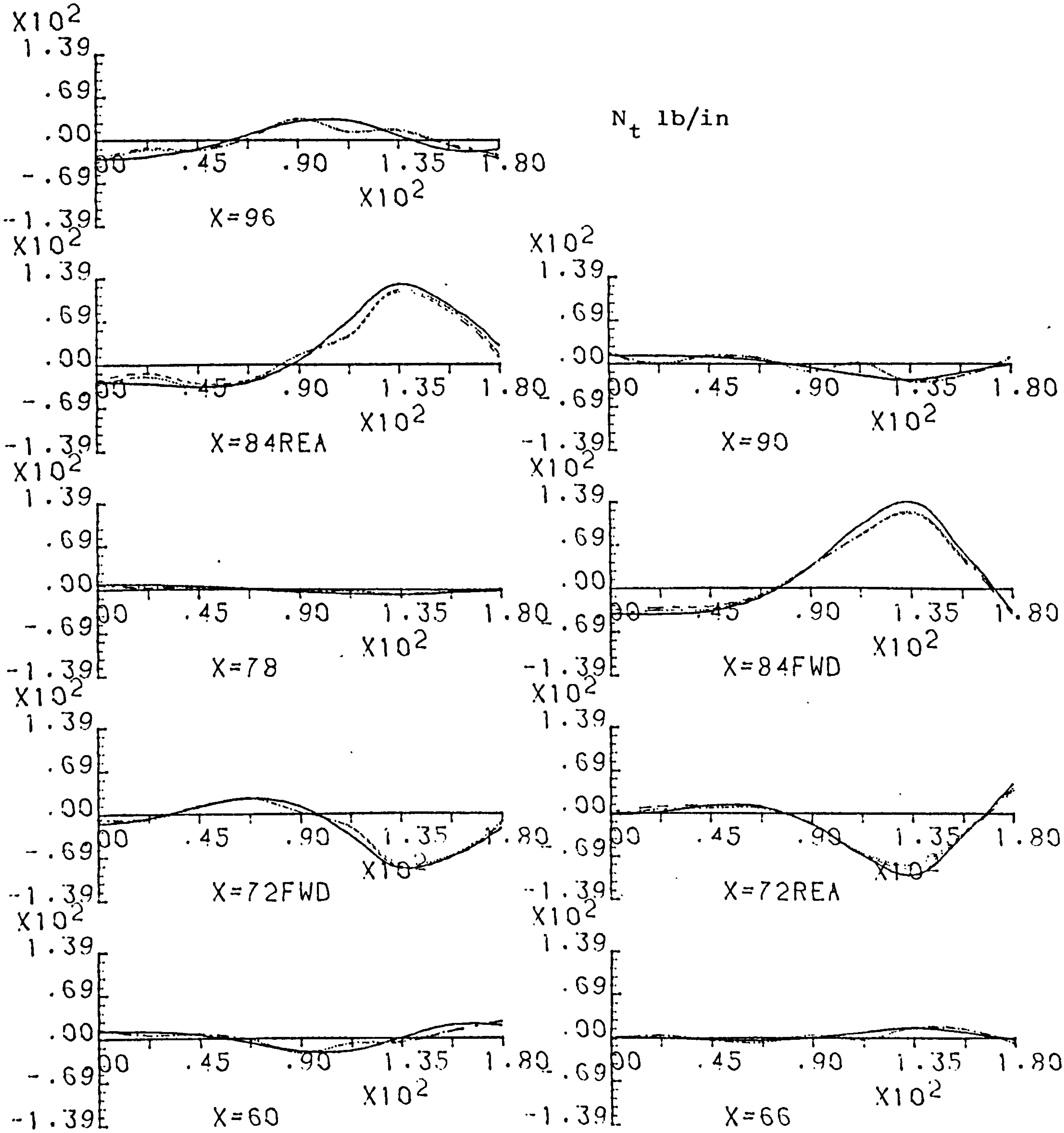

NO STRINGER — As=0.2 (Nstr=4) — As=1.125 (4)

Fig.6.2.15 EFFECT OF STRINGER AREA CHANGE - HOOP STRESS

CENTRE BODY (12R, Nstr=4, 72-12-60): SYM. TAIL (F=400LBF)
1f=0.8 Af=2.0 1r=0.08 Lrsp=12. 180 deg PICK UP

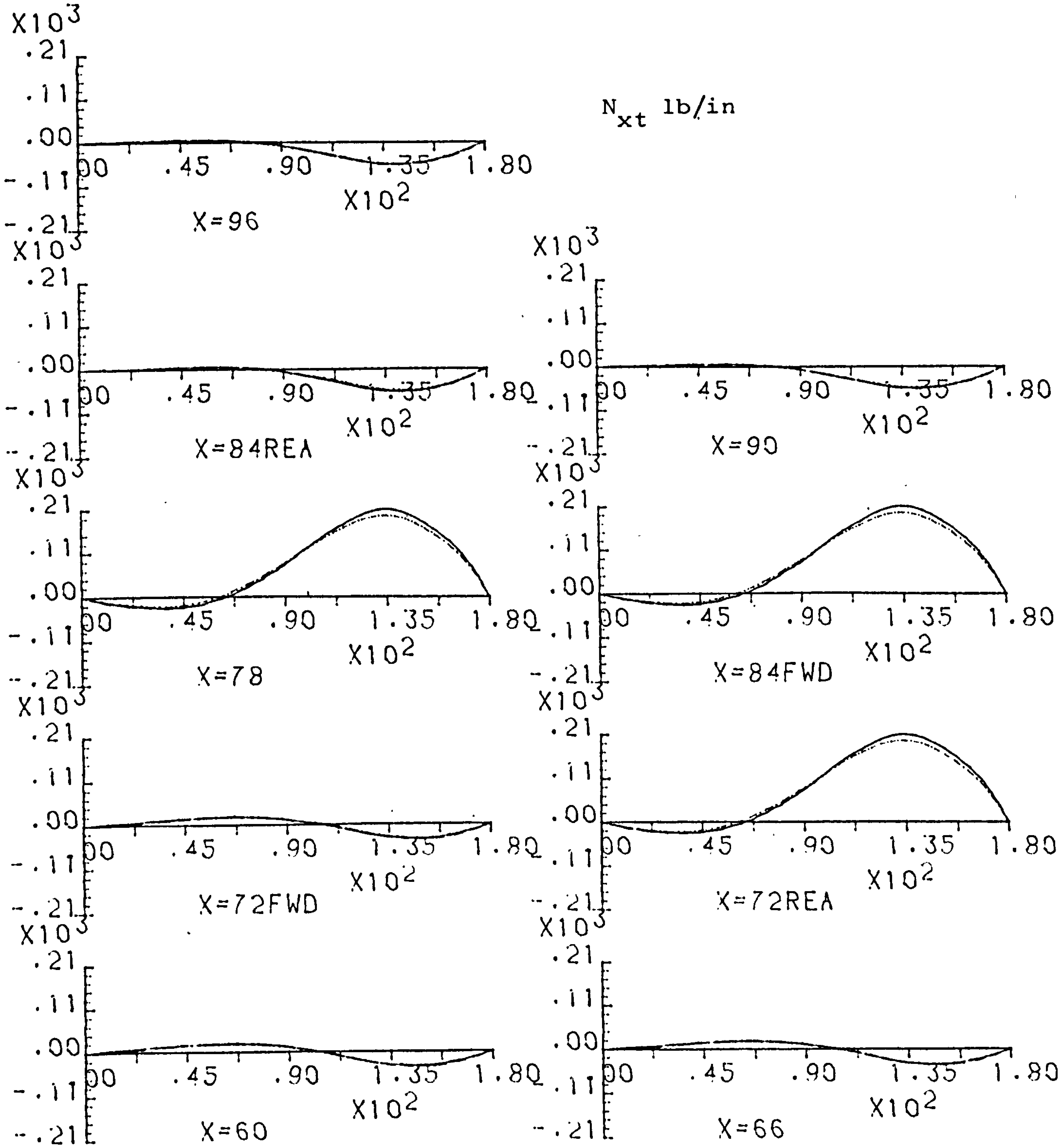

NO STRINGER — As=0.2(Nstr=4) — As=1.125(4)

Fig.6.2.16 EFFECT OF STRINGER AREA CHANGE - SHEAR FLOW

Table. 6.1 Effect of Stringer Area on the circumferential Distribution of Direct Stress at Middle of Two Frames under 800Lbf Tail Load.

R=12.0 t=0.06 Ar=0.2 Ir=0.08 Lrsp=12.0

Ring Frames I_f=0.8

Nx(lb/in)

As \ θ	0.	22.5	45.0	67.5	90.0	112.5	135.0	157.5	180.0
1.125	-40.0	-38.3	-29.7	-18.7	-0.3	15.0	29.7	41.0	43.7
0.20 (%)	-24.3 (60.8)	-23.3 (60.9)	-17.0 (57.3)	-15.7 (66.1)	-0.7	8.3 (55.6)	16.7 (56.2)	25.7 (62.6)	28.0 (63.8)

$$\frac{I_{0.2}}{I_{1.125}} = \frac{384.64}{650.04} = 0.59$$

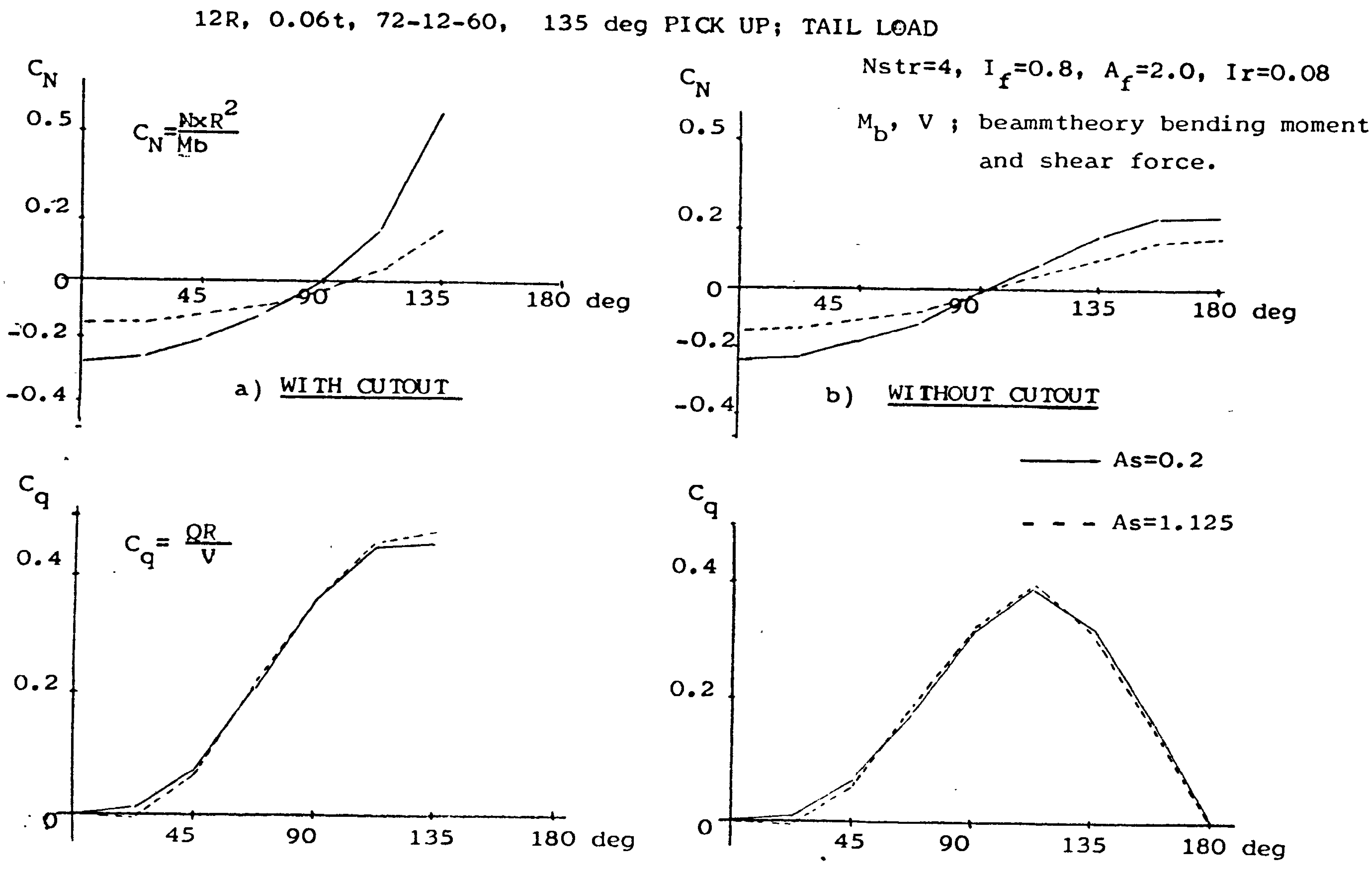

Fig.6.2.17 Effect of stringer area variation at middle of two frames.

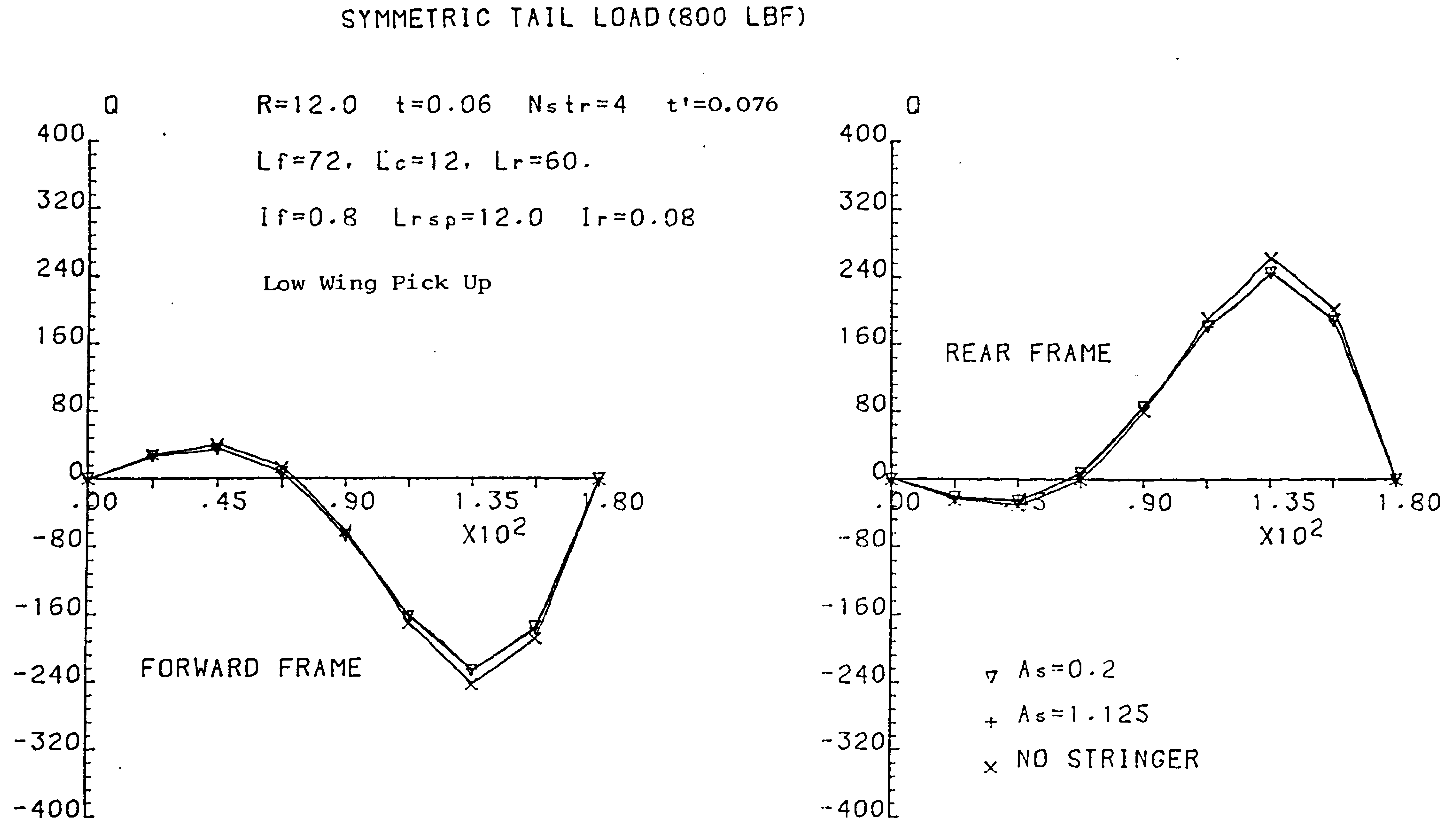

Fig.6.2.18SHEAR FLOW FROM SHELL TO FRAME -STRINGER ARE CHANGE

12R, 0.06t, 72-12-60, 135 deg PICK UP; TAIL LOAD(800lbf)

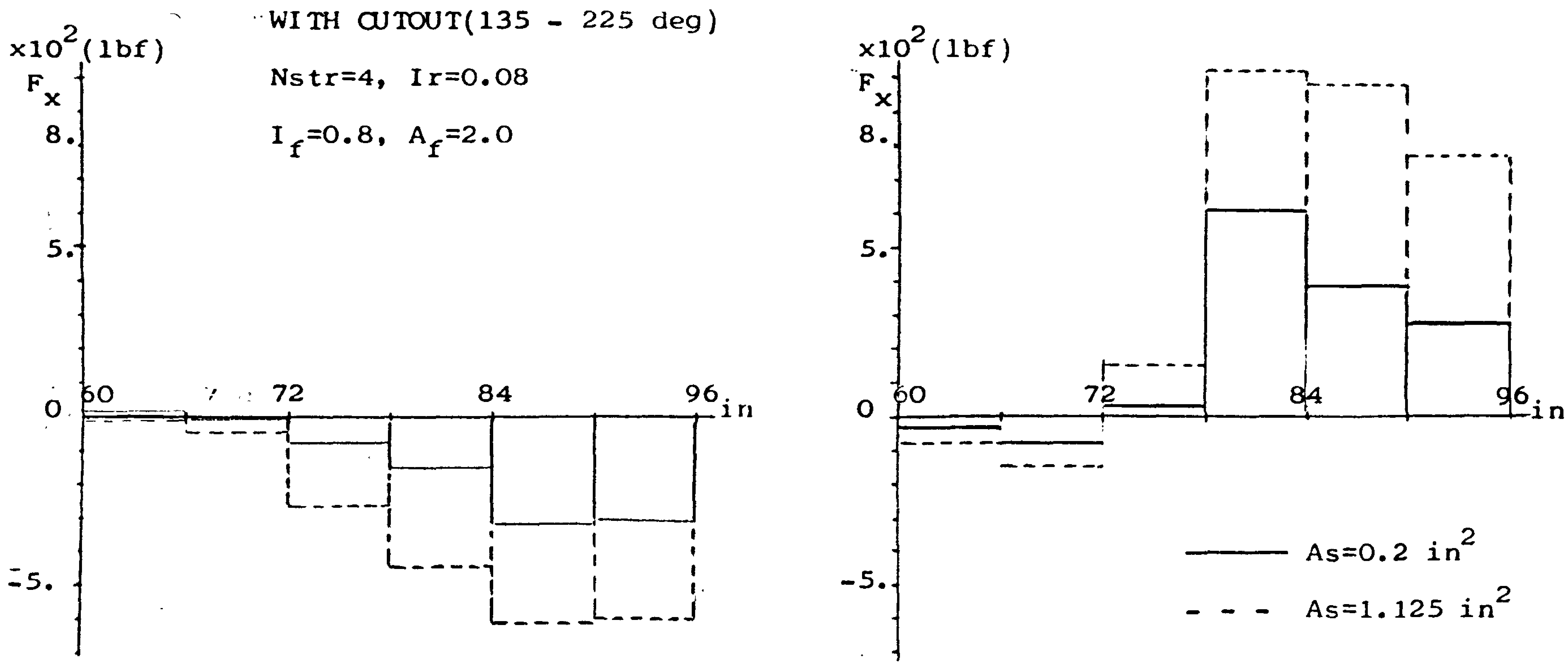

a) UPPER BOOM(45 deg)

b) LOWER BOOM(135 deg)

Fig.6.2.19 . Axial load distributions of stringer element.

Fig.6.2.20 SHEAR FLOW FROM THE SHELL TO RING FRAME; STRINGER STIFFNESS VARIATION

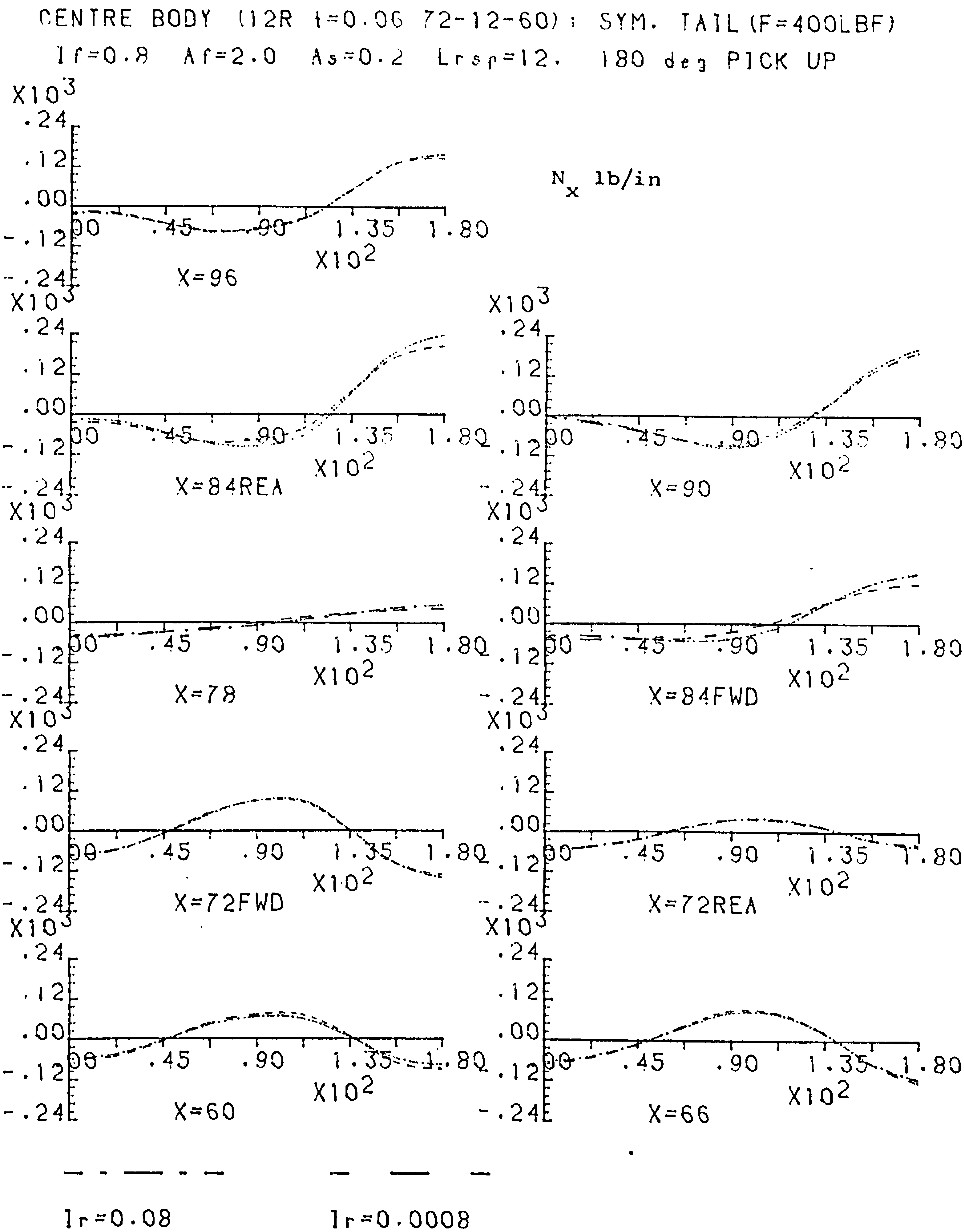

Fig.6.3.1 EFFECT OF RING Ir CHANGE - <u>DIRECT STRESS</u>

* refer paragraph (ii) of section 3.9.

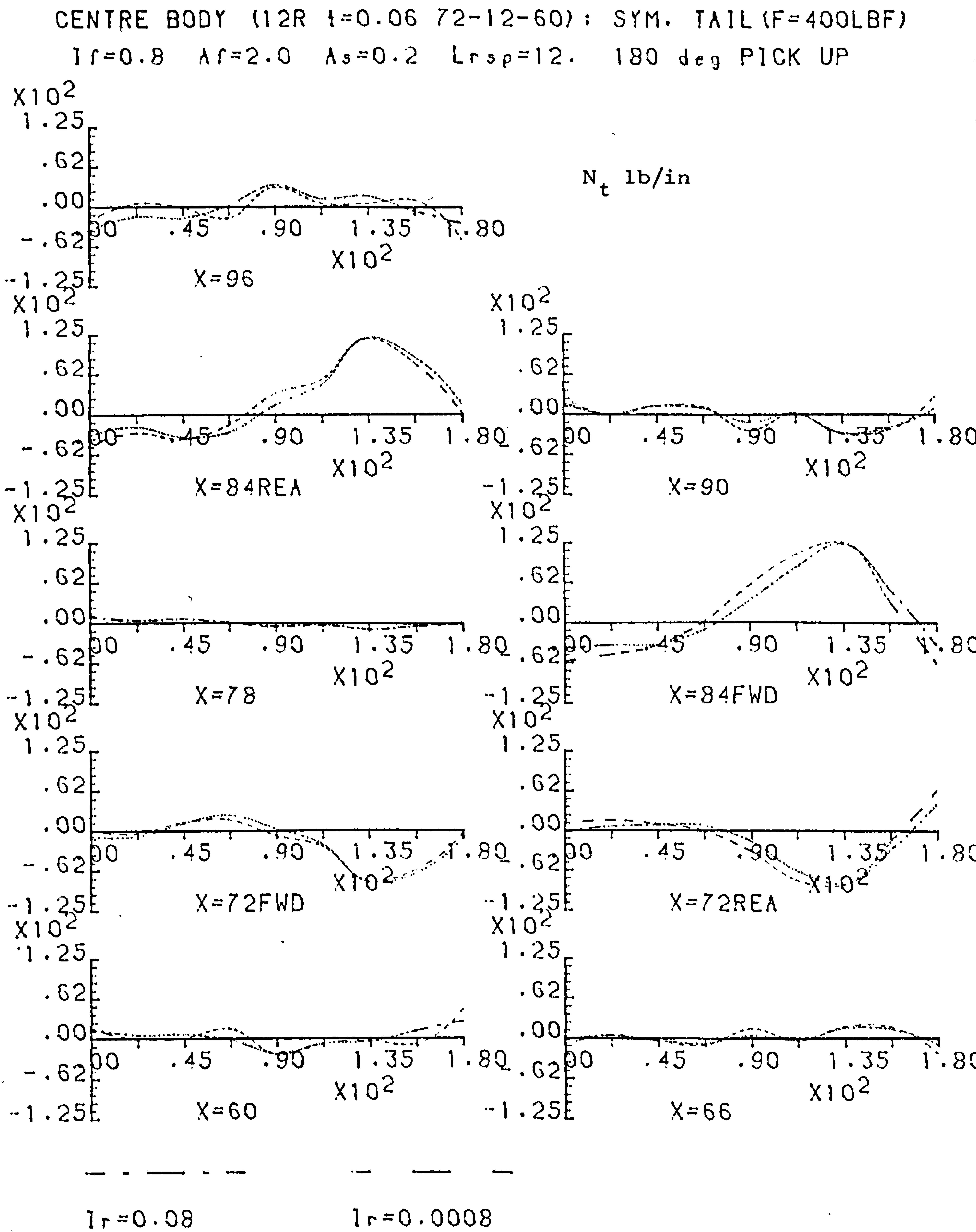

Fig.6.3.2 EFFECT OF RING Ir CHANGE - HOOP STRESS

CENTRE BODY (12R t=0.06 72-12-60): SYM. TAIL (F=400LBF)

If=0.8 Af=2.0 As=0.2 Lrsp=12. 180 deg PICK UP

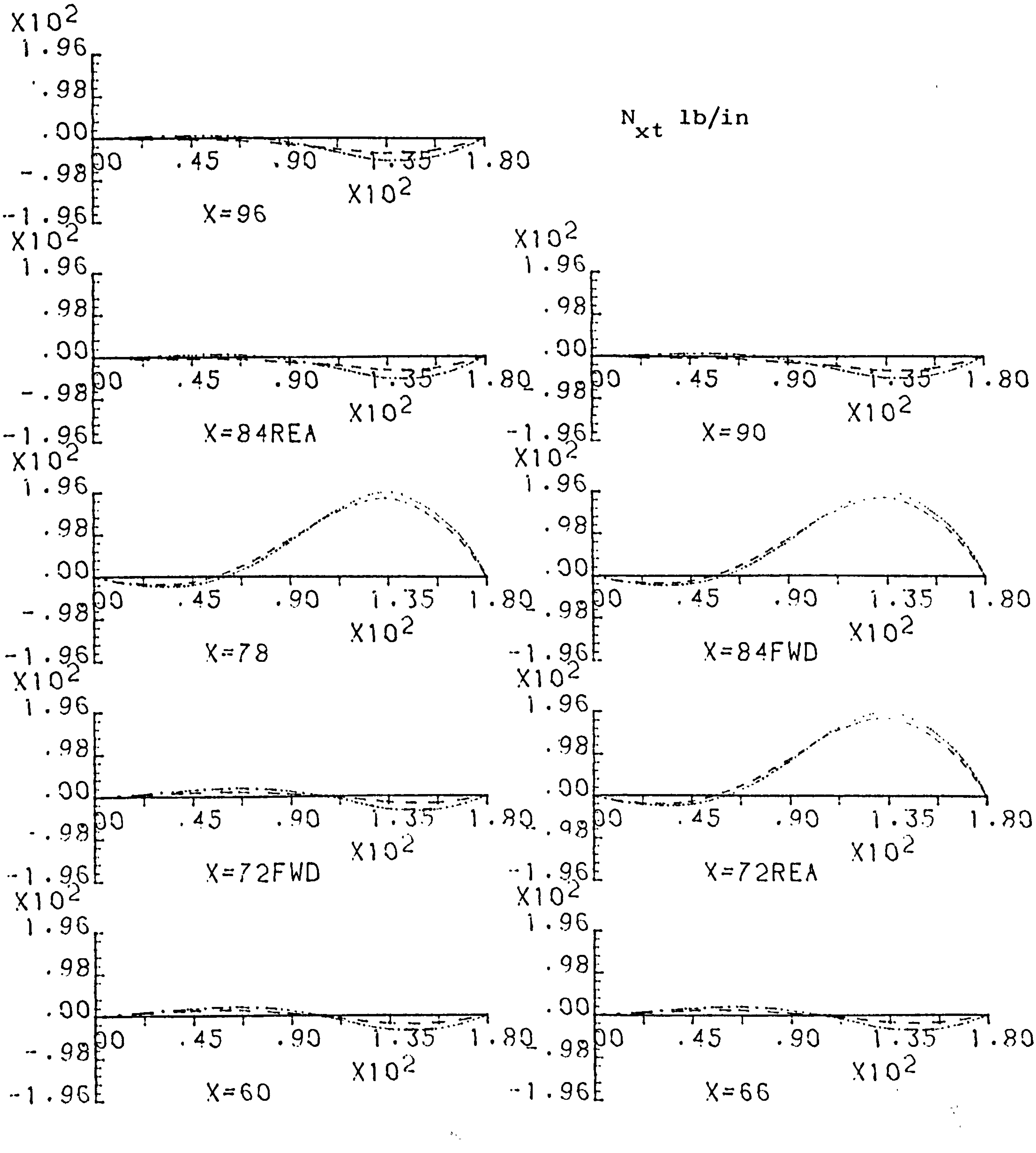

Ir=0.08 Ir=0.0008

Fig.6.3.3 EFFECT OF RING Ir CHANGE - SHEAR FLOW

Fig.6.3.4 SHEAR FLOW FROM THE SHELL TO FRAME : RING STIFFNESS CHANGE

Fig.6.3.5 SHEAR FLOW FROM THE SHELL TO FRAME : RING STIFFNESS CHANGE

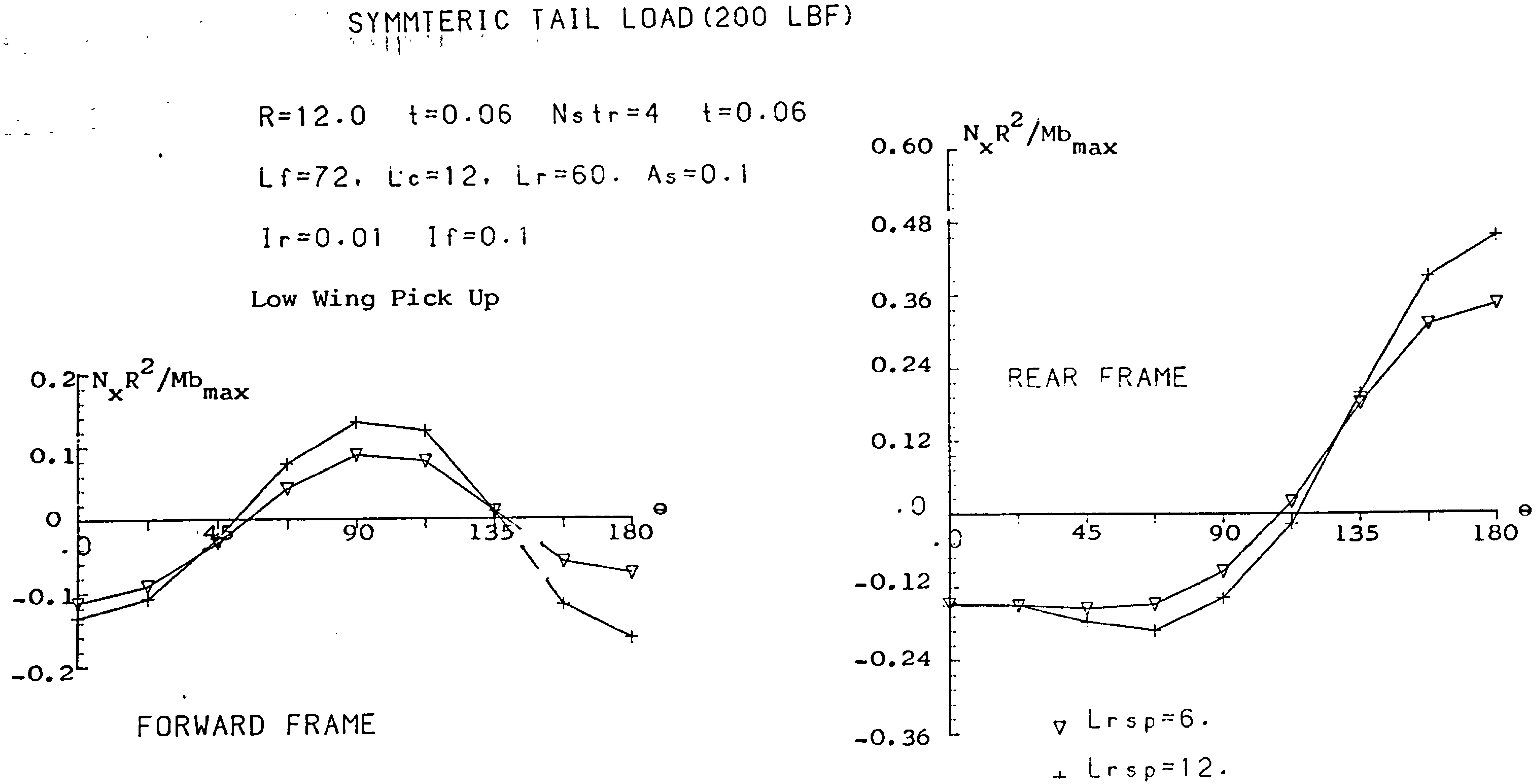

* Mb_{max}; Maximum bending moment
=12000 lbf-in.

Fig.6.3.6 DIRECT STRESS AT FRAME STATIONS - RING SPACING EFFECT

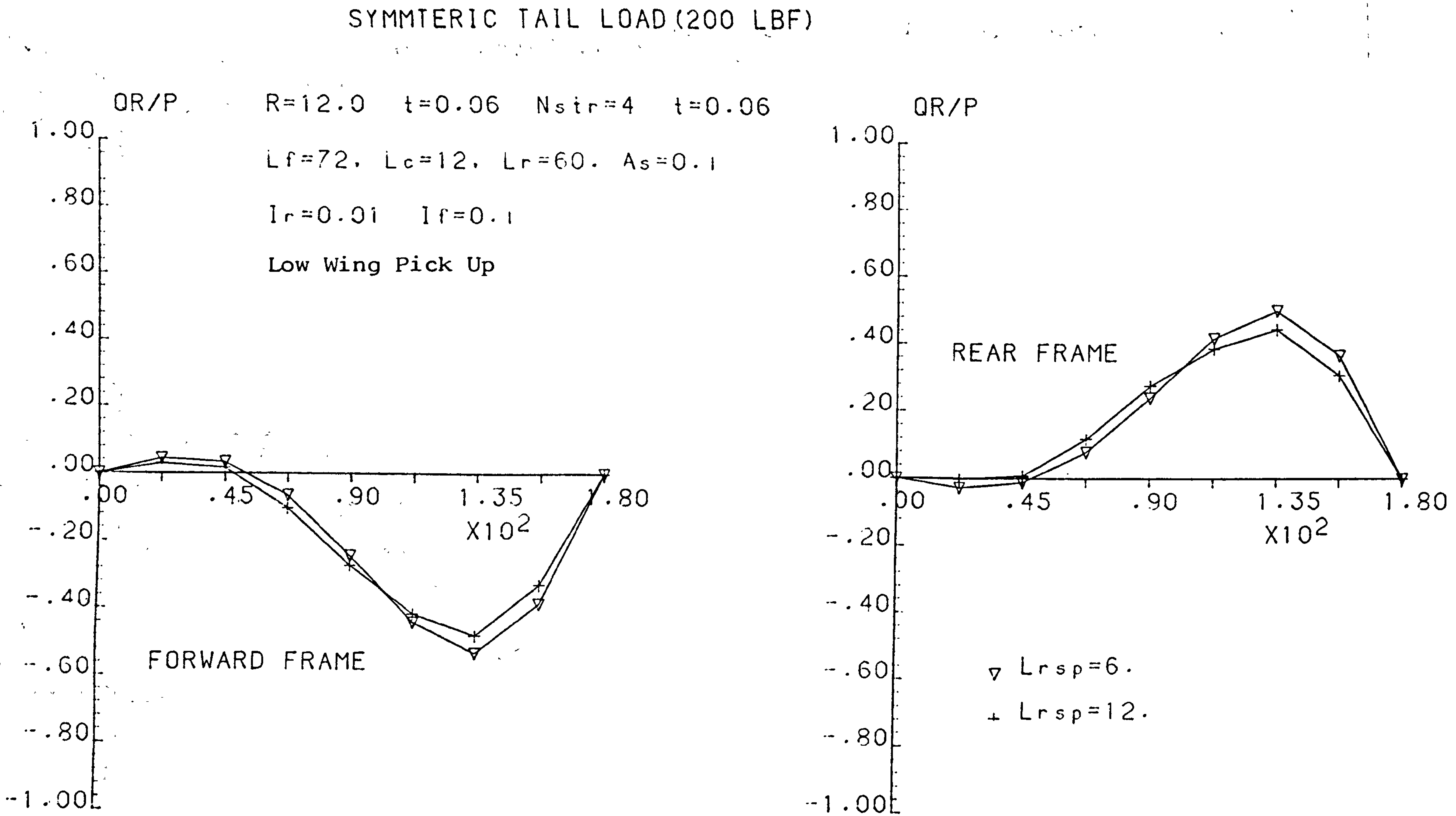

Fig.6.3.7 SHEAR FLOW FROM SHELL TO FRAME - RING SPACING VAIATION

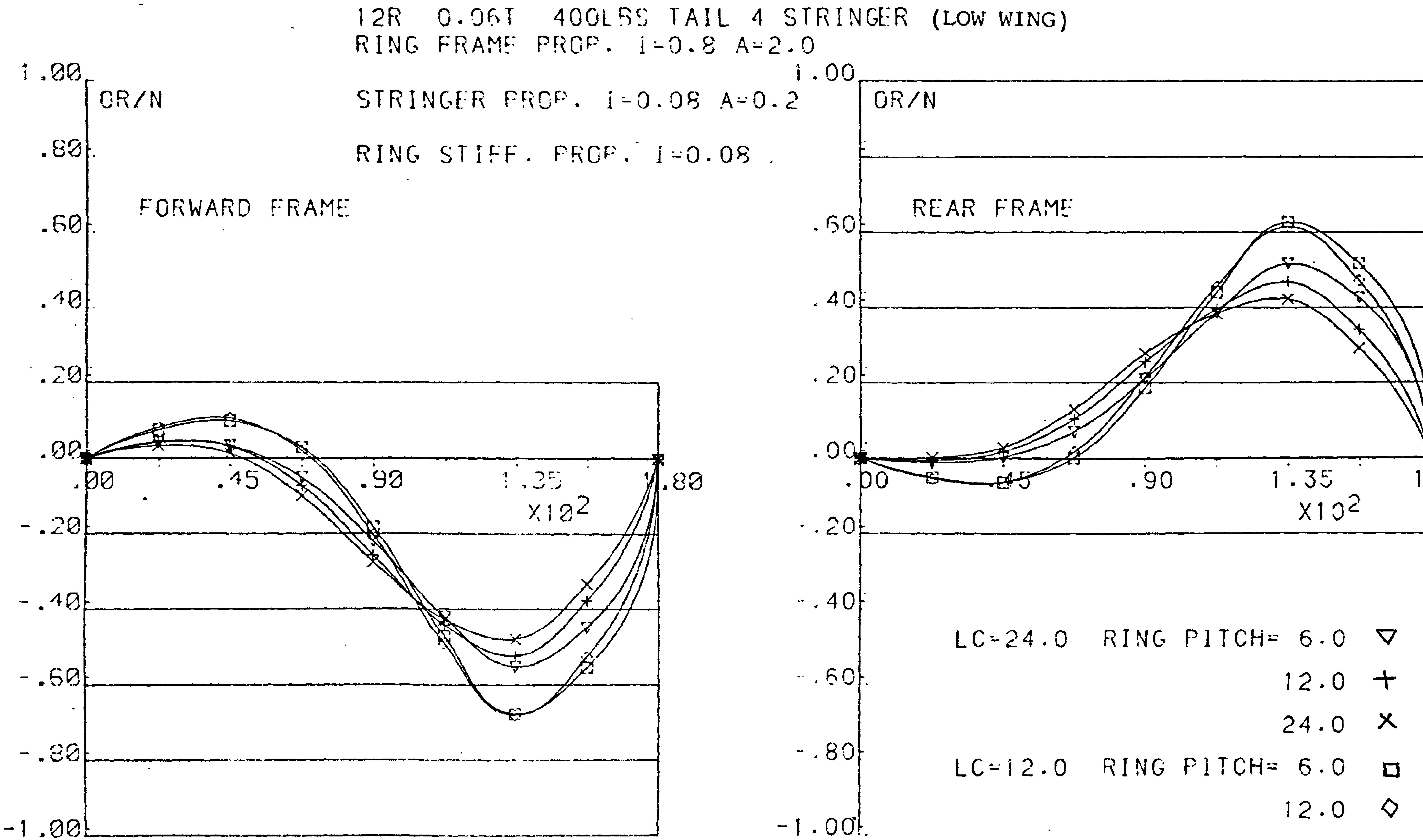

Fig.6.3.8 SHEAR FLOW FROM THE SHELL TO RING FRAME: STD. RING PITCH VARIATION

CENTRE BODY (72-L_c-60): TAIL LOAD

R=6. t=0.06 Astr=Ar=If=0.1 Ir=0.01 Nstr=4

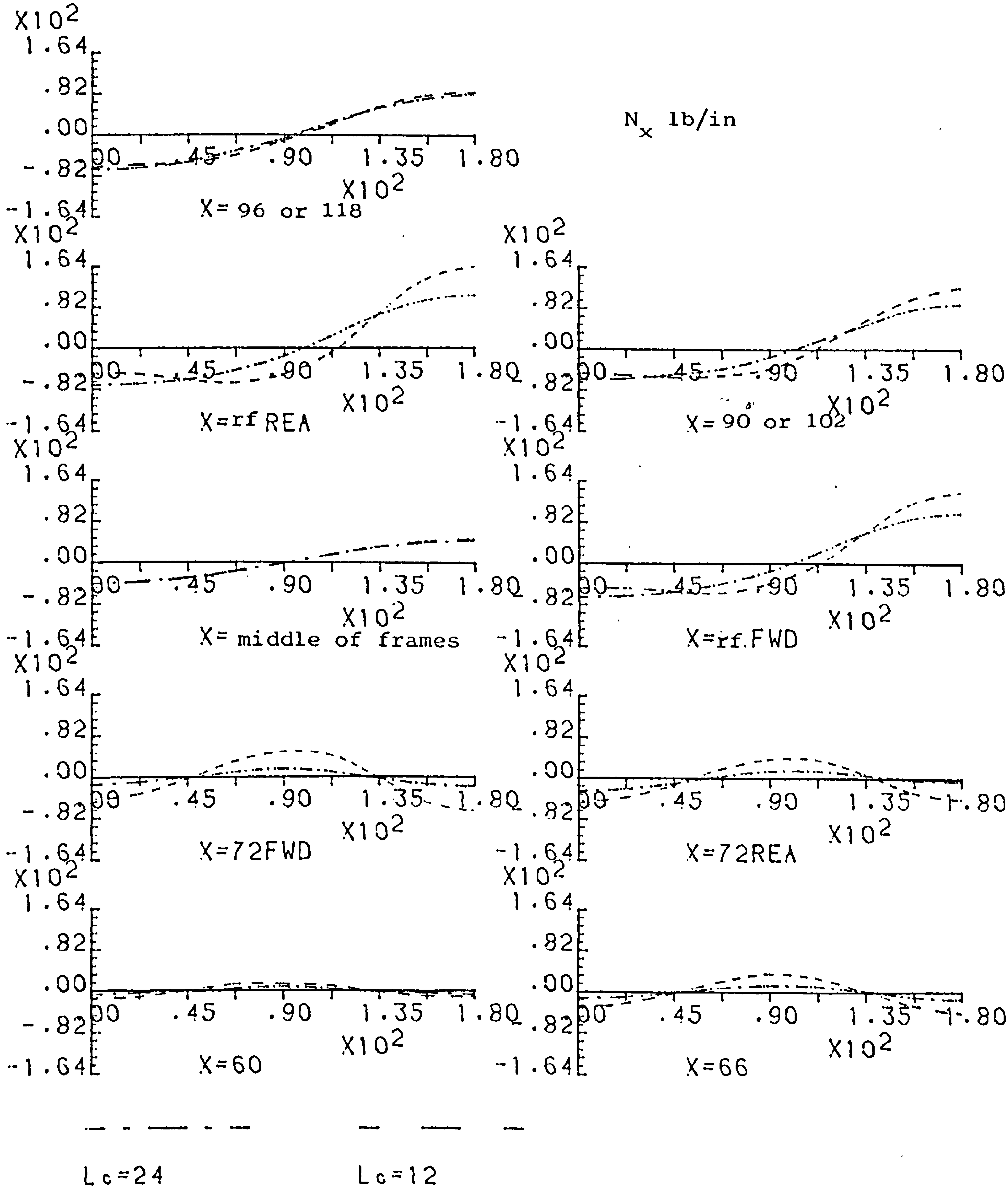

Fig.6.4.1 EFFECT OF FRAME PITCH CHANGE - <u>DIRECT STRESS</u>

CENTRE BODY (72- L_c-60) : TAIL LOAD

R=6. t=0.06 Astr=Ar=If=0.1 Ir=0.01 Nstr=4

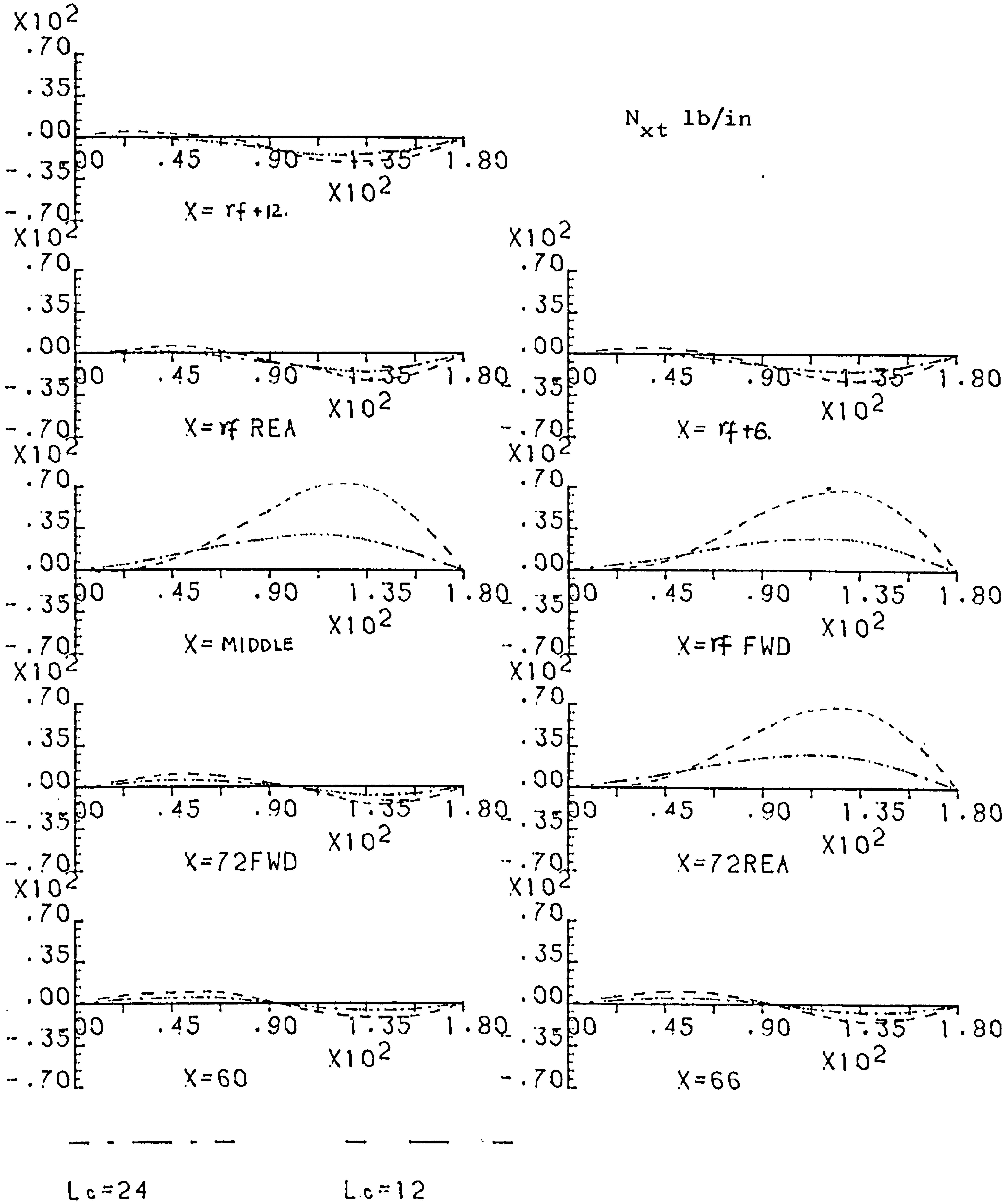

Fig.6.4.2 EFFECT OF FRAME PITCH CHANGE - <u>SHEAR</u>

Fig.6.4.3 <u>SHEAR FLOW</u> AT FRAME STATION - FRAME PITCH CHANGE

Fig.6.4.4 SHEAR FLOW FROM THE SHELL TO FRAME; RADIUS/FRAME. PITCH EFFECT

BOOM-WEB-BOOM TYPE FRAMED SHELL(72-12-60); SYMM. TAIL LOAD

R=6.0 T=0.06 Ir=0.01 Astr=Ar=0.1 Nstr=4 LOW WING

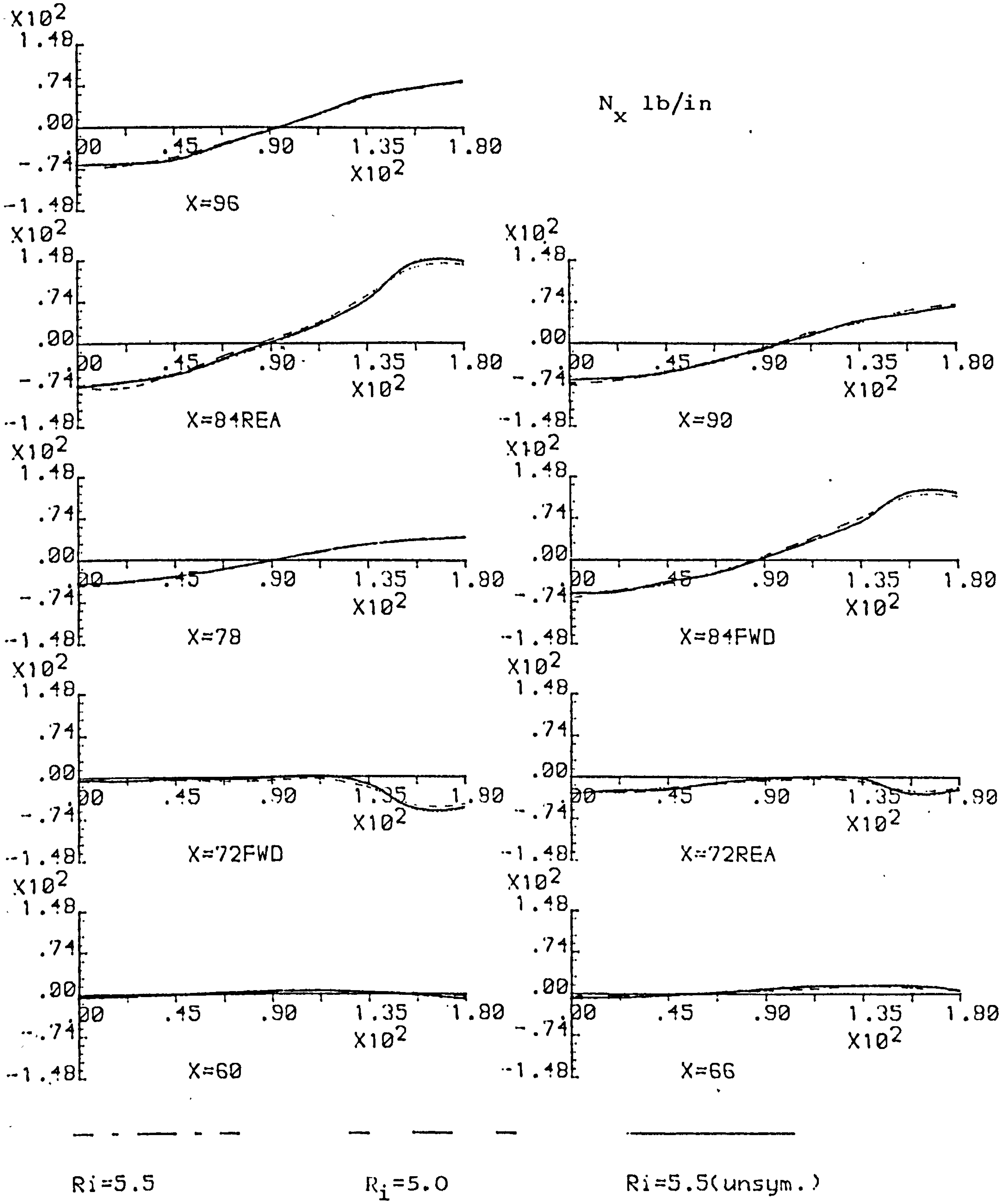

Fig.6.5.1 EFFECT OF FRAME DEPTH CHANGE - DIRECT STRESS

BOOM-WEB-BOOM TYPE FRAMED SHELL(72-12-60); SYMM. TAIL LOAD

R=6.0 T=0.06 Ir=0.01 Astr=Ar=0.1 Nstr=4 LOW WING

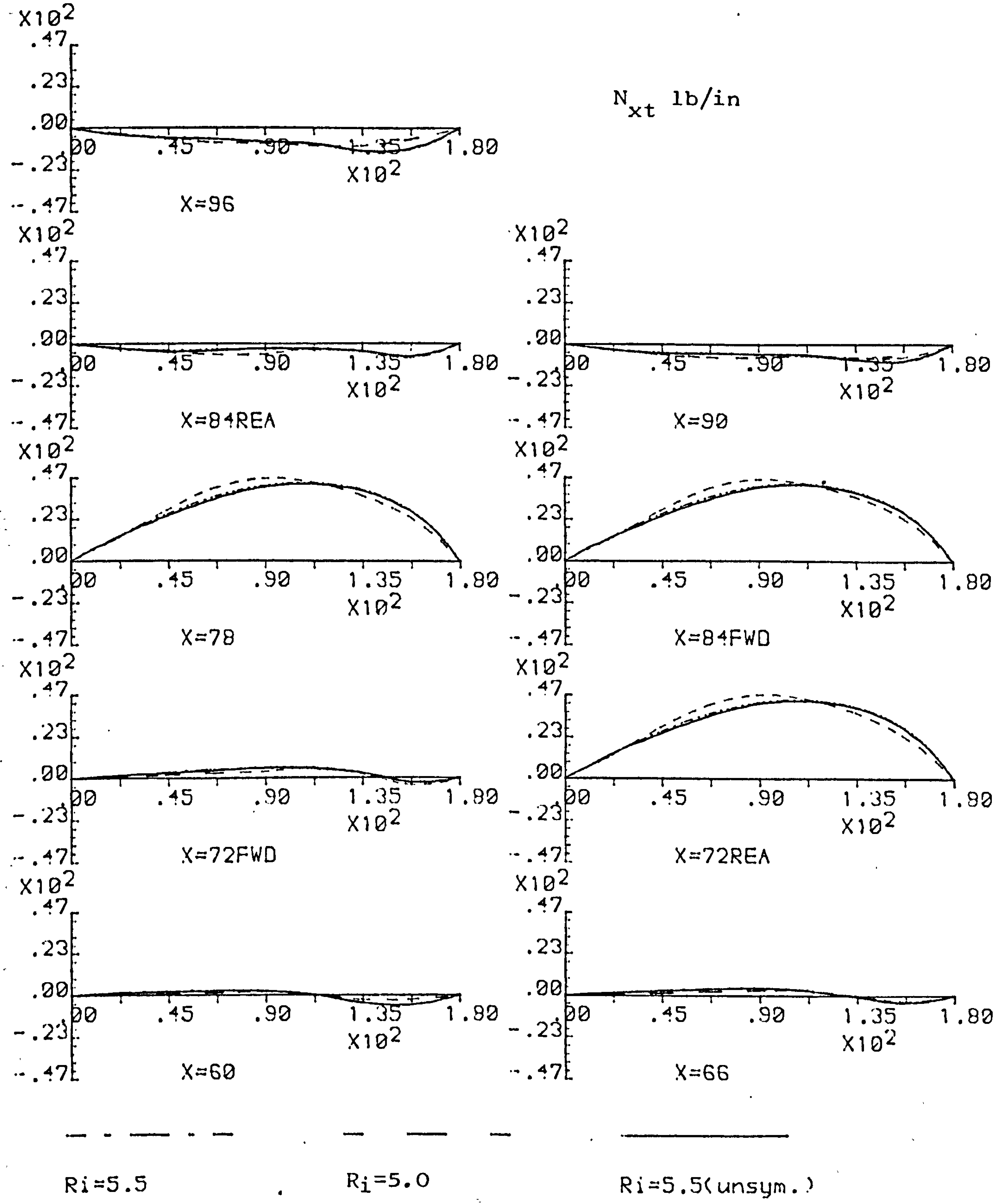

Fig.6.5.2 EFFECT OF FRAME DEPTH CHANGE - shear

Fig.6.5.3 SHEAR FLOW AT FRAME STATIONs - FRAME DEPTH VARIATION

TAIL LOADING(PFF=1000, Prf=1200)

SYMMETRIC - LOW/HIGH WING (180 deg)

R=6.0 t=0.06 LF=72 Lc=12 Lr=60

As=Ar=0.1 Is=Ir=0.01 Nstr=4 IF=0.1

sc; Shear cntre, cg=centroid, sh=shell

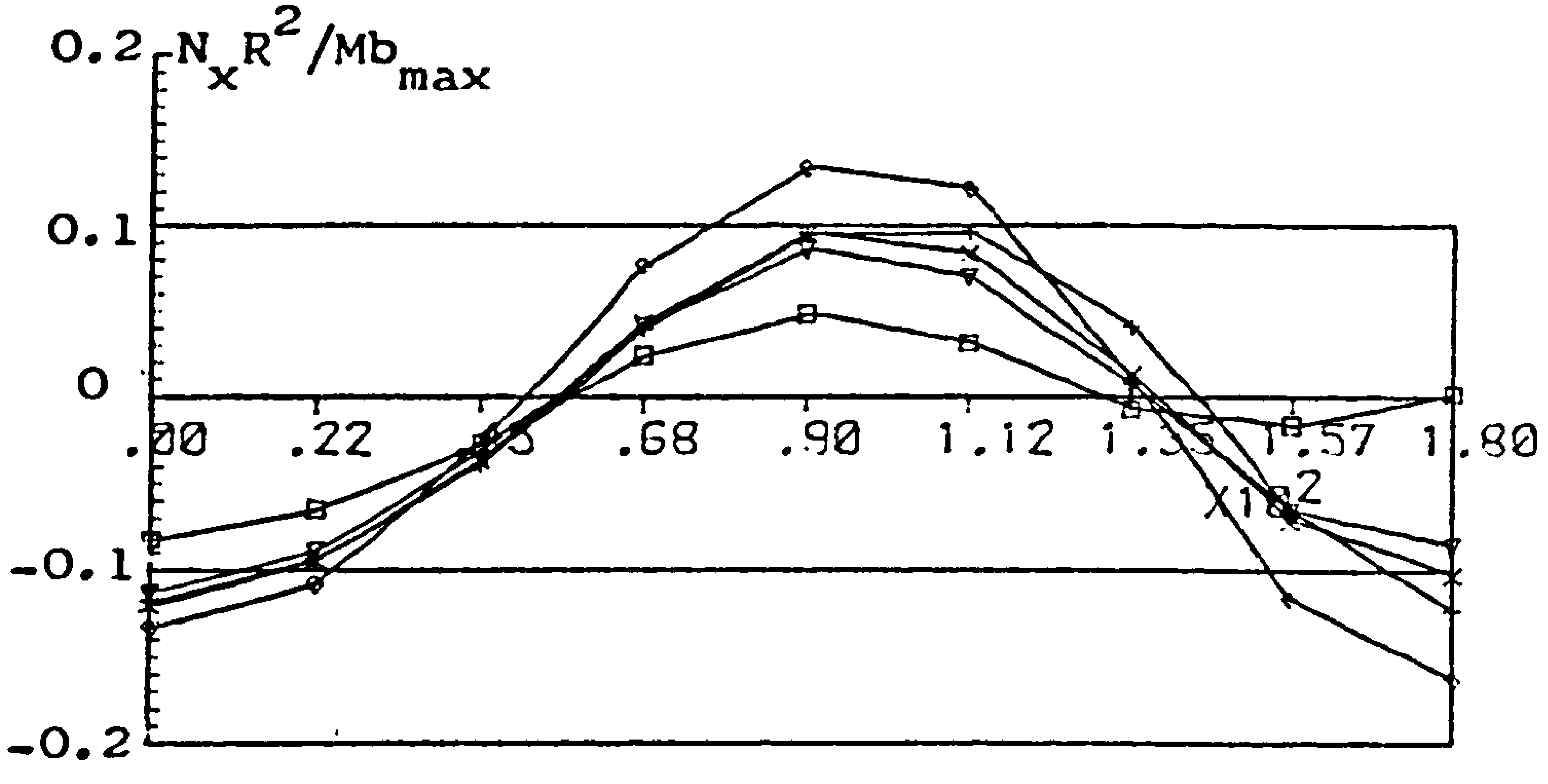

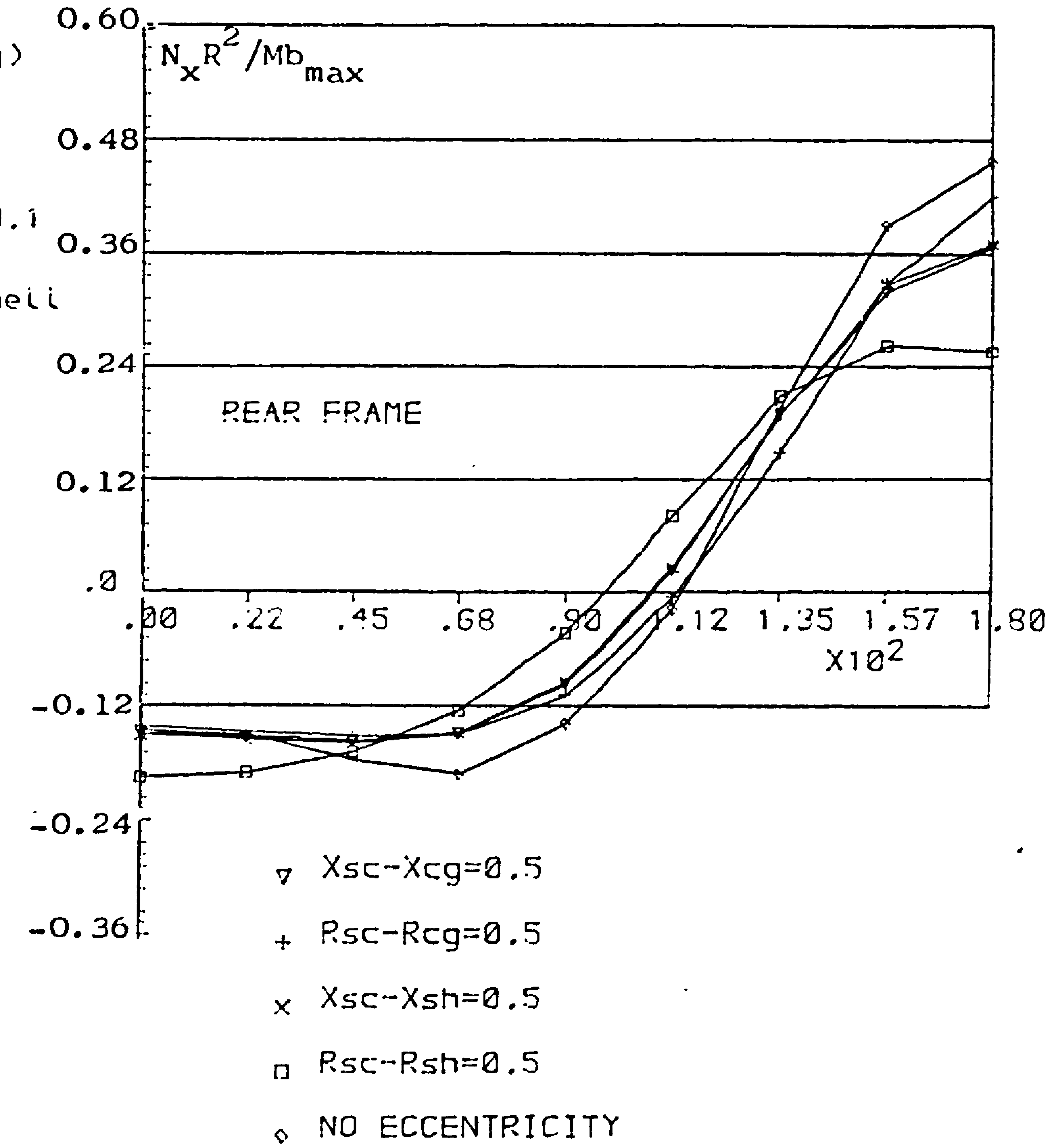

* Mb_{max}= Maximum bending moment ; 12000 lbf-in.

Fig.6.5.4DIRECT STRESS RESULTANT DISTR. AT FRAME STA. - FRAME OFFSET EFF.

Fig.6.5.5 SHEAR FLOW FROM THE SHELL TO THE FRAME - FRAME OFFSET EFFECT

Fig.6.5.6 SHEAR FLOW FROM THE SHELL TO FRAME : FRAME PROPERTY CHANGE

Table 6.2 Effect of the Rear Body Length to the Shell Stress under Tail Load.

Tail plan position; 90^{o}

$R = 6.0$ inch, $t = 0.06$ inch, $L_{rsp} = 12.0$ inch

$L_f = 72$ inch, $L_c = 12$ inch

$P_t = 200$ lbf

a) Direct Stress ($N \times R^2/Mb$) at X = 84.0 inch

L_r \ θ	0	22.5	45	67.5	90	112.5	135	157.5	180
60.0	-0.15	-0.15	-0.18	-0.19	-0.14	-0.02	0.20	0.39	0.46
24.0	-0.12	-0.13	-0.15	-0.16	-0.11	0.03	0.18	0.32	0.36

b) Shear Stress (QR/V) at X = 78.0 inch.

L_r \ θ	0	22.5	45	67.5	90	112.5	135	152.5	180
60.0	0	-0.01	0.05	0.16	0.29	0.42	0.42	0.26	0
24.0	0	-0.02	0.02	0.13	0.28	0.41	0.44	0.29	0

CENTRE BODY (6R t=0.06 24-12-24.): SYM. TAIL LOAD

If=0.1 Af=1.0 Ir=0.01 Lrsp=12. Nstr=4 As=0.1 LOW WING

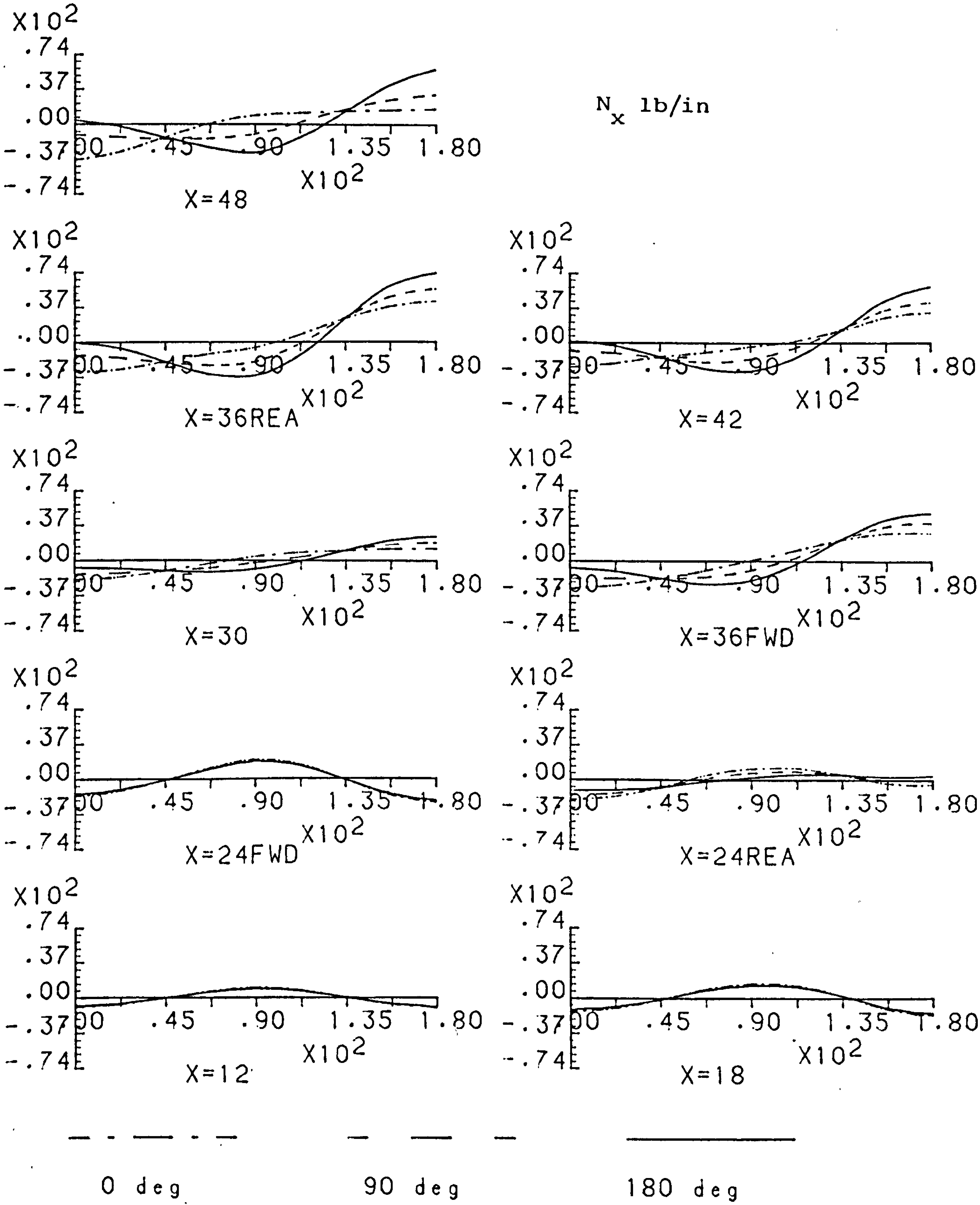

Fig.6.7.1 EFFECT OF TAIL POSITION POSITION CHANGE - DIRECT

CENTRE BODY (6R t=0.06 24-12-24.); SYM. TAIL LOAD

If=0.1 Af=1.0 Ir=0.01 Lrsp=12. Nstr=4 As=0.1 LOW WING

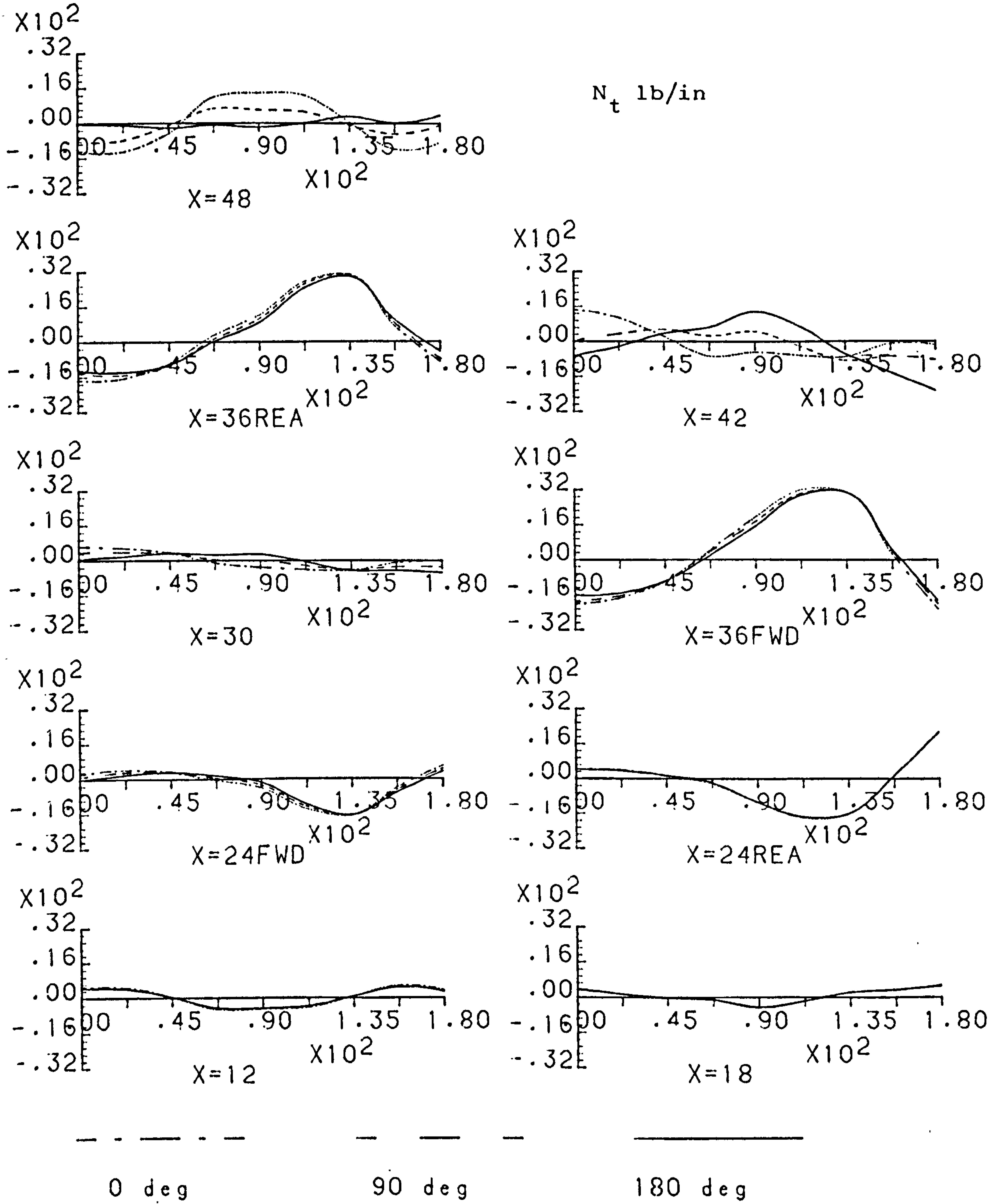

Fig.6.7.2 EFFECT OF TAIL POSITION POSITION CHANGE - <u>HOOP</u>

CENTRE BODY (6R t=0.06 24-12-24.); SYM. TAIL LOAD
If=0.1 Af=1.0 Ir=0.01 Lrsp=12. Nstr=4 As=0.1 LOW WING

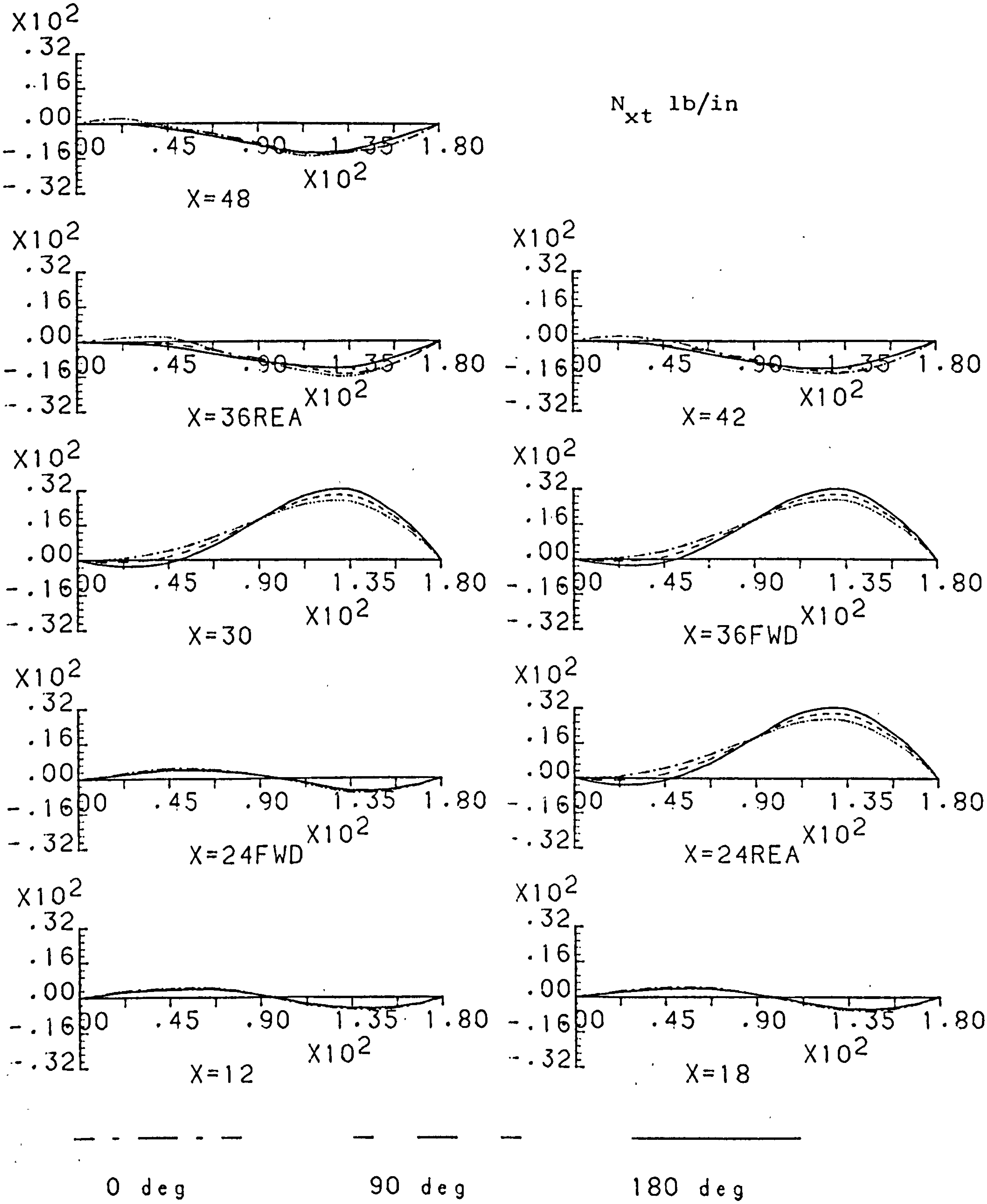

Fig. 6.7.3 EFFECT OF TAIL POSITION POSITION CHANGE - SHEAR

CENTRE BODY (6R t=0.06 24-12-24.): SYM. TAIL LOAD

If=0.1 Af=1.0 Ir=0.01 Lrsp=12. Nstr=4 As=0.1 LOW WING

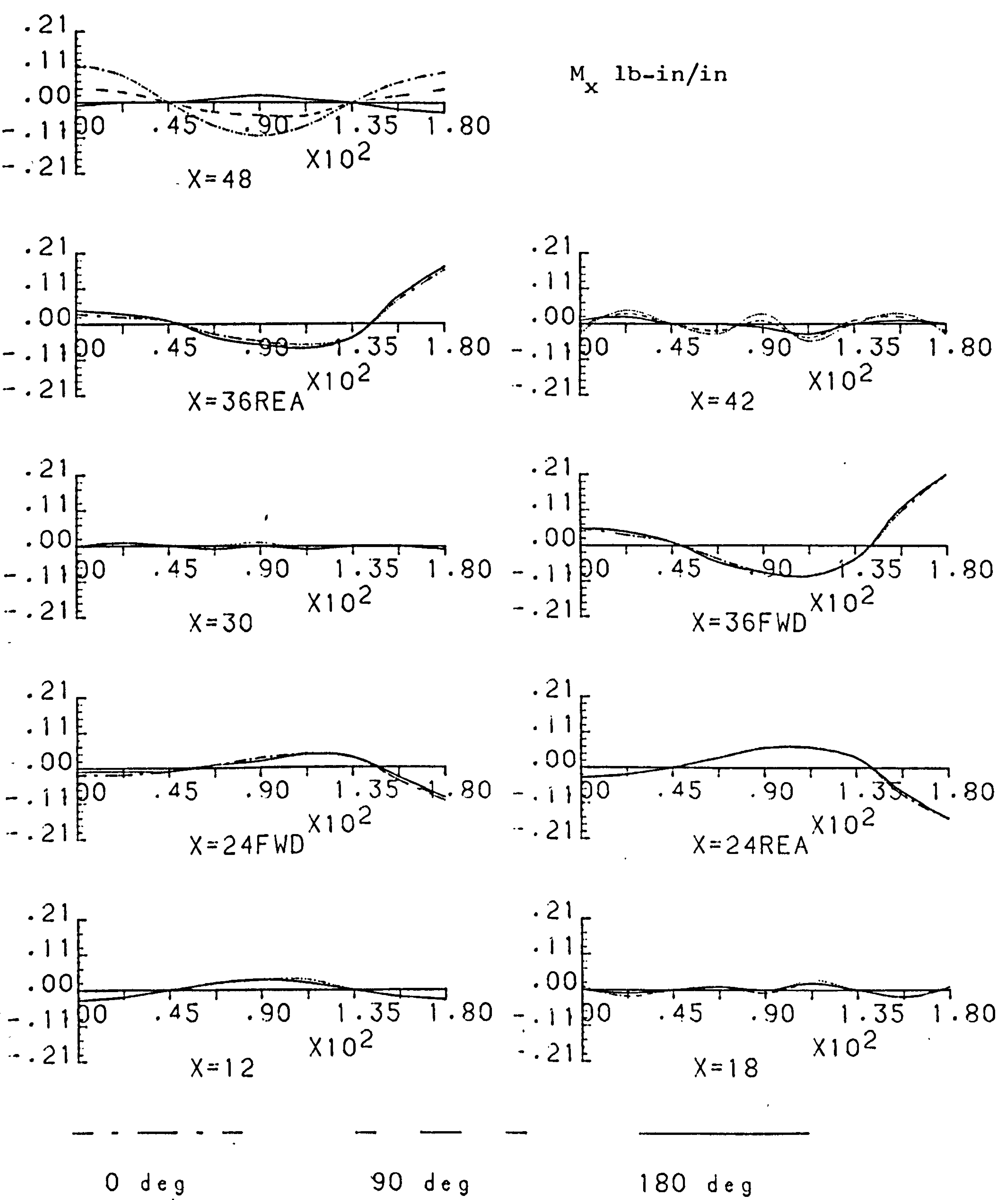

Fig.6.7.4 EFFECT OF TAIL POSITION POSITION CHANGE - AXIAL BEND.

CENTRE BODY (6R t=0.06 24-12-24.); SYM. TAIL LOAD
If=0.1 Af=1.0 Ir=0.01 Lrsp=12. Nstr=4 As=0.1 LOW WING

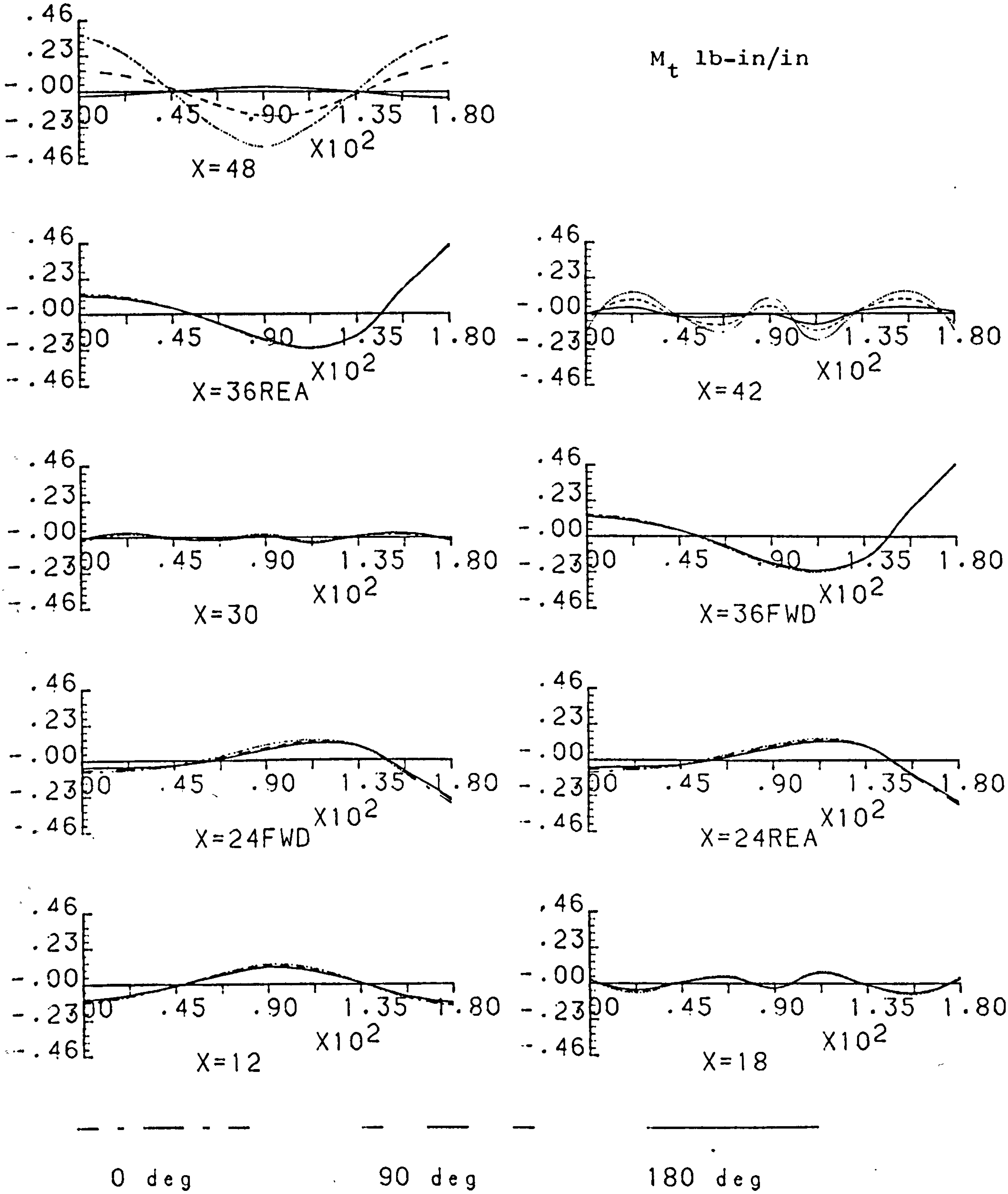

Fig.6.7.5 EFFECT OF TAIL POSITION POSITION CHANGE - CIRC. BEND.

CENTRE BODY (6R t=0.06 24-12-24.); SYM. TAIL LOAD

If=0.1 Af=1.0 Ir=0.01 Lrsp=12. Nstr=4 As=0.1 LOW WING

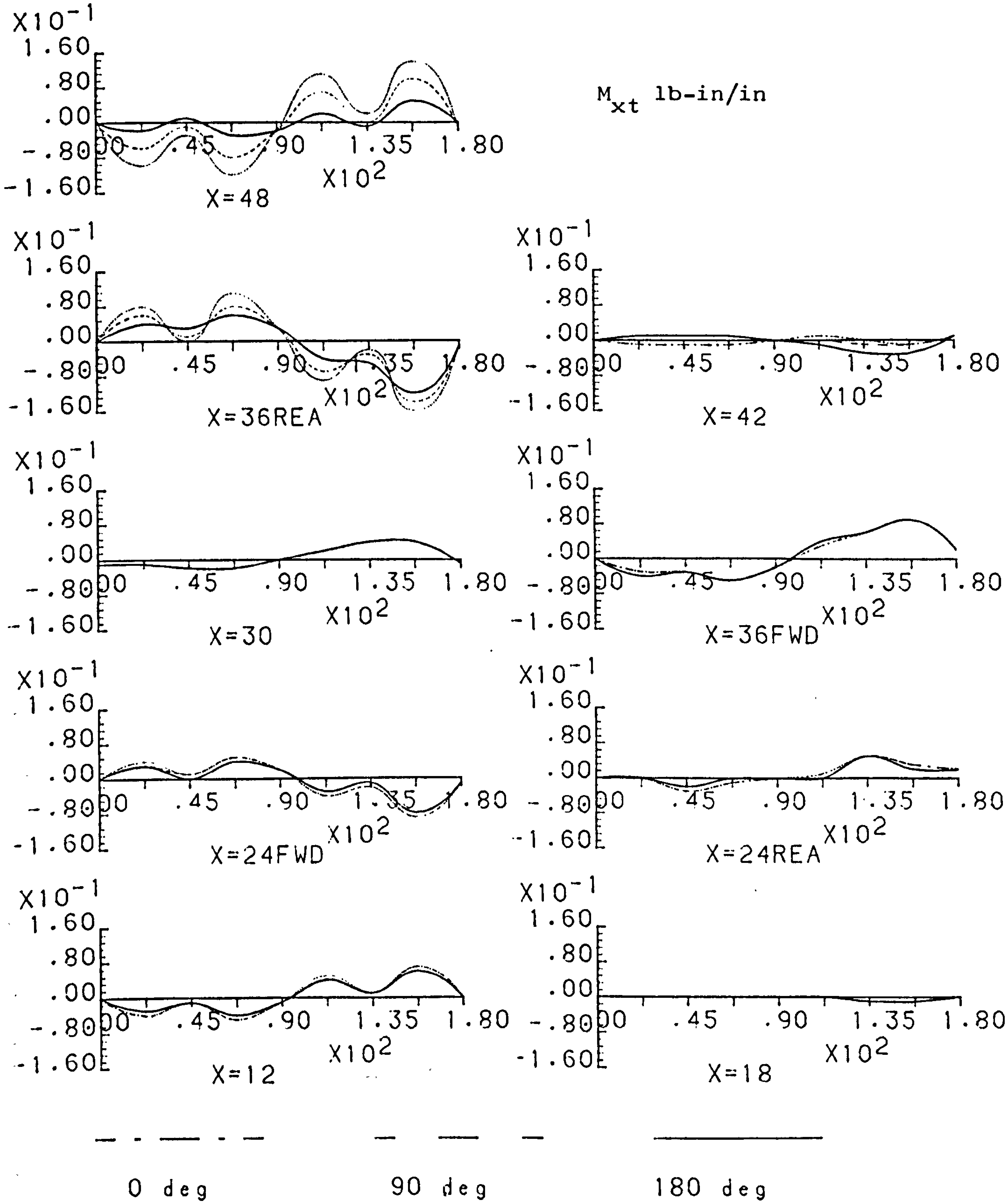

Fig. 6.7.6 EFFECT OF TAIL POSITION POSITION CHANGE - TWIST

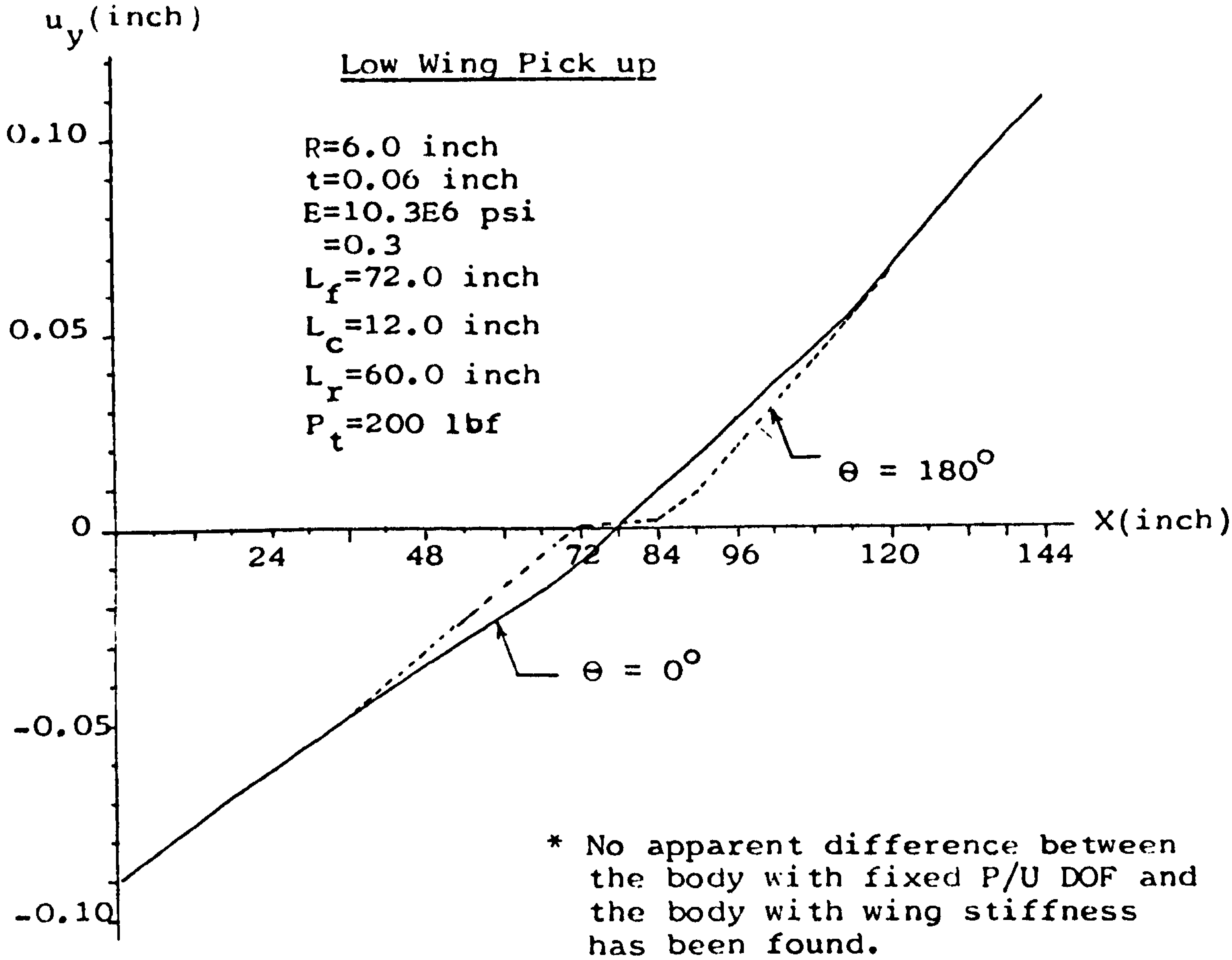

U_y x100inch

	θ \ x	66	72	78	84	90
with Wing	0	-1.643	-0.874	0.068	1.008	1.933
	180	-0.782	-0.053	0.071	0.076	0.879
without Wing	0	-1.610	-0.826	0.013	1.090	2.029
	180	-0.742	0.	0.007	0.	0.968

Fig.6.8.1 Radial Displacement Distribution along the Longitudinal Axis.

72-12-60; 135 deg Pick Up

12 R, 0.06t, Nstr=4, Lrsp=12.0

Tail Load.

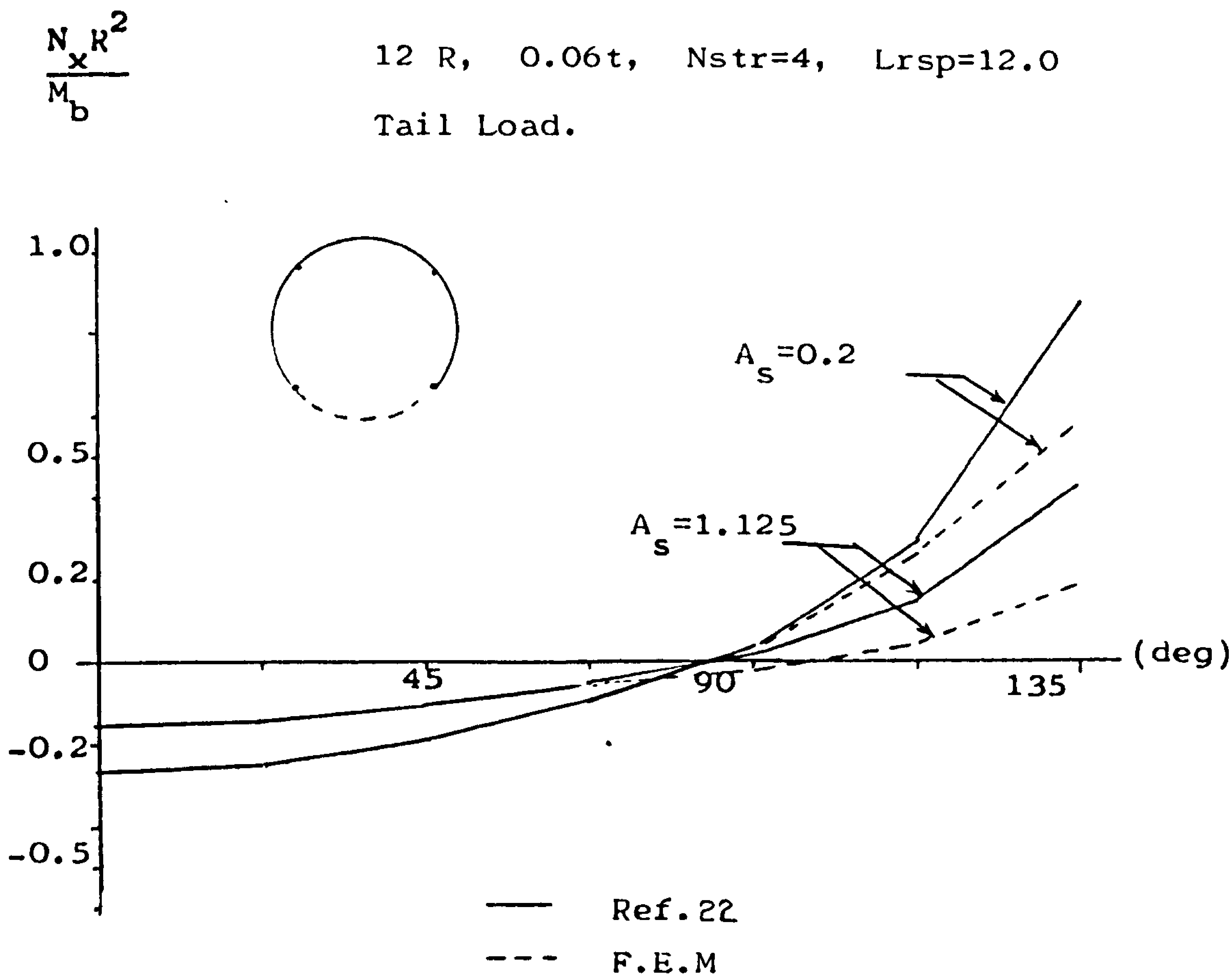

Fig.6.9.1 Axial Stress at the Middle of Two Frame
Two Framed-Shell with Cutout

STRESS RESULT.(C/O AT 135-225 DEG & 72-84 IN); TAIL
R=6.0 T=0.06 Ir=0.01 Astr=Ar=0.1 Nstr=4, 72-12-60

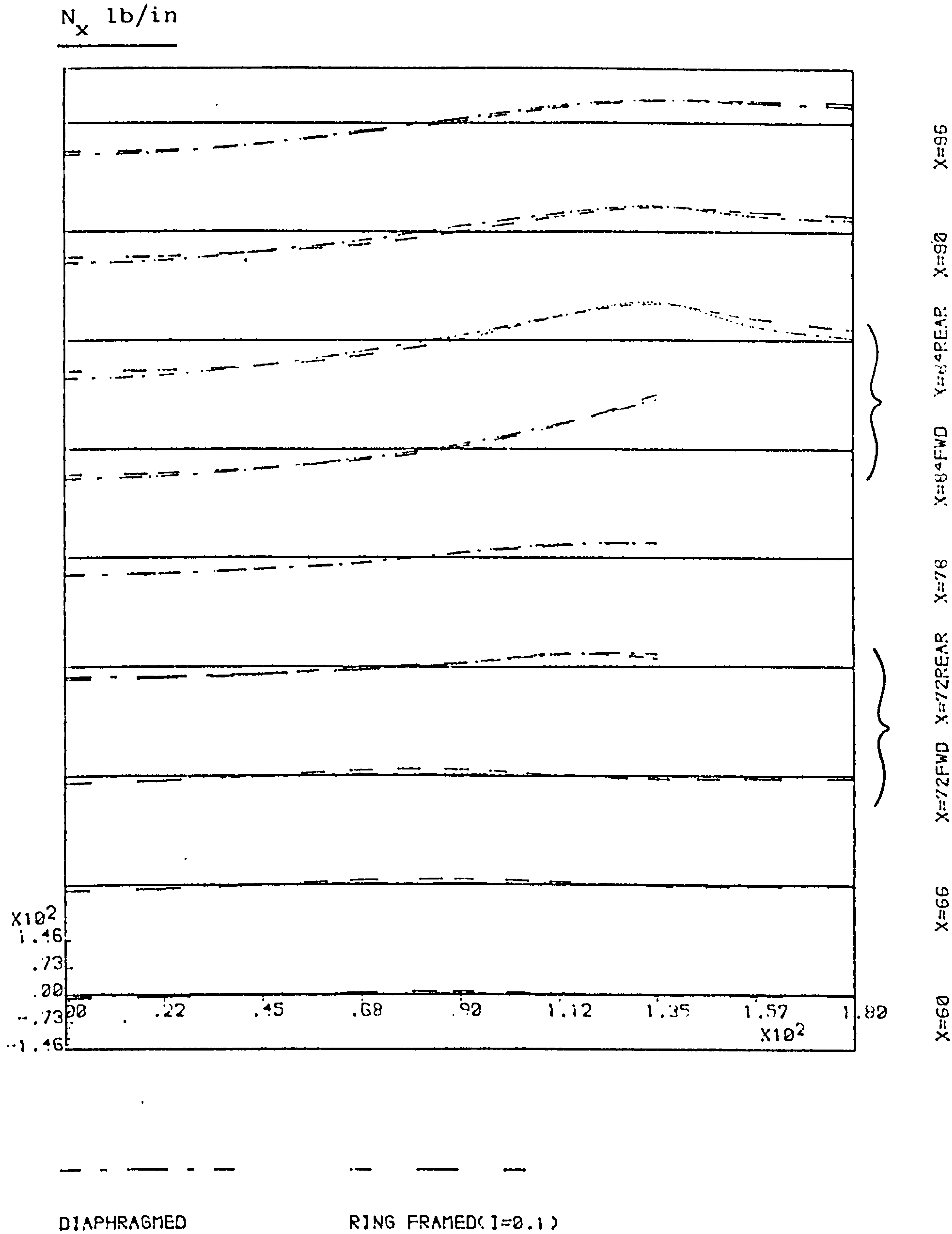

Fig. 6.9.2 EFFECTS OF FRAME TYPE WITH CUTOUT- DIRECT STR.

STRESS RESULT.(C/O AT 135-225 DEG & 72-84 IN); TAIL
R=6.0 T=0.06 Ir=0.01 Astr=Ar=0.1 Nstr=4, 72-12-60

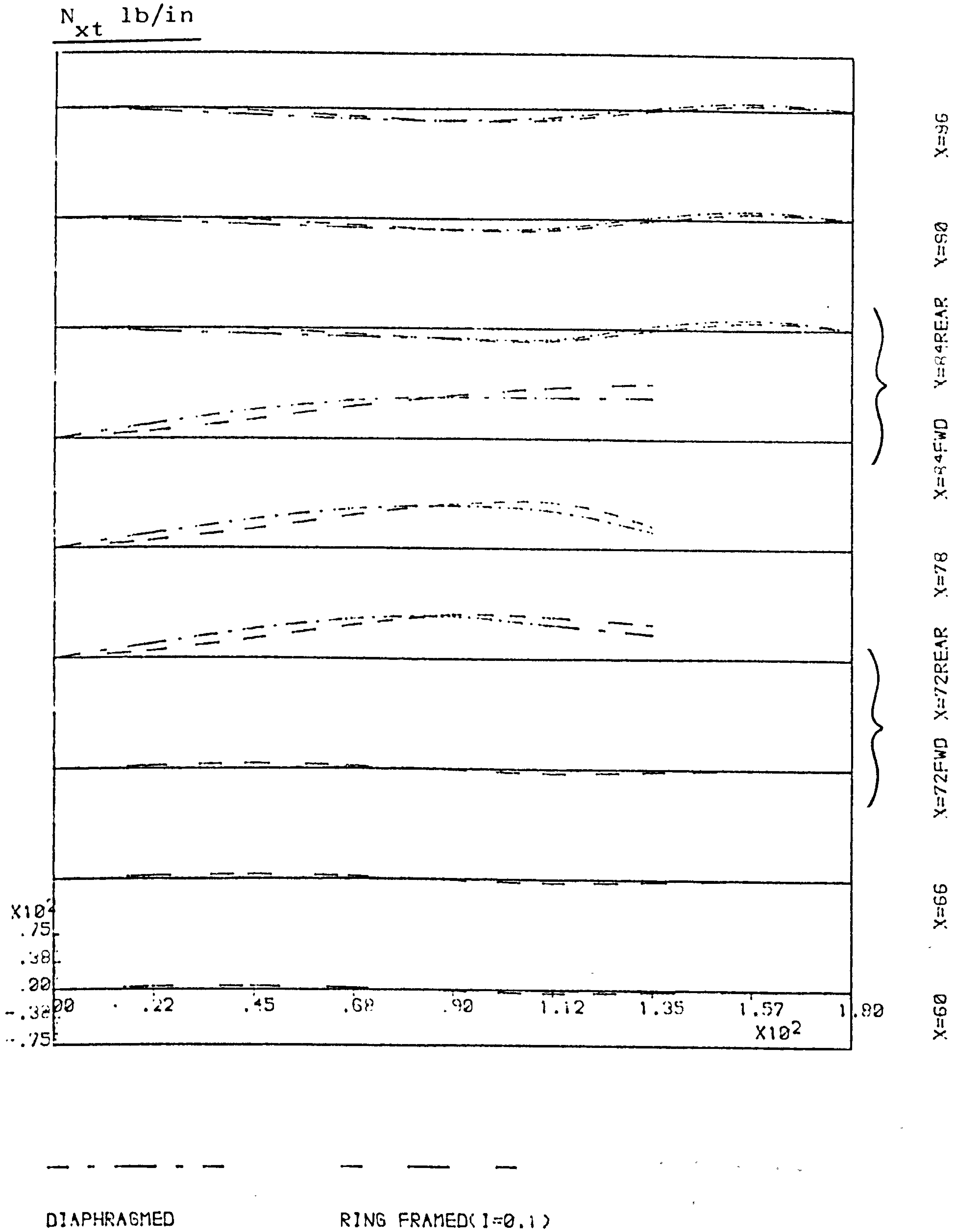

Fig.6.9.3 EFFECTS OF FRAME TYPE WITH CUTOUT - SHEAR FLOW

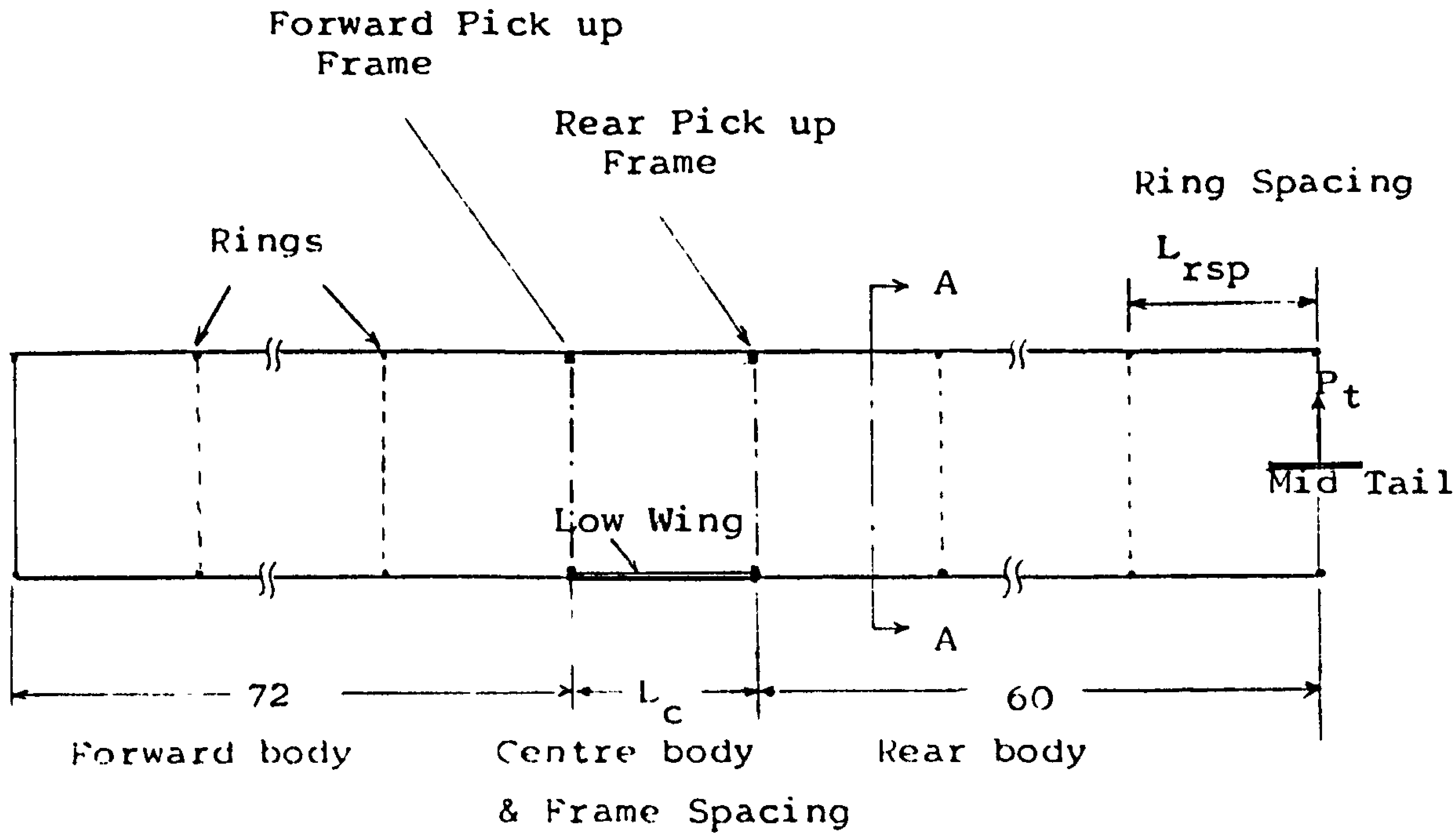

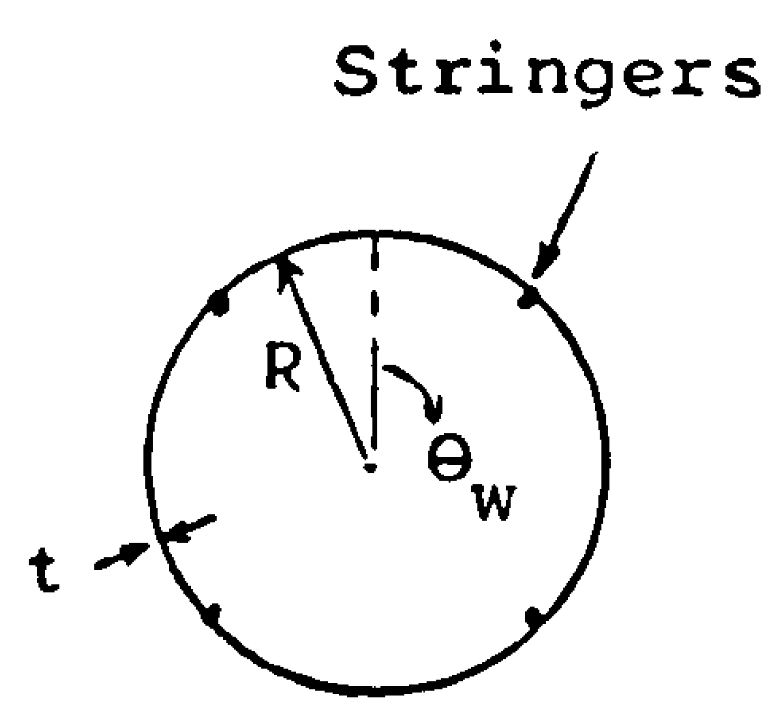

section A-A

Symbols;

A_s; Area of stringer (in^2).

I_f; Second moment of area of frame (in^4).

I_r; Second moment of area of ring stiffener (in^4).

L_{rsp}; Spacing of standard ring stiffeners (in).

N_{str}; Number of stringer (=4).

R; Radius of shell (in).

t; Thick ness of shell skin (in).

t'; Effective skin thickness for direct stress (in).

P_t; Normal force on the tail (lbf).

$Z(Lc)= GtR^4/EI_fL_c$.

N_x; Direct stress (lbf/in).

Q ; Shear stress (lbf/in).

72-Lc-60; Length of body sections(in).

θ_w; Wing position angle (deg).

$\zeta = 1/(\pi + 2A_s/Rt)$ for N_{str}=4.

Fig.7.1.1 Geometry and notations considered.

$72\text{-}L_c\text{-}60$; Tail Load

$R=6.$ $R/t=200$ $A_s/Rt=0.2778$ $I_r/I_f=0.1$ $L_{rsp}=12.$

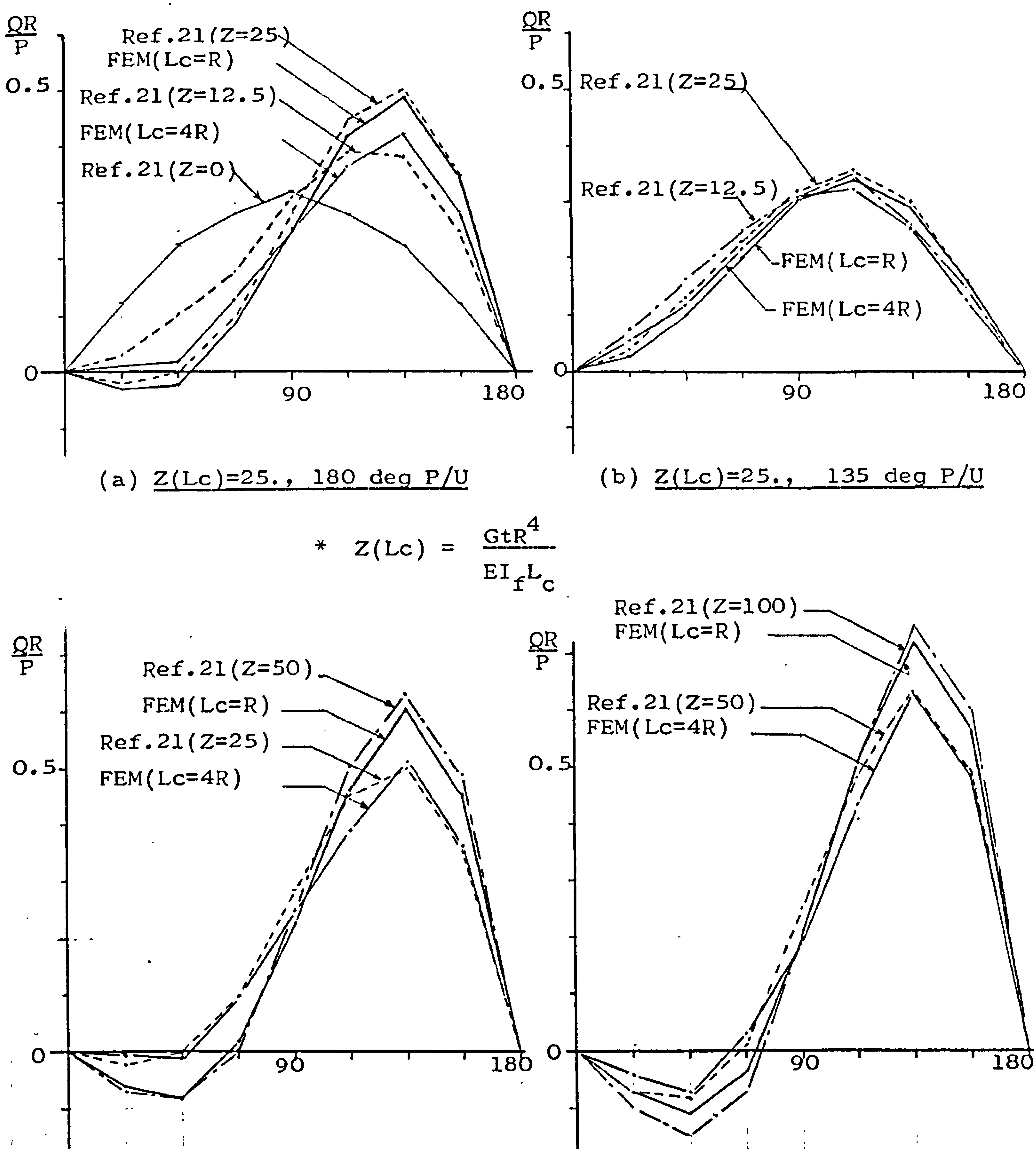

(a) Z(Lc)=25., 180 deg P/U

(b) Z(Lc)=25., 135 deg P/U

$$* \quad Z(Lc) = \frac{GtR^4}{EI_f L_c}$$

(c) Z(Lc)=50., 180 deg P/U

(d) Z(Lc)=100., 180 deg P/U

Fig.7.2.1 Shear flow distributions on the rear frame.

Table 7.1 Effect of variations in the stringer area on the rear pick up frame shear flow distributions.

- o Low wing , tail load, 72-12-60
- o $I_r/I_f = 0.1$, $GtR^4/EI_fL_c = 25.$

i) $R=12.0$ $t=0.06$ $I_f=1.6$ $L_{rsp}=12.$

ii) $R=3.0$ $t=0.03$ $I_f=0.00313$ $L_{rsp}=6.$

$\frac{QR}{P}$

	A_s \ θ	0.	22.5	45.	67.5	90.	112.5	135.	157.5	180.	t'
12R	0.4	0.	-0.033	-0.018	0.076	0.249	0.423	0.503	0.363	0.	.082
	0.2	0.	-0.030	-0.013	0.074	0.246	0.417	0.500	0.363	0.	.0706
3R	0.025	0.	0.003	0.014	0.128	0.252	0.370	0.443	0.289	0.	.0353
	0.0125	0.	0.006	0.014	0.127	0.257	0.366	0.438	0.287	0.	.0326

$GtR^4/EI_fL_c = 25.$; Tail load, 180 deg Pick up

Rear Frame station

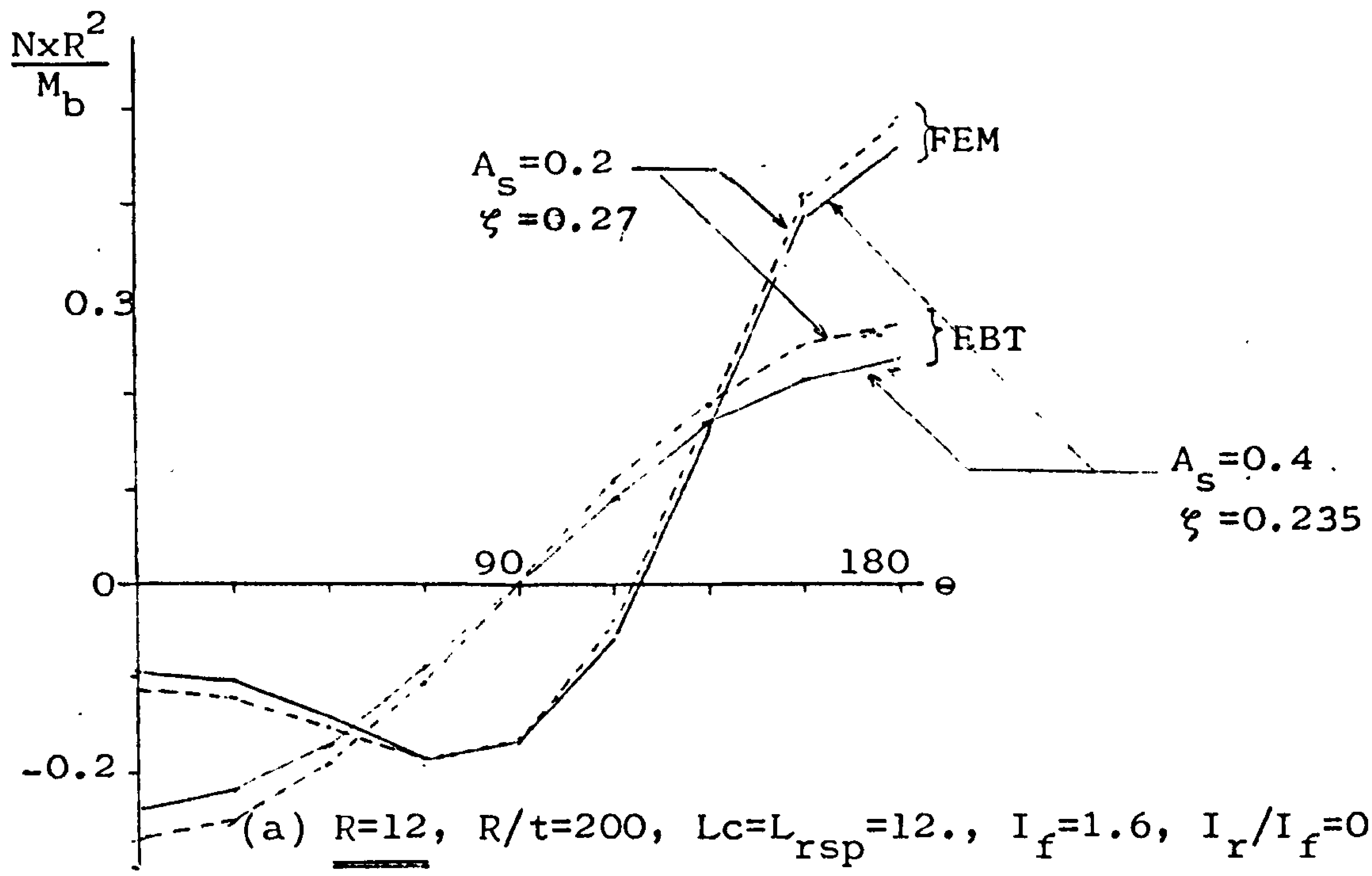

(a) R=12, R/t=200, Lc=L_{rsp}=12., I_f=1.6, I_r/I_f=0.1

$\xi = 1/(\pi + 2A_s/Rt)$

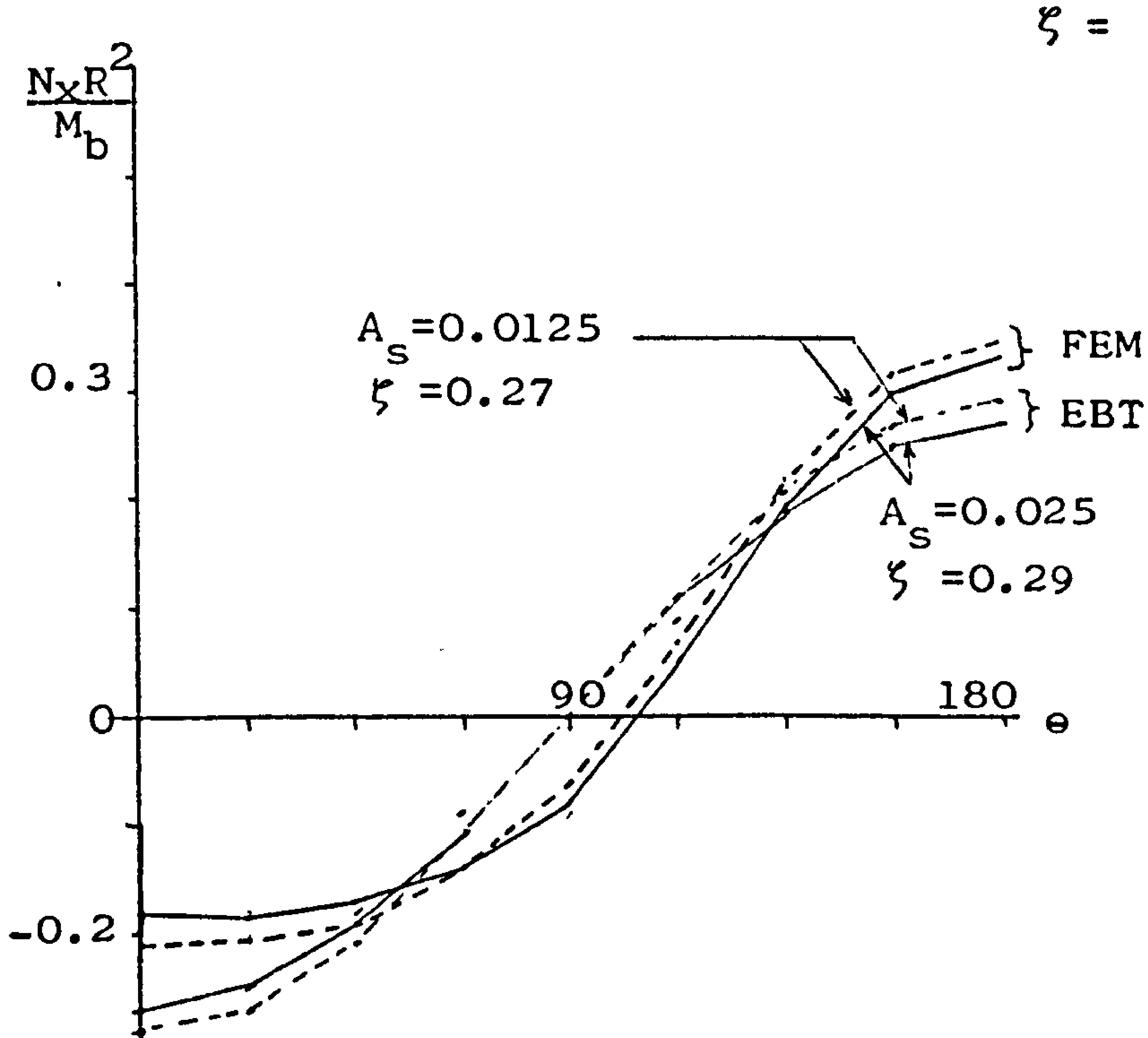

(b) R=3, R/t=100, L_c=12, L_{rsp}=6, I_r/I_f=0.1

Fig.7.2.2 Effect of stringer area on direct stress.

72-Lc-60 , Tail Load

$GtR^4/EI_fL_c = 25.$

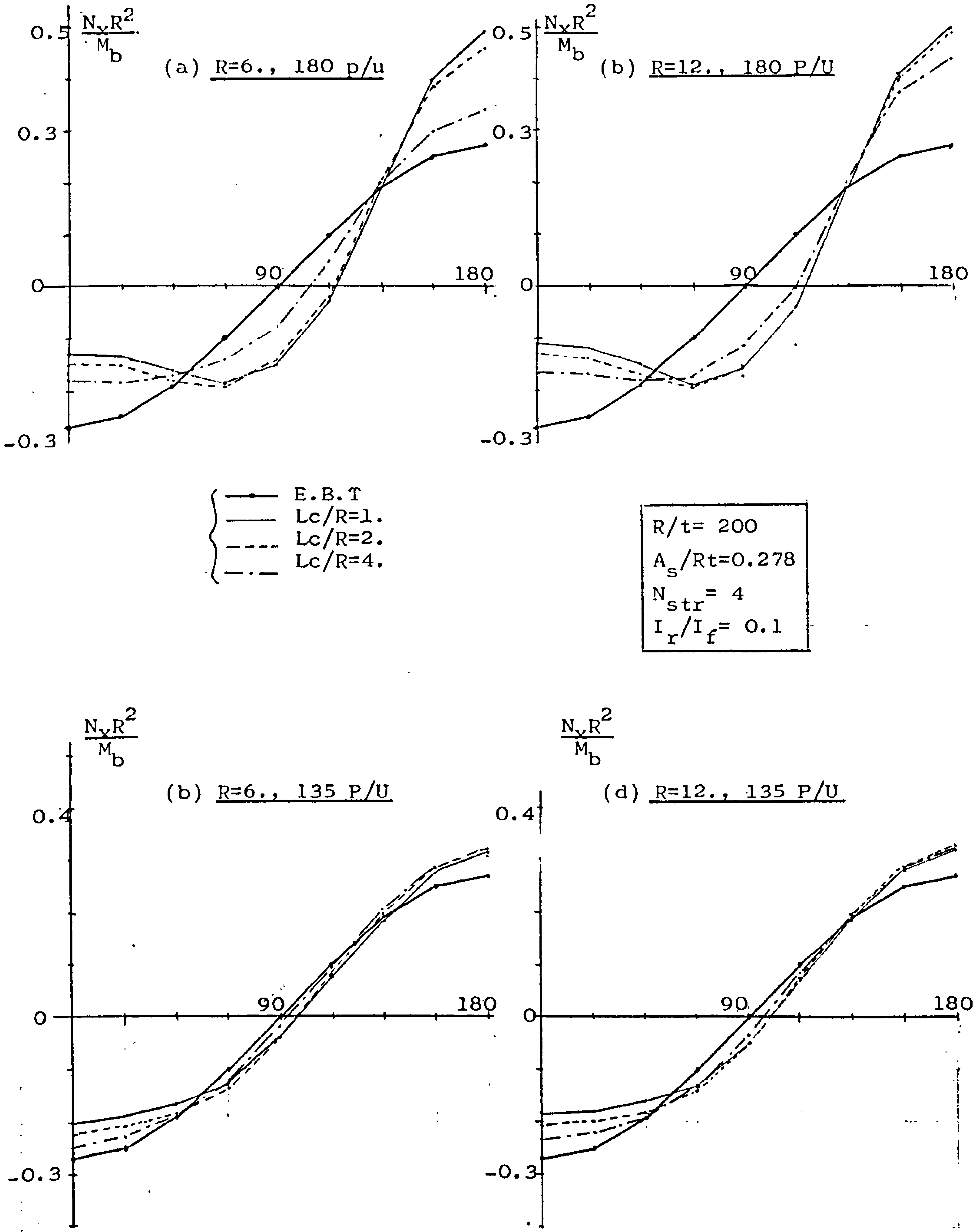

Fig.7.3.1 Direct stress distribution on rear pick up.

Z(Lc)=25.

$GtR^4/EI_f L_c = 25.$, 72-Lc-60, Tail Load

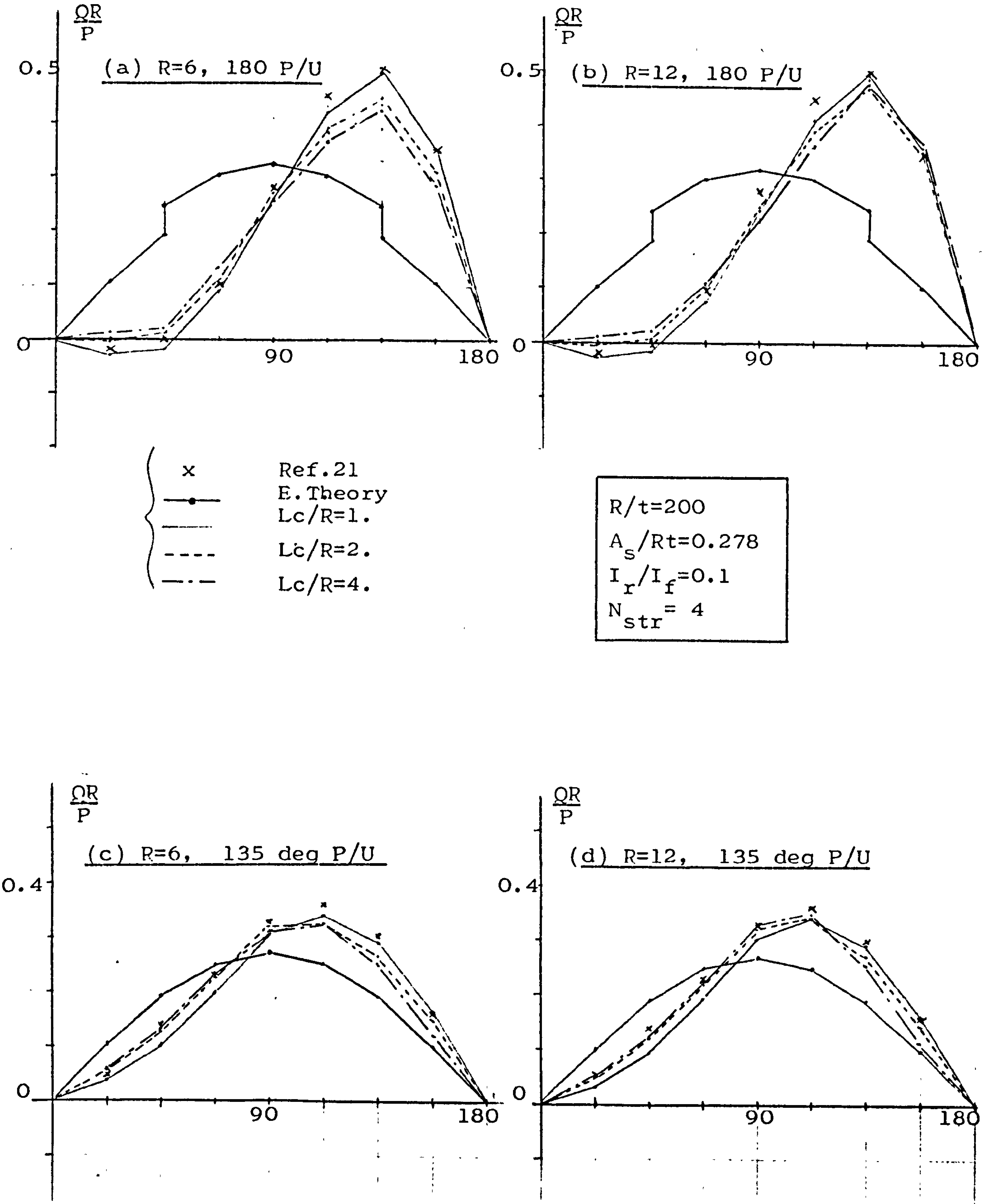

Fig.7.3.2 Shear flow distribution on Rear Frame; Z(Lc)=25.

R=6. R/t=200 $A_s/Rt=0.2778$ $I_r/I_f=0.1$; 180 P/U, Tail load

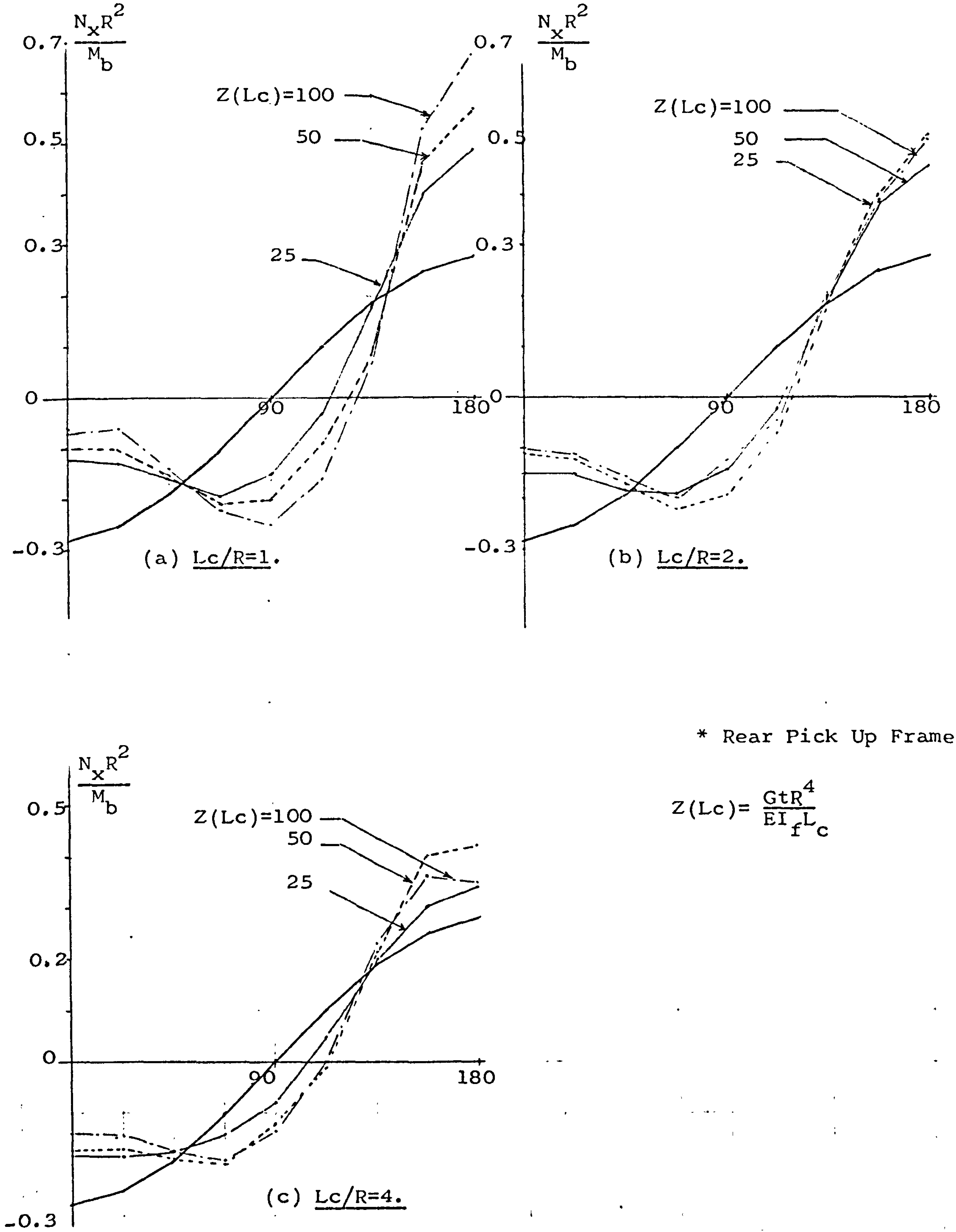

Fig.7.3.3 Effect of variation of Lc/R and Z(Lc) on N_x

R=6. R/t=200 $A_s/Rt=0.2778$ $I_r/I_f=0.1$; 180 P/U, Tail Load

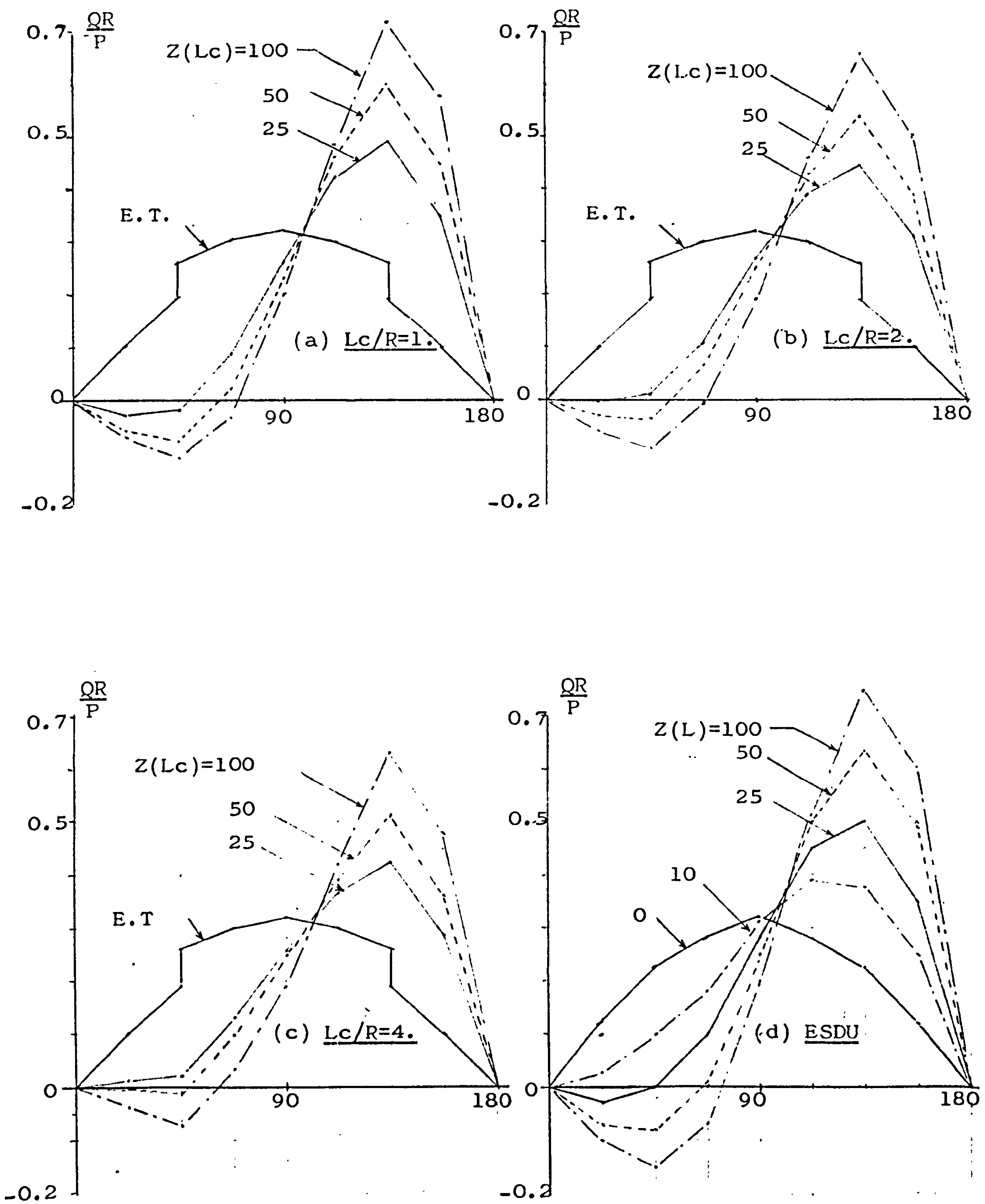

Fig.7.3.4 Effect of variations in Lc/R and Z(Lc); Shear Flow

$72\text{-}L_c\text{-}60$ 180 deg Pick Up Tail Loading

$R/t=200$ $A_s/Rt=0.2778$ $N_{str}=4$ $I_r/I_f=0.1$ $L_{rsp}=12.$

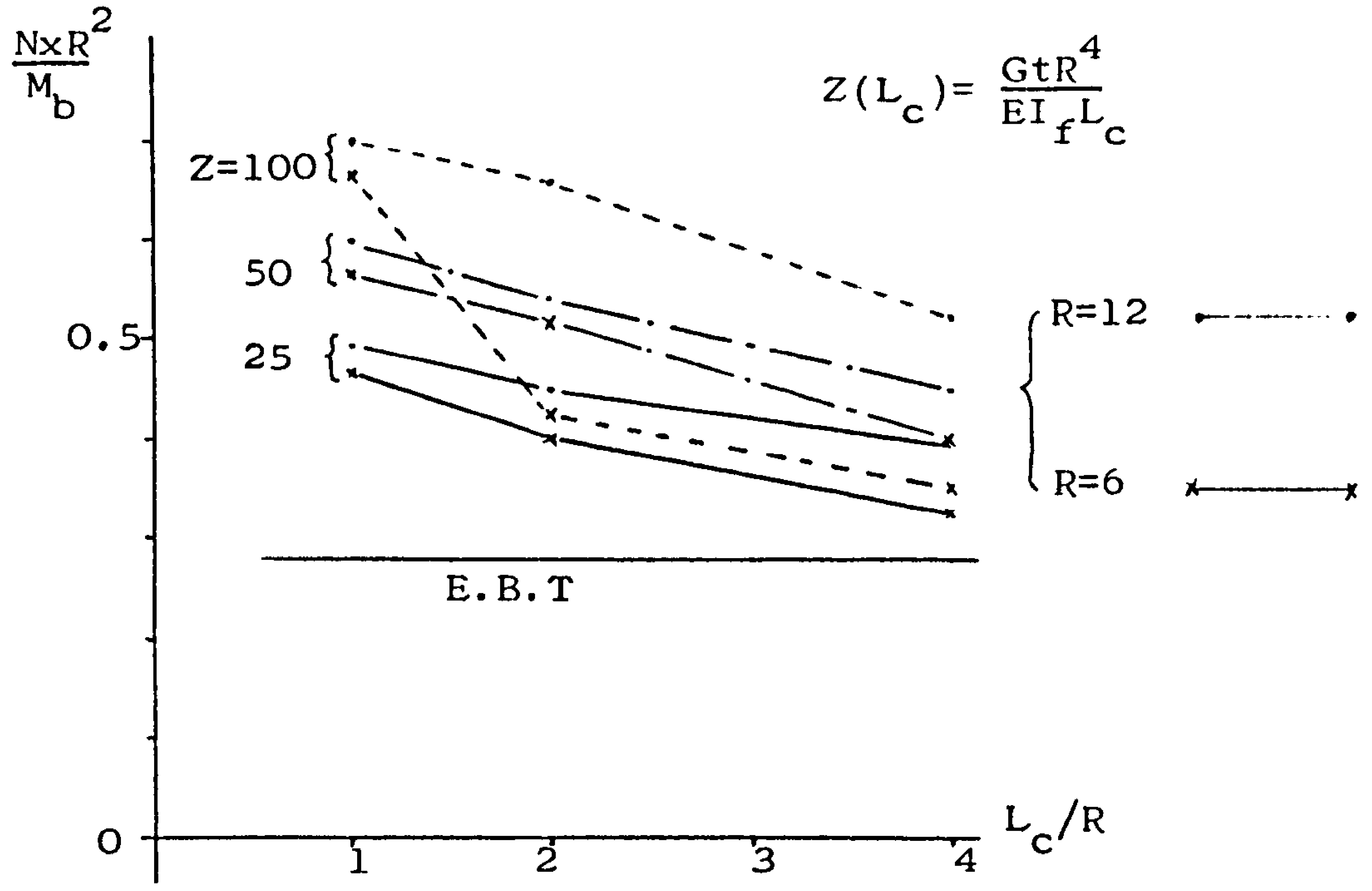

(a)

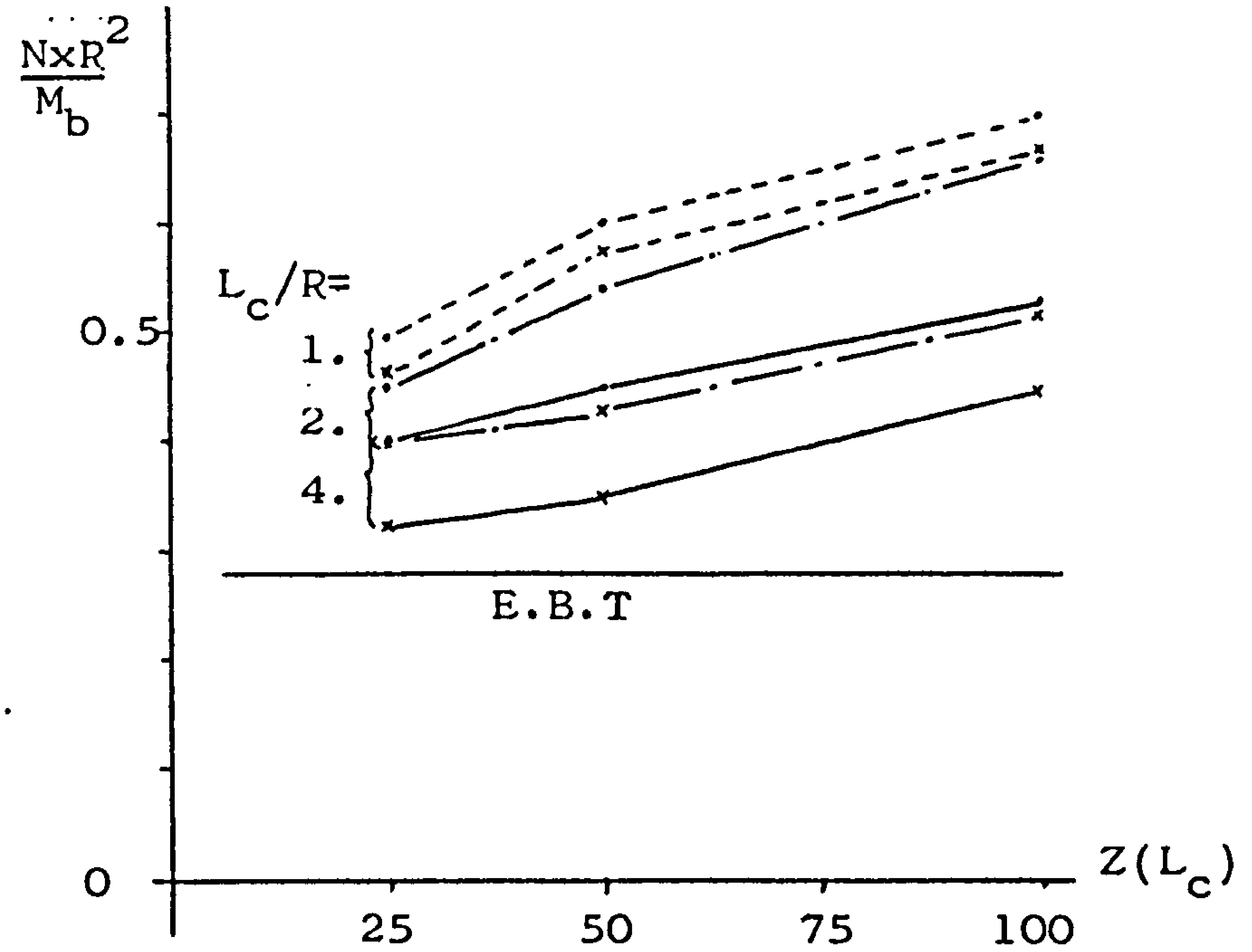

(b)

Fig.7.3.5 Direct stress at 180° on the rear pick up frame.

$72\text{-}L_c\text{-}60$ 180 deg Pick Up ; Tail Loading

$R/t=200$ $A_s/Rt=0.2778$ $N_{str}=4$ $I_r/I_f=0.1$ $L_{rsp}=12$

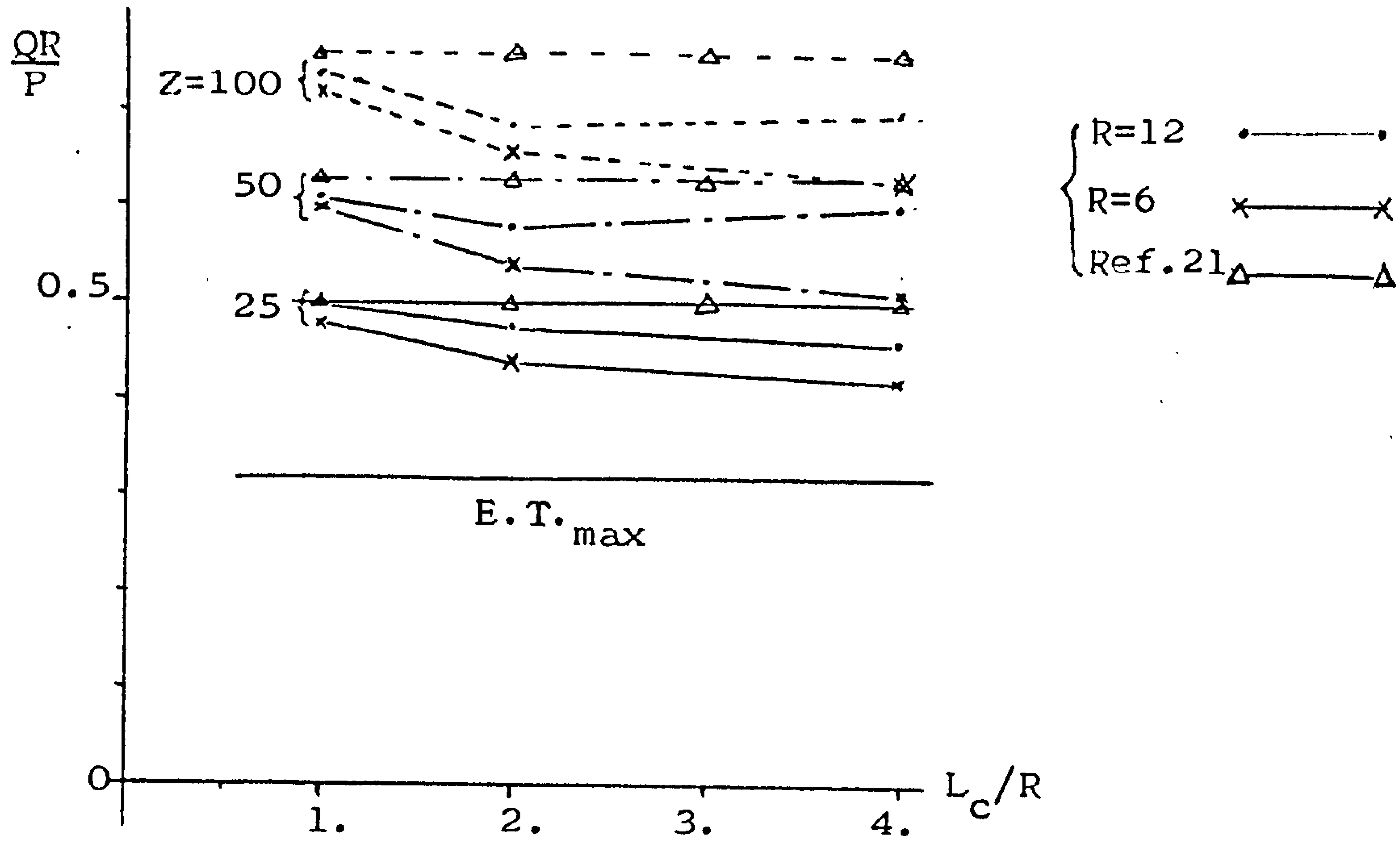

(a)

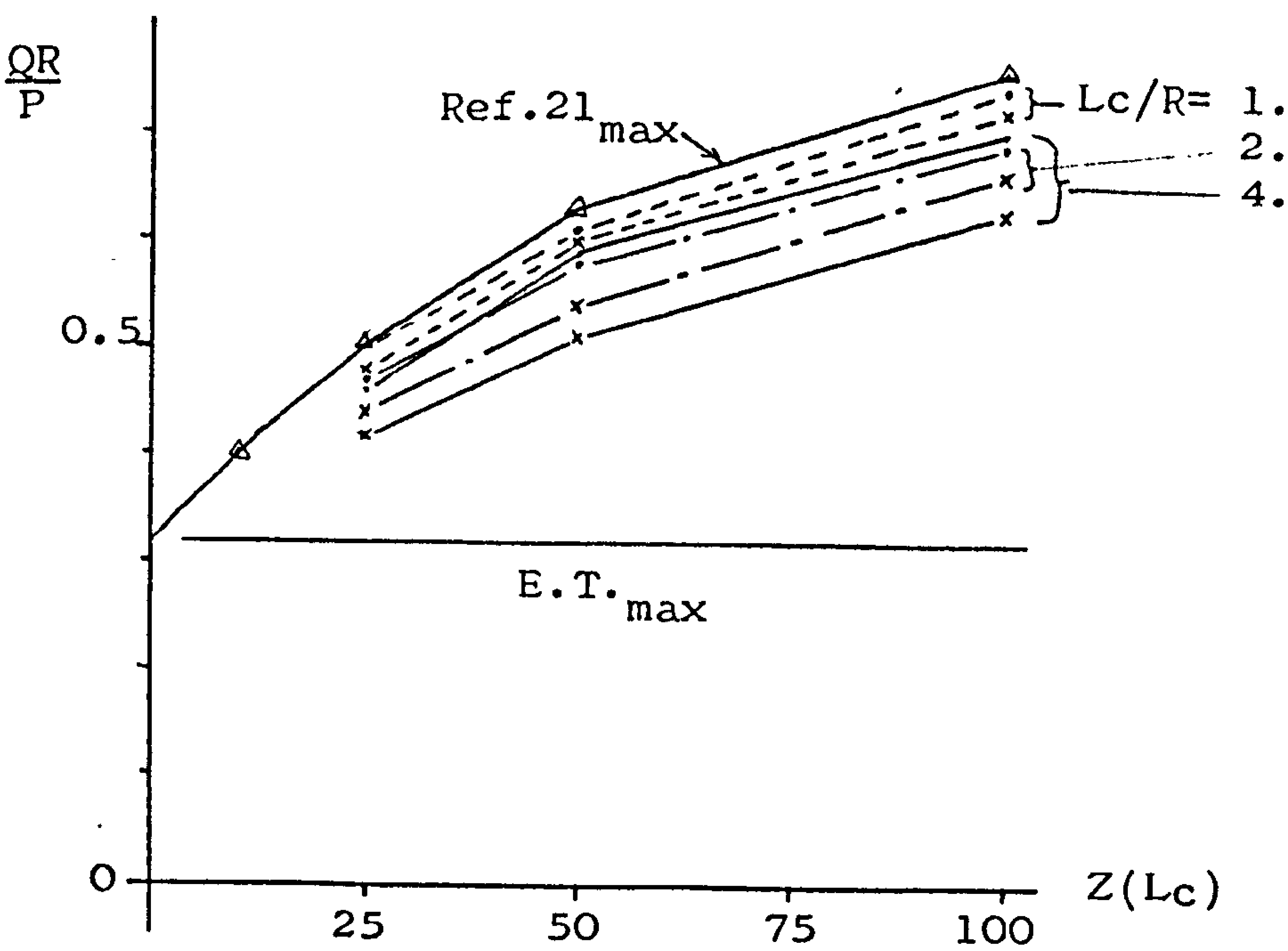

(b)

$$Z(L_c) = \frac{GtR^4}{EI_f L_c}$$

Fig.7.3.6 Variation of maximum shear flow on the rear frame.

$Z(Lc)=25.$ $R=6.$ $t=0.03$ $A_s=0.05$ $Lc=12$ $I_f=0.05$

Rear Frame Station.

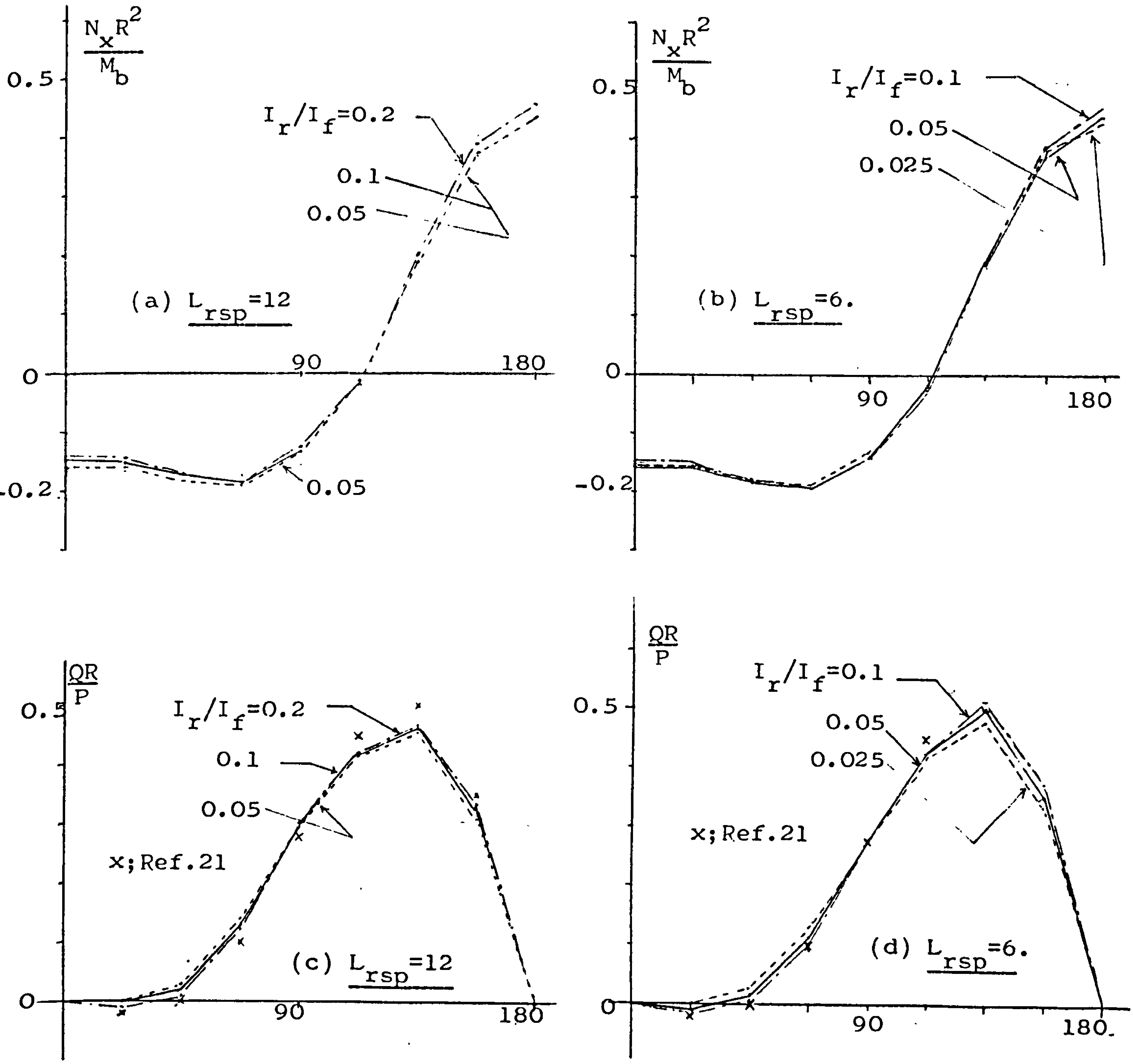

Fig.7.4.1 Effect of variation of I_r/I_f

$GtR^4/EI_f L_c = 25.$ $R=6.$ $R/t=200$ $A_s=0.05$ $I_f=0.05$ $Lc=12$

72-12-60, 180 deg P/U ; Tail Load.

Constant $I_r/L_{rsp}=0.00042$ in^3

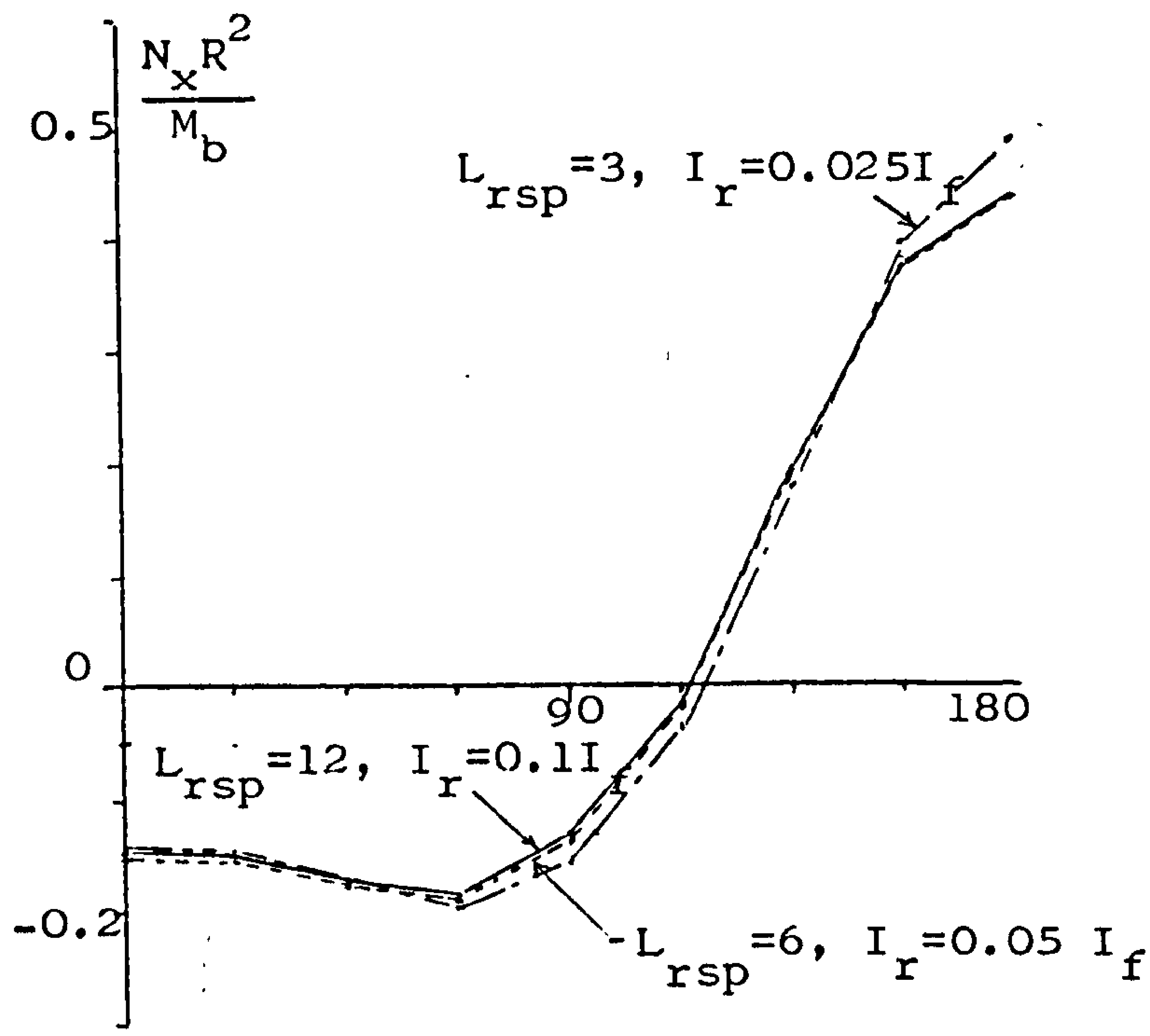

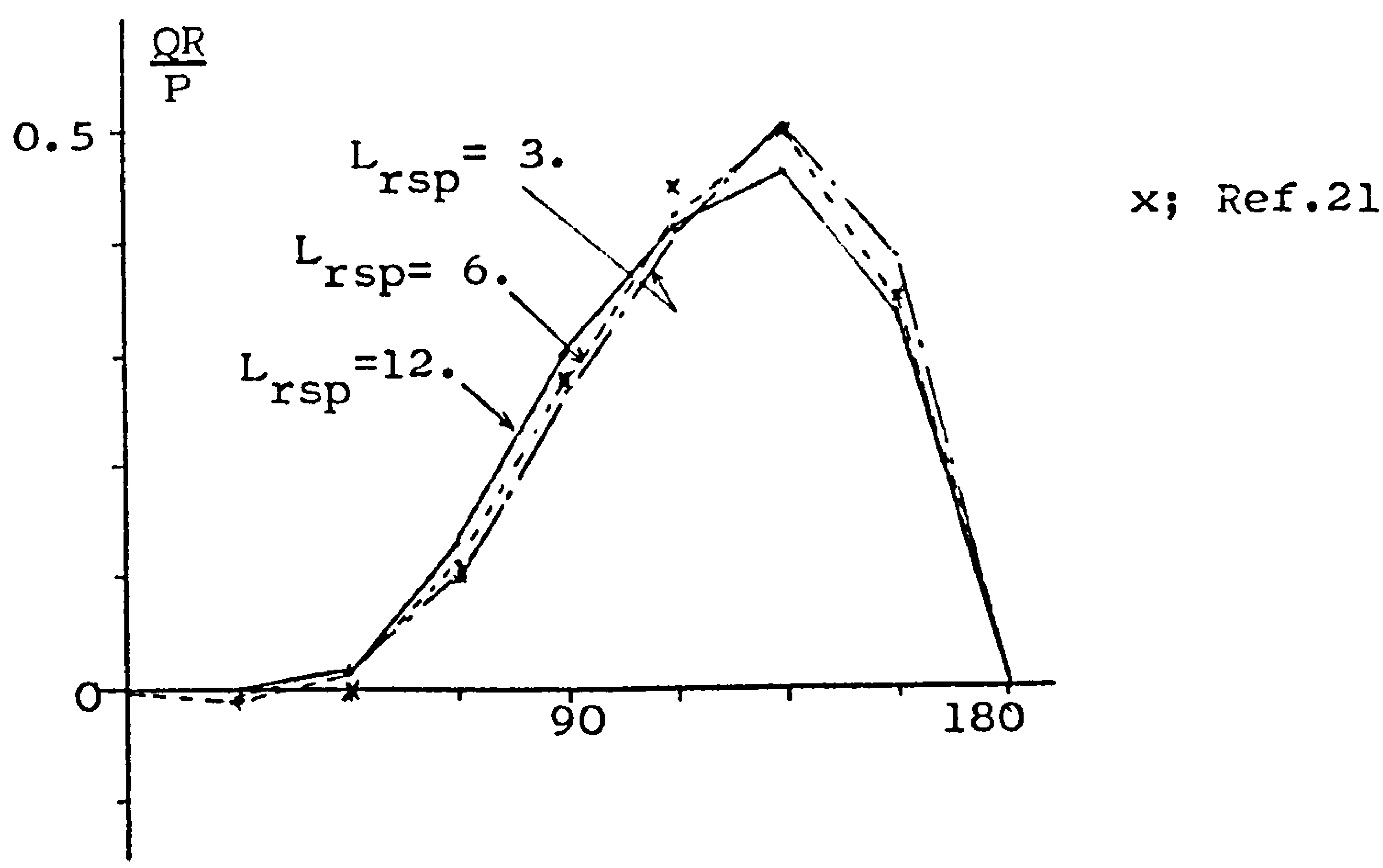

Fig.7.4.2 Effect of Ring spacing variation ; constant I_r/L_{rsp}